TOWARDS A LOCAL REALIST VIEW OF THE QUANTUM PHENOMENON

EDITED BY: Alberto Casado, Ana Maria Cetto, Karl Hess and Andrea Valdés-Hernández

PUBLISHED IN: Frontiers in Physics

frontiers Research Topics

ISSN 1664-8714
ISBN 978-2-88966-641-6
DOI 10.3389/978-2-88966-641-6

About Frontiers

Frontiers is more than just an open-access publisher of scholarly articles: it is a pioneering approach to the world of academia, radically improving the way scholarly research is managed. The grand vision of Frontiers is a world where all people have an equal opportunity to seek, share and generate knowledge. Frontiers provides immediate and permanent online open access to all its publications, but this alone is not enough to realize our grand goals.

Frontiers Journal Series

The Frontiers Journal Series is a multi-tier and interdisciplinary set of open-access, online journals, promising a paradigm shift from the current review, selection and dissemination processes in academic publishing. All Frontiers journals are driven by researchers for researchers; therefore, they constitute a service to the scholarly community. At the same time, the Frontiers Journal Series operates on a revolutionary invention, the tiered publishing system, initially addressing specific communities of scholars, and gradually climbing up to broader public understanding, thus serving the interests of the lay society, too.

Dedication to Quality

Each Frontiers article is a landmark of the highest quality, thanks to genuinely collaborative interactions between authors and review editors, who include some of the world's best academicians. Research must be certified by peers before entering a stream of knowledge that may eventually reach the public - and shape society; therefore, Frontiers only applies the most rigorous and unbiased reviews.
Frontiers revolutionizes research publishing by freely delivering the most outstanding research, evaluated with no bias from both the academic and social point of view. By applying the most advanced information technologies, Frontiers is catapulting scholarly publishing into a new generation.

What are Frontiers Research Topics?

Frontiers Research Topics are very popular trademarks of the Frontiers Journals Series: they are collections of at least ten articles, all centered on a particular subject. With their unique mix of varied contributions from Original Research to Review Articles, Frontiers Research Topics unify the most influential researchers, the latest key findings and historical advances in a hot research area! Find out more on how to host your own Frontiers Research Topic or contribute to one as an author by contacting the Frontiers Editorial Office: frontiersin.org/about/contact

TOWARDS A LOCAL REALIST VIEW OF THE QUANTUM PHENOMENON

Topic Editors:
Alberto Casado, University of Seville, Spain
Ana Maria Cetto, Universidad Nacional Autónoma de México, Mexico
Karl Hess, University of Illinois at Urbana-Champaign, United States
Andrea Valdés-Hernández, National Autonomous University of Mexico, Mexico

Citation: Casado, A., Cetto, A. M., Hess, K., Valdés-Hernández, A., eds. (2021). Towards a Local Realist View of the Quantum Phenomenon. Lausanne: Frontiers Media SA. doi: 10.3389/978-2-88966-641-6

Table of Contents

frontiers in Physics

EDITORIAL
published: 19 February 2021
doi: 10.3389/fphy.2021.651127

Editorial: Towards a Local Realist View of the Quantum Phenomenon

Ana María Cetto[1]*, *Alberto Casado*[2], *Karl Hess*[3] and *Andrea Valdés-Hernández*[1]

[1]Instituto de Física, Universidad Nacional Autónoma de México, Ciudad de México, Mexico, [2]Escuela Técnica Superior de Ingeniería, Departamento de Física Aplicada III, Universidad de Sevilla, Sevilla, Spain, [3]Center for Advanced Study, University of Illinois, Urbana, IL, United States

Keywords: quantum mechanics, realism, locality, contextuality, Bell theorem, zero-point field, de Broglie wave, particle trajectories

Editorial on the Research Topic

Towards a Local Realist View of the Quantum Phenomenon

Quantum mechanics (QM) stands apart from other physical theories inasmuch as its elegant and powerful mathematical formalism conceals the lack of a unique, complete, and coherent conceptual frame in which to accommodate the physical elements that should be put into correspondence with the mathematical objects. Excessive mathematization, blurred physics, and the abandonment of principles on which the remainder of physics rests—such as realism, determinism, locality, objectivity or descriptiveness—have been a discomforting signature in the legacy of QM as we know it.

An aim of this Research Topic was to promote discussions of the physics of QM as seen from different perspectives. Authors were invited to take a closer look beyond the formal apparatus, and point towards new paths for a more physical and realist reframing of QM. The 15 articles included in this issue represent different endeavors to identify underlying physical laws and causal connections, propose a possible "subquantum" theoretical description, revise the rules of correspondence between theory and observation, or offer logical arguments viz. concrete models that question the impossibility theorems.

The introductory statement by Gerard 't Hooft (Hooft) carries the torch for many an article in this issue: "Without wasting time and effort on philosophical justifications and implications, we write down the conditions for the Hamiltonian of a quantum system for rendering it mathematically equivalent to a deterministic system." The natural flow and simplicity of 't Hooft's article are signatures of great mastership that raises the question why we have considered in the past all these philosophical justifications. The answer is, of course, that they trace their origin to the writings of Heisenberg, Bohr, and Einstein. There exists in addition a massive literature on Bell-type inequalities that claims to go beyond philosophy. Bell's theorem has been circumvented by extreme interpretations of experiments with atomic and subatomic entities. One extreme is the increasingly fashionable inference of superluminal "influences" (not information transfer), and the other extreme is the super-determinism as discussed in more palatable forms in the article of Hossenfelder and Palmer (Hossenfelder and Palmer).

Bell's theorem has come to represent a major stumbling block in the search of local realist and deterministic descriptions of our world. Several contributions to this issue, however, demonstrate that it does not constitute the unmovable obstacle that it was thought to be, because it is not only difficult to relate to any actual experiments but also contains questionable physical assumptions. Oaknin (Oaknin) demonstrates that the derivation of Bell-type inequalities suffers from deep physical problems related to the gauging of Bell's variables, which requires an absolute frame of

OPEN ACCESS

Edited and reviewed by:
José S. Andrade,
Federal University of Ceara, Brazil

Correspondence:
Ana María Cetto
ana@fisica.unam.mx

Specialty section:
This article was submitted to Mathematical and Statistical Physics, a section of the journal Frontiers in Physics

Received: *08 January 2021*
Accepted: *18 January 2021*
Published: *19 February 2021*

Citation:
Cetto AM, Casado A, Hess K and Valdés-Hernández A (2021) Editorial: Towards a Local Realist View of the Quantum Phenomenon. Front. Phys. 9:651127. doi: 10.3389/fphy.2021.651127

reference. He shows further that the constraint that Bell-type inequalities supposedly force on the statistics of experimental outcomes may be removed by considering the involvement of gauge symmetries and geometric phases. De Raedt et al. (De Raedt et al.) construct a subquantum model of the Einstein–Podolsky–Rosen–Bohm experiment. Their work uses a digital computer and a discrete-event simulation as a metaphor for idealized, realizable laboratory experiments. All of their variables, including those representing macroscopic events, have definite values and change in time according to an Einstein-local, causal process. Willsch et al. (Willsch et al.) demonstrate further that their Einstein-local simulation models in which particles follow well-defined trajectories, reproduce the results of quantum walk experiments.

A recurrent idea in the present volume is that realism need not be abandoned if one gets rid of concepts such as non-disturbing measurements and non-contextuality. In particular, the evidence against local non-contextual hidden variables offered by many spin–polarization correlation experiments may coexist with a local, causal, realist description of Nature. The possibility of describing physical phenomena with these cherished principles has not been ruled out by some clicks on detectors. Kupczynski (Kupczynski) presents an overview of arguments in support of the idea that the violation of Bell-type inequalities does not necessarily imply the existence of spooky actions at a distance, nor a compulsory renounce to an objective physical reality, provided contextual setting-dependent parameters are included in the description. Such violation simply shows us that "entangled photon pairs cannot be described as pairs of socks nor as pairs of fair dice." Jung (Jung) demonstrates that the strong polarization correlation of entangled photon pairs produced in parametric down conversion can be calculated from wave-like considerations, by assuming a fixed relative phase of the two associated wave packets at the source. As a consequence, the distance between detectors in the Bell-inequality test of local realism becomes irrelevant, and the consideration of faster-than-light communication has no sense at all.

Also Sulis (Sulis) insists in a contextual reality, and proposes an ontological model that incorporates a minimalistic definition of generated reality, possesses a non-Kolmogorov probability structure, and is consistent with nonrelativistic QM. In this scenario, nonrelativistic QM appears as an effective, approximate theory, and the Hilbert-space formalism—extraordinarily useful for the practical purpose of performing calculations—fails in providing an ontological model of QM, ultimately leading to many of its conundrums. The problem lies not with reality but rather with the mathematical tools employed to represent it. All of these facts reaffirm Gerard 't Hooft's enunciation against wasting time and efforts on perceived obstacles that lie outside the direct mathematical physics.

A further specific local realistic interpretation of the entangled photon pairs is offered by Santos (Santos), who studies the generation of polarization-entangled photon pairs produced in parametric down conversion using the Weyl–Wigner formalism in the Heisenberg picture, a more formal approach of quantum optics than the one used by the author and coworkers in previous articles. The picture that emerges resembles classical optics by taking into account the zero-point radiation field entering the nonlinear crystal as a real stochastic field, and entanglement corresponds to a correlation of fluctuations between a signal and a vacuum field in distant places. A detailed discussion is made about the detection process and the relationship of this approach to local realism. Further, in a study by Casado et al. (Casado et al.) the Wigner representation in the Heisenberg picture is used for the study of the quintessential experiment on quantum teleportation, the Innsbruck experiment. The visible presence of the zero-point field is stressed, and new physical insights are given that lead to a deeper knowledge of this experiment. Concretely, entanglement and the collapse postulate are replaced by the consideration of the quadruple correlation properties of the field corresponding to the propagation of two couples of independent photon pairs. The role of the vacuum inputs in Bell-state analysis is investigated, with its presence reinforcing the idea of the zero-point amplitudes as "hidden variables."

Consideration of the effects of the zero-point field on the dynamics takes us to the realm of stochastic electrodynamics (SED), which has been developed to provide a concrete local realistic explanation of the quantum behavior of matter. Cole (Cole) uses a new technique based on SED, to successfully calculate probability–density and n-point correlation functions, both for the complete Planckian field including the zero-point component, and for an electric dipole oscillator embedded in it. The H atom, however, turns out to be far more difficult to deal with. Cole's elaborate but transparent method makes an interesting contrast to Feynman's path-integral approach—where also the H atom appeared to be intractable for more than 3 decades. Considering the importance of finding a proper treatment of SED to describe the H atom, Nieuwenhuizen (Nieuwenhuizen) makes a renewed attempt to avoid self-ionization by studying the atom's ground state perturbed by the zero-point field and using several renormalization schemes that suppress high-frequency tails, which however do not lead to a satisfactory solution. While in the approaches of Cole and Nieuwenhuizen the zero-point field merely perturbs the classical motion, de la Peña et al. (Peña et al.) argue that its influence is far more profound and leads to a nonclassical dynamics. The contact made between SED and stochastic quantum mechanics serves to demonstrate that Newton's second law is modified in an essential way by stochasticity, which is at the core of the transition to the quantum dynamics. The interplay of diffusion and radiation reaction allows the system to converge towards a balance regime, thus offering an explanation for atomic stability.

The wave element, from the outset present in SED, provides a natural bridge to the work by Durey and Bush (Durey and Bush), who ably harness insights gained from the hydrodynamic walking-droplet system to further develop their de Broglie-inspired model of quantum dynamics, and thus lay the foundations for deeper study of what they term hydrodynamic quantum field theory. A complex and detailed analysis, both theoretical and numerical, serves to show that the pilot wave is a combination of short, Compton-scale waves that propagate away from the moving particle, and a de Broglie-scale carrier wave—just as envisaged by de Broglie and reaffirmed in SED. Finally, that the wave–particle duality can be discussed in the light of a causal and objectively realist model of the electron is demonstrated by Avner and Boillot (Avner and Boillot). Their

relativistic electrodynamical model of the subatomic particle at rest involves charged sub-particles following definite trajectories, and stands in sharp contrast with the Heisenberg (widespread) belief that only the abstract (mathematical) description of particles exists. The authors thus direct their attention to explore the gears of one of the most emblematic quantum particles, within an approach that supports the principles of determinism, causality, and objective reality.

AUTHOR CONTRIBUTIONS

All authors listed have made a substantial, direct, and intellectual contribution to the work and approved it for publication.

ACKNOWLEDGMENTS

Partial funding from DGAPA-UNAM through Project PAPIIT IN113720 is acknowledged.

Conflict of Interest: The authors declare that the research was conducted in the absence of any commercial or financial relationships that could be construed as a potential conflict of interest.

frontiers in Physics

ORIGINAL RESEARCH
published: 29 July 2020
doi: 10.3389/fphy.2020.00253

Deterministic Quantum Mechanics: The Mathematical Equations

*Gerard 't Hooft**

Institute for Theoretical Physics, Utrecht University, Utrecht, Netherlands

Without wasting time and effort on philosophical justifications and implications, we write down the conditions for the Hamiltonian of a quantum system for rendering it mathematically equivalent to a deterministic system. These are the equations to be considered. Special attention is given to the notion of "locality." Various examples are worked out, followed by a systematic procedure to generate classical evolution laws and quantum Hamiltonians that are exactly equivalent. What is new here is that we consider interactions, keeping them as general as we can. The quantum systems found, form a dense set if we limit ourselves to sufficiently low energy states. The class is discrete, just because the set of deterministic models containing a finite number of classical states, is discrete. In contrast with earlier suspicions, the gravitational force turns out not to be needed for this; it suffices that the classical system act at a time scale much smaller than the inverse of the maximum scattering energies considered.

Keywords: determinism, Hamiltonian, cellular automaton, locality, ontology, interaction, quantum

OPEN ACCESS

Edited by:
Karl Hess,
University of Illinois at Urbana-Champaign, United States

Reviewed by:
Hans-Thomas Elze,
University of Pisa, Italy
Luis De La Peña,
National Autonomous University of Mexico, Mexico

***Correspondence:**
Gerard 't Hooft
g.thooft@uu.nl

Specialty section:
This article was submitted to Mathematical and Statistical Physics, a section of the journal Frontiers in Physics

Received: *19 May 2020*
Accepted: *09 June 2020*
Published: *29 July 2020*

Citation:
't Hooft G (2020) Deterministic Quantum Mechanics: The Mathematical Equations. Front. Phys. 8:253. doi: 10.3389/fphy.2020.00253

1. INTRODUCTION: ONTOLOGICAL QUANTUM MECHANICS

Discussions of the interpretation of quantum mechanics [1–20] seem to be confusing and endless. This author prefers to consider the mathematical equations that make the difference. Having the equations will make the discussion a lot more straightforward. Here, we reduce the theory of quantum mechanics to a mathematical language describing structures that may well evolve deterministically. The language itself is equally suitable for any system with classical or quantum evolution laws[1].

Every state a system can be in is represented by a unit vector. We are interested in distinguishing "ontological states." These are unit vectors that are mutually orthogonal and have norm one; they form an orthonormal basis of Hilbert space. We can distinguish finite dimensional Hilbert spaces and infinite dimensional ones. A system is said to be deterministic if ontological states evolve into ontological states [21–23].

We use Dirac's bra-ket notation [1] both for classically evolving systems and for quantum mechanical ones. A state is indicated as $|n\rangle$, where n stands short for some description of this state. Often, we simply enumerate all available states, choosing $n \in \mathbb{Z}$, the set of integers. Alternatively, we can have states $|x\rangle$, where x takes the values of all real numbers, or we can have vectors, $|\vec{x}\,\rangle$, $|\vec{n}\,\rangle$, ...

The first models we consider will seem to be too simplistic to represent all interesting and relevant quantum systems in general. These basic models must be looked upon as building blocks for a more complete theory for deterministic quantum mechanics[2]. At the end they will be coupled by (deterministic) interaction Hamiltonians. What is produced in this paper is a generic machinery

[1]Systems that are irreversible in time can also be described this way but require adaptations not considered in this paper.
[2]The words "deterministic" and "ontological," or "ontic" for short, are almost interchangeable in this paper.

to be employed in these constructions. We do realize that further streamlining will make our fundamental observations more transparent.

Determinism can be recognized by analysing the eigenvalue spectrum of the Hamiltonian [21]. At first sight, it seems that only Hamiltonians that are linear in the momenta can represent ontological systems, but this happens only if one assumes the system to be strictly continuous. If we assume the time coordinate to be on a (very dense) lattice, the Hamiltonian eigenvalues are periodic, i.e., these eigenvalues can be forced to sit on a finite interval. If temporarily we limit ourselves to a single, isolated, elementary building block of a more general quantum system, allowing for only a finite number of states, we may assume it to be periodic in time. As we shall observe, deterministic periodic systems can be identified with quantum harmonic oscillators; these have quite realistic Hamiltonians complete with one stable ground state. If time is quantized, we find a useful internal $SU(2)$ symmetry. In that case, there is not only a vacuum state (the state with lowest energy), but there is also an "antivacuum," the state with highest energy. Antivacua may play an important role in black hole physics [24].

Special attention is needed for the concept of locality. For instance, in a free quantum particle in one spacial dimension, with a fairly general expression of the kinetic energy function $T(p)$, we can define an appropriate ontological operator, its "beable," but it is a non-local function of x and p. Such models cannot directly be applied to physically realistic scenarios; instead, they are used as intermediate steps toward more satisfactory procedures, as will be explained. We claim that locally ontological and deterministic systems can be constructed that nevertheless feature quantum mechanical properties, including models as complex as the Standard Model. These deterministic systems take the form of "cellular automata" [25–28]. Formally, there is a limit to the accuracy by which this can be done, but if, as is suspected, the scale at which determinism becomes manifest, is the Planck scale, then we shall have an enormous range of ontological theories that can reproduce all known data quite accurately. They will all be fully quantum mechanical in the usual [29–31] sense.

This includes the Born interpretation of the absolute squares of amplitudes as representing probabilities [32]. Here, we are still free to use various different definitions of what "probability" might mean; in all cases, the definition will be passed on to the wave functions being considered. In our case: *probability in* = *probability out*: the probability for the outcome of an experiment is directly related to the probability for the initial state that was chosen. The Schrödinger equation just passes on that concept of probability from initial to final state.

Second quantization will be a natural ingredient, a process that restores not only local causality, but also positivity of the Hamiltonian; in principle, it works just as in Dirac's formalism for quantized fields, but in our formalism, the interactions are taken care of in a way that is somewhat more complicated than in the Standard Model. We find that second quantization serves a double purpose: it restores special relativity without generating negative energy states [33–36], and it also restores locality without sacrificing ontology. Second quantization in our formalism has been elucidated in [21].

Our paper is set up as follows. Deterministic models may be seen as consisting of elementary cells inside which the data just oscillate in periodic orbits. We first explain such cells in section 3. We explain and exploit the $SU(2)$ symmetry that shows up and comes out handy, because this symmetry is so well-known and studied.

The idea that deterministic systems of this kind can be described *as if* they were quantum mechanical, is briefly illustrated in section 4. Hilbert space is an extremely useful device, but it should *not* be taken for granted that Hilbert space is prerequisite in elementary quantum theory. In contrast however, the notion that energies, momenta, and even space-time coordinates, are *quantized*, is very essential, and consequences of this are immensely important for our understanding of nature.

We then go into the direction of thinking about particles in an ontological language. This should be possible, but it seems to give a serious clash with the most elementary concepts of locality. A single quantum particle of the kind we frequently encounter in atomic physics, in solids, and in most of the elementary particles, behaves in a way that does not seem to allow directly for a deterministic interpretation. We do describe what happens in sections 5 and 6. A single, isolated particle can be well described if its kinetic energy is just a linear function of its momentum; if the kinetic energy is anything more general than that, we do have an interesting ontological variable, but it is non-local. This jeopardizes any attempt to add some kind of ontological potential term for the particle.

Section 7 sets the stage for what comes next, and then comes the most important part of this paper. A reader who wants to go directly into the deep should mainly be interested in sections 8 and 9. Here, we join our elementary cells into a construction where they interact, again allowing only deterministic interaction laws. We do things that are normally not considered: allow for evolution laws that directly exchange ontological states. Surprisingly perhaps, this leads to interaction Hamiltonians that are as general and as complicated as what we usually only encounter in genuine quantum systems. We emphasize that this proves that the distinction between "quantum interactions" and "classical interactions" is artificial, and was the result of our lack of phantasy concerning the interactions that are possible, even if we limit ourselves to what usually is called "deterministic." As will be seen explicitly in section 9, what is normally thought of as being "quantum mechanics" can be attributed to the effect of fast, almost hidden, variables.

A picture emerges of quantum mechanics being an auxiliary device, it is a scheme allowing us to perform statistical investigations far beyond the usual procedures in condensed matter physics and thermodynamics. What is found can be referred to as a "deterministic local field theory," which might be able to dethrone "quantum field theory."

Our mathematics may hint at what might be the main fundamental cause of the apparently true "quantum" nature of our world. The source of the apparent indeterminism in quantum mechanics appears to be *timing*. When two systems, just slightly separated from one another, are allowed to interact, we have to

realize that both systems contain internal parts that oscillate at time scales that are very small even according to time standards used in elementary particle physics. The only way to register what happens when they interact, is to project away the ultra fast time components of both systems. This can only be done by selecting sufficiently low energy eigen states of the Hamiltonian, which is a procedure that can only be done by introducing Hilbert space. Today, physicists only have access to the very lowest energy states, and these can only be addressed in quantum mechanical language. We leave it to the philosophers to expand on such observations or suspicions.

2. THE STANDARD QUANTUM MECHANICAL HAMILTONIAN FOR CONTINUOUS SYSTEMS

Historically, quantum mechanics was first studied for continuous systems, that is, coordinates and momenta are continuously defined on $\mathbb{R}^n$ spaces. The generic Hamiltonian H is then written as

$$H = T(\vec{p}\,) + V(\vec{x}\,) + \vec{A}(\vec{x}\,)\cdot p \tag{1}$$

where $\vec{x}$ and $\vec{p}$ are the usual, continuously defined, coordinates and momenta, obeying

$$[x_i,\, p_j] = i\delta_{ij}\,. \tag{2}$$

the third term is actually the simplest. A Hamiltonian having *only* this term, describes a completely deterministic system, since the Hamilton equations then read:

$$H = \vec{A}(\vec{x}\,)\cdot\vec{p} \qquad \frac{\mathrm{d}}{\mathrm{d}t}\vec{x} = \frac{\partial H}{\partial \vec{p}} = \vec{A}(\vec{x})\,, \tag{3}$$

while the time derivative of $\vec{p}$ is not directly needed. We point out that, in some elementary sense, *all* deterministic evolution laws can be cast in the form (3), so this is actually a very important case.

In the usual quantum systems, we have as a central unit the kinetic term $T(\vec{p}\,)$. Usually, but not always, it takes the form $T(\vec{p}\,) = \frac{1}{2}\vec{p}^{\,2}$. In that case, the "magnetic" term $\vec{A}\cdot\vec{p}$ plays a more secondary role. This case is already considered "essentially quantum mechanical," displaying the characteristic interference patterns. Still, particles that basically move in straight lines might not be the most interesting physical things, so the third term, $V(\vec{x})$, where the function V can be almost anything, would be needed to cover almost all systems of physical interest. This is the most difficult case from the present point of view.

In our discussion, we take one important step backwards: space, time, and often also momentum, will be kept discrete. The continuum limit can always be considered at some later stage. The question is, whether we can handle the interesting case of the general Hamiltonian (1), as the continuum limit of the models that will be discussed now. These models typically describe only a finite-dimensional vector space, for the time being.

3. THE PERIODIC MODEL, AND ITS *SU*(2) SYMMETRY

Our elementary building block will be a system or device that updates itself at every time step, of duration δt, and, after a period $T = N\,\delta t$, it returns to its initial position. The elementary, ontological states are $|k\rangle^{\mathrm{ont}}$, where k is an integer, $k = 0, \ldots N-1$. Note that, at this stage, there is no quantum mechanics in the usual sense, but we shall use quantum mechanics merely as a language [21]. The ontological states considered here are closely related to the concept of "coherent states" that have a long history going back to Glauber [37].

The evolution operator over one time step, $U(\delta t)$, is simply defined by

$$|k\rangle^{\mathrm{ont}}_{t+\delta t} \;=\; U(\delta t)\,|k\rangle^{\mathrm{ont}}_{t} = |k+1 \mod N\rangle^{\mathrm{ont}}_{t}\,.$$
$$U(\delta t) \;=\; \begin{pmatrix} 0 & \cdots & 0 & 1 \\ 1 & \cdots & 0 & 0 \\ \vdots & \ddots & & \vdots \\ 0 & \cdots & 1 & 0 \end{pmatrix}\,. \tag{4}$$

The matrix U is easily diagonalized by using the finite Fourier transformation:

$$|k\rangle^{\mathrm{ont}} \;=\; \tfrac{1}{\sqrt{N}}\sum_{n=0}^{N-1} e^{-2\pi i nk/N}|n\rangle^{E}$$
$$|n\rangle^{E} \;=\; \tfrac{1}{\sqrt{N}}\sum_{k=0}^{N-1} e^{2\pi i nk/N}|k\rangle^{\mathrm{ont}} \tag{5}$$

where $|n\rangle^E$ are the energy eigenstates. We have

$$U(\delta t)|n\rangle^{E} = e^{-2\pi i n/N}|n\rangle^{E} \tag{6}$$

and we can define the Hamiltonian matrix H by imposing

$$U_{\delta t} = e^{-iH\delta t} \qquad H|n\rangle^{E} = \tfrac{2\pi n}{N\delta t}\,|n\rangle^{E} = n\omega\,|n\rangle^{E} \qquad \omega = \tfrac{2\pi}{T} \tag{7}$$

(Note that the *ground state energy* has been tuned to zero here; we shall also do this when the harmonic oscillator is discussed; the reader may always consider "corrected" definitions where the ground state has energy $\frac{1}{2}\omega$).

With the Fourier transform (5), one can easily determine how H acts on the ontological states $|k\rangle^{\mathrm{ont}}$.

Our mathematical machinery becomes more powerful when we realize that the energy eigenstates may be regarded as the eigenstates $|m\rangle$ of L_3 in a three dimensional rotator. Let the total angular momentum quantum number ℓ be given by

$$N \equiv 2\ell + 1 \qquad n = m + \ell \qquad H = \omega(L_3 + \ell)\,. \tag{8}$$

Then define the (modified) operators p and x by

$$L_1 \equiv p\sqrt{\ell} \quad L_2 \equiv x\sqrt{\ell} \quad [\,x,\,p\,] = -iL_3/\ell = i(1 - H/\omega\ell) \tag{9}$$
$$\ell(\ell+1) = L_1^2 + L_2^2 + L_3^2 \;\rightarrow\; H = \tfrac{\omega}{1-H/2\omega\ell}\,\tfrac{1}{2}(p^2 + x^2 - 1) \tag{10}$$

and we see that, when ℓ tends to be large (while the energy H and the fundamental time step δt are kept small), this reduces to the standard Schrödinger equation for the harmonic oscillator (the ground state value $\frac{1}{2}\omega$ has been subtracted from this Hamiltonian). Both x and p take $2\ell+1$ values, and they span the entire Hilbert space, but they are not ontological. We identify the original states $|k\rangle^{\rm ont}$ [Equation (4)], as our ontological states.

The operators $L_\pm = L_1 \pm iL_2$ play the role of creation and annihilation operators: they add or subtract one unit ω to the energy of a state. However, in the upper half of the spectrum, $L_\pm$ interchange their positions: the algebra is such that L_+ can no longer add energy above the limit $m=+\ell$, so that the energy spectrum stretches over the finite interval $[0,\ 2\ell\omega]$. There is an obvious symmetry $H \leftrightarrow 2\ell\omega - H$. And therefore,

the vacuum state $|0\rangle^E$ has a counterpart, the "antivacuum" $|\,2\ell\,\rangle^E$, where the energy is maximal.

Not only in second quantization, but also in black hole physics, such states play an important role. This is an inevitable consequence of our desire to find a finite dimensional theory for quantum mechanics.

Both x and p are discrete operators, just like the Hamiltonian:

$$H=\omega n\,,\quad x=r/\sqrt{\ell}\quad p=s/\sqrt{\ell},\quad r,s \text{ are integers } \in [\,-\ell,\,\ell\,] \tag{11}$$

but, due to the modification (9) in their commutation rule, the unitary operator linking the eigen states $|r\rangle^x$ and $|s\rangle^p$ is more complicated than usual. This happens as long as the elementary time step δt is kept finite. In the limit $\delta t \to 0$ we recover the usual harmonic oscillator. The ontological states then run continuously along a circle. The unitary operator linking the p basis to the x basis for finite ℓ can be obtained from the matrix elements of the operator $e^{\frac{1}{2}i\pi L_1}$ in the basis where L_3 is diagonal. Going to the conventional notation of (ℓ, m) states, one can show that

$${}^x\langle r|s\rangle^p = \langle m|e^{\frac{1}{2}i\pi L_1}|m'\rangle \quad \text{where} \quad m=r,\ m'=s \tag{12}$$

this is derived by first noting that L_1 is diagonal in a basis that is rotated by 90° in angular momentum space, compared to the basis where L_2 is diagonal, and then interchanging L_1, L_2 and L_3. The matrix elements ${}^x\langle r|s\rangle^p$ can be deduced from recursion relations [3] such as

$$\begin{aligned} 2r\,{}^x\langle r|s\rangle^p \;=\; &\sqrt{(\ell+1-s)(\ell+s)}\;{}^x\langle r|s-1\rangle^p \\ &+\sqrt{(\ell+1+s)(\ell-s)}\;{}^x\langle r|s+1\rangle^p \end{aligned} \tag{13}$$

in combination with ${}^x\langle r|s\rangle^p = {}^p\langle s|r\rangle^{x\,*}$ and more. The result can be pictured as in **Figure 1**.

We can define beables $S_\pm$ as

$$S_\pm|k\rangle^{\rm ont} = e^{\mp 2\pi ik/N}|k\rangle^{\rm ont} \quad S_\pm|n\rangle^E = |n\pm 1 \mod N\rangle^E \tag{14}$$

see Equation (5). They are related to $L_\pm$ as follows:

$$L_+ = \sqrt{(n+1)(2\ell-n)}\,S_+ \quad L_- = \sqrt{n(2\ell+1-n)}\,S_-. \tag{15}$$

[3]There is some freedom of phase factors in the definition of the states $|r\rangle^x$ and $|s\rangle^p$.

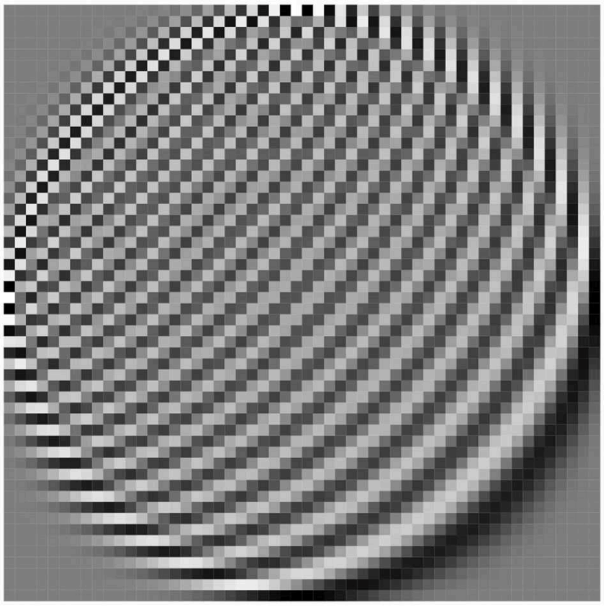

FIGURE 1 | The matrix (12), for the case $\ell = 53/2$. The values of a real solution for the matrix elements are shown. Black is maximal, gray ≈ 0, white is minimal. Notice that, these elements quickly converge to zero outside the circle $m^2 + m'^2 = \ell^2$ (obtained using Mathematica to integrate Equation (13)).

We see here that, due to the factors inside the square roots, the quantum numbers n are now limited both from below ($n \geq 0$) and from above ($n \leq 2\ell$), but these same square roots imply that the numbers k for the ontological states do not represent the eigen states of any of the angular momentum operators L_i, they are superimposed to form such eigen states, so that $L_\pm$ aren't beables, and neither are L_1 and L_2, or p and x (Equation 9).

In the limit $\ell \to \infty$, the second factors in the square roots (15) become constants, so that, indeed, $L_\pm$ act as creation operator $a^\dagger$ and annihilation operator a. The square root of H that one may recognize in Equation (15), relating beables with the more familiar x and p coordinates, will be encountered again in section 6.

We elaborated on these mathematical rules in this section, just because angular momenta are so familiar, and also to emphasize that the finite periodic model (the system with both δt and the period T finite) can be examined using this well-known algebra.

The limit $\delta t \to 0$ turns this system into a point moving continuously along a circle, which in every respect behaves just like the standard harmonic oscillator, as we shall see in section 7, but this limit must be taken with some care.

4. ON THE WAVE FUNCTION GENERATED BY A PERIODIC ONTOLOGICAL SYSTEM

The periodic ontological system is characterized by a classical kinetic variable defined on a finite interval with periodic boundary conditions. No generality is lost if we assume this to

be an angle φ defined on the period $[\,0,\,2\pi\,]$, implying $\varphi(t) = 2\pi k/N$. In the continuum limit, we define the evolution to be $\mathrm{d}\varphi(t)/\mathrm{d}t = \omega$, with ω fixed.

To understand what the quantum wave function here means, we have to assume time to be sliced in small and equal time steps $\delta t = 2\pi/N\omega$, where N is a large integer. In the previous section, it was found that the energy E must then lie in an interval of length ωN. We do have the freedom to define the phase factors of the energy eigen states, and those of the ontological states $|\varphi\rangle$, such that this interval is exactly $[0,\ \omega N]$. The importance of this choice is that an energy eigen state with energy $n\omega$ evolves as

$$\psi_n \ \propto\ e^{-i\omega nt} \ \propto\ \left(e^{-i\varphi(t)}\right)^n \tag{16}$$

and writing $z \equiv e^{-i\varphi}$ one finds that all energy eigen states are positive powers of z. Any wave function expanded in these energy eigen modes is therefore regular for all z that lie inside the unit circle. To arrive at this insight it was crucial that we start with a discrete lattice in the time variable, where the time spacings δt may be chosen arbitrarily small but not zero.

Our motivation for writing this short section was to demonstrate how the elementary building blocks for deterministic models generate the basis elements of complex-valued wave functions in Hilbert space[4].

5. MASSLESS PARTICLE IN A BOX

The harmonic oscillator is closely related to a massless relativistic particle on a lattice (lattice length δx) inside a box with length $R = \ell\,\delta x$, with hard walls at the edges:

$$H = |p| \equiv \sigma\, p \qquad x = \tilde{k}\,\delta x \quad \tilde{k} \in [\,0,\,\ell\,]. \quad \tilde{k}\ \text{integer}. \tag{17}$$

Here, the ontological variables are $\tilde{k}$, and $\sigma = \pm 1$; they are related to the variable k in Equation (4), except that we take the particle to bounce to and fro:

$$k(\tilde{k},\sigma) = \ell + \sigma(\tilde{k} - \ell) \qquad \tilde{k} \in [\,0,\,\ell\,] \quad k \in [\,0,\,2\ell\,]. \tag{18}$$

This says that $0 \le \tilde{k} < \ell$, while the velocity $\partial H/\partial p$ flips when $\tilde{k}$ reaches a wall.

We see that now, in the $\ell \to \infty$ limit, this becomes a model for the free, relativistic massless particle on an infinitely fine one-dimensional lattice, with walls at its edges. The velocity is fixed apart from its sign σ. Keep in mind that the position operator x and the momentum operator p used here differ from x and p that we used for the oscillator (Equation 9), which is why now the Hamiltonian looks different. This section is merely to point out that one system can be transformed into the other. A possible advantage of the description in this section is that, here, x itself is ontological.

Note that the energy spectrum of a relativistic massless particle in the box is linear in the momentum p, and the eigenvalues of p in the box are equidistant, and this is why this system can be mapped easily onto the harmonic oscillator[5]. See also the last paragraph of this paper.

6. MOMENTUM DEPENDENT KINETIC TERM

As already stated in section 2, one might wish to find an ontological interpretation of systems having a Hamiltonian of the form

$$H = T(\vec{p}\,) + V(\vec{x}\,) + \vec{A}(\vec{x}\,)\cdot\vec{p}. \tag{19}$$

In the general case, neither x nor p can be considered to be ontological, since they both evolve as superpositions. However, in some special cases, a variable $y(t)$ can be found that is ontological. The general rule is that we should search for operators such that they commute with themselves at all times, and also with the commutator of the Hamiltonian and these observables (that is, their time derivatives).

We now consider the Hamiltonian (19) in the continuum case, in one dimension (so that we omit the vector symbols) and with $V(x) = 0$. In this case, the vector potential field $A(x)$ can be gauge transformed away, therefore we also put $A(x) = 0$. Define accolades to symmetrize an expression:

$$\{A\ B\} \equiv \tfrac{1}{2}(AB + BA). \tag{20}$$

Then we define the operator $y(t)$ as

$$y \equiv \{x\,\frac{1}{v(p)}\} \qquad v(p) = \mathrm{d}T(p)/\mathrm{d}p. \tag{21}$$

It can be inverted:

$$x = \{y\,v(p)\}. \tag{22}$$

One easily derives that, indeed,

$$\frac{\mathrm{d}}{\mathrm{d}t}y(t) = 1. \tag{23}$$

Demanding both the operator $v(p)$ and its inverse $v^{-1}(p)$ to be sufficiently regular and unambiguous, forces us to keep the sign of $v(p)$ constant.

Note that, in the case where $T(p)$ is quadratic in the momentum p, $v(p)$ is proportional to the square root of the energy; here again, we observe this square root relating the ontological variable with the more familiar x coordinate that we saw in section 3.

[4]It might be interesting that in the "classical like rewriting" of standard QM by [38], used in essential ways in [39], the complex-valued wave functions arise as $\psi = x + ip$, where x and p are integer valued conjugated "coordinate" and "momentum" variables for linear cellular automata.

[5]An apparent degeneracy of the Hamiltonian (17) with σ can be lifted by carefully imposing the boundary conditions needed for realizing the reflections at the edges. We did not include these here in order to avoid inessential complications, but the reader can derive them by unfolding the box where $\tilde{k}$ is living, to become the periodic box for k that has twice that length (see Equation 18).

It is an interesting exercise to compute the inner product between the eigenstates of this ontological parameter y and those of the conventional x operator:

$$\langle x|y\rangle = \int \mathrm{d}p \langle x|p\rangle \langle p|y\rangle = \frac{1}{2\pi}\int \mathrm{d}p \sqrt{\nu(p)}\, e^{i(xp-yT(p))}. \quad (24)$$

It reduces to a Dirac delta function as soon as $T(p)$ is linear in p. In the more general case, unitarity demands that the function $T(p)$ can be inverted, since only then the Cauchy integrals needed to prove unitarity of Equation (24) close. If $T(p)$ can only be inverted on a finite interval of the values for T (or as the half-line rather than all values on the real line), then y is restricted to the values dual to that set.

We decided not to pursue this analysis further since there seems to be a more imminent problem: the operator $y(t)$, as defined in Equation (21), in general, seems to be quite non-local. This is why the ontological variables derived here will not be used to replace space-like coordinates, but rather field-like variables, as in second-quantized field theories, which are explored in sections 7 and 8.

Of course we would also like to understand systems that do have effective potential functions $V(x)$, and they should apply to higher dimensions as well. We shall home in to the completely general Hamiltonian in these last two sections, where we shall see that extra, high energy degrees of freedom will be needed in general.

7. BEABLES, CHANGEABLES, AND SUPERIMPOSABLES

What we call ontological, or deterministic, quantum mechanics is a particularly interesting subset of quantum systems where Hilbert space can be set up in terms of operators we call *beables*, a phrase that was introduced by Bell [40–42]. These are (a set of) operators that all commute with one another at all times, so that, if we have a coordinate frame where at time $t = 0$ all beables are diagonalized, they continue to be diagonalized at all times[6], and consequently, the evolution is completely classical. In this basis, the evolution operator $U(t) = e^{-iHt}$, at distinct times $t = t_i$, is a matrix containing only ones and zeros (see Equation 4). We then refer to operators H and $U(t)$ as *changeables*: they act on the eigen states of the beables merely by replacing these eigen states with other eigen states. Both beables and changeables form small subsets of all possible operators. The generic operators are superpositions of different possible beables and changeables, and so we refer to these remaining operators as *superimposables*.

In section 3, the beables are the operators k, and their eigen states are $|k\rangle_t^{\rm ont}$. The operators $U(\delta t)$ (where δt may have to be chosen to form a time-like lattice) and the associated Hamiltonian H, or L_3, are changeables, while operators such as L_1 and L_2 are superimposables.

In section 5, $\tilde{k}$, σ, and k are beables, while H and p are changeables. In section 6, the operator y is the beable. $T(p)$ is the Hamiltonian, and as such may serve as a changeable. The original position operator x is merely a superimposable.

Consider in particular the harmonic oscillator. Its mathematics is exactly as in section 3, if now we take the limit $\delta t \to 0$. The equations for the harmonic oscillator are written in terms of the familiar annihilation operator a and creation operator $a^\dagger$:

$$\begin{aligned} H = \tfrac{1}{2}\omega(p^2+x^2-1) = \omega\, a^\dagger a \qquad & a = \tfrac{1}{\sqrt{2}}(p-ix) \quad a^\dagger = \tfrac{1}{\sqrt{2}}(p+ix) \\ & p = \tfrac{1}{\sqrt{2}}(a+a^\dagger) \quad x = \tfrac{i}{\sqrt{2}}(a-a^\dagger). \\ & [\,x,\,p\,] = i \quad [\,a,\,a^\dagger] = 1. \end{aligned} \quad (25)$$

In conventional quantum mechanics, all known operators are superimposables, except possibly for the Hamiltonian, which could be a changeable, if we would have been able to identify the complete set of beables. According to the *cellular automaton theory of quantum mechanics* [21–23], the complete Hamiltonian of all physics in our universe happens to be a changeable. This theory can only be verified if we can also identify the ontological variables, the beables, and in practice this is hard. This paper is an attempt to pave the way to such a description of our universe.

In the next section, we seek to describe the beables and changeables in terms of the operators such as x, p, and H of finite, periodic cells. We are now in the limit $N \to \infty$, which means that we have $\ell \to \infty$, so that the 'angular momenta' of section 3 are almost classical. In practice, one frequently needs to switch between the strictly continuous case[7] and the case with finite time steps δt.

In the continuous case, the easiest changeable operator is $H = \omega a^\dagger a = \frac{1}{2}\omega(p^2+x^2-1)$. When δt is taken to be finite, one needs the evolution operator $U(\delta t)$ to describe the motion of a beable k forward by one step (see section 3):

$$U(\delta t)|k\rangle^{\rm ont} = e^{-iH\delta t}|k\rangle^{\rm ont} = |k+1 \mod N\rangle^{\rm ont}. \quad (26)$$

We can also say that the ontological angle φ in section 4 is rotated by an angle $2\pi/N$. Its angular rotation frequency is ω. This rotation is also generated by L_3.

What is the angle φ in terms of the standard harmonic oscillator operators? From Equation (5) in section 3, we see that

$$e^{i\varphi}|n\rangle^E = |n+1\rangle^E \quad (27)$$

and since $a^\dagger|n\rangle^E = \sqrt{\frac{H}{\omega}}\,|n+1\rangle^E$, we find[8]

$$e^{i\varphi} = (\tfrac{H}{\omega})^{-1/2}\, a^\dagger \qquad e^{-i\varphi} = (\tfrac{H}{\omega}+1)^{-1/2}\, a. \quad (28)$$

[6] A special piece of insight is that *measurement devices* will also be diagonalized, so that a measurement will always give unique, "beable" answers. In constructing models for experimental set-ups, one is free to choose the initial state as any wave function one likes, but if the beables are not all diagonalized, the final result will also come as a superposition. However, if we postulate that the universe started in an eigenstate of all beables, the final measurement will also be unique. This can be used as a natural explanation for the "collapse of the wave function."

[7] From a physical point of view, the distinction between continuous and step-wise evolution laws is less significant than one might think. One may or may not be interested in what happens between two distinct time steps, while what really matters is what happens after longer amounts of time.

[8] There is no problem here with the zero eigenvalues of H, since in both Equations (28), the number inverted is always 1 or bigger.

φ is the beable of the harmonic oscillator. By taking powers of the operators $e^{\pm i\varphi}$, we get $\cos\kappa\varphi$ and $\sin\kappa\varphi$ that, together, contain all desirable information concerning the ontological state the oscillator is in. It also applies to the relativistic particle in a box, section 5.

Next, let us construct a complete list of all changeables. One changeable is easy to recognize: the Hamiltonian itself. However, in the next section, we set up the procedures to obtain all possible interaction Hamiltonians, and for that, we need different changeables. Consider the basis of all ontological states, called $|k\rangle^{\rm ont}$ in section 3. Then a generic changeable operator interchanges two such elements, say $|k_1\rangle$ and $|k_2\rangle$. We write it as [9]

$$G_{12} = |k_1\rangle\langle k_2| + |k_2\rangle\langle k_1|. \tag{29}$$

The combination of the two terms in Equation (29) will be needed to preserve hermiticity, as will be clear in the next section. G_{12} is just one possible changeable. If we combine it with all other expressions of the same form, G_{ij}, we may obtain the complete set of all unitary permutations.

One further generalization is conceivable: if we have *many* independent harmonic oscillators (or periodic subsystems), we get a more generalized system with an ontological evolution law. The interchange operators G_{ij} must then be allowed to interchange the states of different oscillators.

In practice, we shall need to consider in particular an operator that only interchanges two states in one given periodic cell/harmonic oscillator, but only if the beables in a neighboring cell—or beables in several neighboring cells—take one particular value. This set is not completely but almost general, so that we can now perform our next step: construct non-trivial interaction Hamiltonians.

The harmonic oscillator Hamiltonian H_0 itself may be regarded as the infinitesimal interchange operator for all pairs of neighboring [10] states $|k_1\rangle^{\rm ont}$ and $|k_1+\delta k\rangle^{\rm ont}$. If we let its amplitude depend on where we are in k space, we have a small but very special class of changeables that we shall also need.

8. ONTOLOGICAL INTERACTIONS

So-far, our models were of an elementary simplicity. Now, we can put them together to obtain physically more interesting systems. Let us start by having a large class of small, independent, ontological "cells," listed by an index i. All of them are so small that, as soon as the influences of other cells are shut off, their own internal motion forces them to be periodic.

In more advanced future approaches, one might wish to avoid these elementary cells, but for our present purpose they appear to be quite useful.

Let the time step δt be 1, and in each cell i we have a variable $k^{(i)}$, with an associated momentum operator $p^{(i)}$. A Hamiltonian H_0 forces all data $k^{(i)}$ to make one step forward at every time step, with periodicity $N^{(i)}$ (allowed to be different for all i):

$$H_0 = \sum_i p_i \quad |k^{(i)}\rangle^{\rm ont}_{t+1} = |k^{(i)}+1\rangle^{\rm ont}_t \quad |N^{(i)}\rangle^{\rm ont} = |0^{(i)}\rangle^{\rm ont}. \tag{30}$$

The basis elements of the combined states are written as

$$|\vec{k}\rangle^{\rm ont}_t = \prod_i |k^{(i)}\rangle^{\rm ont}_t. \tag{31}$$

The ontological interaction to be considered next is an extra term to be added to H_0 such that the $k^{(i)}$ evolve in a more complicated way. First, consider just one cell, $i=1$, and consider two special values, k_1 and k_2, with $k_2 > k_1$. We now ask for an extra term such that, as soon as the value $k = k_1$ or k_2 is reached, it switches to the other value $k = k_2$ or k_1 (by adding the difference, $\Delta k = \pm(k_2 - k_1)$ to the value of k). In addition to this exchange process, we keep the term H_0 in the Hamiltonian, which ensures that at all times also $k \to k+1$ (there is a danger with the non-commutativity of the two terms, but in the continuum limit this ambiguity disappears, while in the discrete case one must ensure unitarity by demanding that every state $|k\rangle$ evolves into exactly one other ket state $|k'\rangle$).

At first sight, this gives a rather trivial effect: either the stretch $[k_1, k_2]$ is skipped, or the system moves within the stretch $[k_1, k_2]$ forever. This means that, physically, we just changed the period of the motion. Nevertheless this is an important interaction, as we shall see. We write the Hamiltonian as

$$H = H_0 \pm \pi|\psi\rangle\langle\psi| \qquad |\psi\rangle = \tfrac{1}{\sqrt{2}}\big(|k_1\rangle - |k_2\rangle\big) \tag{32}$$

both signs are allowed. One may derive that[11], indeed, the evolution operator $U_{\delta t=1}$ contains an extra factor $e^{-\pi i} = -1$ whenever the (normalized) state $|\psi\rangle$ is encountered. The state $|\phi\rangle = \frac{1}{\sqrt{2}}\big(|k_1\rangle + |k_2\rangle\big)$ is orthogonal to $|\psi\rangle$ and is therefore not effected. One sees immediately that the net effect of $U_{\delta t=1}$ is that all k values made one step forward, while $|k_1\rangle \leftrightarrow |k_2\rangle$.

Thus, we introduce the interaction term $H^{\rm int} = \pi|\psi\rangle\langle\psi|$ as an ontological interaction. However, its effect is very strong (it only works with the factor π in front), whereas in general, in quantum physics, we encounter interaction terms of variable strengths, whose effects can be much more general.

Therefore, we consider a further modification. Let us impose the condition that

[9] We often suppress signs and phase factors, when these have no effect on what happens physically in the ontological system. In general, adding phase factors will not help us to describe more general physical systems; at a later stage, however, phase factors can serve some important mathematical purpose.

A reader might wonder how *complex numbers arise in the Hamiltonian?* This "mystery" disappears when complex numbers are treated as pairs of real numbers. In practice, complex amplitudes are often linked to the conservation of matter, or more precisely: baryon number.

[10] to describe the continuum limit, we need to scale the variable k so that the steps δk are no longer 1, as before, but infinitesimal.

[11] The situation becomes more delicate in case more of such terms are added to the Hamiltonian while $\delta t = 1$. To do this right, it will be advisable to keep the continuum limit $\delta t \to 0$ and ensure that the exchanges are kept at a well-defined order. On the other hand we can guarantee that for any ontological (classical) interaction, a well-defined quantum Hamiltonian exists.

the interchange $k_1^{(1)} \leftrightarrow k_2^{(1)}$ only happens if in a neighboring cell, say cell #2, $k^{(2)}$ has a given value, say $k^{(2)} = r$:

$$H^{\rm int} = \pi\, |r^{(2)}\rangle\, \langle r^{(2)}|\, |\psi^{(1)}\rangle\, \langle \psi^{(1)}|. \tag{33}$$

Intuitively, one might suppose that this interaction is much smaller, since in the majority of cases, when $k^{(1)}$ takes the value k_1 or k_2, it must be rather unlikely that $k^{(2)}$ equals r. Does this argument make sense?

Yes, indeed it does, in the following way:
In the real world, δt will be extremely tiny, perhaps as small as the Planck time, some 10^{-44} seconds. Suppose that we only know the interaction Hamiltonian of our 'Standard Model' up to some maximum energy $E^{\rm max}$ of all scattering processes. In practice,

$$E^{\rm max} \ll 1/\delta t. \tag{34}$$

If we limit ourselves to states composed of lower energies only, we can never make Gaussian peaks much sharper than

$$\langle k^{(2)}|\psi^{(2)}\rangle \approx \left(\tfrac{\alpha}{\pi}\right)^{1/4} e^{-\frac{1}{2}\alpha(k^{(2)}-r)^2} \tag{35}$$

where $\alpha = \mathcal{O}(E^{\rm max})^{-2}$. This implies that the amplitude of the interaction Hamiltonian (33) will be very tiny indeed. We can add many such terms to our Hamiltonian before the effects become sizeable.

We should not be concerned that integrating many of such interaction terms to obtain the elementary evolution operator $U_{\delta t}$ over one time step, might add terms of higher order in δt that violate the condition that this term is ontological. Although such considerations may well be important for actual calculations, they do not affect the principle that we can generate a large class of interaction Hamiltonians along these lines.

Which Hamiltonians can we obtain now? the answer may come as a surprise: *All Hamiltonians acting in elementary cells, and generating interactions between neighboring cells, can be obtained from ontological interactions along these lines!* They certainly do not need to commute.

Suppose we have been adding ontological interactions of the type described above, but we still need one matrix element $\langle x_1|H|x_2\rangle$, where $|x_1\rangle$ and $x_2\rangle$ are elements of any basis one may wish to employ. Then all we have to do is take the set of ontological states $|\vec{k}\rangle$ that we started from. Apply the unitary matrix $\langle x|\vec{k}\rangle$ that links the basis of ontological states $|k\rangle^{\rm ont}$ to the states $|x\rangle$, to rewrite the desired Hamiltonian in the ontological basis. Consider any of its off diagonal terms $\langle k_1^{(1)}|H^{\rm int}|k_2^{(1)}\rangle$. Then, according to Equation (33), the missing term can be reproduced by an ontological exchange contribution of these two states in this particular cell.

As for the Standard Model itself, we know that its Hamiltonian does not connect cells far separated from one another, because the Hamiltonian density of all quantum field theories are known to be local in the sense of what is called "no Bell telephone" among philosophers:

The Hamiltonian density $\mathcal{H}(\vec{x})$ in 3-space $\vec{x}$, is such that, at different locations $\vec{x}$, these Hamiltonian density functions commute:

$$[\mathcal{H}(\vec{x}),\, \mathcal{H}(\vec{x}')] = 0 \quad \text{if} \quad \vec{x} \neq \vec{x}'. \tag{36}$$

If the speed of signals is bounded, this leads to commutation of operators outside the light cone.

Bell himself [41, 42] called this "local commutativity," but insisted that tighter definitions of causality—forward and backwards in time—are needed if one wants to compare quantum mechanics with deterministic models. He was criticized on this point [43, 44], and also the present author disagrees; here we just remark that further equations that would be tighter than Equation (36) are not needed. We derive from that equation that off-diagonal matrix elements of the Hamiltonian vanish when they refer to states in cells that are separated far from one another (far meaning far in units of the Planck length!). We connect this with our interaction Equation (33) to conclude that exchange interactions between ontological states that are far separated form one another are not deeded. Our models should violate Bell's theorem and the inequalities arrived at by Clauser et al. [45] simply because our interactions appear to generate quantum field theories.

We do note that, besides generating one off-diagonal term of the interaction Hamiltonian matrix, and its Hermitian conjugate, the interaction Hamiltonian (33) also affects the diagonal terms at $k_1^{(1)}$ and $k_2^{(1)}$. therefore, we might have to readjust all diagonal terms of the Hamiltonian. In the continuum limit, $\delta t \to 0$, this is easy. It just means that the speed at which a given ontological state may make a transition to the next state, may have to be modified.

We also obtained a bonus: the ontological theory is local up to Planckian distance scales, as soon as the commutator rule (36) is obeyed by the quantum system that we wish to reproduce in ontological terms.

We find that by including ontological exchange interactions between the ontological states, and by adjusting the speed of the evolution, we can create a quite generic quantum mechanical Hamiltonian. The model we get is a *cellular automaton* [25–28], exactly as we described in [21], but now we find the systematic prescription needed to let this automaton act as any given local quantum field theory.

It seems now that almost any basic interaction can be obtained, but there are important questions that we have not been able to answer:

We started with cells having no mutual interaction at all. In terms of elementary particle theories, this means that we start with infinitely heavy elementary particles. Then kinetic terms can be added that should lead to finite mass particles. What is the most efficient way from here to realistic quantum particle theories?

Our difficulty is that we do not quite understand how to construct ontological free field theories, describing light or even

massless particles. We need a theory starting from ontological *harmonically coupled* oscillators that obey some form of locality. This seems to be a purely technical problem now, which ought to be resolved.

Another question:

The theory for the interactions between elementary particles features quite a few continuous symmetry properties. How can we reproduce such symmetries? Since our cells tend to be discrete, it is hard to impose continuous symmetries, in particular Lorentz invariance. On the other hand, it is generally expected that most if not all *global* continuous symmetries cannot be exactly valid.

9. HOW A SIEVE CAN CONNECT CLASSICAL THEORIES WITH QUANTUM MECHANICAL ONES

Note that our sieve mechanism can easily be generalized to do the following:

Given two different ontological theories, with Hamiltonians H_1 and H_2, which do not have to commute. Then, adding a fast "sieve" variable enables us to describe a system that, at sufficiently low energies, is described by a Hamiltonian

$$H_3 = \alpha H_1 + \beta H_2 \tag{37}$$

where indeed quantum effects might lead to quantum interference, while, at the microscopic level, the theory is still deterministic.

Such a result seems almost too good to be true. Can we really re-write quantum mechanical systems in terms of deterministic ones? *How does it go in practice?* Which calculations turn a classical system, with exchange interactions and sieves or whatever else, into quantum mechanics? We here briefly analyse how to address this question.

We consider the simplest model of a sieve, giving rise to a Hamiltonian that generates superpositions as soon as the sieve is turned on, and then compare the quantum system with the classical one. The most important feature is that we have two (time) scales.

Our model is sketched in **Figure 2**. Its states are described as $|x\rangle$ where the fundamental, ontological variable x sits in a box with size L and periodic boundary conditions, $|x+L\rangle = |x\rangle$.

x starts out being a beable. The unperturbed Hamiltonian is $H_0 = p_x$, so the velocity is 1, the system circles around in its box. Now, we wish to turn it into a real quantum variable as in the previous section. We add the term $\alpha\pi|\psi\rangle\langle\psi|$, with $|\psi\rangle = \frac{1}{\sqrt{2}}\big(|0\rangle - |A\rangle\big)$ to the Hamiltonian, that had the value $H_0 = p_x$ in the unperturbed case. If $\alpha = 0$ we have the original model. If $\alpha = 1$, the Hamiltonian generates the exchange $|0\rangle \leftrightarrow |A\rangle$ in x-space. In that case, the x variable either stays inside the region $[0, A]$ or inside the region $[A, L]$ This makes it also a beable.

However, if α has any other value, the Hamiltonian contains a non-diagonal element, together with its Hermitian conjugate, resulting in quantum interference. According to section 8, we can mimic the suppression factor α by adding a fast variable y, such that only in the fraction α of all states y can be in, the exchange takes place. This we describe by replacing

$$\alpha = \sum |r\rangle\langle r| \tag{38}$$

in y space. The period of y is here taken to be 1, much shorter than the period L for x.

Classically, if the variable y takes one of the values r of the projection operator (38), precisely at the moment when $x = 0$ or at the moment when $x = A$, the exchange $|0\rangle \leftrightarrow |A\rangle$ takes place, otherwise it does not.

We argued in section 8 that, as long as the variable y stays in its lowest energy state, the equations of motion for the quantum system and the classical system are the same. Now, we are in a position to check this.

The unperturbed Hamiltonian is now $H_0 = p_x + p_y$; x and y move at the same speed $v = 1$, but y makes many oscillations during the time x makes one oscillation. Thus, the system moves in the direction of the arrows in **Figure 2**.

We claim that, in quantum language, the x variable obeys its effective Hamiltonian equations, i.e., the Schrödinger equation—including superposition effects (when $\alpha \neq 0$ and $\neq 1$. What happens classically?

The system evolves along the diagonal arrows in **Figure 2**. The boundary conditions are: x is periodic with period L and y is periodic with period 1. Then, we have the "sieve," consisting of two partial walls of length α in the y direction, one at $x = 0$ and one at $x = A$. The rule is that, if $x = 0$ or $x = A$ while $0 < y < \alpha$ then the states $|0, y\rangle$ and $|A, y\rangle$ are interchanged, after which the evolution continues in the direction of the arrows. We see that, classically, an infinite orbit results. If the lengths A and L have an irrational ratio, the orbit never closes. If we write this in terms of a wave function $\langle x, y|\psi(t)\rangle$, we get some sort of fractal.

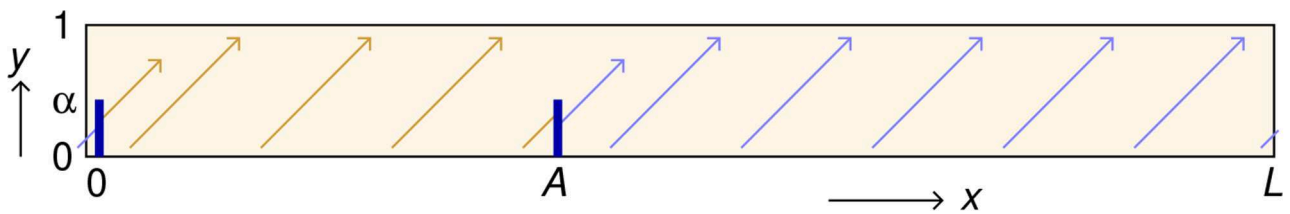

FIGURE 2 | The variables x (horizontal, period $L \gg 1$) and the sieve variable y (vertical, period 1), together moving in the direction of the arrows. See text.

The same orbit can now be described in quantum notation. In the bulk region, we have a wave function, which we write as

$$\psi(x,y,t)=\psi(x-t,y-t,0)=\sum_{n=0}^{\infty}\psi_n(x,t)\,e^{2\pi iny-2\pi int}. \quad (39)$$

We must restrict ourselves to non-negative n, as should be clear from the earlier sections of this paper: there is a lowest energy mode, which was tuned to the value $n=0$ (a procedure that we can also apply to the x coordinate, but for the time being, we keep the x-space notation as is).

Now here is how we can see the effect of the sieve. We consider the waves ψ^{0-} near the point $x=0$ entering at $x<0$ and the waves ψ^{A-} near $x=A$, entering at $x<A$. At $x>0$ the waves ψ^{0+} are leaving, and at $x>A$ the waves ψ^{A+} are leaving. Write

$$\begin{aligned}\psi^{1\pm}&=\tfrac{1}{\sqrt{2}}(\psi^{0\pm}+\psi^{A\pm})\quad\text{and}\\ \psi^{2\pm}&=\tfrac{1}{\sqrt{2}}(\psi^{0\pm}-\psi^{A\pm}).\end{aligned}\quad (40)$$

Then, at the sieve,

$$\begin{aligned}&\psi^{1+}=\psi^{1-}\quad\text{for all } y\\ &\psi^{2+}=\psi^{2-}\quad\text{if}\quad\alpha<y<1\qquad\psi^{2+}=-\psi^{2-}\quad\text{if}\quad 0<y<\alpha.\end{aligned}\quad (41)$$

This is now easy to rephrase in terms of properties of the functions $\psi_n(x,t)$. We also split these into functions $\psi_n^{1\pm}$ and $\psi_n^{2\pm}$. Since

$$\begin{aligned}\psi_n(x)&=\int_0^1 \mathrm{d}y\,e^{-2\pi iny}\,\psi(x,y)\\ \text{and}\quad\int_0^1\mathrm{d}y\,e^{2\pi i\ell y}\,\mathrm{sign}(y-\alpha)&=\frac{-i}{\pi\ell}\big(1-e^{2\pi i\ell\alpha}\big)\quad\text{if}\quad\ell\text{ integer}\neq 0\\ &=1-2\alpha\quad\text{if}\quad\ell=0\end{aligned}\quad (42)$$

we derive

$$\begin{aligned}\psi_n^{1+}&=\psi_n^{1-}\\ \psi_n^{2+}&=(1-2\alpha)\psi_n^{2-}+\sum_{\ell\neq 0}\frac{i}{2\pi\ell}\big(1-e^{2\pi i\ell\alpha}\big)\psi_{n+\ell}^{2-}\end{aligned}\quad (43)$$

so that we find

$$\begin{aligned}\psi_n^{0+}&=\psi_n^{0-}(1-\alpha)+\alpha\,\psi_n^{A-}\\ &\quad+\sum_{\ell\neq n}\frac{i}{4\pi\ell}(1-e^{2\pi i\ell\alpha})(\psi_{n+\ell}^{0-}-\psi_{n+\ell}^{A-})\\ \psi_n^{A+}&=\psi_n^{A-}(1-\alpha)+\alpha\,\psi_n^{0-}\\ &\quad+\sum_{\ell\neq n}\frac{i}{4\pi\ell}(1-e^{2\pi i\ell\alpha})(\psi_{n+\ell}^{A-}-\psi_{n+\ell}^{0-}).\end{aligned}\quad (44)$$

We see that the first terms contain the effect of a quantum superposition. Only when $\alpha=0$ or 1, this represents classical motion in x-space. For the other values of α (Equation 44) looks quantum mechanical. Now we know that, provided we include the extra terms, this is classical motion after all. But the extra terms only contain the high energy states ψ_n. We see in Equation (39) that the $n>0$ modes carry a large amount of energy, so that ignoring them does not affect much the physical nature of these transitions.

10. CONCLUSIONS

We conclude that an ontological theory for the basic interactions is quite conceivable. We find that one can postulate the existence of "cells" that each contain one or more variables; these variables are postulated each to move in periodic orbits (circles) as long as other interactions are absent. Then, we carefully postulate two kinds of interactions, together generating behavior that is sufficiently general to mimic any fundamentally quantum structure. One fundamental force is generated when a variable in one particular cell changes position with a variable in either the same cell or in its immediate vicinity. This exchange interaction will be associated with non-diagonal terms in what later will be our Hamiltonian. To weaken the force, and to make it fundamentally quantum mechanical, we need a sieve, in one or more cells, again in the immediate vicinity (or in the same cell). The ontological variable(s) of the sieve cell will only allow for the given exchange process if the sieve variable takes some pre-assigned value(s). Since we can choose which variables to exchange, as well as the strength of the sieve, this process will generate almost any Hamiltonian.

To then adjust the diagonal terms of the Hamiltonian, all that needs to be done is to adjust the velocities of the variables, depending on their positions in the cells. All taken together, we have as many degrees of freedom to adjust, as there are terms in our (Hermitian) Hamiltonian. This gives us confidence that our procedure will work, regardless the quantum model we are attempting to "explain" in ontological terms.

Actually, we still have a lot of freedom: we can derive which exchange interactions between elementary, ontological states will be needed in order to obtain agreement with today's Standard Model, but the details of the sieve, being the constraints imposed by cells neighboring a given cell, as the ones of the cell # 2 described in Equation (33), will be difficult to derive or even guess. It is clear however, that the effects of the sieves will be almost continuously adjustable, depending on the maximal energies that we allow for our particle-like degrees of freedom (low energies will imply that most sieves are shut off, so that the effects of quantum forces get weak at energies very low compared to the elementary scales of our cells).

Mathematical tools of the kind presented in this paper will be useful to study the constraints imposed on any "unified field theory" by the condition that, at some special time- and distance scale, our world is controlled by ontological forces.

Hopefully, our general strategy (as published during a few decades by now) is becoming more transparent with these demonstrations. Our "cells" are labeled by an index i, and we set up models for particles by arranging such cells in a lattice, called a "cellular automaton." The ontological degrees of freedom, $k^{(i)}$

are the positions of these points on their orbits. What has been achieved in this paper is that we identified a way to characterize generic ontological interactions between the cells, using the *language* of quantum mechanics. The generic interactions, of which one may add a large number at each lattice point, take the following form:

$$H = H_0 + H^{\rm int} \qquad H_0 = \sum_{\text{cells } i} p^{(i)} \tag{45}$$

where $[k^{(i)},\, p^{(j)}] = i\delta_{ij}$, and

$$H^{\rm int} = \pi \sum |r\rangle\, \langle r|\, |\psi^{(i)}\rangle\, \langle\psi^{(i)}| \tag{46}$$

$$|\psi^{(i)}\rangle = \tfrac{1}{\sqrt{2}}\big(|k_1^{(i)}\rangle - |k_2^{(i)}\rangle\big). \tag{47}$$

Here, the notation used was the one describing discrete states. These must be replaced by the continuous states when the $\delta t \to 0$ limit is taken. Hence, for now, the coefficient π has to be 3.14…, since only with this unique strength, the system exchanges position $|k_1^{(i)}\rangle$ with position $|k_2^{(i)}\rangle$ in a deterministic manner. To make the interaction sufficiently small so that it can be inserted in a perturbative quantum field theory, we use one or more other state(s) $|r\rangle$ as projectors (calling them "sieves"). The strength of the interaction then reduces by factors $\mathcal{O}(\sqrt{E^{\rm max}})$ in units where the time step δt is one. This is why we are led to consider the case where all particle energies are low compared to the energies associated to the very tiny time scale of δt.

We saw in section 9, that any strength of the off diagonal terms of the Hamiltonian can be obtained by adding fast variables to the classical system, and although extra terms do arise, the fundamentally quantum nature of the interactions is not jeopardized. We find this result very important, it should be regarded as a strong indication that this is the way to interpret what goes on in our quantum world.

We have high energy modes, which are claimed not to ruin the quantum nature of the results of our calculation. This is also where thermodynamics may enter the picture: if we ignore high energy modes, those are exactly what is left of a fast moving auxiliary variable [12]. Today, in practice, we have too little information to be able to make fundamental distinctions between quantum mechanical and classical behavior: we only know the outcome of scattering experiments as long as the total energy is kept below the limit $E^{\rm max}$. All our experiments are at temperatures too low to allow us to do the timing of dynamical variables sufficiently accurately. We are too close to just one physical state: the vacuum. Thus, we must tolerate uncertainties in our descriptions. These are the quantum uncertainties.

[12]The question was asked by Hossenfelder and Palmer [20].

Since quantum mechanical language was used throughout, and since the states $|\psi^{(i)}\rangle$ connect different basis elements, we see that non commuting interaction Hamiltonians emerge. The only important constraint on $|\psi^{(i)}\rangle$ is that it should connect only nearby ontological states, since only then the resulting Hamiltonian operator obeys locality, which is expressed uniquely in terms of commutators vanishing outside the light cone (Equation 36).

What remains to be done is to achieve more experience in constructing realistic models along these lines, check how these models perform, and reach consensus about their usefulness.

The most important message, we believe, is that quantum mechanics should not be considered as mysterious, it is not fundamentally impossible to understand it from the perspective of classical logic, and the origin of the uncertainty relations can be understood. It all amounts to *timing*, that is, if fast moving, space-like separated, variables are involved in an interaction, it is fundamentally impossible to adjust their time variables sufficiently accurately.

The question whether time is discrete or continuous is physically unimportant; as soon as some description of a system clarifies it sufficiently well, there will be no need to split the time variable into even smaller segments. There is a practical difficulty: only one variable needs to be handled as if continuous: the dynamics of the variable that is used as our clock. All other variables will be limited in number, as one may conclude from black hole physics: black holes can only come in a finite number of quantum states. This implies that, in contrast with our clock, the other variables may have to be kept on a discrete time lattice. So where does our clock come from? In our models, we can choose whatever pleases us, but to guess the right model may be not easy.

Some of our readers may find it difficult to believe that points running around on circles are equivalent to harmonic oscillators. Here, we would like to use an analogy with the science of planets. We can study distant planets through our telescopes, and detect many interesting properties, for which we can find equations. Yet there is one thing we shall never detect: their names. Similarly, we can never tell whether a harmonic oscillator is actually a point moving on a circle. The equations are equivalent. Everything else is name giving.

DATA AVAILABILITY STATEMENT

All datasets presented in this study are included in the article/supplementary material.

AUTHOR CONTRIBUTIONS

The author confirms being the sole contributor of this work and has approved it for publication.

REFERENCES

1. Dirac PAM. *The Principles of Quantum Mechanics*. Oxford: Clarendon Press. (1930).

2. Einstein A, Podolsky B, Rosen N. Can quantum mechanical description of physical reality be considered complete? *Phys Rev.* (1935) **47**:777. doi: 10.1103/PhysRev.47.777

3. Bohm D. A suggested interpretation of the quantum theory in terms of "Hidden Variables, I". *Phys Rev.* (1952) **85**:166–79. doi: 10.1103/PhysRev.85.166
4. Bohm D. A suggested interpretation of the quantum theory in terms of "Hidden Variables, II". *Phys Rev.* (1952) **85**:180–93. doi: 10.1103/PhysRev.85.180
5. Everett H. Relative state formulation of quantum mechanics. *Rev Mod Phys.* (1957) **29**:454. doi: 10.1103/RevModPhys.29.454
6. Jammer M. *The Conceptual Development of Quantum Mechanics*. Mc. New York, NY: Graw-Hill (1966).
7. DeWitt BS. Quantum mechanics and reality. *Phys Today.* (1970) **23**:30–40. doi: 10.1063/1.3022331
8. DeWitt BS. The many-universes interpretation of quantum mechanics. In: *Proceedings of the International School of Physics "Enrico Fermi" Course IL: Foundations of Quantum Mechanics*. New York, NY: Academic Press (1972).
9. Pais A. *Inward Bound, of Matter and Forces in the Physical World*. New York, NY: Clarendon Press; Oxford University Press (1986).
10. Ghirardi GC, Rimini A, Weber T. Unified dynamics for microscopic and macroscopic systems. *Phys Rev D.* (1986) **34**:470.
11. Pais A. *Niels Bohr's Times, in Physics, Philosophy, and Polity*. Oxford: Clarendon Press (1991).
12. Wallace D. Everettian rationality: defending Deutsch's approach to probability in the Everett interpretation. *Stud Hist Philos Sci Part B.* (2003) **34**:415–439. doi: 10.1016/S1355-2198(03)00036-4
13. Kumar M. *QUANTUM, Einstein, Bohr and the Great Debate About the Nature of Reality*. Cambridge: Icon Books Ltd. (2008).
14. Conway J, Kochen S. The free will theorem. *Found Phys*. (2006) **36**:1441. doi: 10.1007/s10701-006-9068-6
15. Zeilinger A. Violation of local realism with freedom of choice. *Proc Natl Acad Sci USA*. (2010) **107**:19708. doi: 10.1073/pnas.1002780107
16. Hossenfelder S. Testing super-deterministic hidden variables theories. *Found Phys.* (2011) **41**:1521. doi: 10.1007/s10701-011-9565-0
17. Hossenfelder S. Testing superdeterministic conspiracy. *J Phys.* (2014) **504**:012018. doi: 10.1088/1742-6596/504/1/012018
18. Schlosshauer M, Kofler J, Zeilinger A. A snapshot of foundational attitudes toward quantum mechanics. *Stud Hist Philos Sci Part B.* (2013) **44**:222–30. doi: 10.1016/j.shpsb.2013.04.004
19. Khrennikov A. *Beyond Quantum*. Singapore: Pan Stanford Publishers Pvt, Ltd. (2014).
20. Hossenfelder S, Palmer T. Rethinking Superdeterminism. *Front Phys.* (2020) **8**:139. doi: 10.3389/fphy.2020.00139
21. 't Hooft G. The cellular automaton interpretation of quantum mechanics. In: *Fundamental Theories of Physics*, Vol. 185. Springer (2016). doi: 10.1007/978-3-319-41285-6
22. Th. Elze H. Quantumness of discrete Hamiltonian cellular automata. In: Invited talk presented at the symposium "Wigner 111 - Colourful and Deep." Budapest (2013).
23. Blasone M, Jizba P, Vitiello G. Dissipation and quantization. *Phys Lett.* (2001) **A287**:205–10. doi: 10.1016/S0375-9601(01)00474-1
24. 't Hooft G. Black hole unitarity and antipodal entanglement. *Found Phys.* (2016) **49**:1185–98. doi: 10.1007/s10701-016-0014-y
25. Ulam SM. Random processes and transformations. *Proc Int Congr Math.* (1952) **2**:264–75.
26. Gardner M. The fantastic combinations of John Conway's new solitary game "life". *Sci Am.* (1970) **223**:120–3. doi: 10.1038/scientificamerican1170-116
27. Gardner M. On cellular automata, self-reproduction, the Garden of Eden and the game of "life". (1971) **224**:112–7.
28. Wolfram S. *A New Kind of Science*. Champaign, IL: Wolfram Media, Inc. (2002).
29. Merzbacher E. *Quantum Mechanics*. New York, NY; London: John Wiley & Sons (1961).
30. Davidov AS. *Quantum Mechanics*. Translated and edited by D. ter Haar. Oxford; London; Edinburgh; New York, NY; Paris; Frankfurt: Pergamon Press (1965).
31. Das A, Melissinos A. *Quantum Mechanics, A Modern Introduction*. New York, NY; London; Paris; Montreux; Tokyo; Melbourne, VIC: Gordon and Breach (1986).
32. Born M. Zur Quantenmechanik der Stoßvorgänge (German) [Toward the quantum mechanics of collision processes]. *J Phys.* (1926) **37**:863–7.
33. Itzykson C, Zuber J-B. *Quantum Field Theory*. Singapore: Mc.Graw-Hill (1980).
34. Ryder LH. *Quantum Field Theory*. Cambridge University Press (1985).
35. de Wit B, Smith J. *Field Theory in Particle Physics*. Vol **I**. Amsterdam; Oxford; New York, NY; Tokyo: North-Holland Elsevier (1986).
36. 't Hooft G. The conceptual basis of quantum field theory. In: Butterfield J, et al., editors. *Handbook of the Philosophy of Science, Philosophy of Physics*. Elsevier. (2007) p. 661–729.
37. Glauber RJ. Coherent and incoherent states of the radiation field. *Phys Rev.* (1963) **131**:2766.
38. Heslot A. Quantum mechanics as a classical theory. *Phys Rev.* (1985) **D31**:1341.
39. Elze HTh. Action principle for cellular automata and the linearity of quantum mechanics. *Phys Rev.* (2014) **A89**:012111. doi: 10.1103/PhysRevA.89.012111
40. Bell JS. On the Einstein podolsky rosen paradox. *Physics.* (1964) **1**:195.
41. Bell JS. On the impossible pilot wave. *Found Phys.* (1982) **12**:989.
42. Bell JS. *Speakable and Unspeakable in Quantum Mechanics*. Cambridge: Cambridge University Press. (1987).
43. Brans CH. Bell's theorem does not eliminate fully causal hidden variables. *Int J Theor Phys.* (1988) **27**:219.
44. Vervoort L. Bell's theorem: two neglected solutions. *Found Phys.* (2013) *arXiv: 1203.6587v2*.
45. Clauser JF, Horne MA, Shimony A, Holt RA. Phys. Rev. Lett. 23, 880. *Erratum Phys. Rev. Lett*. (1970) **24**:549. doi: 10.1103/PhysRevLett.23.880

Conflict of Interest: The author declares that the research was conducted in the absence of any commercial or financial relationships that could be construed as a potential conflict of interest.

frontiers in Physics

ORIGINAL RESEARCH
published: 06 May 2020
doi: 10.3389/fphy.2020.00139

Rethinking Superdeterminism

Sabine Hossenfelder[1] *and Tim Palmer*[2]*

[1] Department of Physics, Frankfurt Institute for Advanced Studies, Frankfurt, Germany, [2] Department of Physics, University of Oxford, Oxford, United Kingdom

Quantum mechanics has irked physicists ever since its conception more than 100 years ago. While some of the misgivings, such as it being unintuitive, are merely aesthetic, quantum mechanics has one serious shortcoming: it lacks a physical description of the measurement process. This "measurement problem" indicates that quantum mechanics is at least an incomplete theory—good as far as it goes, but missing a piece—or, more radically, is in need of complete overhaul. Here we describe an approach which may provide this sought-for completion or replacement: Superdeterminism. A superdeterministic theory is one which violates the assumption of Statistical Independence (that distributions of hidden variables are independent of measurement settings). Intuition suggests that Statistical Independence is an essential ingredient of any theory of science (never mind physics), and for this reason Superdeterminism is typically discarded swiftly in any discussion of quantum foundations. The purpose of this paper is to explain why the existing objections to Superdeterminism are based on experience with classical physics and linear systems, but that this experience misleads us. Superdeterminism is a promising approach not only to solve the measurement problem, but also to understand the apparent non-locality of quantum physics. Most importantly, we will discuss how it may be possible to test this hypothesis in an (almost) model independent way.

Keywords: superdeterminism, Bell theorem, causality, free will, quantum measurement, quantum mechanics

OPEN ACCESS

Edited by:
Karl Hess,
University of Illinois at Urbana-Champaign, United States

Reviewed by:
Babak Shiri,
Neijiang Normal University, China
Gerard't Hooft,
Utrecht University, Netherlands

***Correspondence:**
Tim Palmer
tim.palmer@physics.ox.ac.uk

Specialty section:
This article was submitted to Mathematical Physics, a section of the journal Frontiers in Physics

Received: *26 January 2020*
Accepted: *08 April 2020*
Published: *06 May 2020*

Citation:
Hossenfelder S and Palmer T (2020) Rethinking Superdeterminism. Front. Phys. 8:139. doi: 10.3389/fphy.2020.00139

1. INTRODUCTION

Until the 1970s, progress in the foundations of physics meant discovering new phenomena at higher energies, or short distances, respectively. But progress in high-energy physics has slowed, and may have run its course as far as finding solutions to the deep fundamental problems of physics is concerned. In the past decades, physicists have not succeeded in solving any of the open problems in the foundations of their field; indeed it's not even clear we are getting closer to solving them. Most notably, we have still not succeeded in synthesizing quantum and gravitational physics, or in unraveling the nature of dark matter, problems that have been known since the 1930s.

In this situation it makes sense to go back and look for the path we did not take, the wrong turn we made early on that led into this seeming dead end. The turn we did not take, we argue here, is resolving the shortcomings of quantum mechanics. At the least, we need a physical description of the measurement process that accounts for the non-linearity of quantum measurement.

The major reason this path has remained largely unexplored is that under quite general assumptions (defined below) any theory which solves the measurement problem in a form consistent with the principles of relativity, makes it impossible to prepare a state independently of the detector that will later measure it. If one is not willing to accept this dependence then—by virtue of Bell's theorem [1]—one necessarily has to conclude that a local, deterministic completion

of quantum mechanics is impossible. This, then, requires us to abandon the principles on which general relativity is based and adds to our difficulty reconciling gravity with the other interactions.

If one is, by contrast, willing to accept the consequences of realism, reductionism, and determinism, one is led to a theory in which the prepared state of an experiment is never independent of the detector settings. Such theories are known as "superdeterministic." We wish to emphasize that superdeterministic theories are *not* interpretations of quantum mechanics. They are, instead, theories more fundamental than quantum mechanics, from which quantum mechanics can be derived.

Superdeterminism is frequently acknowledged as an experimentally unclosed loophole (see e.g., [2]) with which one can explain deterministically the observed violations of Bell's inequality. However, for a variety of reasons, many physicists think Superdeterminism is a non-starter. For example, they argue that Superdeterminism would turn experimenters into mindless zombies, unable to configure their experimental apparatuses freely. A similar argument has it that Superdeterminism implies the existence of implausible conspiracies between what would otherwise be considered independent processes. Alternatively, it would seemingly lead to causes propagating backwards in time. Above all, so it is claimed, Superdeterminism would fatally undermine the notion of science as an objective pursuit. In short, Superdeterminism is widely considered to be dead in the water.

The aim of this paper is to re-examine the arguments against Superdeterminism. We will argue that, rather than being an implausible and dismissible loophole, the neglected option of Superdeterminism is the way forward; it's the path we did not take.

2. WHY?

The way it is commonly taught, quantum mechanics has two ingredients to its dynamical law: the Schrödinger equation and the measurement prescription. The measurement prescription is a projection on a detector eigenstate, followed by re-normalizing the new state to 1.

This measurement prescription (also sometimes referred to as the "update" or "collapse" of the wave-function) is not a unitary operation. It preserves probabilities by construction, but it is neither reversible nor linear. The lack of reversibility is not a serious problem: one may interpret irreversibility as a non-physical limit in which one has ignored small but finite residuals that would otherwise make the measurement process reversible.

Rather, the major problem with the measurement process is that it is non-linear. If we have a prepared initial state $|\Psi_1\rangle$ that brings the detector into eigenstate $|\chi_1\rangle$, and another initial state $|\Psi_2\rangle$ that brings the detector into eigenstate $|\chi_2\rangle$, then a linear evolution law would bring a superposition $(|\Psi_1\rangle + |\Psi_2\rangle)/\sqrt{2}$ into a superposition of detector eigenstates—but this is not what we observe.

This is problematic because if quantum mechanics was the correct theory to describe the behavior of elementary particles, then what macroscopic objects like detectors do should be derivable from it. The problem is not merely that we do not know how to make this derivation, it's far worse: the observed non-linearity of the measurement process tells us that the measurement postulate is in contradiction with the linear Schrödinger equation.

However, there is a simple resolution of this problem of non-linearity. In its density matrix form, the Schrödinger equation is remarkably similar to the classical Liouville equation. So much that, in this form, the Schrödinger equation is sometimes referred to as the Schrödinger-Liouville or Quantum-Liouville equation, though the historically more correct term is the von Neumann-Dirac equation:

$$\text{Liouville equation:} \qquad \frac{\partial \rho}{\partial t} = \{H, \rho\}, \tag{1}$$

$$\text{von Neumann-Dirac equation:} \qquad i\hbar \frac{\partial \rho}{\partial t} = [H, \rho]\,. \tag{2}$$

Here, H is the classical/quantum Hamiltonian of the system, the curly brackets are Poisson brackets, and the square brackets are commutators. ρ is the classical/quantum (probability) density, respectively.

The classical Liouville equation is linear in the probability density due to conservation of probability. But this linearity says nothing whatsoever about whether the dynamics of the underlying system from which the probability density derives is also linear. Hence, for example, chaotic dynamical systems, despite their non-linear dynamics, obey the same linear equation for probability density. To us, this close formal similarity between the two equations strongly suggests that quantum physics, too, is only the linear probabilistic description of an underlying non-linear deterministic system.

From this point of view, pursuing an Everettian approach to quantum physics is not the right thing to do, because this idea is founded on the belief that the Schrödinger equation is fundamental; that nothing underpins it. Moreover, it does not make sense to just append non-linear dynamics to the Schrödinger equation in situations when state decoherence becomes non-negligible, because it is not the Schrödinger equation itself that needs to become non-linear. Spontaneous collapse models do not help us either because these are not deterministic[1]. Pilot-wave theories do, in some sense, solve the measurement problem deterministically. However, pilot-wave formulations of quantum mechanics are based on an explicitly non-local ontology, and this non-locality makes it difficult to reconcile such theories with special relativity and, with that, quantum field theory.

What, then, does it take to describe quantum physics with a deterministic, local theory that is reductionist in the sense that the theory allows us to derive the behavior of detectors from the behavior of the theory's primitive elements? The Pusey-Barrett-Rudolph (PBR) theorem [3, 4] tells us that such a theory must violate the Preparation Independence Postulate, according to which the state space of a composite system can

[1]One may, however, expect spontaneous collapse models to appear as effective descriptions of a non-linear collapse process in suitable limits.

be described as a product state whose factors are independent of each other. Violating Preparation Independence entails that either the systems making up the product state are correlated with each other, or that the composite system cannot be described as a product state to begin with. This lack of independence between the prepared state and the detector is the hallmark of Superdeterminism.

3. WHAT?

We define a superdeterministic theory as a Psi-epistemic, deterministic theory that violates Statistical Independence but is local in the sense of respecting Continuity of Action [5], i.e., there is no "action at a distance" as Einstein put it. In the remainder of this section we will explain what these words mean.

1. Psi-epistemic: That a theory is Psi-epistemic means that the wave-function in the Schrödinger equation (or the density-matrix, respectively) does not itself correspond to an object in the real world, i.e., is not ontic. The Copenhagen interpretation and Neo-Copenhagen interpretations are Psi-epistemic because they postulate the wave-function merely encodes knowledge about the state of the system, rather than itself corresponding to a property of the system. However, a theory may also be Psi-epistemic because the wavefunction is emergent, for example as a statistical representation of a more fundamental theory. The theories we will be dealing with here are Psi-epistemic in the latter sense.

Needless to say, the wavefunction derived in any such theory should obey the Schrödinger equation up to current measurement precision and hence reproduce the so-far tested predictions of quantum mechanics. But of course the point of seeking a theory from which to derive quantum mechanics is not to reproduce quantum mechanics, but to make predictions beyond that.

2. Deterministic: By deterministic we will mean that the dynamical law of the theory uniquely maps states at time t to states at time t' for any t and t'. This map, then, can be inverted.

Since the theory we look for should be deterministic and the wavefunction derives from it, we are dealing with a so-called hidden-variable theory. We can ask what exactly are these hidden variables, which in the following are collectively represented by the symbol λ. The answer depends on the specific model one is dealing with, but loosely speaking λ contains all the information that is required to determine the measurement outcome (except the "not hidden" variables that are the state preparation). In this picture, quantum mechanics is not deterministic simply because we do not know λ.

It is important to realize that these hidden variables are not necessarily properties intrinsic to or localized within the particle that one measures; they merely have to determine the outcome of the measurement. To see the distinction, consider the following example. You are standing in a newborn ward in a hospital and look at a room full of screaming infants. On your mind are two questions: What's their blood type? and Will they ever climb Mount Everest? In a deterministic theory, answers to both questions are encoded in the state of the universe at the present time, but they are very different in terms of information availability. A baby's blood type is encoded locally within the baby. But the information about whether a baby will go on to climb Mount Everest is distributed over much of the hypersurface of the moment the baby is born. It is not, in any meaningful sense, an intrinsic property of the baby. This example also illustrates that just because a theory is deterministic, its time evolution is not necessarily predictable.

3. Violation of Statistical Independence: The most distinctive feature of superdeterministic theories is that they violate Statistical Independence. As it is typically expressed, this means that the probability distribution of the hidden variables, $\rho(\lambda)$, is not independent of the detector settings. If we denote the settings of two detectors in a Bell experiment as **a** and **b**, we can write this as

$$\rho(\lambda|\mathbf{a},\mathbf{b}) \neq \rho(\lambda). \tag{3}$$

For example, in the CHSH version of Bell's Theorem [6], **a** and **b** each take one of two discrete orientations, which we can represent here as 0 or 1. To derive Bell's inequality, one assumes $\rho(\lambda|\mathbf{a},\mathbf{b}) = \rho(\lambda)$, a requirement that is also often referred as "Free Choice" (this terminology is profoundly misleading as we will discuss in section 4.1).

While it is straightforward to write down Statistical (In)dependence as a mathematical requirement, the physical interpretation of this assumption less clear. One may be tempted to read the probability encoded by ρ as a frequency of occurrence for different combinations of $(\lambda, \mathbf{a}, \mathbf{b})$ that happen in the real world. However, without further information about the theory we are dealing with, we do not know whether any particular combination ever occurs in the real world. E.g., in the case that a pair of entangled particles is labeled by a unique λ, for any value of λ only one pair of values for **a** and **b** would actually be realized in the real world.

At the very least, whether these alternative combinations of hidden variables and detector settings ever exist depends both on the state space of the theory and on whether dynamical evolution is ergodic on this state space. It is easy to think of cases where dynamical evolution is not ergodic with respect to the Lebesgue measure on state space. Take for example a classical, non-linear system, like the iconic Lorenz model [7]. Here, the asymptotic time evolution is constrained to an attractor with fractal measure, of a dimension lower than the full state space. For initial conditions on the attractor, large parts of state space are never realized.

Neither can we interpret ρ as a probability in the Bayesian sense[2], for then it would encode the knowledge of agents and thereby require us to first define what "knowledge" and "agents" are. This interpretation, therefore, would bring back the very difficulty we set out to remove, namely that a fundamental theory for the constituents of observers should allow us to derive macroscopic concepts.

We should not, therefore, interpret Statistical Independence as a statement about properties of the real world, but understand it as a mathematical assumption of the model with which we

[2] As is the idea behind QBism [8].

are dealing. This point was made, implicitly at least, by Bell himself [1]:

> "I would insist here on the distinction between analyzing various physical theories, on the one hand, and philosophizing about the unique real world on the other hand. In this matter of causality it is a great inconvenience that the real world is given to us once only. We cannot know what would have happened if something had been different. We cannot repeat an experiment changing just one variable; the hands of the clock will have moved, and the moons of Jupiter. Physical theories are more amenable in this respect. We can *calculate* the consequences of changing free elements in a theory, be they only initial conditions, and so can explore the causal structure of the theory. I insist that [Bell's Theorem] is primarily an analysis of certain kinds of theory." (emphasis original)

In summary, Statistical Independence is not something that can be directly tested by observation or by experiment because it implicitly draws on counterfactual situations, mathematical possibilities that we do not observe and that, depending on one's model or theory, may or may not exist.

4. Locality: Finally, we will assume that the superdeterministic theory respects Continuity of Action (for extensive discussion of the term, see Wharton and Argaman [5]). Continuity of Action (hereafter CoA) means that to transfer information from one space-time region to another, disjoint, region, the same information has to also be present on any closed (3-dimensional) surface surrounding the first region (see **Figure 1**). Information, here, refers to quantities that are locally measurable. We make this assumption because both general relativity and quantum field theories respect this criterion.

As laid out in Wharton and Argaman [5], the definition of locality by CoA is not as strong as the locality assumptions entering Bell's theorem. Besides Statistical Independence, the assumptions for Bell's theorem are

1. **Output Independence**
   This assumption states that the measurement outcome is determined by hidden variables, λ, and that the hidden variables are the origin of statistical correlations between distant measurement outcomes. Formally it says that the distribution for the measurement outcomes $x_{\mathbf{a}}$ of detector $\mathbf{a}$ does not depend on the distribution of outcomes $x_{\mathbf{b}}$ at detector $\mathbf{b}$ and vice versa, i.e., $\rho_{\mathbf{ab}}(x_{\mathbf{a}}, x_{\mathbf{b}}|\mathbf{a}, \mathbf{b}, \lambda) = \rho_{\mathbf{a}}(x_{\mathbf{a}}|\mathbf{a}, \mathbf{b}, \lambda)\rho_{\mathbf{b}}(x_{\mathbf{b}}|\mathbf{a}, \mathbf{b}, \lambda)$.
2. **Parameter Independence**
   Parameter independence says that the probability distribution of measurement outcomes at one detector does not depend on the settings of the other detector, i.e., they can be written as $\rho_{\mathbf{a}}(x_{\mathbf{a}}|\mathbf{a}, \mathbf{b}, \lambda) = \rho_{\mathbf{a}}(x_{\mathbf{a}}|\mathbf{a}, \lambda)$ and $\rho_{\mathbf{b}}(x_{\mathbf{a}}|\mathbf{a}, \mathbf{b}, \lambda) = \rho_{\mathbf{b}}(x_{\mathbf{b}}|\mathbf{b}, \lambda)$.

These two assumptions together are also known as "Factorization." The observed violations of Bell's inequality then imply that at least one of the three assumptions necessary to derive the inequality must be violated. Quantum mechanics respects Statistical Independence and Parameter Independence but violates Outcome Independence. Superdeterminism violates Statistical Independence. Bell-type tests cannot tell us which of the two options is correct.

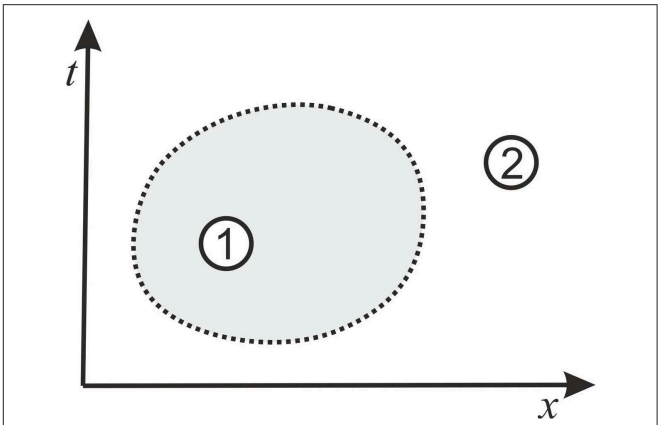

FIGURE 1 | Continuity of Action. If information from event 1 can influence event 2, then this information must affect any closed three surface around 1.

All three assumptions of Bell's theorem—Statistical Independence, Output Independence, and Parameter Independence—are sometimes collectively called "local realism" or "Bell locality." However, Bell's local realism has little to do with how the term "locality" is used in general relativity or quantum field theory, which is better captured by CoA. It has therefore been proposed that Bell locality should better be called Bell separability [9]. However, that terminology did not catch on.

The issue of whether Factorization is a suitable way to encode locality and causality is similar to the issue with interpreting Statistical Independence: It draws on alternative versions of reality that may not ever actually occur. Factorization requires us to ask what the outcome of a measurement at one place would have been given another measurement elsewhere (Outcome Independence) or what the setting of one detector would have been had the other detector's setting been different (Parameter Independence). These are virtual changes, expressed as state-space perturbations. The changes do therefore not necessarily refer to real events happening in space-time. By contrast, Continuity of Action, is a statement about processes that do happen in space-time: its definition does not necessarily invoke counterfactual worlds.

To make this point in a less mathematical way, imagine Newton clapping his hands and hearing the sound reflected from the walls of his College quad (allowing Newton to estimate the speed of sound). He might have concluded that the reflected sound was caused by his clap either because:

- if he had not clapped, he would not have heard the sound;
- the clapping led to the excitation of acoustic waves in the air, which reflected off the wall and propagated back to vibrate Newton's ear drums, sending electrical signals to his brain.

The first definition of causality here depends on the existence of counterfactual worlds and with that on the mathematical structure of one's theory of physics. It makes a statement that is impossible to experimentally test.

The second of these definitions, in contrast, identifies a causal connection between the clap and the cognitive recognition: there is no closed region of space-time surrounding the clap that is not affected by either the acoustic wave or the electrical signal. It is a statement about what actually happens.

This tension between space-time based notions of causality and the assumptions of Bell's theorem was recently highlighted by a new variant of Bell's theorem for temporal order [10]. While the authors suggest their theorem shows that a quantum theory of gravity (under certain assumptions listed in the paper) must lack causal order, the theorem equivalently says that if one wants the weak-field limit of quantum gravity to have a well-defined causal order, then Statistical Independence must be violated.

In summary, by relying on Continuity of Action instead of Factorization we avoid having to make statements about non-observable versions of our world.

3.1. Retrocausality and Future Input Dependence

The violation of Statistical Independence, which superdeterministic theories display, implies a correlation between the detector and the prepared state (as defined by λ), typically in space-like separated regions. These regions, however, are contained in a common causal diamond, so there are events in the past which have both regions in their causal future, and there are events in the future which have both regions in the past.

The possibility that both detector and prepared state are correlated because of a common event in the past is commonly referred to as the "locality loophole" (to Bell's theorem). One can try to address it (to some extent) by choosing the detector settings using events in the far past. An extreme version of this has been presented in Handsteiner et al. [11] where light from distant quasars was used to select detector settings. We have more to say about what this experiment does and does not prove in section 4.3.

The possibility that detector and prepared state are correlated because of an event in the future is often referred to as "retrocausality" or sometimes as "teleology." Both of these terms are misleading. The word "retrocausality" suggests information traveling backward in time, but no superdeterministic model has such a feature. In fact, it is not even clear what this would mean in a deterministic theory. Unless one explicitly introduces an arrow of time (eg from entropy increase), in a deterministic theory, the future "causes" the past the same way the present "causes" the future. The word "teleology" is commonly used to mean that a process happens to fulfill a certain purpose which suffices to explain the process. It is misleading here because no one claims that Superdeterminism is explanatory just because it gives rise to what we observe; this would be utterly non-scientific. A superdeterministic theory should of course give rise to predictions that are not simply axioms or postulates.

For this reason, it was suggested in Wharton and Argaman [5] to use the more scientific expression "Future Input Dependence." This term highlights that to make predictions with a superdeterministic model one may use input on a spacelike hypersurface to the future of system preparation, instead of using input at the time of preparation. This is possible simply because these two slices are connected by a deterministic law. Relying on "future input" may sound odd, but it merely generalizes the tautologically true fact that to make a prediction for a measurement at a future time, one assumes that one makes a measurement at a future time. That is, we use "future input" every time we make a measurement prediction. It is just that this input does not normally explicitly enter the calculation.

We wish to emphasize that Future Input Dependence is in the first place an operational property of a model. It concerns the kind of information that one needs to make a prediction. In contrast with the way we are used to dealing with models, Future Input Dependence allows the possibility that this information may arise from a boundary condition on a future hypersurface. Of course one does not actually know the future. However, drawing on future input allows one to make conditional statements, for example of the type "if a measurement of observable O takes place, then …" Here, the future input would be that observable O will be measured in the first place (of course in that case one no longer predicts the measurement of O itself).

Now, in a deterministic theory, one can in principle formulate such future boundary conditions in terms of constraints on an earlier state. The hidden variables at the future hypersurface can be expressed through those at an earlier time, or, more generally, the two sets are correlated. But the constraint on the earlier state may be operationally useless. That is to say, whether or not one allows Future Input Dependence can make the difference between whether or not a model has explanatory power (see section 4.2 for more on that).

Future Input Dependence is related to Superdeterminism because constraints on a future hypersurface will in general enforce correlations on earlier hypersurfaces; i.e., future input dependent theories generically violate Statistical Independence.

In summary, superdeterministic models are not necessarily either retrocausal or teleological (and indeed we are not aware of any model that exhibits one of these properties). But superdeterministic models may rely on future input to make conditional predictions.

3.2. Disambiguation

The reader is warned that the word "Superdeterminism" has been used with slightly different meaning elsewhere. In all these meanings, Statistical Independence is violated and the corresponding theory should prohibit action at a distance. But some authors [5, 12] distinguish Superdeterminism from retrocausality (or Future Input Dependence, respectively). Further, not everyone also assumes that a superdeterministic theory is deterministic in the first place. We here assume it is, because this was historically the motivation to consider this option, and because if the theory was not deterministic there would not be much point in considering this option.

4. COMMON OBJECTIONS TO SUPERDETERMINISM

In this section we will address some commonly raised objections to Superdeterminism found in various places in the literature and online discussions.

4.1. Free Will and Free Choice

The Statistical Independence assumption is often referred to as "Free Choice," because it can be interpreted to imply that the experimenter is free to choose the measurement setting independently of the value of the hidden variables. This has had the effect of anthropomorphizing what is merely a mathematical assumption of a scientific hypothesis. Let us therefore have a look at the relation between Statistical Independence and the physical processes that underlie free choice, or free will more generally.

Ever since Hume [13], the notion of free will has been defined in two different ways:

- as an ability to have done otherwise;
- as an absence of constraints preventing one from doing what one wishes to do.

As in our previous discussion of causality, these definitions are profoundly different in terms of physical interpretation. An ability to have done otherwise presumes that a hypothetical world where one did do otherwise is a physically meaningful concept. That is to say, the scientific meaningfulness of the notion of "an ability to have done otherwise" depends on the extent to which one's theory of physics supports the notion of counterfactual worlds: as discussed below, theories may vary as to this extent.

The second definition, by contrast, does not depend on the existence of counterfactual worlds. It is defined entirely in terms of events or processes occurring in spacetime. For example, what one "wishes to do" could be defined in terms of a utility function which the brain attempts to optimize in coming to what we can call a "choice" or "decision." This second definition is often referred to as the compatibilist definition of free will.

Statistical Independence relies on the first of these definitions of free will because (as discussed above) it draws on the notion of counterfactual worlds. The absence of Statistical Independence does not, however, violate the notion of free will as given by the second definition. We do not usually worry about this distinction because in the theories that we are used to dealing with, counterfactuals typically lie in the state space of the theory. But the distinction becomes relevant for superdeterministic theories which may have constraints on state-space that rule out certain counterfactuals (because otherwise it would imply internal inconsistency). In some superdeterministic models there are just no counterfactuals in state space (for an example, see section 5.2), in some cases counterfactuals are partially constrained (see section 5.1), in others, large parts of state-space have an almost zero measure (5.3).

One may debate whether it makes sense to speak of free will even in the second case since a deterministic theory implies that the outcome of any action or decision was in principle fixed at the beginning of the universe. But even adding a random element (as in quantum mechanics) does not allow human beings to choose one of several future options, because in this case the only ambiguities about the future evolution (in the measurement process) are entirely unaffected by anything to do with human thought. Clearly, the laws of nature are a constraint that can prevent us from doing what we want to do. To have free will, therefore, requires one to use the compatibilist notion of free will, even if one takes quantum mechanics in its present form as fundamental. Free will is then merely a reflection of the fact that no one can tell in advance what decisions we will make.

But this issue with finding a notion of free will that is compatible with deterministic laws (or even partly random laws) is not specific to Superdeterminism. It is therefore not an argument that can be raised against Superdeterminism. Literally all existing scientific theories suffer from this conundrum. Besides, it is not good scientific practice to discard a scientific hypothesis simply because one does not like its philosophical implications.

Let us look at a simple example to illustrate why one should not fret about the inability of the experimenter to prepare a state independently of the detector. Suppose you have two fermions. The Pauli exclusion principle tells us that it is not possible to put these two particles into identical states. One could now complain that this violates the experimenter's free will, but that would be silly. The Pauli exclusion principle is a law of nature; it's just how the world is. Violations of Statistical Independence, likewise, merely tell us what states can exist according to the laws of nature. And the laws of nature, of course, constrain what we can possibly do.

In summary, raising the issue of free will in the context of Superdeterminism is a red herring. Superdeterminism does not make it any more or less difficult to reconcile our intuitive notion of free will with the laws of nature than is the case for the laws we have been dealing with for hundreds of years already.

4.2. The Conspiracy Argument

This argument has been made in a variety of ways, oftentimes polemically. Its most rigorous version can be summarized as follows. In any deterministic theory one can take a measurement outcome and, by using the law of time-evolution, calculate the initial state that would have given rise to this outcome. One can then postulate that since this initial state gave rise to the observation, we have somehow "explained" the observation. If one were to accept this as a valid argument, this would seemingly invalidate the science method in general. For then, whenever we observe any kind of regularity—say a correlation between X-ray exposure and cancer—we could say it can be explained simply because the initial state happened to be what it was.

The more polemic version of this is that in a superdeterministic theory, the universe must have been "just so" in order that the decisions of experimenters happen to reproduce the predictions of quantum mechanics every single time. Here, the term "just so" is invoked to emphasize that this seems intuitively extremely unlikely and therefore Superdeterminism relies on an implausible "conspiracy" of initial conditions that does not actually explain anything.

To address this objection, let us first define "scientific explanation" concretely to mean that the theory allows one to calculate measurement outcomes in a way that is computationally simpler than just collecting the data. This notion of "scientific explanation" may be too maths-centric to carry over to other disciplines, but will serve well for physics. The criticism leveled at Superdeterminism is, then, that if one were to accept explaining an observation merely by pointing out that an initial state and a deterministic law exists, then one would have to put all the

information about the observation already in the initial state, meaning the theory is not capable of providing a scientific explanation in the above defined sense.

One problem with this argument is that just by knowing a theory violates Statistical Independence one cannot tell anything about its explanatory power. For this one needs to study a concrete model. One needs to know how much information one has to put into the initial state and the evolution law to find out whether a theory is or is not predictive.

Let us look at a specific example from Bell himself [14]. Bell himself realized that free will was a red herring (see section 4.1) and for that reason his arguments against Superdeterminism are framed in a completely deterministic setting. He imagines that the measurement setting ($\mathbf{a} = \mathbf{0}$ or $\mathbf{a} = \mathbf{1}$) is determined by a pseudo-random number generator whose output is exquisitely sensitive to its input x in the sense that the setting depends on the parity of the millionth digit in the decimal expansion of x. Bell concludes that whilst the millionth digit indeed determines the measurement settings, it seems implausible to imagine that it systematically influences, or is systematically influenced by, anything else in the universe—the particle's hidden variables in particular.

Of course "it seems implausible" is not a convincing argument, as Bell himself conceded, writing [14]:

> Of course it might be that these reasonable ideas about physical randomizers are just wrong—for the purpose at hand. A theory may appear in which such conspiracies inevitably occur, and these conspiracies may then seem more digestible than the non-localities of other theories. When that theory is announced I will not refuse to listen, either on methodological or other grounds.

But Bell's intuition rests on the assumption that because worlds which differ only in the millionth digits of the random numbers are very similar to each other, they are necessarily "close" to each other. Such statements therefore implicitly depend on the notion of a distance in state-space. We intuitively tend to assume distance measures are Euclidean, but this does not need to be so in state-space.

Such conspiracy arguments are also often phrased as worries about the need to "fine-tune"—i.e., choose very precisely—the initial conditions (see Wood and Spekkens [15] for a quantifiable definition). The reference to fine-tuning, however, is misleading. There need be nothing *a priori* unscientific about a fine-tuned theory [16]. A fine-tuned theory *may* be unscientific if one needs to put a lot of information into the initial condition thereby losing explanatory power. But this does not necessarily have to be the case. In fact, according to currently accepted terminology both the standard model of particle physics and the concordance model of cosmology are "fine-tuned" despite arguably being scientifically useful.

One way to avoid that fine-tuning leads to a lack of explanatory power is to find a measure that can be defined in simple terms and that explains which states are "close" to each other and/or which are distant and have measure zero, i.e., are just forbidden (see Almada et al. [17] for an example of how this negates the problem of Wood and Spekkens [15]).

Bell's and similar examples that rest on arguments from fine-tuning (or sensitivity, or conspiracy) all implicitly assume that there is no simple way to mathematically express the allowed (or likely) initial states that give rise to the predictions of quantum mechanics. See also section 7 for further discussion on the notion of "closeness" in state-space and section 5.1 for an example of a theory where intuitive Euclidean ideas about closeness of worlds fail.

But assuming that something is impossible does not prove that it is impossible. Indeed, it is provable that it is unprovable to show such theories are unscientific because that is just a rephrasement of Chaitin's incompleteness theorem [18]. This theorem, in a nutshell, says that one can never tell that there is no way to further reduce the complexity of a string (of numbers). If we interpret the string as encoding the initial condition, this tells us that we cannot ever know that there is not some way to write down an initial state in a simpler way.

This is not to say that we can rest by concluding that we will never know that a useless theory cannot be made more useful. Of course, to be considered scientifically viable (not to mention interesting) a superdeterministic theory must actually have an explanatory formulation. We merely want to emphasize that the question whether the theory is scientific cannot be decided merely by pointing out that it violates Statistical Independence.

4.3. The Cosmic Bell Test and the BIG Bell Test

In the Cosmic Bell Test [11], measurement settings are determined by the precise wavelength of light from distant quasars, sources which were causally disconnected at the time the photons were emitted. It is without doubt a remarkable experimental feat, but this (and similar) experiments do not—cannot—rule out Superdeterminism; they merely rule out that the observed correlations in Bell-type tests were locally caused by events in the distant past. It is, however, clear from the derivation of Bell's theorem that violations of Bell's inequality cannot tell us whether Statistical Independence was violated. Violations of Bell's inequality can only tell us that at least one of the assumptions of the theorem was violated.

The belief that such tests tell us something about (the implausibility of) Superdeterminism goes back, once again, to the idea that a state which is intuitively "close" to the one realized in nature (eg, the wavelength of the light from the distant quasar was a little different, all else equal) is allowed by the laws of nature and likely to happen. However, in a superdeterministic theory what seems intuitively like a small change will generically result in an extremely unlikely state; that's the whole point. For example, in a superdeterministic theory, a physically possible counterfactual state in which the wave-length of the photon was slightly different may also require changes elsewhere on the past hypersurface, thereby resulting in the experimenter's decision to not use the quasar's light to begin with.

Similar considerations apply to all other Bell-type tests [19, 20] that attempt to close the freedom-of-choice loophole, like the BIG Bell test [21]. This experiment used input from 100,000 human participants playing a video game to choose detector settings,

thereby purportedly "closing the "freedom-of-choice loophole" (the possibility that the setting choices are influenced by "hidden variables" to correlate with the particle properties)". Needless to say, the experiment shows nothing of that type; one cannot prove freedom of choice by assuming freedom of choice.

In fact, the details of these experiments do not matter all that much. One merely has to note that measuring violations of Bell's inequality, no matter how entertaining the experimental setup, cannot tell us which of the assumptions to the theorem were violated.

4.4. The Tobacco Company Syndrome

Finally, let us turn to the claim that the assumption of Statistical Independence in Bell's theorem can be justified by what it would imply in classical physics. This argument is frequently put forward with the example of using a randomized trial to demonstrate that lung cancer is linked to smoking. If one were to allow violations of Statistical Independence in Bell-type experiments, so the argument goes, tobacco companies could claim that any observed correlation between lung cancer and smoking was due to a correlation between the randomization and the measured variable (i.e., the incidence of cancer). We do not know where this argument originated, but here are two examples:

> "It is like a shill for the tobacco industry first saying that smoking does not cause cancer, rather there is a common cause that both predisposes one to want to smoke and also predisposes one to get cancer (this is already pretty desperate), but then when confronted with randomized experiments on mice, where the mice did not choose whether or not to smoke, going on to say that the coin flips (or whatever) somehow always put the mice already disposed to get lung cancer into the experimental group and those not disposed into the control. This is completely and totally unscientific, and it is an embarrassment that any scientists would take such a claim seriously."—Tim Maudlin [22]

> "I think this assumption [of Statistical Independence] is necessary to even do science, because if it were not possible to probe a physical system independently of its state, we couldn't hope to be able to learn what its actual state is. It would be like trying to find a correlation between smoking and cancer when your sample of patients is chosen by a tobacco company."—Mateus Araújo [23]

One mistake in the argument against Superdetermism is the claim that theories without the assumption of Statistical Independence are unscientific because they are necessarily void of explanatory power. We already addressed this in subsection 4.2. However, the tobacco company analogy brings in a second mistake, which is the idea that we can infer from the observation that Statistical Independence is useful to understand the properties of classical systems, that it must also hold for quantum systems. This inference is clearly unjustified; the whole reason we are having this discussion is that classical physics is not sufficient to describe the systems we are considering.

We have already mentioned an example of how our classical intuition can fail in the quantum case. This example provides a further illustration. For the tobacco trial, we have no reason to think that multiple realizations of the randomization are impossible. For example, two different randomly drawn sub-ensembles of volunteers (say the first drawn in January, the second in February) can be expected to be statistically equivalent. It is only when our theoretical interpretation of an experiment requires us to consider counterfactual worlds, that differences between classical and quantum theories can emerge.

It is further important to note that the assumption of Statistical Independence does not require ensembles of different, actually occurring experiments (as opposed to virtual experiments that only appear in the mathematics) to have different statistical properties. Consider two ensembles of quantum particles, each measured with different measurement settings (say the first in January, the second in February). Since there is no reference to counterfactuals in this description, we cannot infer that the statistical properties of the hidden variables are any different in the January and February ensembles, even in a theory of quantum physics which violates Statistical Independence. At this level, therefore, there is no difference between the quantum and classical example. In a theory that violates Statistical Independence, one merely cannot infer that if February's ensemble of particles had been measured with January's measurement settings, the result would have been statistically identical. By contrast, if February's volunteers had been tested in January, we would, by classical theory, have expected statistically identical results. In this sense, the tobacco trial analogy is misleading because it raises the impression that the assumption of Statistical Independence is more outlandish than it really is.

5. HOW?

The history of Superdeterminism is quickly told because the topic never received much attention. Already Bell realized that if one observes violations of his inequality, this does not rule out local[3], deterministic hidden variable models because Statistical Independence may be violated [14]. It was later shown by Brans that if Statistical Independence is violated, any Bell-nonlocal distribution of measurement outcomes can be obtained in EPR-type experiments [24]. It has since been repeatedly demonstrated that it requires only minute violations of Statistical Independence to reproduce the predictions of quantum mechanics locally and deterministically [25–27].

The scientific literature contains a number of toy models that provide explicit examples for how such violations of Statistical Independence can reproduce quantum mechanics [24, 28, 29] which have been reviewed in Hall [9] (section 4.2). Toy models which violate Statistical Independence through future input dependence [30–33] have recently been surveyed in Wharton and Argaman [5] (section 6). We will here not go through these toy models again, but instead briefly introduce existing approaches to an underlying theory that give rise to Superdeterminism.

These approaches, needless to say, are still in their infancy. They leave open many questions and it might well turn out that none of them is the right answer. We do believe, however, that

[3] In the sense of Continuity of Action, see section 3.

they present a first step on the way toward a satisfactory solution of the measurement problem.

5.1. Invariant Set Theory

Invariant Set Theory (IST) [34, 35] arose from an earlier realization [36] that, suitably formulated, non-linear dynamics could provide the basis for a deterministic theory of quantum physics which was not counterfactually complete and therefore could violate Statistical Independence thus avoiding non-locality. More specifically, IST is a deterministic theory based on the assumption that the laws of physics at their most primitive derive from the geometry of a fractal set of trajectories, or histories, I_U, in state space. States of physical reality—the space-time that comprises our universe and the processes which occur in space-time—are those and only those belonging to I_U; other states in the Euclidean space in which I_U is embedded, do not correspond to states of physical reality. Dynamical evolution maps points on I_U to other points on I_U, whence I_U is invariant under dynamical laws of evolution. In this theory, the basic element of I_U is a fractal helix (in the sense that each trajectory in the helix, like a strand of rope, is itself a helix of finer-scale trajectories).

The link to quantum mechanics is made through the statistical properties of the helices which can be represented by complex Hilbert vectors and tensor products, where squared amplitudes and complex phases of the Hilbert vectors are necessarily described by rational numbers.

IST provides some possible understanding of a key difference between the Liouville equation and the von Neumann-Dirac equation: the factor $i\hbar$. Planck's constant has the dimension of state space (momentum times position) and hence provides an inherent size to any geometric structure in state space, such as I_U. This inherent size is provided by the radius of a helix of I_U. Based on the $U(1) \sim SO(2)$ isomorphism, the square root of minus one is consistent with a rotational symmetry of the helical nature of the trajectories of I_U.

Since it is formulated in terms of complex Hilbert states, IST violates Bell inequalities exactly as does quantum theory. It does this not only because Statistical Independence is violated (the fractal gaps in I_U correspond to states of the world associated with certain counterfactual measurement settings, which by construction are not ontic), it also violates the Factorization assumption of Bell's theorem and hence is Bell-nonlocal. Because the set of helices has fractal structure, the p-adic metric, rather than Euclidean metric is a natural measure of distance in state space.

Importantly, violation of Statistical Independence and Factorization only occur when one considers points which do not lie on I_U. From a Hilbert state perspective, they are associated with Hilbert States where either squared amplitudes or complex phases of Hilbert States cannot be described by rational numbers. Hence, the violations of Statistical Independence and Factorization in IST arise because certain putative counterfactual states are mathematically undefined; without these violations there would be mathematical inconsistency. Importantly, such counterfactual states do not correspond to physically possible processes in space-time. If Statistical Independence and Factorization are weakened to only allow processes which are expressible in space time and hence are physically possible ("Statistical Independence on I_U" and "Factorization on I_U"), then IST is consistent with both free choice and locality.

In IST, the measurement process is described by state-space trajectories that cluster together near detector eigenstates. In this approach, the measurement problem has been largely nullified because the statistical state space of the trajectory segments that lead to those detector eigenstates is no longer the whole Hilbert space, but instead the space whose elements have finite squared amplitudes and complex phases. In this sense, IST does not "complete" quantum theory. Rather, it is a replacement for quantum theory, even at the pre-measurement unitary stage of evolution.

The fractal attractor which defines I_U can be considered a future asymptotic property of some more classical like governing differential equations of motion: start from any point in state space and the trajectory will converge onto it only as $t \to \infty$. The invariant set is therefore operationally incomputable in much the same way that the event horizon of a black hole is.

5.2. Cellular Automata

The Cellular Automata approach to Superdeterminism [37] is a model that employs a time-evolution which proceeds in discrete time-steps on a grid. It uses a language similar to quantum mechanics, in that the state-space is spanned by vectors in a Hilbert-space. These vectors can, as usual, be brought into superpositions. However, it is then postulated that states which result in superpositions that we do not observe are not ontic. It follows from this that an initial state which gave rise to an unobserved outcome was not ontic either. A variety of simple toy models have been discussed in 't Hooft [37].

In this approach there is strictly speaking only one ontic state in the theory, which is the state that the universe is in. The requirement that the final state must correspond to the classical reality which we observe induces constraints at earlier times. These constraints give rise to non-local correlations which result in a violation of Statistical Independence.

The challenge for this approach is to render this theory predictive. As was noted in 't Hooft [37], selecting the ontological state requires a measure for the initial states of the universe:

> "Bell's theorem requires more hidden assumptions than usually thought: *The quantum theory only contradicts the classical one if we assume that the 'counterfactual modification' does not violate the laws of thermodynamics.* In our models, we must assume that it does." (emphasis original)

It is presently unclear from where such a thermodynamic-like measure comes.

5.3. Future-Bounded Path Integrals

The path integral approach to Superdeterminism [38] rests on the observation that the Feynman path integral has a future input dependence already, which is the upper time of the integration. However, in the usual path integral of quantum mechanics (and, likewise, of quantum field theory), one does not evaluate what is the optimal future state that the system can evolve into. Instead,

one posits that all of the future states are realized, which results in a merely probabilistic prediction.

The idea is then to take a modified path integral for the combined system of detector and prepared state and posit that in the underlying theory the combined system evolves along merely one possible path in state space that optimizes a suitable, to-be-defined, function. This function must have the property that initial states which evolve into final states containing superpositions of detector eigenstate states are disfavored, in the sense that they do not optimize the function. Instead, the optimal path that the system will chose is one that ends up in states which are macroscopically classical. One gets back normal quantum mechanics by averaging over initial states of the detector.

This approach solves the measurement problem because the system does deterministically evolve into one particular measurement outcome. Exactly which outcome is determined by the degrees of freedom of the detector that serve as the "hidden variables." Since it is generically impossible to exactly know all the detector's degrees of freedom, quantum mechanics can only make probabilistic predictions.

The challenge of this approach is to find a suitable function that actually has this behavior.

6. EXPERIMENTAL TEST

It is clear that the above discussed theoretical approaches to Superdeterminism require more work. However, such theories have general properties that, with some mild assumptions, tell us what type of experiment has the potential to reveal deviations from quantum mechanics.

To see this, we first note that typical experiments in the foundations of quantum mechanics probe physics at low energies, usually in the range of atomic physics. It is, however, difficult to come up with any model that equips known particles with new degrees of freedom accessible at such low energies. The reason is that such degrees of freedom would change the phase-space of standard model particles. Had they been accessible with any experiment done so far, we would have seen deviations from the predictions of the standard model, which has not happened.

It is well possible to equip standard model particles with new degrees of freedom if those are only resolvable at high energies (examples abound). But in this case the new degrees of freedom do not help us with solving the measurement problem exactly because we assumed that they do not play a role at the relevant energies.

If one does not want to give up on this separation of scales, this leaves the possibility that the hidden variables are already known degrees of freedom of particles which do not comprise the prepared state. Moreover, they are only those degrees of freedom that are resolvable at the energy scales under consideration.

The next thing we note is that all presently known deterministic, local theories have the property that states that were close together at an initial time will remain close for some while. In a superdeterministic theory, states with different measurement settings are distant in state-space, but changes to the hidden variables that do not also change the measurement setting merely result in different measurement outcomes and therefore correspond to states close to each other.

Since the theory is deterministic, this tells us that if we manage to create a time-sequence of initial states similar to each other, then the measurement outcomes should also be similar. This means concretely that rather than fulfilling the Born-rule, such an experiment would reveal time-correlations in the measurement outcomes. The easiest way to understand this is to keep in mind that if we were able to exactly reproduce the initial state, then in a superdeterministic theory the measurement outcome would have to be the same each time, in conflict with the predictions of quantum mechanics.

This raises the question how similar the initial states have to be for this to be observable. Unfortunately, this is not a question which can be answered in generality; for this one would need a theory to make the corresponding calculation. However, keeping in mind that the simplest case of hidden variables are the degrees of freedom of other particles and that the theory is local in the way we are used to it, the obvious thing to try is minimizing changes of the degrees of freedom of the detecting device. Of course one cannot entirely freeze a detector's degrees of freedom, for then it could no longer detect something. But one can at least try to prevent non-essential changes, i.e., reduce noise.

This means concretely that one should make measurements on states prepared as identically as possible with devices as small and cool as possible in time-increments as small as possible.

This consideration does not change much if one believes the hidden variables are properties of the particle after all. In this case, however, the problem is that preparing almost identical initial states is impossible since we do not know how to reproduce the particle's hidden variables. One can then try to make repeated measurements of non-commuting observables on the same states, as previously laid out in Hossenfelder [39].

The distinction between the predictions of quantum mechanics and the predictions of the underlying, superdeterministic theory is not unlike the distinction between climate predictions and weather forecasts. So far, with quantum mechanics, we have made predictions for long-term averages. But even though we are in both cases dealing with a non-linear and partly chaotic system, we can in addition also make short-term predictions, although with limited accuracy. The experiment proposed here amounts to recording short-term trends and examining the data for regularities that, according to quantum mechanics alone, should not exist.

Needless to say, the obvious solution may not be the right one and testing Superdeterminism may be more complicated than that. But it seems reasonable to start with the simplest and most general possibility before turning to model-specific predictions.

7. DISCUSSION

The reader may have noticed a running theme in our discussion of Superdeterminism, which is that objections raised against it are

deeply rooted in intuition that is, ultimately, based on the classical physics we experience with our own senses.

But these intuitions can mislead us. For an illustration, consider Penrose's impossible triangle (see **Figure 2**, bottom). If we see a two-dimensional drawing of the triangle, we implicitly assume that any two arms come closer as they approach a vertex. This raises the impression that the object is impossible to realize in 3-dimensional space. However, the supposedly impossible triangle can be built in reality. The object shown in **Figure 2**, top, seen from the right direction, reproduces what is shown in the 2-dimensional drawing. From any other direction, however, it becomes clear that our intuition has led us to improperly assume two arms necessarily become close as they approach a common vertex.

We believe that the uneasiness we bring to considering Superdeterminism stems from a similar intuitive, but ultimately wrong, idea of closeness. In this case, however, we are not talking about closeness in position space but about closeness in the state-space of a theory.

Faced with trying to quantify the "distance" between two possible states of the universe our intuition is to assume that it can be measured in state space by the same Euclidean metric we use to measure distance in physical space. This indeed is the basis of Lewis's celebrated theory of causality by counterfactuals: of two possible counterfactual worlds, the one that resembles reality more closely is presumed closer to reality [40]. But is this really so? In number theory there is an alternative to the class of Euclidean metrics (and indeed according to Ostrowsky's theorem it is the only alternative): the p-adic metric [41]. The p-adic metric is to fractal geometry as the Euclidean metric is to Euclidean geometry. The details do not need to concern us here, let us merely note that two points that are close according to the Euclidean metric may be far away according to the p-adic metric.

This means from the perspective of the p-adic metric, the distance between the actual world where the parity of the millionth digit of the input to Bell's pseudo-random number generator was, say, 0, and the counterfactual world where the parity was a 1 could be very large, even though it is small using an Euclidean measure of distance. A theory that seems fine-tuned with respect to the latter metric would not be fine-tuned with respect to the former metric. Like with Penrose's triangle, the seemingly impossible becomes understandable if we are prepared to modify our intuition about distance.

But our intention here was not merely to draw attention to how classical intuition may have prevented us from solving the measurement problem. Resolving the measurement problem with Superdeterminism may open the door to solving further problems in the foundations of physics. As has been previously noted [42], our failure to find a consistent quantum theory of gravity may be due, not to our lacking understanding of gravity, but to our lacking understanding of quantization. The same problem may be behind some of the puzzles raised by the cosmological constant. It is further a long-standing conjecture that dark matter is not a new type of particle but instead due to a modification of gravity. We know from observations that such a modification of gravity is parametrically linked to dark energy [43]. The reasons for this connection are currently not well-understood, but completing quantum mechanics, or replacing it with a more fundamental theory, might well be the key to solving these problems.

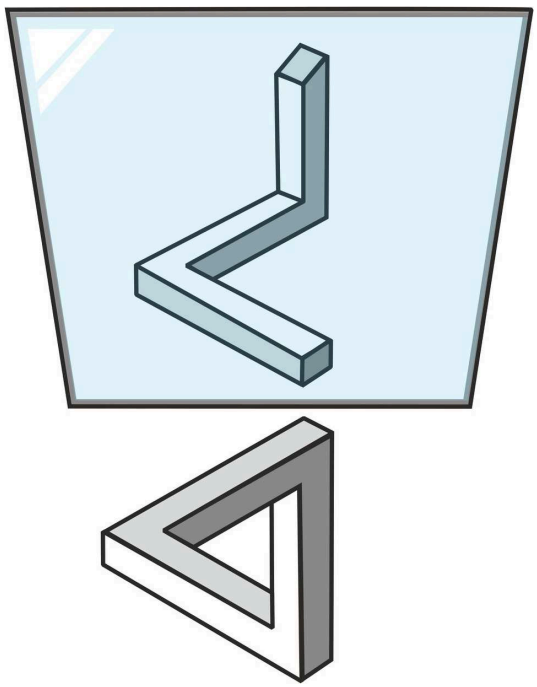

FIGURE 2 | Penrose's "impossible" triangle, placed in front of a mirror, turns out to be not so impossible.

Finally, let us point out that the technological applications of quantum theory become more numerous by the day. Should we discover that quantum theory is not fundamentally random, should we succeed in developing a theory that makes predictions beyond the probabilistic predictions of quantum mechanics, this would likely also result in technological breakthroughs.

8. CONCLUSION

We have argued here that quantum mechanics is an incomplete theory and completing it, or replacing it with a more fundamental theory, will necessarily require us to accept violations of Statistical Independence, an assumption that is sometimes also, misleadingly, referred to as Free Choice. We have explained why objections to theories with this property, commonly known as superdeterministic, are ill-founded.

Since the middle of the past century, progress in the foundations of physics has been driven by going to shorter and shorter distances, or higher and higher energies, respectively. But the next step forward might be in an entirely different direction, it might come from finding a theory that does not require us to hand-draw a line between microscopic and macroscopic reality.

DATA AVAILABILITY STATEMENT

The datasets generated for this study are available on request to the corresponding author.

AUTHOR CONTRIBUTIONS

All authors listed have made a substantial, direct and intellectual contribution to the work, and approved it for publication.

ACKNOWLEDGMENTS

SH gratefully acknowledges support from the Franklin Fetzer Fund. TP gratefully acknowledges support from a Royal Society Research Professorship. This manuscript has been released as a pre-print at arXiv.org [44].

REFERENCES

1. Bell JS. On the Einstein-Podolsky-Rosen paradox. *Physics* (1964) **1**:195.
2. Gallicchio J, Friedman AS, Kaiser DI. Testing Bell's inequality with cosmic photons: closing the setting-independence loophole. *Phys Rev Lett.* (2014) **112**:110405. doi: 10.1103/PhysRevLett.112.110405
3. Pusey MF, Barrett J, Rudolph T. On the reality of the quantum state. *Nat Phys.* (2012) **8**:476. doi: 10.1038/nphys2309
4. Leifer MS. Is the quantum state real? A review of ψ-ontology theorems. *Quanta* (2014) **3**:67–155. doi: 10.12743/quanta.v3i1.22
5. Wharton KB, Argaman N. Bell's theorem and spacetime-based reformulations of quantum mechanics. *arXiv [preprint]* (2019). 1906.04313.
6. Clauser JF, Horne MA, Shimony A, Holt RA. Proposed experiment to test local hidden-variable theories. *Phys Rev Lett.* (1969) **23**:880–4.
7. Lorenz EN. Deterministic nonperiodic flow. *J Atmos Sci.* (1963) **20**:130–41.
8. Fuchs CA, Schack R. Quantum-Bayesian coherence. *arXiv [preprint]* (2019). 09
06.2187.
9. Hall MJW. The significance of measurement independence for Bell inequalities and locality. In: Asselmeyer-Maluga T, editor. *At the Frontier of Spacetime*. Cham: Springer (2016). p. 189–204.
10. Zych M, Costa F, Pikovski I, Brukner Č. Bell's theorem for temporal order. *Nat Commun.* (2019) **10**:3772. doi: 10.1038/s41467-019-11579-x
11. Handsteiner J, Friedman AS, Rauch D, Gallicchio J, Liu B, Hosp H, et al. Cosmic Bell test: measurement settings from milky way stars. *Phys Rev Lett.* (2017) **118**:060401. doi: 10.1103/PhysRevLett.118.060401
12. Price H, Wharton K. A live alternative to quantum spooks. *arXiv [preprint]* (2015). 1510.06712.
13. Hume D. *A Treatise of Human Nature*. Oxford; New York, NY: Oxford University Press (2000).
14. Bell JS. *Speakable and Unspeakable in Quantum Mechanics. Collected Papers on Quantum Philosophy*. Cambridge: Cambridge University Press (1987).
15. Wood CJ, Spekkens RW. The lesson of causal discovery algorithms for quantum correlations: causal explanations of Bell-inequality violations require fine-tuning. *New J Phys.* (2015) **17**:033002. doi: 10.1088/1367-2630/17/3/033002
16. Hossenfelder S. Screams for explanation: finetuning and naturalness in the foundations of physics. *Synthese.* (2019) 1–9. doi: 10.1007/s11229-019-02377-5
17. Almada D, Ch'ng K, Kintner S, Morrison B, Wharton KB. Are retrocausal accounts of entanglement unnaturally fine-tuned? *Int J Quantum Found.* (2016) **2**:1–16.
18. Chaitin G. *The Limits of Mathematics*. London, UK: Springer (1994).
19. Leung C, Brown A, Nguyen H, Friedman AS, Kaiser DI, Gallicchio J. Astronomical random numbers for quantum foundations experiments. *Phys Rev A.* (2018) **97**:042120. doi: 10.1103/PhysRevA.97.042120
20. Rauch D, Handsteiner J, Hochrainer A, Gallicchio J, Friedman AS, Leung C, et al. Cosmic Bell test using random measurement settings from high-redshift quasars. *Phys Rev Lett.* (2018) **121**:080403. doi: 10.1103/PhysRevLett.121.080403
21. The BIG Bell Test Collaboration. Challenging local realism with human choices. *Nature.* (2018) **557**:212–6. doi: 10.1038/s41586-018-0085-3
22. Maudlin T. *Comment on Electrons Don't Think. Blogentry on "BackRe(Action)"* (2019). Available online at: https://bit.ly/33InZZD (accessed December 1, 2019).
23. Araújo M. *Understanding Bell's Theorem Part 1: The Simple Version. Blogentry on "More Quantum"* (2016). Available online at: https://bit.ly/2rGjyky (accessed December 1, 2019).
24. Brans CH. Bell's theorem does not eliminate fully causal hidden variables. *Int J Theor Phys.* (1988) **27**:219.
25. Barrett J, Gisin N. How much measurement independence is needed in order to demonstrate nonlocality? *Phys Rev Lett.* (2011) **106**:100406. doi: 10.1103/PhysRevLett.106.100406
26. Hall MJW. Relaxed Bell inequalities and Kochen-Specker theorems. *Phys Rev A.* (2011) **84**:022102. doi: 10.1103/PhysRevA.84.022102
27. Friedman AS, Guth AH, Hall MJW, Kaiser DI, Gallicchio J. Relaxed Bell inequalities with arbitrary measurement dependence for each observer. *Phys Rev A.* (2019) **99**:012121. doi: 10.1103/PhysRevA.99.012121
28. Degorre J, Laplante S, Roland J. Simulating quantum correlations as a distributed sampling problem. *Phys Rev A.* (2005) **72**:062314. doi: 10.1103/PhysRevA.72.062314
29. Hall MJW. Local deterministic model of singlet state correlations based on relaxing measurement independence. *Phys Rev Lett.* (2010) **105**:250404. doi: 10.1103/PhysRevLett.105.250404
30. Argaman N. Bell's theorem and the causal arrow of time. *Am J Phys.* (2010) **78**:1007–13. doi: 10.1119/1.3456564
31. Di Lorenzo A. A simple model for the spin singlet: mathematical equivalence of non-locality, slave will and conspiracy. *J Phys A.* (2012) **45**:265302. doi: 10.1088/1751-8113/45/26/265302
32. Argaman N. A lenient causal arrow of time? *Entropy.* (2018) **20**:294. doi: 10.3390/e20040294
33. Wharton KB. A new class of retrocausal models. *Entropy.* (2018) **20**:410. doi: 10.3390/e20060410
34. Palmer TN. The invariant set postulate: a new geometric framework for the foundations of quantum theory and the role played by gravity. *Proc R Soc A.* (2009) **465**. doi: 10.1098/rspa.2009.0080
35. Palmer TN. Discretization of the bloch sphere, fractal invariant sets and Bell's theorem. *Proc. R Soc A.* (2020) **476**:20190350. doi: 10.1098/rspa.2019.0350
36. Palmer TN. A local deterministic model of quantum spin measurement. *Proc R Soc A.* (1995) **451**:585–608.
37. 't Hooft G. *The Cellular Automaton Interpretation of Quantum Mechanics*. Cham: Springer (2016). doi: 10.1007/978-3-319-41285-6
38. Donadi S, Hossenfelder S. In preparation.
39. Hossenfelder S. Testing super-deterministic hidden variables theories. *Found Phys.* (2011) **41**:1521. doi: 10.1007/s10701-011-9565-0
40. Lewis D. *Counterfactuals*. Oxford: Blackwell (1973).

41. Katok S. *p-adic Analysis Compared With Real*. Student Mathematical Library (Book 37), Providence, RI: American Mathematical Society (2007).
42. Hossenfelder S. A possibility to solve the problems with quantizing gravity. *Phys Lett B*. (2013) **725**:473. doi: 10.1016/j.physletb.2013.07.037
43. Lelli F, McGaugh SS, Schombert JM, Pawlowski MS. One law to rule them all: the radial acceleration relation of galaxies. *Astrophys J*. (2017) **836**:152. doi: 10.3847/1538-4357/836/2/152
44. Hossenfelder S, Palmer TN. Rethinking superdeterminism. *arXiv*. 1912.06462.

Conflict of Interest: The authors declare that the research was conducted in the absence of any commercial or financial relationships that could be construed as a potential conflict of interest.

frontiers in Physics

ORIGINAL RESEARCH
published: 12 May 2020
doi: 10.3389/fphy.2020.00142

The Bell Theorem Revisited: Geometric Phases in Gauge Theories

*David H. Oaknin**

Rafael Ltd, Haifa, Israel

The Bell theorem stands as an insuperable roadblock in the path to a very desired intuitive solution of the EPR paradox and, hence, it lies at the core of the current lack of a clear interpretation of the quantum formalism. The theorem states through an experimentally testable inequality that the predictions of quantum mechanics for the Bell's polarization states of two entangled particles cannot be reproduced by any statistical model of hidden variables that shares certain intuitive features. In this paper we show, however, that the proof of the Bell theorem involves a subtle, though crucial, assumption that is not required by fundamental physical principles and, hence, it is not necessarily fulfilled in the experimental setup that tests the inequality. Indeed, this assumption can neither be properly implemented within the standard framework of quantum mechanics. Namely, the proof of the theorem assumes that there exists a preferred absolute frame of reference, supposedly provided by the lab, which enables to compare the orientation of the polarization measurement devices for successive realizations of the experiment and, hence, to define jointly their response functions over the space of hypothetical hidden configurations for all their possible alternative settings. We notice, however, that only the relative orientation between the two measurement devices in every single realization of the experiment is a properly defined physical degree of freedom, while their global rigid orientation is a spurious gauge degree of freedom. Hence, the preferred frame of reference required by the proof of the Bell theorem does not necessarily exist. In fact, it cannot exist in models in which the gauge symmetry of the experimental setup under global rigid rotations of the two detectors is spontaneously broken by the hidden configurations of the pair of entangled particles and a non-zero geometric phase appears under some cyclic gauge symmetry transformations. Following this observation, we build an explicitly local model of hidden variables that reproduces the predictions of quantum mechanics for the Bell's states.

Keywords: Quantum Mechanics, EPR paradox, Bell's inequality, hidden variables, locality, rotational symmetry, gauge symmetries, spontaneous symmetry breaking

OPEN ACCESS

Edited by:
Karl Hess,
University of Illinois at Urbana-Champaign, United States

Reviewed by:
Guendelman Eduardo,
Ben-Gurion University of the Negev, Israel
Michael Revzen,
Technion Israel Institute of Technology, Israel

***Correspondence:**
David H. Oaknin
d1306av@gmail.com

Specialty section:
This article was submitted to Mathematical Physics, a section of the journal Frontiers in Physics

Received: *20 March 2020*
Accepted: *09 April 2020*
Published: *12 May 2020*

Citation:
Oaknin DH (2020) The Bell Theorem Revisited: Geometric Phases in Gauge Theories. Front. Phys. 8:142. doi: 10.3389/fphy.2020.00142

1. INTRODUCTION

The Bell theorem is one of the fundamental theorems upon which relies the widespread belief that quantum mechanics is the ultimate mathematical framework within which the hypothetical final theory of the fundamental building blocks of Nature and their interactions should be formulated. The theorem states through an experimentally testable inequality (the Bell inequality) that statistical models of hidden variables that share certain intuitive features cannot reproduce the

predictions of quantum mechanics for the entangled polarization states of two particles (Bell's states) [1, 2]. These predictions have been confirmed beyond doubt by very carefully designed experiments [3–12].

In these experiments a source emits pairs of particles whose polarizations are arranged in a Bell's entangled state:

$$|\Psi_\Phi\rangle = \frac{1}{\sqrt{2}}\left(|\uparrow\rangle^{(A)}|\downarrow\rangle^{(B)} - e^{i\Phi}|\downarrow\rangle^{(A)}|\uparrow\rangle^{(B)}\right), \quad (1)$$

where $\{|\uparrow\rangle, |\downarrow\rangle\}^{(A,B)}$ are eigenstates of Pauli operators $\sigma_Z^{(A,B)}$ along locally defined Z-axes for each one of the two particles. The two emitted particles travel off the source in opposite directions toward two widely separated detectors, which test their polarizations. The orientation of each one of the detectors can be freely and independently set along any arbitrary direction in the XY-plane perpendicular to the locally defined Z-axis. Upon detection each particle causes a binary response of its detector, either $+1$ or -1. Thus, each pair of entangled particles produces an outcome in the space of possible events $\mathcal{P} \equiv \{(-1,-1),(-1,+1),(+1,-1),(+1,+1)\}$. We refer to each detected pair as a single realization of the experiment.

Quantum mechanics predicts that the statistical correlation between the binary outcomes of the two detectors in a long sequence of realizations of the experiment is given by:

$$E(\Delta,\Phi) = -\cos(\Delta-\Phi), \quad (2)$$

where Δ is the relative angle between the orientations of the two detectors. In particular, when $\Delta - \Phi = 0$ we get that $E = -1$, so that all outcomes in the sequence must be either $(-1,+1)$ or $(+1,-1)$.

The Bell theorem states that prediction (2) cannot be reproduced by any model of hidden variables that shares certain intuitive features. In particular, the CHSH version of the theorem states that for the said generic models of hidden variables the following inequality is fulfilled for any set of values $(\Delta_1, \Delta_2, \delta)$ [13]:

$$\left|E(\Delta_1) + E(\Delta_2) + E(\Delta_1-\delta) - E(\Delta_2-\delta)\right| \leq 2. \quad (3)$$

On the other hand, according to quantum mechanics the magnitude in the left hand side of the inequality reaches a maximum value of $2\sqrt{2}$, known as Tsirelson's bound [14], for certain values of Δ_1, Δ_2 and δ— e.g., $\Delta_1 = -\Delta_2 = \frac{1}{2}\delta = \frac{\pi}{4}$. As it was noted above, carefully designed experiments have confirmed that the CHSH inequality is violated according to the predictions of quantum mechanics and, therefore, have ruled out all the generic models of hidden variables constrained by the Bell inequality (3).

In this paper we show, however, that the generic models of hidden variables constrained by the Bell theorem all share a subtle crucial feature that is not necessarily fulfilled in the actual experimental tests of the Bell inequality. Indeed, the considered feature cannot be derived from fundamental physical principles and may even be at odds with the fundamental principle of relativity. Moreover, this feature neither can be properly implemented within the standard framework of quantum mechanics. We follow this observation to explicitly build a local model of hidden variables that does not share the disputed feature and, thus, it is capable to reproduce the predictions of quantum mechanics for the Bell's polarization states of two entangled particles.

Our model puts forward for consideration the possibility that quantum mechanics might not be the ultimate mathematical framework of fundamental physics. In fact, it is interesting to notice that the way how our model solves the apparent "non-locality" associated to entanglement in the standard quantum formalism is very similar to the way how General Relativity solves the "non-locality" of Newton's theory of gravitation: in our model quantum entanglement is the result of a curved metric in the space in which the hypothetical hidden variables live.

2. OUTLINE

Any local statistical model of hidden variables that aims to describe the Bell's experiment consists of some space $\mathcal{S}$ of possible hidden configurations for the pair of entangled particles, labeled here as $\lambda \in \mathcal{S}$, together with a well-defined (density of) probability $\rho(\lambda)$ for each one of them to occur in every single realization. The model must also specify well-defined binary functions $s^{(A)}_{\Omega_A}(\lambda) = \pm 1$, $s^{(B)}_{\Omega_B}(\lambda) = \pm 1$ to describe the outcomes that would be obtained at detectors A and B when the pair of entangled particles occurs in the hidden configuration $\lambda \in \mathcal{S}$ and their polarizations are tested along directions Ω_A and Ω_B, respectively.

The proof of the CHSH inequality (3) involves two well-defined possible orientations Ω_A and Ω'_A for the polarization test of particle A and two well-defined possible orientations Ω_B and Ω'_B for the polarization test of particle B, and assumes that the considered model of hidden variables assigns to each possible hidden configuration $\lambda \in \mathcal{S}$ a 4-tuple of binary values $\left[s^{(A)}_{\Omega_A}(\lambda), s^{(A)}_{\Omega'_A}(\lambda), s^{(B)}_{\Omega_B}(\lambda), s^{(B)}_{\Omega'_B}(\lambda)\right] \in \{-1,+1\}^4$ to describe the outcomes that would be obtained in each one of the two detectors in case that it would be set along each one of its two available orientations. Hence, it is straightforward to obtain that for any $\lambda \in \mathcal{S}$,

$$s^{(A)}_{\Omega_A}(\lambda)\cdot\left(s^{(B)}_{\Omega_B}(\lambda) + s^{(B)}_{\Omega'_B}(\lambda)\right) + s^{(A)}_{\Omega'_A}(\lambda)\cdot\left(s^{(B)}_{\Omega_B}(\lambda) - s^{(B)}_{\Omega'_B}(\lambda)\right) = \pm 2, \quad (4)$$

since the first term is non-zero only when $s^{(B)}_{\Omega_B}(\lambda)$ and $s^{(B)}_{\Omega'_B}(\lambda)$ have the same sign, while the second term is non-zero only when they have opposite signs. The CHSH inequality (3) is then obtained by averaging (4) over the whole space $\mathcal{S}$ of all possible hidden configurations, since

$$\left|\int d\lambda\ \rho(\lambda)\ \left\{s^{(A)}_{\Omega_A}(\lambda)\cdot\left(s^{(B)}_{\Omega_B}(\lambda) + s^{(B)}_{\Omega'_B}(\lambda)\right) + s^{(A)}_{\Omega'_A}(\lambda)\cdot\left(s^{(B)}_{\Omega_B}(\lambda) - s^{(B)}_{\Omega'_B}(\lambda)\right)\right\}\right| \leq 2, \quad (5)$$

while

$$\int d\lambda\, \rho(\lambda)\, s^{(A)}_{\Omega_A}(\lambda) \cdot s^{(B)}_{\Omega_B}(\lambda) \;=\; E(\Delta_1), \tag{6}$$

$$\int d\lambda\, \rho(\lambda)\, s^{(A)}_{\Omega_A}(\lambda) \cdot s^{(B)}_{\Omega'_B}(\lambda) \;=\; E(\Delta_2), \tag{7}$$

$$\int d\lambda\, \rho(\lambda)\, s^{(A)}_{\Omega'_A}(\lambda) \cdot s^{(B)}_{\Omega_B}(\lambda) \;=\; E(\Delta_1 - \delta), \tag{8}$$

$$\int d\lambda\, \rho(\lambda)\, s^{(A)}_{\Omega'_A}(\lambda) \cdot s^{(B)}_{\Omega'_B}(\lambda) \;=\; E(\Delta_2 - \delta). \tag{9}$$

In this argument the orientations Ω_A, Ω'_A, Ω_B, and Ω'_B seem to be fixed with respect to some external frame of reference supposedly provided by the labs. Nonetheless, the data collected in such an experimental setup could be alternatively analyzed within frames of reference aligned, for example, with the magnetic axis of the Sun or the rotational axis of the Galaxy, with respect to which the orientations of the detectors for different realizations of the experiment are not fixed anymore. Obviously, the conclusions of the analysis must remain the same, independently of the chosen lab frame. Indeed, the proof of the CHSH inequality actually requires only three well-defined angles, $\Delta_1 \equiv \angle(\Omega_B, \Omega_A)$, $\Delta_2 \equiv \angle(\Omega'_B, \Omega_A)$, and $\delta \equiv \angle(\Omega'_A, \Omega_A)$, which correspond, respectively, to the relative orientations of Ω_B, Ω'_B, and Ω'_A with respect to Ω_A, which serves as a reference direction. The reference direction Ω_A serves also to define the hidden configuration $\lambda \in \mathcal{S}$ of the pair of entangled particles in every single realization of the experiment, since the description of a physical state must necessarily be done with respect to a reference frame. Otherwise, the orientation with respect to any external lab frame, either the optical table or the stars in the sky, of this reference direction Ω_A at different single realizations of the Bell's experiment is absolutely irrelevant: it is an spurious gauge degree of freedom, which can be set to zero (see **Figure 1**).

The proof of the CHSH inequality, thus, seems straightforward and unavoidable. Nonetheless, the main claim of this paper is that this proof, as well as the proofs of all other versions of the Bell inequality, involve a subtle, though crucial, implicit assumption that cannot be derived from fundamental physical principles and, indeed, it might not be fulfilled in the actual experimental setup that tests the inequality. Namely, in each realization of a Bell's experiment the polarization of each one of the two entangled particles is tested along a single direction. Hence, the relative orientation Δ of the two measurement devices in each single realization of the experiment is a properly defined physical magnitude, which can be set to values Δ_1, Δ_2, or any other desired value. On the other hand, the definition of the angle δ that appears in the proof of the CHSH inequality requires a comparison of the global rigid orientation of the measurement devices for different realizations of the Bell's experiment and, thus, it requires the existence of an absolute preferred frame of reference with respect to which this global orientation could be defined. Otherwise, we could choose the orientation of, say, detector A as the reference direction for every single realization of the experiment and define the orientation of the other detector with respect to it, in which case the proof of the Bell theorem does not necessarily hold as we shall show later. Obviously, such an absolute preferred frame of reference would not be needed if the polarization of each one of the two entangled particles could be tested along two different directions at once in every single realization of the experiment, but this is certainly not the case. Similar concerns regarding the way how different settings of the detectors are compared within the framework of the Bell theorem and the crucial role that this comparison plays in the proof of the inequality are also raised by Hess in [15, 16], and much earlier in a different but related context in Hess and Philipp [17, 18] and Hess et al. [19].

The said preferred frame of reference needed to prove the Bell theorem is supposedly provided by the lab. However, the conditions that a reference frame must fulfill in order to qualify as a preferred absolute frame are far from obvious and, in any case, its existence is an overbold assumption whose fulfillment has never been explored neither theoretically or experimentally. In fact, the existence of an absolute preferred frame of reference would be clearly at odds with Galileo's principle of relativity. Moreover, it is straightforward to show that this assumption cannot be properly implemented within the standard framework of quantum mechanics either. The argument goes as follows. The Bell's state (1) that describes the pair of entangled particles is defined in terms of the bases $\{|\uparrow\rangle, |\downarrow\rangle\}^{(A,B)}$ of eigenstates of the Pauli operators $\sigma_Z^{(A,B)}$ along locally defined Z-axes for each one of the particles. Since these eigenstates are defined up to a global phase, the phase Φ in expression (1) cannot be properly defined with respect to a lab frame. In order to properly define it we need to choose an arbitrary setting of the two detectors that test the polarizations of the pair of entangled particles as a reference. This reference setting defines *parallel* directions along the XY-planes at the sites where each one of the two particles are detected. Then, the phase Φ of the entangled state (1) can be properly defined with respect to this reference setting with the help of the measured correlations between the outcomes of the two detectors, $E = -\cos(\Phi)$. Furthermore, we can use this reference setting to properly define a relative rotation Δ of the orientations of the two measurement devices. On the other hand, since we must use an arbitrary setting of the detectors as a reference, their absolute orientation is an unphysical gauge degree of freedom (see **Figure 2**). In summary, in order to describe the setting of the measurement devices in a Bell's experiment within the standard framework of quantum mechanics we need to specify both Φ and Δ with respect to some otherwise arbitrary reference setting of the detectors. Nonetheless, only their difference $\Delta - \Phi$ is independent of the chosen reference setting and, hence, the correlation between the outcomes of the two devices can only depend on this difference (2).

In the absence of an absolute preferred frame of reference the global rigid orientation of the two detectors is, as we have already noticed before, an spurious (unphysical) gauge degree of freedom and, hence, the proof of the CHSH inequality (as well as of all other versions of the Bell inequality) holds only for models in which the considered hidden configurations are symmetrically invariant under a rigid rotation of the two measuring devices. On the other hand, we shall show below that the proof of the inequality does not necessarily hold when this symmetry

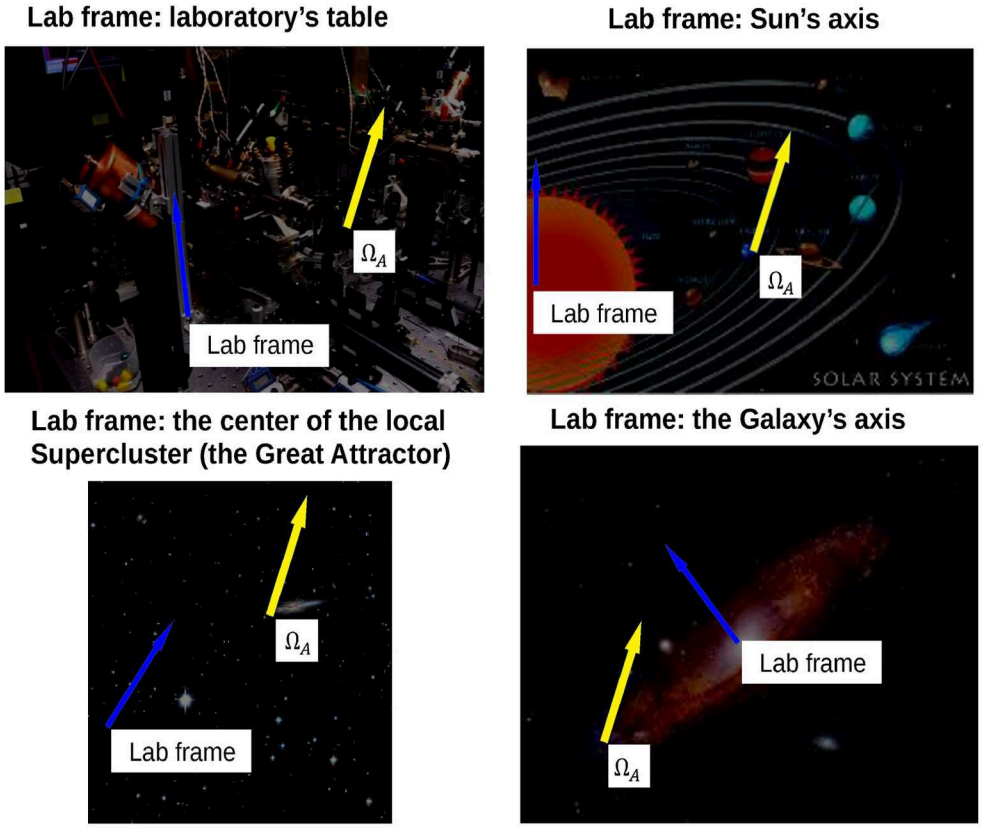

FIGURE 1 | The orientation of the reference direction Ω_A with respect to the chosen lab frame is a spurious gauge degree of freedom.

is (spontaneously) broken by the hidden configuration of the entangled particles, since then a non-zero geometric phase may appear under cyclic gauge transformations. Indeed, the crucial role of the angle δ in the proof of the CHSH inequality is an obvious indication that in order to violate it the gauge symmetry under a rigid rotation of the two detectors must be spontaneously broken.

In fact, it is obvious from the correlation (2) that the entanglement of the two particles explicitly breaks the symmetry of the system under a rotation of the relative orientation of the two detectors. Since a reference direction is needed for this symmetry to get broken, the gauge symmetry under a rigid rotation of the two detectors must be also spontaneously broken. From this perspective the phase Φ that appears in the description of the source (1) seems to play the role of a Goldstone mode associated to the spontaneously broken gauge symmetry, that is, the phase Φ appears instead of the spurious gauge degree of freedom δ that would describe the global rigid orientation of the two detectors. Under these circumstances, it is not possible to compare different settings of the detectors with respect to an external lab frame of reference: they can only be compared with respect to a frame in which they all share the same preferred direction, e.g., the reference frame set by the orientation of one of the detectors. This requirement can be explained as follows.

In the proof of the CHSH inequality it is implicitly assumed, as we have already noticed above, that there exists a preferred frame of reference, which defines a set of coordinates $\lambda \in \mathcal{S}$ over the space $\mathcal{S}$ of all possible hidden configurations that can be used to describe the response function of each one of the two detectors in each one of its two available orientations (defined with respect to the said preferred frame). Above we denoted these response functions as $s^{(A)}_{\Omega_A}(\lambda), s^{(A)}_{\Omega'_A}(\lambda), s^{(B)}_{\Omega_B}(\lambda), s^{(B)}_{\Omega'_B}(\lambda)$. Nonetheless, in general, we should allow for each one of the two detectors to define its proper set of coordinates over the space $\mathcal{S}$. Thus, for a given setting of the detectors we shall denote as λ_A and λ_B the sets of coordinates associated to detector A and detector B, respectively, so that their responses would be given as $s(\lambda_A)$ and $s(\lambda_B)$ by some universal function $s(\cdot)$ of the locally defined coordinate of the hidden configuration. Since these two sets of coordinates parameterize the same space of hidden configurations $\mathcal{S}$ there must exist some invertible transformation that relates them:

$$\lambda_B = -L(\lambda_A;\ \Delta - \Phi), \tag{10}$$

which may depend parametrically on the relative orientation $\Delta - \Phi$ between the two detectors. This transformation must fulfill the constraint

$$d\lambda_A\ \rho(\lambda_A) = d\lambda_B\ \rho(\lambda_B), \tag{11}$$

in order to guarantee that the probability of every hidden configuration to occur remains invariant under a change of coordinates, while the (density of) probability $\rho(\cdot)$ is functionally invariant for both sets of coordinates. However, these constraints do not forbid the possibility that the set of coordinates accumulates a non-zero geometric phase $\alpha \neq 0$ through certain cyclic gauge transformations:

$$\left(-L_{\bar{\Delta}_2}\right) \circ \left(-L_{\bar{\Delta}_2-\bar{\delta}}\right) \circ \left(-L_{\bar{\Delta}_1-\bar{\delta}}\right) \circ \left(-L_{\bar{\Delta}_1}\right) \neq \mathbb{I}, \tag{12}$$

In such a case there does not exist a single set of coordinates that can be used to define the response functions of each one of the two detectors in its two available orientations (defined with respect to an external frame), as required by the proof of the inequality (3). Therefore, in order to compare the four different experiments involved in the CHSH inequality we must choose the orientation of one of the detectors as a reference direction, as we do below in (13), so that they all may be described within a common set of coordinates. The appearance of a non-zero geometric phase under a cyclic transformation is a well-known phenomena in physical models involving gauge symmetries [20] and, therefore, we should not rule out the possibility that it also occurs in models of hidden variables for the Bell's states. The Bell theorem, however, cannot account for such models.

Following these observations we were able to explicitly build a local model of hidden variables that reproduces the predictions of quantum mechanics for the Bell polarization states. In our model the hidden configurations of the pair of entangled particles are described by a *pointer*, which sets an arbitrarily oriented preferred direction and, thus, spontaneously breaks the symmetry of the setup under rigid rotations of the two detectors. As we have just noticed, and we shall show later on in further detail, in order to compare different realizations of the experiment within the framework of such a model we must choose a common reference direction, which can be either the orientation of the hidden configuration of the pair of entangled particles or, alternatively, the orientation of one of the detectors, say, detector A. Since the former may not be directly experimentally accessible, we are left only with the latter option. Thus, in such a model we only need to specify the binary values for $s(\lambda_A)$, $s(\lambda_B)$, $s(\lambda'_B)$, $s(\lambda''_B)$, and $s(\lambda'''_B)$ for each possible hidden configuration $\lambda_A \in \mathcal{S}$ of the pair of entangled particles, where $\lambda_B = -L(\lambda_A; \Delta_1)$, $\lambda'_B = -L(\lambda_A; \Delta_2)$, $\lambda''_B = -L(\lambda_A; \Delta_1 - \delta)$, $\lambda'''_B = -L(\lambda_A; \Delta_2 - \delta)$. It is then straightforward to notice that the magnitude

$$s(\lambda_A) \cdot \left(s(\lambda_B) + s(\lambda'_B) + s(\lambda''_B) - s(\lambda'''_B)\right), \tag{13}$$

which comes instead of (4), can take values out of the interval $[-2, 2]$. Hence, these models are not constrained by the CHSH inequality (3). A simplified version of these arguments is presented in **Figure 3** with the help of a toy model.

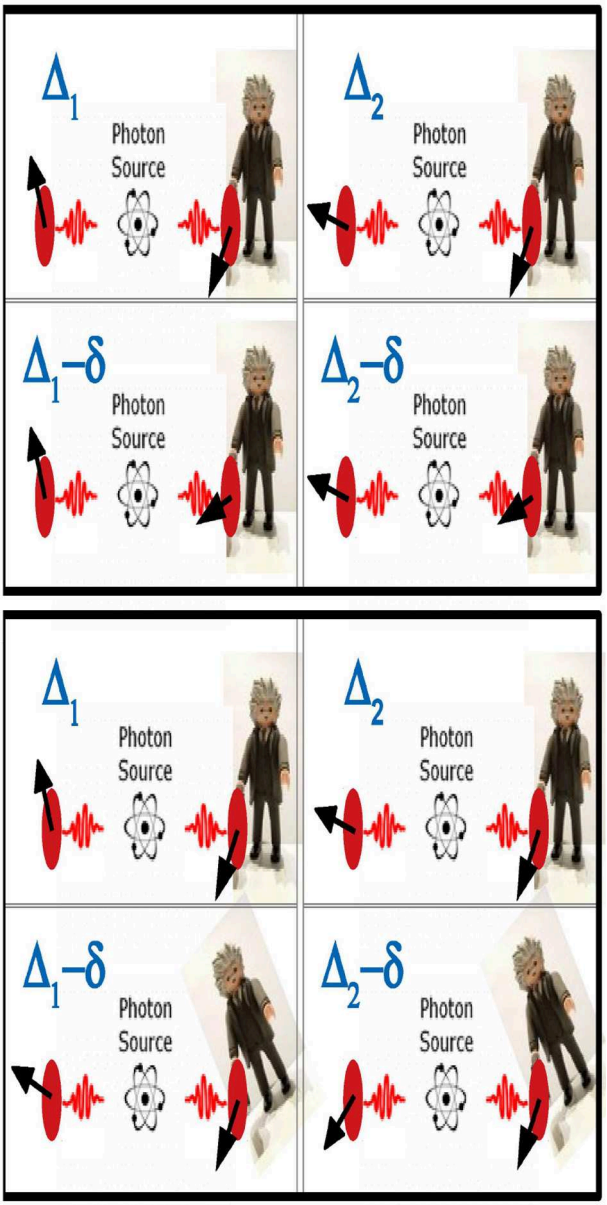

FIGURE 2 | Two descriptions of the experimental setup required for testing the Bell inequality. In the description above the lab frame is taken to be fixed, while in the description below the orientation of detector A is taken to be fixed. The relative angle between the two detectors is set at four possible values Δ_1, Δ_2, $\Delta_1 - \delta$, and $\Delta_2 - \delta$. When considering models in which the hypothetical hidden configurations of the pairs of entangled particles spontaneously break the symmetry under rigid rotations of the orientations of the two measurement devices, only the latter choice allows to properly compare the four different settings.

These arguments can be stated in more abstract terms as follows. Quantum predictions for the Bell experiment are commonly described as a set of conditional probabilities $p(a, b|A, B)$, where $a = \pm 1$ and $b = \pm 1$ are the two possible outcomes at each one of the two detectors and $A = \pm 1$ and

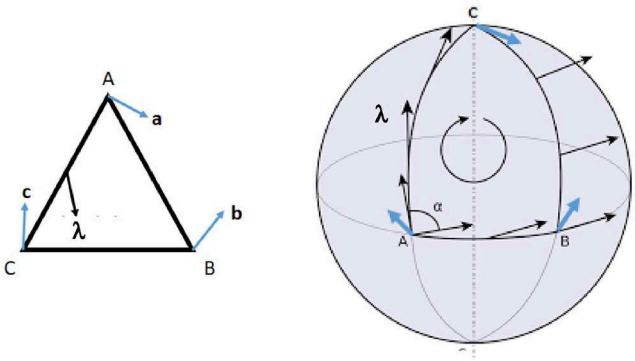

FIGURE 3 | Two closely related, though intrinsically different, random games: the game on the left hand side is constrained by the Bell inequality, while the one on the right hand side is not necessarily constrained by the inequality. In both games we have reference unit vectors, labeled, respectively as $\vec{a}$, $\vec{b}$, and $\vec{c}$, drawn at each one of the vertices, labeled as A, B, and C, of a triangle. In the game on the left the triangle is drawn on a plane surface and the reference unit vectors are contained within the plane, while in the game on the right the "triangle" is defined on the surface of a sphere by segments of three great circles and the three reference unit vectors lay within the corresponding tangent planes. Two copies of a randomly oriented unit vector $\vec{\lambda}$ are generated at random at the center of one of the three segments of the triangle with density of probability $\rho(\vec{\lambda})$, and detected, respectively, at the two detectors located at the ends of the segment. In the game on the left the vector $\vec{\lambda}$ is contained within the plane surface, while in the game on the right the vector $\vec{\lambda}$ is tangent to the sphere. The binary responses of the detectors are locally defined by parallelly transporting the unit vector $\vec{\lambda}$ along the segment of the triangle to its end, and comparing its orientation to the orientation of the corresponding reference unit vector: $A(\vec{a},\vec{\lambda}) = \text{sign}(\vec{a}\cdot\vec{\lambda})$, $B(\vec{b},\vec{\lambda}) = \text{sign}(\vec{b}\cdot\vec{\lambda})$, $C(\vec{c},\vec{\lambda}) = \text{sign}(\vec{c}\cdot\vec{\lambda})$. It is then straightforward to prove the Bell inequality for the game on the left, since for any settings $\vec{a},\vec{b},\vec{c}$ and any random vector $\vec{\lambda}$ the following equality holds:
$\left|A(\vec{a},\vec{\lambda})\cdot B(\vec{b},\vec{\lambda}) + A(\vec{a},\vec{\lambda})\cdot C(\vec{c},\vec{\lambda})\right| = 1 + B(\vec{b},\vec{\lambda})\cdot C(\vec{c},\vec{\lambda})$. Therefore, after integrating over the whole space of possible hidden configurations:
$\left|\int d\vec{\lambda}\ \rho(\vec{\lambda})\left[A(\vec{a},\vec{\lambda})\cdot B(\vec{b},\vec{\lambda}) + A(\vec{a},\vec{\lambda})\cdot C(\vec{c},\vec{\lambda})\right]\right| \leq$
$\int d\vec{\lambda}\ \rho(\vec{\lambda})\left|A(\vec{a},\vec{\lambda})\cdot B(\vec{b},\vec{\lambda}) + A(\vec{a},\vec{\lambda})\cdot C(\vec{c},\vec{\lambda})\right| =$
$\int d\vec{\lambda}\ \rho(\vec{\lambda})\left|A(\vec{a},\vec{\lambda})\cdot B(\vec{b},\vec{\lambda}) + A(\vec{a},\vec{\lambda})\cdot B(\vec{b},\vec{\lambda})\cdot B(\vec{b},\vec{\lambda})\cdot C(\vec{c},\vec{\lambda})\right| =$
$1 + \int d\vec{\lambda}\ \rho(\vec{\lambda})\, B(\vec{b},\vec{\lambda})\cdot C(\vec{c},\vec{\lambda})$, and therefore,
$\left|E^{A,B}(\vec{a},\vec{b}) + E^{A,C}(\vec{a},\vec{c})\right| \leq 1 + E^{B,C}(\vec{b},\vec{c})$. This proof, nonetheless, does not hold for the random game on the right hand side, since the orientation of a vector $\vec{\lambda}$ parallelly transported along the closed contour of the triangle ABC gets rotated by a geometric phase α due to the curvature of the sphere. In fact, in the game on the right the three bipartite correlations are constrained by the inequality $\left|E^{A,B}(\vec{a},\vec{b}) + E^{A,C}(\vec{a},\vec{c})\right| \leq 1 + E^{B,C}(\vec{b},\hat{\mathcal{R}}_\alpha\vec{c})$, where $\hat{\mathcal{R}}_\alpha\vec{c}$ denotes the rotation of vector $\vec{c}$ by an angle α.

$B = \pm 1$ describe two possible choices for the setting of each one of the two detectors. It is then proven that these conditional probabilities cannot be obtained in terms of a local model of hidden variables, defined by its configuration space $\lambda \in \mathcal{S}$, its density of probability $\rho(\lambda)$ and its local response functions $a = f(\lambda, A)$, $b = f(\lambda, B)$ [2].

This statement can be clearly illustrated with the help of the toy model described in **Table 1** [21], where conditional probabilities for each one of the four possible results of an experiment with two binary outcomes $a, b = \pm 1$ (columns) are given for each one of four possible settings, defined by

TABLE 1 | Conditional probabilities for a toy model with two binary inputs and two binary outcomes that cannot be reproduced by a realistic and local underlying theory [21].

Outcome setting	**a** = +1 **b** = +1	**a** = +1 **b** = −1	**a** = −1 **b** = +1	**a** = −1 **b** = −1
$A = +1$ $B = +1$	p_1	0	0	$1-p_1$
$A = +1$ $B = -1$	p_2	0	0	$1-p_2$
$A = -1$ $B = +1$	p_3	0	0	$1-p_3$
$A = -1$ $B = -1$	0	p_4	$1-p_4$	0

TABLE 2 | Conditional probabilities for a toy model with a single input with four possible values and two binary outcomes.

Outcome setting	**a** = +1 **b** = +1	**a** = +1 **b** = −1	**a** = −1 **b** = +1	**a** = −1 **b** = −1
$D = 1$	p_1	0	0	$1-p_1$
$D = 2$	p_2	0	0	$1-p_2$
$D = 3$	p_3	0	0	$1-p_3$
$D = 4$	0	p_4	$1-p_4$	0

They can be reproduced by an underlying theory.

two independent binary inputs $A, B = \pm 1$ (rows). For these probabilities to be properly defined we require that $p_1, p_2, p_3, p_4 \in [0, 1]$. It can be readily checked that for each set of input values (rows) the sum of the probabilities for all possible results of the experiment (columns) equals 1. These conditional probabilities, however, cannot be obtained within the framework of an underlying local model of hidden variables: the conditional probabilities listed in the first three rows would imply $a = b$, that is, the outcomes of the two detectors in any of their four possible settings must have the same sign, which is obviously inconsistent with the conditional probabilities listed in the fourth row.

Nonetheless, it is straightforward to identify in this abstract reformulation of the Bell theorem the same unjustified implicit assumption that we have noticed above, namely, that there are two well-defined choices for the setting of each one of the detectors. We have noticed above that we can properly define and measure only the conditional probabilities $p(a, b|D)$, where $a = \pm 1$ and $b = \pm 1$ are, as before, the outcomes at each one of the two detectors and $D = 1, 2, 3, 4$ defines four possible relative orientations between them. We did notice also that quantum mechanics as well makes theoretical predictions only for these conditional probabilities $p(a, b|D)$. Under these looser constraints the Bell theorem does not necessarily hold.

Consider, for example, the toy model described in **Table 2**. The conditional probabilities are identical to those described in **Table 1** for each one of the four possible results of the experiment, but the setting of the measurement devices is now described by a single parameter $D = 1, 2, 3, 4$. Each input value corresponds to

a given relative orientation of the two devices. The new model simply states that when the devices are set at $D = 1, 2, 3$ their outcomes must have the same sign, and when they are set at $D = 4$ their outcomes must have opposite signs. Obviously, this latter model is not necessarily in contradiction with an underlying local model of hidden variables.

A straightforward proof of the inequalities that constraint the correlations that can be obtained in any model of hidden variables with two binary inputs and two binary outcomes is presented in Revzen [22] using only Boolean logic. The analysis relies on the observation that any such model makes a prediction for the correlations $\langle AB\rangle$, $\langle AB'\rangle$, $\langle A'B\rangle$, and $\langle A'B'\rangle$, and also for the correlations $\langle AA'\rangle$ and $\langle BB'\rangle$ that would be obtained in the hypothetical case that the polarization of each one of the two entangled particles could be tested along two different orientations at once. It can be immediately noticed that these constraints do not hold for the model of hidden variables discussed in this paper, for which the correlations $\langle AA'\rangle$ and $\langle BB'\rangle$ cannot be jointly bounded.

3. THE MODEL

We shall now build an explicitly local statistical model of hidden variables that reproduces the predictions of quantum mechanics for the Bell's states (1) and, hence, it is not constrained by the Bell inequality (3). The fundamental ideas of the model were first discussed in Oaknin [30]. As we have already noticed above, the crux of the model is the spontaneous breaking of the gauge symmetry of the experimental setup under global rigid rotations of the orientation of the detectors. The symmetry is broken by the hidden configuration of the pair of entangled particles. Furthermore, we allow for a non-zero geometric phase (12) to accumulate through cyclic gauge transformations. Under these circumstances there does not exist an absolute preferred frame, other than the orientation of one of the detectors, to which we can refer in order to compare different realizations of the experiment (see **Figure 3**).

The gauge symmetry is spontaneously broken because in the considered model the hidden configuration of the pair of entangled particles has a preferred direction randomly oriented over a unit circle $\mathcal{S}$ in the XY-plane. This orientation is carried by each one of the particles of the entangled pair. Each one of the two detectors defines over this circle $\mathcal{S}$ a frame of reference with its own set of associated coordinates, which we shall denote as $\lambda_A \in [-\pi, +\pi)$ for detector A and $\lambda_B \in [-\pi, +\pi)$ for detector B. Since the two sets of coordinates parameterize the same space $\mathcal{S}$, they must be related by some transformation law:

$$\lambda_B = -L(\lambda_A;\ \Delta - \Phi), \tag{14}$$

where Δ is the relative angle between the two detectors and Φ is the phase that characterizes the source of entangled particles as defined above. This transformation law states that a hidden configuration whose preferred direction is oriented along an angle λ_A with respect to detector A, it is oriented along an angle λ_B with respect to detector B.

The transformation law (14) does not violate neither locality nor causality: it may well be a fundamental law of Nature. Indeed, the notions of locality and causality in special relativity stem from a similar relationship $v' = T(v;\ V)$ between the velocities v and v' of a point particle with respect to two different inertial frames moving with relative velocity V. Moreover, (14) is only a generalization of the Euclidean linear relationship that states that in a flat space given two detectors whose orientations form an angle Δ, then a pointer oriented along an angle ω with respect to one of them is oriented along an angle $\omega - \Delta$ with respect to the other detector.

In order to reproduce the predictions of quantum mechanics we define the transformation law (14) as follows:

- If $\bar{\Delta} \in [0, \pi)$,

$$L(\lambda;\bar{\Delta}) = \begin{cases} q(\lambda-\bar{\Delta})\cdot\arccos\left(-\cos(\bar{\Delta})-\cos(\lambda)-1\right), \\ \qquad\qquad \text{if} \quad -\pi \quad \le \lambda < \bar{\Delta}-\pi, \\ q(\lambda-\bar{\Delta})\cdot\arccos\left(+\cos(\bar{\Delta})+\cos(\lambda)-1\right), \\ \qquad\qquad \text{if} \ \bar{\Delta}-\pi \ \le \lambda < \ 0, \\ q(\lambda-\bar{\Delta})\cdot\arccos\left(+\cos(\bar{\Delta})-\cos(\lambda)+1\right), \\ \qquad\qquad \text{if} \quad 0 \quad \le \lambda < \ \bar{\Delta}, \\ q(\lambda-\bar{\Delta})\cdot\arccos\left(-\cos(\bar{\Delta})+\cos(\lambda)+1\right), \\ \qquad\qquad \text{if} \quad \bar{\Delta} \quad \le \lambda < +\pi, \end{cases} \tag{15}$$

- If $\bar{\Delta} \in [-\pi, 0)$,

$$L(\lambda;\bar{\Delta}) = \begin{cases} q(\lambda-\bar{\Delta})\cdot\arccos\left(-\cos(\bar{\Delta})+\cos(\lambda)+1\right), \\ \qquad\qquad \text{if} \quad -\pi \quad \le \lambda < \bar{\Delta}, \\ q(\lambda-\bar{\Delta})\cdot\arccos\left(+\cos(\bar{\Delta})-\cos(\lambda)+1\right), \\ \qquad\qquad \text{if} \quad \bar{\Delta} \quad \le \lambda < \ 0, \\ q(\lambda-\bar{\Delta})\cdot\arccos\left(+\cos(\bar{\Delta})+\cos(\lambda)-1\right), \\ \qquad\qquad \text{if} \quad 0 \quad \le \lambda < \bar{\Delta}+\pi, \\ q(\lambda-\bar{\Delta})\cdot\arccos\left(-\cos(\bar{\Delta})-\cos(\lambda)-1\right), \\ \qquad\qquad \text{if} \quad \bar{\Delta}+\pi \le \lambda < +\pi, \end{cases} \tag{16}$$

where

$$q(\lambda-\bar{\Delta}) = \text{sign}((\lambda-\bar{\Delta})\text{mod}([-\pi,\pi))),$$

$\bar{\Delta} = \Delta - \Phi$ and the function $y = \arccos(x)$ is defined in its main branch, such that $y \in [0, \pi]$ while $x \in [-1, +1]$. In **Figure 4**, the transformation $L(\lambda;\bar{\Delta})$ is graphically shown for the particular case $\bar{\Delta} = \pi/3$. It is straightforward to check that the transformation law (14) is strictly monotonic and fulfills the differential relationship

$$\left|d\left(\cos(\lambda_B)\right)\right| = d\lambda_B\left|\sin(\lambda_B)\right| = d\lambda_A\left|\sin(\lambda_A)\right| = \left|d\left(\cos(\lambda_A)\right)\right|, \tag{17}$$

while the parameter $\bar{\Delta}$ plays the role of an the integration constant.

Locality is explicitly enforced in our model by requiring that the outcome of each one of the detectors in response to the hidden configuration of the pair of entangled particles depends only on its locally defined orientation, that is, $s(\lambda_A) = \pm 1$ for detector A and $s(\lambda_B) = \pm 1$ for detector B, where λ_B and λ_A are related by relationship (14) and $s(\cdot)$ is the binary response

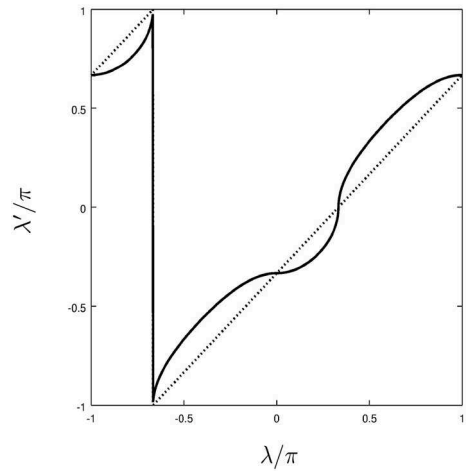

FIGURE 4 | Plot of the transformation law $\lambda \to \lambda' = L(\lambda; \Delta)$ for $\Delta = \pi/3$ (solid line), compared to the corresponding linear transformation (dotted line).

function of the detectors, which for the sake of simplicity we define here as

$$s(l) = \begin{cases} +1, & \text{if } l \in [0, +\pi), \\ -1, & \text{if } l \in [-\pi, 0). \end{cases} \tag{18}$$

In order to complete our statistical model we need to specify also the (density of) probability $\rho(l)$ of each hidden configuration $l \in \mathcal{S}$ over the space $\mathcal{S}$ to occur in every single realization of the pair of entangled particles. By symmetry considerations this density of probability must be functionally identical from the point of view of both detectors, independently of their relative orientation. Moreover, the condition of "free-will" demands that the probability of each hidden configuration to occur in any single realization of the experiment cannot depend on the parameterizations of the space $\mathcal{S}$ associated to each one of the two detectors. This condition can be precisely stated as:

$$d\lambda_A \; \rho(\lambda_A) = d\lambda_B \; \rho(\lambda_B). \tag{19}$$

It is straightforward to show from (17) that this condition is fulfilled if and only if the probability density $\rho(l)$ is given by:

$$\rho(l) = \frac{1}{4} \left| \sin(l) \right|. \tag{20}$$

We can now compute within the framework of this model the statistical correlations expected between the outcomes of the two detectors as a function of their relative orientation. The binary outcomes of each one of the two detectors define a partition of the phase space $\mathcal{S}$ of all the possible hidden configurations into four coarse subsets,

$$\begin{aligned} (s^{(A)} = +1; s^{(B)} = +1) &\iff \lambda_A \in [0, \Delta - \Phi) \\ (s^{(A)} = +1; s^{(B)} = -1) &\iff \lambda_A \in [\Delta - \Phi, \pi) \\ (s^{(A)} = -1; s^{(B)} = +1) &\iff \lambda_A \in [\Delta - \Phi - \pi, 0) \\ (s^{(A)} = -1; s^{(B)} = -1) &\iff \lambda_A \in [-\pi, \Delta - \Phi - \pi), \end{aligned}$$

where we have assumed without any loss of generality that $\Delta - \Phi \in [0, \pi)$. Each one of these four coarse subsets happen with a probability given by:

$$\begin{aligned} p(+1,+1) &= \int_0^{\Delta-\Phi} \rho(\lambda_A)\, d\lambda_A &&= \tfrac{1}{4}\left(1 - \cos(\Delta - \Phi)\right), \\ p(+1,-1) &= \int_{\Delta-\Phi}^{\pi} \rho(\lambda_A)\, d\lambda_A &&= \tfrac{1}{4}\left(1 + \cos(\Delta - \Phi)\right), \\ p(-1,+1) &= \int_{\Delta-\Phi-\pi}^{0} \rho(\lambda_A)\, d\lambda_A &&= \tfrac{1}{4}\left(1 + \cos(\Delta - \Phi)\right), \\ p(-1,-1) &= \int_{-\pi}^{\Delta-\Phi-\pi} \rho(\lambda_A)\, d\lambda_A &&= \tfrac{1}{4}\left(1 - \cos(\Delta - \Phi)\right). \end{aligned}$$

These conditional probabilities reproduce the predictions of quantum mechanics (2):

$$\begin{aligned} E(\Delta, \Phi) &= p(+1,+1) + p(-1,-1) - p(+1,-1) - p(-1,+1) \\ &= -\cos(\Delta - \Phi). \end{aligned}$$

Finally, we notice that in spite of the non-trivial transformation law (14) our model complies with the trivial demand that a relative rotation of the measurement apparatus by an angle Δ followed by a second relative rotation by an angle Δ' results into a final rotation by an angle $\Delta + \Delta'$. Consider, for example, an initial reference setting $\mathcal{T}_0$ in which the outcomes of the two measurement apparatus are correlated by an amount $E = -\cos(\Phi)$. The angular coordinates of the hidden configurations with respect to each one of the two measurement devices, λ_A and λ_B, would be related in this reference setting by the relationship:

$$\lambda_B = -L(\lambda_A; -\Phi). \tag{21}$$

We now define a new measurement setting $\mathcal{T}_1$ obtained from the initial setting $\mathcal{T}_0$ by rotating the relative orientation of the two apparatus by an angle Δ. The angular coordinates λ_A and λ'_B defined with respect to this new setting would be related by:

$$\lambda'_B = -L(\lambda_A; \Delta - \Phi). \tag{22}$$

A third measurement setting $\mathcal{T}_2$ is obtained from the intermediate setting $\mathcal{T}_1$ by rotating the relative orientation of the two apparatus by an additional angle Δ'. In the intermediate setting $\mathcal{T}_1$, which is now taken as reference to define the second rotation, the pair of particles appears to be in a polarization state characterized by a phase $\Phi' = -\Delta + \Phi$. Hence, the angular coordinates λ_A and λ''_B defined with respect to the setting $\mathcal{T}_2$ would be related by the transformation law:

$$\lambda''_B = -L(\lambda_A;\, \Delta' - \Phi') = -L(\lambda_A;\, \Delta' + \Delta - \Phi). \tag{23}$$

By comparison of the transformation law (21) for the initial setting $\mathcal{T}_0$ and the transformation law (23) for the setting $\mathcal{T}_2$, we realize that the latter has been obtained from the initial setting by rotating the apparatus by an angle $\Delta' + \Delta$, as we had demanded.

In order to complete the description of the Bell's experiment we define two new settings $\mathcal{T}_3$ and $\mathcal{T}_4$, which are obtained, respectively, from $\mathcal{T}_1$ and $\mathcal{T}_2$ by canceling the phase Φ in the reference setting $\mathcal{T}_0$. Hence, in these settings the angular coordinates of the hidden configurations with respect to the two measurement apparatus are related by the relationships:

$$\lambda'''_B = -L(\lambda_A;\, \Delta). \tag{24}$$

and

$$\lambda''''_B = -L(\lambda_A;\, \Delta' + \Delta), \tag{25}$$

respectively. Thus, we could intuitively think about the four settings of the detectors involved in a Bell's experiment as corresponding to two possible values for the relative angle Δ and two possible values for the phase Φ, while they all four share the orientation of one the two detectors, say detector A, taken as reference.

Finally, let us notice that when we substitute the coherent source of pairs of entangled particles (1) by the incoherent *classical* source (where all the mixed coherent sources are defined with respect to the same arbitrary setting of the two detectors):

$$\begin{aligned}\hat{\mu} &= \int_{2\pi} d\Phi\, |\Psi_\Phi\rangle\langle\Psi_\Phi| \\ &= |\uparrow\rangle\langle\uparrow|^{(A)} \otimes |\downarrow\rangle\langle\downarrow|^{(B)} + |\downarrow\rangle\langle\downarrow|^{(A)} \otimes |\uparrow\rangle\langle\uparrow|^{(B)},\end{aligned} \tag{26}$$

the broken rotational symmetries are statistically restored and the outcomes of the two measurement devices become uncorrelated for all settings. Only then, when the rotational symmetries are restored, we can safely define separately the orientations of each one of the measurement devices with respect to some external reference frame and, thus, describe the phase space of its possible settings with the help of these two angles (Ω_A, Ω_B).

4. A PROPOSAL FOR AN EXPERIMENTAL TEST

The statistical model of hidden configurations described in the previous section reproduces the quantum mechanical prediction for the correlation (2) between the binary outcomes of projective polarization measurements performed on each one of the two particles of every entangled pair, as a function of the angular parameter $\Delta - \Phi$ that characterizes the experimental setting. However, with the help of additional weak polarization measurements the predictions of this statistical model can still be experimentally distinguished from those of the standard framework of quantum mechanics.

Let us consider as before a source of pairs of entangled particles prepared in a Bell state (1) and a pair of measuring devices that test their polarizations through projective measurements at a relative angle $\Delta - \Phi = \pi/4$, so that the correlation between their binary outcomes is $E_{A_1,B_2} = E(\pi/4) = -1/\sqrt{2}$. For reasons that will be immediately clear we denote this correlation as E_{A_1,B_2}. This correlation is only very slightly modified if we perform on particle B a very weak polarization measurement before the projective polarization test [23, 24]. If we design the weak measurement on particle B so that it is oriented along a relative angle $\Delta - \Phi = -\pi/4$ with respect to the projective polarization measurement on particle A, the correlation between their outcomes in a long sequence of repetitions will be given by $E_{A_1,B_1} = E(-\pi/4) = -1/\sqrt{2}$.

We can now ask ourselves what would be the correlation $E_{B1,B2}$ between the outcomes of the weak measurement performed on particle B and the projective measurement performed on the same particle later on. According to quantum mechanics their correlation should be

$$E^{QM}_{B1,B2} = \cos(\pi/2) = 0, \tag{27}$$

while in the statistical model presented in the previous section their correlation would be [33]

$$\begin{aligned}E^{SM}_{B1,B2} &= 4\left(\int_{\pi/4}^{\pi/2} \rho(\lambda)\, d\lambda - \int_0^{\pi/4} \rho(\lambda)\, d\lambda\right) = \\ &= \int_{\pi/4}^{\pi/2} \left|\sin(\lambda)\right|\, d\lambda - \int_0^{\pi/4} \left|\sin(\lambda)\right|\, d\lambda = \\ &= -\cos(0) + \cos(\pi/4) - \cos(\pi/2) + \cos(\pi/4) = \\ &= \sqrt{2} - 1 \simeq 0.41 \neq E^{QM}_{B1,B2}.\end{aligned} \tag{28}$$

5. DISCUSSION

The Bell theorem is one of the pillars upon which relies the widely accepted belief that quantum mechanics is the ultimate mathematical framework within which the hypothetical final theory of the fundamental building blocks of Nature and their interactions must be formulated. The theorem proves through an experimentally testable inequality (the Bell inequality) that the predictions of quantum mechanics for the Bell polarization states of two entangled particles cannot be reproduced by any underlying theory of hidden variables that shares certain intuitive features.

In this paper we have shown, however, that these intuitive features include a subtle, though crucial, assumption that is not required by fundamental physical principles and, hence, it is not necessarily fulfilled in the actual experimental setup that tests the inequality. In fact, the disputed assumption cannot be implemented within the framework of standard quantum mechanics either.

Namely, the proof of the Bell theorem requires the existence of a preferred frame of reference, supposedly provided by a lab, with respect to which the orientations of each one of the two measurement devices can be independently defined for every single realization of the experiment. This preferred frame is

required in order to compare the orientations of the detectors in a sequence of repetitions of the experiment, since in every realization each particle's polarization can be tested along a single orientation.

Notwithstanding, the existence of a preferred frame of reference is at odds with Galileo's fundamental principle of relativity and, indeed, it cannot exist when the hidden configurations of the pair of entangled particles spontaneously break the rotational symmetry of the experimental setup under rigid rotations of the two detectors and a non-zero geometric phase accumulates through cyclic gauge transformations. In such a case, in order to compare different realizations of the experiment, we must pick the orientation of one of the detectors as a common reference direction, with respect to which the relative orientation of the second detector is defined. Under these conditions the Bell theorem does not necessarily hold [see (13), **Figures 2**, **3**].

Following these ideas we explicitly built a model of hidden variables for the Bell's states of two entangled particles that reproduces the predictions of quantum mechanics. Further details of the model are discussed in Oaknin [30]. In two additional accompanying papers we have used these same ideas to build explicit local models of hidden variables for the GHZ state of three entangled particles [31] and also for the qutrit [32].

The derivation of a model of local hidden variables for the entangled states of two or more qubits means that entanglement, the quintessential quantum phenomenon, can be fully described without the quantum formalism. Indeed, the model shows that entanglement can be described in terms of classical statistical concepts, with the help of the well-understood classical notions of curved spaces and gauge degrees of freedom. Thus, the model proves that there are not mysterious fundamental differences between classical and quantum correlations.

Furthermore, the model of hidden variables presented here opens the window to the possible existence of an unexplored physical reality that might underlay the laws of quantum mechanics [25] and, thus, it might lead to a whole new area of research in physics in quest for the fundamental laws of this underlying reality. The existence of such a reality was first suggested 85 years ago by Einstein, Podolsky and Rosen through their famous EPR paradox [26, 27], but following Bell's arguments it had been thought that an underlying reality was incompatible with quantum mechanics [28, 29].

Finally, we wish to notice that our model of hidden variables is built upon fundamental physical concepts shared by the formalism of General Relativity and, thus, it might eventually lead to a unified description of quantum phenomena and gravitation.

DATA AVAILABILITY STATEMENT

The raw data supporting the conclusions of this article will be made available by the authors, without undue reservation.

AUTHOR CONTRIBUTIONS

The author confirms being the sole contributor of this work and has approved it for publication.

ACKNOWLEDGMENTS

This manuscript has been released as a pre-print at https://arxiv.org/abs/1912.06349, DO [34].

REFERENCES

1. Bell JS. On the Einstein-Podolsky-Rosen paradox. *Physics*. (1964) **1**:195–200.
2. Fine A. Hidden variables, joint probability, and the Bell inequalities. *Phys Rev Lett*. (1982) **48**:291.
3. Hensen B, Bernien H, Dréau AE, Reiserer A, Kalb N, Blok MS, et al. Loophole-free Bell inequality violation using electron spins separated by 1.3 kilometres. *Nature*. (2015) **526**:682–6. doi: 10.1038/nature15759
4. Aspect A, Dalibard J, Roger G. Experimental test of Bell's inequalities using time-varying analyzers. *Phys Rev Lett.* (1982) **49**:1804. doi: 10.1103/PhysRevLett.49.1804
5. Tittel W, Brendel J, Zbinden H, Gisin N. Violation of bell inequalities by photons more than 10 km apart. *Phys Rev Lett.* (1998) **81**:3563. doi: 10.1103/PhysRevLett.81.3563
6. Weihs G, Jennewein T, Simon C, Weinfurter H, Zeilinger A. Violation of Bell's inequality under strict Einstein locality conditions. *Phys Rev Lett*. (1998) **81**:5039–43. doi: 10.1103/PhysRevLett.81.5039
7. Rowe MA, Kielpinski D, Meyer V, Sackett CA, Itano WM, Monroe C, et al. Experimental violation of a Bell's inequality with efficient detection. *Nature*. (2001) **409**:791–4. doi: 10.1038/35057215
8. Giustina M, Mech A, Ramelow S, Wittmann B, Kofler J, Beyer J, et al. Bell violation using entangled photons without the fair-sampling assumption. *Nature*. (2013) **497**:227–30. doi: 10.1038/nature12012
9. Christensen BG, McCusker KT, Altepeter J, Calkins B, Gerrits T, Lita T, et al. Detection-loophole-free test of quantum nonlocality, and applications. *Phys Rev Lett*. (2013) **111**:130406. doi: 10.1103/PhysRevLett.111.130406
10. Giustina M, Versteegh MAM, Wengerowsky S, Handsteiner J, Hochrainer A, Phelan K, et al. A significant-loophole-free test of Bell's theorem with entangled photons. *Phys Rev Lett*. (2015) **115**:250401. doi: 10.1103/PhysRevLett.115.250401
11. Shalm LK, Meyer-Scott E, Christensen BG, Bierhorst P, Wayne MA, Stevens MJ, et al. A strong loophole-free test of local realism. *Phys Rev Lett*. (2015) **115**:250402. doi: 10.1103/PhysRevLett.115.250402
12. Wiseman H. Quantum physics: death by experiment for local realism. *Nature*. (2015) **526**:649. doi: 10.1038/nature15631
13. Clauser JF, Horne MA, Shimony A, Holt RA. Proposed experiment to test local hidden variables theories. *Phys Rev Lett.* (1969) **23**:880–4. doi: 10.1103/PhysRevLett.23.880
14. Cirelson BS. Quantum generalizations of Bell's inequality. *Lett Math Phys*. (1980) **4**:93.
15. Hess K. Bell's theorem and Instantaneous influences at a distance. *arXiv:1805.04797*. doi: 10.4236/jmp.2018.98099
16. Hess K. Kolmogorov's probability spaces for 'entangled' data subsets of EPRB experiments: no violation of Einstein's separation principle. *J Modern Physics*. (2020).
17. Hess K, Philipp W. Bell's theorem and the problem of decidability between the views of Einstein and Bohr. *Proc Natl Acad Sci USA*. (2001) **98**:14228–33. doi: 10.1073/pnas.251525098
18. Hess K, Philipp W. Breakdown of Bell's theorem for certain objective local parameter spaces. *Proc Natl Acad Sci USA*. (2004) **101**:1799–805. doi: 10.1073/pnas.0307479100

19. Hess K, De Raedt H, Michielsen K. From Boole to Leggett-Garg inequality: epistemology of Bell-type inequalities. *Adv Math Phys.* (2016) **2016**:4623040. doi: 10.1155/2016/4623040
20. Wilczek F, Shapere A, editors. *Geometric Phases in Physics.* Singapore: World Scientific (1989).
21. Popescu S, Rohrlich D. Quantum nonlocality as an axiom. *Found Phys.* (1994) **24**:379–85. doi: 10.1007/BF02058098
22. Revzen M. Kolmogorov proof of the Clauser-Horne-Shimony-Holt inequalities. *Int J Quant Inform* (2018) **16**:1850013. doi: 10.1142/S0219749918500132
23. White TC, Mutus JY, Dressel J, Kelly J, Barends R, Jeffrey E, et al. Preserving entanglement during weak measurement demonstrated with a violation of the Bell-Leggett-Garg inequality. *NPJ Quant Inform*. (2016) **2**:15022. doi: 10.1038/npjqi.2015.22
24. Dressel J, Korotkov AN. Avoiding loopholes with hybrid Bell-Leggett-Garg inequalities. *Phys Rev A*. (2014) **89**:012125. doi: 10.1103/PhysRevA.89.012125
25. Ball P. Exorcising Einstein's spooks *Nature*. doi: 10.1038/news011129-15
26. Einstein A, Podolsky B, Rosen N. Can quantum mechanical description of physical reality be considered complete? *Phys Rev.* (1935) **47**:777–80. doi: 10.1103/Phys.Rev.47.777
27. Bohm D. *Quantum Theory*. New York, NY: Prentice-Hall (1951).
28. Bell JS. On the problem of hidden variables in quantum mechanics. *Physics.* (1966) **38**:447–52.
29. Kochen S, Specker EP. The problem of hidden variables in quantum mechanics. *J Math Mech*. (1967) **17**:59–87.
30. Oaknin DH. Solving the EPR paradox: an explicit statistical local model of hidden variables for the singlet state. *arXiv:1411.5704.*
31. Oaknin DH. Solving the Greenberger-Horne-Zeilinger paradox: an explicit local model of hidden variables for the GHZ state. *arXiv:1709.00167.*
32. Oaknin DH. Bypassing the Kochen-Specker theorem: and explicit non-contextual model of hidden variables for the qutrit. *arXiv:1805.04935.*
33. Oaknin DH. Comment on 'White, T., Mutus, J., Dressel, J. et al., "Preserving entanglement during weak measurement demonstrated with a violation of the Bell-Leggett-Garg inequality". *npj Quantum Inf.* (2016) **2:**15022.
34. Oaknin DH. The Bell inequality revisited: geometric phases in gauge theories. *arXiv:1912.06349.* doi: 10.3389/fphy.2020.00142

Conflict of Interest: DO was employed by the company RAFAEL Advanced Defense Systems.

frontiers in Physics

ORIGINAL RESEARCH
published: 12 May 2020
doi: 10.3389/fphy.2020.00160

Discrete-Event Simulation of an Extended Einstein-Podolsky-Rosen-Bohm Experiment

Hans De Raedt[1,2]*, *Manpreet S. Jattana*[1,3], *Dennis Willsch*[1], *Madita Willsch*[1], *Fengping Jin*[1] *and Kristel Michielsen*[1,3]

[1] *Jülich Supercomputing Centre, Institute for Advanced Simulation, Forschungszentrum Jülich, Jülich, Germany,* [2] *Zernike Institute for Advanced Materials, University of Groningen, Groningen, Netherlands,* [3] *RWTH Aachen University, Aachen, Germany*

We use discrete-event simulation to construct a subquantum model that can reproduce the quantum-theoretical prediction for the statistics of data produced by the Einstein-Podolsky-Rosen-Bohm experiment and an extension thereof. This model satisfies Einstein's criterion of locality and generates data in an event-by-event and cause-and-effect manner. We show that quantum theory can describe the statistics of the simulation data for a certain range of model parameters only.

Keywords: subquantum model, Einstein-Podolsky-Rosen-Bohm experiments, discrete-event simulation, quantum theory, local realist model

OPEN ACCESS

Edited by:
Karl Hess,
University of Illinois at Urbana-Champaign, United States

Reviewed by:
Andrei Khrennikov,
Linnaeus University, Sweden
Juergen Jakumeit,
Access e.V., Germany

***Correspondence:**
Hans De Raedt
deraedthans@gmail.com

Specialty section:
This article was submitted to Mathematical Physics, a section of the journal Frontiers in Physics

Received: *18 March 2020*
Accepted: *17 April 2020*
Published: *12 May 2020*

Citation:
De Raedt H, Jattana MS, Willsch D, Willsch M, Jin F and Michielsen K (2020) Discrete-Event Simulation of an Extended Einstein-Podolsky-Rosen-Bohm Experiment. Front. Phys. 8:160. doi: 10.3389/fphy.2020.00160

1. INTRODUCTION

The Einstein-Podolsky-Rosen thought experiment was introduced to question the completeness of quantum theory [1], "completeness" being defined in reference [1]. Bohm proposed a modified version that employs the spins instead of coordinates and momenta of a two-particle system [2], and is experimentally realizable [3–10]. A key issue in the foundations of physics is whether there exist "local realist" models that yield the statistical results of the quantum-theoretical description of the Einstein-Podolsky-Rosen-Bohm (EPRB) experiment.

In this paper, we take, as operational definition of a local realist model, any model for which

1. all variables, including those representing events which occur at specific locations and specific times, always have definite values,
2. all variables change in time according to an Einstein-local, causal process.

In the literature, one often finds the statement that Bell's theorem [11, 12] rules out **any** local realist model for the EPRB experiments. In references [11, 12], Bell gives a proof that a correlation $C(\mathbf{a},\mathbf{b})$ of the form

$$C(\mathbf{a},\mathbf{b}) = \int d\lambda\ \mu(\lambda)A(\mathbf{a},\lambda)B(\mathbf{b},\lambda)\ , \quad |A(\mathbf{a},\lambda)| \leq 1\ , \quad |B(\mathbf{b},\lambda)| \leq 1\ ,\ 0 \leq \mu(\lambda),$$
$$\int d\lambda\ \mu(\lambda) = 1\ , \tag{1}$$

cannot arbitrarily closely approximate the correlation $-\mathbf{a}\cdot\mathbf{b}$ *for all* unit vectors $\mathbf{a}$ and $\mathbf{b}$. According to Bell (see reference [12]), this is the theorem. On the other hand, the quantum-theoretical description of the EPRB experiment in terms of two spin-1/2 particles in the singlet state yields

the correlation $-\mathbf{a}\cdot\mathbf{b}$. Clearly, there is a conflict between the quantum-theoretical model of the EPRB experiment and the model defined by Equation (1). While there can be no doubt about the mathematical correctness of Bell's theorem, the physical relevance of the theorem and its applicability to the data gathered in laboratory EPRB experiments has been under scrutiny since its conception [13–49]. A fundamental problem with the application of Bell's model Equation (1) to this data is the following.

Evidently, in a laboratory EPRB experiment, before one can even think about computing correlations of particle properties, it is necessary to first classify a detection event as corresponding to the arrival of a particle or as something else. Any laboratory EPRB experiment with photons employs a specific, well-defined procedure to identify photons [3–10]. Such a procedure is **definitely missing** in the model Equation (1) proposed and analyzed by Bell [12]. If the aim is to describe the outcome of a laboratory EPRB experiment, then not incorporating such a procedure in the model is a fallacy which, logically speaking, is not much different from trying to model electrodynamics in terms of electrical phenomena without taking into account the magnetic phenomena. Although it is good practice to analyze the most primitive model first, the observation that it does not agree with experimental results only suggests that it is **too primitive**. The failure of the primitive model to account for the identification process is the fundamental reason why Bell's theorem cannot have the status of a "no-go" theorem for the existence of a local realist model for a laboratory EPRB experiment.

In this paper, we use the term "subquantum model" to refer to a local realist model of an experiment which satisfies the requirements 1 and 2 and

3. the model can reproduce the statistical results of the quantum-theoretical description of the experiment in an event-by-event, cause-and-effect manner.

The main aim of this paper is to present a subquantum model for the EPRB experiment and an extended version thereof. The latter, which we abbreviate by EEPRB, differs from the standard EPRB experiment in that all the measurements for the four different pairs of settings, required to perform Bell-inequality tests, can be made in one single run instead of four runs of the experiment. As such, the EEPRB experiment is not vulnerable to the contextuality loophole [44]. We adopt the discrete-event simulation (DES) approach, introduced in reference [50], to construct a subquantum model for both the EPRB and EEPRB experiment. This approach has proven fruitful for constructing subquantum models for many fundamental quantum-physics experiments with photons and neutrons [51].

2. DISCRETE-EVENT SIMULATION: GENERAL ASPECTS

DES is a general methodology for modeling the time evolution of a system as a discrete sequence of consecutive events [52, 53]. DES is used in many different branches of science, engineering, economics, finance, etc. [52], but has only fairly recently been adopted as a methodology to construct subquantum models for basic, fundamental quantum physics experiments [50, 51].

In the following, whenever we use the term DES, we mean DES modeling applied to quantum physics problems, not DES in general. The salient features of this particular application of DES are the following.

- Events are the basic building blocks of any DES model, just as points are the basic building blocks of Euclidean geometry. In DES an event is a **defined** concept, represented by a model variable taking a particular value (e.g., a bit changing from zero into one) at a specific point in time. In contrast to quantum theory, there is no need to invoke the elusive wave function collapse to "explain" how quantum theory may eventually be reconciled with the fact that a measurement yields a definite yes/no answer, or to appeal to Born's rule.
- It may be difficult to analyze the behavior of a DES model by means of differential equations, probability theory, or other mathematical techniques of theoretical physics. Of course, we may use e.g., probability or quantum theory to model the statistics of the data produced by a DES.
- It is not practicable to perform a DES without using a digital computer. A digital computer itself is a physical device that changes its internal state (all the bits of the CPU and memory) in a discrete, step-by-step (clock cycle) manner. Therefore, a DES algorithm running on a digital computer (which we assume is error-corrected and operating flawlessly) can be viewed as a metaphor for an idealized experiment on a physical device (the digital computer) [54]. All aspects of such an experiment are under the control of a programmer. In the context of EPRB experiments, this means that any loophole [55] can be opened or closed at the discretion of the programmer. For instance, the so-called contextuality loophole, which is impossible to avoid in a laboratory EPRB experiment [49], can be trivially closed in a DES (see below).
- The outcomes of genuine laboratory experiments are subject to unknown influences but in a DES on a digital computer (operating flawlessly), there are no such influences. If there were, it would not be possible to exactly reproduce the results of a DES. Therefore, DES is "the experiment" to confront a theory with facts obtained under the same premises as those on which the theory is based.
- Although a DES algorithm changes the state of a physical device (the digital computer), the events and variables in a DES are only metaphors for the "real" detector click, etc. On the other hand, once it has been established that a DES of a subquantum model yields the correct results, one could build a macroscopic mechanical device that performs exactly the same as DES.
- DES on a digital computer complies with the notion of realism, meaning that at any time during the DES, the internal state of the digital computer is known exactly, all variables of the simulation model taking definite values. Of course, we can always "hide" an algorithm and data on purpose. For instance, we can do this to create the illusion that the "visible" data is unpredictable (a standard technique to generate pseudo-random numbers).

- In a digital computer, there are no signals traveling faster than light. Therefore, on the most basic level, the internal operation of a digital computer complies with Einstein's notion of local causality. However, there is nothing that prevents us from performing an acausal analysis of the data. For instance, if we generate and store a sequence of numbers and then wish to compute the sum, we may do this by summing the numbers in the reverse order of how they were generated. This trivial example shows that one has to distinguish between the generation of the raw data and the processing of this data. For the purpose of constructing a local realist DES model, it is essential that the process that generates the raw data complies with Einstein's notion of local causality. It is not permitted to accumulate data, perform e.g., a discrete Fourier transform or compute acausal correlations, and use the results to describe a quantum physics experiment. While both these techniques are very useful for a wide variety of data processing tasks [56], they are "forbidden" in a DES of a subquantum model.
- Consistency of the DES methodology demands that a subquantum model for, say, a beam splitter, must be re-used, without modification, for all experiments in which this beam splitter is used. Our DES approach seems to satisfy this requirement of consistency, at least for a vast number of fundamental quantum-physics experiments with photons and neutrons [51]. Our motivation for considering both the EPRB and extended EPRB (EEPRB) experiments is to scrutinize the consistency of the DES approach for this category of experiments.

Finally, to head off misunderstandings, the DES models that we construct do not, in any way, make use of the quantum-theoretical predictions for the statistics of the data. Instead, a DES builds up these statistics by an event-by-event, cause-and-effect, Einstein-local process. Under appropriate conditions, these statistics can be described by quantum theory, while in other cases they cannot (see below).

3. EXTENDED EINSTEIN-PODOLSKY-ROSEN-BOHM EXPERIMENT: THEORY

3.1. Thought Experiment

Figure 1 shows the layout of an extended Einstein-Podolsky-Rosen-Bohm (EEPRB) experiment with spin-1/2 particles [26]. A source is emitting a pair of particles in two spatially separated directions toward beam splitters BS1 and BS2. In this idealized experiment, all beam splitters are assumed to be identical, performing selective (filtering) measurements [57, 58]. Selective measurements allow us to attach an attribute with definite value (e.g., the direction of the magnetic moment or of the polarization) to the particle. For instance, assuming that BS1, BS3, and BS4 perform ideal selective measurements, a particle leaving BS1 along path $S_1 = +1$ ($S_1 = -1$) will always leave BS3 (BS4) along path $S_3 = +1$ ($S_3 = -1$) if $\mathbf{c} = \mathbf{a}$. In case of selective measurements, we can attach an attribute to the particle, the value of this attribute being given by S_1. We use the same procedure for attaching attributes to particles leaving the other beam splitters.

Particles leaving BS3, ..., BS6 are registered by detectors. All detectors are assumed to be identical and to have a 100% detection efficiency (we relax this assumption later). The binary variables $x_{i,j} = 0, 1$ for $i = 1, \ldots, 4$ and $j = 1, 2$ (see **Figure 1**) indicate which of the four detectors at the left ($j = 1$) and right ($j = 2$) fire. For each pair of emitted particles, exactly one of

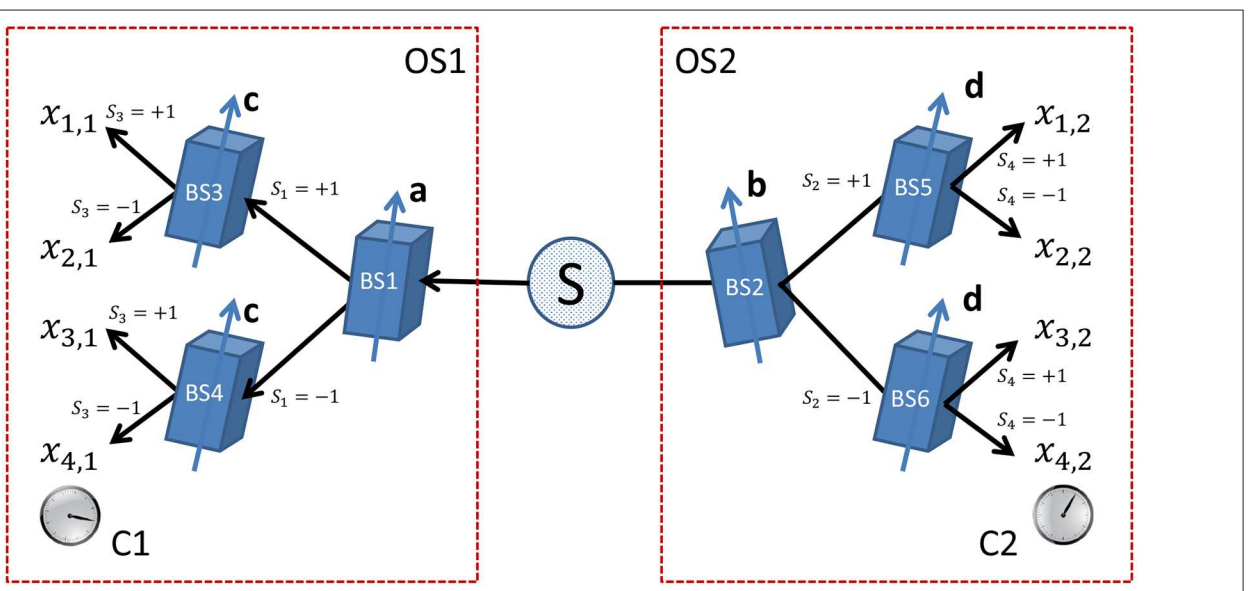

FIGURE 1 | Layout of the extended Einstein-Podolsky-Rosen-Bohm experiment with spin-1/2 particles emitted by the source S. The observation station OS1 (OS2) contains three beam splitters BS1, BS3, and BS4, (BS2, BS5, and BS6) and a clock C1 (C2). The directions of the beam splitters BS1, BS2, BS3, BS4, BS5, and BS6 are represented by vectors **a**, **b**, **c**, **c**, **d**, and **d**, respectively.

the detectors on the left and exactly one of the detectors on the right side of the source will register a particle. This implies that for $j = 1, 2$, only one of $x_{1,j}$, $x_{2,j}$, $x_{3,j}$, and $x_{4,j}$ can be non-zero. The four new variables defined by

$$\begin{aligned} S_1 &= x_{1,1} + x_{2,1} - x_{3,1} - x_{4,1} \,, \\ S_2 &= x_{1,2} + x_{2,2} - x_{3,2} - x_{4,2} \,, \\ S_3 &= x_{1,1} - x_{2,1} + x_{3,1} - x_{4,1} \,, \\ S_4 &= x_{1,2} - x_{2,2} + x_{3,2} - x_{4,2} \,, \end{aligned} \tag{2}$$

all take values $+1$ or -1 (see **Figure 1**). Clearly, S_1 and S_3 (S_2 and S_4) encode, in a unique manner, the path that the left (right) going particle took. In the following, we use the S's to formulate the DES model.

For practical reasons, most laboratory EPRB experiments are carried out with photons [3–10], the polarization of the photons playing the role of the spin. From a quantum-theoretical viewpoint, there is no loss of generality in doing so because mathematically, the description of the photon polarization is in terms of Pauli-spin matrix algebra. In the following, to keep the discussion concise and concrete, we only focus on (E)PRB experiments that employ the photon polarization as the "quantum system" of interest.

A source is emitting a pair of photons in two spatially separated directions toward beam splitters BS1 and BS2. BS1 sends one photon of the pair to either BS3 or BS4. BS2 sends the other photon of the pair to either BS5 or BS6. In an ideal model, all beam splitters are identical. Each beam splitter represents a combination of wave plates, an electro-optical modulator (EOM), and a polarizing beam splitter (PBS), see for example Figure 1C in reference [9]. The EOM acts as a switchable (voltage controlled) polarization rotator, the rotation being characterized by a two-dimensional unit vector (indicated by the arrow through the beam splitter), relative to local frames of reference attached to the observation stations OS1 and OS2, respectively.

It is expedient to introduce the vectors $\mathbf{a} = (\cos a, \sin a)$, $\mathbf{a}_\perp = (-\sin a, \cos a)$, $\mathbf{b} = (\cos b, \sin b)$, $\mathbf{b}_\perp = (-\sin b, \cos b)$, $\mathbf{c} = (\cos c, \sin c)$, $\mathbf{c}_\perp = (-\sin c, \cos c)$, $\mathbf{d} = (\cos d, \sin d)$, and $\mathbf{d}_\perp = (-\sin d, \cos d)$. Photons leave BS1 with linear polarization along either $\mathbf{a}$ ($S_1 = +1$) or $\mathbf{a}_\perp$ ($S_1 = -1$). For the other beam splitters, we have similar relations between the direction of the linear polarization of the photons that leave the beam splitters and the value of the corresponding S-variable.

3.2. Classical Electrodynamics

It is instructive to first consider the case in which the detector signal is linearly proportional to the intensity of the impinging light. This case is covered by classical optics, described by Maxwell's theory of electrodynamics.

According to empirical evidence, the intensity of light passing through a polarizer is given by Malus' law $I = I_0 \cos^2(\phi - \psi)$, where ϕ is the polarization of the light beam and ψ is the rotation of the polarizer, both relative to a laboratory frame of reference. I_0 is the intensity of the incident light.

We assume that the source emits "special" randomly polarized light toward BS1 and BS2, special in the sense that the difference between the polarizations of the two beams ϕ_0 is fixed in time. Then, using Malus' law for BS1 and BS2, the correlated intensity for one particular, random realization of the polarization angle ϕ is given by

$$\begin{aligned} &I_1(S_1, S_2|\mathbf{a}, \mathbf{b}, \phi, \phi_0) \\ &= I_0^2 \frac{1 + S_1 \cos 2(\phi - a)}{2} \frac{1 + S_2 \cos 2(\phi - b + \phi_0)}{2} \,, \end{aligned} \tag{3}$$

where I_0 denotes the light intensity of a single beam. Integrating over all polarizations ϕ with a uniform density $1/2\pi$ yields

$$I_1(S_1, S_2|\mathbf{a}, \mathbf{b}, \phi_0) = \frac{I_0^2}{4}\Big[1 + \frac{1}{2} S_1 S_2 \cos 2(a - b + \phi_0)\Big] \,. \tag{4}$$

Repeated use of Malus' law and exploiting the fact that the polarizations of the two beams leaving a beam splitter are orthogonal, the correlated intensity of the different beams is then given by

$$\begin{aligned} I(S_1, S_2, S_3, S_4|\mathbf{a}, \mathbf{b}, \mathbf{c}, \mathbf{d}, \phi_0) = &\frac{I_0^2}{16}\Big[1 + \frac{1}{2} S_1 S_2 \cos 2(a - b + \phi_0)\Big] \\ &\Big[1 + S_1 S_3 \cos 2(a - c)\Big] \\ &\Big[1 + S_2 S_4 \cos 2(b - d)\Big] \,. \end{aligned} \tag{5}$$

The moments of the correlated intensity Equation (5) are

$$\begin{aligned} \widehat{K}_i &= \sum_{S_1,S_2,S_3,S_4=\pm 1} S_i I(S_1, S_2, S_3, S_4|\mathbf{a}, \mathbf{b}, \mathbf{c}, \mathbf{d}, \phi_0) = 0, \\ &\qquad i = 1, 2, 3, 4 \,, \\ \widehat{K}_{ij} &= \sum_{S_1,S_2,S_3,S_4=\pm 1} S_i S_j I(S_1, S_2, S_3, S_4|\mathbf{a}, \mathbf{b}, \mathbf{c}, \mathbf{d}, \phi_0), \\ &\qquad 1 \le i < j \le 4 \,, \\ \widehat{K}_{ijk} &= \sum_{S_1,S_2,S_3,S_4=\pm 1} S_i S_j S_k I(S_1, S_2, S_3, S_4|\mathbf{a}, \mathbf{b}, \mathbf{c}, \mathbf{d}, \phi_0) = 0, \\ &\qquad i \ne j \ne k \ne i \,, \\ \widehat{K}_{1234} &= \sum_{S_1,S_2,S_3,S_4=\pm 1} S_1 S_2 S_3 S_4 I(S_1, S_2, S_3, S_4|\mathbf{a}, \mathbf{b}, \mathbf{c}, \mathbf{d}, \phi_0) \\ &= I_0^2 \cos 2(a - c) \cos 2(b - d) \,. \end{aligned} \tag{6}$$

For $\phi_0 = \pi/2$ (orthogonally polarized beams) and $I_0 = 1$, the explicit expressions for the two-S correlations are

$$\begin{aligned} &\widehat{K}_{12} = -\frac{1}{2} \cos 2(a - b), \quad \widehat{K}_{13} = \cos 2(a - c), \\ &\widehat{K}_{14} = -\frac{1}{2} \cos 2(a - b) \cos 2(b - d), \\ &\widehat{K}_{23} = -\frac{1}{2} \cos 2(a - b) \cos 2(a - c), \\ &\widehat{K}_{24} = \cos 2(b - d), \\ &\widehat{K}_{34} = -\frac{1}{2} \cos 2(a - b) \cos 2(a - c) \cos 2(b - d). \end{aligned} \tag{7}$$

The factor 1/2 which appears in Equation (4) and in four of the six second moments $\widehat{K}_{ij}$ is characteristic of the correlation of two

light intensities. Here and in the following, we use the hat on top of the symbols to emphasize that the expressions have been obtained from a theoretical model.

3.3. Quantum Theory

Classical electrodynamics describes the intensity of light and does not discriminate between individual events. In contrast, quantum theory can be used to describe the statistics of events, particularly in cases, such as the EPRB experiment, where detectors can discriminate between them.

For a pair of photons whose polarizations are described by the singlet state, **Appendix A** shows that the joint probability to observe one photon in the path labeled by S_1 and the other one in the path labeled by S_2 is given by De Raedt et al. [59]

$$P(S_1, S_2|\mathbf{a}, \mathbf{b}, Z) = \frac{1 - S_1 S_2 \ \cos 2(a-b)}{4}, \tag{8}$$

where Z denotes a valid proposition that represents all conditions under which the experiment is performed with the exception of $\mathbf{a}$ and $\mathbf{b}$. Note that for $\phi_0 = \pi/2$, Equation (4) differs from Equation (8) through the factor 1/2 only.

In **Appendix A**, we show that the joint probability to observe one photon in the path labeled by (S_1, S_3) and the other in the path labeled by (S_2, S_4) is given by

$$\begin{aligned} P(S_1, S_2, S_3, S_4|\mathbf{a}, \mathbf{b}, \mathbf{c}, \mathbf{d}, Z) = &\frac{1}{16}\big[1 - S_1 S_2 \cos 2(a-b)\big] \\ &\big[1 + S_1 S_3 \cos 2(a-c)\big] \\ &\big[1 + S_2 S_4 \cos 2(b-d)\big]. \end{aligned} \tag{9}$$

As already mentioned in the introduction, a subquantum model for the EEPRB experiment must not make use of Equation (9) to generate the quadruples (S_1, S_2, S_3, S_4).

Note that the only non-trivial difference between Equations (5) and (9) is that in the former case, the absolute value of the pre-factor of the $S_1 S_2$ term never exceeds 1/2 whereas in the latter case, it is equal to -1. The expressions of the second moments of Equation (9) read

$$\begin{aligned} &\widehat{E}_{12} = -\cos 2(a-b), \quad \widehat{E}_{13} = \cos 2(a-c), \\ &\widehat{E}_{14} = -\cos 2(a-b)\cos 2(b-d), \\ &\widehat{E}_{23} = -\cos 2(a-b)\cos 2(a-c), \quad \widehat{E}_{24} = \cos 2(b-d), \\ &\widehat{E}_{34} = -\cos 2(a-b)\cos 2(a-c)\cos 2(b-d), \end{aligned} \tag{10}$$

which are not all equal to the corresponding expressions of the $\widehat{K}$'s, see Equation (7). From Equation (9) it follows that $\widehat{E}_1 = \widehat{E}_2 = \widehat{E}_3 = \widehat{E}_4 = \widehat{E}_{123} = \widehat{E}_{124} = \widehat{E}_{134} = \widehat{E}_{234} = 0$ and $\widehat{E}_{1234} = \cos 2(a-c)\cos 2(b-d)$.

Clearly, in order to have a subquantum model generate data that agrees either with Maxwell's theory Equation (5) or quantum theory Equation (9), we only have to construct a subquantum model in which we can control the pre-factor of the $S_1 S_2$ term in Equation (5). Thinking of light as a collection of photons, in sections 3.4 and 4, we explain how this control naturally results from the simple fact that we have to classify individual events as photons or something else, whereas in the "classical" case this classification is not an issue. At this point, it should be mentioned that within the context of the classical and quantum theory of light, changing the prefactor 1/2 of the $S_1 S_2$ term in Equation (5) is a subtle issue, intimately related to the amount of second-order coherence one can observe by measuring either intensities or by counting clicks of a detector [60]. A discussion of this important issue is out of the scope of this paper and we refer the reader who is interested in these aspects to the in-depth analysis given in reference [60]. In our paper, Equations (5) and (9) are only used to provide the classical/quantum results which any valid subquantum model for the (E)EPRB experiment has to reproduce.

An important feature of this EEPRB experiment is that all the correlations that are required to test for violations of Bell/Clauser-Horne-Shimony-Holt (CHSH) inequalities [12, 61] are obtained in a single run (instead of three/four runs) of the experiment [26]. The EEPRB experiment does not suffer from the contextuality loophole [49]. As $0 \leq P(S_1, S_2, S_3, S_4|\mathbf{a}, \mathbf{b}, \mathbf{c}, \mathbf{d}, Z) \leq 1$, it follows directly that all Bell-type inequalities, including all variants of the CHSH inequality, can never be violated [62]. This is easily seen by evaluating the sum $\sum_{S_1,S_2,S_3,S_4=\pm 1} g(S_1, S_2, S_3, S_4) P(S_1, S_2, S_3, S_4|\mathbf{a}, \mathbf{b}, \mathbf{c}, \mathbf{d}, Z)$ for various choices of the function $g(S_1, S_2, S_3, S_4)$, such as $-1 \leq g(S_1, S_2, S_3, S_4) = S_1 S_2 + S_1 S_3 + S_2 S_3 \leq 3$, or $-2 \leq g(S_1, S_2, S_3, S_4) = S_1 S_3 + S_1 S_4 + S_2 S_3 - S_2 S_4 \leq 2$, for example. In words, the quantum-theoretical description of the EEPRB experiment predicts that all Bell/CHSH inequalities are satisfied, in stark contrast to the case in which the correlations that enter the Bell/CHSH inequalities are computed from the quantum-theoretical description of the EPRB experiment.

3.4. Practical Realization: Photon Identification Problem

The exposition in subsection 3.1 assumes that each emitted pair of particles triggers exactly two detectors, namely only one of the four detectors at OS1 and one of the four detectors at OS2. In a laboratory experiment with Stern-Gerlach magnets and magnetic billiard balls, this assumption may hold true. However, it is not at all evident to have a source which only creates correlated pairs of elementary particles, such as photons which upon hitting a detector, will trigger exactly one detector at OS1 and exactly one detector at OS2.

With the exception of two experiments [9, 10], EPRB experiments with photons use time coincidence to identify photon pairs [3–8]. The two EPRB experiments [9, 10] that do not rely on time coincidence employ local, adjustable voltage thresholds to identify photons. This procedure is mathematically equivalent to attaching a local time tag to each particle, or to using time coincidence [63]. Therefore, in the following, we only discuss the subquantum model that uses local time tags as the vehicle for identifying pairs of photons. The modifications required to deal with voltage thresholds are trivial [63].

As explained above, a minimal theoretical model of a laboratory (E)EPRB experiment with photons should include a procedure to identify (pairs of) photons. Specifically, not including the data by which the photons and/or pairs

are identified opens the so-called photon identification loophole [63]. By design, the EPRB experiments that claim to be loophole free [8–10] all suffer from this loophole.

As shown in **Figure 1**, observation stations OS1 and OS2 are equipped with local clocks C1 and C2, respectively. The time t_1 (t_2) at which a detector in OS1 (OS2) fires is read off from the local clock C1 (C2). The clocks C1 and C2 are synchronized before the source starts to emit pairs of particles and, being ideal clocks, remain synchronized for the duration of the experiment. Similarly, the frames of reference of OS1 and OS2 are aligned before the source starts to emit pairs of particles and do not change afterwards.

Concretizing the aim of this paper, in the next section, we describe a local realist model of the (E)EPRB experiment that reproduces the statistical predictions of quantum theory given by Equations (8) and (9). In formulating the DES model, we call the agents that carry the information from the source to the observation stations "photons" and use the language of optics.

4. SUBQUANTUM MODEL

Before describing all the components of the subquantum model, we recall the basic strategy that we adopt in constructing such a model. As quantum theory describes the most ideal version of the (E)EPRB experiment and as our aim is to show that the subquantum model reproduces the results of the former, we construct a DES of the most ideal version of the (E)EPRB experiment. The DES model for the EEPRB experiment that we describe next contains the ideal implementation of EPRB laboratory experiments.

In concert with our general strategy to set up the subquantum model, we assume that the source emits pairs of photons only and this at regular time intervals Δ. The time at which the nth pair is emitted is given by $T_n = n\Delta$. The time it takes for a photon to travel from the source to BS1 or BS2 is assumed to be constant and the same for all photons traveling to OS1 and OS2. We denote this time of flight by $T'_{\rm TOF}$. Similarly, the time of flight from BS1 to BS3 or BS4 (BS2 to BS5 or BS6) and the time of flight from BS3, BS4, BS5, or BS6 to the corresponding detectors are denoted by $T''_{\rm TOF}$ and $T'''_{\rm TOF}$, respectively. The total time of flight is then $T_{\rm TOF} = T'_{\rm TOF} + T''_{\rm TOF} + T'''_{\rm TOF}$.

In the DES model, the polarization of the photon traveling to BS1 (BS2) is represented by a two-dimensional unit vector $\mathbf{x}_1 = (\cos\phi, \sin\phi)^{\rm T}$ ($\mathbf{x}_2 = (-\sin\phi, \cos\phi)^{\rm T}$). The angle ϕ is chosen to be uniformly random from the interval $[0, 2\pi)$. As $\mathbf{x}_1^{\rm T}\cdot\mathbf{x}_2 = 0$, the polarizations of the photons of each pair are orthogonal, that is, they are maximally anticorrelated and randomly distributed over the unit circle.

In the following, we specify the DES rules for BS1 only. The rules for the other beam splitters are identical and are obtained by a simple change of symbols. In the DES model, the operation of beam splitter BS1 is defined by the rules

$$S_1 = \begin{cases} +1 \text{ if } \cos^2(\phi - a) > r \\ -1 \text{ if } \cos^2(\phi - a) \le r \end{cases}, \; x'_1 = \begin{cases} \mathbf{a} & \text{if } S_1 = +1 \\ \mathbf{a}_\perp & \text{if } S_1 = -1 \end{cases}, \quad (11)$$

where $0 < r < 1$ denotes a uniform pseudo-random number. Here and in the following, it is implicitly understood that a new instance of the pseudo-random number r is generated with each invocation of an equation in which r appears. The unit vector $\mathbf{x}'_1$ denotes the polarization of the photon leaving BS1. It is not difficult to see that the model defined by Equation (11) generates $S_1 = +1$ ($S_1 = -1$) events with a relative frequency given by $\cos^2(\phi - a)$ ($\sin^2(\phi - a)$), i.e., Equation (11) produces data that is in concert with Malus' law if the polarization of the incident photon is constant in time.

Optical components, such as wave plates and EOMs contain birefringent material which changes the polarization by retarding (or delaying) one component of the polarization with respect to its orthogonal component. In the DES, this retardation effect is accounted for by assuming that as a photon passes through a beam splitter, it may suffer from a time delay which may depend on the direction of the beam splitter relative to the polarization of the photon.

Obviously, the law of retardation in the subquantum model cannot be derived from Maxwell's theory or quantum theory. We can only find the subquantum law of retardation by trial and error. Fortunately, from earlier work we already know the subquantum law of retardation for the EPRB experiment [64, 65] and we only need to extend this law slightly to have the DES reproduce the quantum-theoretical results for both the EPRB and EEPRB experiment. Specifically, for BS1, the two DES rules for the subquantum law of retardation read

$$\begin{aligned} \tau_1 &= \tau_{\rm EPRB}(\mathbf{x}_1, \mathbf{a}) \left|\frac{1 - \mathbf{x}_1\cdot\mathbf{u}_1}{2}\right|^\beta \\ &= r' T_{\max} \left|\sin 2(\phi - a)\right|^\alpha \left|\frac{1 - \mathbf{x}_1\cdot\mathbf{u}_1}{2}\right|^\beta \quad , \quad \mathbf{u}_1 \leftarrow \mathbf{x}_1 \, , \end{aligned} \quad (12)$$

where $\mathbf{x}_1$ (or equivalently ϕ) is the polarization of the incoming photon, $0 < r' < 1$ is another uniform pseudo-random number, $T_{\max}$ is an adjustable parameter specifying maximum retardation, and $\alpha > 0$ is an adjustable parameter controlling the dependence of the retardation on the difference between the photon polarization $\mathbf{x}_1$ and the orientation of the beam splitter $\mathbf{a}$. As indicated by the subscript EPRB, $\tau_{\rm EPRB} = r' T_{\max} \left|\sin 2(\phi - a)\right|^\alpha$ suffices to reproduce the quantum-theoretical results of the EPRB experiment [54, 59, 63–65].

The new features are the last factor in Equation (12), $\beta > 0$ being an adjustable parameter, and the rule $\mathbf{u}_1 \leftarrow \mathbf{x}_1$ which updates the two-dimensional vector $\mathbf{u}_1$. The initial value of $\mathbf{u}_1$ can be any vector that has a norm ≤ 1. This vector is attached to the beam splitter and may be thought of as representing (on a subquantum level) the electrical polarization of the material [51].

The purpose of the factor $|(1 - \mathbf{x}_1\cdot\mathbf{u}_1)/2|^\beta$ in Equation (12) is to turn off the generation of random retardation times if the polarization of the incoming photons is constant. To see how this works, first consider the case that the polarization of the incoming photons is constant, say $\mathbf{x}_1 = \widetilde{\mathbf{x}}_1$. Then, after the first photon has passed by, $\mathbf{u}_1 = \widetilde{\mathbf{x}}_1$ and $|(1 - \mathbf{x}_1\cdot\mathbf{u}_1)/2|^\beta = 0$ for all photons that follow. Next, assume that the polarization of the

photons entering BS1 is randomly distributed over the unit circle. Then, because $\mathbf{x}_1$ and $\mathbf{u}_1$ (which is equal to the polarization $\mathbf{x}_1$ of the previous photon) are independent, $|(1-\mathbf{x}_1\cdot\mathbf{u}_1)/2|^\beta$ is just a random variable in $[0,1]$ multiplying $\tau_{\rm EPRB}$. The idea to store and use the value of the polarization of the previous photon has also been used to reproduce, by DES, the quantum-theoretical results for a large variety of single-photon and single-neutron experiments [50, 51]. The capability of the subquantum model to disable the generation of random retardation times if the polarization of the incoming photons is constant is essential for reproducing the quantum-theoretical results of both the EPRB and EEPRB experiments with the same subquantum model.

At this point, it may be of interest to mention that on the basis of the statistics (i.e., averages and correlations) only, it is not possible to make statements about the uniqueness of the subquantum law of retardation. As a matter of fact, in the case at hand, replacing Equation (12) by the rules

$$\begin{aligned}\tau_1 &= \tau_{\rm EPRB}(\mathbf{x}_1,\mathbf{a})\left|\frac{1-\mathbf{u}_1\cdot\mathbf{u}_1}{2}\right|^\beta \qquad (13)\\ &= r' T_{\max}\left|\sin 2(\phi-a)\right|^\alpha\left|\frac{1-\mathbf{u}_1\cdot\mathbf{u}_1}{2}\right|^\beta,\\ \mathbf{u}_1 &\leftarrow \gamma\mathbf{u}_1+(1-\gamma)\mathbf{x}_1\,, \qquad (14)\end{aligned}$$

works equally well.

Equation (14) defines a deterministic learning machine (DLM) [50, 51], which learns, event-by-event, the time average of the polarizations $\mathbf{x}_1$ carried by the photons. The speed and accuracy by which $\mathbf{u}_1$ approaches the time average of the $\mathbf{x}_1$'s is controlled by the parameter $0<\gamma<1$ [51]. The order in which Equations (13) and (14) are executed is irrelevant. The DLM defined by Equation (14) is the same as the one that has been used to reproduce, by DES, the quantum-theoretical results for a large variety of single-photon and single-neutron experiments [50, 51]. If the polarizations of the incoming photons are constant, say $\widetilde{\mathbf{x}}_1$, and a certain number (depending on γ) of photons has passed by, we have $\mathbf{u}_1\approx\widetilde{\mathbf{x}}_1$ and $|(1-\mathbf{u}_1\cdot\mathbf{u}_1)/2|^\beta\approx 0$. If the polarizations of the photons entering BS1 are randomly distributed over the unit circle, $\mathbf{u}_1\to 0$ and $|(1-\mathbf{u}_1\cdot\mathbf{u}_1)/2|^\beta\approx 1$. Then, just as in the case of Equation (12), the factor $|(1-\mathbf{u}_1\cdot\mathbf{u}_1)/2|^\beta$ in Equation (4) is used to turn off the generation of random retardation times if the polarizations of the incoming photons are constant.

In our idealized experiment, all detectors are assumed to be identical and to have a 100% detection efficiency. After a photon has passed BS3 or BS4 (BS5 or BS6), it may trigger one and only one detector in OS1 (OS2), symbolized by one of $x_{1,1}$, $x_{2,1}$, $x_{3,1}$, or $x_{4,1}$ ($x_{1,2}$, $x_{2,2}$, $x_{3,2}$, or $x_{4,2}$) being equal to one and the other ones being equal to zero. The time t_1 (t_2) at which a detector in OS1 (OS2) fires is read off from the local clock C1 (C2). These local clocks C1 and C2 are synchronized before the source starts to emit pairs of photons and, being ideal clocks, remain synchronized for the duration of the experiment. For the nth emitted pair, the arrival times are given by

$$t_{1,n} = T_{\rm TOF}+n\Delta+\tau_{1,n}+\begin{cases}\tau_{3,n} & \text{if } S_1=+1\\ \tau_{4,n} & \text{if } S_1=-1\end{cases}, \qquad (15)$$

$$t_{2,n} = T_{\rm TOF}+n\Delta+\tau_{2,n}+\begin{cases}\tau_{5,n} & \text{if } S_2=+1\\ \tau_{6,n} & \text{if } S_2=-1\end{cases}, \qquad (16)$$

where we have attached the subscript n to keep track of which pair of the emitted pairs we are dealing with. For each pair-emission event $n=1,\ldots,N$, Equations (11)–(16) generate the data $(S_{1,n},S_{3,n},t_{1,n})$ and $(S_{2,n},S_{4,n},t_{2,n})$. Note that OS1 and OS2 only share the angle of polarization ϕ characterizing the pair of photons, nothing else.

In each triple in $(S_{i,n},S_{i+2,n},t_{i,n})$, we replace the time variable by a (local) binary variable $w_{i,n}$ to indicate whether a detection event is classified as a photon ($w_{i,n}=1$) or not ($w_{i,n}=0$). Specifically, the rule to decide whether a detection event corresponds to the observation of a photon or of something else is given by

$$w_{i,n}=\begin{cases}1 \text{ if } 0\le t_{i,n}-T_{\rm TOF}-n\Delta\le W, & \text{"a photon"}\\ 0 \text{ if } t_{i,n}-T_{\rm TOF}-n\Delta>W, & \text{"something else"}\end{cases} \qquad i=1,2, \quad (17)$$

where W is the time window (an adjustable parameter). We emphasize that the decision process defined by Equation (17) only involves variables that are local to the observation stations.

Equations (11)–(17) define the rules by which the subquantum model generates the data sets

$$\begin{aligned}\mathscr{S}_1 &= \left\{(S_{1,n},S_{3,n},w_{1,n})\mid n=1,\ldots,N\right\} \quad \text{and}\\ \mathscr{S}_2 &= \left\{(S_{2,n},S_{4,n},w_{2,n})\mid n=1,\ldots,N\right\}, \qquad (18)\end{aligned}$$

collected by OS1 and OS2, respectively. From the data sets $\mathscr{S}_1$ and $\mathscr{S}_2$, we compute the single- and two-particle averages

$$\begin{aligned}K_i &= \frac{1}{N}\sum_{n=1}^N S_{i,n}, \quad E_i=\frac{\sum_{n=1}^N w_{1,n}w_{2,n}S_{i,n}}{\sum_{n=1}^N w_{1,n}w_{2,n}}, \quad i=1,2,3,4\\ K_{ij} &= \frac{1}{N}\sum_{n=1}^N S_{i,n}S_{j,n}, E_{ij}=\frac{\sum_{n=1}^N w_{1,n}w_{2,n}S_{i,n}S_{j,n}}{\sum_{n=1}^N w_{1,n}w_{2,n}},\\ (i,j) &= (1,2),(1,3),(1,4),(2,3),(2,4),(3,4)\,, \qquad (19)\end{aligned}$$

without (K's) and with (E's) the photon identification process in place.

5. SIMULATION RESULTS

Below, we specify the DES parameters that have been used, discuss the data shown in **Figures 2**, **3**, and provide additional information about simulation data that we do not show.

- The number of emitted pairs is $N=1,000,000$ per setting $(\mathbf{a},\mathbf{b},\mathbf{c},\mathbf{d})$.
- The maximum retardation time was chosen to be $T_{\max}=5,000$ (dimensionless units). Pairs of particles are emitted with a time interval $\Delta>2T_{\max}$. In line with our strategy to perform an ideal experiment, this choice eliminates the possibility of

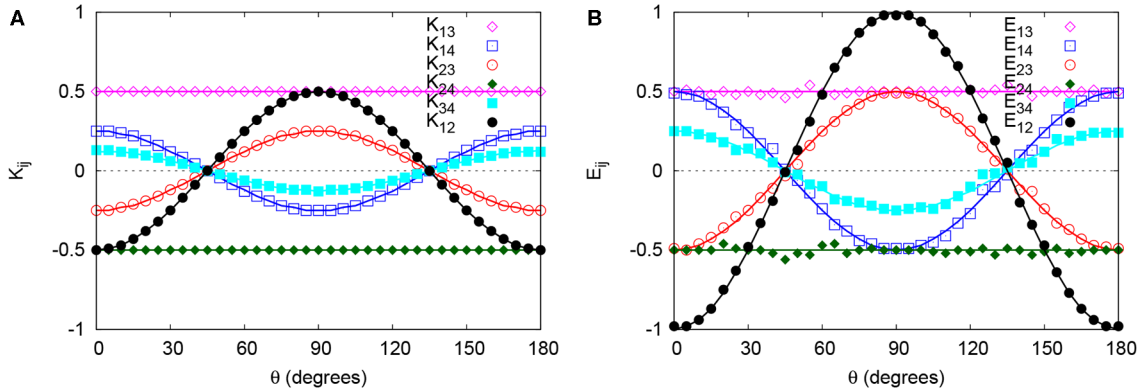

FIGURE 2 | DES results for the correlations between all pairs of the S-variables as a function of $\theta = a - b$, with $b = 0$, $c = a + \pi/6$, and $d = \pi/3$. The source emits pairs of photons with orthogonal polarizations chosen randomly. Ignoring statistical fluctuations, the averages of all S-variables (not shown) are zero. **(A)** The correlations K_{ij} computed without photon identification (markers) are in excellent agreement with the corresponding correlations $\widehat{K}_{ij}$ [see Equation (7)] predicted by Maxwell's theory (solid lines) for two light beams with orthogonal, random polarization ($\phi_0 = \pi/2$); **(B)** The correlations E_{ij} computed with photon identification (markers) are in excellent agreement with the corresponding correlations $\widehat{E}_{ij}$ predicted by quantum theory [solid lines, see Equation (10)] for two spin-1/2 particles in a singlet state.

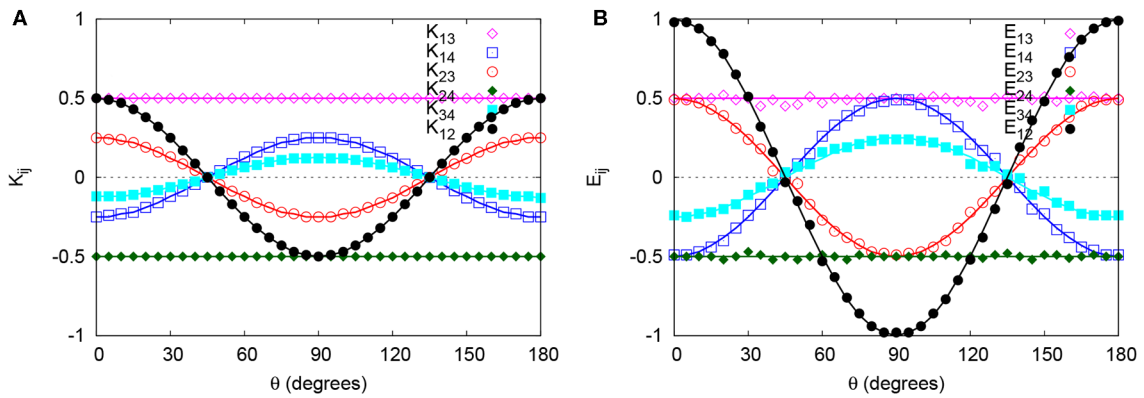

FIGURE 3 | Same as **Figure 2** except that the source emits pairs of photons with the same instead of orthogonal polarizations chosen randomly. **(A)** The correlations K_{ij} computed without photon identification (markers) are in excellent agreement with the corresponding correlations $\widehat{K}_{ij}$ (solid lines) predicted by Maxwell's theory for two light beams with the same, random polarization ($\phi_0 = 0$); **(B)** The correlations E_{ij} computed with photon identification (markers) cannot be obtained from quantum theory for two spin-1/2 particles (see **Appendix B**) but are in excellent agreement with the corresponding correlations (solid lines) obtained from the expression Equation (9) in which the factor $[1 - S_1 S_2 \cos 2(a - b)]$ is replaced by $[1 + S_1 S_2 \cos 2(a - b)]$.

misidentifying pairs and also ensures that at each instant of time, there is only one photon in transit to OS1 and only one other photon en route to OS2. For $T_{\rm TOF}$ we can take any non-negative value. In fact, from Equation (17) it follows that the actual values of Δ and $T_{\rm TOF}$ do not enter in the DES algorithm.

- In **Figure 2A**, we show the DES results for the case without photon identification (that is if $W > T_{\rm max}$ or $\alpha = \beta = 0$). Then the DES reproduces the results of Maxwell's theory, **by an event-by-event process** [66]. Specifically, if the polarization of the incoming photon is constant, the DES model of the beam splitter itself generates data according to Malus' law. The DES model of the EEPRB experiment with randomly polarized light produces data that, ignoring statistical fluctuations, is in excellent agreement with Equation (7) (see **Figure 2A**).
- Using a local time window $W = 1$ (dimensionless units) and for $\alpha = 4$ and $\beta = 1/2$, the **event-by-event process** yields results (see **Figure 2B**) for the E's which are in excellent agreement with quantum theory (data for the first, third, and fourth moments are not shown). The ratio of identified photon pairs to emitted pairs depends on a and b and varies between $\sim 11\%$ for $a = b$ and 0.1% for $|a - b| = \pi/4$. For $W = 8$, this ratio changes to $\sim 18\%$ for $a = b$ and 0.8% for $|a - b| = \pi/4$, while the agreement with quantum theory is still very good (data not shown).
- The data obtained by identifying photons using time coincidence instead of local time windows are almost the same and are therefore not shown. In the limit $W/T_{\rm max} \to 0$, $N \to \infty$, and $\alpha = 4$, it has been proven analytically that the DES model of the EPRB experiment yields the correlation $E_{12} = -\cos 2(a - b)$ exactly [65].
- Using the same pseudo-random sequence for each choice of settings renders the DES compliant with the notion of

a counterfactually definite theory. In this case, the DES results (data not shown) are, for all practical purposes, the same as those obtained by using different pseudo-random sequences for each choice of settings. Operating in this mode, the subquantum model of the EPRB experiment does not suffer from the contextuality loophole [49] nor of any other known loopholes [55]. This confirms the conclusion of an earlier work [54], which adopted a different approach to realize counterfactually-definite compliant simulations. The demonstration that there exist both counterfactually-definite and non-counterfactually-definite compliant computer models for the EPRB experiments that produce results in complete agreement with those of quantum theory implies that, for the case of EPRB experiments, counterfactual definiteness is not incompatible with quantum physics [63].

- In the DES, it is trivial to account for the detection efficiency $0 \leq \eta \leq 1$. For each detection event, we generate a pseudo-random number r'' and remove the detection event from the data set if $r'' > \eta$. We find that the only effect of reducing η is to increase the statistical fluctuations (data not shown). The agreement with quantum theory is not affected.
- In **Figure 3**, we show the DES results for the case in which the source emits photons with the same polarization chosen randomly. In this case, the DES reproduces the results of Maxwell's theory (**Figure 3A**). A corresponding quantum-theoretical result does not exist, see **Appendix B**. However, the DES data are in excellent agreement with a **non-quantum** probabilistic theory in which the factor $\left[1 - S_1 S_2 \cos 2(a-b)\right]$ in Equation (9) is replaced by $\left[1 + S_1 S_2 \cos 2(a-b)\right]$ (see **Figure 3B**).
- Replacing the rules Equation (12) by the rules Equations (13) and (14), and repeating the DES with the same value of α and β also yields data (not shown) that are in excellent agreement with the quantum-theoretical description, for γ in the range $[0.1, 0.98]$.
- Our DES model also reproduces the theoretical results (see **Appendix C**) if the two photons of each pair have a fixed polarization (results not shown). In Maxwell's theory, this case is described by light beams with fixed polarizations. In quantum theory, this case is described by an (uncorrelated) product state.

Table 1 gives a compact overview of the agreement between the DES results and the theoretical descriptions of the (E)EPRB experiments.

6. DISCUSSION AND SUMMARY

Laboratory EPRB experiments unavoidably require a procedure to classify a detection event as corresponding to a photon or as something else. Independent of the precise nature of this procedure (voltage threshold, local time window, time coincidence, etc.), any model that aims at describing an EPRB experiment should, from the start, account for this procedure by introducing additional variables into the description. In contrast, Bell's model, while charmingly simple, does not account for an essential aspect of laboratory EPRB experiments, namely the classification of detection events in terms of photons or something else. Consequently, any subquantum model that aims at reproducing the results of quantum theory for the (E)EPRB experiment should have features that are not included in Bell's model. As a matter of fact, a quick glance at how the data of laboratory EPRB experiments are being processed reveals that it is the photon identification process which is lacking in Bell's model. Including this process implies that correlations between events are calculated only from subsets of the data, in which case Bell's theorem does not apply. Using only subsets of the data, there is only the constraint that the correlation should, in absolute value, be ≤ 1. Apart from that "almost everything" is possible [20, 67–69], including a subquantum model that, in the appropriate limit, yields the correlation of the singlet state [64, 65].

Clearly, on the basis of the statistical data alone, it is not possible to reject subquantum models of the EPRB and EEPRB experiments presented in this paper. The relevant question is how a laboratory experiment can rule out or confirm that (i) a subquantum level description is possible and/or (ii) the rules by which the DES model of the beam splitter operates provide a reasonable description.

Regarding (i): If we consider it as irrelevant to ask what kind of process gives rise to the statistics of events, it seems very difficult to beat quantum theory in terms of descriptive power [70]. Therefore, it is clear that addressing (i) requires the analysis of the data on the level of individual events, without being biased by what quantum theory predicts for the statistics.

Regarding (ii): The DES model defined by Equations (11) and (12) or Equations (11), (13), and (14) produces data in concert with Malus' law, i.e., with the experiment, and therefore seems solid. The additional feature of the DES model (which allows us to reproduce the statistics of the EPRB and EEPRB experiments as given by quantum theory) is the subquantum law of retardation, defined by Equation (12) or Equations (13)

TABLE 1 | Overview of the agreement between the DES results and the theoretical descriptions of the (E)EPRB experiments.

	Without photon identification		With photon identification	
Photon pair polarization	**EPRB**	**EEPRB**	**EPRB**	**EEPRB**
Orthogonal + random	MT [Equation (4), $\phi_0 = \pi/2$]	MT [Equation (5), $\phi_0 = \pi/2$]	QT [Equation (8)]	QT [Equation (9)]
Parallel + random	MT [Equation (4), $\phi_0 = 0$]	MT [Equation (5), $\phi_0 = 0$]	?	?
Fixed	MT [Equation (C1)]	MT [Equation (C2)]	QT [Equation (C1)]	QT [Equation (C2)]

*MT, DES results agree with Maxwell's theory of electrodynamics; QT, DES results agree with quantum theory of a pair of spin-1/2 particles. Question mark: DES results cannot be described by quantum theory of a pair of spin-1/2 particles (see **Appendix B**).*

and (14). At first sight, there is no experimental support for such a law. However, let us look at the EPRB experiment from a slightly different perspective, namely, as a setup to characterize the response of the observation stations to very feeble, randomly anticorrelated light. Then, our DES data and also the analysis of experimental data [65] support the hypothesis that the EPRB experiment demonstrates that the statistics of the detection events that have been classified as photons depend on the settings.

What if we try to measure the retardation by an experiment that uses feeble light with fixed polarization? As explained in section 4, in our subquantum model the retardation time does not depend on the setting of the beam splitter if the polarization is constant in time. Only if the polarization is not fixed in time, our subquantum model yields retardation times that depend on the setting of the beam splitter. This is precisely what the EPRB experiment does: through the correlation, it provides information about the retardation as a function of the setting of the beam splitter. Therefore, to rule out the subquantum law of retardation used in our DES, it is necessary to perform both the experiments with feeble, randomly polarized light and with feeble light of fixed polarization.

Summarizing, we have proposed a subquantum model which satisfies Einstein's criterion of locality and which generates, event-by-event, data that agrees with the quantum-theoretical description of the Einstein-Podolsky-Rosen-Bohm and the extended Einstein-Podolsky-Rosen-Bohm experiments. This demonstration does not build on the traditional methods of theoretical physics but instead uses a digital computer and a discrete-event simulation as a metaphor for idealized, realizable laboratory experiments.

DATA AVAILABILITY STATEMENT

The datasets generated for this study are available on request to the corresponding author.

AUTHOR CONTRIBUTIONS

KM, HD, MJ, and FJ contributed to the conception and design of the DES models. MJ, MW, DW, KM, FJ, and HD contributed to the writing of the manuscript. MJ, MW, DW, and HD independently performed all the simulations.

REFERENCES

1. Einstein A, Podolsky A, Rosen N. Can quantum-mechanical description of physical reality be considered complete? *Phys Rev.* (1935) **47**:777–80. doi: 10.1103/PhysRev.47.777
2. Bohm D. *Quantum Theory*. New York, NY: Prentice-Hall (1951).
3. Kocher CA, Commins ED. Polarization correlation of photons emitted in an atomic cascade. *Phys Rev Lett.* (1967) **18**:575–7. doi: 10.1103/PhysRevLett.18.575
4. Clauser JF, Shimony A. Bell's theorem: experimental tests and implications. *Rep Prog Phys.* (1978) **41**:1881–927. doi: 10.1088/0034-4885/41/12/002
5. Aspect A, Dalibard J, Roger G. Experimental test of Bell's inequalities using time-varying analyzers. *Phys Rev Lett.* (1982) **49**:1804–7. doi: 10.1103/PhysRevLett.49.1804
6. Weihs G, Jennewein T, Simon C, Weinfurther H, Zeilinger A. Violation of Bell's inequality under strict Einstein locality conditions. *Phys Rev Lett.* (1998) **81**:5039–43. doi: 10.1103/PhysRevLett.81.5039
7. Christensen BG, McCusker KT, Altepeter JB, Calkins B, Lim CCW, Gisin N, et al. Detection-Loophole-Free test of quantum nonlocality, and applications. *Phys Rev Lett.* (2013) **111**:130406. doi: 10.1103/PhysRevLett.111.130406
8. Hensen B, Bernien H, Dreau AE, Reiserer A, Kalb N, Blok MS, et al. Loophole-free Bell inequality violation using electron spins separated by 1.3 kilometres. *Nature.* (2015) **526**:682–6. doi: 10.1038/nature15759
9. Giustina M, Versteegh MAM, Wengerowsky S, Handsteiner J, Hochrainer A, Phelan K, et al. Significant-Loophole-Free test of Bell's theorem with entangled photons. *Phys Rev Lett.* (2015) **115**:250401. doi: 10.1103/PhysRevLett.115.250401
10. Shalm LK, Meyer-Scott E, Christensen BG, Bierhorst P, Wayne MA, Stevens MJ, et al. Strong Loophole-Free test of local realism. *Phys Rev Lett.* (2015) **115**:250402. doi: 10.1103/PhysRevLett.115.250402
11. Bell JS. On the Einstein-Podolsky-Rosen paradox. *Physics.* (1964) **1**:195–200. doi: 10.1103/PhysicsPhysiqueFizika.1.195
12. Bell JS. *Speakable and Unspeakable in Quantum Mechanics*. Cambridge: Cambridge University Press (1993).
13. de la Peña L, Cetto AM, Brody TA. On hidden-variable theories and Bell's inequality. *Lett Nuovo Cim.* (1972) **5**:177–81. doi: 10.1007/BF02815921
14. Fine A. On the completeness of quantum theory. *Synthese.* (1974) **29**:257–89. doi: 10.1007/BF00484961
15. Fine A. Some local models for correlation experiments. *Synthese.* (1982) **50**:279–94. doi: 10.1007/BF00416904
16. Fine A. Hidden variables, joint probability, and Bell inequalities. *Phys Rev Lett.* (1982) **48**:291–5. doi: 10.1103/PhysRevLett.48.291
17. Fine A. Joint distributions, quantum correlations, and commuting observables. *J Math Phys.* (1982) **23**:1306–10. doi: 10.1063/1.525514
18. de Muynck WM. The Bell inequalities and their irrelevance to the problem of locality in quantum mechanics. *Phys Lett A.* (1986) **114**:65–7. doi: 10.1016/0375-9601(86)90480-9
19. Kupczyński M. On some tests of completeness of quantum mechanics. *Phys Lett A.* (1986) **116**:417–9. doi: 10.1016/0375-9601(86)90372-5
20. Brans CH. Bell's theorem does not eliminate fully causal hidden variables. *Int J Theor Phys.* (1987) **27**:219–26. doi: 10.1007/BF00670750
21. Jaynes ET. Clearing up mysteries—the original goal. In: Skilling J, editor. *Maximum Entropy and Bayesian Methods*. Vol. 36. Dordrecht: Kluwer Academic Publishers (1989). p. 1–27. doi: 10.1007/978-94-015-7860-8_1
22. Brody T. *The Philosphy Behind Physics*. Berlin: Springer (1993). doi: 10.1007/978-3-642-78978-6
23. Pitowsky I. George Boole's 'conditions of possible experience' and the quantum puzzle. *Br J Phil Sci.* (1994) **45**:95–125. doi: 10.1093/bjps/45.1.95
24. Fine A. *The Shaky Game: Einstein Realism and the Quantum Theory*. Chicago, IL: University of Chicago Press (1996).
25. Khrennikov AY. *Interpretations of Probability*. Utrecht: VSP Int. Sc. Publishers (1999). doi: 10.1515/9783110213195
26. Sica L. Bell's inequalities I: an explanation for their experimental violation. *Opt Comm.* (1999) **170**:55–60. doi: 10.1016/S0030-4018(99)00417-4
27. De Baere W, Mann A, Revzen M. Locality and Bell's theorem. *Found Phys.* (1999) **29**:67–77. doi: 10.1023/A:1018865120111
28. Hess K, Philipp W. Bell's theorem and the problem of decidability between the views of Einstein and Bohr. *Proc Natl Acad Sci USA.* (2001) **98**:14228–33. doi: 10.1073/pnas.251525098
29. Hess K, Philipp W. A possible loophole in the theorem of Bell. *Proc Natl Acad Sci USA.* (2001) **98**:14224–77. doi: 10.1073/pnas.251524998
30. Hess K, Philipp W. Bell's theorem: critique of proofs with and without inequalities. *AIP Conf Proc.* (2005) **750**:150–7. doi: 10.1063/1.1874568
31. Accardi L. Some loopholes to save quantum nonlocality. *AIP Conf Proc.* (2005) **750**:1–20. doi: 10.1063/1.1874552
32. Kracklauer AF. Bell's inequalities and EPR-B experiments: are they disjoint? *AIP Conf Proc.* (2005) **750**:219–27. doi: 10.1063/1.1874573

33. Santos E. Bell's theorem and the experiments: increasing empirical support to local realism? *Stud Hist Phil Mod Phys.* (2005) **36**:544–65. doi: 10.1016/j.shpsb.2005.05.007
34. Kupczyński M. Entanglement and Bell inequalities. *J Russ Las Res.* (2005) **26**:514–23. doi: 10.1007/s10946-005-0048-7
35. Morgan P. Bell inequalities for random fields. *J Phys A.* (2006) **39**:7441–5. doi: 10.1088/0305-4470/39/23/018
36. Khrennikov AY. A mathematicians viewpoint to Bell's theorem: in memory of Walter Philipp. *AIP Conf Proc.* (2007) **889**:7–17. doi: 10.1063/1.2713442
37. Adenier G, Khrennikov AY. Is the fair sampling assumption supported by EPR experiments. *J Phys B Mol Opt Phys.* (2007) **40**:131–41. doi: 10.1088/0953-4075/40/1/012
38. Nieuwenhuizen TM. Where Bell went wrong. *AIP Conf Proc.* (2009) **1101**:127–33. doi: 10.1063/1.3109932
39. Matzkin A. Is Bell's theorem relevant to quantum mechanics? On locality and non-commuting observables. *AIP Conf Proc.* (2009) **1101**:339–48. doi: 10.1063/1.3109959
40. Hess K, Michielsen K, De Raedt H. Possible experience: from Boole to Bell. *Europhys Lett.* (2009) **87**:60007. doi: 10.1209/0295-5075/87/60007
41. Khrennikov AY. *Contextual Approach to Quantum Formalism*. Berlin: Springer (2009). doi: 10.1007/978-1-4020-9593-1
42. Graft DA. The Bell inequality cannot be validly applied to the Einstein-Podolsky-Rosen-Bohm (EPRB) experiments. *Phys Essays.* (2009) **22**:534–42. doi: 10.4006/1.3231944
43. Khrennikov AY. On the role of probabilistic models in quantum physics: Bell's inequality and probabilistic incompatibility. *J Comput Theor Nanosci.* (2011) **8**:1006–10.
44. Nieuwenhuizen TM. Is the contextuality loophole fatal for the derivation of Bell inequalities? *Found Phys.* (2011) **41**:580–91. doi: 10.1007/s10701-010-9461-z
45. Hess K. *Einstein Was Right!* Singapore: Pan Stanford Publishing (2015). doi: 10.1201/b16809
46. Kupczyński M. EPR paradox, quantum nonlocality and physical reality. *J Phys Conf Ser.* (2016) **701**:012021. doi: 10.1088/1742-6596/701/1/012021
47. Kupczyński M. Can we close the Bohr-Einstein quantum debate? *Phil Trans R Soc A.* (2017) **375**:20160392. doi: 10.1098/rsta.2016.0392
48. Hess K, De Raedt H, Michielsen K. Analysis of Wigner's set theoretical proof for Bell-type inequalities. *J Mod Phys.* (2017) **8**:57–67. doi: 10.4236/jmp.2017.81005
49. Nieuwenhuizen TM, Kupczyński M. The Contextuality Loophole is fatal for the derivation of Bell inequalities: reply to a comment by I. Schmelzer. *Found Phys.* (2017) **47**:316–9. doi: 10.1007/s10701-017-0062-y
50. De Raedt K, De Raedt H, Michielsen K. Deterministic event-based simulation of quantum phenomena. *Comp Phys Comm.* (2005) **171**:19–39. doi: 10.1016/j.cpc.2005.04.012
51. Michielsen K, De Raedt H. Event-based simulation of quantum physics experiments. *Int J Mod Phys C.* (2014) **25**:01430003. doi: 10.1142/S0129183114300036
52. Banks J, Carson II JS, Nelson BL, Nicol DM. *Discrete-Event System Simulation*. New York, NY: Pearson (1996).
53. Leemis LM, Park SK. *Discrete-Event Simulation: A First Course*. New York, NY: Pearson (2006).
54. De Raedt H, Michielsen K, Hess K. The digital computer as a metaphor for the perfect laboratory experiment: Loophole-free Bell experiments. *Comp Phys Comm.* (2016) **209**:42–7. doi: 10.1016/j.cpc.2016.08.010
55. Larsson JÅ. Loopholes in Bell inequality tests of local realism. *J Phys A Math Theor.* (2014) **47**:424003. doi: 10.1088/1751-8113/47/42/424003
56. Press WH, Flannery BP, Teukolsky SA, Vetterling WT. *Numerical Recipes*. Cambridge: Cambridge University Press (2003).
57. Schwinger J. The algebra of microscopic measurements. *Proc Natl Acad Sci USA.* (1959) **45**:1542–53. doi: 10.1073/pnas.45.10.1542
58. Ballentine LE. *Quantum Mechanics: A Modern Development*. Singapore: World Scientific (2003).
59. De Raedt H, De Raedt K, Michielsen K, Keimpema K, Miyashita S. Event-by-event simulation of quantum phenomena: application to Einstein-Podolosky-Rosen-Bohm experiments. *J Comput Theor Nanosci.* (2007) **4**:957–91. doi: 10.1166/jctn.2007.2381
60. Khrennikov A. Quantum versus classical entanglement: eliminating the issue of quantum nonlocality. *Found. Phys.* (2020). doi: 10.1007/s10701-020-00319-7
61. Clauser JF, Horn MA, Shimony A, Holt RA. Proposed experiment to test local hidden-variable theories. *Phys Rev Lett.* (1969) **23**:880–84. doi: 10.1103/PhysRevLett.23.880
62. De Raedt H, Hess K, Michielsen K. Extended Boole-Bell inequalities applicable to quantum theory. *J Comput Theor Nanosci.* (2011) **8**:1011–39. doi: 10.1166/jctn.2011.1781
63. De Raedt H, Michielsen K, Hess K. The photon identification loophole in EPRB experiments: computer models with single-wing selection. *Open Phys.* (2017) **15**:713–33. doi: 10.1515/phys-2017-0085
64. De Raedt K, Keimpema K, De Raedt H, Michielsen K, Miyashita S. A local realist model for correlations of the singlet state. *Eur Phys J B.* (2006) **53**:139–42. doi: 10.1140/epjb/e2006-00364-9
65. Zhao S, De Raedt H, Michielsen K. Event-by-event simulation model of Einstein-Podolsky-Rosen-Bohm experiments. *Found Phys.* (2008) **38**:322–47. doi: 10.1007/s10701-008-9205-5
66. Michielsen K, Jin F, De Raedt H. Event-based corpuscular model for quantum optics experiments. *J Comput Theor Nanosci.* (2011) **8**:1052–80. doi: 10.1166/jctn.2011.1783
67. Pearle PM. Hidden-variable example based upon data rejection. *Phys Rev D.* (1970) **2**:1418–25. doi: 10.1103/PhysRevD.2.1418
68. Pascazio S. Time and Bell-type inequalities. *Phys Lett A.* (1986) **118**:47–53. doi: 10.1016/0375-9601(86)90645-6
69. Pascazio S. On emission lifetimes in atomic cascade tests of the Bell inequality. *Phys Lett A.* (1987) **126**:163–7. doi: 10.1016/0375-9601(87)90452-X
70. De Raedt H, Katsnelson MI, Michielsen K. Quantum theory as the most robust description of reproducible experiments. *Ann Phys.* (2014) **347**:45–73. doi: 10.1016/j.aop.2014.04.021
71. De Raedt H, De Raedt K, Michielsen K, Keimpema K, Miyashita S. Event-based computer simulation model of aspect-type experiments strictly satisfying Einstein's locality conditions. *J Phys Soc Jpn.* (2007) **76**:104005. doi: 10.1143/JPSJ.76.104005

Conflict of Interest: The authors declare that the research was conducted in the absence of any commercial or financial relationships that could be construed as a potential conflict of interest.

APPENDIX A: QUANTUM THEORY OF THE (E)EPRB EXPERIMENT

For reference, we briefly review the quantum-theoretical description of the EPRB and EEPRB experiment. In this appendix, for the sake of generality, we first consider magnetic spin-1/2 particles passing through Stern-Gerlach magnets.

In the context of (E)EPRB experiments, the case of interest is a system of two spins in the singlet state, described by the density matrix

$$\rho = \frac{\mathbb{1} - \boldsymbol{\sigma}_1 \cdot \boldsymbol{\sigma}_2}{4} = \frac{1}{2}\begin{pmatrix} 0 & 0 & 0 & 0 \\ 0 & +1 & -1 & 0 \\ 0 & -1 & +1 & 0 \\ 0 & 0 & 0 & 0 \end{pmatrix} = \left(\frac{|\uparrow\downarrow\rangle - |\downarrow\uparrow\rangle}{\sqrt{2}}\right)\left(\frac{\langle\uparrow\downarrow| - \langle\downarrow\uparrow|}{\sqrt{2}}\right). \tag{A1}$$

A selective measurement on the spin-1/2 particle is described by the operator Ballentine [58]

$$M(S, \boldsymbol{\sigma}, \mathbf{x}) = \frac{\mathbb{1} + S\,\boldsymbol{\sigma}\cdot\mathbf{x}}{2} = M^2(S, \boldsymbol{\sigma}, \mathbf{x}), \tag{A2}$$

projecting a state of the spin-1/2 system onto the eigenstate of $\boldsymbol{\sigma}\cdot\mathbf{x}$ with eigenvalue $S = \pm 1$.

The probabilities to observe the outcomes S_1 and S_2 in an EPRB experiment are given by Ballentine [58]

$$\begin{aligned} P(S_1|\mathbf{a}) &= \mathbf{Tr}\, M(S_1, \boldsymbol{\sigma}_1, \mathbf{a})\ \rho\ M(S_1, \boldsymbol{\sigma}_1, \mathbf{a}) = \mathbf{Tr}\ \rho\ M(S_1, \boldsymbol{\sigma}_1, \mathbf{a})\,, \\ P(S_2|\mathbf{b}) &= \mathbf{Tr}\, M(S_2, \boldsymbol{\sigma}_2, \mathbf{b})\ \rho\ M(S_2, \boldsymbol{\sigma}_2, \mathbf{b}) = \mathbf{Tr}\ \ \rho\ M(S_2, \boldsymbol{\sigma}_2, \mathbf{b})\,, \end{aligned} \tag{A3}$$

respectively. For two spin-1/2 particles in the singlet state Equation (A1), we have $P(S_1|\mathbf{a}) = \langle\boldsymbol{\sigma}_1\cdot\mathbf{a}\rangle = 1/2$ and $P(S_2|\mathbf{b}) = \langle\boldsymbol{\sigma}_2\cdot\mathbf{b}\rangle = 1/2$, The probability to observe the joint event (S_1, S_2) is given by Ballentine [58]

$$\begin{aligned} &P(S_1, S_2|\mathbf{a}, \mathbf{b}) \\ &= \mathbf{Tr}\, M(S_2, \boldsymbol{\sigma}_2, \mathbf{b}) M(S_1, \boldsymbol{\sigma}_1, \mathbf{a})\ \rho\ M(S_1, \boldsymbol{\sigma}_1, \mathbf{a}) M(S_2, \boldsymbol{\sigma}_2, \mathbf{b}) \\ &= \mathbf{Tr}\ \rho\ M(S_1, \boldsymbol{\sigma}_1, \mathbf{a}) M(S_2, \boldsymbol{\sigma}_2, \mathbf{b}), \end{aligned} \tag{A4}$$

where we used the fact that $[M(S_1, \boldsymbol{\sigma}_1, \mathbf{a}), M(S_2, \boldsymbol{\sigma}_2, \mathbf{b})] = 0$ for all $\mathbf{a}$ and $\mathbf{b}$. For two spin-1/2 particles in the singlet state Equation (A1), Equation (A4) becomes

$$P(S_1, S_2|\mathbf{a}, \mathbf{b}) = \frac{1 - S_1 S_2\ \mathbf{a}\cdot\mathbf{b}}{4}. \tag{A5}$$

Similarly, the probability to observe the joint event (S_1, S_2, S_3, S_4) is given by

$$\begin{aligned} P(S_1, S_2, S_3, S_4|\mathbf{a}, \mathbf{b}, \mathbf{c}, \mathbf{d}) &= \mathbf{Tr}\left[M(S_4, \boldsymbol{\sigma}_2, \mathbf{d}) M(S_3, \boldsymbol{\sigma}_1, \mathbf{c})\right. \\ &\quad M(S_2, \boldsymbol{\sigma}_2, \mathbf{b}) M(S_1, \boldsymbol{\sigma}_1, \mathbf{a}) \rho\ M(S_1, \boldsymbol{\sigma}_1, \mathbf{a}) \\ &\quad \left. M(S_2, \boldsymbol{\sigma}_2, \mathbf{b}) M(S_3, \boldsymbol{\sigma}_1, \mathbf{c}) M(S_4, \boldsymbol{\sigma}_2, \mathbf{d})\right] \\ &= \mathbf{Tr}\left[\rho\ M(S_1, \boldsymbol{\sigma}_1, \mathbf{a}) M(S_3, \boldsymbol{\sigma}_1, \mathbf{c})\right. \\ &\quad M(S_1, \boldsymbol{\sigma}_1, \mathbf{a}) M(S_2, \boldsymbol{\sigma}_2, \mathbf{b}) M(S_4, \boldsymbol{\sigma}_2, \mathbf{d}) \\ &\quad \left. M(S_2, \boldsymbol{\sigma}_2, \mathbf{b})\right]. \end{aligned} \tag{A6}$$

Performing the matrix multiplications and calculating the trace we obtain

$$\begin{aligned} P(S_1, S_2, S_3, S_4|\mathbf{a}, \mathbf{b}, \mathbf{c}, \mathbf{d}, Z) = &\frac{1}{16}\left[1 - S_1 S_2\ \mathbf{a}\cdot\mathbf{b}\right] \\ &\left[1 + S_1 S_3\ \mathbf{a}\cdot\mathbf{c}\right] \\ &\left[1 + S_2 S_4\ \mathbf{b}\cdot\mathbf{d}\right]. \end{aligned} \tag{A7}$$

The derivation of the quantum-theoretical description of an experiment with photon polarization instead of magnetic spin-1/2 particles is not much different, for details see reference [71]. The upshot is that we only have to replace $\mathbf{a}\cdot\mathbf{b}$ by $\cos 2(a-b)$ etc. Thus, in the case of an EEPRB experiment that uses the polarization of the photons, the probability to observe the joint event (S_1, S_2, S_3, S_4) is given by

$$\begin{aligned} P(S_1, S_2, S_3, S_4|\mathbf{a}, \mathbf{b}, \mathbf{c}, \mathbf{d}, Z) = &\frac{1}{16}\left[1 - S_1 S_2 \cos 2(a-b)\right] \\ &\left[1 + S_1 S_3 \cos 2(a-c)\right] \\ &\left[1 + S_2 S_4 \cos 2(b-d)\right]. \end{aligned} \tag{A8}$$

APPENDIX B: A LIMITATION OF QUANTUM THEORY FOR TWO SPIN-1/2 PARTICLES

If the random polarizations of particles that enter BS1 and BS2 are the same instead of orthogonal, the DES generates data which, within the usual statistical fluctuations, is characterized by $E_1 = E_2 = 0$, and $E_{12} = +\cos 2(a-b)$. In this appendix, we prove that a two-particle system with single-particle averages $\widehat{E}_1 = \widehat{E}_2 = 0$, and pair correlation $\widehat{E}_{12} = +\cos 2(a-b)$ cannot be described by the quantum theory of two spin-1/2 particles. As in **Appendix A**, we consider the general case of two spin-1/2 particles and deal with the case of photon polarization at the end.

Using the Pauli-matrices and the 2×2 unit matrix as a basis of the vector space of 2×2 matrices, we can, without loss of generality, write the 4×4 density matrix of the two-spin system as

$$\widehat{\rho} = \frac{1}{4}\left(\mathbb{1} + \sum_{k=x,y,z} u_k \sigma_1^k + \sum_{k=x,y,z} v_k \sigma_2^k + \sum_{k,l=x,y,z} \sigma_1^k w_{k,l} \sigma_2^l\right), \tag{B1}$$

where the u's and v's are real numbers and the w's are the elements of a Hermitian matrix. According to quantum theory, we then have

$$\begin{aligned} \widehat{E}_1 &= \langle\boldsymbol{\sigma}_1\cdot\mathbf{a}\rangle = \mathbf{Tr}\,\widehat{\rho}\,\boldsymbol{\sigma}_1\cdot\mathbf{a} = \mathbf{u}\cdot\mathbf{a} \\ \widehat{E}_2 &= \langle\boldsymbol{\sigma}_2\cdot\mathbf{b}\rangle = \mathbf{Tr}\,\widehat{\rho}\,\boldsymbol{\sigma}_2\cdot\mathbf{b} = \mathbf{v}\cdot\mathbf{b} \\ \widehat{E}_{12} &= \langle\boldsymbol{\sigma}_1\cdot\mathbf{a}\ \boldsymbol{\sigma}_2\cdot\mathbf{b}\rangle = \mathbf{Tr}\,\widehat{\rho}\,\boldsymbol{\sigma}_1\cdot\mathbf{a}\ \boldsymbol{\sigma}_2\cdot\mathbf{b} = \mathbf{a}^{\mathrm{T}}\cdot\mathbf{w}\cdot\mathbf{b}\,. \end{aligned} \tag{B2}$$

If *for all* unit vectors $\mathbf{a}$ and $\mathbf{b}$ we have $\langle\boldsymbol{\sigma}_1\cdot\mathbf{a}\rangle = \langle\boldsymbol{\sigma}_2\cdot\mathbf{b}\rangle = 0$ and $\langle\boldsymbol{\sigma}_1\cdot\mathbf{a}\ \boldsymbol{\sigma}_2\cdot\mathbf{b}\rangle = -q\,\mathbf{a}\cdot\mathbf{b}$, then $\mathbf{u} = \mathbf{v} = 0$ and $\mathbf{w} = -q\,\mathbb{1}$, implying that

$$\widehat{\rho}_q = \frac{\mathbb{1} - q\,\boldsymbol{\sigma}_1\cdot\boldsymbol{\sigma}_2}{4}\,. \tag{B3}$$

The four eigenvalues of $\boldsymbol{\sigma}_1 \cdot \boldsymbol{\sigma}_2$ are 1, 1, 1, and -3. Therefore, $\widehat{\rho}_q$ has a negative eigenvalue if $q < -1/3$ and in this case $\widehat{\rho}_q$ does not qualify as a density matrix whereas $\widehat{\rho}_{q=1} = (\mathbb{1} - \boldsymbol{\sigma}_1 \cdot \boldsymbol{\sigma}_2)/4$ does (and represents the singlet state).

In summary, there does not exist a quantum-theoretical description in terms of a 4×4 density matrix that yields $\widehat{E}_1 = \widehat{E}_2 = 0$ and $\widehat{E}_{12} = +|q|\mathbf{a}\cdot\mathbf{b}$ or for all unit vectors $\mathbf{a}$ and $\mathbf{b}$ and $|q| > 1/3$. This includes the special case for which $\widehat{E}_{12} = +\cos 2(a-b)$ and $\widehat{E}_1 = \widehat{E}_2 = 0$.

APPENDIX C: PRODUCT STATE

For completeness, we give the expressions for the probabilities for the case that the two photons of each pair leave the source with fixed polarization $\mathbf{p}$ and $\mathbf{q}$, respectively. Instead of Equation (8), we have

$$P(S_1, S_2|\mathbf{a}, \mathbf{b}, Z) = \frac{1 + S_1 \ \cos 2(a-p)}{2} \frac{1 + S_2 \ \cos 2(b-q)}{2}, \tag{C1}$$

and instead of Equation (9), we have

$$\begin{aligned} P(S_1, S_2, S_3, S_4|\mathbf{a}, \mathbf{b}, \mathbf{c}, \mathbf{d}, Z) = &\frac{1}{16}\big[1 + S_1 \ \cos 2(a-p)\big] \\ &\big[1 + S_2 \ \cos 2(b-q)\big] \\ &\big[1 + S_1 S_3 \cos 2(a-c)\big] \\ &\big[1 + S_2 S_4 \cos 2(b-d)\big]. \end{aligned} \tag{C2}$$

Note that Equations (C1) and (C2) also apply to the case of classical optics with $I_0 = 1$.

frontiers in Physics

ORIGINAL RESEARCH
published: 07 May 2020
doi: 10.3389/fphy.2020.00145

Discrete-Event Simulation of Quantum Walks

Madita Willsch[1], *Dennis Willsch*[1], *Kristel Michielsen*[1,2] *and Hans De Raedt*[1,3]*

[1] Jülich Supercomputing Centre, Institute for Advanced Simulation, Forschungszentrum Jülich, Jülich, Germany, [2] RWTH Aachen University, Aachen, Germany, [3] Zernike Institute for Advanced Materials, University of Groningen, Groningen, Netherlands

We use discrete-event simulation on a digital computer to study two different models of experimentally realizable quantum walks. The simulation models comply with Einstein locality, are as "realistic" as the one of the simple random walk in that the particles follow well-defined trajectories, are void of concepts, such as particle-wave duality and wave-function collapse, and reproduce the quantum-theoretical results by means of a cause-and-effect, event-by-event process. Our simulation model for the quantum walk experiment presented in Robens et al. [1] reproduces the result of that experiment. Therefore, the claim that the result of the experiment "rigorously excludes (i.e., falsifies) any explanation of quantum transport based on classical, well-defined trajectories" needs to be revised.

Keywords: quantum walk, quantum theory, subquantum models, discrete event simulation (DES), computer simulation

OPEN ACCESS

Edited by:
Karl Hess,
University of Illinois at Urbana-Champaign, United States

Reviewed by:
Martin Warnke,
Leuphana University, Germany
Theo Nieuwenhuizen,
University of Amsterdam, Netherlands

***Correspondence:**
Hans De Raedt
h.a.de.raedt@rug.nl

Specialty section:
This article was submitted to Mathematical Physics, a section of the journal Frontiers in Physics

Received: *08 March 2020*
Accepted: *14 April 2020*
Published: *07 May 2020*

Citation:
Willsch M, Willsch D, Michielsen K and De Raedt H (2020) Discrete-Event Simulation of Quantum Walks. Front. Phys. 8:145. doi: 10.3389/fphy.2020.00145

1. INTRODUCTION

A particle is said to perform a simple random walk (SRW) over a set of lattice points (enumerated by integers) when at each time step, it jumps to one of its neighboring points, and the direction of the jump is determined by a random variable [2, 3]. Random walks find applications in many diverse fields, too many to list them here.

The term "quantum random walk" was introduced in 1993 [4] and emphasizes the analogy to the simple random walk on a lattice. However, the time evolution of a "quantum random walk" is deterministic and reversible [5], not random at all, so the term *quantum walk* (QW) is more apt. There are various kinds of proposals and implementations of QWs using optical lattices [1, 6, 7], ion traps [8–10], microwave cavities [11], or optical networks [12–14]. A review covering various aspects of QWs is given in Kempe [15].

The basic idea of the QW is similar to that of the SRW. Instead of using a random variable to decide which way to jump, an internal degree of freedom (e.g., spin or polarization) is used to determine the direction of the jump. This internal degree of freedom changes its state according to the rules of quantum theory, that is by a unitary transformation.

For simplicity, in this paper, we consider the case where this state is described by a 2-dimensional Hilbert space (e.g., spin up $|\uparrow\rangle$ and spin down $|\downarrow\rangle$) and the particle makes nearest-neighbor hops on a one-dimensional lattice. Compared to the SRW, the new feature is that at each jump, the state of the spin changes by a unitary transformation, e.g., a Hadamard transformation. The particle moves to the right if the projection of the spin (along the z-axis by convention) is up $|\uparrow\rangle$ and moves to the left if its spin is down $|\downarrow\rangle$.

In symbols, this process is formalized as follows. The basis states of the Hilbert space are $|x, s\rangle$, where $x \in \{-L, \ldots, L\}$ labels the position on the one-dimensional lattice of $X = 2L + 1$ sites, and $s \in \{\uparrow, \downarrow\}$ labels the eigenstates of the z-component of the Pauli matrices describing the internal degree of freedom. In terms of the basis states, the wave function at step l reads

$$|\Phi^{(l)}\rangle = \sum_{x=-L}^{L} \phi^{(l)}_{x,\uparrow}|x,\uparrow\rangle + \phi^{(l)}_{x,\downarrow}|x,\downarrow\rangle \quad , \qquad \sum_{x=-L}^{L} \left|\phi^{(l)}_{x,\uparrow}\right|^2 + \left|\phi^{(l)}_{x,\downarrow}\right|^2 = 1, \tag{1}$$

and is related to the initial state $|\Phi^{(0)}\rangle = |0,\uparrow\rangle$ by

$$|\Phi^{(l)}\rangle = (SH)^l |\Phi^{(0)}\rangle, \tag{2}$$

where

$$S = \sum_{x=-L+1}^{L} |x-1,\uparrow\rangle\langle x,\uparrow| + \sum_{x=-L}^{L-1} |x+1,\downarrow\rangle\langle x,\downarrow| \tag{3}$$

is the operator that implements the particle jump,

$$|\uparrow\rangle\langle\uparrow| = \begin{pmatrix} 1 & 0 \\ 0 & 0 \end{pmatrix}, \quad |\downarrow\rangle\langle\downarrow| = \begin{pmatrix} 0 & 0 \\ 0 & 1 \end{pmatrix}, \quad |\uparrow\rangle\langle\downarrow| = \begin{pmatrix} 0 & 1 \\ 0 & 0 \end{pmatrix}, \quad |\downarrow\rangle\langle\uparrow| = \begin{pmatrix} 0 & 1 \\ 0 & 0 \end{pmatrix} \tag{4}$$

are the spin projection operators, and

$$H = \frac{1}{\sqrt{2}} \begin{pmatrix} 1 & 1 \\ 1 & -1 \end{pmatrix} \tag{5}$$

is the Hadamard operation, acting on the spin degree-of-freedom only. We only consider the case that the number of steps is smaller than or equal to L, meaning that the particle initially localized at $x = 0$ never goes beyond the boundaries of the lattice.

QWs are different from SRWs in that the latter cannot display interference phenomena whereas the former, being described in terms of the evolution of a wave function, can. In addition, the probability distribution of a QW (starting from the initial state $|\Phi^{(0)}\rangle = |0,\uparrow\rangle$) is not necessarily symmetric w.r.t. $x = 0$, unlike the probability distribution of a SRW for a particle initially at $x = 0$. Furthermore, the variance of x is non-linear in the number of steps L [15].

There are two distinct views of the formulation of the QW. The first uses the particle picture to spell out the rules by which a particle changes its position and spin. Although the spin is often regarded as a characteristic quantum feature, if there is only one spin in play, we can equally well represent this spin by a unit vector on a Bloch sphere, a genuine classical-mechanical construct. The quantization of the spin only enters through the digitalization of its projection on the z-axis, a process very similar to the tossing of a coin, which during its flight usually rotates. This pictorial description of the motion of a **single** particle is as "realistic" as the one of the SRW. Indeed, at any time the particle is at a definite position and the measurement of the internal degree of freedom yields an unpredictable outcome (the mapping of the unit vector to "spin-up" or "spin-down"), determining the direction of the jump.

In the second view of the formulation of the QW, use of wave mechanics is made in order to describe the evolution of a collection of particles, prepared in the same initial state (position and spin). The realistic view is lost when we impose that the time evolution of a single particle and its internal degree of freedom are to be described in terms of a wave function that evolves in time according to the rules of quantum theory, Equation (2) in the case at hand.

2. AIM OF THE PAPER

In this paper, we demonstrate that QWs can be modeled without ever having to resort to the notion of particle-wave duality, the wave function of the particle, the update rule Equation (2), etc. Specifically, we show that it is possible to construct a discrete-event simulation (DES) that is as realistic as the model of the SRW, complies with Einstein's notion of local causality [16], and reproduces the results of quantum theory without using expressions, such as Equations (1) or (2). In this respect, DES constitutes a "subquantum" model that agrees with the statistical results of quantum theory but additionally gives a description in terms of individual events in contrast to quantum theory which only gives collective, statistical predictions.

DES is a general methodology for simulating the time evolution of a system as a discrete sequence of consecutive events. In the application at hand, there are four different kinds of events, namely a particle starting its walk, an operation acting on the second degree of freedom (e.g., the spin) of a particle, a particle moving from one lattice site to the next according to the state of the second degree of freedom, and a particle being counted and removed by detectors positioned at each of the lattice sites and activated after a particle made the maximum number of allowed jumps.

Simulation of a SRW is one of the simplest applications of DES. In the DES of both the SRW and the QW, each walker follows a well-defined trajectory but in contrast to the former, the latter yields distributions of particles over the lattice which agree with the quantum-theoretical prediction, not with a distribution originating from a diffusion process.

We also use DES to reproduce the experimental data of a particular QW experiment with atoms [1], which "rigorously excludes (i.e., falsifies) any explanation of quantum transport based on classical, well-defined trajectories," in blatant contradiction with the fact that each of the particles in the DES follows a well-defined trajectory and the DES reproduces the experimental data. In particular, we show that the DES can produce data that either violates or does not violate the Leggett-Garg inequality (LGI) [17], depending on the treatment of the data [18, 19]. This implies that the QW by itself is not the cause of a violation of the LGI. Note that in DES it is trivial to perform non-invasive measurements, an essential requirement for the application of the LGI [17].

3. DISCRETE-EVENT SIMULATION

For our demonstration, we build on the DES approach introduced in De Raedt et al. [20], which reproduces the

experimental and quantum-theoretical results of many fundamental quantum-physics experiments with photons and neutrons [21]. In essence, we use DES on a digital computer as a metaphor for a perfect laboratory experiment [22]. A salient feature of any DES implementation is that all variables which enter the model have definite values and are known at all times. The application of DES to the QW is based on the following ideas:

1. The moving object is treated as a particle carrying a unit vector and making nearest-neighbor jumps on a one-dimensional lattice.
2. There are "processing units" which can be thought of as being placed on the lattice sites. Depending on the unit vector that the particle carries when it enters a processing unit, the latter may rotate the unit vector and tell the particle where to jump to.
3. Each particle can only take one definite path. In this sense, our DES of a QW is as "realistic" as the DES of a SRW.
4. A particle can arrive at only one detector. The function of the detector is to count the particle and to remove it from the lattice. Each detection event is caused by exactly one particle making a walk. Of course, being a simulation on a digital computer, during the DES, the position of the particle and its unit vector can be "read out" at any time, without disturbing anything.
5. A particle is not allowed to start its walk as long as there is another particle present on the lattice, implying that there can be no direct interaction between particles.
6. Interference results from the adaptive dynamics of the processing units. In the case at hand, a processing unit models a beam splitter with two input and two output ports (see below). Input to such a processing unit are the port at which the particle enters and the orientation of the unit vector. The adaptive dynamics changes the internal state of the processing unit in a deterministic manner. The internal state determines the output port by which a particle leaves the processing unit.
7. After processing many particles (100,000 in the case at hand), the relative frequencies of the detector counts agree with the probabilities obtained from the quantum-theoretical description.

In a DES, we can read off, at any time, the value of a physical quantity without changing the state of the system and we explicitly exclude from consideration DES implementations that violate Einstein's criterion of local causality. Specifically, our DES models satisfy the locality criteria of category 0, as defined in Hess [16], that is they are void of interactions (such as those appearing in the hydrodynamic/Bohm interpretation of quantum theory [23, 24]) that violate Einstein's criterion of local causality. In summary, our DES approach satisfies the criteria for a local realist model.

Our DES is manifestly "non-quantum mechanical" in the sense that there is no wave function describing the state of the particle in space-time but instead there are definite particle trajectories. Still the rules by which these trajectories are formed cannot be described by "Newtonian mechanics." Clearly, without calling upon magic, one cannot have individual particles following well-defined trajectories interfere unless there is a mechanism at work that provides some form of indirect communication between successive particles starting their walk. As mentioned in 6 above, in our DES approach, this indirect communication is the result of the adaptive (non-Newtonian) dynamics of the processing unit.

At this point of the discussion, we wish to draw attention to a paper of Duane [25]. Duane proposed that, in addition to the quantum rules for energy and angular momentum, there is a similar rule for the linear momentum and then showed that with this rule one can explain the diffraction of X-rays from a crystal without reference to interference of waves [25]. In plain words, the key point of Duane's work may be formulated as follows: there is no reason to attach a wave function to a particle if there is plenty of wave-like motion in the crystal with which the X-rays interact. At the time of the development of quantum theory, the latter experiment was generally taken as strong evidence for the dual particle-wave character. An extensive discussion of the negative impact of the particle-wave duality and the development of a deeper understanding of where quantum theory comes from and what it entails is given by Landé in a series of papers [26–29] and a book [30].

We mention Duane's work [25] here because in essence, a similar idea is also used to construct the rules of operation for the processing units in our DES. Indeed, a quick glance at the structure of the DES algorithm for a beam splitter [20, 21] shows that the internal state of this unit is represented by a real-valued vector of length two and a complex-valued vector of length four. The decision about the port at which the particle leaves the beam splitter involves the combination of these two vectors and a multiplication by a 4×4 unitary matrix. In other words, we have attached a kind of "wave function" to the material (of the beam splitter), meaning that this "wave function" is local to the device. In the case of a beam splitter for light, the internal state, the "wave function," is just another word for the electrical polarization vector of the material [21] and has little relation to the particle wave function that appears in quantum theory. An essential ingredient of the processing unit, its capability of adapting (learning) its state from the particles that it receives on its input ports, as well as the rule to send particles out, cannot be inferred from the work of Duane. They are designed such that the DES is able to reproduce, event-by-event (particle-by-particle), in a cause-and-effect manner, the values of the probabilities predicted by quantum theory [20, 21].

4. DISCRETE-EVENT SIMULATION OF A QW

In this section, we present the results of a DES for a QW on a line which can be implemented by a network of beam splitters, phase shifters and photodetectors [12]. An interesting point of this implementation is that light waves can be used to simulate the QW, i.e., we can use Maxwell's equations for electromagnetic waves to simulate a quantum system. Of course, this is not really a surprise as the description of beam splitters, phase shifters etc.,

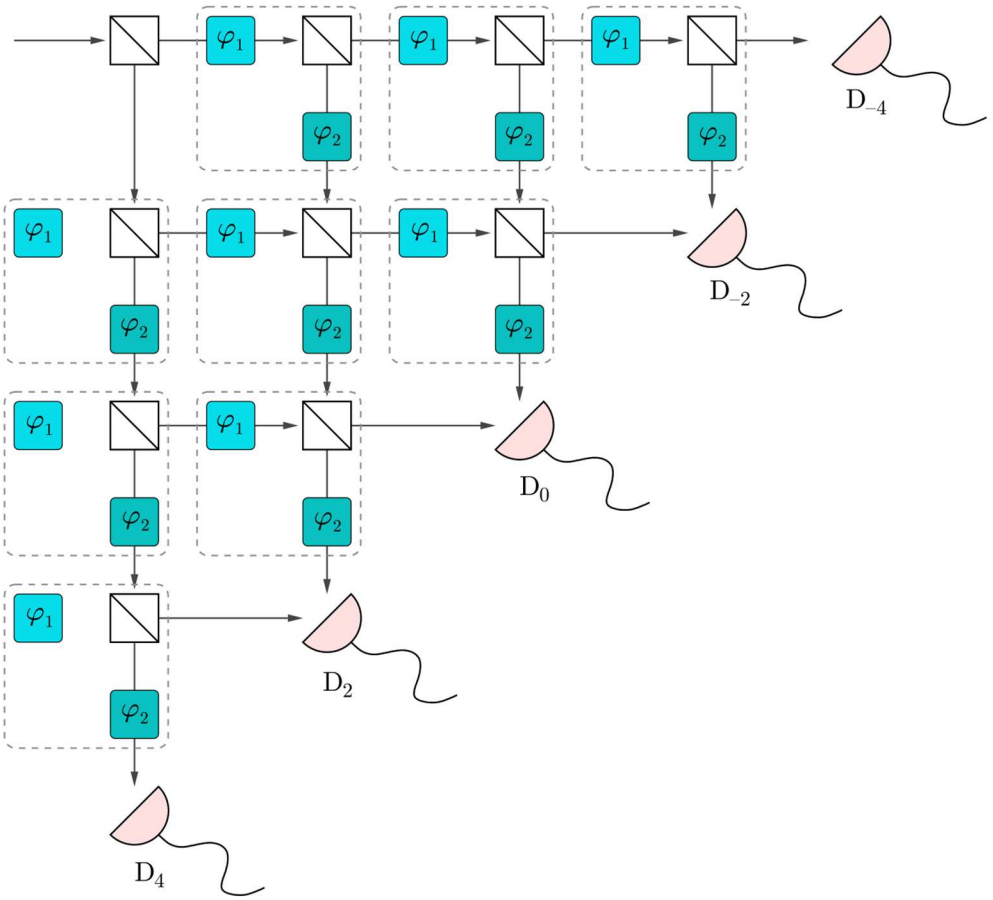

FIGURE 1 | Setup of a realization of a QW experiment [12] on a line of $L = 4$ levels ($X = 9$ lattice sites). The solid (cyan) boxes represent phase shifters, shifting the phase of the wave by angles φ_1 or φ_2, respectively. Open squares with a diagonal line represent 50:50 beam splitters. Half circles (pink) with a tail denote detectors at level 4, placed at lattice sites $x = -4, -2, 0, 2, 4$. Each group of three processing units, marked by a dashed border, causes the particle to jump left or right.

uses Jones-vector calculus which is, in essence, the same as the quantum-theoretical description in terms of Equations (1)–(5). As explained earlier, the main point of performing a DES for a QW is that it uses an event-by-event, particle-based approach that is as realistic as the description of a SRW and does not rely on the quantum formalism embodied in Equations (1)–(5).

The layout of the proposed experiment is shown in **Figure 1**. The function of the beam splitters is to create the superposition of the two input modes. In Jones-vector calculus or quantum theory (see **Appendix A**), the matrix describing the operation of a beam splitter is given by

$$M_{\mathrm{BS}} = \frac{1}{\sqrt{2}} \begin{pmatrix} 1 & i \\ i & 1 \end{pmatrix}. \tag{6}$$

Two phase shifters, with their Jones matrix representation given by

$$M_{\varphi_1} = \begin{pmatrix} e^{i\varphi_1} & 0 \\ 0 & 1 \end{pmatrix} \quad \text{and} \quad M_{\varphi_2} = \begin{pmatrix} 1 & 0 \\ 0 & e^{i\varphi_2} \end{pmatrix}, \tag{7}$$

respectively, change the phase difference between the two partial waves leaving the beam splitter.

Table 1 summarizes the theoretical results for the QW and the corresponding SRW. For both types of walks, detectors with an odd (even) number x will only register particles if l is also odd (even). From the expressions in **Table 1** it also follows that the probabilities to observe a particle do not depend on φ_1. For more than two steps ($l > 2$) the dependence on φ_2 is sinusoidal, a characteristic feature of interference. Furthermore, the variance is larger than for the SRW and the peak of the distributions is not at the center anymore.

Implementing a DES for a network, such as the one shown in **Figure 1** is straightforward. We simply reuse, over-and-over again and without modification, the event-based algorithms that have been developed to simulate the beam splitter, phase shifter, and detector [21] and connect outputs to inputs of these algorithms strictly according to the diagram in **Figure 1**. As the algorithms for all the different components and the method to stitch them together have been discussed extensively and at great length elsewhere [21], we omit the discussion of these aspects. The reader interested in setting up her/his own DES should

TABLE 1 | Quantum theoretical results for the probabilities of the quantum walk after $l = 1, \ldots, 5$ steps (see **Appendix A** for details on the calculation) for a particle initially localized at $x = 0$.

Step	Lattice site (detector number) x										
l	−5	−4	−3	−2	−1	0	1	2	3	4	5
1	0	0	0	0	$\frac{1}{2}$	0	$\frac{1}{2}$	0	0	0	0
2	0	0	0	$\frac{1}{4}$	0	$\frac{2}{4}$	0	$\frac{1}{4}$	0	0	0
3	0	0	$\frac{1}{8}$	0	$\frac{3}{8}+\frac{2\cos\varphi_2}{8}$	0	$\frac{3}{8}-\frac{2\cos\varphi_2}{8}$	0	$\frac{1}{8}$	0	0
4	0	$\frac{1}{16}$	0	$\frac{4}{16}+\frac{2+4\cos\varphi_2}{16}$	0	$\frac{6}{16}-\frac{4}{16}$	0	$\frac{4}{16}+\frac{2-4\cos\varphi_2}{16}$	0	$\frac{1}{16}$	0
5	$\frac{1}{32}$	0	$\frac{5}{32}+\frac{6+6\cos\varphi_2}{32}$	0	$\frac{10}{32}-\frac{6}{32}$	0	$\frac{10}{32}-\frac{6}{32}$	0	$\frac{5}{32}+\frac{6-6\cos\varphi_2}{32}$	0	$\frac{1}{32}$

*The probabilities only depend on φ_2, not on φ_1. For $l = 1$ and $l = 2$, the probabilities are identical to the ones of the SRW (the first or only term in each column) which are given by $2^{-l}\binom{l}{(x+l)/2}$ if $x+l$ is even and are zero otherwise. For more than two steps, the probabilities in each row exhibit a $\varphi_2 \to \varphi_2+\pi$ symmetry w.r.t. $x = 0$. Interference leads to the differences (red) between the probabilities of the SRW and the QW. The case $\varphi_1 = \pi/2$ and $\varphi_2 = -\pi/2$ is shown in **Figure 1**.*

consult Michielsen and De Raedt [21] and papers cited therein. Details of the implementation, specific for the application to QWs, can be found in Nocon [31]. An example implementation in PYTHON is given in **Appendix B** and available online[1].

Our implementation of the DES of the QW experiment shown in **Figure 1** allows for more than $L = 5$ levels ($X = 11$ sites). In general, the larger the number of beam splitters in the diagram, the larger the number of particles has to be in order for the processors mimicking the beam splitters to adapt sufficiently well to the ratio of particles arriving at the two input ports, i.e., representing the two sides at which photons can enter a beam splitter [20, 21]. Numerical experiments show that sending $N = 100,000$ particles through the network is more than sufficient to go up to $L = 7$ levels ($X = 15$ sites) and to obtain data with good statistics. **Figures 2A–F** shows DES results after $l = 2$ up to $l = 7$ steps and for the phase shifts $\varphi_1 = \pi/2$ and $\varphi_2 = -\pi/2$, as well as the results obtained from the quantum-theoretical description (asterisks). Other asymmetric cases are considered below and in Nocon [31] and can be generated using the program given in **Appendix B**.

The DES outcomes are in full agreement with the quantum-theoretical results. In conclusion, the DES provides a local realist model that reproduces the quantum-theoretical results of the QW.

5. DISCRETE-EVENT SIMULATION OF A QW EXPERIMENT WITH ATOMS [1]

Robens et al. experimentally implemented a four-level QW with cesium atoms in a state-dependent optical potential [1]. They made use of the fact that the two hyperfine states of the electronic ground state of the cesium atom, $|F = 4, m_F = 4\rangle$ (pseudo-spin up) and $|F = 3, m_F = 3\rangle$ (pseudo-spin down), experience a different lattice potential [1]. A microwave pulse can change the superposition of these two hyperfine states, and the difference in sensitivity of the $|F = 4, m_F = 4\rangle$ and $|F = 3, m_F = 3\rangle$ states to left- and right-handed polarized light can be used to manipulate the position of the cesium atoms in the state-dependent potential [1].

[1]Available online at: https://jugit.fz-juelich.de/qip/quantum-walk (accessed April 25, 2020).

In the DES, a cesium atom with its two hyperfine states is represented by a particle carrying a two-state spin system. Although we should not think of particles in the DES as objects observed in Nature, to build a mental picture of what the DES is actually doing, it may, for the present purpose, be very helpful to think of a particle and its spin as a single photon and its polarization [32]. Therefore, and also for the uniformity of presentation, we will formulate the DES model of the cesium-atom experiment using the language of optics, using terms like beam splitters, phase shifters, etc. As a matter of fact, as long as the dimension of the Hilbert space is finite, it is always possible to reformulate the original problem as a problem of photons traversing a network of optical components [33] or, equivalently, as a quantum gate circuit [34].

The basic ingredients of the DES are then the following [31]. Distinguishing the cesium atoms on the basis of their hyperfine state is implemented as the action of a polarizing beam splitter, separating h and v polarized photons (relative to the entrance surface of the first polarizing beam splitter in **Figure 3**). In the context of the experiment, h (v) corresponds to the hyperfine states $|F = 4, m_F = 4\rangle$ ($|F = 3, m_F = 3\rangle$). The creation of the superposition of the hyperfine states is realized by Hadamard transformations, i.e., a combination of half-wave plates and $\pi/2$ phase shifters [21, 31]. As h and v polarized photons do not interfere, instead of the 50:50 beam splitters used in the DES of the QW model studied in section 4, we use polarizing beam splitters in order to let h and v polarized photons interfere [31]. A sample implementation of the DES is given in **Appendix B**.

The "photonics" DES network that corresponds to the experiment with the cesium atoms [1] is depicted in **Figure 3**. Looking at **Figure 3**, it is easy to see that some of the polarizing beam splitters (those that show only one input and one output line) can be removed without affecting the operation of the network. However, in our DES, we do not "optimize" the network for computational efficiency. As a matter of fact, the DES of the network in **Figure 3** is so fast that optimization is not worth the effort (the original implementation was written in C++ [31], but even the demonstration in PYTHON given in **Appendix B** only takes a few seconds).

Figures 4A–C shows that the DES reproduces the experimental results of Robens et al. [1]. For convenience,

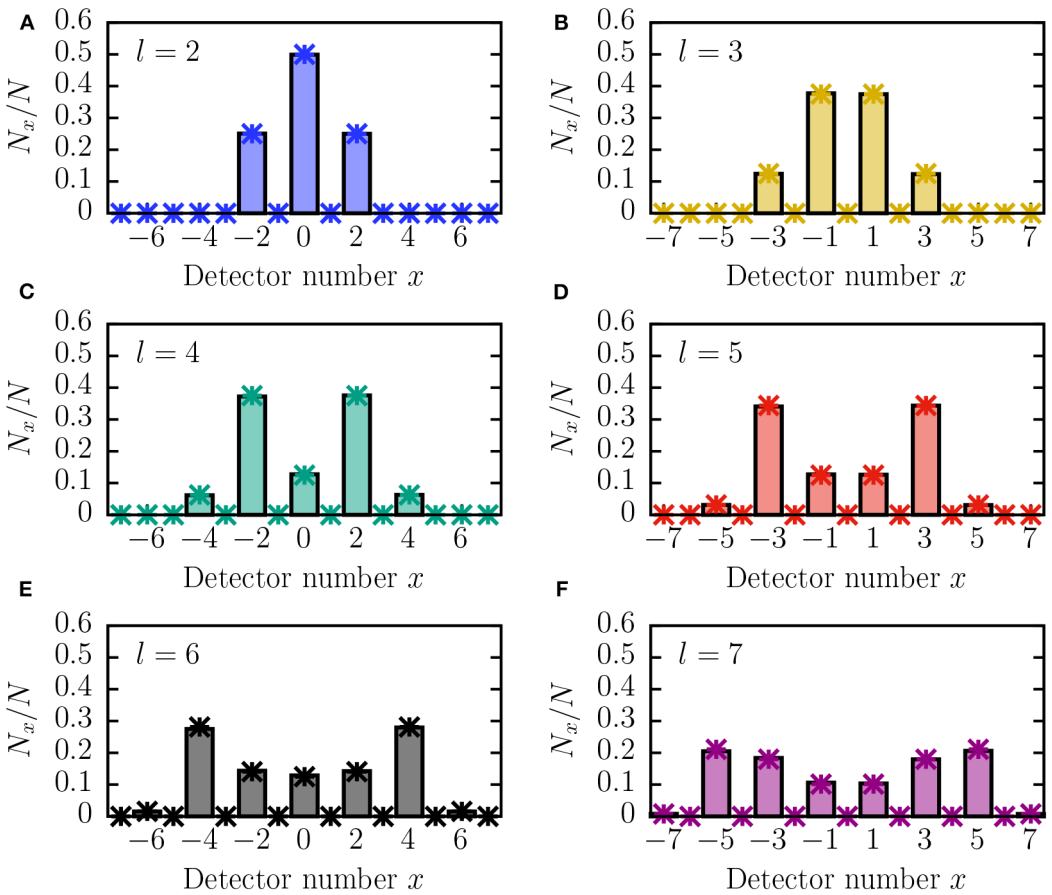

FIGURE 2 | Results for the normalized number of detector counts N_x/N as a function of the detector number x, obtained by a DES of the QW for $N = 100,000$ repetitions, $\varphi_1 = \pi/2$ and $\varphi_2 = -\pi/2$ and for different numbers of steps $l = 2, \ldots, 7$, corresponding to **(A–F)**. The distributions from the DES (bars) match with the analytical results for the QW (asterisks, see **Table 1**). For more than 3 steps, the distributions of the QW are broader than those of the SRW (see **Table 1**) because of interference effects.

the experimental data have been read off from Figures 3A–C of Robens et al. [1], normalized, and plotted as striped bars in **Figures 4A–C**. Furthermore, we see that the DES produces the quantum-theoretical results of the asymmetric four-step QW (asterisks).

The agreement between the DES and experimental data proves that, in contrast to the claim made in Robens et al. [1], it is possible, to describe a QW without a particle wave function, but with particles following individual trajectories that are as well-defined as in the case of a SRW, and local "wave functions" attached to each polarizing beam splitter [21]. We remark that the `learningrate` parameter of the beam splitters (see **Appendix B**) can be used to tune the "quantumness" of the DES such that `learningrate` $= 0$ yields the SRW and $0.9 \leq$ `learningrate` ≤ 0.98 yields the QW.

Obviously, the agreement between the DES and experimental data seems to be in conflict with the common lore that local realist models, such as a DES cannot reproduce certain results of quantum physics. It is therefore of interest to explore whether this conflict is fundamental or not. Recall that by construction, our DES model of the QW complies with the category 0 locality criteria, as defined in Hess [16].

Robens et al. support their claim that the QW experiment "rigorously excludes (i.e., falsifies) any explanation of quantum transport based on classical, well-defined trajectories" by demonstrating a violation of a LGI [1]

$$K = \langle Q(t_2)Q(t_1)\rangle + \langle Q(t_3)Q(t_2)\rangle - \langle Q(t_3)Q(t_1)\rangle \leq 1, \qquad (8)$$

where the $Q(t_i)$ are real numbers with $|Q(t_i)| \leq 1$ and t_i denote the position at which the measurements are performed (equivalent to the time in the original formulation of the LGI). We demonstrate, by means of a DES of their experiment, that their claim is unfounded.

5.1. Procedure Applied in the Experiment [1]

Robens et al. set $t_1 = 0$ (initial state preparation $|\Phi^{(0)}\rangle = |x = 0, \uparrow\rangle$, start of a single-particle walk), $t_2 = 1$ (after the first single-atom jump), and $t_3 = 4$ (after the fourth single-atom jump). In **Figure 3**, each single-atom jump corresponds to

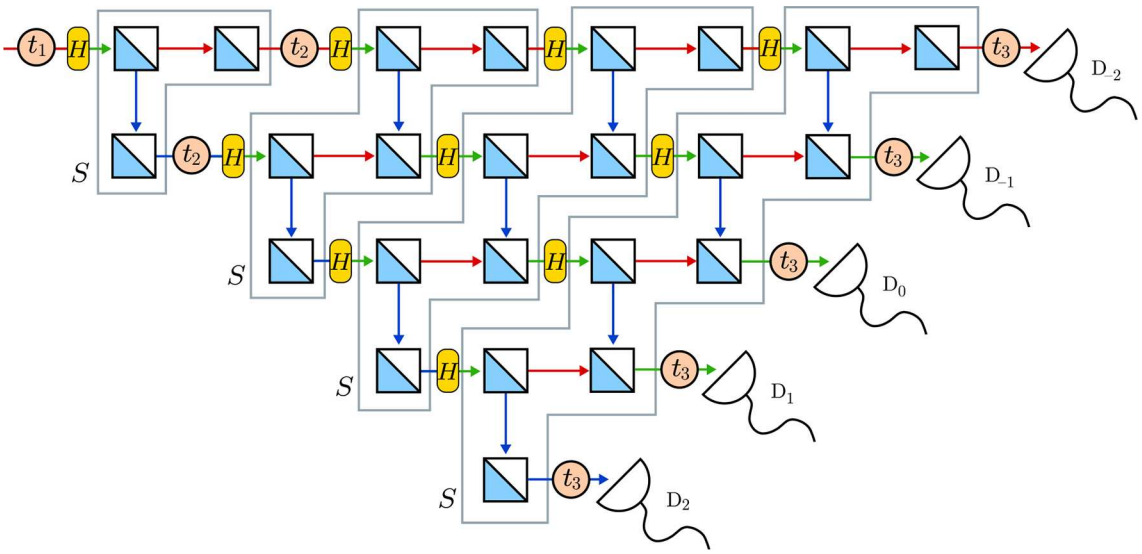

FIGURE 3 | DES setup for the QW with polarized single photons of the same energy. Red horizontal (blue vertical) lines show the path of *h* (*v*) polarized photons. Green lines represent the path of photons with a linear combination of *h* and *v* polarization. The input to the network consists of *h* polarized photons only. Square (blue/white) boxes represent polarizing beam splitters. The oval (yellow) boxes perform a Hadamard transformation on the photon polarization. Each gray region corresponds to a single-atom jump operation in the QW experiment [1]. In quantum theory, the *H* boxes correspond to Equation (5) and the *S* regions correspond to Equation (3). Circles with labels t_1, t_2, and t_3 denote the positions of the $Q(t_1)$, $Q(t_2)$, and $Q(t_3)$ measurements, respectively.

a transition from one gray region to the next. Circles with the labels t_1, t_2, and t_3 indicate the corresponding positions in the DES. Robens et al. proceed by choosing $Q(t_1) = Q(t_2) = 1$ and assign $Q(t_3) = +1$ if at the fourth step, the particle is observed at $x > 0$, and $Q(t_3) = -1$ otherwise [1]. With these simplifications, Equation (8) reduces to

$$K = 1 + \langle Q(t_3)Q(t_2)\rangle - \langle Q(t_3)\rangle \leq 1. \tag{9}$$

In order to estimate $\langle Q(t_3)\rangle$, Robens et al. repeat the QW experiment about 400 times, and compute the average of the measured $Q(t_3)$ [1]. To estimate $\langle Q(t_3)Q(t_2)\rangle$, Robens et al. need to repeat the same QW procedure two times in addition. In the first (second) repetition, they measure the position at t_2, by what they believe is an ideal negative measurement, and remove atoms that are measured at position $x = 1$ ($x = -1$). We cannot question the extent to which they really implemented an ideal negative measurement in their experiment. In our DES of this experiment, however, it is trivial to perform an ideal negative measurement. In both cases, the atoms continue their walk and are finally measured at t_3, yielding either $Q(t_3) = -1$ or $Q(t_3) = +1$. The average of the $Q(t_3)$'s is then denoted by $\langle Q(t_3)\rangle_{x_2}$ where $x_2 \in \{-1, +1\}$ indicates which atoms are kept at t_2.

With this data in hand, Robens et al. compute the left-hand side of Equation (9) as

$$K = 1 + \sum_{x_2=\pm 1} P(x_2;\ t_2)\langle Q(t_3)\rangle_{x_2} - \langle Q(t_3)\rangle, \tag{10}$$

where $P(x_2;\ t_2)$ denotes the probability that the atom was at position $x_2 = \pm 1$ at t_2, the theoretical values being 1/2 (see the $l = 1$ row of **Table 1**). Plugging in the experimentally obtained data, Robens et al. find that [1]

$$K = 1.435 \pm 0.074 > 1, \tag{11}$$

and conclude that the "reported violation of the LG inequality proves that the concept of a well-defined, classical trajectory is incompatible with the results obtained in a quantum-walk experiment [1]." This conclusion is unjustified, as we now show.

5.2. Refutation of the Claim

Our demonstration consists of two steps. First, we show that a DES of the QW performed with the same measurement procedure as the one used by Robens et al. reproduces their experimental results and therefore also produces a violation of the LGI. In this case, the DES also reproduces the results of the quantum-theoretical model in which we block the corresponding path labeled by t_2. Second, because in a DES performing non-invasive measurements is not an issue, there is no need to perform three different runs to measure all the quantities which appear in Equation (9). In fact, one DES run suffices to compute all the quantities that enter the LGI. In this case, the DES also reproduces the quantum-theoretical results of the QW.

In the first step, we adopt the same procedure as in the real experiment [1], namely we perform three DESs for a four-step QW. In each DES run, the number of particles is $N = 100,000$. In the first run, we compute $\langle Q(t_3)\rangle$ without removing particles at position t_2. For the other two runs, at position t_2, we simulate an ideal negative measurement by removing the particles traveling to the right (*h* polarization) and downwards (*v* polarization), respectively, as Robens et al. do in their experiment with the cesium atoms.

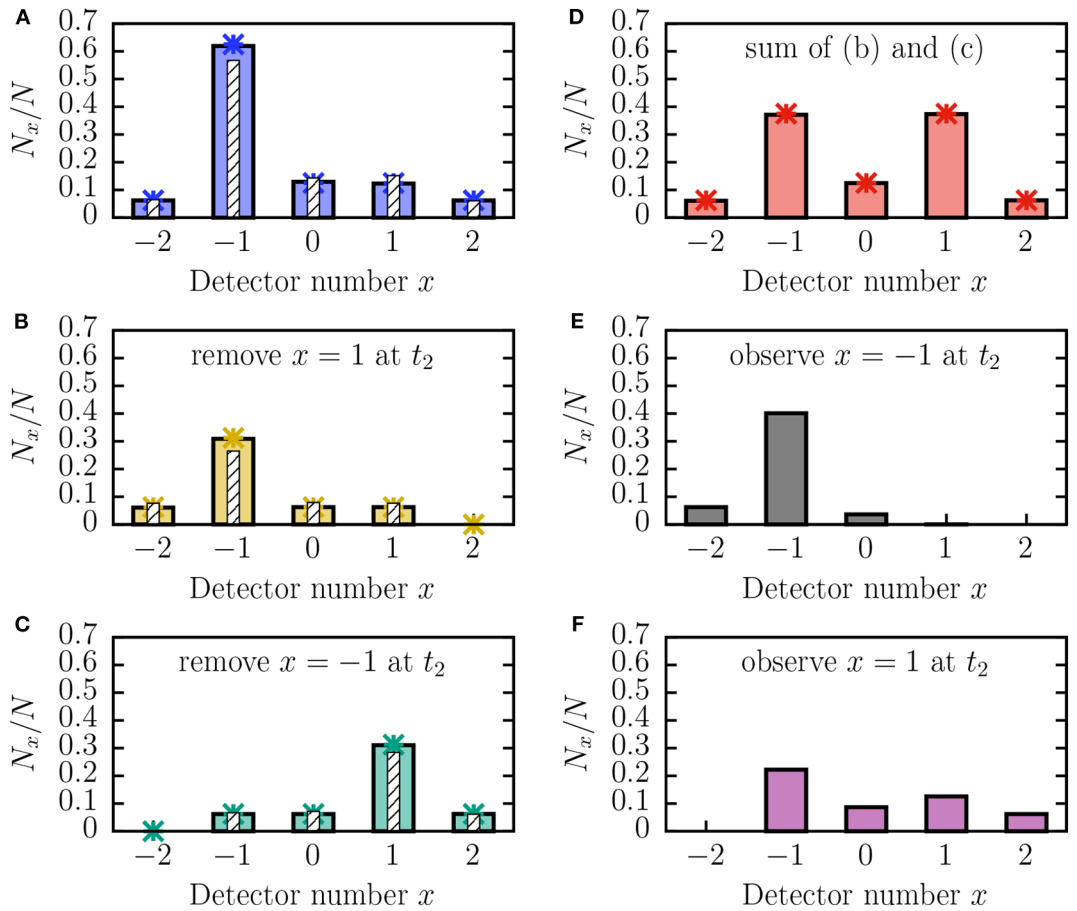

FIGURE 4 | DES results (solid bars) of the normalized detector counts N_x/N as a function of the detector position x. In each run, $N = 100,000$ particles were sent through the network shown in **Figure 3**. In **(A–C)**, the solid bars represent the distribution where at position t_2, **(A)** no particles, **(B)** particles at $x = 1$, **(C)** particles at $x = -1$ have been removed. In **(D)**, the sum of **(B,C)** is shown to be symmetric and equal to the four-step QW shown in **Figure 2C** (for $x \mapsto x/2$). **(E,F)** Show the distributions resulting from only observing (and not removing) the particle at t_2. As their sum yields the distribution in **(A)**, the observation does not affect the result and is thus non-invasive. Asterisks represent the ideal result obtained from quantum theory, i.e., $\sum_s |\langle 2x, s|(SH)^3|\psi\rangle|^2$ where $|\psi\rangle$ is given by **(A)** $SH|0,\uparrow\rangle$, **(B)** $|-1,\uparrow\rangle/\sqrt{2}$, or **(C)** $|+1,\downarrow\rangle/\sqrt{2}$ (see also Equations 2–5). There are no asterisks in **(E,F)** because this information is only accessible in the subquantum model. The corresponding experimental data presented in Figures 3A–C of Robens et al. [1] is (up to a normalization factor) indicated by the striped bars in **(A–C)**.

Direct confirmation that the DES reproduces the experimentally observed results follows from comparing the data obtained using the removal process (see **Figures 4A–C**) with the corresponding data presented in Figures 3A–C of Robens et al. [1]. Up to normalization factors, all results agree. Furthermore, the DES reproduces the quantum-theoretical results for the QW starting at $(t_1, x = 0)$, $(t_2, x = -1)$, and $(t_2, x = +1)$, shown as asterisks in **Figures 4A–C**, respectively.

Next, we compute K as given in Equation (10) from the data of the three different runs. We estimate the statistical error on the value of K by repeating the three different runs ten times and obtain

$$K = 1.497 \pm 0.006 > 1, \tag{12}$$

violating the LGI by several standard deviations. In fact, the value of $K = 1.497 \pm 0.006$ is compatible with the theoretical maximum violation of $K = 1.5$, achievable by this type of experiment [1].

For the second step, we use the DES to perform truly ideal non-invasive "measurements" at t_2. Instead of performing three DES runs (two of them removing certain particles), we perform a single DES run, and only observe the particle's position at t_2 (see Listing 2 in **Appendix B**). We emphasize that in DES, this observation is truly non-invasive.

The resulting counts of the DES are shown in **Figures 4E,F**. From a comparison of **Figures 4B,C** with **Figures 4E,F**, it is immediately clear that there is a significant difference between the counts obtained by the three-run and single-run procedures. Furthermore, the distributions in **Figures 4E,F** add up to the original result in **Figure 4A**. In contrast, the sum of the distributions in **Figures 4B,C**, obtained by the invasive procedure, add up to the symmetric distribution in **Figure 4D**, which is identical to the four-step QW shown in **Figure 2C**.

The relevant question is whether Equation (9) can still be violated. We compute K from the data collected in a single DES of the QW and obtain

$$K = 0.999 \pm 0.002, \tag{13}$$

implying that there is no violation of Equation (9) (up to statistical fluctuations).

The clear difference between results of the three-run and single-run procedure proves that the violation of the LGI by the three-run procedure is not a property of the QW itself. Instead, in the case at issue, the violation of the LGI is the result of using three different experimental scenarios with three different experimental data sets to compute the single quantity K.

It is worth mentioning that the data analysis used in other experiments that report violations of Bell-type inequalities shares similar features, in that correlations are computed from different subsets of a larger data set [22], which has been discussed in terms of the contextuality loophole [18]. Such a procedure can, as Simpson's paradox nicely illustrates [3], lead to all kinds of interesting, paradoxical conclusions.

6. DISCUSSION AND CONCLUSION

In this paper, we have proposed a subquantum model for quantum walks. The model is as realistic as the model for a simple random walk and satisfies Einstein's criterion of locality, and uses a digital computer and a discrete-event simulation algorithm as a metaphor for realizable quantum walk experiments [1, 12]. The subquantum model generates, event-by-event, data that agrees with the quantum-theoretical description of a quantum walk [12].

The subquantum model also reproduces the results of a quantum walk experiment with cesium atoms [1]. In our simulation, the trajectories of each individual particle can be followed. Therefore, the conclusion made in Robens et al. [1] "that the concept of a well-defined, classical trajectory is incompatible with the results obtained in a quantum-walk experiment" is unjustified. The results presented in this paper can be reproduced with the PYTHON programs provided in **Appendix B** and online[1].

Our subquantum model based on discrete-event simulation can reproduce the experimental data of quantum walk experiments as well as many other optics and neutron-interferometry experiments [20–22, 31]. This suggests that standardized software that allows for simulations of single events observed in (quantum) physics experiments may lead to a new kind of theory. Whether the discrete-event simulation approach can be modified/generalized to attain the descriptive power of a theory, formulated in terms of software (i.e., a well-defined set of rules stated in terms of a programming language) rather than in the conventional language of theoretical physics, is a challenging project for future research.

Being a realistic and Einstein-local model, a salient feature of our simulation approach is the absence of concepts, such as particle-wave duality, Born's rule, and other concepts which are characteristic of quantum theory. Regarding the foundations of the latter, it is of interest to mention that one of the rules by which the discrete-event simulation operates requires attaching a kind of "local wave function" to some of the event-based processing units (such as the beam splitters) [20, 21]. This is very reminiscent of a proposal by Duane, who showed that one can explain the diffraction of X-rays from a crystal without reference to interference of waves, by adding, to the quantum rules for energy and angular momentum, a similar rule for the linear momentum [25]. In essence, Duane suggested that instead of invoking the particle-wave character, for model building it may be more effective to let particles (not waves) interact with the multitude of wave-like motion that is already present in the crystal [26]. As we have shown in this paper, this idea can be combined with discrete-event simulation to yield a local realist model for a quantum walk.

DATA AVAILABILITY STATEMENT

The datasets generated for this study are available on request to the corresponding author.

AUTHOR CONTRIBUTIONS

MW, KM, and HD contributed to the conception and design of the DES models. MW, DW, KM, and HD contributed to the writing of the manuscript. DW wrote the python code provided in the Appendix. MW and DW independently performed all simulations.

SUPPLEMENTARY MATERIAL

The Supplementary Material for this article can be found online at: https://www.frontiersin.org/articles/10.3389/fphy.2020.00145/full#supplementary-material

REFERENCES

1. Robens C, Alt W, Meschede D, Emary C, Alberti A. Ideal negative measurements in quantum walks disprove theories based on classical trajectories. *Phys Rev X*. (2015) **5**:011003. doi: 10.1103/PhysRevX.5.011003
2. Pearson K. The problem of the random walk. *Nature*. (1905) **72**:294. doi: 10.1038/072294b0
3. Grimmet GR, Stirzaker DR. *Probability and Random Processes*. Oxford: Clarendon Press (2001).
4. Aharonov Y, Davidovich L, Zagury N. Quantum random walks. *Phys Rev A*. (1993) **48**:1687. doi: 10.1103/PhysRevA.48.1687
5. Knight PL, Roldán E, Sipe JE. Quantum walk on the line as interference phenomena. *Phys Rev A*. (2004) **68**:020301(R). doi: 10.1103/PhysRevA.68.020301

6. Dür W, Raussendorf R, Kendon VM, Briegel HJ. Quantum walks in optical lattices. *Phys Rev A*. (2002) **66**:052319. doi: 10.1103/PhysRevA.66.052319
7. Karski M, Förster L, Choi JM, Steffen A, Alt W, Meschede D, et al. Quantum walk in position space with single optically trapped atoms. *Science*. (2009) **325**:174. doi: 10.1126/science.1174436
8. Travaglione BC, Milburn GJ. Implementing the quantum random walk. *Phys Rev A*. (2002) **65**:032310. doi: 10.1103/PhysRevA.65.032310
9. Schmitz H, Matjeschk R, Schneider C, Glueckert J, Enderlein M, Huber T, et al. Quantum walk of a trapped ion in phase space. *Phys Rev Lett*. (2009) **103**:090504. doi: 10.1103/PhysRevLett.103.090504
10. Zähringer F, Kirchmair G, Gerritsma R, Solano E, Blatt R, Roos CF. Realization of a quantum walk with one and two trapped ions. *Phys Rev Lett*. (2010) **104**:100503. doi: 10.1103/PhysRevLett.104.100503
11. Sanders BC, Bartlett SD. Quantum quincunx in cavity quantum electrodynamics. *Phys Rev A*. (2003) **67**:042305. doi: 10.1103/PhysRevA.67.042305
12. Jeong H, Paternostro M, Kim MS. Simulation of quantum random walks using the interference of a classical field. *Phys Rev A*. (2004) **69**:012310. doi: 10.1103/PhysRevA.69.012310
13. Schreiber A, Cassemiro KN, Potoček V, Gábris A, Mosley PJ, Andersson E, et al. Photons walking the line: a quantum walk with adjustable coin operations. *Phys Rev Lett*. (2010) **104**:050502. doi: 10.1103/PhysRevLett.104.050502
14. Broome MA, Fedrizzi A, Lanyon BP, Kassal I, Aspuru-Guzik A, White AG. Discrete single-photon quantum walks with tunable decoherence. *Phys Rev Lett*. (2010) **104**:153602. doi: 10.1103/PhysRevLett.104.153602
15. Kempe J. Quantum random walks–an introductory overview. *Contemp Phys*. (2003) **44**:307. doi: 10.1080/0010715031000110776
16. Hess K. Categories of nonlocality in EPR theories and the validity of Einstein's separation principle as well as Bell's theorem. *J Mod Phys*. (2019) **10**:1209–21. doi: 10.4236/jmp.2019.1010080
17. Leggett AJ, Garg A. Quantum mechanics versus macroscopic realism: is the flux there when nobody looks. *Phys Rev Lett*. (1985) **9**:857–60. doi: 10.1103/PhysRevLett.54.857
18. Nieuwenhuizen TM. Is the contextuality loophole fatal for the derivation of Bell inequalities? *Found Phys*. (2011) **41**:580–91. doi: 10.1007/s10701-010-9461-z
19. Hess K. *Einstein Was Right!* Singapore: Pan Stanford Publishing (2015). doi: 10.1201/b16809
20. De Raedt K, De Raedt H, Michielsen K. Deterministic event-based simulation of quantum phenomena. *Comp Phys Comm*. (2005) **171**:19–39. doi: 10.1016/j.cpc.2005.04.012
21. Michielsen K, De Raedt H. Event-based simulation of quantum physics experiments. *Int J Mod Phys C*. (2014) **25**:01430003. doi: 10.1142/S0129183114300036
22. De Raedt H, Michielsen K, Hess K. The digital computer as a metaphor for the perfect laboratory experiment: loophole-free Bell experiments. *Comp Phys Comm*. (2016) **209**:42–7. doi: 10.1016/j.cpc.2016.08.010
23. Madelung E. Quantentheorie in hydrodynamischer Form. *Z Phys*. (1927) **40**:322–6. doi: 10.1007/BF01400372
24. Bohm D. A suggested interpretation of the quantum theory in terms of "Hidden" variables. I. *Phys Rev*. (1952) **85**:166–79. doi: 10.1103/PhysRev.85.166
25. Duane W. The transfer of quanta of radiation momentum to matter. *Proc Nat Acad Sci USA*. (1923) **9**:158–64. doi: 10.1073/pnas.9.5.158
26. Landé A. Quantum fact and fiction. *Am J Phys*. (1965) **33**:123–7. doi: 10.1119/1.1971264
27. Landé A. Quantum fact and fiction. II. *Am J Phys*. (1966) **34**:1160–3. doi: 10.1119/1.1972539
28. Landé A. Quantum fact and fiction. III. *Am J Phys*. (1969) **34**:701–4. doi: 10.1119/1.9717
29. Landé A. Quantum fact and fiction. IV. *Am J Phys*. (1975) **43**:701–4.
30. Landé A. *New Foundations of Quantum Mechanics*. Cambridge: Cambridge University Press (2015).
31. Nocon M. *Discrete-Event Simulations of Quantum Random Walks, Quantum Key Distribution, and Related Experiments*. RWTH Aachen (2016). Available online at: http://juser.fz-juelich.de/record/819152
32. Zhao Z, Du J, Li H, Yang T, Chen ZB, Pan JW. Implement quantum random walks with linear optics elements. *arXiv*. (2002) quant-ph/0212149.
33. Reck M, Zeilinger A, Bernstein HJ, Bertani P. Experimental realization of any discrete unitary operator. *Phys Rev Lett*. (1994) **73**:58–61. doi: 10.1103/PhysRevLett.73.58
34. Nielsen M, Chuang I. *Quantum Computation and Quantum Information*. Cambridge: Cambridge University Press (2000).

Conflict of Interest: The authors declare that the research was conducted in the absence of any commercial or financial relationships that could be construed as a potential conflict of interest.

frontiers in Physics

REVIEW
published: 23 September 2020
doi: 10.3389/fphy.2020.00273

Is the Moon There If Nobody Looks: Bell Inequalities and Physical Reality

*Marian Kupczynski**

Département d'informatique et d'ingénierie, Université du Québec en Outaouais, Gatineau, QC, Canada

Bell-CHSH inequalities are trivial algebraic properties satisfied by each line of an Nx4 spreadsheet containing ±1 entries, thus it is surprising that their violation in some experiments allows us to speculate about the existence of non-local influences in nature and casts doubt on the existence of the objective external physical reality. Such speculations are rooted in incorrect interpretations of quantum mechanics and in a failure of local realistic hidden variable models to reproduce quantum predictions for spin polarization correlation experiments (SPCE). In these models, one uses a counterfactual joint probability distribution of only pairwise measurable random variables (A, A′, B, B′) to prove Bell-CHSH inequalities. In SPCE, Alice and Bob, using 4 incompatible pairs of experimental settings, estimate imperfect correlations between clicks registered by their detectors. Clicks announce the detection of photons and are coded by ±1. Expectations of corresponding random variables—E (AB), E (AB′), E (A′B), and E (A′B′)—are estimated and compared with quantum predictions. These estimates significantly violate CHSH inequalities. Since variables (A, A′) and (B, B′) cannot be measured jointly, neither Nx4 spreadsheets nor a joint probability distribution of (A, A′, B, B′) exist, thus Bell-CHSH inequalities may not be derived. Nevertheless, imperfect correlations between clicks in SPCE may be explained in a locally causal way, if contextual setting-dependent parameters describing measuring instruments are correctly included in the description. The violation of Bell-CHSH inequalities may not therefore justify the existence of a spooky action at the distance, super-determinism, or speculations that an electron can be both here and a meter away at the same time. In this paper we review and rephrase several arguments proving that such conclusions are unfounded. Entangled photon pairs cannot be described as pairs of socks nor as pairs of fair dice producing in each trial perfectly correlated outcomes. Thus, the violation of inequalities confirms only that the measurement outcomes and 'the fate of photons' are not predetermined before the experiment is done. It does not allow for doubt regarding the objective existence of atoms, electrons, and other invisible elementary particles which are the building blocks of the visible world around us.

Keywords: quantum non-locality, counterfactual definiteness, local realism, non-invasive measurability, Tsirelson bound, EPR paradox, Bell-CHSH inequalities

OPEN ACCESS

Edited by:
Ana Maria Cetto, Universidad Nacional Autónoma de México, Mexico

Reviewed by:
Sisir Roy, National Institute of Advanced Studies, India
Theo Nieuwenhuizen, University of Amsterdam, Netherlands

***Correspondence:**
Marian Kupczynski
marian.kupczynski@uqo.ca

Specialty section:
This article was submitted to Mathematical and Statistical Physics, a section of the journal Frontiers in Physics

Received: *24 April 2020*
Accepted: *18 June 2020*
Published: *23 September 2020*

Citation:
Kupczynski M (2020) Is the Moon There If Nobody Looks: Bell Inequalities and Physical Reality. Front. Phys. 8:273. doi: 10.3389/fphy.2020.00273

INTRODUCTION

External physical reality existed before we were able to probe it with our senses and experiments. From early childhood, we learn that the objects surrounding us continue to exist even when we stop looking at them.

Another notion imprinted in our genes is the notion of a local causality. If a baby elephant or a baby antelope does not stand up immediately after their birth, they will die. Several events which we observe may be connected by causal chains. The amazing migration patterns and courtship rituals of birds and butterflies are encoded in their genes.

Our brains, evolved over millions of years, allow us to understand that the external physical reality should be governed by natural laws which we can try to discover. We succeeded in explaining observable properties of macroscopic objects assuming the existence of invisible atoms and molecules. Later, we discovered electrons, nuclei, elementary particles, resonances, and various fields that play an important role in the Standard Model. Various conservation laws are obeyed in macroscopic and in quantum phenomena.

Information about the invisible world is indirect and relative to how we probe it. Invisible charged elementary particles leave traces of their passage in photographic emulsion or in different chambers (sparks, bubble, multi-layer, etc.). They also produce clicks on detectors.

We accelerate electrons, protons, and ions and by projecting them on various targets we probe more deeply into the structure of the matter over smaller and smaller distances. We succeeded in trapping electrons and ions. We constructed atomic clocks and ion chips for quantum computing.

It is therefore surprising that the violation of various Bell-type inequalities [1–5] by some correlations between clicks on the detectors observed in spin polarization correlation experiments (SPCE) [6–11] may lead to the conclusion that that there is no objective physical reality, that the electron may be both here and a meter away at the same time, that a measurement performed by Alice in a distant location may change instantaneously an outcome of Bob's measurement or that apparently random choices of experimental settings in SPCE are predetermined due to super-determinism.

The fact that such conclusions are unfounded has been pointed out by several authors [12–83]. The violation of the inequalities confirms only that "*unperformed experiments have no outcomes*" [84], that one may not neglect the interaction of a measuring instrument with a physical system and that the "*non-invasive measurability*" assumption is not valid. It confirms the existence of quantum observables which can only be measured in incompatible experimental contexts.

It also proves that entangled photon pairs, produced in SPCE, may not be described as pairs of socks (local realistic hidden variable models- LRHVM) or as pairs of fair dice (stochastic hidden variable models-SHVM) [1–4].

We are unable to create any consistent *mental picture* of a "photon." We have the same problem with many other elementary particles, but the lack of *mental pictures* does not mean that they do not exist. These invisible particles are building blocks of the visible world around us, including ourselves.

A completely new approach is needed in order to reconcile the quantum theory with the theory of general relativity, and it is not certain whether we are smart enough to find it. We will surely not discover it, however, if we accept *quantum magic* as the explanation of phenomena which we do not understand.

The question in the title of this article was first asked by Einstein during his promenade with Pauli, after it was rephrased in different contexts by Leggett and Garg [85] and Mermin [86]. In this paper, we defend Einstein's position [87–89] as we believe that the moon continues to exist if nobody looks at it.

The paper is organized as follows:

In section Experimental Spreadsheets and Bell-Type Inequalities we show that Bell-CHSH, Leggett-Garg, and Boole inequalities [34, 70, 78, 90] are trivial arithmetic properties of some Nx3 or Nx4 spreadsheets containing ± 1 entries.

In section Local Realistic Models for EPR-Bohm Experiment we define LRHVM and explain why these models cannot reproduce quantum predictions for ideal EPRB experiments which are impossible to implement.

In section Contextual Description of Spin Polarization Correlation Experiments we show how, by incorporating in an LRHVM setting dependent parameters describing measuring instruments, we may explain in a locally causal way correlations between distant outcomes observed in SPCE.

In section Subtle Relationship of Probabilistic Models With Experimental Protocols we explain why Bell-1971 model [2, 91] and Clauser-Horne model [4] are inconsistent with experimental protocols used in SPCE.

In section Quantum Mechanics and CHSH Inequalities we define *quantum CHSH inequality* [92, 93] and Tsirelson bound [92] and we reproduce Khrennikov's recent arguments [43] that the violation of quantum CHSH inequality confirms the local incompatibility of some quantum observables.

In section The Roots of Quantum Non-locality we show that speculations about quantum non-locality are in fact rooted in the incorrect interpretation of von Neumann/Lüders projection postulates [94, 95].

In section Apparent Violations of Bell-Boole Inequalities in Elastic Collision Experiments we discuss simple experiments with elastically colliding metal balls [54] and we explain an apparent violation of Bell-Boole inequalities in these experiments. These experiments allow us to better understand LRHVM and why they fail to describe SPCE.

Section Conclusions contains some conclusions.

EXPERIMENTAL SPREADSHEETS AND BELL-TYPE INEQUALITIES

Let us examine properties of a spreadsheet with four columns each containing N entries ± 1. We may have N-identical rows or 16 different rows permuted in an arbitrary order. The entries may be coded values representing outcomes of some random experiment (e.g., flipping of four fair coins). They may display the results of some population survey or represent daily variations of

some stocks. They also may be created by an artist as a particular visual display. Thus, the columns in the spreadsheet may be finite samples of a particular discrete time-series of data or they can be devoid of any statistical meaning.

If each line of the spreadsheet contains measured values (a. a, b, b′) of jointly distributed random variables (A, A′, B, B′) taking the values ±1 then b = b′ or b = –b′and then:

$$\begin{aligned} |s| &= |ab - ab' + a'b + a'b'| \\ &= |a(b - b')| + |a'(b + b')| \leq 2. \end{aligned} \quad (1)$$

From (1) we immediately obtain CHSH inequality:

$$\begin{aligned} |s| &\leq \sum_{a,a',b,b'} |ab - ab' + a'b + a'b'| \mathrm{p(a, a', b, b')} \\ &\leq |\mathrm{E(AB) - E(AB')}| + |\mathrm{E(A'B) + E(A'B')}| < 2 \end{aligned} \quad (2)$$

where p(a, a, b, b′) is a joint probability distribution of (A, A′, B, B′) and $E(AB) = \sum_{a,b} abp(a, b)$ is a pairwise expectation of A and B obtained using a marginal probability distribution $p(a, b) = \sum_{a',b'} p(a, a', b, b')$.

If A′ = B and B′ = C then E(BB) = 1 and we obtain from (2) Boule and Leggett-Garg inequalities satisfied by three jointly distributed variables (A,B,B′):

$$\begin{aligned} |\mathrm{E(AB)} &- \mathrm{E(AC)}| + 1 + \mathrm{E(BC)} \leq 2 \Rightarrow |\mathrm{E(AB)} \\ &- \mathrm{E(AC)}| \leq 1 - \mathrm{E(BC)} \end{aligned} \quad (3)$$

The Bell (64) inequality $|P(\vec{a}, \vec{b}) - P(\vec{a}, \vec{c})| \leq 1 + P(\vec{b}, \vec{c})$ is a Boole inequality (3) for $P(\vec{a}, \vec{b}) = -E(AB)$, $P(\vec{a}, \vec{c}) = -E(AC)$ and $P(\vec{b}, \vec{c}) = -E(BC)$.

All these inequalities are deduced using the inequality (1) obeyed by any four numbers equal to ±1. The inequalities (2) and (3) are in fact necessary and sufficient conditions for the existence of a joint probability distribution of only pairwise measurable ±1-valued random variables [18, 19].

The inequalities (2) and (3) are of course also valid if |A|≤1, |A′|≤1|, |B|≤1, and |B′|≤1.

LOCAL REALISTIC MODELS FOR EPR-BOHM EXPERIMENT

In physics, Bell-CHSH inequalities [2] were derived in an attempt to reproduce quantum predictions for impossible to implement ideal EPRB experiments [96].

In EPRB experiments a source produces a steady flow of electron- or photon- pairs [60] prepared in a quantum spin-singlet state. One photon is sent to Alice and another to Bob in distant laboratories where they measure photons' spin projections in directions **a** and **b** (**||a||=||b||=1**) and the outcomes "spin up" or "spin down" are coded ±1. There are no losses and for any pair of experimental settings Alice's and Bob's measuring stations output correlated pairs of outcomes.

If Alice and Bob perform their experiments using four pairs of settings [(**a**, **b**); (**a′**, **b**); (**a**, **b′**); and (**a′**, **b′**)], then outcomes ±1 are the values of corresponding 4 binary random variables A_a, $A_{a'}$, B_b, and $B_{b'}$. In [1, 2] these values are determined by some ontic parameters λ (hidden variables) describing pairs of photons when they arrive at Alice's and Bob's measuring stations. Pairwise expectations of measured random variables, in different settings, are all expressed in terms of a unique probability distribution p(λ) defined on an unspecified probability space Λ:

$$\begin{aligned} E(A_aB_b) &= \sum_{\lambda\in\Lambda} A_a(\lambda)B_b(\lambda)p(\lambda) \\ &= \sum_{\lambda} A(\vec{a}, \lambda)B(\vec{b}, \lambda)p(\lambda) \end{aligned} \quad (4)$$

$$\begin{aligned} E(A_aB_{b'}) &= \sum_{\lambda\in\Lambda} A_a(\lambda)B_{b'}(\lambda)p(\lambda) \\ &= \sum_{\lambda} A(\vec{a}, \lambda)B(\vec{b}', \lambda)p(\lambda) \end{aligned} \quad (5)$$

$$\begin{aligned} E(A_{a'}B_b) &= \sum_{\lambda\in\Lambda} A_{a'}(\lambda)B_b(\lambda)p(\lambda) \\ &= \sum_{\lambda} A(\vec{a}', \lambda)B(\vec{b}, \lambda)p(\lambda) \end{aligned} \quad (6)$$

$$\begin{aligned} E(A_{a'}B_{b'}) &= \sum_{\lambda\in\Lambda} A_{a'}(\lambda)B_{b'}(\lambda)p(\lambda) \\ &= \sum_{\lambda} A(\vec{a}', \lambda)B(\vec{b}', \lambda)p(\lambda) \end{aligned} \quad (7)$$

If in (1) we replace $a = A_a(\lambda) = A(\mathbf{a}, \lambda)$, $a' = A_{a'}(\lambda) = A(\mathbf{a'}, \lambda)$, $b = B_b(\lambda) = B(\mathbf{b}, \lambda)$, and $b' = B_{b'}(\lambda) = B(\mathbf{b'}, \lambda)$ we obtain:

$$\begin{aligned} |S| &= \sum_{\lambda} |A(\vec{a}, \lambda)B(\vec{b}, \lambda) - A(\vec{a}, \lambda)B(\vec{b}', \lambda) + A(\vec{a}, \lambda)B(\vec{b}, \lambda) \\ &+ \mathrm{A}(\vec{a}, \lambda)B(\vec{b}', \lambda)|p(\lambda) \leq 2 \end{aligned} \quad (8)$$

Therefore, the expectations (4–7) obey the inequality (2).

Bell used the integration over hidden variables instead of the summation. In agreement with QM, he insisted that one cannot measure simultaneously or in a sequence different spin projections of the same photon, thus the expectations $E(A_a A_{a'} B_b B_{b'})$ have no physical meaning. Nevertheless, the existence of those counterfactual non-vanishing expectations is necessary in order to prove (8). Namely there exists a mapping:

$$\lambda \rightarrow (A_a(\lambda), A_{a'}(\lambda), B_b(\lambda), B_{b'}(\lambda)) = (a, a', b, b') \quad (9)$$

which defines a joint probability distribution p(a, a′, b, b′) and a non-vanishing counterfactual expectation $E(A_a A_{a'} B_b B_{b'})$ [56, 97].

If a joint probability distribution p (a, a′, b, b′) does not exist, the inequalities (2) and (8) cannot be derived. According to QM, such joint probability distributions do not exist in EPRB, thus, for some settings, quantum predictions violate CHSH inequalities.

For an ideal EPRB experiment, QM predicts: $E(A_a B_b) = -\mathbf{a}\cdot\mathbf{b} = -\cos\theta$ and $E(A_a) = E(B_b) = 0$. If **b** and **b′** are arbitrary orthogonal unit vectors (**b·b′ = 0**), **a = (b′-b)/$\sqrt{2}$** and **a′ = (b + b′)/$\sqrt{2}$** then **S=[(b′-b)·(b′-b)+(b′ + b)·(b′ + b]/$\sqrt{2}$ =** $4/\sqrt{2} = 2\sqrt{2}$. This value significantly violates CHSH and saturates the

Tsirelson's bound [92], which we discuss in section Quantum Mechanics and CHSH Inequalities.

According to QM: $E(A_aB_a) = -1$ and $E(A_aB_{-a}) = 1$ for any vector **a.** Thus, Alice and Bob when measuring spin projections using the settings (**a**, **a**) and (**a**, **–a**) should obtain perfectly anti-correlated or correlated outcomes, respectively. At the same time, these outcomes are believed to be produced in an *irreducible random way*, thus one encounters an impossible to resolve paradox:

"a pair of dice showing always perfectly correlated outcomes."

In order to reproduce perfect correlations in LRHVM, one abandons the irreducible randomness and assumes that Alice's and Bob's outcomes are predetermined before measurements are done. Therefore, there exists a counterfactual joint probability distribution of all these predetermined outcomes and CHSH inequalities may not be violated [86, 97–99].

Fortunately, this paradox exists only on paper because an ideal EPRB experiment does not exist and in SPCE we neither observe strict correlations nor anti-correlations between clicks.

In the next section we show how imperfect correlations between clicks in SPCE may be explained in a locally causal way without evoking quantum magic.

CONTEXTUAL DESCRIPTION OF SPIN POLARIZATION CORRELATION EXPERIMENTS

In SPCE, correlated signals/photons, sent by some sources, arrive at distant measuring stations and produce clicks on the detectors. There are black counts, laser intensity drifts, photon registration time delays, etc. Detected clicks have time tags which are different for Alice and Bob. One has to identify clicks corresponding to photons that are members of the same entangled "pair of photons" which is a setting- dependent complicated task. Correlated clicks are rare events and estimated correlations depend on the photon-identification procedure used. A detailed discussion regarding how data is gathered and coincidences determined may be found, for example in Hess and Philipp [22], De Raedt et al. [80, 82], Adenier and Khrennikov [100, 101], and Larsen [102].

Even if all the above-mentioned difficulties had not existed, QM would not have predicted perfect correlations for real experiments. Settings of realistic polarizers may not be treated as mathematical vectors [47], but rather as small spherical angles; therefore instead of $E(A_a B_b) = -\mathbf{a}\cdot\mathbf{b} = -\cos\theta$ we obtain:

$$E(A_aB_b = \eta(\vec{a})\eta\vec{b}\int_{Oa}\int_{Ob} -\vec{u}\cdot\vec{v}d\vec{u}d\vec{v} \tag{10}$$

where $O_a = \{\vec{u} \in S^{(2)};\ |1-\vec{u}\cdot\vec{a}| \le \varepsilon\}$ and $O_b = \{\vec{v} \in S^{(2)};\ |1-\vec{v}\cdot\vec{b}| \le \varepsilon\}$

In order to estimate correlations, Alice and Bob have to choose correlated time windows. They retain only pairs of windows containing two types of events: "a click on a detector 1 and a click on a detector 2" or "a click on only one of the detectors." Therefore, in SPCE, random variables describing outcomes of these experiments have three possible values coded as ±1 or 0.

To make a comparison with the notation used in [60] easier, where more details may be found, we denote different pairs of settings by (x, y),…, (x′, y′) and $E(A_xB_y) = E(AB|x,y)$.

Imperfect correlations estimated in SPCE may be reproduced by the following locally causal contextual hidden variable model [59, 60]:

$$E(A_xB_y) = \sum_{\lambda\in\Lambda_{xy}} A_x(\lambda_1,\lambda_x)B_y(\lambda_2,\lambda_y)p_x(\lambda_x)p_y(\lambda_y)p(\lambda_1,\lambda_2) \tag{11}$$

$$E(A_xB_{y'}) = \sum_{\lambda\in\Lambda_{xy'}} A_x(\lambda_1,\lambda_x)B_{y'}(\lambda_2,\lambda_{y'})p_x(\lambda_x)p_{y'}(\lambda_{y'})p(\lambda_1,\lambda_2) \tag{12}$$

$$E(A_{x'}B_y) = \sum_{\lambda\in\Lambda_{x'y}} A_{x'}(\lambda_1,\lambda_{x'})B_y(\lambda_2,\lambda_y)p_{x'}(\lambda_{x'})p_y(\lambda_y)p(\lambda_1,\lambda_2) \tag{13}$$

$$E(A_{x'}B_{y'}) = \sum_{\lambda\in\Lambda_{x'y'}} A_{x'}(\lambda_1,\lambda_{x'})B_{y'}(\lambda_2,\lambda_{y'})p_{x'}(\lambda_{x'})p_{y'}(\lambda_{y'})p(\lambda_1,\lambda_2) \tag{14}$$

$$E(A_x) = \sum_{\lambda\in\Lambda_{xy}} A_x(\lambda_1,\lambda_x)p_x(\lambda_x)p_y(\lambda_y)p(\lambda_1,\lambda_2) \tag{15}$$

$$E(B_y) = \sum_{\lambda\in\Lambda_{xy}} B_y(\lambda_2,\lambda_y)p_x(\lambda_x)p_y(\lambda_y)p(\lambda_1,\lambda_2) \tag{16}$$

where $A_x(\lambda_1, \lambda_x) = 0,\pm1$, $A_{x'}(\lambda_1, \lambda_{x'}) = 0,\pm1$, $B_y(\lambda_2, \lambda_y) = 0,\pm1$, and $B_{y'}(\lambda_2, \lambda_{y'}) = 0,\pm1$. Please note that $A_x(\lambda_1, \lambda_{x'})$, $A_{x'}(\lambda_1, \lambda_x)$, $B_y(\lambda_2, \lambda_{y'})$, and $B_{y'}(\lambda_2, \lambda_y)$ are undefined. The experiments performed in incompatible settings are described by dedicated probability distributions defined on 4 disjoint hidden variable spaces:

$$\begin{aligned}\Lambda_{xy} &= \Lambda_{12}\times\Lambda_x\times\Lambda_y\,;\,\Lambda_{x'y} = \Lambda_{12}\times\Lambda_{x'}\times\Lambda_y\,;\,\Lambda_{xy'}\\ &= \Lambda_{12}\times\Lambda_x\times\Lambda_{y'}\,;\,\Lambda_{x'y'} = \Lambda_{12}\times\Lambda_{x'}\times\Lambda_{y'}\end{aligned} \tag{17}$$

where $\Lambda_x\bigcap\Lambda_{x'} = \Lambda_y\bigcap\Lambda_{y'} = \varnothing$. Therefore, counterfactual expectations $E(A_x A_{x'})$, $E(B_y B_{y'})$, $E(A_x A_{x'} B_y B_{y'})$ do not exist and Bell and CHSH inequalities may not be derived.

The efficiency of detectors is not 100% and it is difficult to establish correct coincidences between distant clicks because of time delays. These two problems, called efficiency and coincidence-time loopholes, were discussed in detail by Larsen and Gill [103] in terms of the sub-domains of hidden variables corresponding to four experimental settings. They found that CHSH inequality has to be modified:

$$\begin{aligned}|E(A_xB_y|\Lambda_{xy}) &- E(A_xB_{y'}|\Lambda_{xy'})| + |E(A_{x'}B_y|\Lambda_{x'y})\\ &+ E(A_{x'}B_{y'}|\Lambda_{x'y'})| \le 4-2\delta\end{aligned} \tag{18}$$

where $\delta \propto p(\Lambda_{xy}\bigcap\Lambda_{xy'}\bigcap\Lambda_{x'y}\bigcap\Lambda_{x'y'})$. In our model $p(\varnothing) = 0$, thus the only constraint for S in our model is a no-signaling bound: $|S|\le4$.

Our model contains enough free parameters to fit any estimated correlations. For example, if we start with k values of λ_1, k values of λ_2, and m values for each λ_x, $\lambda_{x'}$, $\lambda_{y,}$, and $\lambda_{y'}$ we have km pairs of (λ_1, λ_x), 3^{km} functions $A_x(\lambda_1, \lambda_x)$, and 3^{km} functions $B_y(\lambda_2, \lambda_y)$. We also have m-1 free parameters

for each $p_x(\lambda_x)$, $p_{x'}(\lambda_{x'})$, $p_y(\lambda_y)$, and $p_{y'}(\lambda_{y'})$ and $\left(\frac{k(k+1)}{2}-1\right)$ free parameters for $p(\lambda_1, \lambda_2)$. Thus, we have 4×3^{km} functions to choose and $4(m-1) + k(k-1)/2$ free parameters to fit 32 probabilities or eight expectations estimated in experiments performed using four pairs of settings. If instead of four pairs of settings Alice and Bob use nine pairs of settings, then we may increase m and k as needed to fit 72 probabilities or 12 expectation values, etc.

In mathematical statistics we concentrate on observable events: outcomes of random experiments or results of a population survey. Joint probability distributions are used only to describe random experiments producing several outcomes in each trial e.g., rolling several dice or various data items describing the same individual drawn from some statistical population. Probabilistic models describe a scatter of these outcomes without entering into the details of how outcomes are created.

Hidden variable probabilistic models introduce some invisible "hidden events" which determine subsequent real outcomes of random experiments. In Bell model (4–7), pairs of photons ("beables") are described by λ before measurements take place. Because clicks are predetermined by the values of λ there exists the mapping (9) and the probability distribution of "hidden events" described by $p(\lambda)$ which may be replaced by a joint distribution $p(a, a', b, b')$.

In contextual model (11–17), an outcome of "a click" or "no-click" is not predetermined and is created in a locally causal way in function of a hidden parameter describing a signal ("photon") arriving at the measuring station and a hidden parameter describing a measuring instrument in the moment of their interaction. The model (11–17) gives an insight into how apparently random outcomes are created in SPCE.

In model (4–7) there exists a joint probability distribution of all hidden events labeled by λ. In the model (14–17), hidden events form 4 disjoint probability spaces and there exist only four distinct joint probability distributions $(p_{xy}(\lambda_x, \lambda_1, \lambda_y, \lambda_2)$ on $\Lambda_{xy}, \ldots, p_{x'y'}(\lambda_{x'}, \lambda_1, \lambda_{y'}, \lambda_2)$ on $\Lambda_{x'y'})$. A joint probability distribution of all possible hidden events $(\lambda_x, \lambda_1, \lambda_y, \lambda_2, \lambda_{x'}, \lambda_{y'}, \lambda_2)$ does not exist because hidden events $(\lambda_x, \lambda_{x'})$ and $(\lambda_y, \lambda_{y'})$ may never occur together. This is why one may not prove CHSH assuming the existence of such probability distribution and a non-vanishing $E(A_x A_{x'} B_y B_{y'})$ used to prove (2–3, 8) does not exist.

SUBTLE RELATIONSHIP OF PROBABILISTIC MODELS WITH EXPERIMENTAL PROTOCOLS

In 1971, Bell [91] pointed out that whilst one may incorporate into his model additional hidden variables describing measuring instruments, it does not invalidate his conclusions because after the averaging over instrument variables the pairwise expectations still have to obey CHSH inequalities. We reproduce his reasoning in the notation consistent with (11–17).

If we average over the variables λ_x and λ_y we obtain:

$$E(A_xB_y) = \sum_{\lambda_1,\lambda_2} \overline{A}_x(\lambda_1)\overline{B}_y(\lambda_2)p(\lambda_1,\lambda_2) \tag{19}$$

$$E(A_xB_{y'}) = \sum_{\lambda_1,\lambda_2} \overline{A}_x(\lambda_1)\overline{B}_{y'}(\lambda_2)p(\lambda_1,\lambda_2) \tag{20}$$

$$E(A_{x'}B_y) = \sum_{\lambda_1,\lambda_2} \overline{A}_{x'}(\lambda_1)\overline{B}_y(\lambda_2)p(\lambda_1,\lambda_2) \tag{21}$$

$$E(A_{x'}B_{y'}) = \sum_{\lambda_1,\lambda_2} \overline{A}_{x'}(\lambda_1)\overline{B}_{y'}(\lambda_2)p(\lambda_1,\lambda_2) \tag{22}$$

where

$$\overline{A}_x(\lambda_1) = \sum_{\lambda_x} A_x(\lambda_1,\lambda_x)p_x(\lambda_x)\ ;\ \overline{B}_y(\lambda_2)$$
$$= \sum_{\lambda_y} B_y(\lambda_2,\lambda_y)p_y(\lambda_y) \tag{23}$$

$$\overline{A}_{x'}(\lambda_1) = \sum_{\lambda_{x'}} A_{x'}(\lambda_1,\lambda_{x'})p_{x'}(\lambda_{x'})\ ;\ \overline{B}_{y'}(\lambda_2)$$
$$= \sum_{\lambda_{y'}} B_y(\lambda_1,\lambda_{y'})p_{y'}(\lambda_{y'}) \tag{24}$$

Since $|A_x(\lambda_1, \lambda_x)| \leq 1$, $|A_{x'}(\lambda_1, \lambda_{x'})| \leq 1$, $|B_y(\lambda_2, \lambda_y)| \leq 1$, $|B_{y'}(\lambda_2, \lambda_{y'}) = | \leq 1$ thus $|\overline{A}_x(\lambda_1)| \leq 1$, $|\overline{A}_{x'}(\lambda_1)| \leq 1$, $|\overline{B}_y(\lambda_2)| \leq 1$, $|\overline{B}_{y'}(\lambda_2)| \leq 1$ and:

$$|\bar{A}_x(\lambda_1)|\overline{B}_y(\lambda_2) - \overline{B}_{y'}(\lambda_2)| + |\bar{A}_{x'}(\lambda_1)|\overline{B}_y(\lambda_2) + \bar{B}_{y'}(\lambda_2)| \leq 2 \tag{25}$$

Although the expectations calculated using the Equations (11–14) and (19–22) have the same values, the two sets of formulas describe different experiments. In the experiment described by the Equations (11–14), pairs of photons arrive sequentially to measuring instruments which produce in a locally causal way "a click" or "no-click," and a counterfactual Nx4 spreadsheet of all possible outcomes does not exist and may not be used to prove CHSH inequalities. Thus, the estimated pairwise expectations may significantly violate (8), which they do.

The Equations (19–22) describe an experiment, impossible to implement, which uses the following two-step experimental protocol:

1. For each arriving pair of photons estimate the averages (23–24).
2. Display estimated values $|\overline{A}_x(\lambda_1)| \leq 1$, $|\overline{A}_{x'}(\lambda_1)| \leq 1$, $|\overline{B}_y(\lambda_2)| \leq 1$, and $|\overline{B}_{y'}(\lambda_2)| \leq 1$ in four columns of a Nx4 spreadsheet.
3. Use all entries of this spreadsheet to estimate expectations (19–22).

Because the entries of each line of this spreadsheet obey the inequality (1), if we could implement this protocol the estimated expectations would obey CHSH for any finite sample.

There is a significant difference between a probabilistic model and a hidden variable model. If we average out some variables in a probabilistic model, we always obtain a marginal probability

distribution describing some feasible experiment. If we average out some hidden variables in a hidden variable model, we may obtain a new hidden variable model which does not correspond to any feasible experiment.

For a similar reason, the experimental protocol of SHVM is inconsistent with the protocol used in SPCE. A much more detailed discussion of a subtle relationship of probabilistic models with experimental protocols may be found in [56].

As we demonstrated with Hans De Raedt [104], different experimental protocols, based on the same probabilistic model, may generate significantly different estimates of various population parameters.

If we want to compare the data obtained in SPCE with quantum predictions, we have to post- select only pairs of ± 1 outcomes which correspond to invisible entangled pairs of photons. Thus, instead of the Equations (11, 15–16) we obtain:

$$E(A_x B_y | A_x \neq 0, B_y \neq 0) = \sum_{\lambda \in \Lambda'_{xy}} A_x(\lambda_1, \lambda_x) B_y(\lambda_2, \lambda_y) p_x(\lambda_x) p_y(\lambda_y) p(\lambda_1, \lambda_2) \tag{26}$$

$$E(A_x | A_x \neq 0, B_y \neq 0) = \sum_{\lambda \in \Lambda'_{xy}} A_x(\lambda_1, \lambda_x) p_x(\lambda_x) p_y(\lambda_y) p(\lambda_1, \lambda_2) \tag{27}$$

$$E(B_y | A_x \neq 0, B_y \neq 0) = \sum_{\lambda \in \Lambda'_{xy}} B_y(\lambda_2, \lambda_y) p_x(\lambda_x) p_y(\lambda_y) p(\lambda_1, \lambda_2) \tag{28}$$

where $\Lambda'_{xy} = \{\lambda \epsilon\ \Lambda_{xy} | A_x(\lambda_1, \lambda_x) \neq 0 \text{ and } B_y(\lambda_2, \lambda_y) \neq 0\}$. In a similar way, we transform the expectations (12–14) into conditional expectations. Using these conditional expectations, we may not derive CHSH; thus our model does not exclude their violations in SPCE. It may also explain in a rational way an apparent violation of no- signaling reported in [79, 80, 100, 101, 105–108]:

$$\begin{aligned} E(A_x | A_x \neq 0, B_y \neq 0) &\neq E(A_x | A_x \neq 0, B_{y'} \neq 0); \\ E(B_y | A_x \neq 0, B_y \neq 0) &\neq E(B_y | A_{x'} \neq 0, B_y \neq 0) \end{aligned} \tag{29}$$

The setting-dependence of these marginal expectations does not prove no-signaling because E (A_x) and E (B_y) defined by (15–16) do not depend on the distant measurement settings.

Please note that the expectations (26) may not be transformed into a factorized form (21).

Naïve quantum predictions for a singlet state cannot explain the correlations observed in SPCE. One has to use much more complicated density matrices [109] containing free parameters, and still some discrepancies between the theoretical predictions and the data persist. A more detailed discussion of how the data are analyzed in SPCE and how the apparent violation of no-signaling may be explained may be found in [60].

Since our description of real data is causally local, all speculations about *quantum non-locality* are unfounded.

In the next section we explain that, contrary to what is believed, probabilistic predictions of QM are not in conflict with local causality.

QUANTUM MECHANICS AND CHSH INEQUALITIES

According to the statistical contextual interpretation [29, 52, 57, 89, 110, 111], QM provides probabilistic predictions for experiments performed in well-defined experimental contexts. In these experiments, identical preparations of physical systems are followed by measurements of physical observables. A class of identical preparations is described by a state vector $|\psi\rangle$ or by a density matrix ρ and a class of equivalent measurements of an observable A is represented by a Hermitian/self-adjoint operator $\hat{A}$. Outcomes of measurements are eigenvalues of these operators. In general, outcomes are not pre-determined and they are created as a result of the interaction of measuring instruments with physical systems. In the same experimental context, only the values of compatible physical observables, represented by commuting operators, give sharp values when measured jointly.

In SPCE, "photon pairs," prepared by a source, are described by a density matrix ρ and physical observables A and B by Hermitian operators $\hat{A}_1 = \hat{A} \otimes I$ and $\hat{B}_1 = I \otimes \hat{B}$ defined on a Hilbert space $H = H_1 \otimes H_2$. The correlations between measured values of these observables are evaluated using a conditional covariance between A and B [56, 58]:

$$\mathrm{cov}(A, B|\rho) = E(AB|\rho) - E(A|\rho)E(B|\rho) \tag{30}$$

where, $E(A|\rho) = Tr\rho\hat{A}_1, E(B|\rho) = Tr\rho A\hat{B}_1$ and $E(AB|\rho) = Tr\rho\hat{A}_1\hat{B}_1$. If ρ is an arbitrary mixture of separable states then quantum correlations have to obey CHSH:

$$|E(AB|\rho) - E(AB'|\rho)| + |E(A'B|\rho) + E(A'B'|\rho)| \leq 2 \tag{31}$$

As we saw in section Experimental Spreadsheets and Bell-Type Inequalities, the inequality (31) may be significantly violated for entangled quantum states if specific incompatible pairs of settings are chosen.

The quantum description is contextual because a triplet $\{\rho, \hat{A}_1, \hat{B}_1\}$ depends explicitly on a preparation of "photon pairs" and on observables (A,B) measured using specific experimental settings. Different incompatible experimental settings are therefore described in QM by different specific Kolmogorov models.

In particular, Cetto et al. [73] have recently demonstrated that expectations E(AB | ψ), for a singlet state $|\psi\rangle \in H$, may be expressed in terms of the eigenvalues of operators $\hat{A} = \vec{\sigma} \cdot \vec{a}$ and $\hat{B} = \vec{\sigma} \cdot \vec{b}$ using specific dedicated probability distributions. We reproduce below their results in our notation:

$$E(AB|\psi) = -\vec{a} \cdot \vec{b} = \sum_{\alpha\beta} \alpha\beta p_{ab}(\alpha, \beta) = E(A_a B_b) \tag{32}$$

where $\hat{A}\otimes\hat{B}|\alpha\beta\rangle_{ab} = \alpha\beta|\alpha\beta\rangle_{ab}$, $p_{ab}(\alpha,\beta) = |\langle\psi|\alpha\beta\rangle_{ab}|^2$ and $\alpha = \pm 1$ and $\beta = \pm 1$. For the remaining settings we obtain:

$$E(AB'|\psi) = -\vec{a}\cdot\vec{b}' = \sum_{\alpha\beta'}\alpha\beta' p_{ab'}(\alpha,\beta') = E(A_{a'}B_b) \quad (33)$$

$$E(A'B|\psi) = -\vec{a}'\cdot\vec{b} = \sum_{\alpha'\beta}\alpha'\beta p_{a'b}(\alpha',\beta) = E(A_{a'}B_b) \quad (34)$$

$$E(A'B'|\psi) = -\vec{a}'\cdot\vec{b}' = \sum_{\alpha'\beta'}\alpha'\beta' p_{a'b'}(\alpha',\beta') = E(A_{a'}B_{b'}) \quad (35)$$

If 4 experiments are performed in incompatible (complementary) contexts then a joint probability distribution $p(\alpha\alpha'\beta\beta')$ and the expectation values $E(A_aA_{a'}B_bB_{b'})$ do not exist in agreement with the contextual model (11–14).

In 1982, Fine [18, 19] demonstrated that Bell-CHSH inequalities are necessary and sufficient conditions for the existence of a joint probability distribution of ±1-valued observables (A,A′,B,B′).

As we saw in section Local Realistic Models for EPR-Bohm Experiment, QM predicts a significant violation of CHSH inequality: $S = 2\sqrt{2}$.

In 1980, Tsirelson [92] proved that $2\sqrt{2}$ is the greatest value of S allowed by QM:

$$|S| = |\left\langle\psi|\hat{S}|\psi\right\rangle| = |\left\langle\psi|\hat{A}\hat{B} - \hat{A}\hat{B}' + \hat{A}'\hat{B} + \hat{A}'\hat{B}'|\psi\right\rangle| \le 2\sqrt{2} \quad (36)$$

where $|\psi\rangle \in H$ is an arbitrary pure state and all Hermitian operators on the left hand side are arbitrary elements of C* algebra having their norms ($\left\|\hat{A}\right\| = \sup_{\|\phi\|\le 1}\left\langle\phi|\hat{A}|\phi\right\rangle$) smaller or equal to 1. In order to prove (36), Tsirelson used a following operator inequality:

$$\hat{S}^2 = \left(\hat{A}\hat{B} - \hat{A}\hat{B}' + \hat{A}'\hat{B} + \hat{A}'\hat{B}'\right)^2 \le 4I + \left[\hat{A},\hat{A}'\right]\left[\hat{B},\hat{B}'\right] \quad (37)$$

From (37) he deduced immediately that $\left\|\hat{S}^2\right\| \le 4 + \left\|\left[\hat{A},\hat{A}'\right]\right\|\left\|\left[\hat{B},\hat{B}'\right]\right\| \le 4 + 2\times 2 = 8$, thus $\left\|\hat{S}\right\| \le 2\sqrt{2}$ proves *quantum CHSH inequality* (36). Landau [93] defined an operator $\hat{C} = \frac{1}{2}\hat{S}$ and noticed that if A, A′. B and B′ are ±1-valued observables ($\hat{A}^2 = I$), then the inequality (37) becomes the equality $\hat{C}^2 = I + \frac{1}{4}\left[\hat{A}_1,\hat{A}_2\right]\otimes\left[\hat{B}_1,\hat{B}_2\right]$ and $\left\|\hat{C}\right\| \le 1$.

Recently, Khrennikov discussed various implications of (37). CHSH inequality may be violated only if both $\left[\hat{A}_1,\hat{A}_2\right] \ne 0$ and $\left[\hat{B}_1,\hat{B}_2\right] \ne 0$. Therefore, the violation of CHSH proves the *local incompatibility* of Alice and Bob's specific physical observables [43] which has nothing to do with *quantum non-locality*.

The *local incompatibility* of some observables allows neither doubt over the *local causality* in nature nor the *"objective"* existence of elementary particles and atoms.

THE ROOTS OF QUANTUM NON-LOCALITY

Mathematical models provide abstract idealized descriptions of physical phenomena and in general are unable to explain, by detailed causal chains, why such a description is successful. For example, in Newton's equations describing the motion of planets, a small change in the position of one planet at time t seems to instantaneously change gravitational forces acting on distant planets. Newton admitted that no intuitive explanation of this mystery existed, but it did not diminish the value of his gravitation theory.

According to the special theory of relativity, the physical influences may not propagate faster than the speed of light c, thus it became clear that Newton's theory of gravitation should be modified. Einstein, by constructing the general theory of relativity, succeeded in reconciling the special theory of relativity with Newton's theory of gravitation which is still used with success by NASA.

Similarly, in a non-relativistic QM, relativistic effects are not important. The theory provides algorithms which allow probabilistic predictions to be made regarding outcomes of experiments performed in well-defined macroscopic contexts. A time-dependent Schrodinger equation describes only a time evolution of a complex valued function (probability amplitude), which, together with Hermitian/self-adjoint operators, is used to provide probabilistic predictions for a scatter of experimental outcomes.

Quantum predictions are consistent with Einsteinian no-signaling. Quantum field theory (QFT) is explicitly relativistic and field operators in space-like regions commute.

The speculations about *quantum non-locality* are only rooted in incorrect "individual interpretations" of QM according to which:

1. a pure state vector/wave function $|\psi\rangle$ is an attribute of an individual physical system;
2. a measurement of a physical observable A instantaneously changes/collapses the initial state vector onto an eigenvector vector $|a_i\rangle$ of the corresponding operator $\hat{A}$ with a probability $p = \langle a_i|\psi\rangle^2$;
3. a measurement outcome is an eigenvalue a_i corresponding to the vector $|a_i\rangle$;
4. if two physical systems, S_1 and S_2, interacted in the past and separated, a measurement of the observable A performed on the system S_1 and yielding a result $A{=}a_i$ determines instantaneously a state vector $|\phi\rangle_{A=a_i}$ of the system S_2 in a distant location.

Using (1–4) one concludes that measurements of observables A and B performed on systems S_1 and S_2 create in an *"irreducible random way"* perfectly correlated outcomes at distant space-like locations, thus we encounter the same paradox: *"a pair of dice showing perfectly correlated outcomes."*

The statistical contextual interpretation of QM (SCI) [52, 57, 89] is free of paradoxes. According to this interpretation, a quantum state vector represents only an ensemble of identically prepared physical systems and, after a von Neumann/Lüders

projection, a new state describes a different ensemble of physical systems. Namely: $|\phi\rangle_{A=a_i}$ describes all the systems S_2 such that measurements of the observable A on their entangled partners (systems S_1) gave the same outcome $A = a_i$.

The statistical interpretation does not claim that QM provides the complete description of individual physical systems and the question of whether quantum probabilities may be deduced from some more detailed description of quantum phenomena is left open [46, 52, 59, 61, 87–89, 112, 113].

Lüders projection and its interpretation have been discussed recently in detail by Khrennikov [44]. We reproduce below a few statements from the abstract of his article:

> "If probabilities are considered to be objective properties of random experiments, we show that the Lüders projection corresponds to the passage from joint probabilities describing all sets of data to some marginal conditional probabilities describing some particular subsets of data. If one adopts a subjective interpretation of probabilities, such as Qbism, then the Lüders projection corresponds to standard Bayesian updating of the probabilities. The latter represents degrees of beliefs of local agents about outcomes of individual measurements which are placed or which will be placed at distant locations. In both approaches, probability-transformation does not happen in the physical space, but only in the information space. Thus, all speculations about spooky interactions or spooky predictions at a distance are simply misleading."

In 1998, Ballentine explained in his book that "individual interpretation" of QM is incorrect: "Once acquired, the habit of considering an individual particle to have its own wave function is hard to break. Even though it has been demonstrated strictly incorrect." Therefore, talking about "passion at the distance," "predictions at the distance," and "steering at the distance" may only lead to incorrect mental pictures and create unnecessary confusion.

In QM, measuring devices always play an active role. Allahverdyan et al. [110, 111] recently solved the dynamics of a particular realistic quantum measurement and discussed what this implies for the interpretation of QM. On page 6 in [110] they wrote:

> "A measurement is the only means through which information may be gained about a physical system. Both in classical and in quantum physics, it is a dynamical process which couples this system S to another system, the apparatus A. Some correlations are thereby generated between the initial (and possibly final) state of S and the final state of A."

Claims that QM is a non-local theory are also based on an incorrect interpretation of a two-slit experiment. In this experiment, a wave function (representing an ensemble of identically prepared electrons) "passes" by two slits, but this does not mean that a single electron may be in two distinct places at the same time. If two detectors are placed in front of the slits, they never click at the same time, thus an electron (but not the electromagnetic field created by an electron) passes by only one slit. According to SCI, a wave function is only a mathematical entity and QM does not provide a detailed space-time description of how the interference pattern on a screen is formed by the impacts of individual electrons.

Another root of *quantum non-locality* is Bell's insistence that the violation of Bell-type inequalities in SPCE would mean that a locally causal description of these experiments is impossible [1]:

> "In a theory in which parameters are added to quantum mechanics to determine the results of *individual measurements, without changing the statistical predictions, there must be a* mechanism whereby the setting of one measuring device can influence the reading of another instrument, however remote. Moreover, the signal involved must propagate instantaneously, so that such a theory could not be Lorentz invariant."

Consider Alice and Bob, both doing a realistic EPRB-type experiment. Theo Nieuwenhuizen brought to my attention that the already nonsensical idea of faster-than-light communication (i.e., non-locality) becomes even more "mind-boggling" when the experiments have different durations.

Bell's statement is correct only if one is talking about an ideal EPRB which does not exist. The violations of various Bell-type inequalities in real SPCE prove only that these experiments may not be described by oversimplified hidden variable models. In SHVM, the outcomes, registered in distant measuring stations, are produced in an irreducible random way, thus the correlations between such outcomes are very limited. In LRHVM and in Eberhard model [5], a fate of a photon/electron is predetermined before the experiment is performed.

As we explained in section Contextual Description of Spin Polarization Correlation Experiments, imperfect correlations in SPCE may be explained in a locally causal way if instrument parameters are correctly included in a probabilistic model, closing the so-called Nieuwenhuizen's *contextuality loophole* [65–67].

Bell-CHSH inequalities may also be violated in social sciences by expectations of ± 1–valued random variables, which can only be measured pairwise but not all together. The violation of these inequalities in social sciences has nothing to say about the physical reality and the locality of nature [16, 37, 38, 114–116]. This is why we agree with Khrennikov [43], that we should get rid of *quantum non-locality* as it is a misleading notion.

In the next section we discuss simple experiments with colliding elastically metal balls in which the experimental outcomes are predetermined but an apparent violation of Bell and Boole inequalities may be proven [54]. We also discuss the violation of inequalities by the estimates obtained using finite samples.

APPARENT VIOLATIONS OF BELL-BOOLE INEQUALITIES IN ELASTIC COLLISION EXPERIMENTS

Let us consider a simple experiment with metal balls colliding elastically:

1. A 4 kg metal ball and a 1 kg metal ball are placed in some fixed positions, P_1 and P_2, on a horizontal perfectly smooth surface.
2. A device D, with a built in random numbers generator, is imparting on a lighter ball a constant rectilinear velocity with a speed described by a random variable V taking values v and distributed according to a probability density $f_V(v) = 1/10$ for $0 < v \leq 10$ and the ball is sliding without friction and without rotating toward the heavier ball.
3. After an elastic head-on collision, the heavier ball starts moving forward with the speed $V_1 = 2v/5$ and the lighter ball rebounds backwards with the speed $V_2 = 3v/5$. It is easy to check that the total linear momentum and energy are conserved: $1v = 4(2v/5) - 1(3v/5)$ and $1v^2 = 4(2v/5)^2 + 1(3v/5)^2$.
4. After the collision, both balls arrive at two distant measuring stations, S_1 and S_2 (treated as black boxes), which for 4 different selected pairs of settings output values (± 1) of only pairwise measurable observables (A, B), (A, C), (B, C), and (B, B).
5. Before each repetition of the experiment, Alice and Bob systematically or randomly choose a pair of settings, simply by pushing appropriate switches on their measuring stations.
6. We assume that boxes function in a locally causal way: the speed of a ball is measured and setting dependent coded values ± 1 are outputted. Thus, A, B, and C denote physical observables, which are measured, which means that in the setting (B, B) the same physical observables are measured by Alice and Bob.

The observables A, B, and C are functions of hidden random variables, V_1 and V_2, which are distributed according to probability distributions $f_{V_1}(v_1) = 1/4$ and $f_{V_2}(v_2) = 1/6$ on the intervals [0, 4] and [0, 6], respectively.

Let us now define the specific functions of A(y), B(y), and C(y), where $y = v_1$ (if Alice is using a setting A) or $y = v_2$ (if (Bob is using a setting A). We have chosen that, after the collision, Alice measures the speed of the heavier ball, but it does change pairwise expectations.

- $A(y) = -1$ if $0 < y \leq 2$ and $A(y) = 1$ if $2 < y$,
- $B(y) = -1$ if $0 < y \leq 3$ and $B(y) = 1$ if $3 < y$,
- $C(y) = 1$ if $0 < y \leq 3$ and $C(y) = -1$ if $3 < y$.

If $V_1 = v_1$ then $V_2 = 3v_1/2$ and the pairwise expectation $E(AB) = \int_0^4 A(v_1)B(3v_1/2)f_{V_1}(v_1)dv_1$. We see immediately, that $E(AB) = \frac{1}{4}\left(\int_0^2 (-1)(-1)dv_1 + \int_2^4 (1)(1)dv_1\right) = 1$ and E (AC) = -E (AB) =-1. In a similar way we evaluate E(BC).

- If $v_1 \leq 2$ then $v_2 < 3$: $B(v_1)C(v_2) = (-1)(1) = -1$.
- If $2 < v_1 \leq 3$ then $3 < v_2 \leq 4.5$: $B(v_1)C(v_2) = (-1)(-1) = 1$.
- If $3 < v_1$ then $4.5 < V_2$: $B(v_1)C(v_2) = (1)(-1) = -1$.

Thus:

$$E(BC) = -\int_0^2 f_{V_1}(v_1)dv_1 + \int_2^3 f_{V_1}(v_1)dv_1 - \int_3^4 f_{V_1}(v_1)dv_1 \quad (38)$$

and $E(BC) = -2/4 + 1/4 - 1/4 = -1/2$ and $E(BB) = -E(BC) = 1/2$.

We see that Bell (+sign) and Boule (-sign) inequalities (3) seem to be violated:

$$|E(AB) - E(AC)| \leq 1 \pm E(BC) \quad (39)$$

because $|1-(-1)| > 1 \pm 1/2$.

The violation of (39) is surprising because the outcomes of our experiments are predetermined.

However, one has to pay attention before checking Bell-Boole-inequalities. Despite the fact that in the settings (A,B) and (B,C) Alice and Bob measure the same physical observable B, the output values ± 1 are the values of 2 different random variables $B(V_1) \neq B(V_2)$. Therefore, the inequalities which are violated are not (39), but inequalities:

$$|E(A(V_1)B(V_2)) - E(A(V_1)C(V_2))| \leq 1 \pm E(B(V_1)C(V_2)) \quad (40)$$

Since for each trial, values of random variables $[A(V_1), B(V_1), B(V_2), C(V_2)]$ are predetermined by a value of the initial speed V imparted on the lighter ball, there exists an "invisible" joint probability distribution of these random variables and CHSH inequalities may not be violated:

$$\begin{aligned} |S| &= |E(A(V_1)B(V_2)) - E(A(V_1)C(V_2)) + E(B(V_1)B(V_2)) \\ &\quad + E(B(V_1)C(V_2))| = 1 + 1 + \frac{1}{2} - \frac{1}{2} \leq 2 \end{aligned} \quad (41)$$

By treating measuring stations as black boxes, Alice and Bob do not know whether this *invisible* joint probability exists and that for each trial the values of measured observables are predetermined. Therefore they display the data obtained in different settings using four Mx2 spreadsheets and they estimate measurable pairwise expectations $E(A(V_1)B(V_2))$, $E(A(V_1)C(V_2))$, $E(B(V_1)C(V_2))$, and $E(B(V_1)B(V_2))$.

These estimates may violate the inequality (41) because, as we demonstrated in section Introduction, only the estimates obtained using all ± 1 entries of Nx4 spreadsheets strictly obey CHSH inequality for any finite sample. Alice and Bob do not know that their outcomes are in fact extracted from specific lines of invisible Nx4 spreadsheet and that the columns of Mx2 spreadsheets are simple random samples drawn from the corresponding complete columns of Nx4 spreadsheet. This is why, if M and N are large, the estimated pairwise expectations may not violate the inequality (41) more significantly than is permitted by sampling errors.

In collision experiments, outcomes are predetermined and the correlations exist due to the energy and momentum conservation. In SPCE, the correlations between signals are created at the source.

There is a big difference between metal balls and photons in SPCE. In collision experiments, metal balls are distinct macroscopic objects with well-defined linear momenta. Measurements of speeds are, with a good approximation, noninvasive, thus measuring stations in fact register passively their preexisting values and output specific coded values ± 1.

In SPCE we cannot observe and follow pairs of photons moving from the source to the measuring stations. By no means

can the passage of a photon through a polarization beam splitter (PBS) be considered as a passive registration of a preexisting "spin up" or spin down" value. Clicks on the detectors are also the results of dynamical processes.

In collision experiments all observables are compatible, therefore Alice's modified measuring station might output in each trial values of (A (V_1), B (V_1)) and Bob's modified station values of (B(V_2), C(V_2)) which might have been displayed using a Nx4 spreadsheet. In SPCE it is impossible because the observables (A, A′) and (B, B′) are not compatible and their joint probability distribution and Nx4 spreadsheet do not exist.

The problem of how significantly finite samples, extracted from a counterfactual spreadsheet Nx4, may violate CHSH inequalities was studied by Gill [117]. Each pair of arriving photons are described by a line (±1,±1,±1,±1) from a counterfactual Nx4 spreadsheet containing predetermined values of observables (A,A′,B,B′). By randomly assigning setting labels to the lines and extracting corresponding pairs of outcomes from these lines, one obtains four simple random samples drawn from the corresponding pairs of complete columns of Nx4 spreadsheet. If these simple random samples are used to estimate pairwise expectations E(AB),E(AB′), E(A′B),E(A′B′) then:

$$\Pr\left(\langle AB\rangle_{obs} + \langle AB'\rangle_{obs} + \langle A'B\rangle_{obs} - \langle A'B'\rangle_{obs} \geq 2\right) \leq \frac{1}{2} \quad (42)$$

where $\langle AB\rangle_{obs}$ is an estimate of E(AB) etc. A more detailed discussion of various finite sample proofs of Bell-type inequalities may be found in [57, 117].

Let us see what happens if we display all experimental data (containing N data items for each pair of settings) in a 4Nx4 spreadsheet and randomly fill the remaining empty spaces by ±1. Pairwise expectations estimated using complete columns of this spreadsheet strictly obey CHSH inequality. One may ask a question: why can real data, being subsets of these columns, violate CHSH more significantly than it is permitted by (42)? The answer is simple: the outcomes obtained in SPCE for each pair of incompatible settings are not **simple random samples** extracted from corresponding columns of the completed 4Nx4 counterfactual spreadsheet.

In [104] we studied the impact of a sample inhomogeneity on statistical inference. In particular we generated two large samples (which were not simple random samples) from some statistical population and we estimated some population parameters. The obtained estimates were dramatically different.

De Raedt et al. [82] generated in a computer experiment quadruplets of raw data (±1,±1,±1,±1). Subsequent setting -dependent photon identification procedures, mimicking procedures used in real experiments, allowed the creation of new data samples containing only pairs (±1,±1) for each experimental settings. Because these new data sets were not simple random samples extracted from the raw data, the estimated values of pairwise expectations, obtained using these setting- dependent samples, could violate CHSH as significantly as it was observed in SPCE.

We personally do not believe that the fate of the photons is predetermined only by the preparation at the source and that the violation of Bell-CHSH inequalities is the effect of unfair sampling during a post selection.

For us, clicks registered by distant measuring stations in SPCE and coded by ±1 are of a completely different nature than the colors and sizes of socks or the positions and linear momenta of balls and electrons. Spin projections and clicks do not exist before the measurements are done. Thus, one may not describe incoming "pairs of photons" by lines of non-existing Nx4 spreadsheet containing ±1 counterfactual outcomes of impossible to perform experiments.

CONCLUSIONS

In this article we explained why the speculations about quantum non-locality and quantum magic are rooted in incorrect interpretations of QM and/or in incorrect "mental pictures" and models trying to explain invisible details of quantum phenomena.

For example, a "mental picture" of an ideal EPRB experiment in which twin photon pairs produce, in an irreducible random way, strictly correlated or anti-correlated clicks on distant detectors creates the impossible to resolve paradox:

"a pair of dice showing always perfectly correlated outcomes."

As we explained in section Local Realistic Models for EPR-Bohm Experiment, we do not need to worry because the ideal EPRB experiment does not exist.

In SPCE, setting directions are not mathematical vectors but only small spherical angles and we neither see nor follow pairs of entangled photons which produce "click" or "no- click" results on Alice's and Bob's detectors. There are black counts, laser intensity drifts, etc. Detected clicks have time tags and correlated time-windows are used to identify and select pairs of clicks created by the photons belonging to the same entangled pair.

Since various photon- identification procedures are setting – dependent, final post-selected data may not be described by the quantum model used to describe the non-existing ideal EPRB. In SPCE, not only do we not have strict correlations or anti-correlations between Alice and Bob's outcomes but marginal single counts distributions also depend on the distant settings that seems to violate Einsteinian no- signaling. This violation is only apparent because single count distributions estimated using raw data do not depend on the distant settings [60].

Raw and post- selected data in SPCE may be described in a locally causal way using a contextual model [59, 60] in which "a click" or "a no-click" are determined using setting dependent parameters describing a measuring instrument and parameters describing a signal arriving at the measuring station at the moment of the measurement. Still, a detailed description of how "Nature gets this done" is the real mystery underlying quantum correlations.

In contrast to LRHVM and SHVM, in the contextual model (11–17) and in QM the outcomes of four incompatible experiments performed in different settings are described by dedicated probability distributions defined on disjoint probability spaces. Only if all the physical observables measured in SPCE were compatible could these dedicated probability

distributions be deduced as marginal probability distributions from a joint probability distribution defined on a unique probability space.

Khrennikov recently explained in [43, 44] that *quantum non-locality* is also rooted in incorrect individual interpretation of QM and in incorrect interpretation of Lüders projection postulate.

Plotnitsky pointed out in [118] that in QM there is no place for *spooky action at a distance*, however his insistence on *spooky predictions at a distance* contributes to general confusion [44].

Other convincing arguments against *quantum non-locality* have recently been given by Jang [119, 120], Bough [121], Wilsch et al. [122], and De Raedt et al. [123].

We want also to mention a recent paper of Griffiths [124] in which he arrives also to the conclusion, that quantum mechanics is consistent with Einstein's locality principle and that the notions of *quantum nonlocality* and of *quantum steering* are misleading and should be abandoned or renamed.

As we mentioned in the introduction, it would be surprising if the violation of Bell-CHSH inequalities, which are proven using simple algebraic inequalities satisfied by any quadruplet of 4 integer numbers equal to ± 1, might have deep metaphysical implications. In fact, such metaphysical implications are quite limited and may be summarized in a few words: "*unperformed experiments have no results*" [84].

Therefore, the violation of various Bell-type inequalities may neither justify the existence of non-local influences nor justify doubts that atoms, electrons, and the Moon are not there when nobody looks.

AUTHOR CONTRIBUTIONS

The author confirms being the sole contributor of this work and has approved it for publication.

ACKNOWLEDGMENTS

We would like to thank the reviewers for several precious suggestions and Rhiannon Schouten for English language proof-reading of my article. We also express my gratitude to Andrei Khrennikov for his kind hospitality extended to me during several Växjö conferences on the Foundations of Quantum Mechanics and for many stimulating discussions.

REFERENCES

1. Bell JS. On the Einstein-Podolsky-Rosen paradox. *Physics.* (1965) **1**:195. doi: 10.1103/PhysicsPhysiqueFizika.1.195
2. Bell JS. *Speakable and Unspeakable in Quantum Mechanics*. Cambridge: Cambridge UP. (2004) doi: 10.1017/CBO9780511815676
3. Clauser JF, Horne MA, Shimony A, Holt RA. Proposed experiment to test local hidden-variable theories. *Phys Rev Lett.* (1969) **23**:880. doi: 10.1103/PhysRevLett.23.880
4. Clauser JF, Horne MA. Experimental consequences of objective local theories. *Phys Rev D*. (1974) **10**:526. doi: 10.1103/PhysRevD.10.526
5. Eberhard PH. Background level counter efficiencies required for a loophole-free einstein-podolsky -rosen experiment. *Phys RevA*. (1993) **47**:747. doi: 10.1103/PhysRevA.47.R747
6. Aspect A, Grangier P, Roger G. Experimental test of Bell's inequalities using time-varying analyzers. *Phys Rev Lett.* (1982) **49**:1804–7. doi: 10.1103/PhysRevLett.49.1804
7. Weihs G, Jennewein T, Simon C, Weinfurther H, Zeilinger A. Violation of Bell's inequality under strict Einstein locality conditions. *Phys Rev Lett.* (1998) **81**:5039–43. doi: 10.1103/PhysRevLett.81.5039
8. Christensen BG, McCusker KT, Altepeter JB, Calkins B, Lim CCW, Gisin N, et al. Detection-loophole-free test of quantum non-locality and applications. *Phys Rev Lett.* (2013) **111**:130406. doi: 10.1103/PhysRevLett.111.130406
9. Hensen B, Bernien H, Dreau AE, Reiserer A, Kalb N, Blok MS, et al. Loopholefree Bell inequality violation using electron spins separated by 1.3 kilometres. *Nature.* (2015) **526**:15759. doi: 10.1038/nature15759
10. Giustina M, Versteegh MAM, Wengerowsky S, Handsteiner J, Hochrainer A, Phelan K, et al. Significant-loophole-free test of Bell's theorem with entangled photons. *Phys Rev Lett.* (2015) **115**:250401. doi: 10.1103/PhysRevLett.115.250401
11. Shalm LK, Meyer-Scott E, Christensen BG, Bierhorst P, Wayne MA, Stevens MJ, et al. Strong loophole-free test of local realism. *Phys Rev Lett.* (2015) **115**:250402. doi: 10.1103/PhysRevLett.115.250402
12. Accardi L. Topics in quantum probability. *Phys Rep.* (1981) **77**:169 −192. doi: 10.1016/0370-1573(81)90070-3
13. Accardi L. Some loopholes to save quantum non-locality. *AIP Conf Proc.* (2005) **750**:1–19. doi: 10.1063/1.1874552
14. Accardi L, Uchiyama S. Universality of the EPR-chameleon model. *AIP Conf Proc.* (2007) **962**:15–27. doi: 10.1063/1.2827299
15. Aerts D. A possible explanation for the probabilities of quantum mechanics. *J Math Phys.* (1986) **27**:202–9. doi: 10.1063/1.527362
16. Aerts D, Aerts Arguelles J, Beltran L, Geriente S, Sassoli de Bianchi M, Sozzo, et al. Quantum entanglement in physical and cognitive systems: a conceptual analysis and a general representation. *Europ Phys J Plus.* (2019) **134**:493. doi: 10.1140/epjp/i2019-12987-0
17. Aerts D, Sassoli de Bianchi M. When Bertlmann wears no socks. Common causes induced by measurements as an explanation for quantum correlations. *arXiv:1912.07596 [quant-ph].* (2020).
18. Fine A. Hidden variables, joint probability and the Bell inequalities. *Phys Rev Lett.* (1982) **48**:291–5. doi: 10.1103/PhysRevLett.48.291
19. Fine A. Joint distributions, quantum correlations, commuting observables. *J Math Phys.* (1982) **23**:1306–10. doi: 10.1063/1.525514
20. K. Hess Philipp W, A possible loophole in the theorem of Bell. *Proc Natl Acad Sci USA*. (2001)**98**:14224–7. doi: 10.1073/pnas.251524998
21. Hess K, Philipp W. A possible loophole in the Bell's theorem and the problem of decidability between the views of Einstein and Bohr. *Proc Natl Acad Sci USA*. (2001) **98**:14228–33. doi: 10.1073/pnas.251525098
22. Hess K, Philipp W. *Bell's Theorem: Critique of Proofs With and Without Inequalities*. *AIP Conf Proc.* (2005) **750**:150–7. doi: 10.1063/1.1874568
23. Hess K. *Einstein Was Right!. Pan*. Singapore: Pan Stanford Publishing (2015). doi: 10.1201/b16809
24. Hess K, Michielsen K, De Raedt H. Possible experience: from boole to bell. *Europhys Lett.* (2009) **87**:60007. doi: 10.1209/0295-5075/87/60007
25. Hess K, De Raedt H, Michielsen K. Hidden assumptions in the derivation of the theorem of Bell. *Phys Scr.* (2012) T**151**:014002. doi: 10.1088/0031-8949/2012/T151/014002
26. Hess K, Michielsen K, De Raedt H. From boole to leggett-garg: epistemology of bell-type inequalities. *Adv Math Phys.* (2016) **2016**:4623040. doi: 10.1155/2016/4623040
27. Jaynes ET. Clearing up mysteries - The original goal. In: Skilling J, editor. *Maximum Entropy and Bayesian Methods Vol. 36.* Dordrecht: Kluwer Academic Publishers. (1989). p. 1–27. doi: 10.1007/978-94-015-7860-8_1
28. Khrennikov AY. *Interpretations of Probability*; *VSP Int*. Tokyo: Sc. Publishers: Utrecht. (1999).

29. Khrennikov A. Non-Kolmogorov probability models and modified Bell's inequality. *J Math Phys.* (2000) **41**:1768–77. doi: 10.1063/1.533210
30. Khrennikov A.Yu Volovich IV. Quantum non-locality, EPR model Bell's theorem. In: Semikhatov A, et al., editors. *Proceedings 3rd International Sakharov Conference on Physics.* Moscow: World Scientific, Singapore. (2003). p. 260–7.
31. Khrennikov A. (Ed.) Växjö interpretation-**2003**: Realism of contexts. In *Quantum Theory: Reconsideration of Foundations.* Växjö: Växjö Univ. Press. (2004). p. 323–38.
32. Khrennikov A. The principle of supplementarity: Contextual probabilistic viewpoint to complementarity, the interference of probabilities, and the incompatibility of variables in quantum mechanics. *Found Phys.* (2005) **35**:1655–93. doi: 10.1007/s10701-005-6511-z
33. Khrennikov AY. Bell's inequality: Non-locality, "death of reality", or incompatibility of random variables. *AIP Conf Proc.* (2007) **962**:121–31. doi: 10.1063/1.2827294
34. Khrennikov AY. Bell-boole inequality: non-locality or probabilistic incompatibility of random variables? *Entropy*. (2008) **10**:19–32. doi: 10.3390/entropy-e10020019
35. Khrennikov AY. Violation of Bell's inequality and nonKolmogorovness. *AIP Conf Proc.* (2009) **1101**:86–99. doi: 10.1063/1.3109976
36. Khrennikov AY. Bell's inequality: Physics meets probability. *Inf Sci.* (2009) **179**:492–504. doi: 10.1016/j.ins.2008.08.021
37. Khrennikov A. *Contextual Approach to Quantum Formalism*. Dordrecht: Springer. (2009). doi: 10.1007/978-1-4020-9593-1
38. Khrennikov A. *Ubiquitous Quantum Structure.* Berlin: Springer. (2010). doi: 10.1007/978-3-642-05101-2
39. Khrennikov A. Bell argument: Locality or realism? *Time to make the choice. AIP Conf Proc.* (2012) (1424) *1*60–175. doi: 10.1063/1.3688967
40. Khrennikov A. CHSH inequality: Quantum probabilities as classical conditional probabilities. *Found Phys.* (2015) **45**:711. doi: 10.1007/s10701-014-9851-8
41. Khrennikov *Probability* A, *Randomness: Quantum Versus Classical*. London: Imperial College Press (2016) doi: 10.1142/p1036
42. Khrennikov AY. After bell. *Fortschr Phys.* (2017) **65**:1600044. doi: 10.1002/prop.201600044
43. Khrennikov A. Get rid of non-locality from quantum physics. *Entropy.* (2019) **21**:806. doi: 10.3390/e21080806
44. Khrennikov A. Two faced janus of quantum non-locality. *Entropy.* (2020) **22**:303. doi: 10.3390/e22030303
45. Kupczynski M. New test of completeness of quantum mechanics. *ICTP preprint IC/84/242.* (1984)
46. Kupczynski M. On some new tests of completeness of quantum mechanics. *Phys Lett A*. (1986) **116**:417–9. doi: 10.1016/0375-9601(86)90372-5
47. Kupczynski M. Pitovsky model complementarity. *Phys Lett A*. (1987) **121**:51–3. doi: 10.1016/0375-9601(87)90263-5
48. Kupczynski M. Bertrand's paradox Bell's inequalities. *Phys Lett A*. (1987) **121**:205–7. doi: 10.1016/0375-9601(87)90002-8
49. Kupczynski M. On the completeness of quantum mechanics. *arXiv:quant-ph/0208061v1*. (2002).
50. Kupczynski M. Contextual observables and quantum information. *arXiv:0710.3510v1 [quant-ph].* (2007).
51. Kupczynski M. Entanglement bell inequalities. *J Russ Laser Res.* (2005) **26**:514–23. doi: 10.1007/s10946-005-0048-7
52. Kupczynski M. Seventy years of the EPR paradox. *AIP Conf Proc.* (2006) **861**:516–23. doi: 10.1063/1.2399618
53. Kupczynski M. EPR paradox, locality and completeness of quantum. *AIP Conf Proc.* (2007) **962**:274–285. doi: 10.1063/1.2827317
54. Kupczynski M. Entanglement and quantum non-locality demystified. *AIP Conf Proc.* (2012) (1508) 253-264. doi: 10.1063/1.4773137
55. Kupczynski M. Causality local determinism versus quantum non-locality. *J Phys Conf Ser.* (2014) **504**:012015. doi: 10.1088/1742-6596/504/1/012015
56. Kupczynski M. Bell inequalities, experimental protocols and contextuality. *Found Phys.* (2015) **45**:735–53. doi: 10.1007/s10701-014-9863-4
57. Kupczynski M. EPR paradox quantum non-locality physical reality. *J Phys Conf Ser.* (2016) **701**:012021. doi: 10.1088/1742-6596/701/1/012021
58. Kupczynski M. On operational approach to entanglement and how to certify it. *Int J Q Inform.* (2016) **14**:1640003. doi: 10.1142/S0219749916400037
59. Kupczynski M. Can we close the Bohr-Einstein quantum debate? *Phil Trans R Soc A*. (2017) **375**:20160392. doi: 10.1098/rsta.2016.0392
60. Kupczynski M. Is Einsteinian no-signalling violated in Bell tests? *Open Physics.* (2017) **15**:739–753. doi: 10.1515/phys-2017-0087
61. Kupczynski M. Quantum mechanics and modeling of physical reality. *Phys Scr.* (2018) **93**:123001. doi: 10.1088/1402-4896/aae212
62. Kupczynski M. Closing the door on quantum non-locality. *Entropy.* (2018) **20**:877. doi: 10.3390/e20110877
63. De Muynck VM, De Baere W, Martens H. Interpretations of quantum mechanics, joint measurement of incompatible observables and counterfactual definiteness. *Found Phys.* (1994) **24**:1589–664. doi: 10.1007/BF02054787
64. De Muynck WM. *Foundations of Quantum Mechanics.* Dordrecht: Kluver Academic (2002). doi: 10.1007/0-306-48047-6
65. Nieuwenhuizen TM. Where Bell went wrong. *AIP Conf Proc.* (2009) **1101**:127–33. doi: 10.1063/1.3109932
66. Nieuwenhuizen TM. Is the contextuality loophole fatal for the derivation of Bell inequalities. *Found Phys.* (2011) **41**:580–91. doi: 10.1007/s10701-010-9461-z
67. Nieuwenhuizen TM, Kupczynski M. The contextuality loophole is fatal for derivation of bell inequalities: reply to a comment by I. Schmelzer. *Found Phys.* (2017) **47**:316–9. doi: 10.1007/s10701-017-0062-y
68. Pascazio Time S. Bell–type inequalities. *Phys Lett A*. (1986)**118**:47–53. doi: 10.1016/0375-9601(86)90645-6
69. Pitovsky I. Deterministic model of spin statistics. *Phys Rev D*. (1983) **27**:2316–26. doi: 10.1103/PhysRevD.27.2316
70. Pitovsky I. George Boole's conditions of possible experience the quantum puzzle. *Brit J Phil Sci.* (1994) **45**:95–125. doi: 10.1093/bjps/45.1.95
71. De la Peña L, Cetto AM, Brody TA. On hidden variable theories and Bell's inequality. *Lett Nuovo Cimento.* (1972) **5**:177. doi: 10.1007/BF02815921
72. Cetto AM, de la Pena L, Valdes-Hernandez A. Emergence of quantization: the spin of the electron. *J Phys Conf Ser.* (2014) **504**:012007. doi: 10.1088/1742-6596/504/1/012007
73. Cetto AM, Valdes-Hernandez A, de la Pena L. On the spin projection operator and the probabilistic meaning of the bipartite correlation function. *Found Phys.* (2020) **50**:27–39. doi: 10.1007/s10701-019-00313-8
74. De Raedt H, De Raedt K, Michielsen K, Keimpema K, Miyashita S. Event-based computer simulation model of Aspect-type experiments strictly satisfying Einstein's locality conditions. *J Phys Soc Jap.* (2007) **76**:104005. doi: 10.1143/JPSJ.76.104005
75. De Raedt K, De Raedt H, Michielsen K. A computer program to simulate Einstein-Podolsky-Rosen-Bohm experiments with photons. *Comp Phys Comm.* (2007) **176**:642–51. doi: 10.1016/j.cpc.2007.01.007
76. De Raedt H, De Raedt K, Michielsen K, Keimpema K, Miyashita S. Event-by-event simulation of quantum phenomena: Application to Einstein-Podolsky-Rosen-Bohm experiments. *J Comput Theor Nanosci.* (2007) **4**:957–91. doi: 10.1166/jctn.2007.2381
77. Zhao S, De Raedt H, Michielsen K. Event-by-event simulation model of Einstein-Podolsky-Rosen-Bohm experiments. *Found Phys.* (2008) **38**:322–47. doi: 10.1007/s10701-008-9205-5
78. De Raedt H, Hess K, Michielsen K. Extended boole-bell inequalities applicable to quantum theory. *J Comp Theor Nanosci.* (2011) **8**:10119. doi: 10.1166/jctn.2011.1781
79. De Raedt H, Michielsen KF. Einstein-podolsky-rosen-bohm laboratory experiments: data analysis and simulation. *AIP Conf Proc.* (2012) **1424**:55–66. doi: 10.1063/1.3688952
80. De Raedt H, Jin F, Michielsen K. Data analysis of Einstein-Podolsky-Rosen-Bohm laboratory experiments. *Proc SPIE.* (2013) **8832**:88321N1–11. doi: 10.1117/12.2021860
81. Michielsen K, De Raedt H. Event-based simulation of quantum physics experiments. *Int J Mod Phys C.* (2014) **25**:1430003–66. doi: 10.1142/S0129183114300036
82. De Raedt H, Michielsen K, Hess K. The photon identification loophole in EPRB experiments:computer models with single-wing selection. *Open Physics.* (2017) **15**:713–33. doi: 10.1515/phys-2017-0085
83. Zukowski M.; Brukner C. Quantum non-locality—It ain't necessarily so. *J Phys A Math Theor.* (2014) **47**:424009. doi: 10.1088/1751-8113/47/42/424009

84. Peres A. Unperformed experiments have no results. *Am J Phys.* (1978) **46**:745–7. doi: 10.1119/1.11393
85. Leggett AJ, Garg A. Quantum mechanics versus macroscopic realism: is the flux there when nobody looks. *Phys Rev Lett.* (1985) **9**:857–60. doi: 10.1103/PhysRevLett.54.857
86. Mermin D. Is the moon there when nobody looks? reality and the quantum theory. *Phys Today.* (1985) **4**:38. doi: 10.1063/1.880968
87. Einstein A. In: Schilpp PA. (ed). *Albert Einstein: Philosopher–Scientist.* Evanston, IL: The Library of Living Philosophers, Inc (1949)
88. Einstein A. Physics and reality. *J Franklin Inst.* (1936) **221**:349. doi: 10.1016/S0016-0032(36)91047-5
89. Ballentine LE. The statistical interpretation of quantum mechanics. *Rev Mod Phys.* (1989) **42**:358–81. doi: 10.1103/RevModPhys.42.358
90. Boole G. On the theory of probabilities. *Philos Trans R Soc Lond.* (1862) **152**:225–52. doi: 10.1098/rstl.1862.0015
91. Bell JS. Introduction to the hidden-variable question. In: *Foundations of Quantum Mechanics.* New York: Academic. (1971) p. 171–81. (reproduced in [2])
92. Cirel'son BS. Quantum generalizations of Bell's inequality. *Lett Math Phys.* (1980) **4**:93–100. doi: 10.1007/BF00417500
93. Landau LJ. On the violation of Bell's inequality in quantum theory. *Phys Lett A.* (1987) **20**:54. doi: 10.1016/0375-9601(87)90075-2
94. Von Neumann J. *Mathematical Foundations of Quantum Mechanics.* Princeton, NJ: Princeton University Press (1955).
95. Lüders G. Über die Zustandsänderung durch den Messprozess. *Ann Phys.* (1951) **8**:322–8. doi: 10.1002/andp.19504430510
96. Bohm D. *Quantum Theory.* New York, NY: Prentice-Hall (1951).
97. Valdenebro A. Assumptions underlying Bell's inequalities. *Eur J Phys.* (2002) **23**:569–77. doi: 10.1088/0143-0807/23/5/313
98. Mermin ND. Hidden variables and the two theorems of John Bell. *Rev Mod Phys.* (1993) **65**:803. doi: 10.1103/RevModPhys.65.803
99. Wiseman H. The two bell's theorems of john bell. *J Phys A Math Theor.* (2014) **47**:424001. doi: 10.1088/1751-8113/47/42/424001
100. Adenier G, Khrennikov AY. Is the fair sampling assumption supported by EPR experiments? *J Phys B Atom Mol Opt Phys.* (2007) **40**:131–41. doi: 10.1088/0953-4075/40/1/012
101. Adenier G, Khrennikov AY. Test of the no-signaling principle in the Hensen loophole-free CHSH experiment. *Fortschr Phys.* (2017) **65**. doi: 10.1002/prop.201600096
102. Larsson J-A. Loopholes in Bell inequality tests of local realism. *J Phys A Math Theor.* (2014) **47**:424003. ?doi: 10.1088/1751-8113/47/42/424003
103. Larsson J-A, Gill RD. Bell's inequality and the coincidence-time loophole. *Europhys Lett.* (2004) **67**:707–13. doi: 10.1209/epl/i2004-10124-7
104. Kupczynski M, De Raedt H. Breakdown of statistical inference from some random experiments. *Comp Phys Commun.* (2016) **200**:168. doi: 10.1016/j.cpc.2015.11.010
105. Bednorz A. Analysis of assumptions of recent tests of local realism. *Phys. Rev. A.* (2017) **95**:042118. doi: 10.1103/PhysRevA.95.042118
106. Lin PS, Rosset D, Zhang Y, Bancal JD, Liang YC. Device-independent point estimation from finite data and its application to device-independent property estimation. *Phys. Rev. A*, (2018) 97:032309. doi: 10.1103/PhysRevA.97.032309
107. Zhang Y, Glancy S, Knill E. Asymptotically optimal data analysis for rejecting local realism. *Phys Rev A.* (2011) **84**:062118. doi: 10.1103/PhysRevA.84.062118
108. Christensen BG, Liang Y-C, Brunner N, Gisin N, Kwiat P. Exploring the limits of quantum non-locality with entangled photons. *Phys Rev X.* (2015) **5**:041052. doi: 10.1103/PhysRevX.5.041052
109. Kofler J, Ramelow S, Giustina M, Zeilinger A. On Bell violation using entangled photons without the fair-sampling assumption. *arXiv:1307.6475v1 [quant-ph].* (2013).
110. Allahverdyan AE, Balian R, Nieuwenhuizen TM. Understanding quantum measurement from the solution of dynamical models. *Phys Rep.* (2013) **525**:1–166. doi: 10.1016/j.physrep.2012.11.001
111. Allahverdyan AE, Balian R, Nieuwenhuizen TM. A sub-ensemble theory of ideal quantum measurement processes. *Ann Phys.* (2017) 376C:324. doi: 10.1016/j.aop.2016.11.001
112. Kupczynski M. Is quantum theory predictably complete? *Phys Scr.* (2009) T**135**:014005. doi: 10.1088/0031-8949/2009/T135/014005
113. Kupczynski M. Time series, stochastic processes completeness of quantum theory. *AIP Conf Proc.* (2011) **1327**:394–400. doi: 10.1063/1.3567465
114. Dzhafarov EN, Kujala JV. Selectivity in probabilistic causality: Where psychology runs into quantum physics. *J Math Psych.* (2012) **56**:54–63. doi: 10.1016/j.jmp.2011.12.003
115. Dzhafarov EN, Kujala JV. No-forcing, and no-matching theorems for classical probability applied to quantum mechanics 2014. *Found Phys.* (2014) **44**:248–65. doi: 10.1007/s10701-014-9783-3
116. Aerts D, Sozzo S, Veloz T. New fundamental evidence of non-classical structure in the combination of natural concepts. *Philosoph Trans R Soc A.* (2015) **374**:20150095. doi: 10.1098/rsta.2015.0095
117. Gill RD. Statistics causality and bell's theorem. *Stat Sci.* (2014) **29**:512–28. doi: 10.1214/14-STS490
118. Plotnitsky A. Spooky predictions at a distance: Reality, complementarity contextuality in quantum theory. *Phil Trans R Soc. A.* (2019) **377**:20190089. doi: 10.1098/rsta.2019.0089
119. Jung K. Violation of Bell's inequality: Must the Einstein locality really be abandoned? *J Phys Conf Ser.* (2017) **880**:012065. doi: 10.1088/1742-6596/880/1/012065
120. Jung K. Polarization correlation of entangled photons derived without using non-local interactions. *Front Phys.* (2020). doi: 10.3389/fphy.2020.00170
121. Boughn S. Making sense of Bell's theorem and quantum non-locality. *Found Phys.* (2017) **47**:640–57. doi: 10.1007/s10701-017-0083-6
122. Willsch M, et al. Discrete-event simulation of quantum walks. *Front Phys.* (2020) doi: 10.3389/fphy.2020.00145
123. De Raedt et al. Discrete-event simulation of an extended einstein-podolsky-rosen-bohm experiment. *Front Phys.* (2020) doi: 10.3389/fphy.2020.00160
124. Griffiths RB. Nonlocality claims are inconsistent with Hilbert-space quantum mechanics. *Phys. Rev. A.* (2020) **101**:022117. doi: 10.1103/PhysRevA.101.022117

Conflict of Interest: The author declares that the research was conducted in the absence of any commercial or financial relationships that could be construed as a potential conflict of interest.

frontiers in Physics

ORIGINAL RESEARCH
published: 19 May 2020
doi: 10.3389/fphy.2020.00170

Polarization Correlation of Entangled Photons Derived Without Using Non-local Interactions

*Kurt Jung**

Fachbereich Physik, Technische Universität Kaiserslautern, Kaiserslautern, Germany

Entangled photons leaving parametric down-conversion sources exhibit a pronounced polarization correlation. The data violate Bell's inequality thus proving that local realistic theories cannot explain the correlation results. Therefore, many physicists are convinced that the correlation can only be brought about by non-local interactions. Some of them even assume that instantaneous influences at a distance are at work. Actually, assuming a strict phase correlation of the photons at the source the observed polarization correlation can be deduced from wave optical considerations. The correlation has its origin in the phase coupling of circularly polarized wave packets leaving the fluorescence photon source simultaneously. The enlargement of the distances between photon source and observers does not alter the correlation if the polarization status of the wave packets accompanying the photons is not changed on their way from the source to the observers. At least with respect to the polarization correlation of entangled photons the principle of locality remains valid.

Keywords: Bell's theorem, violation of Bell's inequality, non-local interactions, instantaneous influence at a distance, polarization correlation, entangled photons, quantum statistics

OPEN ACCESS

Edited by:
Karl Hess,
University of Illinois at Urbana-Champaign, United States

Reviewed by:
Juergen Jakumeit,
Access e.V., Germany
Daniel Luiz Nedel,
Universidade Federal da Integração Latino-Americana, Brazil

***Correspondence:**
Kurt Jung
jung@physik.uni-kl.de

Specialty section:
This article was submitted to Mathematical Physics, a section of the journal Frontiers in Physics

Received: *03 March 2020*
Accepted: *22 April 2020*
Published: *19 May 2020*

Citation:
Jung K (2020) Polarization Correlation of Entangled Photons Derived Without Using Non-local Interactions. Front. Phys. 8:170. doi: 10.3389/fphy.2020.00170

1. INTRODUCTION

In 1935 Einstein et al. [1] initiated a discussion whether quantum mechanics is complete or not. In the following years one could not find concrete hints for the occurrence of hidden variables. In 1964 Bell [2] showed on the basis of two spin 1/2 particles that local realistic theories can principally not reproduce the results of quantum mechanics. In 1969 Clauser et al. [3] proposed an experiment to test local hidden variable theories with entangled photons. Already 3 years later Freedman and Clauser presented first measurements proving that local realistic theories were not able to describe the experimental results [4].

More elaborate experiments on the polarization correlation of entangled photons [5–12] showed that the experimental results are fully reproduced by quantum mechanics.

All experiments providing polarization correlation data with good statistics are performed in such a way that the detection processes of two distant observers are spacelikely separated. Thus, the publications on these experiments generally suggest that the results can only be induced by superluminal signals between the observers. Especially Salart et al. [9] emphasize that the violation of Bell's inequality seems to prove that quantum mechanics make use of non-local interactions.

Discrepancies between the results of local realistic theories and quantum mechanics are also discussed for more complicated quantum systems with more than two particles [13]. Many of these publications insinuate that faster-than-light communication might be possible. The drawback of all these attempts to prove the occurrence of non-local interactions is that until now no concrete results could be presented which reproduce the experimental findings.

In the last few years several recognized physicists try to prove that quantum mechanics does not use non-local interactions [14–21]. The authors show that some mathematical operations like the reduction of a quantum state seem to have non-local consequences. On closer examination these operations only cause changes of the observer's knowledge on the quantum state. The changes thus do not take place in physical space but merely in information space.

In fact, the results of the experiments with parametric down-conversion photon sources can be derived from wave optical and quantum statistical considerations without using superluminal signals. There are good arguments to assume that the experiments of Aspect and coworkers with entangled photons emerging from a specific decay cascade of calcium [5, 6] can also be explained without using non-local interactions. However, additional tests on the polarization status of the photons would be helpful in order to conclusively answer the question.

2. PHOTON PAIRS ARISING FROM DOWN-CONVERSION SOURCES

In the last 22 years several polarization correlation experiments with parametric down-conversion sources have been performed [7–12]. If necessary experimental details are taken from the doctor thesis of Weihs [22]. In a BBO crystal ultraviolet photons are converted into two phase coupled circularly polarized green photons with equal energies.

The circularly polarized wave packets are immediately decomposed into two linearly polarized wave packets with orthogonal polarization directions. The ordinary beam is vertically polarized. The extraordinary beam is horizontally polarized. Due to the different propagation directions the emission cones of ordinary and extraordinary beam appear on the exit plane as two off-centered circles which intersect each other at two points (see **Figure 1**). After traversing a compensation plate the reassembled circularly polarized wave packets leave nearly unchanged the two intersection zones.

In the polarization correlation experiments with parametric down-conversion sources only the so-called singlet-configuration has been studied. In this configuration the polarization planes of associated photons rotate in the same direction. In statistical average about one half of the photon pairs rotate clockwisely, the other half counterclockwisely.

3. DETECTION OF POLARIZED PHOTONS BY ALICE AND BOB

Photons emerging from the two exit sites of the source are guided by optical fibers to the observers. After leaving the optical fibers the wave packets traverse an electro-optical modulator arranged between two suitably oriented quarter-wave plates. In combination the three optically active elements twist linearly polarized waves by an arbitrarily choosable angle proportional to the applied voltage. The detector unit is fixed in space. The twist of the plane waves by the electro-optical modulator simulates a virtual twist of the detector unit. For the sake of convenience it will be assumed in the following that the twisting units are omitted and that the detectors are really twisted in space.

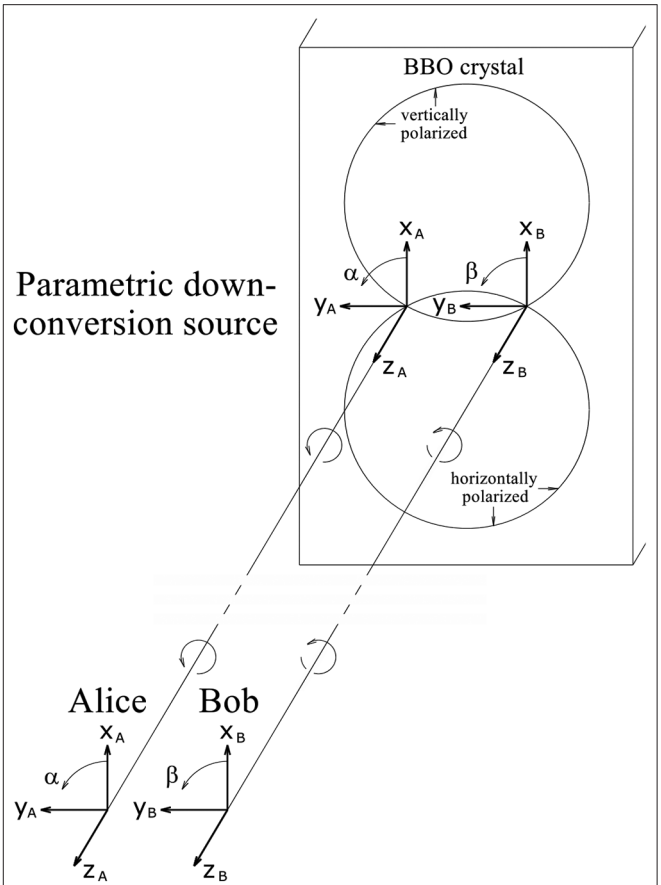

FIGURE 1 | Schematic diagram of a simple experimental setup suited to determine polarization correlations. In the top right corner a BBO source is shown which provides entangled photons both rotating in the same direction. The coordinate systems of the observers Alice and Bob shown in the bottom left corner are both right-handed. The angles α and β indicate the orientations of the linear polarizations looked for by Alice and Bob, respectively. The thin lines between source and observers denote optical fibers. The distance between Alice and Bob is usually chosen large enough to ensure that two associated photon detection processes are spacelikely separated.

By the use of Wollaston prisms Alice and Bob split the incoming wave packets into two equally large components with orthogonal polarization directions. The linearly polarized components hit altogether four detectors which should be highly sensitive in order to detect nearly all incoming photons [11, 12]. When the apparatus is thoroughly adjusted the count rates of the detectors should no longer depend on the polarization direction.

In the four detector channels each registered pulse is saved together with an individual time stamp. After having finished the measurement the four data lists are compared in order to determine four coincidence rates namely $I(\alpha, \beta)$, $I(\alpha, \beta + 90°)$, $I(\alpha + 90°, \beta)$, and $I(\alpha + 90°, \beta + 90°)$. Let I_0 be the coincidence rate when the selecting filters are removed on both sides of the experiment. If the losses in the filters are negligible I_0 is also the coincidence rate summed up in the four channels. The two

coincidence rates $I(\alpha, \beta)$ and $I(\alpha, \beta + 90^\circ)$ add up to $I_0/2$. The same is true for the coincidence rates $I(\alpha + 90^\circ, \beta)$ and $I(\alpha + 90^\circ, \beta + 90^\circ)$. Thereby one has to bear in mind that coincidence rates exhibit statistical uncertainties.

In this article particle as well as wave aspects will be addressed because the correlation of photons detected by Alice and Bob depends on the relative phase of the circularly polarized wave packets accompanying the photons. The derivation of the polarization correlation is mainly based on wave arguments but if necessary particle aspects will also be considered.

The terms "wave" and "light" are often used for convenience. In fact, a light beam will always be understood as a stream of independent wave packets with limited coherence length. Only wave packet pairs incorporating entangled photon pairs are strictly phase coupled when they leave the photon source. In the experiment of Weihs [22, p. 63] the coherence length has been estimated to be about 0.1 m. Thus, the wave packets leaving the photon source are very short in comparison with the distance between Alice and Bob thus precluding wave based non-local interactions between the observers.

4. FORMAL DERIVATION OF THE POLARIZATION CORRELATION

In wave optics and quantum mechanics one often asks for the phase relation of interfering waves in the detection plane in order to get the interference pattern. In correlation experiments, however, one has to ask for the phase relation of two associated wave packets at the source. The relative phase at the source manifests itself in the overlap integral of the two normalized wave packets.

The two wave packets simultaneously leaving outputs A and B have a phase shift of $\pm 90^\circ$ at the source. The sign reveals which of the wave packets is leading. In **Figure 1** the phase shift is indicated by twisted rotation vectors. If $\alpha \neq \beta$ an additional phase shift of $\pm(\alpha - \beta)$ has to be taken into account. The sign depends on the rotational direction of the two circularly polarized wave packets. Thus, the total phase shift of the two linearly polarized partial waves looked for by the two observers is

$$\varphi = \pm 90^\circ \pm (\alpha - \beta). \tag{1}$$

Neglecting the envelope function one has to evaluate the overlap integral of the two normalized functions

$$\begin{aligned} f(t) &= \sqrt{\omega/\pi}\, sin(\omega t) \\ g(t) &= \sqrt{\omega/\pi}\, sin(\omega t \pm 90^\circ \pm (\alpha - \beta)). \end{aligned} \tag{2}$$

The second function divided by the normalizing factor can be converted by using trigonometrical addition theorems twice

$$\begin{aligned} &sin(\omega t \pm 90^\circ \pm (\alpha - \beta)) = \\ &sin(\omega t) cos(\pm 90^\circ \pm (\alpha - \beta)) + \\ &cos(\omega t) sin(\pm 90^\circ \pm (\alpha - \beta)) = \\ &\pm sin(\omega t) sin(\alpha - \beta) \\ &\pm cos(\omega t) cos(\alpha - \beta) \end{aligned} \tag{3}$$

By using the definite integrals

$$\begin{aligned} \frac{\omega}{\pi} \int_0^{2\pi/\omega} sin(\omega t) sin(\omega t) dt = 1 \\ \frac{\omega}{\pi} \int_0^{2\pi/\omega} sin(\omega t) cos(\omega t) dt = 0 \end{aligned} \tag{4}$$

one can easily calculate the overlap integral

$$\int_0^{2\pi/\omega} f(t) g(t) dt = \pm\, sin(\alpha - \beta). \tag{5}$$

The (absolute) square of the overlap integral of the two normalized phase coupled wave packets is proportional to the coincidence rate. As has been explained in the previous chapter the coincidence rates $I(\alpha, \beta)$ and $I(\alpha, \beta + 90^\circ)$ add up to $I_0/2$. Therefore, the proportionality factor must be $I_0/2$.

Thus the coincidence rate is given by

$$I(\alpha, \beta) = I_0\, sin^2(\alpha - \beta)/2 \tag{6}$$

and the correlation is given by

$$C(\alpha, \beta) = \frac{I(\alpha, \beta)}{I(\alpha, \beta) + I(\alpha, \beta + 90^\circ)} = sin^2(\alpha - \beta). \tag{7}$$

With this rather simple consideration the experimentally found correlations of entangled photons have been fully reproduced.

5. WORKING OUT QUANTUM STATISTICAL ASPECTS

Quantum statistics will become much clearer if each of the two circularly polarized light beams A and B leaving the source is formally splitted into two commensurate linearly polarized beams with orthogonal polarization directions. A circularly polarized wave can always be understood as the superposition of two equally sized linearly polarized partial waves with orthogonal polarization directions. The two partial waves are phase shifted with respect to each other by $\pm 90^\circ$. The orientations of the linear polarizations ϑ and $\vartheta + 90^\circ$ can be freely chosen.

The photons contained in the two partial beams form two disjunct groups. If a photon has been assigned to a linearly polarized partial beam it will always stay in that beam. There is no intermixing between the two photon groups on their way from the source to the observers even if the photons and the accompanying wave packets traverse electro-optical modulators and quarter-wave plates.

All modern experiments are planned with the aim that selection and detection processes carried out by the two observers are spacelikely separated. Therefore, the splitting is performed just in front of the detectors. The rather late fixing of the angles α and β even concerns photons leaving the source much earlier. Thus, the splitting of the circularly polarized beams admittedly needs non-local information but certainly no non-local interaction because the two streams of photons propagating toward Alice and Bob are not modified by the repeated change

of the detection angles. Before the photons reach the associated Wollaston prism the splitting procedure is a purely mathematical but not a physical process.

Due to their common origin entangled photon pairs are phase coupled when they leave the source. In case of parametric down-conversion processes the two entangled photons are in phase but the two associated circularly polarized wave packets are phase shifted by $\pm 90^\circ$.

As the optical pathes from the source to Alice and Bob will generally not be balanced the initial phase information cannot be recovered by simply comparing the arrival times of the entangled photons. This would merely be impossible due to the limited time resolution of external clocks and to the jitter of the detection electronics.

Fortunately the two beams are equipped with synchronized internal clocks which can be easily read off by the observers. Within one wave cycle the polarization plane performs a full turn. Thus, the relative phase of the photons at the source up to multiples of 180° can be recovered from the difference of the polarization angles looked for by the two observers. The modulo 180° term comes from the 180° periodicity of the polarizer's transmittance.

The polarization correlation with due regard to the particle aspect will be derived in two steps. At first the case $\alpha = \beta$ will be discussed. This step covers the crucial point in the line of arguments explaining why the entangled photons are statistically distributed to only two of the four possible coincidence channels.

The two partial beams $A(\alpha)$ and $B(\alpha + 90^\circ)$ are in phase (or opposite in phase) at the source. The same is true for the partial beams $A(\alpha + 90^\circ)$ and $B(\alpha)$. As the photons are in phase at the source they must be found either in the coincidence channel $A(\alpha)/B(\alpha + 90^\circ)$ or in the coincidence channel $A(\alpha + 90^\circ)/B(\alpha)$. As the two coincidence channels are equivalent the probabilities to find the entangled photon pairs in these two coincidence channels must be equal.

In contrast, the partial beams $A(\alpha)$ and $B(\alpha)$ are phase shifted at the source by $\pm 90^\circ$. That means they are orthogonal to each other. The same is true for the partial beams $A(\alpha + 90^\circ)$ and $B(\alpha + 90^\circ)$. Therefore, there will be no coincidences in these two coincidence channels.

For each angle α the coincidence rates in the four conceivable channels are thus given by

$$\begin{aligned} I(\alpha, \beta = \alpha + 90^\circ) &= I_0/2 \\ I(\alpha, \beta = \alpha) &= 0 \\ I(\alpha + 90^\circ, \beta = \alpha) &= I_0/2 \\ I(\alpha + 90^\circ, \beta = \alpha + 90^\circ) &= 0. \end{aligned} \tag{8}$$

The correlations $C(\alpha, \beta = \alpha)$, $C(\alpha, \beta = \alpha + 90^\circ)$, $C(\alpha + 90^\circ, \beta = \alpha + 90^\circ)$, and $C(\alpha + 90^\circ, \beta = \alpha)$ are either zero or unity. That means entangled photons are strictly anticorrelated. This statement is valid for each single pair of entangled photons, not only for a statistical ensemble of entangled photon pairs.

The considerations above prove that the two entangled photons are both contained either in the partial wave pair $A(\alpha)$ and $B(\alpha + 90^\circ)$ or in the partial wave pair $A(\alpha + 90^\circ)$ and $B(\alpha)$. Whether the photon is detected by detector $A(\alpha)$ or by detector $A(\alpha + 90^\circ)$ is purely accidental. One cannot predict which detector will be hit by individual photons. However, after the detection of the first photon of a photon pair for example on Alice's side it will be clear which one of the two detectors on Bob's side will be hit by the second photon.

Only the anti-correlation of entangled photons is predefined but not the polarization of individual photons [23]. This is why the polarization direction should not be thought of as an element of reality.

The phase relation of partial beams at the source thus leads to the strong polarization correlation although the information on the polarization status is not a hidden property of the photons. Einstein et al. [1] had claimed that a property equally found in two no longer interacting quantum states must be an element of reality. The pronounced polarization correlation of entangled photons seems to be a counterexample.

The wrong estimate of Einstein and his coworkers has entailed the erroneous approach of Bell [2] who assumed that the polarization directions are real properties of the photons. In fact, the phase coupling only predefines the interrelationship but not the property itself. In consequence Bell's inequalities are irrelevant.

The extension of the consideration to the case $\alpha \neq \beta$ is rather trivial and exclusively rests on an optical law discovered by Etienne Louis Malus in 1810. Malus' law says: If light linearly polarized in direction γ traverses a polarization filter with its polarization axis oriented in direction δ its intensity is reduced by the factor

$$cos^2(\gamma - \delta).$$

One cannot predict which one of the photons will traverse the polarization filter because Malus' law has a purely statistical character. The law is valid not only for light leaving a classical light source but also for laser light. That means it does not depend on second-order coherence properties of a photon stream. It is also experimentally proven in case of low intensity when the beam intensity is measured by single photon detectors. Brukner and Zeilinger explicitly show that Malus' law is also valid in the quantum regime [24]. In one of his recent publications Khrennikov has also used Malus' law when he derived the polarization correlation of entangled photons starting from quantum mechanical considerations [16, p. 3].

The first of Equation (8) means that if one of the entangled photons has been recorded by detector $A(\alpha)$ the associated photon will certainly be contained in the partial beam $B(\alpha + 90^\circ)$. Therefore, one has to apply Malus' law for $\gamma = \alpha + 90^\circ$ and $\delta = \beta$. That means the coincidence rate $I_0/2$ is reduced by the factor $cos^2(\alpha + 90^\circ - \beta) = sin^2(\alpha - \beta)$. Therewith the coincidence rate $I(\alpha, \beta)$ is given by

$$I(\alpha, \beta) = I_0 \, sin^2(\alpha - \beta)/2. \tag{9}$$

in accordance with Equation (6).

The role of Alice and Bob can be exchanged. If the circularly polarized beams are splitted into partial beams linearly polarized

in the directions β and $\beta + 90^\circ$ the results presented above will be reproduced.

For $\alpha \neq \beta$ Malus' law with its inherently statistical character has to be applied on Alice's or on Bob's side. In this case the correlation $C(\alpha, \beta)$ is larger than zero and smaller than unity. Thus, the correlation is not defined for a single pair of entangled photons but only for a sufficiently large group of entangled photon pairs.

As has been proven above the piece of information responsible for the emergence of the pronounced correlation is the phase shift of two associated wave packets when they leave the source. Traditionally quantum mechanics strictly takes into account phase differences of wave functions contained in a matrix element. Therefore, it can be assumed for sure that the phase difference of the two entangled photons will also be considered in quantum mechanics.

It is not relevant whether the correlation problem is handled classically or quantum mechanically. It is only relevant whether the phase information is used or not.

The calculations based on local realistic theories do not consider phase relations. They only try to reproduce the polarization correlation by assuming that the polarization directions of the entangled photons are encoded in the photons as hidden variables. In explaining the strong polarization correlation of entangled photons only their relative phase at the source is relevant.

6. GENERAL REMARKS

The pronounced correlation of entangled photons is neither superprising nor mysterious. It solely depends on the initial phase shift of the circularly polarized waves accompanying the entangled photons. One only has to make sure that the polarization directions α and β looked for by the two observers are associated with corresponding polarization angles at the source. This condition is fulfilled in each of the experiments. Hereby it is not relevant at what time the polarization directions have been chosen. The purely conceptual splitting of the two partial beams and the detection of the photons have no effect on the parametric down-conversion process. The relative phase of the entangled photons has been fixed inside the source. The observers only decide which polarization directions they look for. There is no need for a superluminal information transfer between the observers. The distance between the observers is absolutely irrelevant.

The relative phase of entangled photons at the source could be declared to be a hidden variable finally revealed by the coincidence detection process. Hidden variables of this type can only be associated with wave packets but not with particles. The decisive point of the argumentation is that the wave intensity and thus also the coincidence rate is proportional to the (absolute) square of the scattering amplitude. Properties are only manifested after squaring the overlap integral. In particle based considerations properties directly act upon counting rates.

Bell's inequality is misleading because it attributes properties like polarization directions to particles and not to waves. Therefore, Bell cannot take into account phase differences of entangled photons. In future one should ignore violations of Bell's theorem because Bell's considerations are not adequate to describe wave phenomena.

7. CORRELATION OF PHOTON PAIRS IN TRIPLET CONFIGURATION

A pronounced correlation of entangled photons should also be observable in triplet configuration. That means that the two circularly polarized waves are rotating in opposite directions. In this case the correlation cannot be derived as easily as in the singlet case. One can figure out that the triplet configuration arises from the singlet configuration by mirroring one of the circularly polarized waves at a vertical plane. This can be performed by a half-wave plate with the optical axis oriented in vertical direction. If the circularly polarized wave packets are phase shifted by $\pm 90^\circ$ the correlation should be

$$C(\alpha, \beta) = sin^2(\alpha + \beta). \tag{10}$$

Thereby the origins of the angles α and β have to lie in the vertical plane. Preliminary measurements of Weihs [22, p. 72] support this result. For example if the two observers both look for polarization directions parallel to 45° the coincidence rate is at a maximum.

In a former publication [25] the sign in the correlation equation for the triplet configuration was minus instead of plus. The sign change has to do with the fact that Bob's coordinate system was left-handed in the previous article. In the consideration above both coordinate systems are right-handed.

8. PROPERTIES OF PHOTON PAIRS ARISING FROM ATOMIC SOURCES

In the experiments with parametric down-conversion sources the two circularly polarized wave packets are phase shifted by $\pm 90^\circ$ leading to a strict anticorrelation of the linear polarizations. In contrast, in the experiments of Aspect et al. [5, 6] the two circularly polarized wave packets are in phase or opposite in phase. Therefore, the correlation is given by

$$C(\alpha, \beta) = cos^2(\alpha - \beta). \tag{11}$$

The two photons produced by a decay cascade of calcium have different frequencies. Only if the rotational frequencies are equal one can define a phase shift. Thus, it should be tested in future experiments whether the rotational frequencies of the two entangled photons are equal or not. With respect to the rotational motion the coherence time of the two photons must be longer than the life time of the intermediate state of the decay cascade.

9. DOES IT HELP TO POSTULATE NON-LOCAL INTERACTIONS?

Is it really helpful to postulate a novel interaction which is in serious conflict with special relativity? Postulating an information

transfer faster than light entails a wealth of new problems. An instantaneous influence at a distance requires that simultaneity can be strictly defined for distant locations in contrast to corresponding assertions of special relativity.

Even if such principal objections are ignored many practical problems arise. How could such a postulated interaction generate correct results? In correlation experiments the ratio of coincidence rates in two complementary channels $I(\alpha, \beta)$ and $I(\alpha, \beta + 90°)$ has to be precisely defined. The newly postulated interaction has to redirect a well-specified percentage of stochastically arriving photons from one channel to the other one. The expected ratio of coincidences in the two channels depends on the difference of the polarization directions α and β? How does the postulated interaction get the information on the angles? In the experiments the twisting angles α and β are generated by applying voltages to electro-optical modulators. How could any theory whatsoever associate a voltage to an angle? The proportionality factor depends on the material, on the orientation of the crystal axis and numerous other experimental details.

Actually, in the optical fibers spurious birefringent effects occur which are manually compensated. How can the postulated new interaction know whether the apparatus is well-adjusted or not? By the way all the twisting processes are frequency dependent. Only light composed of photons like those used in the experiment can gain the information on the adjustment status and on the angles α and β.

The experiment of Salart et al. [9, p. 863] shows that the postulated "spooky" interaction must be at least 50,000 times faster than the speed of light. If the lengthes of the optical fibers differ distinctly from each other the superluminal signal has to wait quite a long, but an extremely well-defined time interval before it redirects individual pulses from one output to the other one. It will be extremely difficult to embed such a delayed reaction in a serious physical theory.

DATA AVAILABILITY STATEMENT

All datasets generated for this study are included in the article/supplementary material.

AUTHOR CONTRIBUTIONS

The author confirms being the sole contributor of this work and has approved it for publication.

ACKNOWLEDGMENTS

I thank Andrei Khrennikov for kindly reading my manuscript. I tried to consider his concerns with respect to quantum statistics.

REFERENCES

1. Einstein A, Podolsky B, Rosen N. Can quantum-mechanical description of physical reality be considered complete? *Phys Rev.* (1935) **47**:777–80.
2. Bell JS. On the Einstein Podolsky Rosen Paradox. *Physics.* (1964) **1**:195–200.
3. Clauser JF, Horne MA, Shimony A, Holt RA. Proposed experiment to test local hidden-variable theories. *Phys Rev Lett.* (1969) **23**:880–4.
4. Freedman SJ, Clauser JF. Experimental test of local hidden-variable theories. *Phys Rev Lett.* (1972) **28**:938–41.
5. Aspect A, Grangier P, Roger G. Experimental tests of realistic local theories via Bell's theorem. *Phys Rev Lett.* (1981) **47**:460–3.
6. Aspect A, Grangier P, Roger G. Experimental realisation of Einstein-Podolsky-Rosen-Bohm *Gedanken experiment*: a new violation of Bell's inequalities. *Phys Rev Lett.* (1982) **49**:91–4.
7. Tittel W, Brendel J, Gisin B, Herzog T, Zbinden H, Gisin N. Experimental demonstration of quantum correlations over more than 10 km. *Phys Rev A.* (1998) **57**:3229–32.
8. Tittel W, Brendel J, Zbinden H, Gisin N. Violation of Bell's inequalities by photons more than 10 km apart. *Phys Rev Lett.* (1998) **81**:3563–6.
9. Salart D, Baas A, Branciard C, Gisin N, Zbinden H. Testing the speed of 'spooky action at a distance'. *Nature.* (2008) **454**:861–4. doi: 10.1038/nature07121
10. Weihs G, Jennewein J, Simon C, Weinfurter H, Zeilinger A. Violation of Bell's inequality under strict Einstein locality conditions. *Phys Rev Lett.* (1998) **81**:5039–43.
11. Giustina M, Versteegh MAM, Wengerowsky S, Handsteiner J, Hochrainer A, Phelan K, et al. (2015) Significant-Loophole-Free test of Bell's theorem with entangled photons. *Phys Rev Lett.* (2015) **115**:250401. doi: 10.1103/PhysRevLett.115.250401
12. Shalm L, Meyer-Scott E, Christensen BG, Bierhorst P, Wayne MA, Stevens MJ, et al. Strong Loophole-Free test of local realism. *Phys Rev Lett.* (2015) **115**:250402. doi: 10.1103/PhysRevLett.115.250402
13. Pan JW, Bouwmeester D, Daniell M, Weinfurter H, Zeilinger A. Experimental test of quantum nonlocality in three-photon Greenberger-Horne-Zeilinger entanglement. *Nature.* (2000) **403**:515–9. doi: 10.1038/35000514
14. Khrennikov A. Get rid of nonlocality from quantum physics. *Entropy.* (2019) **21**:806. doi: 10.3390/e21080806
15. Khrennikov A. Quantum versus classical entanglement: eliminating the issue of quantum nonlocality. *Found Phys.* (2020) doi: 10.1007/s10701-020-00319-7. [Epub ahead of print].
16. Khrennikov A. Two faced Janus of quantum nonlocality. *Entropy.* (2020) **22**:303. doi: 10.3390/e22030303
17. Kupczynski M. Closing the door on quantum nonlocality. *Entropy.* (2018) **20**:877. doi: 10.3390/e20110877
18. Hess K. Bell's theorem and instantaneous influence at a distance. *J Mod Phys.* (2018) **9**:1573–90. doi: 10.4236/jmp.2018.98099
19. Hess K. Categories of nonlocality in EPR theories and the validity of Einstein's separation principle as well as Bell's theorem. *J Mod Phys.* (2019) **10**:1209–21. doi: 10.4236/jmp.2019.1010080
20. Boughn S. Making sense of Bell's theorem and quantum nonlocality. *Found Phys.* (2017) 47:640–57. doi: 10.1007/s10701-017-0083-6
21. Griffiths RB. Nonlocality claims are inconsistent with Hilbert-space quantum mechanics. *Phys Rev A.* (2020) **101**:022117. doi: 10.1103/PhysRevA.101.022117
22. Weihs G. *Ein Experiment zum Test der Bellschen Ungleichung unter Einsteinscher Lokalität* (Dissertation), Universität Wien (1999). Available

online at: https://www.uibk.ac.at/exphys/photonik/people/gwdiss.pdf (accessed March 1, 2020).
23. Khrennikov A. Towards a resolution of dilemma: nonlocality or nonobjectivity. *Int J Theor Phys.* (2012) **51**:2488–502. doi: 10.1007/s10773-012-1129-3
24. Brukner Š, Zeilinger A. Malus' law and quantum information. *Acta Phys Slov.* (1999) **49**:647–52.
25. Jung K. Violation of Bell's inequality: must the Einstein locality really be abandoned? *J Phys Conf Ser.* (2017) **880**:1–8. doi: 10.1088/1742-6596/880/1/012065

Conflict of Interest: The author declares that the research was conducted in the absence of any commercial or financial relationships that could be construed as a potential conflict of interest.

frontiers in Physics

ORIGINAL RESEARCH
published: 15 September 2020
doi: 10.3389/fphy.2020.00360

Locality Is Dead! Long Live Locality!

*William Sulis**

Collective Intelligence Laboratory, Department of Psychiatry and Behavioural Neuroscience, McMaster University, Hamilton, ON, Canada

Several decades of theory and experiment into EPR correlations have led to the widely held belief that reality is non-local, in spite of the fact that this violates special relativity. To date, no experiment has shown a violation of special relativity, and EPR experiments do not demonstrate the existence of superluminal information exchange, merely correlations which violate certain inequalities. Every "loophole" in these hidden variable theories has been thought plugged. However, there is much confusion in the literature due to conflation of the terms "locality," "realism," "hidden variables," "non-contextuality." The presence of local hidden variables is thought to necessarily lead to a Kolmogorov probability structure (hence non-contextuality), but this is an assumption, one which is not true in general once context effects are taken into account. Treated as an observational theory, several authors have shown no incompatibility between quantum mechanics and locality, and that the Bell scenario is actually about whether reality is contextual. This paper proposes a descriptive theory by assuming a generated reality (following Whitehead's Process Theory) which can violate the principle of continuity and possess non-Kolmogorov probability structure, and reproduce the results of non-relativistic quantum mechanics, while allowing only causally local information exchange without hidden variables. A generated reality is thus compatible with both quantum mechanics and special relativity, reproducing all of the results expected from quantum mechanics while still maintaining causally local realism. This process model thus appears to be an ideal candidate for developing theories for the unification of quantum mechanics and general relativity.

Keywords: local realism, contextuality, process algebra, process model, non-relativistic quantum mechanics

OPEN ACCESS

Edited by:
Andrea Valdés-Hernández, National Autonomous University of Mexico, Mexico

Reviewed by:
Theo Nieuwenhuizen, University of Amsterdam, Netherlands
Emmanuel E. Haven, Memorial University, Canada
Robert Bruce Mann, University of Waterloo, Canada

***Correspondence:**
William Sulis
sulisw@mcmaster.ca

Specialty section:
This article was submitted to Mathematical and Statistical Physics, a section of the journal Frontiers in Physics

Received: *24 April 2020*
Accepted: *28 July 2020*
Published: *15 September 2020*

Citation:
Sulis W (2020) Locality Is Dead! Long Live Locality!. Front. Phys. 8:360. doi: 10.3389/fphy.2020.00360

INTRODUCTION

The debate as to whether reality at its fundamental level conforms to the tenets of local realism has been decided decisively in the negative. Non-locality has won. Locality is dead! Or is it? In spite of an ever more sophisticated series of hidden variable theorems and dramatic experimental results, has the issue of local realism truly been laid to rest? In the years following the seminal paper of Einstein, Podolsky and Rosen (EPR) [1], the concept of local realism has become equated with the concept of (deterministic) local, non-contextual, hidden variables (LNHV). The assumption of LNHV leads to inequalities on measurement correlations, which experiments have shown are violated. The conclusion is that LNHV do not exist.

The restriction of local hidden variables to *deterministic* LNHV was unnecessary, likewise, the restriction of local realism to LNHV is also excessive. Arguments in support of this will be provided and an explicit model of non-relativistic quantum mechanics (NRQM), the Process Algebra model, will be demonstrated. The Process Algebra model is a local, realist, generative, contextual, and

discrete model of NRQM without hidden variables in which NRQM appears as an effective theory in the continuum limit as Planck length and time are taken to zero [2–6]. It has been argued that the Process Algebra model provides a true completion of NRQM [4]. The Process Algebra provides a nuanced framework for representing interactions between fundamental entities which the standard Hilbert space formulation lacks. It suggests that the quantum paradoxes and conundrums are due to a failure of the usual Hilbert space formalism to correctly represent particle interactions.

THE ARGUMENTS AGAINST LOCAL HIDDEN VARIABLES

The story against local realism begins with the 1935 EPR paper [1], which tackled two questions, that of the completeness of quantum mechanics as a physical theory and that of the nature of reality. As to completeness, they wrote: "Whatever the meaning assigned to the term *complete,* the following requirement for a complete theory seems to be a necessary one: *every element of the physical reality must have a counterpart in the physical theory."* They later suggested the following as a plausible, sufficient but not necessary definition of reality: "*If, without in any way disturbing a system, we can predict with certainty (i.e., with probability equal to unity) the value of a physical quantity, then there exists an element of physical reality corresponding to this physical quantity* (SIC)."

Nowadays quantum mechanics is considered to be complete *mathematically (or epistemologically)*, because no addition to quantum mechanics results in a probabilistically better theory [7]. Whether or not it is complete *ontologically*, thus providing a complete description of physical reality is no longer a criterion [8].

The EPR argument was not about locality *per se* but against contextuality, the inability to perform simultaneous measurements of incompatible (non-commuting) observables. Locality was inferred from the requirement that the systems should not interact with one another in any manner.

Subsequently Bohm [9], Bohm and Aharonov [10], Bell [11], and Clauser, Horne, Shimony, Holt [12] introduced refinements to the EPR argument which brought the scenario (or a version thereof) closer to experimental scrutiny and explicitly addressed the issues of locality and hidden variables. The idea of hidden variables refers to the existence of some unknown parameter space Λ, such that all measurements A and probabilities p associated with an experiment are functions of values, that is, $A(x,\lambda), p(x,\lambda)$, where x refers to all of the overt variables associated with the experiment. Early papers focused on deterministic hidden variables, but as Bell pointed out [11], the question of deterministic, non-deterministic, or stochastic is irrelevant; the real question is whether or not the assumption of hidden variables can explain the observations. The Bell scenario involves two quantum systems, I, II, which interact to form an entangled state, ensuring that the states of the two systems are correlated. The systems then propagate to space-like separated locations, *X, Y*, which, if special relativity (and therefore locality) holds, should ensure that they are unable to interact with one another in any manner. Next two independent observers, conventionally Alice and Bob, are allowed to carry out measurements, Alice of system I, Bob of system II, of (usually non-commuting) observables *A,B*, respectively, each parameterized by *a,b*, respectively. After collecting their data, Alice and Bob then determine various correlations among their measurements and then test these results against a specific inequality, namely $-2 \leq E(a',b') + E(a',b'') + E(a'',b') - E(a'',b'') \leq 2$ where $E(x,y)$ is the expectation value of the product of the outcomes of measurements of the two systems when Alice's observable setting is x and Bob's observable setting is y ([13], chapter 8).

Bell [11], Jarrett [14], and Shimony [13] emphasized that one of the key components of the argument leading to the inequality is that the probability distribution given by the hidden variables must satisfy a factorizability condition. Following Shimony [13] and Jarrett [14], let $p^i(x/k,a,b)$ denote the probability of observer i measuring outcome x given complete state k, Alice's setting a and Bob's setting b. $p(m,n/k,a,b)$ is the joint probability when Alice obtains measurement m and Bob obtains measurement n. $p^i(x/k,a,b,y)$ is the conditional probability when the second observer obtains measurement y. Jarrett defined two independence conditions:

Parameter Independence

$$p^i(m/k,a,b) = p^1(m/k,a)$$
$$p^2(n/k,a,b) = p^2(n/k,b)$$

Outcome Independence

$$p^1(m/k,a,b,n) = p^1(m/k,a,b)$$
$$p^2(n/k,a,b,m) = p^2(n/k,a,b)$$

Jarrett showed that the assumption of both independence conditions leads to the factorizability condition: $p(m,n/k,a,b) = p^1(m/k,a)p^2(n/k,b)$. This condition is an essential component of most hidden variable arguments [10, 11, 15–18]. When true, the hidden variables are non-contextual with a Kolmogorov probability structure, unlike quantum mechanics which has a non-Kolmogorov probability structure by virtue of the Born rule. All hidden variable arguments assume factorizability. Assuming factorizability, Fine [19, 20] showed that the presence of deterministic LNHV implies the existence of a joint probability distribution for even non-commuting observables, violating the predictions of quantum mechanics.

Kolmogorov [21] himself emphasized that probability theory was fundamentally a contextual theory. Probability distributions were context dependent. Fine [20] developed some criteria for when a joint probability distribution exists but years earlier Vorob'ev [22] had presented a complete set of criteria for the existence of joint distributions in the general case and several examples where his criteria failed to be satisfied. This clearly showed that the factorizability condition is an assumption, not a necessity. The fundamental question is whether hidden variables are non-contextual (factorizable) or contextual.

Another approach to the EPR scenario has focused upon contextuality directly. EPR [1] and others [23] define realism to mean that every element of reality possesses, a priori, a definite value for every possible observable. Contextuality asserts that not all observables can have pre-existing values. Realism is then equated with non-contextuality. A succession of ever more powerful results (von Neumann [24], Gleason [25], Mackey [26], Kochen-Specker [27], Mermin [28]) have shown quite conclusively that quantum mechanics, in its Hilbert space formulation, is a contextual theory. Dispersion-free measures do not exist, so that it is impossible through acts of measurement to assign definite values to all possible observables to single physical entities. If realism is equivalent to non-contextuality, then quantum mechanics shows that realism does not exist. One is left with Wheeler's famous dictum that "no phenomenon is a phenomenon until it is an observed phenomenon" [29], so that there is no external reality; the actions of an observer cause reality to manifest. The realist perspective attempts to avoid falling down this particular philosophical rabbit hole.

It took nearly 50 years to develop the technology to allow testing of these theories. Most experiments have involved entangled photons although a few have used entangled electrons [30–38]. Since the first experiments of Aspect and Grangier [30] showed that the Bell inequality was indeed violated, a number of possible "loopholes" have been proposed related to experimental factors such as detector accuracy, propagation losses, detector distance, superdeterminism, all of which have been eliminated by subsequent experiments [31–36]. Even free will have been challenged [39]. Bell's inequality has been violated in all of these experiments to a statistical level of at least 11 standard deviations, and any presumed non-local influence must propagate with a speed of at least 50,000c. Bell type experiments have now become school demonstrations [37]. There is now an experiment which visualizes correlations referred to in Bell's theorem [38].

For those who accept Bell's argument and its variations, the issue would appear to be put to rest. LNHV do not exist and reality, if it even exists, is non-local.

THE ARGUMENTS AGAINST THE ARGUMENTS AGAINST LOCAL HIDDEN VARIABLES

Or is it? As in every walk of life, things are not as simple as they first appear.

Khrennikov [40], drawing on work of Hertz and Boltzmann, divides theories into two general kinds: descriptive, and observational. Descriptive (ontological) theories attempt to describe the entities (causes) that give rise to observed phenomena. Observational (epistemological) theories attempt to merely provide a predictive framework for these same phenomena. Quantum mechanics is, mostly, an observational theory. The arguments against local hidden variable described above are framed within an observational framework.

The Bell scenario involves three distinct stages: interaction, propagation, measurement. The literature has focused primarily upon the measurement stage, simply assuming the first two stages as given. Nevertheless, the derivation of the inequalities depends upon assumptions made regarding these initial stages. Quantum mechanics is not involved in this derivation. Experiments have been performed which show that the inequalities are violated. Logically then, there must be errors in the assumptions leading to the inequalities. This is not necessarily a vindication of quantum mechanics.

From an observational/epistemological perspective the key problem is the assumption of factorizability of the probability associated with whatever variables are assumed to be present in the description of the measurement situation. A factorizable probability leads inevitably to a joint distribution for the measurements, regardless of whether they are compatible or complementary. Is the assumption of factorizability necessary for any model of local realism?

Khrennikov [40], following earlier work of Landau [41], constructed a quantum mechanical analog of the CHSH inequality. Given 4 observables, A_1, A_2 for system 1 and B_1, B_2 for system 2, he considered:

$< \mathcal{B} >= \frac{1}{2}(<A_1B_1> + <A_1B_2> + <A_2B_1> - <A_2B_2>)$. After some algebra he obtained the Landau identity $\widehat{\mathcal{B}}^2 = 1 - \frac{1}{4}[\hat{A}_1, \hat{A}_2][\hat{B}_1, \hat{B}_2]$. If either the A or B operators are compatible, then $| < \mathcal{B} > | \leq 1$. He then showed that there exists a quantum state such that $||\widehat{\mathcal{B}}||^2 \geq (1 + \mu) > 1$ so that quantum mechanics violates the above inequality. Khrennikov argued that the quantum analog of the CHSH inequality measures the degree of incompatibility among the observables being measured on each system and is not a reflection of non-locality. Similarly, Cabello [42] has demonstrated formally that the generalized Bell inequality and Kochen-Specker contextuality are equivalent in quantum mechanics. Nieuwenhuizen [43] also examined the CHSH inequality and showed that the probability measures required to calculate the various correlation functions were subject to contextuality effects, so that no joint probability distribution, required to make meaningful the resulting inequality, exists. He referred to this as the *contextuality loophole,* and also argued for its universality. Kupczynski [44] advocates for an purely epistemological, ensemble interpretation of quantum mechanics, and also argues that the Bell argument is invalid because it fails to take into account the contextual nature of the probability distributions associated with these ensembles.

Khrennikov has developed an extension of Kolmogorov probability theory called *contextual probability theory* [45]. Contextual probability theory does for probability theory what non-Euclidean geometry did for geometry. The point of departure from Kolmogorov probability is the *sum rule*, which takes the form $p^b_C(\beta) = \sum_\alpha p^a_C(\alpha)p_{\beta|\alpha} + 2\lambda(\beta|\alpha, C)\sqrt{\prod_\alpha p^a_C(\alpha)p_{\beta|\alpha}}$ where

λ is the probabilistic measure of interference and the p terms are various conditional probabilities over contexts (C) and observables a,b. In Kolmogorov probability, $\lambda = 0$, otherwise λ can be a trigonometric function or a hyperbolic function. Contextual probability has been applied to a number of classical level phenomena in biology, psychology, and economics [45–51] and to the Bell situation [52, 53]. The appearance of

non-Kolmogorov probability at a classical level demonstrates empirically that the assumption that any probability associated with local hidden variables *must* be Kolmogorov is prima facie false. Hidden variables may be non-contextual or contextual at both classical and quantum levels. This does not necessitate non-locality or a failure of realism.

Dzhafarov et al. [54], Dzhafarov and Kon [55], and Dzhafarov and Kujala [56] has presented an alternative approach to that of Khrennikov termed *Contextuality by Default*. Following the notation in [57], each random variable is associated with the quantity q being measured and the context a within which the measurement is made, and denoted, R^a_q. Consider two measurements, q,q' and two contexts a,b. For a fixed context a, the pair $R^a_q, R^a_{q'}$ is termed *bunch,* representing the collection of measurements associated to a specific context. It is reasonable to believe that such a pair is jointly distributed. For a fixed measurement q, the pair R^a_q, R^b_q is termed a *connection* for q.

The most basic form of contextuality occurs when no joint distribution can be found for a connection. In such a case they are said to be *inconsistently connected*. This is the situation of *contextuality by default*. Dzhafarov considers this to be the most trivial form of contextuality since it is so ubiquitous. Dzhafarov has developed a more restricted notion of contextuality in line with contextuality in physics. He considers couplings between bunches. For example, given two bunches $R^a_q, R^a_{q'}$ and $R^b_q, R^b_{q'}$, a coupling is a set of jointly distributed random variables (A,B,X,Y), subject to certain constraints, such that (A,B) is distributed as $R^a_q, R^a_{q'}$ and (X,Y) is distributed as $R^b_q, R^b_{q'}$. The constraints involve A,X and B,Y which correspond to measurements of q and q', respectively. A measurement q is considered to be *context independent* if among all couplings (A,B,X,Y), we have $Pr(A \neq X) = 0$. It can be shown that such a coupling may not exist even if the system is consistently connected.

Now consider all couplings (A,X) for just the connection $R^a_q, R^b_{q'}$ and find the minimal value m' for $Pr(A \neq X)$. Then consider the global coupling (A,B,X,Y) and again find the minimal value m for $Pr(A \neq X)$. If m = m' the system is non-contextual and if $m > m'$ then the system is contextual. This form of contextuality is analogous to that found in physics and gives rise to similar types of inequalities.

Contextuality by default has been observed experimentally [57]. Moreover, two recent studies [58, 59] have demonstrated the strong form of contextuality in a social psychological setting [58] and in individuals [59]. Contextuality in the form observed in quantum mechanical settings is thus not unique to the quantum domain but can occur in classical settings as well. Dzhafarov and Kon [55] have analyzed the Bell scenario within the contextuality-by-default model, and showed that it can be understood using wholly classical (albeit contextual) probability theory.

Dzharfarov and Kujala [60] applied Contextuality by Default analysis to the double slit experiment. They pointed out that "Contextuality or non-contextuality is a property of a system of random variables representing an empirical situation rather than of the empirical situation itself." They presented a very general model of the two slit situation, using Kolmogorov probability together with the addition of a context parameter, much as Kolmogorov originally argued [21], and obtained the usual statistics. Dzhafarov argued that the Bell argument is not about the nature of physical reality but rather about the failure to take context effects into account when creating a Kolmogorov type probability model of a situation.

The role of context in probability theory has not always been ignored. Kolmogorov [21] and von Mises [61] understood that probability theory was contextual. Pitowski [62, 63] analyzed the Bell situation and presented a model based on a form of contextual probability. In his model "The relative frequencies violate Bell's inequality the way they do *because* the locality principle is *true*" (SIC) [63]. Later, Pitowski [64] developed a deterministic model of spin statistics using the concept of non-measureable sets. He argued [63] that quantum mechanics is essentially a probability theory, which in Khrennikov's language would be viewed as a trigonometric contextual probability theory. Gudder [65] applied a generalized probability theory similar to that of Pitowski to the problem of spin statistics and showed that such a model was compatible with local hidden variables. Gudder [66] had already shown that a hidden variable model of the Bell scenario was possible so long as contextual hidden variables were used, a line of thought supported a few years later by Ballentine [67]. Local contextual hidden variable models have also been developed by Durdevic [68, 69]. Recently Griffiths [70], using a coherent histories approach, has reaffirmed that quantum mechanics is a local theory, the inequalities are a consequence of the contextuality of quantum mechanics, and the correlations that are detected in a typical Bell experiment arise due to a common *quantum* cause [71]. These models seem to have been ignored in the mainstream literature. The belief that the probability theory of the classical world is necessarily Kolmogorov and non-contextual has achieved the status of dogma, and it has proved extremely difficult to disabuse people of this.

A different approach was proposed by Palmer [72] who developed a deterministic model of the spin scenario but where, crucially, there was a non-linear dynamics in place. The consequence of this was the impossibility of forming the correlation functions required for the Bell inequality. Experimentally, correlations can always be calculated but they need not be meaningful [73]. He suggested that the inequalities said nothing about the nature of reality, since the correlation functions involved did not exist.

Remarkably, contextual hidden variable theories have not gained much traction within the foundations community. In spite of their ability to reproduce the quantum mechanical results while preserving locality, they have, for the most part, been ignored in favor of the quasi-mystical notion of non-locality. Shimony ([13], chapter 10) defined two types of contextual hidden variables: environmental, which include experimental conditions, and algebraic, referring to models on quantum logics or lattices. He rejected both types of contextual hidden variables of the environmental type ([14], chapter 10), arguing that they would still satisfy a factorizability condition, but without proof. Shimony appeared to reject locality, evading special relativity by

his "passion at a distance." He argued that a breach of outcome independence did not imply superluminal signaling, but outcome dependence reflects contextuality, not necessarily non-locality.

LOCAL REALISM NEED NOT IMPLY NON-CONTEXTUAL LOCAL HIDDEN VARIABLES

If the observational approach to theory suffices, then it appears clear that measurement is a contextual act. Non-disturbing, non-contextual, "objective" measurements do not exist universally. The classical notion of objectivity does not hold true. This does not, however, imply that an act of measurement *creates* reality, merely that reality may be *altered* by such an act. Reality appears to be interactive, and thus characterized by a weak form of subjectivity. This appears easier to accept than non-locality, since evidence for contextuality is all around us, while evidence for non-locality is profoundly lacking. Griffiths writes [70] "To be sure, those who claim that instantaneous non-local influences are present in the quantum world will generally admit that they cannot be used to transmit information; this is known as the 'no-signaling' principle, widely assumed in quantum information theory. This means that such influences (including wave function collapse) cannot be directly detected in any experiment. The simplest explanation for their lack of influence is that such influences do not exist."

Pusey, Barrett and Rudolph [74] have argued that the wave function is ontological, and experiments visualizing Bell-type non-local behavior [38], quantum jumps [75], quantum measurement processes [76], quantum trajectories [77], quantum wave functions [78], and single photons [79] would seem to support this. Evidence that quantum jumps [75] and quantum measurements [76] evolve over a period of time suggests that there is an actual "something" out there corresponding to such behavior. This suggests that a purely observational theory is inadequate and a descriptive theory is also needed to explain contextuality and the presence of long range correlations.

The dominant viewpoint, however, is that the wave function is merely epistemological, and that quantum mechanics deals only with the statistics and behaviors of ensembles. The ability to carry out single photon and single particle experiments demonstrates that this is not a necessity [80, 81]. The ensemble approach focuses on the density matrix ρ, defined as $\rho = \sum_i p_i |\phi_i><\phi_i|$ where the $|\phi_i>$ are pure states [82]. Moreover, the density matrix involves two different kinds of probability: an explicit classical probability in the form of the real valued p_i and an implicit non-Kolmogorov probability in the form of the squared modulus of the complex valued amplitudes of the pure states. These two considerations suggest that ensembles should be treated ontologically as supervening on pure states. Thus, questions of ontology should reference pure states.

The challenge in finding an ontological model of pure states in quantum mechanics lies not with the measurement problem (for which a detailed model within the usual quantum mechanical framework has been proposed [83, 84]) but rather in providing an ontological understanding of superposition. A naïve attribution of measurements to a single particle in a superposition state leads to confusion and paradox, causing many to abandon an ontological interpretation of the wave function and sometimes reality itself.

Norsen [85] has pointed out that dispensing with the idea of realism, broadly considered, results in the end of scientific inquiry, because without some notion of a "reality," what is it that scientists have to talk about? But must realism be identified with classical objectivity? Zeilinger et al. write "objects have physical properties independent of measurement (the assumption of realism)"([34], p. 250401-1). But this is just the definition of non-contextuality. This definition of realism seems to beg the question.

Rosen [86] suggested that physics' focus on inanimate matter has resulted in an unnecessarily limited world view. Experience with emergent systems in biology, psychology, and economics [87, 88] has demonstrated that many naturally occurring systems and phenomena are transient, open, multiscale, emergent, generated and generative, contextual, and subjective. It is doubtful that anyone seriously considers these systems to be "real" only as a result of "observation." It is not realism that needs to be abandoned—rather concepts such as ideal object, ideal non-disturbing measurement, and non-contextuality must go.

A metaphysics with subjective elements was proposed by Whitehead [89] nearly a century ago. It is a *process* model of reality which emphasizes its transient, generated, generative, emergent, and contextual features. Several authors have proposed process models of physics [2–6, 90–99] and even Shimony [13] wrote about Whitehead's idea of process.

Consider an alternative definition of realism. To begin, why is it necessary that an element of reality *possess* a priori all of the properties that can be measured on it? Measurement is an act, and always involves an interaction between a system and a measuring apparatus. It is generated *in the moment* as the interaction takes place. There is no need to assume that *something* corresponding to this measurement exists in the system prior to its interaction with the measurement apparatus. It is only necessary that the system possesses the potential to determine such a measurement when it interacts with a measurement apparatus. It is equally unreasonable to assert that *nothing* exists prior to the interaction with the measurement apparatus. The system must exist or what exactly does the measurement apparatus interact with? Moreover, the interaction with the system results in a *systematic difference* which ensures that only particular measured values are returned with particular frequencies. If the measurement apparatus creates the measurement, then why just these values and no others? The system must possess a potentiality which becomes realized in any interaction with a measurement apparatus.

Why too is it necessary that for something to be real it must be knowable to a human observer. Quantum mechanics appears obsessed with the idea of measurement, yet events occur in nature without any obvious "measurement" taking place and without any "observer." A theory of natural processes should, reasonably, describe the evolution of such processes as they occur "*in vivo*," and not merely "*in vitro*," in a laboratory. Moreover,

such a theory should be able to deal with single entities, not merely ensembles.

At a bare minimum, any entity must possess some propensity to determine a difference in the state or future history of at least one of the entities that it interacts with. For, if something is thought to exist, but in any interaction with anything whatsoever, in any manner and for all time, it never determines any difference whatsoever, then it might just as well not exist, since its existence will never be noted. Of course an entity may never have an opportunity to interact with another entity, so it is not essential that a difference be realized, only that the entity possesses a propensity to determine a difference, should a suitable interaction occur. These two considerations suggest the following minimalist definition of realism:

An entity is real if it exhibits a propensity to determine a systematic difference. An entity or phenomenon can determine a difference in only a single interaction for a single time, or across many interactions over multiple times. It may determine the *same* difference at multiple times, or it may determine *different* differences on *different* occasions, but these should be systematic in some manner. With respect to the same initial conditions, the difference may be deterministic (fixed single value), non-deterministic (fixed set of values), or stochastic (fixed probability distribution). There is no need for an observer, particularly a human observer. Previous comments aside, if this potentiality is never realized then its reality is rather moot. Thus, there is a need for an entity with which it can interact so as to realize this potentiality and thus register its reality. It may be that this additional entity is itself, and that self-interaction might provide the most basic interaction realizing a potentiality, perhaps that of bare existence. The realization of other potentialities requires interactions with wholly separate entities. The minimum requirement for such entities is that they can register a difference in either state or history, a concept referred to as salience [100]. There is no need for consciousness or agency.

The determination of a difference requires interaction; it is relational. Some differences may be private, specific to an individual entity (for example quarks and gluons) or public, accessible to many entities (for example photons). The idea of reality being a propensity to determine a difference has much in common with the pragmatism of John Dewey [101] and the process view of Whitehead [89]. Propensity drives home the point that it is the capacity to determine a difference which matters, not which difference it is which is determined.

A quantum system determines a potentiality to obtain certain measured values through an act of measurement. These values are only realized through an interaction with a measurement apparatus. It is not necessary that the quantum system possess these measured values, merely that it possess the propensity to determine them, if only in a statistical manner. It is a set of dispositions. Since only select measurements are made possible, it makes a difference, and by the definition proposed here, it is real. It might be associated with a particular measurement on one occasion, but this need not be the same on a subsequent occasion. That will depend upon the intervening interaction history. Properties can be real, they can be contextual, they simply need not be eternal.

Measurements are not specific properties of the system but propensities, one of which may be realized following a measurement act. The system does not possess these properties but rather, together with a suitable measurement apparatus, acts as a generator of properties. Thus, quantum systems should not be thought of as "objects" but rather as "processes." Since processes make a difference, somewhat, somewhere, sometime, processes are held to be elements of reality. They are ontological entities but with characteristics such as transience, emergence, generativity, agency, contextuality, and locality.

Some quantum properties have a universal character, such as whether their wave function is scalar, spinor, vector, tensor, or their charge, rest mass, and so on. These can be attributed to the system itself. Many other properties, however, are contextual in character and thus should be treated as generative propensities. For example, whether a quantum system is to be considered wave-like or particle-like is contextual. Indeed, Ionicioiu et al. [18] showed that the wave-particle distinction is not compatible with a non-contextual hidden variable representation. The tracks of fundamental particles are also contextual in that they do not occur in the absence of a detector. Mott [102] showed that the formation of particle tracks in a bubble chamber was an emergent feature of the interaction between the particle and the atoms in the bubble chamber. There are no tracks without the bubble chamber. The formation of tracks is a propensity of the particle, not a property of the particle.

Consider again the Bell correlations. Reichenbach [103] formulated the principle of the common cause, which states that if an improbable coincidence has occurred, there must exist a common cause. In the Bell scenario, the common cause is presumed to occur at the time at which measurements on the two systems take place. However, consider the following Gedanken experiment. Consider a source which produces a pair of spin-entangled particles I, II, with opposite momenta $\boldsymbol{p}$, $\boldsymbol{-p}$, which are allowed to move to locations a distance d apart, where there are placed detectors for Alice and Bob. The detectors of Alice and Bob are space-like separated. The outcome of each measurement is sent to a common location at a distance h from each detector where there is a recording device which measures the outcome from each detector simultaneously. A common trigger is established at a distance r from each detector. When a signal from the trigger is sent, each detector makes a measurement, thus ensuring simultaneity. In the interval between trigger signals, Alice and Bob are free to alter the specific measurement being made by their detector.

The output from the source has a wave function of the form

$$|\Psi(\mathbf{r}_1,\mathbf{r}_2)>=\frac{1}{\sqrt{2}}[|\phi_1:\rho_1(\mathbf{r}_1,\mathbf{r}_2)>+|\phi_2:\rho_2(\mathbf{r}_1,\mathbf{r}_2)>].$$

The question is: at what point in this situation is the supposed passion at distance to play out?

The unusual notation for the wave function is intentional. In part it follows Mott's [102] argument in which he emphasized that the wave function for the interaction between particle and bubble chamber fluid possessed a complex, non-separable dependence on both the particle and the atom with which it is interacting. It is also meant to emphasis the algebraic aspect of Hilbert space expressed in the bra-ket notation and the representation of this algebra by means of the wave function. This will be important later in the discussion of the Process Algebra. Note that knowledge of this wave function comes from outside Alice and Bob. From Alice's point of view, there is a single particle whose wave function is $|\Psi_1(\mathbf{r}_1) >= \frac{1}{\sqrt{2}}(|\phi_1(\mathbf{r}_1) > +|\phi_2(\mathbf{r}_1) >)$, while Bob sees a single particle with wave function $|\Psi_2(\mathbf{r}_2) >= \frac{1}{\sqrt{2}}(|\rho_1(\mathbf{r}_2) > +|\rho_2(\mathbf{r}_2) >)$.

If they were to pool their descriptions they would assume that the combined wave function is $|\Psi(\mathbf{r}_1, \mathbf{r}_2) >= |\Psi_1(\mathbf{r}_1) > |\Psi_2(\mathbf{r}_2) >$, which is clearly inconsistent with the actual case and also with what is observed by the recorder. Why then are we so quick to assume that the entangled wave function

$$|\Psi(\mathbf{r}_1, \mathbf{r}_2) >= \frac{1}{\sqrt{2}}[|\phi_1 : \rho_1(\mathbf{r}_1, \mathbf{r}_2) > +|\phi_2 : \rho_2(\mathbf{r}_1, \mathbf{r}_2) >]$$
$$= \frac{1}{\sqrt{2}}[|\phi_1(\mathbf{r}_1) > |\rho_1(\mathbf{r}_2) > +|\phi_2(\mathbf{r}_1) > |\rho_2(\mathbf{r}_2)] >?$$

Alice and Bob will make their measurements simultaneously, at exactly the same proper times for each particle. If Alice were to carry out her measurement slightly earlier than Bob, Alice would presumably collapse the wave function of particle I and cause the wave function of particle II to collapse to the corresponding entangled state, and conversely if Bob measures first. Here, however, the measurements are carried out simultaneously. So what will happen? If nothing exists prior to the simultaneous measurements of Alice and Bob, then it is not clear at all how this is to be resolved. Alice and Bob believe that they are working with free particles yet the recorder will obtain correlated measurements. A definite difference will be observed. Thus, according to the definition of realism being considered here, a definite *something* must exist *prior* to the measurements taking place.

The entangled system exhibits a propensity to determine two simultaneous correlated measurements which make a difference, and thus it is reasonable to consider that the entangled system represents a single element of reality. The error lies in assuming that one has two quantum systems which are somehow correlated. That seems possible only through the passage of some signal between them, but in the case of simultaneous measurements, what could such a signal convey? Such a signal not only must be instantaneous, but it must also effect a choice. This seems implausible.

A simpler explanation is that there is only one system, but it produces two measurements. This could occur in one of two ways. First of all, when the entangled state is created, entangled particles are emitted in either of the two entangled states, $|\phi_1 : \rho_1(\mathbf{r}_1, \mathbf{r}_2) >$ or $|\phi_2 : \rho_2(\mathbf{r}_1, \mathbf{r}_2) >$, and then propagated. In that case the wave function is merely epistemological, describing a statistical ensemble of entangled particles. The second possibility is more interesting. At the moment of measurement the entangled system has the propensity to manifest either state $|\phi_1 : \rho_1(\mathbf{r}_1, \mathbf{r}_2) >$ or $|\phi_2 : \rho_2(\mathbf{r}_1, \mathbf{r}_2) >$, never both, with 50–50 frequency. In either of these cases there is no need for quasi-mystical instantaneous signals to be passing back and forth between measurement devices.

Now suppose that the experimental situation is rescaled, so that all distances diminish by a proportion p. The above argument can be repeated and again, the entangled system exhibits the propensity to manifest either state $|\phi_1 : \rho_1(\mathbf{r}_1, \mathbf{r}_2) >$ or $|\phi_2 : \rho_2(\mathbf{r}_1, \mathbf{r}_2) >$, never both. It follows that this must hold true for every moment of time. Since, at every such moment of time, the entangled system has the propensity to determine a difference, there must be an element of reality present at each moment of time. The entangled system is thus the generators of these momentary propensities.

Since the wave function appears to be at least partially ontological, the simplest explanation for this propensity is that at each moment of time, the entangled particle system *actually* manifests either state $|\phi_1 : \rho_1(\mathbf{r}_1, \mathbf{r}_2) >$ or $|\phi_2 : \rho_2(\mathbf{r}_1, \mathbf{r}_2) >$, never both, and that the state may change from moment to moment.

If one believes in the principle of continuity then this is quite problematic and perplexing. If time is continuous then the evolution of the entangled system must be neither smooth, nor continuous. For if H is the Hamiltonian and time evolution is given by the usual operator, $U(t) = \exp[-itH/\hbar]$, then assume that there is some time interval $[t_1, t_2]$ on which the entangled state is constant. Then $U(t)=I$ for every $t \leq t_2 - t_1$, and hence $U(t)=I$ for all t. It appears that one must abandon the principle of continuity. Bancal et al. [17] and Gisin [104] and colleagues addressed this problem in the context of a Bell scenario. They studied the case of 4 quantum observers and, by assuming the principle of continuity and a constant, finite but unspecified superluminal speed v ($c < v < \infty$) of propagation of any hidden signals, were able to find an inequality involving various correlated measurements, as well as a quantum state which violated the inequality. They concluded that either the principle of continuity must be violated, or superluminal signaling must be possible. Gisin wrote "Note that the finding of such a speed would falsify both quantum theory and relativity, a result not many physicists are willing to envisage" [104, pg 10] thus favoring abandoning the principle of continuity. Bancal et al. wrote "This gives further weight to the idea that quantum correlations somehow arise from outside spacetime, in the sense that no story in space and time can describe how they occur" ([17], pg. 4).

The theory of special relativity has survived multiple experimental tests and has yet to be violated. The principle of continuity, however, is frequently violated at smaller scales, so why should it not be violated at the smallest scale? This would appear to provide far less of a shock to our conceptual system than the assumption of instantaneous transmission of undetectable signals. Indeed a recent paper argues that there is an upper limit to the frequency of any physical process, including

any "clock," with the shortest temporal interval on the order of 10^{-33} s [105].

Local realism, according to the new definition, appears to be perfectly tenable provided one accepts contextuality and abandons the principle of continuity. The remainder of this paper is devoted to describing just such a locally realist model of non-relativistic quantum mechanics (NRQM) without hidden variables.

PROCESS AND THE PROCESS ALGEBRA MODEL

One way to implement a descriptive theory together with the new definition of realism is through the concept of process. This has its origins in the writings of Heraclitus and Siddhartha Gautama and its modern version in Whitehead's process theory. A propensity to determine differences can be accommodated if those differences are generated. A process is viewed as a generator of primitive events called *actual occasions*, the base elements of reality. By the new definition of realism, if a process is responsible for determining differences, manifesting as actual occasions, then a process must be accorded the same ontological status, that is, the same degree of reality, as those occasions.

Whitehead considered a process to be a sequence of events having a coherent temporal structure in which relations between the events are more fundamental than the events themselves. Whitehead viewed process as being ontologically prior to substance and becoming to be a fundamental aspect of being. Becoming is fundamental to process, and fundamental to becoming is transience. In process theory events have a transient existence, coming into being, manifesting briefly, then fading away. Each actual occasion exists only long enough to *prehend* the realities of the previous events and to form a response to them, thereby immediately passing out of existence and becoming data for subsequent events. Actual occasions, the basic elements of reality, are held to be inseparable occasions-in-connection, giving reality a holistic aspect. The act of prehension underscores that information plays a fundamental role in the unfolding of reality, and that in particular, it is meaning that is necessary to give rise to coherence among events [90]. Reality is emergent, arising out of a lower level of actual occasions as are the fundamental physical entities, which are viewed as emergent configurations of actual occasions [13, 89].

Actual occasions do not *occur* in space-time, nor do they *move* in space-time. Instead, actual occasions *form* space-time. They are the primitive "events" upon which natural entities supervene and from which they emerge. Processes, being generators of actual occasions, are thus generators of space-time itself. Logically, processes do not exist *within* space-time, they stand *outside* of it, thus fulfilling the suggestion of Bancal et al. [17].

In keeping with the descriptive perspective, actual occasions constitute the signs by means of which processes implement their propensity to determine differences. An actual occasion marks a specific expression of this propensity, determining one of whatever many differences the process may determine. Actual occasions thus mark whichever difference is being determined, *in the moment*, and this difference may vary from moment to moment.

The idea of process depends crucially upon the idea of becoming, and that in turn requires a transient now. Such a concept is thought to be incompatible with special relativity, but this is a misunderstanding of what special relativity implies. As Wigner pointed out [106], what special relativity demonstrated is the non-existence of *global* frames of reference. All global frames of reference are mathematical fictions. Simultaneity, and thus a transient now, can exist, but co-moving observers within the universe will not agree about this. Denying simultaneity is another example of misplaced omniscience. Reality may unfold according to a transient now even if human observers cannot detect it. Several authors have argued that it is not the block universe which is a necessity but rather some form of presentism [107–110].

Similar to the actual occasions that they generate, processes shift between periods of activity and inactivity. While active, they express a propensity to determine differences, manifesting in distinct attributes and functionality. Processes interact with one another according to their attributes and functionalities and the actual occasions that they manifest, and these interactions are triggered by the manifesting of particular actual occasions.

Process ideas can be seen in Finkelstein's quantum relativity [92, 95], Noyes's bit-string physics [94], Bastin and Kilmister's combinatorial physics [96], Hiley's process physics [93], Cahill's process physics [97]. Emergent models of physics include Nelson [111], Adler [112], Levin and Wen [113], and two time models such as stochastic quantization [114] and Bars' two time physics [115].The process algebra model has many roots: Sorkin's causal sets [116] (whose basic elements could be reinterpreted as actual occasions), Lee's discrete time dynamics [117], Kempf's interpolation model of QFT [118] (which suggested that NRQM could be emergent from a discrete space). Related models include the cellular automata models of 't Hooft [119] and Elze [120], which appear to be special cases of process algebra models. Trofimova [98, 99] has proposed several process algebra based formalisms for describing the principles of transience which govern processes in functional constructivism. Her approach to process algebra uses several functional differentiation classes, a concept of "performance" and several universal process-trends. It applies particularly to complex, adaptive, multiscale systems. Her work has provided much inspiration for the author.

The next few pages describe the process algebra model in terse detail. A more leisurely discussion can be found in [2, 4]. The process algebra model considered here views quantum mechanics as an (incomplete) effective theory, being the asymptotic limit as spatiotemporal scales become infinitesimal. The Hilbert space formalism is considered to be mathematically coarse, blurring the distinction between ontological and epistemological, and leading to a great deal of unnecessary confusion.

Since von Neumann, the use of the language of Hilbert spaces for formulating NRQM has become dogma [24]. The Process Algebra model starts from the realization that the Hilbert space of NRQM is a reproducing kernel Hilbert space [121]. Given a reproducing kernel Hilbert space $H(X)$ with base space X, one can find a discrete subspace Y of X (sampling subspace), and a

Hilbert space $H(Y)$ on Y, such that each function in $H(Y)$ can be lifted to a function in $H(X)$ via interpolation. Interpolation means that if $\Psi(z)$ is a function in $H(X)$, then for each $y \in Y$ there exists an interpolation function $\Psi_y(z)$ on H(X) such that $\Psi(z) = \sum_{y\in Y} \Psi(y)\Psi_y(z)$. In general there are usually an infinite number of these sampling subspaces. The interpolations functions are not unique. They are usually chosen by reason of goodness of fit. In the case that the subspace Y has the form of a regular lattice the interpolation functions may be taken to be sinc functions ($\sin x/x$) [90]. If the subspace has an irregular structure with density matching the Beurling density [122], Fechtinger-Gröchenik interpolation theory may be used instead [121, 123]. Interpolation does not reproduce all functions on $H(X)$ but rather a more limited set of band-limited functions, that is, functions whose Fourier transform is limited to a bounded set, ensuring the existence of a natural ultraviolet cutoff.

In interpolation theory, *H(X)* is considered to be fundamental while *H(Y)* is derived, a result of a sampling procedure. The Process Algebra model reverses this relationship. The discrete subsets Y are considered to be fundamental, their elements representing the actual occasions of Whitehead's process theory. The elements of *H(Y)* are the ontological wave functions, and the elements of *H(X)* are derived (emergent) through an (arbitrary) interpolation procedure. The elements of Y are considered to be generated by process, **P**, and the value $\Psi(y)$ assigned to a point y in Y is also generated by P by causally propagating specific information from prior actual occasions to nascent actual occasions by means of a causal propagator, **K**. The resulting wave function $\Psi(z) = \sum_{y\in Y} \Psi(y)\Psi_y(z)$ is thus emergent. The discrete subsets are called *causal tapestries* and their individual points are called *informons*. The triad of prior causal tapestry, process, nascent causal tapestry forms a compound present.

It is essential to understand that *all* of the physics takes place on the causal tapestry Y. The space X is treated as emergent. Interpolation may be used to recover all of the physics on the emergent space X. The informons represent the fundamental elements of reality. Information among the elements is propagated only in a locally causal manner. Note that these informons do not constitute hidden variables. There is no additional parameter space associated with these informons. They constitute the fundamental elements of space-time, and their causal relationships *are* space-time. Moreover, they are the wave function. The wave function $\Psi(\mathbf{z})$ is *not* a *function* of these informons, it *is* these informons. The process model thus possesses local realism *without* hidden variables. This is an important distinguishing feature from other contextual hidden variable models. Moreover, the wave function in the process algebra framework is both ontological and epistemological. More about this will be discussed later. As informons are the formal representation of actual occasions, it is important to note that informons *do not move* in space-time. Information propagates, informons do not. They merely come into existence and then fade away. Informons may be generated in a discontinuous manner. This does not violate special relativity since no information is transferred between the informons that comprise a causal tapestry, only causally from prior to nascent causal tapestry.

A simple visual analogy might help. Think of space-time like an LED display, with each active LED element representing an actual occasion. These LED elements are lit at random, but on an ultrafast, imperceptible time scale. The resulting image represents our observable reality. Processes are represented by the signal which determines which elements are lit.

Each informon takes the form: $[n]{<}\mathbf{p}_n;\mathbf{m}_n{:}\phi_n(\mathbf{z});\Gamma_n{>}\{\mathbb{G}_n\}$ where

1) n is a heuristic mathematical label,
2) $\mathbf{p}_n$ is a structured set of intrinsic properties,
3) $\mathrm{m}_{\boldsymbol{n}}\boldsymbol{:}\boldsymbol{\phi_n}(\mathrm{z})$ is a pair of extrinsic properties,
4) Γ_n is the local coupling effectiveness,
5) $\mathbb{G}_n$ is a causally ordered collection of informons, with causal metric ρ, called the content (based on an idea of Markoupoulou [124]). The union of content sets over all informons in the causal tapestry must itself form a causal set [116, 124, 125]. The causal distance is related to the depth of the causal structure, and the delay in formation flow (important in the case of non-zero rest mass).

The brackets [,],<,>,{,} are simply delimiters.

The local process strength at an informon n is given as $\Gamma_n^*\Gamma_n$. The information residing in the informons of the content is utilized by the generating process to create the informon. The intrinsic properties $\mathbf{p}_n$ are attributed to the generating process **P** and imparted to each informon generated by **P**. The extrinsic properties are unique to each informon but are frame dependent. Each informon n is interpreted as a point $\mathbf{m}_n$ (*causal manifold interpretation or embedding*) in some causal manifold $\boldsymbol{M}$. Its content set $\mathbb{G}_n$ causally embeds into $\boldsymbol{M}$. Each causal tapestry forms a causal antichain in $\boldsymbol{M}$, and thus represents a discrete sampling of a spacelike hypersurface in $\boldsymbol{M}$. Each informon n is associated with a *local Hilbert space interpretation* of the form $\phi_n(\mathbf{r}) = \Gamma_n f_n(\mathbf{r}, \mathbf{m}_m)$, the Hilbert space $H(\boldsymbol{M})$ being that over the causal manifold $\boldsymbol{M}$. Each causal tapestry I is associated with two different maps: a *tapestry realization* (or allowing a slight misnomer, a *tapestry "wave function"*) of the form $\Omega(n) = \Gamma_n$, and a *global Hilbert space interpretation* over the causal manifold of the form $\Psi(\mathbf{r}) = \sum_{n\in I} \Gamma_n f_n(\mathbf{r}, \mathbf{m}_n)$. When the informons of a causal tapestry embed into the causal manifold as a discrete lattice, it is possible to replace each $f_n(\mathbf{r}, \mathbf{m}_n)$ by a spatial translation ($T_{\mathbf{m}_n} f(\mathbf{r}) = f(\mathbf{r} - \mathbf{m}_n)$) of a single generic sinc function $g(\sigma, \mathbf{z}) = \sin\sigma\mathbf{z}/\sigma\mathbf{z}$, so that $\Psi(\mathbf{r}) = \sum_{n\in I} \Gamma_n T_{\mathbf{m}_n} g(\sigma, \mathbf{r})$. The lattice spacing must be consistent with the Beurling density [122]. Maymon and Oppenheim [126] have shown that non-uniform embeddings still provide a highly accurate approximation using sinc interpolation so long as the spatiotemporal density is large enough. A more realistic model requires the use of non-uniform embeddings and more sophisticated interpolation techniques, such as Fechtinger-Gröchenik theory [121].

A tapestry realization is analogous to a space representation of a wave function. There is a dual causal tapestry which can be

formed using the duals of the content sets and which gives rise to an analog of the momentum representation, but this construction will not be needed here.

A process generates individual informon in a series of short rounds, collectively forming a round, in which information is propagated. A causal tapestry is generated in a series of rounds, forming a complete generation. Processes possess three additional intrinsic characteristics:

1) r, the number of prior informons whose information is incorporated into an informon *n*. It is also the cardinality of $\mathbb{G}_n$, and the number of short rounds needed to form *n*.
2) N, the number of informons in each generation, and thus the number of rounds and the cardinality of the causal tapestry I.
3) R, the number of informons generated per round. A *primitive* process has R=1. Otherwise the process is *compound*.

Process properties include invariants such as charge, rest mass, mathematical type (scalar, spinor, vector, tensor, real, complex, quaternion etc.) as well as conserved quantities such as energy, momentum, angular momentum. Conserved quantities are not considered fundamental but rather result from symmetries of the causal propagator [90, 127]. A process can possess a well-defined energy or momentum but there is no dispersion free measure because the informons which are generated by the process are dispersed in space-time. The Heisenberg Uncertainty relations still hold.

The action of a process involves:

1) The assignment of a new informon label
2) The assignment of property set $\mathbf{p}_n$
3) The assignment of causal relations and distances to prior informons
4) The assignment of a content set $\mathbb{G}_n$
5) The propagation of information from prior informons.
6) Determination of local coupling effectiveness by propagating the local coupling effectiveness from each informon in $\mathbb{G}_n$ forward to *n* according to the rule $\Gamma_n = \sum_{m\in I} K(n,m)\Gamma_m$ where the propagator *K* will depend upon the causal distance $\rho(n,m)$. The propagator will be determined by particle and interacting potentials.

The dispersion of informons and subsequent causal diffusion of their information is consistent with the interpretation of the Schrödinger equation as describing a diffusion process [128]. One particular version of the process algebra model can be shown to be equivalent to Feynman path integrals [2–4, 129], but without the interpretation of motion along all possible paths. Moreover, it can be shown that if the propagator is relativistically invariant, then the generation of informons is also relativistically invariant [2–6].

Interactions between processes are conjectured as being triggered by the generation of informons according to the compatibility between the processes. Compatibility between interacting complex systems is an idea first proposed by Trofimova [130]. In the current context it can be thought of as a generalization of the idea of coupling factors. Compatibility $\Xi(\mathbf{P},\mathbf{M})$ is conjectured to be a function of fixed factors such as mass, charge, coupling constants, and of the local compatibilities. The probability of an interaction taking place $\mathbf{\Pi}(\mathbf{P},\mathbf{M})$ is in turn a function of the compatibility, $\mathbf{\Pi}(\mathbf{P},\mathbf{M}) = \chi(\Xi(\mathbf{P},\mathbf{M}))$. The precise form of these functions depends upon the particular case. The Born rule is expected to arise from these interactions and from the compatibility, but a precise derivation is not yet in hand. If one naively applies the Born rule, then probability will be proportional to the local process strength. If so then it will be non-Kolmogorov by virtue of the presence of interaction terms

$$\begin{aligned}\Gamma_n^*\Gamma_n &= \sum_{m\in I} K(n,m)^*\Gamma_m^* \sum_{m'\in I} K(n,m')\Gamma_{m'} \\ &= \sum_{m\in I} K(n,m)^*K(n,m)\Gamma_m^*\Gamma_m + \\ &\sum_{m\in I}\sum_{m'\in I, m\neq m'} K(n,m)^*K(n,m')\Gamma_m^*\Gamma_{m'}\end{aligned}$$

The global Hilbert space interpretation is an ontological wave function, in that it describes the informons generated during one complete action of a process, and so one possible history of a quantum system. To carry out calculations, however, it is necessary to consider all possible histories. To do so requires the use of the process graph defined in the next section. It essentially is a combinatorial tool which keeps track of every possible history of the system as it evolves under a process from a fixed prior causal tapestry. Each possible history yields a distinct global Hilbert space interpretation. The *Process Covering Map* $\mathcal{P}(I)$ gathers together these interpretations into a single set valued map. From this one can form a combinatorial interpretation which can be used for calculations involving single systems. When multiple systems are involved, the process graph must be extended into a configuration space graph together with its associated configuration space covering map [2–4]. The details can be found elsewhere and are not needed for the arguments to follow.

It can be shown [2–4] that for a primitive process **P** and prior causal tapestry I, in the asymptotic limit as Planck length and Planck time tend to 0; $r, N \rightarrow \infty$, $\mathcal{P}(I)$ $\{\Psi(\mathbf{r})\}$, tends to a single function. Thus, in the case of a primitive process, in the asymptotic limit, the process generates only a single wave function which corresponds to the usual NRQM wave function. For a primitive process the wave function becomes *both* ontological and computational. This is not true for compound processes, so that the ontological wave function (global Hilbert space interpretation) which describes a single instance of reality, and the computational wave function which is used for making predictions, are no longer the same [2–4]. This failure to distinguish between these cases may be the source of much confusion about the interpretation of the wave function.

The process covering map gives rise to a correspondence between processes and (set-valued) operators on the space of global Hilbert space interpretations. The standard operator formalism is thus an emergent feature of the Process Algebra model arising in the asymptotic limit of infinite information and infinitesimal scale [2, 4, 90].

An important concept is that of *epistemological equivalence*. Epistemological equivalence of two processes **P** and **Q** means that their global Hilbert space interpretations, $\Psi^P(\mathbf{r}), \Psi^Q(\mathbf{r})$, respectively, are equal as functions over the causal manifold. In other words,

$$\Psi^P(\mathbf{r}) = \sum_n \Gamma_n f_n(\mathbf{r}, \mathbf{m}_n) = \sum_m \Gamma_m f_m(\mathbf{r}, \mathbf{m}_m) = \Psi^Q(\mathbf{r}).$$

If two processes are epistemologically equivalent then the specifics of informon generation do not matter in so far as NRQM is concerned. They generate the same emergent wave functions and therefore will yield the same NRQM predictions. This is useful because processes can be modeled heuristically based upon mathematical convenience just so long as they are epistemologically equivalent to any real processes. In particular one can use processes based upon combinatorial games which have particularly valuable characteristics [131–133]. Epistemological equivalence may also possess ontological implications in that it might be impossible on principle for macroscopic observers to be able to access information about this most fundamental level. To use a computer analogy, it is generally inadvisable for a computer program to be able to access and change its own code. Perhaps that is the case for nature as well.

THE PROCESS ALGEBRA

The various paradoxes and conundrums posed by NRQM can be addressed through the Process Algebra. Processes can interact in a myriad of ways and the Process Algebra provides the formal language for describing these interactions. The power of epistemological equivalence is that it allows for many different representations of process to be considered based on heuristic, computational, or conceptual reasons, and it ensures that the results of calculations will still agree with one another. In this it is akin to the concept of gauge invariance. The most useful such representation to date is based upon combinatorial game theory. These games have been used for decades for generating mathematical structures [130–132] and are used heuristically as a model for how processes generate informons.

Processes may influence one another in two different ways. The first (*coupling*) involves the generation of individual informons, their relative timing as well as the sources of information which enters into their generation. Coupling results in epistemologically equivalent processes, so properties are unaltered. The second (*interaction*) involves the activation or inactivation of individual processes and the creation of new processes. Epistemological equivalence is broken and properties are altered.

Two processes $\mathbf{P_1,P_2}$ may be independent, meaning that the neither constrains the actions of the other in any way. This relationship is denoted simply by the comma ",". Compound processes (R >1) can be formed from primitive processes (R = 1) by various coupling operations. A coupling affects timing and information flow. Two processes may generate informons concurrently (*products*) during each round, or sequentially (*sums*), with only one process generating informons during a given round. Information from either or both processes may enter into the generation of a given informon (free) or information incorporated into an informon by a process may only come from informons previously generated by that process (*exclusive*). This leads to four possible operators:

1. Free sequential (free sum): $\mathbf{P}_1 \hat{\oplus} \mathbf{P}_2$
2. Exclusive sequential (exclusive sum): $\mathbf{P}_1 \oplus \mathbf{P}_2$
3. Free concurrent (free product): $\mathbf{P}_1 \hat{\otimes} \mathbf{P}_2$
4. Exclusive concurrent (exclusive product): $\mathbf{P}_1 \otimes \mathbf{P}_2$

The operation of concatenation is used to denote processes that act in successive generation cycles. Thus, $\mathbf{P}_1 \cdot \mathbf{P}_2$ (or simply $\mathbf{P}_1\mathbf{P}_2$) indicates that $\mathbf{P}_1$ acts during the first generation cycle, while $\mathbf{P}_2$ acts during the second generation cycle.

Interactions break epistemological equivalence and can do so in myriad ways. Interactions between processes may activate an inactive process or inactivate an active process. In addition, an interaction among processes $\mathbf{P_1,P_2,..,P}_\mathrm{n}$ may generate a new process, **P**, which can be described in functional form as $\mathrm{F}(\mathbf{P_1,P_2,..,P}_\mathrm{n}) = \mathbf{P}$. If $\Theta(\mathbf{P_1,P_2,..,P}_\mathrm{n})$ describes a coupling among $\mathbf{P_1,P_2,..,P}_\mathrm{n}$ then the functional relation may be described using the operation of concatenation, as $\Theta(\mathbf{P_1,P_2,..,P}_\mathrm{n})\ \mathbf{P}$.

Since there are potentially so many different types of interactions, a set of generic operators are used to indicate the presence of an interaction with the specifics to be spelled out if known. Thus, there are

1. Free sequential (free interactive sum): $\mathbf{P}_1 \hat{\boxplus} \mathbf{P}_2$
2. Exclusive sequential (exclusive interactive sum): $\mathbf{P}_1 \boxplus \mathbf{P}_2$
3. Free concurrent (free interactive product): $\mathbf{P}_1 \hat{\boxtimes} \mathbf{P}_2$
4. Exclusive concurrent (exclusive product): $\mathbf{P}_1 \boxtimes \mathbf{P}_2$

Independence, sums and products are commutative, associative and distributive operations. Concatenation is non-commutative and non-associative in general. The zero process, **O**, is the process that does nothing.

An important and special form of interaction is the *coupling interaction*. Such interactions respect epistemological equivalence and thus are potentially reversible through a subsequent coupling interaction. An example is a rotation to a different eigenbasis as a result of an engagement with a measurement apparatus.

If the propagator is spatio-temporal invariant, so is the associated process. Since processes are independent of space-time, their actions too are independent of any extrinsic causal manifold interpretation. They will act in the same manner regardless of where the embeddings into the causal manifold occur. Thus, if the propagator is invariant under space and time translations, so is the associated process.

Another point worth mentioning is that due to the non-commutativity of concatenation generally, there is an intrinsic temporal asymmetry within the process algebra model. Temporal evolution according to the process algebra model is not time reversible. It is quite permissible for two processes $\mathbf{P}, \mathbf{Q}$ to be time reversible individually, but yet their concatenation is not time reversible. Assume that $\mathbf{QP} \neq \mathbf{PQ}$. If T is the time reversal operator (which means that if **P** assigns an informon

the causal manifold interpretation $(t, \mathbf{z})$, then $T[\mathbf{P}]$ assigns it the interpretation $(-t, \mathbf{z})$), then $T[\mathbf{P}] = \mathbf{P}$ and $T[\mathbf{Q}] = \mathbf{Q}$ but $T[\mathbf{PQ}] = T[\mathbf{Q}]T[\mathbf{P}] = \mathbf{QP} \neq \mathbf{PQ}$.

Unlike NRQM where multi-particle systems require tensor products, and QFT uses the Fock space, the multi-particle representation of the Process Algebra requires the use of a categorical co-product space. This space consists of formal, rather than arithmetic, sums of global Hilbert space interpretations. Thus, process algebra sums correspond to arithmetic sums while products correspond to co-product (formal) sums. Tensor products appear in the configuration space covering map, which again highlights the difference between the ontological global Hilbert space interpretation and the epistemological process and configuration space covering maps.

The impact of these different operations is best demonstrated using a *process graph*. The process graph $G(\mathbf{P})$ of a process **P** is defined as follows: rounds 0 to N are laid out in order. At round 0 one places the informons of the prior causal tapestry. At round k, place each informon n that was generated during round k and draw a directed line from each prior informon in its content set G_n to n and label it withthe causal distance between the two informons. Note that no lines link informons of the prior causal tapestry to one another or nascent informons to one another since no information passes among them. Let $G(\mathbf{P})n = \{n\} \cup G_n$, the subgraph of $G(\mathbf{P})$ consisting of n and its content set. The process graph is used to determine the causal manifold interpretation of the nascent causal tapestry and the global Hilbert space interpretation. If a process acts on the same prior causal tapestry it may produce a different process graph, thus a different history. The process covering map gathers together the global Hilbert space interpretations of these different process graphs, thus all of the possible histories required for a sum over histories calculation. A configuration space graph and configuration space covering map can be defined for products of processes.

Let $|\mathbf{P}|$ denote the total number of informons generated during the *current* generation cycle. For any two processes **P,Q** we have

$$|\mathrm{P}| = N_P, |\mathrm{Q}| = N_Q$$

$$|\mathrm{P}\hat{\oplus}\mathrm{Q}| = |\mathrm{P} \oplus \mathrm{Q}| = \max\{|\mathrm{P}|, |\mathrm{Q}|\}$$

$$|\mathrm{P}, \mathrm{Q}| = |\mathrm{P}\hat{\otimes}\mathrm{Q}| = |\mathrm{P} \otimes \mathrm{Q}| = |\mathrm{P}| + |\mathrm{Q}|$$

$$|\mathrm{P} \cdot \mathrm{Q}| = |\mathrm{Q}|$$

In addition we have

$$G(\mathrm{P}, \mathrm{Q}) = \mathrm{G}(\mathrm{P}) \cup \mathrm{G}(\mathrm{Q})$$

$$G(\mathrm{P}) \cup G(\mathrm{Q}) = G(\mathrm{P} \oplus \mathrm{Q}) \subset G(\mathrm{P}\hat{\oplus}\mathrm{Q})$$

$$G(\mathrm{P}) \times G(\mathrm{Q}) = G(\mathrm{P} \otimes \mathrm{Q}) \subset G(\mathrm{P}\hat{\otimes}\mathrm{Q})$$

$$G(\mathrm{P} \cdot \mathrm{Q}) = G(\mathrm{Q})$$

This highlights some of the subtle differences between these operations.

The basic rules for applying these operations in combining processes are the following:

1 The free sum is only used for single systems and combining states which possess identical property sets (pure states).
2 The exclusive sum is used for single systems and combining states which possess distinct property sets (mixed states).
3 The free product is used for multiple systems which possess distinct character (scalar, spinorial, vectorial, and so on) such as coupling a boson and a fermion. It is unclear whether two bosons might couple via a free product.
4 The exclusive product is used for multiple systems which possess the same character such as coupling two bosons or two fermions.

The Process Algebra can be represented in many different ways as an algebra of processes, as an algebra of combinatorial games in one model of process, as an algebra of causal tapestry realizations, as a Hilbert space of global Hilbert space representations. Note that the latter representation is not faithful, that is it does not possess all of the structure of the Process Algebra. As stated previously, this results in a loss of causally meaningful information. To emphasize these different representations, one can describe Process Algebra elements as $|\mathbf{P}>$, $|G_P>$, $|\Omega_P(n)>$, $|\Psi_P(\mathbf{r})>$.

CALCULATIONS IN THE PROCESS ALGEBRA MODEL

To illustrate the difference in Hilbert space and Process Algebra approaches, consider first how the process algebra approach deals with superpositions. The linearity of the Schrödinger equation allows for two solutions $\Psi_1(\mathbf{r}), \Psi_2(\mathbf{r})$ to be summed together to yield a new solution $\Psi(\mathbf{r}) = \alpha_1\Psi_1(\mathbf{r}) + \alpha_2\Psi_2(\mathbf{r})$ of the same equation, and therefore a possible state. In the Hilbert space of NRQM note that every space-time point **r** possesses wave function contributions from *both* states $\Psi_1(\mathbf{r}), \Psi_2(\mathbf{r})$ and so if interpreted ontologically this means that the system at the point **r** is manifesting *both* states simultaneously, regardless of what those states entail. This is not a problem if the wave function is interpreted epistemologically (statistically) since in that case it is merely a tool to calculate the probability of being observed in either of the two states at the point **r.** This works for an ensemble of particles, but what of a single particle? How does one explain fixed probabilities if, unlike in classical probability, the object being observed

possesses no definite attributes until after being observed? How is it that *every* observer determines the same attributes and probabilities?

By contrast consider the process algebra approach. Each component state $\Psi_1(\mathbf{r}), \Psi_2(\mathbf{r})$ is generated by its own process $\mathbf{P}_1, \mathbf{P}_2$, respectively. The superposition process is represented in the Process Algebra by the exclusive sum, $\mathbf{P} = \alpha_1\mathbf{P}_1 \oplus \alpha_2\mathbf{P}_2$ so that each sub-process generates a unique, distinct causal tapestry, I_1, I_2 ($I_1 \cap I_2 = \varnothing$), respectively, and *no* information from one process enters into the generation of any informon of the other process. The two causal tapestries embed into disjoint regions of the causal manifold. The causal tapestries are thus physically and informationally isolated from one another. The causal tapestry for $\mathbf{P}$ is $I = I_1 \cup I_2$ and on this causal tapestry the causal tapestry wave function $\Omega(n)$ for $\mathbf{P}$ takes the form $\Omega_1(n) + \Omega_2(n)$, where each $\Omega_i(n)$ is extended to I by setting $\Omega_i(n) = 0$ for $n \in I/I_i$, Note that although the algebraic sum is used there is no ontological confusion since for any n, $\Omega(n)$ receives contributions from either $\Omega_1(n)$ or $\Omega_2(n)$ but never both. Note though that the co-product free sum could also be used. This causal tapestry wave function describes a single system which manifests in either of the two states, which remain distinct, yet whose wave functions are *intertwined*. The informons that support these causal tapestry wave functions are generated sequentially, never concurrently, and so at any given moment only one of the two states is manifesting, so it only ever appears in a single state. The intertwining of the wave functions creates the impression of a mixed reality state at the macro-level, yet that is never the case at the micro-level.

In a superposition of processes, $\mathbf{P} = \alpha_1\mathbf{P}_1 \oplus \alpha_2\mathbf{P}_2$ the effect of each modifier α_i is to modify the value of the local coupling effectiveness ($\Gamma_n \rightarrow \alpha_i\Gamma_n$ for example) so that $\Omega(n) = \alpha_1\Omega_1(n) + \alpha_2\Omega_2(n)$ and the global Hilbert space interpretation is formed in the usual manner, $\Psi(\mathbf{r}) = \alpha_1\Psi_1(\mathbf{r}) + \alpha_2\Psi_2(\mathbf{r})$.

The combined global Hilbert space interpretation thus takes the form

$$\Psi(\mathbf{r}) = \sum_{n\in I_1\cup I_2} \Gamma_n f_n(\mathbf{r}, \mathbf{m}_n) = \sum_{n\in I_1} \alpha_1\Gamma_n f_n(\mathbf{r}, \mathbf{m}_n) + \sum_{n\in I_2} \alpha_2\Gamma_n f_n(\mathbf{r}, \mathbf{m}_n) = \alpha_1\Psi_1(\mathbf{r}) + \alpha_2\Psi_2(\mathbf{r}),$$

This is a map in the Hilbert space $H(\boldsymbol{M})$ over the causal manifold, the same Hilbert space where the NRQM wave function resides, and it constitutes the Process Algebra approximation to the NRQM wave function. Note that in moving to the Hilbert space, causal ontological information is lost since now the wave function is over space-time locations, *not* informons, and contributions from the sub-processes are now summed, *not* intertwined. This information could be preserved if the algebraic sum above were replaced by a co-product free sum, but that is not a Hilbert space property. However, it would not be possible to carry out the usual NRQM calculations in that case.

The concept of informon being new, there is currently no direct evidence to suggest a particular model ofr their generation. Epistemological equivalence, however, allows one to side step that for the moment, and any strategy resulting in an epistemologically equivalent model suffices. Several such models have been presented in the literature [2–6, 90]. Work is underway to model informon generation as a diffusion process as has been suggested in the literature for the Schrödinger equation [111, 114, 128]. The discussion here is meant as an in-principle demonstration of the Process Algebra framework and not a final theory.

The causal tapestry wave function is ontological, representing a single complete action of a process in generating informons (and thus a region of space-time events). The causal tapestry wave function represents the outcome of interactions with other processes only with respect to that single process. Statistical calculations require the use of the process and configuration space graphs and covering maps. The compatibility between processes is conjectured to be a function of the local coupling effectiveness Γ_n, which in turn reflects the effect of myriad local interactions. If the effect of these interactions is summarized in a potential, then it seems reasonable, as an initial approximation, to assume that the local coupling effectiveness will depend in some manner upon the Lagrangian. The probability of an interaction, triggered by the generation of informons, must be positive real valued and is conjectured to depend on the compatibility. It seems reasonable, therefore, to conjecture that the compatibility (hence probability) should depend on the local process strength, $\Gamma_n^*\Gamma_n$ which is both positive real and relativistically invariant. Therefore, making the simplest assumption, the local probability is assumed to be given by the Born rule, $P_n = \Gamma_n^*\Gamma_n$. If an interaction depends upon the presence of several informons $A = \{n_i\}$, then the probability depends upon $P_A = \sum_{m\in A} \Gamma_n^*\Gamma_n$, the local process strength over A. As in NRQM these local coupling effectiveness values can be normalized relative to the global process strength $P_I = \sum_{n\in I} \Gamma_n^*\Gamma_n = |\Omega(n)|^2$. Recall from a previous section that interaction effects are already encoded within the Γ_n. By analogy with Dirac's bra-ket formalism, one can introduce a scalar product on the causal tapestry wave function of the form $< \Omega(n)|\Omega'(m) >= \sum_{n,m\in I} \Omega^*(n)\Omega'(m)\delta(n,m)$ where $\delta(n,m)$ is akin to a differential. The percentage of contribution to the strength by the process generating $\Omega(n)$ to the process generating $\Omega'(m)$ is given by $| < \Omega(n)|\Omega'(m) > |^2$. The global strength is given as $|\Omega(n)|^2 = \sum_{n\in I}\sum_{m\in I} \Omega^*(n)\Omega(m)\delta(n,m) = \sum_{n\in I} \Gamma_n^*\Gamma_n$.

For example if $\Omega(n) = \alpha_1\Omega_1(n) + \alpha_2\Omega_2(n)$ then $<\Omega_2(n)|\Omega(n)> = \sum_{n\in I_2}\sum_{m\in I_1\cup I_2} \Omega_2^*(n)\Omega(n)\delta(n,m) = \alpha_2 \sum_{n\in I_2} \Gamma_n^*\Gamma_n = \alpha_2|\Omega_2(n)|^2 = \alpha_2$
assuming suitable normalization of the process strength

These calculations can also be carried out using the global Hilbert space interpretation with the usual Hilbert space scalar product $< \Psi(\mathbf{r})|\Psi'(\mathbf{r}) >= \int_M \Psi^*(\mathbf{r})\Psi'(\mathbf{r})d\mathbf{r}$.

Conisder a region $\hat{A}$ of the causal manifold containing causal manifold interpretations of informons in the set A. Then we may define

$$P_{\hat{A}} = \int_{\hat{A}} \Psi^*(\mathbf{r})\Psi(\mathbf{r})d\mathbf{r} = \int_{\hat{A}} \sum_{n,n' \in I} \Gamma_n^* \Gamma_{n'} f_n(\mathbf{r}, \mathbf{m_n}) f_{n'}(\mathbf{r}, \mathbf{m_{n'}})d\mathbf{r} =$$

$$\int_{\hat{A}} \sum_{n,n' \in A} \Gamma_n^* \Gamma_{n'} f_n(\mathbf{r}, \mathbf{m_n}) f_{n'}(\mathbf{r}, \mathbf{m_{n'}})d\mathbf{r}$$
$$+ \int_{\hat{A}} \sum_{n,n' \notin A} \Gamma_n^* \Gamma_{n'} f_n(\mathbf{r}, \mathbf{m_n}) f_{n'}(\mathbf{r}, \mathbf{m_{n'}})d\mathbf{r} \approx$$

$$\int_{\hat{A}} \sum_{n,n' \in A} \Gamma_n^* \Gamma_{n'} f_n(\mathbf{r}, \mathbf{m_n}) f_{n'}(\mathbf{r}, \mathbf{m_{n'}})d\mathbf{r}$$

since the f_n decrease in value rapidly away from A. Similarly,

$$\int_{M} \sum_{n,n' \in A} \Gamma_n^* \Gamma_{n'} f_n(\mathbf{r}, \mathbf{m_n}) f_{n'}(\mathbf{r}, \mathbf{m_{n'}})d\mathbf{r} =$$

$$\int_{\hat{A}} \sum_{n,n' \in A} \Gamma_n^* \Gamma_{n'} f_n(\mathbf{r}, \mathbf{m_n}) f_{n'}(\mathbf{r}, \mathbf{m_{n'}})d\mathbf{r}$$
$$+ \int_{M/\hat{A}} \sum_{n,n' \in A} \Gamma_n^* \Gamma_{n'} f_n(\mathbf{r}, \mathbf{m_n}) f_{n'}(\mathbf{r}, \mathbf{m_{n'}})d\mathbf{r} \approx$$

$$\int_{\hat{A}} \sum_{n,n' \in A} \Gamma_n^* \Gamma_{n'} f_n(\mathbf{r}, \mathbf{m_n}) f_{n'}(\mathbf{r}, \mathbf{m_{n'}})d\mathbf{r}.$$

Thus

$$\int_{\hat{A}} \sum_{n,n' \in I} \Gamma_n^* \Gamma_{n'} f_n(\mathbf{r}, \mathbf{m_n}) f_{n'}(\mathbf{r}, \mathbf{m_{n'}})d\mathbf{r} \approx$$
$$\int_{M} \sum_{n,n' \in A} \Gamma_n^* \Gamma_{n'} f_n(\mathbf{r}, \mathbf{m_n}) f_{n'}(\mathbf{r}, \mathbf{m_{n'}})d\mathbf{r} = \sum_{n \in A} \Gamma_n^* \Gamma_n$$

again since the f_n are orthogonal to one another. Likewise

$$< \Psi_2(\mathbf{r})|\Psi(\mathbf{r}) >= \int_{\mathbf{r}} \sum_{n \in I_2} \Gamma_n^* f_n(\mathbf{r}, \mathbf{m}_n)(\sum_{m \in I_1} \alpha_1 \Gamma_m f_m(\mathbf{r}, \mathbf{m}_m)$$
$$+ \sum_{m' \in I_2} \alpha_2 \Gamma_{m'} f_{m'}(\mathbf{r}, \mathbf{m}_{m'}))d\mathbf{r} = \alpha_2 \sum_{n \in I_2} \Gamma_n^* \Gamma_n = \alpha_2$$

Thus, the basic calculations can all be carried out on the causal tapestry itself and so as stated previously, all of the relevant physics occurs on the causal tapestry. The global Hilbert space interpretation provides an observer dependent link to the NRQM Hilbert space which facilitates some calculations and comparisons to NRQM but is not necessary for the physics.

Each causal tapestry wave function $\Omega(n)$ provides an ontological representation of the action of a single process, and thus the history of one occurrence of that process. This is insufficient to carry out computations because only N informons will be generated out of a possible infinitude. The causal tapestry wave function may suffice for primitive processes under certain asymptotic conditions, but it fails for compound processes as it generates only N informon tuples whereas at least N^R must be determined. For computations one must resort to the process covering graph. There all possible causal tapestry histories are gathered (by union) into a single causal graph and the causal tapestry wave function is generated on this graph, as is the global Hilbert space interpretation. These maps now contain sufficient information about all possible evolutions to make calculations possible. However, the process graph and its wave functions are *not* ontological; they are merely epistemological structures used to carry out calculations.

The information incorporated into the local coupling effectiveness (and local process strength) takes into account local effects both of and upon the generating process. In the course of generating informons it is presumed that there will be interactions with other processes. When these other processes give rise to relatively persistent macroscopic or classical-like entities it is convenient to summarize these local effects in terms of field notions such as the potential field. The local coupling coefficients should take these effects into account so a natural first choice is to try a Lagrangian approach.

Assume now that a suitable strategy for generating informons has been adopted and that the informons are generated so as to form points on a 4D lattice with lattice spacing $(l_P)^4$ where l_P is the Planck length. For simplicity, assume further that one has a primitive process (R=1) in some energy eigenstate (so we need only consider a single causal tapestry) and that N=r=$|c|$, the value of c to the nearest integer and stripped of its units. Assume that each generation of an informon occurs in Planck time t_P and that each complete action of the process generates $|c|$ informons in time $|c|t_P$. This time interval corresponds to a length ct_P=l_P. Thus, each causal tapestry is separated from the next by an interval ct_P=l_P, hence the choice of lattice spacing. Label each causal tapestry by its generation number n so that the time coordinate for the nth tapestry is n$|c|t_P$ and each causal tapestry corresponds to a 3D spatial lattice.

Initial states are generally assumed in NRQM. In the Process Algebra framework, since causal tapestries are generated, so must initial states, and so the question of initial states is actually rather important and subtle within the Process Algebra framework. However, a discussion of this problem would detract from the main focus and an initial causal tapestry I_0 will simply be assumed with causal tapestry wave function $\Omega_0(n)$, global Hilbert space interpretation $\Psi_0(\mathbf{r})$ and corresponding NRQM wave function $\hat{\Psi}_0(\mathbf{r})$ satisfying $\Psi_0(\mathbf{m}_n) = \hat{\Psi}_0(\mathbf{m}_n)$ on the embedding sites of informons. Each subsequent causal tapestry is labeled by its generation number n and denote the corresponding 3D sublattice as L_n.

An effective space-time approach is due to Feynman [129]. However, this is presented here only to provide an "in-principle" demonstration. The Feynman propagator allows for long range

transfer of information (long range "paths") and is suitable for NRQM where causal has a different definition but it is not causal in the relativistic sense. Restricting the number of informons being generated serves to truncate the calculation and avoid this problem but then to be precise more definite estimates of the Kernel approximation are needed to determine the size of the resulting amplitude error. These details warrant another paper. If the Lagrangian for a scalar particle of mass m is $\mathcal{L} = p^2/2m - V$then on the causal tapestry one might expect it to take the form $\mathcal{L}(n,n') = md(n,n')^2/2|c|^2t_P^2 - V(n)$ where n and n' refer to informons on the nascent and current tapestries, respectively, and d is the causal tapestry distance. Then $S[n,n'] = \mathcal{L}(n,n')|c|t_P$ so the propagator may be written as $\mathcal{P}_{n,n'} = \frac{l_P^3}{A^3}e^{i/\hbar S[n,n']}$ Note that this is defined entirely on the causal tapestry.

The tapestry wave function can be extended from the tapestry I_n to the sublattice L_n by the convention that $\Omega_m(n) = 0$ if $n \notin I_n$ and that $\mathcal{P}_{n,n'} = 0$ if no information propagates from n to n'. Assume that the process has generated tapestries up to generation m and consider generation $m+1$. Assume that N informons have been generated and consider the causal tapestry wave function $\Omega_{m+1}(n)$. The value of the local coupling effectiveness at the informon n^{m+1} is ${\Gamma^{m+1}}_{n^{m+1}} = \sum_{n^m \in I_m} \mathcal{P}_{n^{m+1},n^m}{\Gamma^m}_{n^m}$. Expanding back to the initial state one has

$$\Gamma^{m+1}_{n^{m+1}} = \sum_{n^m \in \mathcal{L}_m} \cdots \sum_{n^0 \in \mathcal{L}_0} \mathcal{P}_{n^{m+1}n^m} \cdots \mathcal{P}_{n^1 n^0}\Gamma^0_{n0} =$$

$$\Gamma^{m+1}_{n^{m+1}} = \sum_{n^m \in \mathcal{L}_m} \cdots \sum_{n^0 \in \mathcal{L}_0} \mathcal{P}_{n^{m+1}n^m} \cdots \mathcal{P}_{n^1 n^0}\hat{\Psi}_0(\mathbf{m}_{n^0}) =$$

$$\sum_{n^m \in \mathcal{L}_m} \cdots \sum_{n^0 \in \mathcal{L}_0} \frac{l_P^3}{A^3}e^{\frac{i}{\hbar}S[n^{m+1},n^m]}\frac{l_P^3}{A^3}e^{\frac{i}{\hbar}S[n^m,n^{m-1}]} \cdots \times \frac{l_P^3}{A^3}e^{\frac{i}{\hbar}S[n^1,n^0]}\hat{\Psi}_0(\mathbf{m}_{n^0}) =$$

$$\sum_{n^m \in \mathcal{L}_m} \cdots \sum_{n^0 \in \mathcal{L}_0} e^{\frac{i}{\hbar}S[n^{m+1},n^m]+S[n^m,n^{m-1}]+\cdots+S[n^1,n^0]} \times \overbrace{\frac{l_P^3}{A^3}\frac{l_P^3}{A^3}\cdots\frac{l_P^3}{A^3}}^{m+1}\hat{\Psi}_0(\mathbf{m}_{n^0}) =$$

(using Feynman's notation)

$$\sum_{n^m \in \mathcal{L}_m} \cdots \sum_{n^0 \in \mathcal{L}_0} e^{\frac{i}{\hbar}S[n^{m+1},n^0]}\overbrace{\frac{l_P^3}{A^3}\frac{l_P^3}{A^3}\cdots\frac{l_P^3}{A^3}}^{m+1}\hat{\Psi}_0(\mathbf{m}_{n^0}) \approx$$

$$\sum_{n^0 \in \mathcal{L}_0}\int_{L_m} \cdots \int_{L_1} e^{\frac{i}{\hbar}S[n^{m+1},n^0]}\overbrace{\frac{dx^{m+1}}{A^3}\cdots\frac{dx^1}{A^3}}^{m}\frac{l_P^3}{A^3}\hat{\Psi}_0(\mathbf{m}_{n^0}) \approx$$

$$\int_{L_m} \cdots \int_{L_0} e^{\frac{i}{\hbar}S[n^{m+1},n^0]}\overbrace{\frac{dx^{m+1}}{A^3}\cdots\frac{dx^0}{A^3}}^{m+1}\hat{\Psi}_0(\mathbf{r}) = \hat{\Psi}_{m+1}(\mathbf{m}_{n^{m+1}})$$

Thus, we find that the global Hilbert space interpretation

$$\Psi_{m+1}(\mathbf{r}) = \sum_{n^{m+1} \in L_{m+1}} {\Gamma^{m+1}}_{n^{m+1}} f_{n^{m+1}}(\mathbf{r}, \mathbf{m}_{n^{m+1}}) \approx$$

$$\sum_{n^{m+1} \in L_{m+1}} \hat{\Psi}_{m+1}(\mathbf{m}_{n^{m+1}}) f_{n^{m+1}}(\mathbf{r}, \mathbf{m}_{n^{m+1}}) \approx \hat{\Psi}_{m+1}(\mathbf{r})$$

The accuracy of the approximation will depend upon N,r and the value of $\frac{l}{p}$. Parzen's theorem [121] can be used to show that it will become increasingly exact as $N, r \to \infty$ and $l_P \to 0$. In the Process Algebra framework, the usual approximation of $^{h\to 0}$ does not lead to the classical realm but merely to NRQM. This is the reason that NRQM is considered to be an effective theory in the limit of infinite information $^{N,r\to\infty}$ and continuity or infinitesimal scale $^{h\to 0}$ Classicality is thought to be a consequence of the complexity process interactions.

The causal tapestry wave function is discrete and finite and so clearly can diverge in values from the corresponding NRQM wave function. These differences can be due to a variety of factors: truncation errors due to the finite number of informon generated, aliasing errors due to the informon density, amplitude errors due to the discrete approaximation to the Kernel integral, time-jitter errors due to non-uniform spacing of informons and information loss if informons are generated non-contiguously [121]. However, if the density of informons exceeds the Beurling density for the NRQM wave function and if the wave function tends to zero at infinity rapidly, then the difference between these two may be surprisingly small. In the case of a primitive process generating a single eigenstate the NRQM wave function can be achieved in one of two ways—either or by the asymptotic procedure described above or by resorting to the process graph and covering map. Both techniques allow for information to divege to infinity, thus capturing all possibly informon generation sequences and therefore, information paths. The causal tapestry itself, however, is always discrete and finite and possesses finite information, which will result in a disagreement between the global Hilbert space interpretation and the NRQM wave function. This error will depend upon the accuracy of the approximation to the integral $\int_{\mathcal{M}} K(\mathbf{r}_{j'}, \mathbf{r}_j)\phi_j(\mathbf{r}_j)d\mathbf{r}_j$, the deviations from uniformity of the informons, the values of N,r and of t_P, l_P. Determining the error in the general case is probably intractable but there are results for special cases, particularly when the informons occupy contiguous sites in a regular lattice such as in the example above. In one dimension, if the NRQM wave function $\hat{\Psi}(t)$ satisfies $|\hat{\Psi}(t)| \leq M|t|^{-\gamma}$ for $0 < \gamma \leq 1$, $|\int_{\mathcal{M}} K(\mathbf{r}_{j'}, \mathbf{r}_j)\phi_j(\mathbf{r}_j)d\mathbf{r}_j - \Psi(\mathbf{r}_{j'})| \leq \epsilon$, the discrepancy between each embedding point and its ideal lattice embedding point is less than δ, and the truncation number $r = 2[W^{1+1/\gamma} + 1] + 1$, then according to a theorem of Butzer [121], the error E satisfies

$$||E||_\infty \leq -K(\Psi, \gamma, \epsilon/l_P, \delta/l_P)l_P \ln l_P$$

where

$$K = (1+\frac{1}{\gamma})\left\{\sqrt{5}e\left[(\frac{14}{\pi}+\delta/l_P+\frac{7}{3\sqrt{5}\pi})||\Psi^{(1)}||_\infty+\dot{o}/l_P\right]+6e(M+||\Psi||_\infty)\right\}$$

Then $||E||_\infty \approx 10^{-33}K$ if l_P is the Planck length.

Ideally, if the discrete approximation to the Kernel integral and the Kernel integral are equal, the informons lie continguously on a uniform lattice, and the informons occupy a cubic spatial region with $N^{1/3}$ informons on one side, then one can use the Yao and Thomas theorem [121] to find a rough estimate for the error *E,* namely

$$|\Phi(\mathbf{r})-\Psi(\mathbf{r})| = |E| \leq \frac{64\max_{\mathcal{M}'}|\Psi(x,y,z)|}{(2\pi)^3 N} \approx \frac{1}{31N}\,(m^{-3/2}).$$

Thus, a value for N of |c| yields an error of $\sim 10^{-10}$ $(m^{-3/2})$ and if N=|c|^3 then the error is $\sim 10^{-30}$ $(m^{-3/2})$.

Thus, even this relatively simple Process Algebra model can reproduce, to a high degree of accuracy, any NRQM wave function which can be calculated using Feynman path integrals and whose energy is bounded by h/2|c|t$_P$.

THE PROCESS ALGEBRA APPROACH TO THE PARADOXES

The paradoxes and dualities of quantum mechanics appear to arise from one of two main factors, either a failure to utilize a contextual probability model when analyzing an experimental situation, or an attempt to interpret a wave function in both ontological and epistemological terms. The former was pointed out by Dzhafarov [60] in his contextuality by default analysis of the two slit experiment. The difference in outcomes is a consequence of contextuality. It can also be seen in the analysis of wave-particle duality by Ionicioiu et al. [18] who used a Bell type argument to try to show that the wave-particle distinction for a particle cannot be non-contextual.

The Process Algebra approach focuses upon the latter factor, the confusion of ontology and epistemology. Only the causal tapestry realization is truly ontological, although the global Hilbert space interpretation preserves ontology at informon embeddings sites. For epistemology one requires the use of the process and configuration space graphs and the set-valued process and configuration space covering maps. These lead to the usual NRQM wave functions, which are viewed as being epistemological. The resolution of the paradoxes is not to be had through an ever more clever or convoluted elaboration of standard quantum mechanics using the Hilbert space. It is not a problem of computation. The problem lies in attempting to use the Hilbert space formalism to provide an ontological model of quantum mechanics. The Hilbert space is simply too coarse grained to carefully distinguish between distinct ontological states. This coarse graining is adequate for carrying out calculations of quantum mechanical statistics, but not for the purpose of ontology. The problem is that the Hilbert space serves as a quotient space relative to the Process Algebra, which results in a loss of ontological information. The Hilbert space conflates information relative to distinct ontological states leading to confusion when attempts are made to provide an ontological interpretation. This does not occur in the Process Algebra framework. Thus, the problem is not with reality, but rather with the mathematical language used to represent reality.

CONCLUSION

Theoretical and experimental evidence strongly points to the end of local non-contextual hidden variables. This, however, is not the end of local realism. The fundamental result is that reality is contextual. This is entirely compatible with locality. There is no need to introduce non-locality or "spooky action at a distance." There need be no conflict between quantum mechanics and relativity. The cost, however, is to abandon the principle of continuity and accept a process generated reality. A specifc model, the Process Algebra model is presented as an in-principle demonstration of model which is generated, causally local, Lorentz invariant, contextual, without hidden variables and which. can reproduce the results of NRQM to as high level of accuracy. It is suggested that the paradoxes that plague quantum mechanics are due to the inability of the Hilbert space formalism to correctly distinguish between ontology and epistemology. The Process Algebra model corrects this deficiency and promises the possibility of a paradox free quantum mechanics. Hopefully this paper will encourage further research.

DATA AVAILABILITY STATEMENT

The original contributions presented in the study are included in the article/supplementary material, further inquiries can be directed to the corresponding author/s.

AUTHOR CONTRIBUTIONS

The sole author is responsible for the literature review, conceptualization, analysis, and preparation of the manuscript. Any errors and omissions are their sole responsibility.

ACKNOWLEDGMENTS

WS wishes to thank Irina Trofimova for countless discussions related to process ideas. WS would also like to thank Andrei Khrennikov and Etibar Dzhafarov for many valuable discussions. Further, WS wishes to thank Robb Mann, Rafael Sorkin and Achim Kempf for their support during the gestation of the early version of these ideas. WS also wishes to thank the reviewers who provided very helpful commentary and additional references which helped to improve the quality of the paper.

REFERENCES

1. Einstein A, Podolsky B, Rosen N. Can quantum mechanical description of reality be considered complete? *Phys Rev.* (1935) **77**:777–80. doi: 10.1103/PhysRev.47.777
2. Sulis W. *A Process Model of Non-Relativistic Quantum Mechanics*. Ph.D. thesis, University orf Waterloo, Waterloo, ON (2014).
3. Sulis W. A process model of quantum mechanics. *J Mod Phys*. (2014) **5**: 1789–95. doi: 10.4236/jmp.2014.516176
4. Sulis W. Completing quantum mechanics. In: Sienicki K, editor. *Quantum Mechanics Interpretations*. Berlin: Open Academic Press (2017) p. 350–421.
5. Sulis W. A process algebra approach to quantum electrodynamics: physics from the top up. In: Martinez R, editor. *Complex Systems: Theory and Applications*. New York, NY: Nova Publishing (2017). p. 1–42.
6. Sulis W. A process algebra approach to quantum electrodynamics. *Int J Theoret Phys.* (2017) **56**:3869–79. doi: 10.1007/s10773-017-3366-y
7. Colbeck R, Renner R. No extension of quantum theory can have improved predictive power. *Nat. Comm.* (2011) **2**:411. doi: 10.1038/ncomms1416
8. Dawid R. *String Theory and the Scientific Method*. Cambridge: Cambridge University Press (2014). doi: 10.1017/CBO9781139342513
9. Bohm D. A suggested interpretation of the quantum theory in terms of "hidden variables". I. *Phys Rev.* (1952) **85**:166–79. doi: 10.1103/PhysRev.85.166
10. Bohm D, Aharonov Y. Discussion of experimental proof for the paradox of Einstein, Rosen, and Podolsky". *Phys Rev*. (1957) **108**:1070. doi: 10.1103/PhysRev.108.1070
11. Bell JS. *Speakable and Unspeakable in Quantum Mechanics*. Cambridge: Cambridge University Press (1987).
12. Clauser J, Horne M, Shimony A, Holt R. Proposed experiment to test local hidden variable theories. *Phys Rev Lett*. (1969) **23**:880–4. doi: 10.1103/PhysRevLett.23.880
13. Shimony A. *Search for a Naturalistic World View, Volume II, Natural Science and Metaphysics*. Cambridge: Cambridge University Press (1993). doi: 10.1017/CBO9780511621147
14. Jarrett J. On the physical significance of the locality conditions in the Bell argument. *Nous*. (1984) **18**:569–89. doi: 10.2307/2214878
15. Clauser J, Shimony A. Bell's theorem : experimental tests and implications. *Rep Prog Phys*. (1978) **41**:1881–927. doi: 10.1088/0034-4885/41/12/002
16. Leggett AJ, Garg A. Quantum mechanics versus macroscopic realism: Is the flux there when nobody looks? *Phys Rev Lett*. (1985) **54**:857–60. doi: 10.1103/PhysRevLett.54.857
17. Bancal JD, Pironio S, Acin A, Liang YC, Scarani V, Gisin N. Quantum nonlocality based on finite-speed causal influences leads to superluminal signalling. *Nature Phys.* (2012) 8: 867–70. doi: 10.1038/nphys2460
18. Ionicioiu R, Jennewein T, Mann RB, Terno, D. Is wave-particle objectivity compatible with determinism and locality? *Nat Comm*. (2014) **5**:3997. doi: 10.1038/ncomms5997
19. Fine, A. Hidden variables, joint probability, and the Bell inequalities. *Phys Rev Lett*. (1982) **48**:291–5. doi: 10.1103/PhysRevLett.48.291
20. Fine A. Joint distributions, quantum correlations, and commuting observables. *J Math Phys*. (1982) **23**:1306–10. doi: 10.1063/1.525514
21. Kolmogorov AN. *Foundations of the Theory of Probability*. New York, NY: Chelsea Publishing (1956).
22. Vorob'ev NN. Consistent families of measures and their extensions. *Theory Prob Appl*. (1962) **7**:147–63. doi: 10.1137/1107014
23. Handsteiner J, Friedman A, Rauch. D, Gallicchio A, Liu B, Hosp H, et al. Cosmic Bell test: measurements settings from Milky Way stars. *Phys Rev Lett*. (2017) **118**:060401. doi: 10.1103/PhysRevLett.118.060401
24. von Neumann, J. *Mathematical Foundations of Quantum Mechanics*. Princeton: Princeton University Press (1955).
25. Gleason AM. Measures on the closed subspaces of a Hilbert space. *J Math Mech*. (1957) **6**:885–93. doi: 10.1512/iumj.1957.6.56050
26. Mackey G. Quantum mechanics and Hilbert space. *Am Math Monthly*. (1957) **64**:45–57. doi: 10.1080/00029890.1957.11989120
27. Kochen S, Specker E. The problem of hidden variables in quantum mechanics. *J Math Mech*. (1967) **17**:59–87. doi: 10.1512/iumj.1968.17.17004
28. Mermin D. Simple unified form for the major no-hidden-variables theorem. *Phys Rev Lett*. (1990) **65**:3373–6. doi: 10.1103/PhysRevLett.65.3373
29. Wheeler JA, ZurekWH. Quantum theory and measurement. Princeton: Princeton University Press (1983).
30. Aspect A. Closing the door on Einstein's and Bohr's quantum debate. *Physics*. (2015) **8**:123–6. doi: 10.1103/Physics.8.123
31. Hensen B, Bernien H, Dréau AE, Reiserer A, Kalb N, Blok MS, et al. Loophole-free Bell inequality violation using electron spins separated by 1.3 kilometres. *Nature*. (2015) **526**:682–6. doi: 10.1038/nature15759
32. Shalam L, Meyer-Scott E, Christensen B, Bierhorst P, Wayne M, Stevens M, et al. Strong loop-hole free test of local realism. *Phys Rev Lett*. (2015) **115**:250402. doi: 10.1103/PhysRevLett.115.250402
33. Giustina M, Versteegh M, Wengerowsky S, Handsteiner J, Hochrainer A, Phelan K, et al. Significant-loophole-free test of Bell's theorem with entangled photons. *Phys Rev Lett*. (2015) **115**:250401. doi: 10.1103/PhysRevLett.115.250401
34. Hensen B, Kalb N, Blok MS, Dréau EA, Reiserer A, Vermeulen RFL, et al. Loophole-free Bell test using electron spins in diamond: second experiment and additional analysis. *Sci Rep*. (2016) **6**:30289. doi: 10.1038/srep30289
35. Rauch D, Handsteiner J, Hochrainer A, Gallicchio J, Friedman A, Leung C, et al. Cosmic Bell test using random measurement settings from high red-shift quasars. *Phys Rev Lett*. (2018) **121**:080403. doi: 10.1103/PhysRevLett.121.080403
36. Proietti M, Pickston A, Graffitti F, Barrow P, Kundys D, Branciard C, et al. Experimental test of local observer-independence. *arXiv [Preprint]*. (2019). arXiv: 1902. 05080v2. doi: 10.1126/sciadv.aaw9832
37. Dhand I, D'Souza A, Narasimhachar V, Sinclair N, Wein S, Zarkeshian P, et al. Understanding quantum physics through simple experiments: from wave-particle duality to Bell's theorem. *arXiv [Preprint]*. (2018).
38. Moreau P-A, Toninelli E, Gregory T, Aspden R, Morris P, Padgett M. Imaging Bell-type nonlocal behavior. *Sci Adv*. (2019) **5**:eaaw2563. doi: 10.1126/sciadv.aaw2563
39. Conway JH, Kochen S. The free will theorem. *arXiv*. (2006). doi: 10.1007/s 10701-006-9068-6
40. Khrennikov A. Getting rid of non-locality from quantum physics. *arXiv [Preprint]*. (2019). arXiv: 1907 02702v3. doi: 10.20944/preprints202004.0547.v1
41. Landau L. On the violation of Bell's inequality in quantum theory. *Phys Lett A*. (1987) **120**:54–6. doi: 10.1016/0375-9601(87)90075-2
42. Cabello A. Generalized Bell nonlocality and Kochen-Specker contextuality are equivalent in quantum theory. *arXiv*. (2019) 1904. 05306v1.
43. Nieuwenhuizen T. Is the contextuality loophole fatal for the derivation of the Bell inequalities. *Found Phys.* (2011) **41**:580–91. doi: 10.1007/s10701-010-9461-z
44. Kupczynski M. Quantum mechanics and modeling of physical reality. *Phys Sci*. (2018) **93**:123001. doi: 10.1088/1402-4896/aae212
45. Khrennikov A. *Ubiquitous Quantum Structure*. New York, NY: Springer (2010). doi: 10.1007/978-3-642-05101-2
46. Asano M, Basieva I, Khrennikov A, Ohya M, Yamato I. A general quantum information model for the contextual dependent systems breaking the classical probability law. *arXiv*. (2011) 1105.4769v1.
47. Khrennikov A. *Probability and Randomness: Quantum Versus Classical*. London: Imperial College Press (2017).
48. Asano M, Basieva I, Khrennikov A, Ohya M, Yamato I. Non-Kolmogorovian approach to the context-dependent systems breaking the classical probability law. *Found Phys.* (2013) **43**:895–911. doi: 10.1007/s10701-013-9725-5
49. Khrennikov A. Vaxjo interpretation of wave function. 2012. *arXiv*. (2012) 1210. 2390v1. doi: 10.1063/1.4773136
50. Busemeyer, J Bruza PD. *Quantum Cognition and Decision*. Cambridge: Cambridge University Press (2012). doi: 10.1017/CBO9780511997716
51. Haven E, Khrennikov A. *Quantum Social Science*. Cambridge: Cambridge University Press (2014).
52. Khrennikov A, Alodjants A. Classical (local and contextual) probability model for Bohm-Bell type experiments: no signaling as independence of random variables. *Entropy*. (2019) **21**:157. doi: 10.3390/e21020157
53. Khrennikov A. Violation of Bell's inequality and postulate on simultaneous measurements of compatible observables. *arXiv*. (2011) 1102. 4 743v1.
54. Dzhafarov E, Kujala J, Cervantes V. Contextuality by default: a brief overview of ideas, concepts, and terminology. In: Atmanspacher H, Filk, T, Pothos,

editors. *Lecture Notes in Computer Science*. New York, NY: Springer (2016). p. 12–23. doi: 10.1007/978-3-319-28675-4_2
55. Dzhafarov E, Kon M. On universality of classical probability with contextually labeled random variables. *J Math Psych.* (2018) **85**:17–24. doi: 10.1016/j.jmp.2018.06.001
56. Dzhafarov E, Kujala J. Context-content systems of random variables: the contextuality-by-default theory. *J Math Psych.* (2016) **74**:11–33. doi: 10.1016/j.jmp.2016.04.010
57. Dzhafarov E, Zhang R, Kujala J. Is there contextuality in behavioral and social systems? *Phil Trans Royal Soc A.* (2015) **374**:20150099. doi: 10.1098/rsta.2015.0099
58. Cervantes V, Dzhafaarov E. Snow queen is evil and beautiful: experimental evidence for probabilistic contextuality in human choices. *Decision.* (2018) **5**:193–204. doi: 10.1037/dec0000095
59. Cervantes V, Dzhafarov E. True contextuality in a psychophysical experiment. *J Math Psych.* (2019) **91**:119–27. doi: 10.1016/j.jmp.2019.04.006
60. Dzhafarov E; Kujala J. Contextuality analysis of the double slit experiment (with a glimpse into three slits). *Entropy.* (2018) **20**:278. doi: 10.3390/e20040278
61. von Mises R. *Probability, Statistics and Truth*. New York, NY: Dover Publications (1981).
62. Pitowski, I. *The Logic of Fundamental Processes: Nonmeasurable Sets and Quantum Mechanics*. Ph.D. dissertation, University of Western Ontario, London, Ontario (1983).
63. Pitowski I. Resolution of the einstein-podolsky-rosen and bell paradoxes. *Phys Rev Lett.* (1982) **48**:1299–302. doi: 10.1103/PhysRevLett.48.1299
64. Pitowski I. Deterministic model of spin and statistics. *Phys Rev D.* (1983) **27**:2316–26. doi: 10.1103/PhysRevD.27.2316
65. Gudder S. Reality, locality, and probability. *Found Phys.* (1984) **14**:997–1010. doi: 10.1007/BF01889250
66. Gudder S. On hidden variable theories. *J Math Phys.* (1970) **11**:431–6. doi: 10.1063/1.1665156
67. Ballentine LE. Probability theory in quantum mechanics. *Am J Phys.* (1986) **54**:883–9. doi: 10.1119/1.14783
68. Durdevic M. Contextual extensions of C* algebras and hidden variable theories. *J Phys A Math Gen.* (1990) **24**:549–5. doi: 10.1088/0305-4470/24/3/013
69. Durdevic M. Quantum field theory and local contextual extensions. *J Phys A Math Gen.* (1992) **25**:665–77. doi: 10.1088/0305-4470/25/3/023
70. Griffiths R. Nonlocality claims are inconsistent with Hilbert space quantum mechanics. *arXiv*. (2020) 1901. 07050v3. doi: 10.1103/PhysRevA.101.022117
71. Allen J-M, Barrett J, Horsman D, Lee C, Spekkens R. Quantum common causes and quantum causal models. *Phys Rev X.* (2017) **7**:031021. doi: 10.1103/PhysRevX.7.031021
72. Palmer T. A local deterministic model of quantum spin measurement. *Proc Math Phys Sci.* (1995) **451**:585–608. doi: 10.1098/rspa.1995.0145
73. Laughlin R. *A Different Universe: Reinventing Physics From the Bottom Down*. New York, NY: Perseus Books (2005).
74. Pusey M, Barrett J, Rudolph T. On the reality of the quantum state. *Nat Phys.* (2012) **8**:475–8. doi: 10.1038/nphys2309
75. Minev SO, Mundhada S, Shankar P, Reinhold R, Gutierrez-Jáuregui RJ, Schoelkopf, et al. To catch and reverse a quantum jump mid-flight. *Nature.* (2019) **570**:200. doi: 10.1038/s41586-019-1287-z
76. Pokorny F, Zhang C, Higgins G, Cabello A, Klienmann M, Hennrich M. Tracking the dynamics of an ideal quantum measurement. *Phys Rev Lett.* (2020) **124**:080401. doi: 10.1103/PhysRevLett.124.080401
77. Kocsis S, Braverman B, Ravets S, Stevens MJ, Mirin RP, Shalm LK, et al. Observing the average trajectories of single photons in a two-slit interferometer. *Science.* (2011) **332**:1170–3. doi: 10.1126/science.1202218
78. Lundeen J, Sutherland B, Patell A, Stewart C, Bamber C. Direct measurement of the quantum wavefunction. *Nat Lett.* (2011) **474**:188–91. doi: 10.1038/nature10120
79. Gariepy G, Krstajic N, Henderson R, Li C, Thomson R, Buller G. Heshmat B, et al. Single-photon sensitive light-in-flight imaging. *Nat Comm.* (2015) **6**:6021. doi: 10.1038/ncomms7408
80. Migdall A, Polyakov S, Fan J, Bienfang J (Editors.). *Single-Photon Generation and Detection*. New York, NY: Academic Press (2013).
81. Rauch H, Werner S. *Neutron Interferometry: Lessons in Experimental Quantum Mechanics*. Oxford: Oxford Science Publications (2000).
82. Weinberg S. *Lectures on Quantum Mechanics*. Cambridge: Cambridge University Press (2013).
83. Allahverdyan A, Balian R, Nieuwenhuizen T. Understanding quantum measurement from the solution of dynamical models. *Phys Rep.* (2013) **525**:1–66. doi: 10.1016/j.physrep.2012.11.001
84. Allahverdyan A, Balian R, Nieuwenhuizen T. A sub-ensemble theory of ideal quantum measurement processes. *Ann Phys.* (2017) **376**:324–52. doi: 10.1016/j.aop.2016.11.001
85. Norsen T. Against "realism". *Found Phys.* (2007) **78**:311–40. doi: 10.1007/s10701-007-9104-1
86. Rosen R. Some epistemological issues in physics and biology. In: Hiley BJ, Peat FD, editors. *Quantum Implications: Essays in Honour of David Bohm*. London: Routledge. (1991) p. 314–27.
87. Sulis W. Naturally occurring computational systems. *World Futures.* (1993) **39**:225–41. doi: 10.1080/02604027.1994.9972406
88. Sulis W. Causality in naturally occurring computational systems. *World Futures.* (1995) **44**:129–48. doi: 10.1080/02604027.1995.9972538
89. Whitehead AN. *Process and Reality*. New York, NY: The Free Press (1978).
90. Sulis W. An information ontology for the process algebra model of non-relativistic quantum mechanics. *Entropy*. (2020) **22**:136. doi: 10.3390/e22020136
91. Eastman TE, Keeton H (Editors.). *Physics and Whitehead: Quantum, Process and Experience*. Albany, NY: SUNY Press (2004).
92. Finkelstein, D. *Quantum Relativity: A Synthesis of the Ideas of Einstein and Heisenberg*. New York, NY: Springer (1997).
93. Hiley BJ. Process, distinction, groupoids and Clifford algebras: an alternative view of the quantum formalism. In: Coecke B, editor. *New Structures for Physics*. Berlin: Springer-Verlag (2001). p. 705–52. doi: 10.1007/978-3-642-12821-9_12
94. Noyes HP. *Bit-String Physics: A Finite and Discrete Approach to Natural Philosophy*. Singapore: World Scientific (2001). doi: 10.1142/4692
95. Selesnick SA. *Quanta, Logic and Spacetime: Variations on Finkelstein's Quantum Relativity*. Singapore: World Scientific (1998). doi: 10.1142/3586
96. Bastin T, Kilmister CW. *Combinatorial Physics*. Singapore: World Scientific (1995). doi: 10.1142/2703
97. Cahill RT. *Process Physics: From Information Theory to Quantum Space and Matter*. New York, NY: Nova Science Publishers (2005).
98. Trofimova I. Functional constructivism: in search of formal descriptors. *Nonlin Dynam Psychol Life Sci.* (2017) **21**:441–74. [Epub ahead of print].
99. Trofimova, I. *Phenomena of Functional Differentiation and Fractal Functionality*. *Complex Systems Theory and Applications*. *WIT Press*. Southhampton (2016). doi: 10.2495/DNE-V11-N4-508-521
100. Sulis W. Archetypal dynamics and emergence. In: Nation J, Trofimova I, Rand J, Sulis W, editors. *Formal Descriptions of Developing Systems*. Dordrecht: Kluwer Press (2002) 185-228.
101. Dewey J. Does reality possess a practical character. In: Thorndike E, editor. *Essays, Philosophical and Psychological, in Honor of William JAMES, Professor in Harvard University, by his Colleagues at Columbia Univeristy*. New York, NY: Longmansm, Green and Co (1908). p. 53–80.
102. Mott NF. The wave mechanics of α-ray tracks. *Proc Royal Soc London A.* (1929) **126**:79–84. doi: 10.1098/rspa.1929.0205
103. Reichenbach H. *The Direction of Time*. Reichenbach M, editors. Berkeley: University of California Press (1991).
104. Gisin N. Quantum correlation in Newtonian space and time: arbitrarily fast communication or nonlocality. *arXiv*. (2013) 1210. 7308v2
105. Wendel G, Martinez L, Bojowald M. Physical implication of a fundamental period of time. *Phys Rev Lett.* (2020) **124**:241301. doi: 10.1103/PhysRevLett.124.241301
106. Wigner, E. *Symmetries and Reflections: Scientific Essays*. Bloomington: Indiana University Press (1967). p. 52.
107. Unger RM, Smolin, L. *The Singular Universe and the Reality of Time*. Cambridge: Cambridge University Press (2015). doi: 10.1017/CBO9781139696487
108. Elitzur, A. Quantum phenomena within a new theory of time. In: Elitzur A, Dolev S, Kolenda, N, editors. *Quo Vadis Quantum Mechanics?* New York, NY: Springer (2005). p. 325–50. doi: 10.1007/b137897

109. Gisin N. Time really passes, science can't deny that. In: Renner R, Stupar S, editors. Time in Physics. Cham: Birkhäuser (2017). P. 1-15. doi: 10.1007/978-3-319-68655-4_1
110. Sorkin R. Relativity does not imply that the future already exists: a counterexample. In: Petkov V, editor. *Relativity and the Dimensionality of the World*. New York, NY: Springer (2007) 153–61. doi: 10.1007/978-1-4020-6318-3_9
111. Nelson, E. Derivation of the Schrödinger equation from Newtonian mechanics. *Phys Rev.* (1966) **150**:1079–85. doi: 10.1103/PhysRev.150.1079
112. Adler, S. *Quantum Theory as an Emergent Phenomenon*. Cambridge: Cambridge University Press (2004). doi: 10.1017/CBO9780511535277
113. Levin M, Wen X.-G. Colloquium: photons and electrons as emergent phenomena. *Rev Mod Phys.* (2005) **77**:871–9. doi: 10.1103/RevModPhys.77.871
114. Damgaard FH, Huffel H. *Stochastic Quantization*. Singapore: World Scientific (1988). doi: 10.1142/0375
115. Bars I. Standard model of particles and forces in the framework of two time physics. *Phys Rev D.* (2006) **74**:081095. doi: 10.1103/PhysRevD.74.085019
116. Bombelli L, Lee J, Meyer D, Sorkin R. Space-time as a causal set. *Phys Rev Lett.* (1987) **59**:521–4. doi: 10.1103/PhysRevLett.59.521
117. Lee TD. Can time be a discrete dynamical variable? *Phys Lett B.* (1983) **122**:217–20. doi: 10.1016/0370-2693(83)90687-1
118. Kempf A. Spacetime could be simultaneously continuous and discrete in the same way that information can. arXiv. (2010) 10104354.v1. doi: 10.1088/1367-2630/12/11/115001
119. 't Hooft G. *The Cellular Automaton Interpretation of Quantum Mechanics*. Berlin: Springer (2014).
120. Elze, H. Quantum models as classical cellular automata. *arXiv*. (2017) 1701.02252v1. doi: 10.1088/1742-6596/845/1/012022
121. Zayed AI. *Advances in Shannon's Sampling Theory*. Boca Raton, FL: CRC Press (1993).
122. Landau, H. Necessary density conditions for sampling and interpolation of certain entire functions. *Acta Mathematica.* (1967) **117**:37–52. doi: 10.1007/BF02395039
123. Bisseling RH, Kosloff R. Multidimensional interpolation and differentiation based on an accelerated sinc interpolation procedure. *Comp Phys Comm.* (1986) **39**:313–32. doi: 10.1016/0010-4655(86)90093-7
124. Markopoulou, F. The internal description of a causal set: what the universe looks like from the inside. *Commun Math Phys.* (2000) **211**:559–83.41. doi: 10.1007/s002200050826
125. Borchers HJ, Sen RN. *Mathematical Implications of Einstein-Weyl Causality*. New York, NY: Springer (2006). doi: 10.1007/3-540-37681-X
126. Maymon S, Oppenheim AV. Sinc interpolation of nonuniform samples. *IEEE Trans Sig Processes.* (2011) **59**:4745–58. doi: 10.1109/TSP.2011.2160054
127. Noether E. Invariante Variationsprobleme. Nachrichten von der Gesellschaft der Wissenschaften zu Göttingen. *Mathematisch-Physikalische Klasse.* (1918). **28**:235–57.
128. Nagasawa M. *Schrödinger Equations and Diffusion Theory*. New York, NY: Birkhauser (1993). doi: 10.1007/978-3-0348-0560-5
129. Feynman R; Hibbs A. *Quantum Mechanics and Path Integrals*. New York, NY: Dover (2010).
130. Trofimova I. Sociability, diversity and compatibility in developing systems: EVS approach. In: Nation J, Trofimova I, Rand J, Sulis W, editors. *Formal Descriptions of Developing Systems* Kluwer: Amsterdam. (2002). p. 231–48. doi: 10.1007/978-94-010-0064-2_13
131. Conway JH. *On Numbers and Games*. Natick, NH: A.K. Peters (2001). doi: 10.1201/9781439864159
132. Hodges W. *Building Models by Games*. New York, NY: Dover Publications (2006).
133. Hirsch R, Hodkinson I. *Relation Algebras by Games*. New York, NY: Elsevier (2002).

Conflict of Interest: The author declares that the research was conducted in the absence of any commercial or financial relationships that could be construed as a potential conflict of interest.

frontiers in Physics

ORIGINAL RESEARCH
published: 03 June 2020
doi: 10.3389/fphy.2020.00191

Local Realistic Interpretation of Entangled Photon Pairs in the Weyl-Wigner Formalism

*Emilio Santos**

Departamento de Física Moderna, Universidad de Cantabria, Santander, Spain

A polarization correlation experiment with two maximally entangled photons created by spontaneous parametric down-conversion is studied in the Weyl-Wigner formalism, that reproduces the quantum predictions. A realistic stochastic interpretation is proposed suggesting that an analysis of the experiments more detailed than the Bell approach may be compatible with local realism. Entanglement appears as a correlation between fluctuations of signal and vacuum fields.

Keywords: local realism, bell inequalities, entangled photons, parametric down-conversion, Weyl-Wigner

OPEN ACCESS

Edited by:
Ana Maria Cetto, National Autonomous University of Mexico, Mexico

Reviewed by:
Herman Batelaan, University of Nebraska-Lincoln, United States
Anouar Ben Mabrouk, University of Kairouan, Tunisia
Kaled Dechoum, Universidade Federal Fluminense, Brazil

***Correspondence:**
Emilio Santos
emilio.santos@unican.es

Specialty section:
This article was submitted to Mathematical Physics, a section of the journal Frontiers in Physics

Received: *05 March 2020*
Accepted: *30 April 2020*
Published: *03 June 2020*

Citation:
Santos E (2020) Local Realistic Interpretation of Entangled Photon Pairs in the Weyl-Wigner Formalism. Front. Phys. 8:191. doi: 10.3389/fphy.2020.00191

1. THE EMPIRICAL REFUTATION OF BELL´S LOCAL REALISM

In 2015, experiments were reported showing for the first time the loophole-free violation of a Bell inequality [1, 2]. The result has been interpreted as the "death by experiment for local realism," this being the hypothesis that "the world is made up of real stuff, existing in space and changing only through local interactions… about the most intuitive scientific postulate imaginable" [3]. This statement, and many similar ones, emphasize both the relevance of *local realism* for our understanding of the physical world and the fact that it has been *refuted empirically*. Nevertheless, it is worth studying the possibility of a loophole in the empirical refutation via a new definition of locality weaker than Bell´s. In this article I search for such a weak locality, compatible with the said experiments [1, 2], that involved photon pairs entangled in polarization produced via spontaneous parametric down conversion. Thus I will analyze such experiments using the Weyl-Wigner formalism of quantum optics, rather than the more usual Hilbert-space formalism. Previously I revisit briefly the origin and meaning of the Bell inequalities [4].

Bell defined "local hidden variables" model, later named "local realistic," to be any model of an experiment where the results of all correlation measurements may be interpreted according to the formulas

$$\langle A\rangle = \int \rho(\lambda)\, d\lambda M(\lambda, A)\,, \langle B\rangle = \int \rho(\lambda)\, d\lambda M(\lambda, B)\,,$$
$$\langle AB\rangle = \int \rho(\lambda)\, d\lambda M(\lambda, A)\, M(\lambda, B)\,, \quad (1)$$

where $\lambda \in \Lambda$ is one or several random ("hidden") variables, $\langle A\rangle, \langle B\rangle$, and $\langle AB\rangle$ being the expectation values of the results of measuring the observables A, B or their product AB, respectively. Here we will consider that the observables correspond to detection, or not, of some signals (e.g., photons) by two parties named Alice and Bob, attaching the values 1 or 0 to these two possibilities. In this case $\langle A\rangle, \langle B\rangle$ correspond to the single and $\langle AB\rangle$ to the coincidence detection rates respectively. The following mathematical conditions are assumed

$$\rho(\lambda) \geq 0, \int \rho(\lambda)\, d\lambda = 1, M(\lambda, A) \in \{0, 1\}, M(\lambda, B) \in \{0, 1\}\,. \quad (2)$$

Equation (2) corresponds to a "deterministic model" where the statistical aspects derive from the probabilistic nature of the hidden random variables $\{\lambda\}$. More general models may be constructed where the whole interval $[0,1]$ is substituted for $\{0,1\}$ in Equation (2). A constraint of locality is included, namely $M(\lambda,A)$ is independent of $M(\lambda,B)$ and $\rho(\lambda)$ independent of both $M(\lambda,A)$ and $M(\lambda,B)$[5]. From these conditions it is possible to derive empirically testable (Bell) inequalities [6, 7]. The tests are most relevant if the measurements performed by Alice and Bob are specially separated in the sense of relativity theory.

In the following sections, I shall shortly review the treatment within the Weyl-Wigner formalism of the polarization correlation measurement of two maximally entangled photons produced via spontaneous parametric down conversion (SPDC). Thus, I continue a theoretical interpretation of SPDC experiments within the WW formalism in the Heisenberg picture, that was initiated in the nineties of the past century [8–18]. In many of those early studies the approach was heuristic and one of the purposes of this article is to provide a more formal foundation. The WW formalism suggests an intuitive picture for photon entanglement and the interpretation of SPDC experiments in terms of random variables and stochastic processes. However, there are difficulties with the picture that will be discussed in section 4 below.

2. THE WEYL-WIGNER FORMALISM IN QUANTUM OPTICS

2.1. Definition

The WW formalism was developed for non-relativistic quantum mechanics, where the basic observables involved are positions, $\hat{x}_j$, and momenta, $\hat{p}_j$, of the particles [19–25]. It may be trivially extended to quantum optics provided we interpret $\hat{x}_j$ and $\hat{p}_j$ to be the sum and the difference of the creation, $\hat{a}_j^\dagger$, and annihilation, $\hat{a}_j$, operators of the j normal mode of the radiation. That is

$$\hat{x}_j \equiv \frac{c}{\sqrt{2}\omega_j}\left(\hat{a}_j+\hat{a}_j^\dagger\right), \hat{p}_j \equiv \frac{i\hbar\omega_j}{\sqrt{2}c}\left(\hat{a}_j-\hat{a}_j^\dagger\right) \quad (3)$$
$$\Rightarrow \hat{a}_j = \frac{1}{\sqrt{2}}\left(\frac{\omega_j}{c}\hat{x}_j+\frac{ic}{\hbar\omega_j}\hat{p}_j\right), \hat{a}_j^\dagger = \frac{1}{\sqrt{2}}\left(\frac{\omega_j}{c}\hat{x}_j-\frac{ic}{\hbar\omega_j}\hat{p}_j\right).$$

Here $\hbar$ is Planck constant, c the velocity of light and ω_j the frequency of the normal mode. In the following, I will use units $\hbar = c = 1$. For the sake of clarity I shall represent the operators in a Hilbert space with a "hat," e.g., $\hat{a}_j, \hat{a}_j^\dagger$, and the amplitudes in the WW formalism without "hat," e.g., a_j, a_j^*.

The connection with the Hilbert-space formalism is made via the Weyl transform as follows. For any trace class operator $\hat{M}$ of the former we define its Weyl transform to be a function of the field operators $\left\{\hat{a}_j, \hat{a}_j^\dagger\right\}$, that is

$$W_{\hat{M}} = \frac{1}{(2\pi^2)^n}\prod_{j=1}^{n}\int_{-\infty}^{\infty}d\lambda_j\int_{-\infty}^{\infty}d\mu_j \exp\left[-2i\lambda_j \mathrm{Re}a_j - 2i\mu_j \mathrm{Im}a_j\right]$$
$$\times Tr\left\{\hat{M}\exp\left[i\lambda_j\left(\hat{a}_j+\hat{a}_j^\dagger\right)+i\mu_j\left(\hat{a}_j-\hat{a}_j^\dagger\right)\right]\right\}.$$

The transform is *invertible* that is

$$\hat{M} = \frac{1}{(2\pi^2)^{2n}}\prod_{j=1}^{n}\int_{-\infty}^{\infty}d\lambda_j\int_{-\infty}^{\infty}d\mu_j \exp\left[i\lambda_j\left(\hat{a}_j+\hat{a}_j^\dagger\right)+i\mu_j\left(\hat{a}_j-\hat{a}_j^\dagger\right)\right]$$
$$\times\prod_{j=1}^{n}\int_{-\infty}^{\infty}d\mathrm{Re}a_j\int_{-\infty}^{\infty}d\mathrm{Im}a_j W_{\hat{M}}\left\{a_j,a_j^*\right\}\exp[-2i\lambda_j \mathrm{Re}a_j - 2i\mu_j \mathrm{Im}a_j].$$

The transform is *linear*, that is if f is the transform of $\hat{f}$ and g the transform of $\hat{g}$, then the transform of $\hat{f}+\hat{g}$ is $f+g$.

It is standard wisdom that the WW formalism is unable to provide any intuitive picture of the quantum phenomena. The reason is that the Wigner function, that may represent a quantum state, is not positive definite in general and therefore cannot be interpreted as a probability distribution (of positions and momenta in quantum mechanics, or field amplitudes in quantum optics). However, we shall see that in quantum optics the formalism in the Heisenberg representation, where the evolution goes in the field amplitudes, allows the interpretation of the experiments using the Wigner function only for the vacuum state, that is positive definite.

The use of the WW formalism in quantum optics has the following features in comparison with the Hilbert-space formalism:

1. It is just quantum optics, therefore the predictions for experiments are the same.
2. The calculations using the WW formalism are generally no more involved than the corresponding ones in Hilbert space, and sometimes might be easier because no problem of non-commutativity arises.
3. The formalism suggests a physical picture in terms of random variables and stochastic processes. In particular the counterparts of creation and annihilation operators look like random amplitudes.

Here we shall use the formalism in the Heisenberg picture, where the evolution appears in the observables. On the other hand the concept of photon, as a particle, does not appear in the WW formalism.

2.2. Properties

All properties of the WW transform in particle systems may be translated to quantum optics via Equation (3). The transform allows getting a function of (c-number) amplitudes for any trace-class operator (e.g., any function of the creation and annihilation operators of "photons"). In particular we may get the (Wigner) function corresponding to any quantum state. For instance the vacuum state, represented by the density matrix $|0\rangle\langle 0|$, is associated with the following Wigner function

$$W_0 = \prod_j \frac{2}{\pi} \exp\left(-2\left|a_j\right|^2\right). \tag{4}$$

This function might be interpreted as a (positive) probability distribution. Hence the picture that emerges is that the quantum vacuum of the electromagnetic field (also named *zeropoint field, ZPF*) consists of stochastic fields with a probability distribution independent for every mode, having a Gaussian distribution with mean energy $\frac{1}{2}\hbar\omega$ per mode.

Similarly there are functions associated with the observables. For instance the following Weyl transforms are obtained

$$\begin{aligned}
\hat{a}_j &\leftrightarrow a_j, \hat{a}_j^\dagger \leftrightarrow a_j^*, \frac{1}{2}\left(\hat{a}_j^\dagger\hat{a}_j + \hat{a}_j\hat{a}_j^\dagger\right) \leftrightarrow a_j a_j^* = \left|a_j\right|^2, \\
\hat{a}_j^\dagger\hat{a}_j &= \frac{1}{2}\left(\hat{a}_j^\dagger\hat{a}_j + \hat{a}_j\hat{a}_j^\dagger\right) + \frac{1}{2}\left(\hat{a}_j^\dagger\hat{a}_j - \hat{a}_j\hat{a}_j^\dagger\right) \leftrightarrow \left|a_j\right|^2 - \frac{1}{2}, \\
\left(\hat{a}_j^\dagger + \hat{a}_j\right)^n &\leftrightarrow \left(a_j + a_j^*\right)^n, \left(\hat{a}_j^\dagger - \hat{a}_j\right)^n \leftrightarrow \left(a_j - a_j^*\right)^n, n \text{ an integer.}
\end{aligned} \tag{5}$$

I stress that the quantities a_j and a_j^* are c-numbers and therefore they commute with each other. The former Equation (5) mean that in expressions *linear in creation and/or annihilation operator* the Weyl transform just implies "*removing the hats*." However this is not the case in nonlinear expressions in general. In fact from the latter two Equations (5) plus the linearity property it follows that for a product in the WW formalism the Hilbert space counterpart is

$$a_j^k a_j^{*l} \leftrightarrow (\hat{a}_j^k \hat{a}_j^{\dagger l})_{sym}, \tag{6}$$

where the subindex *sym* means writing the product with all possible orderings and dividing for the number of terms. Hence the WW field amplitudes corresponding to products of field operators may be obtained putting the operators in symmetrical order via the commutation relations. Particular instances that will be useful latter are the following

$$\begin{aligned}
\hat{a}_j^\dagger\hat{a}_j &\rightarrow \left|a_j\right|^2 - \frac{1}{2}, \hat{a}_j\hat{a}_j^\dagger \rightarrow \left|a_j\right|^2 + \frac{1}{2}, \hat{a}_j{}^2 \rightarrow a_j^2, \hat{a}_j^{\dagger 2} \rightarrow \hat{a}_j^{*2} \\
\hat{a}_j^\dagger\hat{a}_j\hat{a}_j^\dagger\hat{a}_j &\rightarrow \left|a_j\right|^4 - \left|a_j\right|^2, \hat{a}_j\hat{a}_j^\dagger\hat{a}_j\hat{a}_j^\dagger \rightarrow \left|a_j\right|^4 + \left|a_j\right|^2, \\
\hat{a}_j^\dagger\hat{a}_j^\dagger\hat{a}_j\hat{a}_j &\rightarrow \left|a_j\right|^4 - 2\left|a_j\right|^2 + \frac{1}{2}, \hat{a}_j\hat{a}_j\hat{a}_j^\dagger\hat{a}_j^\dagger \rightarrow \left|a_j\right|^4 + 2\left|a_j\right|^2 + \frac{1}{2}.
\end{aligned} \tag{7}$$

Other properties may be easily obtained from well known results of the standard Weyl-Wigner formalism in particle quantum mechanics. I will present them omitting the proofs.

Expectation values may be calculated in the WW formalism as follows. In the Hilbert-space formalism they read $Tr(\hat{\rho}\hat{M})$, or in particular $\langle\psi \mid \hat{M} \mid \psi\rangle$, whence the translation to the WW formalism is obtained taking into account that the trace of the product of two operators becomes

$$Tr(\hat{\rho}\hat{M}) = \int W_{\hat{\rho}}\left\{\hat{a}_j, \hat{a}_j^\dagger\right\} W_{\hat{M}}\left\{\hat{a}_j, \hat{a}_j^\dagger\right\} \prod_j d\mathrm{Re}a_j d\mathrm{Im}a_j.$$

That integral is the WW counterpart of the trace operation in the Hilbert-space formalism. Particular instances are the following expectations that will be of interest later on

$$\begin{aligned}
\left\langle\left|a_j\right|^2\right\rangle &\equiv \int d\Gamma W_0\left|a_j\right|^2 = \frac{1}{2}, \left\langle a_j^n a_j^{*m}\right\rangle = 0 \text{ if } n \neq m. \\
\left\langle 0\left|\hat{a}_j^\dagger\hat{a}_j\right|0\right\rangle &= \int d\Gamma(a_j^* a_j - \frac{1}{2}) W_0 = 0, \\
\left\langle 0\left|\hat{a}_j\hat{a}_j^\dagger\right|0\right\rangle &= \int d\Gamma(\left|a_j\right|^2 + \frac{1}{2}) W_0 = 2\left\langle\left|a_j\right|^2\right\rangle = 1, \\
\left\langle\left|a_j\right|^4\right\rangle &= 1/2, \left\langle\left|a_j\right|^n \left|a_k\right|^m\right\rangle = \left\langle\left|a_j\right|^n\right\rangle\left\langle\left|a_k\right|^m\right\rangle \text{ if } j \neq k.
\end{aligned} \tag{8}$$

where W_0 is the Wigner function of the vacuum (Equation 4). This means that in the WW formalism the field amplitude a_j (coming from the vacuum) behaves like a complex random variable with Gaussian distribution and mean square modulus $\left\langle\left|a_j\right|^2\right\rangle = 1/2$. I point out that the integral for any mode not entering in the function $M\left(\left\{a_j, a_j^*\right\}\right)$ gives unity in the integration due to the normalization of the Wigner function (Equation 4). An important consequence of Equation (8) is that *normal (antinormal) ordering of creation and annihilation operators in the Hilbert space formalism becomes subtraction (addition) of 1/2 in the WW formalism. The normal ordering rule is equivalent to subtracting the vacuum contribution.*

2.3. Evolution

In the Heisenberg picture of the Hilbert-space formalism the density matrix is fixed and any observable, say $\hat{M}$, evolves according to

$$\frac{d}{dt}\hat{M} = i\left(\hat{H}\hat{M} - \hat{M}\hat{H}\right), \hat{M} = \hat{M}(t),$$

where $\hat{H}$ is the Hamiltonian. Translated to the WW formalism this evolution of the observables is given by the Moyal equation with the sign changed. The standard Moyal equation applies to the evolution of the Wigner function, that represents a quantum state being the counterpart of the density matrix in the Schrödinger picture of the Hilbert space formalism. Thus, in the WW formalism we have

$$\begin{aligned}
\frac{\partial W_{\hat{M}}}{\partial t} &= 2\{\sin\left[\frac{1}{4}\left(\frac{\partial}{\partial\mathrm{Re}a_j'}\frac{\partial}{\partial\mathrm{Im}a_j''} - \frac{\partial}{\partial\mathrm{Im}a_j'}\frac{\partial}{\partial\mathrm{Re}a_j''}\right)\right] \\
&\times W_{\hat{M}}\left\{a_j', a_j^{*\prime}, t\right\} H\left(a_j'', a_j^{*\prime\prime}\right)\}_{a_j},
\end{aligned} \tag{9}$$

where $\{\}_{a_j}$ means making $a_j' = a_j'' = a_j$ and $a_j^{*\prime} = a_j^{*\prime\prime} = a_j^*$ after performing the derivatives.

A simple example is the free evolution of the field amplitude of a single mode. The Hamiltonian in the WW formalism may be trivially obtained translating the Hamiltonian of the Hilbert-space formalism, that is

$$\hat{H}_{free} = \omega_j\hat{a}_j^\dagger\hat{a}_j = \frac{1}{2}\omega_j(\hat{a}_j^\dagger\hat{a}_j + \hat{a}_j\hat{a}_j^\dagger) - \frac{1}{2}\omega_j$$

$$\rightarrow H_{free} = \omega_j(\left|a_j\right|^2 - \frac{1}{2}) = \omega_j\left[(\mathrm{Re}a_j)^2 + (\mathrm{Im}a_j)^2 - \frac{1}{2}\right],$$

where we have taken the first Equation (8) into account. This leads to

$$\begin{aligned}\frac{d}{dt}a_j &= \frac{1}{2}\omega_j\left[2(\mathrm{Im}a_j) - 2\left(\mathrm{Re}a_j\right)i\right] \\ &= -i\omega_j a_j \Rightarrow a_j(t) = a_j(0)\exp\left(-i\omega_j t\right) \end{aligned} \quad (10)$$

Another example is the down-conversion process in a nonlinear crystal. Avoiding a detailed study of the physics inside the crystal [12, 26] we shall study a single mode problem with the model Hamiltonian[27]

$$\hat{H}_I = A\hat{a}_s^\dagger\hat{a}_i^\dagger\exp(-i\omega_P t) + A^*\hat{a}_s\hat{a}_i\exp(i\omega_P t), \quad (11)$$

when the laser is treated as classically prescribed, undepleted, and spatially uniform field of frequency ω_P. The parameter A is proportional to the pump amplitude and the nonlinear susceptibility. In the WW formalism this Hamiltonian becomes (see Equation 5)

$$H_I = Aa_s^*a_i^*\exp(-i\omega_P t) + A^*a_sa_i\exp(i\omega_P t),$$

whence taking Equation (9) and (10) into account we have

$$\begin{aligned}\frac{d}{dt}a_s &= -i\omega_s a_s - iAa_i^*\exp(-i\omega_P t), \quad (12)\\ \frac{d}{dt}a_i &= -i\omega_i a_i - iAa_s^*\exp(-i\omega_P t).\end{aligned}$$

We shall assume that the vacuum field a_s evolves as in Equation (10) before entering the crystal and then according to Equation (12) inside the crystal, that is during the time T needed to cross it. In order to get the radiation intensity to second order in $AT \equiv C$ (see below section 2.4) we must solve these two coupled equations also to second order. After some algebra this leads to

$$\begin{aligned}a_s(t) &= \left(1 + \frac{1}{2}|C|^2\right)a_s(0)\exp(-i\omega_s t) - iCa_i^*(0)\exp[i(\omega_i - \omega_P)t] \\ &= [\left(1 + \frac{1}{2}|C|^2\right)a_s(0) - iCa_i^*(0)]\exp(-i\omega_s t), \quad (13)\end{aligned}$$

and the latter equality takes the "energy conservation" into account, that in the WW formalism looks like a condition of frequency matching, $\omega_P = \omega_s + \omega_i$, with no reference to photon energies.

Equation (13) gives the time dependence of the relevant mode of signal after crossing the crystal, but we should take account of the field dependence on position including a factor $\exp(i\mathbf{k}_s\cdot\mathbf{r})$, that is a phase depending on the path length. Therefore, the correct form of Equation (13) would be, modulo a global phase,

$$a_s(\mathbf{r},t) = [\left(1 + \frac{1}{2}|C|^2\right)a_s(0) - iCa_i^*(0)]\exp(i\mathbf{k}_s\cdot\mathbf{r} - i\omega_s t). \quad (14)$$

A similar result is obtained for $a_i(t)$, that is

$$a_i(\mathbf{r},t) = [\left(1 + \frac{1}{2}|C|^2\right)a_i(0) - iCa_s^*(0)]\exp(i\mathbf{k}_i\cdot\mathbf{r} - i\omega_i t). \quad (15)$$

Equations (14) and (15) may be interpreted saying that the interaction of the vacuum signal with the pumping laser produces an additional field that travels in the direction of the idler. Similarly the vacuum idler produces a field that travels in the direction of the signal. Therefore, it has sense adding the initial vacuum signal plus the amplification of the idler.

We may perform a change from C to the new parameter $D = \left(1 + \frac{1}{2}|C|^2\right)^{-1}C$, whence Equation (7) become, to order $O\left(|D|^2\right)$,

$$\begin{aligned}E_s^+ &= \left(1 + \frac{1}{2}|C|^2\right)\left[a_s + Da_i^*\right]\exp(i\mathbf{k}_s\cdot\mathbf{r} - i\omega_s t), \quad (16)\\ E_i^+ &= \left(1 + \frac{1}{2}|C|^2\right)\left[a_i + Da_s^*\right]\exp(i\mathbf{k}_i\cdot\mathbf{r} - i\omega_i t), |D| << 1,\end{aligned}$$

and I will ignore the constant global factor $\left(1 + \frac{1}{2}|C|^2\right) \sim 1$ because we will be interested in calculating *relative* detection rates.

Equations (14) and (15), although good enough for calculations, are bad representations of the physics. In fact a physical beam corresponds to a superposition of the amplitudes, $a_{\mathbf{k}}^*$, of many modes with frequencies and wavevectors close to ω_s and $\mathbf{k}_s$, respectively. For instance we may represent the positive frequency part of the idler beam created in the crystal, to first order in D, as follows

$$\begin{aligned}E_i^{(+)}(\mathbf{r},t) &= -iD\int f_i(\mathbf{k})\,d^3\mathbf{k}a_{\mathbf{k}}^*\exp[i(\mathbf{k}-\mathbf{k}_s) \\ &\quad\cdot\mathbf{r} - i(\omega - \omega_s)t] + E_{ZPF}^{(+)}, \quad (17)\end{aligned}$$

where $\omega = \omega(\mathbf{k})$ and $f_i(\mathbf{k})$ is an appropriate function, with domain in a region of $\mathbf{k}$ around $\mathbf{k}_s$. The field $E_{ZPF}^{(+)}$ is the sum of amplitudes of all vacuum modes, including the one represented by a_s in Equation (14). (We have neglected a term of order $|C|^2$ so that $E_i^{(+)}$ is correct to order $|C|$ or what is equivalent order $|D|$). These vacuum modes have fluctuating amplitudes with a probability distribution given by the vacuum Wigner function (Equation 4). It may appear that the amplitude a_s is lost "as a needle in the haystack" within the background of many radiation modes, but it is relevant in correlation experiments. In fact the vacuum amplitude a_s in Equations (13) or (14) is fluctuating and the same fluctuations appear also in the signal amplitude a_s^* of Equation (15). Therefore, coincidence counts will be favored when large positive fluctuations of the fields (Equations 13, 15) arrive simultaneously to Alice and Bob detectors. In the Hilbert-space formalism this fact is named "entanglement between a signal and the vacuum." In the WW formalism of quantum optics *this entanglement appears as a correlation of fluctuations between a signal and a vacuum field in distant places.*

The mentioned properties of the WW formalism are sufficient for the interpretation of experiments involving pure radiation

field interacting with macroscopic bodies, these defined by their bulk electric properties like the refraction index or the nonlinear electrical susceptibility. Within the WW formalism the interaction between the fields (either signals or vacuum fields) and macroscopic bodies may be treated as in classical electrodynamics. This is for instance the case for the action of a laser on a crystal with nonlinear susceptibility, studied elsewhere [12, 26].

3. PHOTON PAIRS ENTANGLED IN POLARIZATION

In this section, I will apply the WW formalism to the description of the polarization correlation of entangled photon pairs produced via spontaneous parametric down-conversion (SPDC). I will assume that the experimental set-up is made so that the fields arriving at the detectors correspond to so called "photon pairs maximally entangled" in polarization. These fields are obtained in the outgoing channels of a beam splitter after sending the signal and idler beams produced by SPDC to the incoming channels. The electromagnetic radiation is a vector field with two possible polarizations and I should take into account this fact including vectors in the description, that we have omitted till now. Thus, I will write the beams produced as follows

$$\begin{aligned}\mathbf{E}_A^+ &= \left(a_s + Da_i^*\right)\exp\left(-i\omega_s t\right)\mathbf{v} + i\left(a_i + Da_s^*\right)\exp\left(-i\omega_i t\right)\mathbf{h},\\ \mathbf{E}_B^+ &= -i\left(a_s + Da_i^*\right)\exp\left(-i\omega_s t\right)\mathbf{h} + \left(a_i + Da_s^*\right)\exp\left(-i\omega_i t\right)\mathbf{v},\end{aligned} \tag{18}$$

where $\mathbf{h}$ is a unit vector horizontal and $\mathbf{v}$ vertical. We have not written explicitly the dependence on position, that could be restored without difficulty (see Equation 17). Furthermore, from now on I will ignore all spacetime dependence that usually contributes phase factors irrelevant for our argument. The complex conjugate of the above fields will be labeled as follows

$$(\mathbf{E}_A^+)^* \equiv \mathbf{E}_A^-, (\mathbf{E}_B^+)^* \equiv \mathbf{E}_B^-$$

The "two photons entangled in polarization," represented by Equation (18) in the Weyl-Wigner formalism, will arrive at the Alice and Bob polarization analyzers put at angles θ and ϕ with the vertical, respectively. Hence the beams emerging from them will have field amplitudes

$$\begin{aligned}E_A^+ &= \left(a_s + Da_i^*\right)\cos\theta + i\left(a_i + Da_s^*\right)\sin\theta,\\ E_B^+ &= -i\left(a_s + Da_i^*\right)\sin\phi + \left(a_i + Da_s^*\right)\cos\phi,\end{aligned} \tag{19}$$

and polarizations at angles θ and ϕ with the vertical, respectively. For later convenience I define the partial fields

$$\begin{aligned}E_{A0}^+ &= a_s\cos\theta + ia_i\sin\theta, E_{B0}^+ = -ia_s\sin\phi + a_i\cos\phi,\\ E_{A1}^+ &= D\left[a_i^*\cos\theta + ia_s^*\sin\theta\right], E_{B1}^+ = D\left[-ia_i^*\sin\phi + a_s^*\cos\phi\right].\end{aligned} \tag{20}$$

The single, P_A, P_B, and coincidence, P_{AB}, detection rates in the WW formalism may be obtained by comparison with the rates calculated in the Hilbert-space formalism. Thus, in the following we revisit briefly the Hilbert-space treatment of the entangled photon pairs. I will start with the quantum fields arriving at Alice and Bob, respectively, that are the counterparts of the WW (Equation 19). It is trivial to get them either from Equation (11) or, taking Equation (5) into account, that is "putting hats" in the WW (Equation 20). We get the field operators

$$\begin{aligned}\hat{E}_A^+ &= \hat{E}_{A0}^+ + \hat{E}_{A1}^+, \hat{E}_B^+ = \hat{E}_{B0}^+ + \hat{E}_{B1}^+,\\ \hat{E}_{A0}^+ &= \hat{a}_s\cos\theta + i\hat{a}_i\sin\theta, \hat{E}_{B0}^+ = -i\hat{a}_s\sin\phi + \hat{a}_i\cos\phi,\\ \hat{E}_{A1}^+ &= D[\hat{a}_i^\dagger\cos\theta + i\hat{a}_s^\dagger\sin\theta], \hat{E}_{B1}^+ = D[-i\hat{a}_i^\dagger\sin\phi + \hat{a}_s^\dagger\cos\phi],\end{aligned} \tag{21}$$

and similar for the Hermitian conjugates. Alice's single detection rate is proportional to the following vacuum expectation (with $\hat{E}_A^- = \left(\hat{E}_A^+\right)^\dagger$)

$$\begin{aligned}P_A &= \langle 0 \mid \hat{E}_A^-\hat{E}_A^+ \mid 0\rangle = |D|^2\langle 0 \mid \hat{E}_{A1}^-\hat{E}_{A1}^+ \mid 0\rangle\\ &= |D|^2\langle 0 \mid (\hat{a}_i\cos\theta - i\hat{a}_s\sin\theta)(\hat{a}_i^\dagger\cos\theta + i\hat{a}_s^\dagger\sin\theta) \mid 0\rangle\\ &= |D|^2\langle 0 \mid \hat{a}_i\hat{a}_i^\dagger\cos^2\theta + \hat{a}_s\hat{a}_s^\dagger\sin^2\theta \mid 0\rangle = |D|^2,\end{aligned} \tag{22}$$

where in the former equality, I have neglected creation $\hat{E}_{A0}^-$ (annihilation $\hat{E}_{A0}^+$) operators appearing on the left (right). A similar result may be obtained for the single detection rate of Bob, that is

$$P_B = \langle 0 \mid \hat{E}_B^-\hat{E}_B^+ \mid 0\rangle = |D|^2, \hat{E}_B^- = \left(\hat{E}_B^+\right)^\dagger. \tag{23}$$

We are assuming ideal detectors, but for real detectors P_A and P_B should be multiplied times the detection efficiencies η_A and η_B, and the coincidence rate P_{AB} times $\eta_A\eta_B$.

In order to get the detection rule for single rates in the WW formalism we should translate Equation (22) taking Equation (8) into account. We get

$$\begin{aligned}P_A &= \left[\left(\langle|a_i|^2\rangle - \frac{1}{2}\right)\cos^2\theta + \left(\langle|a_s|^2\rangle - \frac{1}{2}\right)\sin^2\theta\right]\\ &\quad + |D|^2\left[\left(\langle|a_s|^2\rangle + \frac{1}{2}\right)\cos^2\theta + \left(\langle|a_i|^2\rangle + \frac{1}{2}\right)\sin^2\theta\right]\\ &= |D|^2\left[\cos^2\theta + \sin^2\theta\right] = |D|^2, \langle a_i a_s^*\rangle = \langle a_s a_i^*\rangle = 0,\end{aligned} \tag{24}$$

that agrees with the result calculated in the Hilbert-space formalism (Equation 22). Now we compare Equation (24) with the average of the field intensity arriving at Alice (see Equation 19), that is

$$\begin{aligned}\langle I_A\rangle &= \left\langle\left|E_A^+\right|^2\right\rangle = \langle|a_i|^2\rangle\cos^2\theta + \langle|a_s|^2\rangle\sin^2\theta\\ &\quad + |D|^2\left[\langle|a_s|^2\rangle\cos^2\theta + \langle|a_i|^2\rangle\sin^2\theta\right] = \frac{1}{2}\left(1 + |D|^2\right).\end{aligned} \tag{25}$$

We see that going from Equation (26) to Equation (24) the signal terms (those of order $|D|^2$) are multiplied times 2, whilst those coming from the vacuum (of order unity) are eliminated. This may be seen as a subtraction of the vacuum (ZPF) and

multiplication of the signal times 2, which leads to the following rule for the single detection rate in the WW formalism:

$$P_A = 2\langle I_A\rangle - 2\langle I_{A0}\rangle, I_A = E_A^+E_A^- = \left|E_A^+\right|^2, I_{A0} = \left|E_{A0}^+\right|^2. \quad (26)$$

The Hilbert-space rule for the coincidence rate is the vacuum expectation value of the product of four field operators in normal order. Here we have two terms

$$P_{AB} = \frac{1}{2}\langle 0 \mid \hat{E}_A^-\hat{E}_B^-\hat{E}_B^+\hat{E}_A^+ \mid 0\rangle + \frac{1}{2}\langle 0 \mid \hat{E}_B^-\hat{E}_A^-\hat{E}_A^+\hat{E}_B^+ \mid 0\rangle, \quad (27)$$

that would be equal if $\hat{E}_A^+$ and $\hat{E}_B^+$ commute. The former expectation may be evaluated to order $|D|^2$ as follows

$$\begin{aligned}\langle 0 \mid \hat{E}_A^-\hat{E}_B^-\hat{E}_B^+\hat{E}_A^+ \mid 0\rangle &= \langle 0 \mid \hat{E}_{A1}^-\hat{E}_B^-\hat{E}_B^+\hat{E}_{A1}^+ \mid 0\rangle = \langle 0 \mid \hat{E}_{A1}^-\hat{E}_{B0}^-\hat{E}_{B0}^+\hat{E}_{A1}^+ \mid 0\rangle \\ &= \langle 0 \mid \hat{E}_{A1}^-\hat{E}_{B0}^- \mid 0\rangle\langle 0 \mid \hat{E}_{B0}^+\hat{E}_{A1}^+ \mid 0\rangle = \left|\langle 0 \mid \hat{E}_{B0}^+\hat{E}_{A1}^+ \mid 0\rangle\right|^2 \\ &= |D|^2\left|\langle 0 \mid \left(-i\hat{a}_s\sin\phi + \hat{a}_i\cos\phi\right)\left(\hat{a}_i^\dagger\cos\theta + i\hat{a}_s^\dagger\sin\theta\right) \mid 0\rangle\right|^2,\end{aligned}$$

where the former equality, similar to Equation (22), removes creation operators on the left and annihilation operators on the right, the second one removes terms of order $|D|^4$ and the rest is trivial. The latter term of Equation (27) gives a similar contribution so that we get

$$\begin{aligned}P_{AB} &= \frac{1}{2}\left|\langle 0 \mid \hat{E}_{B0}^+\hat{E}_{A1}^+ \mid 0\rangle\right|^2 + \frac{1}{2}\left|\langle 0 \mid \hat{E}_{A0}^+\hat{E}_{B1}^+ \mid 0\rangle\right|^2 \\ &= |D|^2\cos^2(\theta-\phi). \end{aligned} \quad (28)$$

Here the creation operators are placed to the right and those of annihilation to the left, so that no subtraction is required in passing to the WW formalism. It is enough to substitute c-number amplitudes multiplied times 2 for the field operators, in order to get the rule for the coincidence rate in the WW formalism. That is

$$\begin{aligned}\left\langle E_{A0}^+E_{B1}^+\right\rangle + \left\langle E_{A1}^+E_{B0}^+\right\rangle &= \left\langle E_A^+E_B^+\right\rangle = D\cos(\theta-\phi) \quad (29)\\ &\Rightarrow P_{AB} = \left|\left\langle E_A^+E_B^+\right\rangle\right|^2 = |D|^2\cos^2(\theta-\phi),\end{aligned}$$

where we have taken Equations (20) and (8) into account. Here the vacuum subtraction is not explicit because the vacuum term would be zero, that is $\left\langle E_{A0}^+E_{B0}^+\right\rangle = 0$.

It is interesting to get the coincidence detection rate in terms of field intensities, rather than amplitudes. To do that we start calculating

$$\langle I_AI_B\rangle = \left\langle E_A^+E_A^-E_B^+E_B^-\right\rangle. \quad (30)$$

In the WW formalism the field amplitudes are c-numbers, therefore they commute, and the averages should be performed as in Equation (8). The expectation (Equation 30) may be obtained taking into account that the fields have the mathematical properties of Gaussian random variables (see Equation 4) (although this section is devoted to calculations and for the moment I am not committed to any physical interpretation). Thus, I apply a well-known property of the average of the product of four Gaussian random variables, that is

$$\begin{aligned}\langle I_AI_B\rangle &= \left\langle E_A^+E_A^-\right\rangle\left\langle E_B^+E_B^-\right\rangle + \left\langle E_A^+E_B^-\right\rangle\left\langle E_A^-E_B^+\right\rangle + \left\langle E_A^+E_B^+\right\rangle\left\langle E_A^-E_B^-\right\rangle \\ &= \langle I_A\rangle\langle I_B\rangle + \left|\langle E_A^+E_B^-\rangle\right|^2 + \left|\left\langle E_A^+E_B^+\right\rangle\right|^2. \end{aligned} \quad (31)$$

A similar procedure but involving the vacuum intensities, gives

$$\langle I_{A0}I_{B0}\rangle = \langle I_{A0}\rangle\langle I_{B0}\rangle + \left|\left\langle E_{A0}^+E_{B0}^-\right\rangle\right|^2 + \left|\left\langle E_{A0}^+E_{B0}^+\right\rangle\right|^2. \quad (32)$$

Here the third term does not contribute and the second one equals the second term of Equation (31) to order $|D|^2$. Hence, we get the rule for the coincidence rate in the WW formalism that in the following I write both in terms of fields and in terms of intensities.

$$P_{AB} = \left|\left\langle E_A^+E_B^+\right\rangle\right|^2 = \langle I_AI_B\rangle - \langle I_A\rangle\langle I_B\rangle - \langle I_{A0}I_{B0}\rangle + \langle I_{A0}\rangle\langle I_{B0}\rangle. \quad (33)$$

4. LOCALITY IN THE EXPERIMENTS WITH ENTANGLED PHOTON PAIRS

4.1. Realistic Interpretation of the Vacuum Radiation Field

I emphasize again that the WW formalism provides an alternative formulation of quantum optics, physically equivalent to the more common Hilbert-space. But it suggests a picture of the optical phenomena quite different from the latter, where photon is the fundamental concept. Indeed the WW picture may provide a local realistic interpretation in terms of random variables and stochastic processes. In the following, I present the main ideas of this interpretation. It rests upon several assumptions as follows.

The fundamental hypothesis is that *the electromagnetic vacuum field is a real stochastic field* (*the zeropoint field, ZPF)*. If expanded in normal modes the ZPF has a (positive) probability distribution of the amplitudes given by Equation (4). According to that assumption any photodetector would be immersed in an extremely strong radiation, infinite if no cut-off existed. Thus, how might we explain that detectors are not activated by the vacuum radiation? Firstly the strong vacuum field is effectively reduced to a weaker level if *we assume that only radiation within some (small) frequency interval is able to activate a photodetector*, that is the interval of sensitivity (ω_1, ω_2). However, the problem is not yet solved because signals involved in experiments have typical intensities of order the vacuum radiation in the said frequency interval so that the detector would be unable to distinguish a signal from the ZPF noise. Our proposal is to assume that *a detector may be activated only when the net Poynting vector (i.e., the directional energy flux) of the incoming radiation is different from zero, including both signal and vacuum fields*. More specifically I will assume that *the detector possesses an active area and the probability of a photocount is proportional to the net radiant energy flux crossing that area from the front side during some activation time, the probability being zero if the net flux crossing the area is in the reverse direction.*

These assumptions allow to understand qualitatively why the signals, but not the vacuum fields, activate detectors. Indeed the ZPF arriving at any point (in particular the detector) would be isotropic on the average, whence its associated mean Poynting vector would be nil, therefore only the signal radiation should produce photocounts. A problem remains because the vacuum fields are fluctuating so that the Poynting vector also fluctuates. Hence we may predict the existence of some dark rate even at zero Kelvin. The problems derived from the fluctuations diminish taking into account that *photocounts are not produced by an instantaneous interaction of the fields with the detectors but the activation requires some time interval*, a known fact in experiments. Therefore the effective activating energy flux is a time average whose fluctuations are plausibly small.

Of course these arguments are qualitative and a quantitative estimate should be worthwhile. However making such an estimate is rather involved and in the following I will just sketch the steps required. We should start calculating the probability distribution of the Poynting vector **P** due to the ZPF at a point **r** in space at time t. If we expand the ZPF in plane waves as usual, the probability of the Z component of **P** may be written as a sum involving all radiation modes, that is

$$Prob\left(P_z\right) = \left[\sum_j \sum_k a_j a_k Prob\left(a_j, a_k\right) \mathbf{E}_j\left(\mathbf{r},t\right) \times \mathbf{B}_k\left(\mathbf{r},t\right)\right] \cdot \mathbf{u}_z, \tag{34}$$

where a_j (a_k) is the amplitude of the mode $j\left(k\right)$, $\mathbf{E}_j$ ($\mathbf{B}_k$) its associated electric (magnetic) field and $\mathbf{u}_z$ is a unit vector in the Z direction. The probability density $Prob\left(a_j, a_k\right)$ is related to Equation (4). We assume that only field components with frequencies in the sensitivity interval (ω_1, ω_2) are effective for detection, whence we should restrict the double sum to modes with frequencies in that interval. Hence we might obtain the probability distribution of the integrated energy flux, Φ, crossing the active area of the detector during the activation time T. Finally we may assume that a detection event takes place whenever Φ surpasses a threshold $\Phi_0 > 0$ related to the detection efficiency, η, of the detector. If the ZPF is isotropic the flux crossing the active area of the detector might be positive or negative with equal probabilities but the ratio Φ/T, would be smaller as T is larger, zero for $T \to \infty$. We may choose Φ_0, as a function of T, so that the ZPF Φ surpasses Φ_0 very rarely. However for any finite T there will be a finite probability that $\Phi > \Phi_0$ thus producing photocounts even in the absence of signals. These spurious counts give a dark rate r usually attributed to thermal fluctuations. Indeed the experimental dark rate is known to decrease with temperature, but we propose that r would remain finite at zero Kelvin. Now we study the case when there is a signal, superimposed to the ZPF, arriving at the detector. The signal may be weak with respect to a typical short-time fluctuation of the ZPF, but it is *positive* at all times because signals arrive at the detector in the positive Z direction. Thus, a positive quantity should be added to the fluctuating energy flux due to the ZPF, calculated via Equation (34). In a particular experiment we should choose T, the sensitivity interval and the threshold Φ_0 such that we have high detection efficiency η and small dark rate r, but there are obvious constraints. For instance in order to have a small r we need high T and/or high Φ_0, but in this case some signals will become undetected leading to a decrease of η. I propose that these constraints are the physical reason for the difficulty of manufacturing very efficient photon counters.

4.2. Interpretation of the Photon Experiments

Our aim is to achieve a realistic local interpretation of the experiments measuring polarization correlation of entangled photon pairs, that we studied with the WW formalism in the previous section. Thus, I will consider two vacuum beams entering the nonlinear crystal, where they give rise to a "signal" and an "idler" beams. After crossing several appropriate devices they produce fields that will arrive at the Alice and Bob detectors. I do not attempt to present a detailed model, that should involve many radiation modes, in order to represent the signals as (narrow) beams (see Equation 17). I will study only detection rates, that may be illustrated with just 2 vacuum modes.

In agreement with our previous hypotheses a photodetection should derive from a relatively large integrated energy flux crossing the active surfaces. In actual experiments the pumping laser is pulsed and it is a fact that the detection rates are far smaller than the pulsing rate. In our interpretation this means that only in a tiny fraction of laser pulses, the flux Φ becomes greater than Φ_0. Thus, I will replace the threshold assumption of the previous subsection, i.e., detection when $\Phi > \Phi_0$, by another assumption, more convenient for the simplicity of calculations, namely that the detection probability is proportional to Φ if $\Phi > 0$, zero otherwise. I believe that the new assumption might be derived from the old one but I omit the proof. In the following it will be convenient to write everything in terms of the Poynting vector $\vec{I}$ rather than the integrated flux, Φ, assuming that the single detection probability per time window, T, by Alice is given by

$$P_A = \left\langle [M_A]_+ \right\rangle, M_A \equiv T^{-1} \int_0^T \vec{n}_A \cdot \vec{I}^A_{total}\left(\mathbf{r}_A,t\right) dt, \tag{35}$$

where $[M]_+ = M$ if $M > 0$, $[M]_+ = 0$ otherwise, and $\vec{n}_A$ is a unit vector in the direction of the incoming signal beam, assumed normal to the active area of the detector. The experimental time window has a duration of the order of a laser pulse, and may be different from the activation time of the detector but I will use the same label T. I shall use units such that both the intensities and the detection rates are dimensionless defining the rate as probability of a photodetection within one time window T. In Equation (35), I include a positivity constraint that I will ignore in the following substituting M_A for $[M_A]_+$. This approximation underestimate the rate. In fact the quantity M_A defined in Equation (35) will be positive in a fraction, say $f < 1$, of the samples and negative in the fraction $1 - f$. In the former case $[M_A]_+ = M_A$, in the latter $[M_A]_+ = 0$. Therefore $\langle M_A \rangle < \left\langle [M_A]_+ \right\rangle$, but we assume that the error is small if the activation time is large as commented in the previous subsection.

In order to provide a quantitative argument, I will consider a simplified model involving just two radiation modes, a_s and

a_i, and follow closely the calculation of the section 3. The fields emerging from the nonlinear crystal, after crossing several appropriate devices, will arrive at the Alice and Bob detectors. Each one of these fields consists of two parts, one large, of order unity and another of order $|D| << 1$. The former, given in Equation (20), is what would arrive at the detectors if there was no pumping laser and therefore no signal. It is just a part of the ZPF, whilst the rest of the ZPF consists of radiation that did not appear explicitly in the equations of section 3 because it was not needed in the calculations. As discussed above the total ZPF should have the property of isotropy, therefore giving an energy flux that may be positive or negative, nil on the average. The terms of order $|D|$, given by Equation (20), correspond to the signal produced in the nonlinear crystal after the modifications introduced by beam splitters and polarizers (and other devices like apertures, filters, lens systems, etc. whose action is not detailed in our simplified model). In summary the Poynting vector of the radiation at the (center of the) active area of Alice´s detector may be written

$$Alice: \vec{I}^{A}_{total}(t) = \vec{I}^{A}_{ZPF}(t) + \vec{I}_{A}(t). \tag{36}$$

$\vec{I}_A$ corresponding to the field E_A, Equation (19) and $\vec{I}^{A}_{ZPF}(t)$ comes from the rest of the ZPF. $\vec{I}_A(t)$ has the direction of $\vec{n}_A$, (Equation 35), whence the radiation intensity equals the modulus of the Poynting vector. Furthermore, its intensity is time independent (the time dependence of the signal fields derives from the sum of many modes as in Equation 17), so that we may write

$$M_A = I^{A}_{ZPF} + I_A, I^{A}_{ZPF} \equiv T^{-1}\int_0^T \vec{n}_A \cdot \vec{I}^{A}_{ZPF}(\mathbf{r}_A,t)\, dt, \tag{37}$$

and similar for Bob´s M_B.

In order to get the Alice single detection rate we need the average of M_A, that we will evaluate by comparison with the case when there is no pumping on the nonlinear crystal. In this case I_A becomes the intensity I_{A0}, Equation (26), and the Poynting vector of all vacuum fields arriving at the detector of Alice, i.e., $\vec{I}^{A}_{ZPF}(t) + \vec{I}_{A0}(t)$, should have nil average due to the isotropy of the *ZPF*. And similar for Bob. As a consequence the intensities I_{A0} and I_{B0}, Equation (26), should fulfill the following equalities

$$\left\langle I^{A}_{ZPF} + I_{A0}\right\rangle = \left\langle I^{B}_{ZPF} + I_{B0}\right\rangle = 0. \tag{38}$$

It would appear that this relation could not be true for all values of the angles θ, ϕ (Equation 20) because the ZPF Poynting vector $\hat{I}^{A}_{ZPF}$ and $\hat{I}^{B}_{ZPF}$ should not depend on our choice of angles whilst I_{A0} and I_{B0} do depend. However, this is flawed, the positions of the polarizers may influence also the ZPZ arriving at the detectors and it is plausible that the total Poynting vector has always zero mean. From Equation (35) to (38) we may derive the single rates of Alice and Bob, that is

$$P_A = \langle M_A\rangle = \langle I_A\rangle - \langle I_{A0}\rangle, P_B = \langle M_B\rangle = \langle I_B\rangle - \langle I_{B0}\rangle. \tag{39}$$

The result agrees with the quantum calculation in the WW formalism except for a factor 2 that derives from a different definition of field amplitudes. I point out that no dark rate appears in Equation (39) due to our approximation $[M]_+ = M$, see comment after Equation (35).

An analysis should be also made for the coincidence detection rates, but it is more involved and will not be included in the present paper (for a preliminary approach see [28]). A sketch is as follows. The coincidence detection probability in a given time window would be given by an extension of Equation (35), that is

$$P_{AB} = \left\langle [M_A]_+ [M_B]_+ \right\rangle.$$

This will give rise to many correlations between the field intensities arriving at Alice and Bob detectors. Determining the correct values of the correlations is a subtle matter, but I hope that an appropriate choice might reproduce the quantum predictions and the empirical results. The relevant achievement in the experiments is the strong correlation, that is the fact that P_{AB} is of the same order as P_A and P_B. Such a strong correlation is crucial for the violation of a Bell inequality. A qualitative argument for that correlation in our model is the following. The vacuum fields arriving at the nonlinear crystal are enhanced by the action of the laser, thus producing the socalled signal and idler fields. That enhancement is rarely strong enough to produce detection events in Alice and Bob detectors. However, from time to time a combination of high values of *both* relevant (fluctuating) vacuum fields, a_s and a_i, will give a relatively intense signal and idler fields that combined in the form of Equation (18) produce high field intensities arriving at both Alice and Bob detectors, giving rise to a coincidence count. The point is that a detection event requires simultaneous high values of a_s and a_i and in this case the signal intensities arriving at Alice and Bob are both large, whence detections are most probably produced in coincidence (provided the angles θ, ϕ in Equation 19 are appropriate).

The WW formalism suggests a quite different picture from the Hilbert-space one in terms of photons. We should not assume that the *small* value of the coupling parameter $|D|^2$ implies that the production probability of "entangled photon pairs" during a time window is small, but that the probability of detection, conditional to the photon production, is of the order of *unity*. (The latter probability is defined as the detection efficiency). In the WW formalism the probability of a photocount by Alice or Bob *does not factorize that way*. Furthermore, the concept of photon does not appear at all, but there are *continuous fluctuating fields including a real ZPF* arriving at the detectors that are activated when the arriving signal intensities are large enough.

Finally I stress that the hypothesis that the quantum vacuum fields are real allows a more detailed model of the experiments than Bell´s approach and the model is local. Indeed, as in the interpretation of single detections rates (Equation 39), the signals (accompanied by vacuum) travel causally from the source to the detectors.

5. DISCUSSION

Bell´s work of 1964 put forward an acute conflict in theoretical physics. The derived Bell inequalities are currently seen as

necessary conditions for any local realistic theory of physics. On the other hand the inequalities are incompatible with some predictions of quantum mechanics. The conclusion is that either local realism does not hold in nature or that quantum mechanics is not valid in all circumstances. Both alternatives are hard to accept.

Realims is a principle that may be stated saying that: *In science we ought to be concerned with what nature does,* not just with predictions of empirical results, so that we may get a picture of the natural world. In physics the picture should be quantitative, and we should interpret the observed phenomena in terms of general laws. In the microscopic domain the laws are those of quantum mechanics. The problem is that for some experiments, like those mentioned in section 1 [1, 2], the evolution of particles and/or fields, seems to require influences traveling at a superluminal velocity. This means a violation of "locality."

Locality (or relativistic causality) was defined and emphatically supported by Einstein. For instance in his authobiographical notes [29] Einstein wrote "On one supposition we should, in my opinion, absolutely hold fast: the real factual situation of the system S2 is independent of what is done with the system S1, which is spatially separated from the former." Thus, the violation of locality by experiments might look as a contradiction between quantum theory and relativity. The present wisdom is that locality has been indeed violated by the recent experiments but the conflict with relativity is minimized by the fact that quantum mechanics does not predict the possibility of sending superluminal signals (no-signaling theorem). However, in the views of many people including this author, a violation of locality is highly unsatisfactory.

In this paper, I offer a possible solution, namely that the Bell analysis sketched in the Introduction section does not apply to the commented experiments. In fact the standard method to do with a system of entangled photon pairs, or entangled quantum subsystems in general, is to start with the quantum representation of the whole system by a quantum state, that is a vector $\mid \psi\rangle$ of the Hilbert space. In the case of two photons entangled in polarization a representation of the quantum state may be

$$\mid \psi\rangle = \frac{1}{\sqrt{1+|c|^2}}\left(\mid V(a)\rangle \mid H(b)\rangle - c \mid H(a)\rangle \mid V(b)\rangle\right), \quad (40)$$

where c is a (nonzero) complex number, $V(a)$ $\left(H(a)\right)$ means that Alice´s photon has vertical (horizontal) polarization and similar for Bob. Checking that the representation (Equation 40) is correct is obtained by several measurements performed, in particular the single rates and the coincidence rate by Alice and Bob for detections after the photons cross polarizers at appropriate angles. The relevant result is that those rates violate a Bell inequality for appropriate choices of angles. Thus assuming that Bell analysis was correct (see section 1), people concludes that local realism has been empirically refuted.

Our criticism to that conclusion is that Bell analysis is not valid for the commented experiments. It is necessary to study in detail all elements involved in the production of the entangled "photon" pairs. (Actually we should speak of entangled radiation modes rather than photons). In particular the action of the quantum vacuum electromagnetic radiation. In some sense the ZPF is taken into account when one studies quantum optics using the standard Hilbert-space formalism in the Heisenberg representation, as revisited in section 2, where a comparison is made with the treatment in the Weyl-Wigner formalism. In the former the quantum vacuum fields are represented by linear combinations of creation and annihilation operators of photons. This abstract treatment leads people to take the vacuum fields as "virtual," that is purely formal devices useful for calculations but devoid of reality. The novelty of the present paper is to assume that the vacuum fields are real stochastic fields, something that appears as quite plausible in the Weyl-Wigner formalism. Thus, I propose that it is possible to interpret the experiments [1, 2] assuming that all quantum fields involved, including the vacuum ones, are real fluctuating (stochastic) fields that propagate causally in space.

DATA AVAILABILITY STATEMENT

The original contributions presented in the study are included in the article/supplementary materials, further inquiries can be directed to the corresponding author/s.

AUTHOR CONTRIBUTIONS

The author confirms being the sole contributor of this work and has approved it for publication.

ACKNOWLEDGMENTS

This manuscript has been released as a pre-print at arXiv:1908.03924 [28].

REFERENCES

1. Shalm LK, Meyer-Scott E, Christensen BG, Bierhorst P, Wayne MA, Stevens MJ, et al. A strong loophole-free test of local realism. *Phys Rev Lett.* (2015) **115**:250402. doi: 10.1103/PhysRevLett.115.250402
2. Giustina M, Versteegh MAM, Wengerowsky S, Handsteiner J, Hochrainer A, Phelan K, et al. A significant loophole-free test of Bell´s theorem with entangled photons. *Phys Rev Lett.* (2015) **115**:250401. doi: 10.1103/PhysRevLett.115.250401
3. Wiseman H. Quantum physics: death by experiment for local realism. *Nature.* (2015) **526**:649–50. doi: 10.1038/nature15631
4. Santos E. Mathematical and physical meaning of the Bell inequalities. *Eur J Phys.* (2016) **37**:055402. doi: 10.1088/0143-0807/37/5/055402
5. Bell JS. On the Einstein, podolsky and rosen paradox. *Physics.* (1964) **1**:195. doi: 10.1103/PhysicsPhysiqueFizika.1.195
6. Clauser JF, Horne M. Experimental consequences of objective local theories. *Phys Rev D.* (1974) **10**:526–35. doi: 10.1103/PhysRevD.10.526
7. Eberhard PH. Background level and counter efficiencies required for a loophole-free Einstein-Podolsky-Rosen experiment. *Phys Rev A.* (1993) **47**:R747–9. doi: 10.1103/PhysRevA.47.R747
8. Casado A, Marshall TW, Santos E. Parametric downconversion experiments in the Wigner representation. *J Opt Soc*

Am. B. (1997) **14**:494–502. doi: 10.1364/JOSAB.14.000494
9. Casado A, Fernández-Rueda A, Marshall TW, Risco-Delgado R, Santos E. Fourth order interference in the Wigner representation for parametric downconversion experiments. *Phys Rev A*. (1997) **55**:3879–90. doi: 10.1103/PhysRevA.55.3879
10. Casado A, Fernández-Rueda A, Marshall TW, Risco-Delgado R, Santos E. Dispersion cancellation and quantum eraser experiments analyzed in the Wigner function formalism. *Phys Rev A*. (1997) **56**:2477–80. doi: 10.1103/PhysRevA.56.2477
11. Casado A, Marshall TW, Santos E. Type II parametric downconversion in the Wigner formalism. Entanglement and Bell´s inequalities. *J Opt Soc Am B.* (1998) **15**:1572–7. doi: 10.1364/JOSAB.15.001572
12. Dechoum K, Marshall TW, Santos E. Parametric down and up conversion in the Wigner representation of quantum optics. *J Mod Opt.* (2000) **47**:1273–87. doi: 10.1080/09500340008232173
13. Casado A, Marshall TW, Risco-Delgado R, Santos E. Spectrum of the parametric down converted radiation calculated in the Wigner function formalism. *Eur Phys J D.* (2001) **13**:109–19. doi: 10.1007/s100530170292
14. Casado A, Guerra S, Plácido J. Wigner representation for experiments on quantum cryptography using two-photon polarization entanglement produced in parametric down-conversion. *J Phys B Mol Opt Phys.* (2008) **41**:045501. doi: 10.1088/0953-4075/41/4/045501
15. Casado A, Guerra S, Plácido J. Partial Bell-state analysis with parametric down conversion in the Wigner function formalism. *Adv Math Phys.* (2010) **2010**:501521. doi: 10.1155/2010/501521
16. Casado A, Guerra S, Plácido J. Wigner representation for polarization momentum hyperentanglement generated in parametric down-conversion, and its application to complete Bell-state measurement. *Eur Phys J D.* (2014) **68**:338–48. doi: 10.1140/epjd/e2014-50368-y
17. Casado A, Guerra S, Plácido J. Wigner representation for entanglement swapping using parametric down conversion: the role of vacuum fluctuations in teleportation. *J Mod Opt.* (2015) **62**:377–86. doi: 10.1080/09500340.2014.983571
18. Casado A, Guerra S, Plácido J. Rome teleportation experiment analysed in the Wigner representation: the role of the zeropoint fluctuations in complete one-photon polarization-momentum Bell-state analysis. *J Mod Opt.* (2018) **65**:1960–74. doi: 10.1080/09500340.2018.1478009
19. Weyl H. Quantenmechanik und Gruppentheorie. *Z Phys*. (1927) **46**:1–46. doi: 10.1007/BF02055756
20. Weyl H. *The Theory of Groups and Quantum Mechanics*. New York, NY: Dover (1931).
21. Wigner EP. On the quantum correction for thermodynamic equilibrium. *Phys Rev.* (1932) **40**:749. doi: 10.1103/PhysRev.40.749
22. Groenewold HJ. On the principles of elementary quantum mechanics. *Physica.* (1946) **12**:405–46. doi: 10.1016/S0031-8914(46)80059-4
23. Moyal JE. Quantum mechanics as a statistical theory. *Proc Cambridge Phil Soc*. (1949) **45**:99–124. doi: 10.1017/S0305004100000487
24. Hillery M, O´Connell RF, Scully MO, Wigner, EP. *Phys Rep.* (1984) **106**:121–68. doi: 10.1016/0370-1573(84)90160-1
25. Zachos CK, Fairlie DB, Curtright TL. *Quantum Mechanics in Phase Space*. Singapore: World Scientic (2005).
26. Casado A, Fernández-Rueda A, Marshall TW, Martínez J, Risco-Delgado R, Santos E. Dependence on crystal parameters of the correlation time between signal and idler beams in parametric down conversion calculated in the Wigner representation. *Eur Phys J D.* (2000) **11**:465–72. doi: 10.1007/s100530070074
27. Ou ZY, Wang LJ, Mandel L. Evidence for phase memory in two-photon down conversion through entanglement with the vacuum. *Phys Rev A.* (1990) **41**:566. doi: 10.1103/PhysRevA.41.566
28. Santos E. Local realistic interpretation of entangled photon pairs in the Weyl-Wigner formalism. *arXiv:1908.03924* (2019).
29. Einstein A. *Albert Einstein: Philosopher-Scientist*. Schilpp PA, Editor. Evanston: Open Court (1949).

Conflict of Interest: The author declares that the research was conducted in the absence of any commercial or financial relationships that could be construed as a potential conflict of interest.

frontiers in Physics

ORIGINAL RESEARCH
published: 11 December 2020
doi: 10.3389/fphy.2020.588415

Innsbruck Teleportation Experiment in the Wigner Formalism: A Realistic Description Based on the Role of the Zero-Point Field

Alberto Casado[1]*, *Santiago Guerra*[2] and *José Plácido*[2]

[1]Departamento de Física Aplicada III, Escuela Técnica Superior de Ingeniería, Universidad de Sevilla, Sevilla, Spain, [2]Grupo de Ingeniería Térmica e Instrumentación, Universidad de Las Palmas de Gran Canaria, Las Palmas de Gran Canaria, Spain

In this article, an undulatory description of the Innsbruck teleportation experiment is given, grounded in the role of the zero-point field (ZPF). The Wigner approach in the Heisenberg picture is used, so that the quadruple correlations of the field, along with the subtraction of the zero-point intensity at the detectors, are shown to be the essential ingredients that replace entanglement and collapse. This study contrasts sharply with the standard particle-like analysis and offers the possibility of understanding the hidden mechanism of teleportation, relying on vacuum amplitudes as hidden variables.

Keywords: teleportation, parametric downconversion, Wigner representation, local realism, zero-point field, Bell state measurement

OPEN ACCESS

Edited by:
Cosmas K Zachos,
Argonne National Laboratory (DOE),
United States

Reviewed by:
Anouar Ben Mabrouk,
University of Kairouan, Tunisia
Ndolane Sene,
Cheikh Anta Diop University, Senegal

***Correspondence:**
Alberto Casado
acasado@us.es

Specialty section:
This article was submitted to Mathematical and Statistical Physics, a section of the journal Frontiers in Physics

Received: *28 July 2020*
Accepted: *22 October 2020*
Published: *11 December 2020*

Citation:
Casado A, Guerra S and Plácido J (2020) Innsbruck Teleportation Experiment in the Wigner Formalism: A Realistic Description Based on the Role of the Zero-Point Field. Front. Phys. 8:588415. doi: 10.3389/fphy.2020.588415

1 INTRODUCTION

Since Bennett et al. proposed teleportation in 1993 [1], quantum state transmission has become essential for developing quantum computing and quantum communication [2, 3]. The standard theoretical approach to teleportation is based on the peculiar properties of Einstein–Podolsky–Rosen (EPR) pairs [4] in the Hilbert space. Entanglement and the projection postulate, along with the classical communication between the sender and receiver, often called Alice and Bob, respectively, constitute the fundamental elements of the teleportation protocol.

In the late 1990s, teleportation was achieved in experiments performed by the Universities of Innsbruck [5] and Rome [6], by using entangled photons generated in parametric downconversion (PDC). There is a discrepancy regarding who first performed genuine quantum teleportation [7]. On the one hand, the Innsbruck experiment used two pairs of entangled photons, and one of the four photons was used as a trigger to generate the single-particle state to be teleported [5, 8]. A remarkable characteristic of the four-photon source is the first experimental implementation of entanglement swapping [9, 10]. Nevertheless, given that the four polarization Bell states of two photons were not distinguishable using entanglement only in one degree of freedom and linear optics [11], the teleportation protocol described in Ref. 1 cannot be accomplished with 100% success in the Innsbruck scheme. Moreover, a controversial aspect of this experiment was the postselective or nonpostselective nature of teleportation [12–14]. On the other hand, in the Rome teleportation experiment, a pair of downconverted photons was used, and the state to be teleported was encoded in one of two degrees of freedom of one photon [15], which made a difference with respect to the work in Ref. 1. In contrast, the Bell state measurement (BSM) was accomplished with 100% success. In Ref. 16, a different implementation of the theoretical proposal given in Ref. 15 was carried out.

The Wigner formalism constitutes a complementary approach to the orthodox formulation in the Hilbert space for the study of quantum optical experiments implemented with PDC [17–25]. The

Wigner function of PDC is positive and allows for an intuitive picture in terms of stochastic processes. In the Wigner representation within the Heisenberg picture (WRHP), the dynamics is contained in the electric field and the Wigner distribution is time-independent, corresponding to the Wigner function of the vacuum state. In this approach, the linearity of the field equations of motion in the setup PDC plus linear optics can be exploited, to achieve relevant conclusions about quantum versus classical electrodynamics, by looking directly at the fields and their correlation properties. Recently, a more formal foundation of PDC has been developed using the Weyl–Wigner formalism [26].

One of the most interesting features of the WRHP approach is that the zero-point field (ZPF) appears in a natural form, which contributes to it being considered as a real stochastic field [27, 28]. The role of ZPF at the nonlinear crystal and idle channels of the optical devices placed between the source and detectors should be analyzed for a deeper understanding of the underlying physics. In this picture, photon entanglement can be understood as an interplay of correlated modes through the contribution of ZPF amplitudes in the polarization components of the field. Moreover, collapse is related to the subtraction of the zero-point intensity at the detectors, so that this approach clearly emphasizes the wave nature of light. The fact that detectors have a threshold gives rise to all nonclassical features of entangled photon pairs generated by PDC.

The standard analysis of a PDC experiment with the WRHP approach consists of the following steps:

i. Expression of the electric field amplitude corresponding to narrow light beams outgoing the nonlinear source is calculated. These beams are a linear transformation of the ZPF entering the crystal [17–19].
ii. Propagation of these fields throughout the experimental setup is conducted, following the rules of classical optics. At this step, the zero-point beams entering the idle channels of the optical devices must be considered.
iii. Calculation of the detection rates constitutes the main difference with respect to classical physics. In the case of single counts, the zero-point intensity is the threshold for detection, but the subtraction is more involved in the case of joint and multiple detection rates.
iv. The detection rates are expressed in terms of the field correlations mediated by the ZPF, allowing for a picture in terms of stochastic processes.
v. New physical insights emerge through the analysis of the different zero-point inputs. The role of the amplitude and phase of the fields in the light intensity at the detectors becomes relevant to the description of an internal mechanism leading to the different results. This analysis cannot be conducted with the standard treatment in the Hilbert space.

The combination of the possibility of transmitting and storing quantum information via the ZPF has revealed that the WRHP formalism is a very useful tool in analyzing the influence of the vacuum field in experiments on optical quantum communication [29–34]. Specifically, this approach has been applied to the analysis of teleportation experiments, such as entanglement swapping [32] and the Rome teleportation experiment [33]. The study of the Rome experiment showed the great importance of the zero-point inputs in BSM [31], in such a way that the distinguishability of the four polarization-momentum Bell states of a single photon can be understood from a sufficient balance between the zero-point inputs at the source of entanglement and those that intervening in the Bell state analyzer. More recently, the role of the zero-point amplitudes as hidden variables on Bell state distinguishability and their application to teleportation [16] have been investigated [34].

In this article, a new picture of the Innsbruck teleportation experiment [5] is given, by using the WRHP approach. The importance of this proposal lies in understanding the physical properties of ZPF inputs that intervene in the experiment and emphasizing the wave nature of light and causal propagation of the fields involved. The article is organized as follows. In **Section 2**, the Wigner formalism in the Heisenberg framework is briefly reviewed. In **Section 3**, a general setup, including the one given in Ref. 5, is analyzed to investigate the relationship between teleportation and quadruple correlations. In **Section 4**, the relationship between different ZPF inputs at the setup and optimality of the BSM at Alice's station is analyzed. **Section 5** is devoted to the calculation of the fourfold detection probabilities in the Innsbruck experiment. Finally, in **Section 6**, the main conclusions of this work are presented along with further steps of this research line.

2 THE WIGNER REPRESENTATION WITHIN THE HEISENBERG PICTURE APPROACH FOR PARAMETRIC DOWNCONVERSION EXPERIMENTS

In this section, the mathematical tools used in the development of this work are described [17–19]. The field radiated by a nonlinear crystal is produced from the coupling between the ZPF and a classical wave representing the laser pumping beam. The vacuum is represented as a sum of two mutually complex conjugate amplitudes as follows:

$$\mathbf{E}_v(\mathbf{r},t) = \mathbf{E}_v^{(+)}(\mathbf{r},t) + \mathbf{E}_v^{(-)}(\mathbf{r},t), \tag{1}$$

with

$$\mathbf{E}_v^{(+)}(\mathbf{r},t) = i\sum_{\mathbf{k},\lambda}\left(\frac{\hbar\omega_{\mathbf{k}}}{2L^3}\right)^{1/2}\alpha_{\mathbf{k},\lambda}\mathbf{u}_{\mathbf{k},\lambda}e^{i(\mathbf{k}\cdot\mathbf{r}-\omega_{\mathbf{k}}t)}, \tag{2}$$

$$\mathbf{E}_v^{(-)}(\mathbf{r},t) = -i\sum_{\mathbf{k},\lambda}\left(\frac{\hbar\omega_{\mathbf{k}}}{2L^3}\right)^{1/2}\alpha^{*}_{\mathbf{k},\lambda}\mathbf{u}_{\mathbf{k},\lambda}e^{-i(\mathbf{k}\cdot\mathbf{r}-\omega_{\mathbf{k}}t)}. \tag{3}$$

The subscripted letter "v" denotes the vacuum field or ZPF. L^3 is the normalization volume, $\alpha_{\mathbf{k},\lambda}(t)$ is the amplitude corresponding to a mode whose wave vector is $\mathbf{k}$ and polarization vector is $\mathbf{u}_{\mathbf{k},\lambda}$, with $\omega_{\mathbf{k}} = c|\mathbf{k}|$, and λ takes values in the set $\{H, V\}$, where $H(V)$ means horizontal (vertical).

Stochastic variables $\alpha^{*}_{\mathbf{k},\lambda}$ and $\alpha_{\mathbf{k},\lambda}$ follow a distribution given by the following Gaussian equation:

$$W(\alpha) = \prod_{\mathbf{k},\lambda} \frac{2}{\pi} \mathrm{e}^{-2\left|\alpha_{\mathbf{k},\lambda}\right|^2}; \alpha \equiv \{\alpha_{\mathbf{k},\lambda}\}. \tag{4}$$

On the other hand, the beam corresponding to the laser is represented by a plane wave with wave vector $\mathbf{k}_p$ and frequency ω_p. We have the following:

$$\mathbf{V}(\mathbf{r},t) = \left(V_p(t)\exp\left[i\left(\mathbf{k}_p\cdot\mathbf{r}-\omega_p t\right)\right] + c.c.\right)\mathbf{u}; \mathbf{u}\perp\mathbf{k}_p, \tag{5}$$

where c.c. denotes complex conjugation. Given that the coherence time of the laser beam is usually large compared to most of the times involved, the amplitude $V_p(t)$ will be considered as a constant.

The electric field corresponding to a (narrow) light beam emitted by a nonlinear crystal is represented by the following slowly varying amplitude:

$$\mathbf{F}^{(+)}(\mathbf{r},t) = i\mathrm{e}^{\omega_s t}\sum_{\mathbf{k}\in[\mathbf{k}]_s,\lambda}\left(\frac{\hbar\omega_{\mathbf{k}}}{2L^3}\right)^{1/2}\alpha_{\mathbf{k},\lambda}(0)\mathbf{u}_{\mathbf{k},\lambda}\mathrm{e}^{i(\mathbf{k}\cdot\mathbf{r}-\omega_{\mathbf{k}}t)}, \tag{6}$$

where ω_s represents the central frequency of the beam and $[\mathbf{k}]_s$ constitutes a set of wave vectors centered at $\mathbf{k}_s$. Amplitude $\alpha_{\mathbf{k},\lambda}(t=0)$ has been calculated elsewhere to second order in a characteristic coupling constant (g) [17–19]. Type II PDC contains amplitudes $\alpha_{\mathbf{k},\lambda}$ ($\mathbf{k}\in[\mathbf{k}]_s$), belonging to the zero-point beam entering the crystal in the direction of the signal, and the amplitudes $\alpha_{\mathbf{k}',\lambda'}$ ($\boldsymbol{k}'\in[\mathbf{k}]_i;\lambda'\neq\lambda$), concerning the zero-point beam corresponding to the so-called idler photon, fulfilling the matching conditions $\omega_{\mathbf{k}}+\omega_{\mathbf{k}'}\approx\omega_p$ and $\mathbf{k}+\boldsymbol{k}'\approx\mathbf{k}_p$. For $t>0$, there is a free evolution. The concrete expression of the fields exiting the crystal and the description of entanglement in the WRHP approach are reviewed in the next section.

Field amplitude $\mathbf{F}^{(+)}$ propagates through free space according to the following expression:

$$\mathbf{F}^{(+)}(\mathbf{r}_2,t) = \mathbf{F}^{(+)}\left(\mathbf{r}_1, t-\frac{r_{12}}{c}\right)\mathrm{e}^{i\omega_s(r_{12}/c)}\ ;\ \mathbf{r}_{12} = |\mathbf{r}_2-\mathbf{r}_1|. \tag{7}$$

Let us now review the theory of photodetection. The single detection probability at a given detector D_a is as follows:

$$P_a(\mathbf{r},t) = K_a\langle I_a(\mathbf{r},t) - I_{v,a}(\mathbf{r})\rangle, \tag{8}$$

where $\langle\ldots\rangle$ represents an average with the Wigner density given in **Eq. 4**. $I_a \propto \mathbf{E}_a^{(+)}\cdot\mathbf{E}_a^{(-)} = \mathbf{F}_a^{(+)}\cdot\mathbf{F}_a^{(-)}$, in appropriate units, is the intensity of light arriving at the detector and $I_{v,a}$ corresponds to the average intensity of the ZPF. On the other hand, K_a is a constant related to the effective efficiency of the detection process at detector D_a.

In experiments involving polarization, the joint detection probability is calculated by using the following expression:

$$P_{ab}(\boldsymbol{r},t;\boldsymbol{r}',t') = K_aK_b\times\sum_{\lambda,\lambda'}\left|\langle F^{(+)}_{a,\lambda}(\phi_a;\boldsymbol{r},t)F^{(+)}_{b,\lambda'}(\phi_b;\boldsymbol{r}',t')\rangle\right|^2, \tag{9}$$

where ϕ_A and ϕ_B, appearing in the cross-correlation $\langle F^{(+)}_{a,\lambda}F^{(+)}_{b,\lambda'}\rangle$, represent setup parameters. In the situation where the operators corresponding to fields in detectors D_a and D_b commute, as in the case of Bell-type experiments [35], the previous expression is equivalent to the average of product $K_aK_b(I_a-I_{v,a})(I_b-I_{v,b})$. Nevertheless, in a general situation, the subtraction of the pure zero-point contribution is more involved.

Finally, in experiments involving fourfold detection, the detection probability can be obtained as the sum of sixteen addends. We have the following:

$$P_{abcd}(\mathbf{r},t;\mathbf{r}',t';\mathbf{r}'',t'';\mathbf{r}''',t''') = K_aK_bK_cK_d \times\sum_{\lambda,\lambda',\lambda'',\lambda'''}\left|\langle F^{(+)}_{a,\lambda}(\phi_a;\mathbf{r},t)F^{(+)}_{b,\lambda'}(\phi_b;\mathbf{r}',t')F^{(+)}_{c,\lambda''}(\phi_c;\mathbf{r}'',t'')F^{(+)}_{d,\lambda'''}(\phi_d;\mathbf{r}''',t''')\rangle\right|^2, \tag{10}$$

where the quadruple correlation $\langle F^{(+)}_{a,\lambda}F^{(+)}_{b,\lambda'}F^{(+)}_{c,\lambda''}F^{(+)}_{d,\lambda'''}\rangle$ can be calculated in terms of the cross-correlation properties of the fields, by taking into account the fact that the field amplitudes in PDC are Gaussian. That is,

$$\langle F^{(+)}_{a,\lambda}F^{(+)}_{b,\lambda'}F^{(+)}_{c,\lambda''}F^{(+)}_{d,\lambda'''}\rangle = \langle F^{(+)}_{a,\lambda}F^{(-)}_{b,\lambda'}\rangle\langle F^{(-)}_{c,\lambda''}F^{(+)}_{d,\lambda'''}\rangle + \langle F^{(+)}_{a,\lambda}F^{(+)}_{c,\lambda''}\rangle \times\langle F^{(+)}_{b,\lambda'}F^{(+)}_{d,\lambda'''}\rangle + \langle F^{(+)}_{a,\lambda}F^{(+)}_{d,\lambda'''}\rangle\langle F^{(+)}_{b,\lambda'}F^{(+)}_{c,\lambda''}\rangle. \tag{11}$$

In actual experiments, **Eqs 8–10** must be integrated over the surface aperture of the detectors and appropriate detection windows.

3 THE MEANING OF TELEPORTATION IN TERMS OF THE QUADRUPLE CORRELATIONS

The standard description of teleportation in the Hilbert space [1] uses three particles, one of them (particle 1) in an unknown quantum state to be teleported, $|\phi\rangle_1 = \alpha|H\rangle_1 + \beta|V\rangle_1$, and two entangled particles (particles 2 and 3) in a singlet state, $|\psi^-\rangle_{23}$. The state of the three-particle system is given by the tensor product:

$$\begin{aligned}|\psi\rangle_{123} &= |\phi\rangle_1|\psi^-\rangle_{23}\\ &= -\frac{1}{2}|\psi^-\rangle_{12}(\alpha|H\rangle_3+\beta|V\rangle_3) - \frac{1}{2}|\psi^+\rangle_{12}(\alpha|H\rangle_3-\beta|V\rangle_3)\\ &\quad+\frac{1}{2}|\phi^-\rangle_{12}(\beta|H\rangle_3+\alpha|V\rangle_3) + \frac{1}{2}|\phi^+\rangle_{12}(\beta|H\rangle_3-\alpha|V\rangle_3),\end{aligned} \tag{12}$$

where the four Bell-base states are

$$|\psi^{\pm}\rangle_{ij} = \frac{1}{\sqrt{2}}\left[|H\rangle_i|V\rangle_j \pm |V\rangle_i|H\rangle_j\right], \tag{13}$$

$$|\phi^{\pm}\rangle_{ij} = \frac{1}{\sqrt{2}}\left[|H\rangle_i|H\rangle_j \pm |V\rangle_i|V\rangle_j\right]. \tag{14}$$

A BSM on particles 1 and 2 leaves particle 3 in a state that can be modified after classical communication, to reproduce the initial state of particle 1. If the BSM indicates the detection of a singlet state of particles 1 and 2, then teleportation is directly achieved.

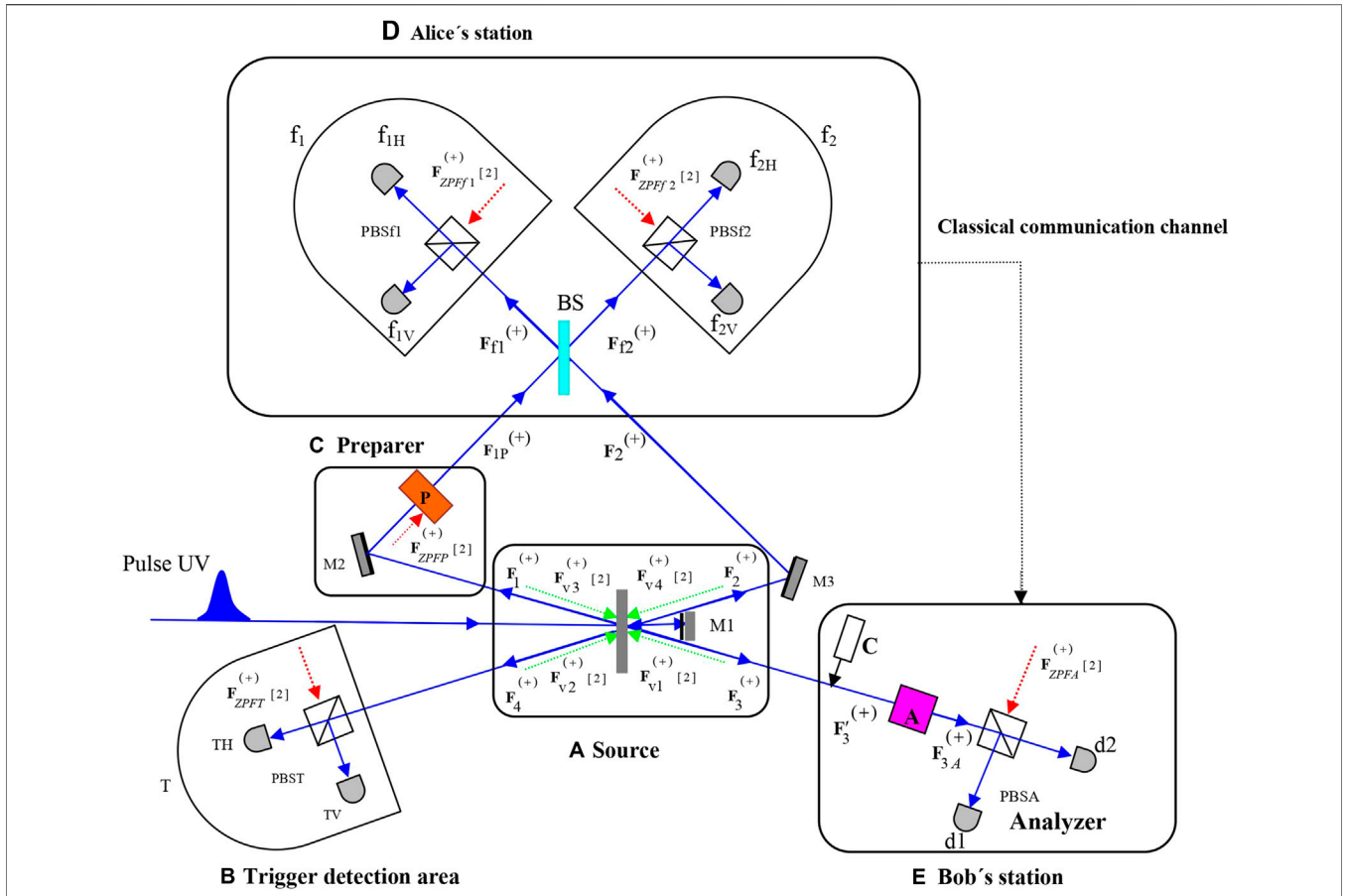

FIGURE 1 | General setup for teleportation based on the Innsbruck experiment, showing the principles involved in quantum teleportation and all the zero-point entries for the analysis with the WRHP approach. The number of sets of ZPF modes is written between brackets. **(A)** Source ($N_{ZPF,S} = 8$). Each of the vacuum inputs at the source contains two sets of ZPF modes. **(B)** Trigger. The first detection is produced at the trigger detection area. The ZPF beam entering the idle channel of PBST introduces two sets of vacuum modes. **(C)** Preparer. Beam $\mathbf{F}_1^{(+)}$ is modified through the action of a linear optical device *P*. In the case of a linear polarizer, a zero-point contribution $\mathbf{F}_{ZPFP}^{(+)}$ must be considered. **(D)** Alice's station. It consists of a balanced beam splitter and two detection areas f_1 and f_2. Each area includes an arrangement with a PBS and two detectors f_{iH} and f_{iV} ($i = \{1, 2\}$). Each of the ZPF inputs, $\mathbf{F}_{ZPFf1}^{(+)}$ and $\mathbf{F}_{ZPFf2}^{(+)}$, introduces two sets of vacuum modes. **(E)** Bob's station. The setup at Bob's side is intended to check that teleportation has been successful. It consists of an optical device *A* and a polarizing beam splitter PBSA followed by two detectors *d*1 and *d*2. The optical device C can be used after classical communication between Alice and Bob.

In the Innsbruck experiment, two independent pairs of downconverted photons are "simultaneously" produced in the state $|\Pi\rangle_{1234} = |\psi^-\rangle_{14}\ |\psi^-\rangle_{23}$. Photon 4 is used as a trigger to generate the state described in **Eq. 12**, once a given transformation is applied on photon 1.

In the WRHP approach, a deep understanding of this experiment requires the analysis of the quadruple correlation properties of the field. Let us consider the sketch of the experimental setup described in **Figure 1**. The notation used in this figure is similar to the one given in Ref. 5, with the goal of an easier reading of this article and the possibility of comparing it with the original setup. In addition, ZPF inputs are represented for understanding the original ideas displayed in this work and its relationship with the standard description in the Hilbert space formulation. Four two-by-two correlated beams represent two couples of polarization-entangled photons. The input fields $\mathbf{F}_{v1}^{(+)}$ and $\mathbf{F}_{v4}^{(+)}$ ($\mathbf{F}_{v2}^{(+)}$ and $\mathbf{F}_{v3}^{(+)}$), each containing two sets of vacuum modes, are coupled with the laser, giving rise to the correlated signals $\mathbf{F}_1^{(+)}$ and $\mathbf{F}_4^{(+)}$ ($\mathbf{F}_2^{(+)}$ and $\mathbf{F}_3^{(+)}$). The quantum information is carried out by eight sets of ZPF modes that are amplified at the source, that is,

$$N_{ZPF,S} = 8. \tag{15}$$

The exiting fields at the center of the nonlinear source can be expressed to second order in the coupling parameter using the following amplitudes (for simplicity, space-time notation is discarded):

$$F_1^{(+)} = \begin{bmatrix} F_s^{(+)} \\ F_p^{(+)} \end{bmatrix} = \begin{bmatrix} (1+g^2|V|^2J)F_{v1,H}^{(+)} + gVGF_{v4,V}^{(-)} \\ (1+g^2|V|^2J)F_{v1,V}^{(+)} + gVGF_{v4,H}^{(-)} \end{bmatrix}, \tag{16}$$

$$F_4^{(+)} = \begin{bmatrix} F_q^{(+)} \\ e^{i\pi}F_r^{(+)} \end{bmatrix} = \begin{bmatrix} (1+g^2|V|^2J)F_{v4,H}^{(+)} + gVGF_{v1,V}^{(-)} \\ e^{i\pi}\left[(1+g^2|V|^2J)F_{v4,V}^{(+)} + gVGF_{v1,H}^{(-)}\right] \end{bmatrix}, \tag{17}$$

$$F_2^{(+)} = \begin{bmatrix} F'^{(+)}_s \\ F'^{(+)}_p \end{bmatrix} = \begin{bmatrix} (1+g^2|V|^2J)F_{v2,H}^{(+)} + gV'GF_{v3,V}^{(-)} \\ (1+g^2|V|^2J)F_{v2,V}^{(+)} + gV'GF_{v3,H}^{(-)} \end{bmatrix}, \tag{18}$$

$$F_3^{(+)} = \begin{bmatrix} F'^{(+)}_q \\ e^{i\pi}F'^{(+)}_r \end{bmatrix} = \begin{bmatrix} (1+g^2|V|^2J)F^{(+)}_{v3,H} + gV'GF^{(-)}_{v2,V} \\ e^{i\pi}\left[(1+g^2|V|^2J)F^{(+)}_{v3,V} + gV'GF^{(-)}_{v2,H}\right] \end{bmatrix}, \tag{19}$$

where G and J are linear operators defined elsewhere [17–19] and are related to the selection of modes fulfilling the matching conditions. On the other hand, $V' = -V$ due to the reflection of the pumping beam at mirror M1. It will be considered that M1 is in a fixed position, such that the condition of temporal overlap at the beam splitter is fulfilled [5].

Equations 16–19 correspond to the WRHP description of the state vector $|\Pi\rangle_{1234} = |\Psi^-\rangle_{14}|\Psi^-\rangle_{23}$, the crucial point being the interplay of correlated fields, through the action of the zero-point amplitudes: the only nonnull cross-correlations are those concerning the labels (p, q) and (r, s) of beams 1–4 and the same for the beams 2–3. This can be easily understood by taking into account the fact that $F^{(+)}_{vj,X}$ $(j = \{1, 2, 3, 4\}, X = \{H, V\})$ is only correlated with $F^{(-)}_{vj,X}$, being a direct consequence of **Eq. 4**. Any of the four cross-correlations can be expressed, at any position and time, in terms of the corresponding one at the center of the nonlinear source (see **Eq. 7**). We have the following:

$$\langle F_p^{(+)}(0,t)F_q^{(+)}(0,t')\rangle = \langle F_r^{(+)}(0,t)F_s^{(+)}(0,t')\rangle = gV\nu(t-t'), \tag{20}$$

where $\nu(t-t')$ is a function that vanishes when $|t-t'| > \tau$, t being the correlation time between the downconverted photons. Similar relations hold for the corresponding primed amplitudes. In addition, the exponential factor $(e^{i\pi})$ in **Eqs 17** and **19** gives rise to a sign difference between the two correlations, corresponding to orthogonal polarization amplitudes, involving the couple of beams 1 − 4 (2–3). This sign difference identifies the physical properties of the singlet state in the WRHP formalism [29, 30].

Moreover, the amplitude $\mathbf{F}_p^{(+)}$ verifies the following autocorrelation property:

$$\langle F_p^{(+)}(0,t)F_p^{(-)}(0,t')\rangle - \langle F^{(+)}_{\nu 1,V}(0,t)F^{(-)}_{\nu 1,V}(0,t')\rangle = g^2|V|^2\mu(t-t'), \tag{21}$$

where $\mu(t-t')$ is a function that goes to zero when $|t-t'| > \tau$. Similar relations hold for the rest of the field amplitudes given in **Eqs 16–19**.

By taking into account **Eq. 20**, the two nonnull cross-correlations concerning beams 1 and 4 can be expressed in the following compact form:

$$\langle F^{(+)}_{4,X}(0,t)F^{(+)}_{1,U}(0,t')\rangle = (-1)^{n(X)}gV\nu(t-t')[1-\delta_{XU}], \tag{22}$$

where X and U can take values in the set $\{H, V\}$. On the other hand, $n(H) = 2$ and $n(V) = 1$. A similar expression holds for the correlations involving beams 2 and 3, that is,

$$\langle F^{(+)}_{2,X}(0,t)F^{(+)}_{3,U}(0,t')\rangle = (-1)^{n(X)+1}gV'\nu(t-t')[1-\delta_{XU}]. \tag{23}$$

The quadruple correlations representing the fields given in **Eqs 16–19** can be calculated using **Eq. 11**. Given that beam 1 (2) is only correlated with 4 (3), there are four nonnull correlations:

$$\begin{aligned}&\langle F^{(+)}_{4,X}(0,t)F^{(+)}_{1,U}(0,t')F^{(+)}_{2,W}(0,t'')F^{(+)}_{3,Z}\left(0,t'''\right)\rangle \\ &\quad = (-1)^{n(X)+n(W)+1}g^2VV'\nu(t-t')\nu\left(t''-t'''\right)[1-\delta_{XU}][1-\delta_{WZ}],\end{aligned} \tag{24}$$

where X, U, Z, and W can take values in the set $\{H, V\}$.

From now on, for notation simplicity, an identical distance between the source and the different detectors will be considered, so that the phase shift in **Eq. 7** will not be considered in the expression of the fields. Moreover, for the time being, the dependence of the fields on position and time will be discarded. Nevertheless, the reader's attention can be drawn, wherever necessary, to any reintroduction of space-time variables.

In the Innsbruck experiment, the first detection is produced at the trigger detector. Let us suppose that the trigger detection area involves a polarizing beam splitter PBST that transmits (reflects) horizontal (vertical) polarization. Two detectors, TH and TV, are placed at each of the exiting channels. The fields at the detectors have a noise component coming from the ZPF entering the idle channel of PBST, that is,

$$F^{(+)}_{TH} = \begin{pmatrix} F^{(+)}_q \\ iF^{(+)}_{ZPFT,V} \end{pmatrix}; F^{(+)}_{TV} = \begin{pmatrix} F^{(+)}_{ZPFT,H} \\ -iF^{(+)}_r \end{pmatrix}. \tag{25}$$

Let us now consider the action of a linear optical device on beam 1. The transmitted field amplitude $\mathbf{F}^{(+)}_{1P}$ is

$$\mathbf{F}^{(+)}_{1P} = \widehat{P}\,\mathbf{F}^{(+)}_1 = \begin{bmatrix} L_H & R_H \\ L_V & R_V \end{bmatrix}\begin{bmatrix} F^{(+)}_s \\ F^{(+)}_p \end{bmatrix} = \begin{bmatrix} L_HF^{(+)}_s + R_HF^{(+)}_p \\ L_VF^{(+)}_s + R_VF^{(+)}_p \end{bmatrix}, \tag{26}$$

where P denotes the word "preparer" and L (R) is the left (right) column of $\widehat{P}$.

In the case of a circular polarizer of angle θ with respect to horizontal, $L_H = \cos^2\theta$, $R_H = L_V = \cos\theta\sin\theta$, and $R_V = \sin^2\theta$. In this situation, a zero-point contribution $\mathbf{F}^{(+)}_{ZPFP}$ must be added in **Eq. 26**. This ZPF amplitude is uncorrelated with the rest of the fields. Thus, $\mathbf{F}^{(+)}_{1P}$ can be generally expressed as follows:

$$\mathbf{F}^{(+)}_{1P} = \begin{bmatrix} P_H\left(F^{(+)}_s, F^{(+)}_p\right) \\ P_V\left(F^{(+)}_s, F^{(+)}_p\right) \end{bmatrix}, \tag{27}$$

where

$$\begin{aligned}P_H\left(F^{(+)}_s, F^{(+)}_p\right) &= L_HF^{(+)}_s + R_HF^{(+)}_p + F^{(+)}_{ZPFP,H}, \\ P_V\left(F^{(+)}_s, F^{(+)}_p\right) &= L_VF^{(+)}_s + R_VF^{(+)}_p + F^{(+)}_{ZPFP,V}.\end{aligned} \tag{28}$$

The general transformation given in **Eq. 28** represents a great variety of experiments with different preparations so that the analysis displayed in this article goes beyond the experimental situation given in Ref. 5, where a linear polarizer acts on beam $\mathbf{F}^{(+)}_1$. As a matter of fact, the previous analysis of entanglement swapping given in Ref. 32, where $\widehat{P} = \widehat{I}$, can be seen as a particular case of the results presented in this work.

Using **Eqs 17**, **20**, **27**, and **28**, we have the following four cross-correlations concerning beams $\mathbf{F}^{(+)}_{1P}$ and $\mathbf{F}^{(+)}_4$:

$$\langle F^{(+)}_{4,X}F^{(+)}_{1P,U}\rangle = (-1)^{n(X)}gV\nu(0)F(X,U), \tag{29}$$

where the bivariate function $F(X,U)$ is given by

$$F(X,U) = L_U\delta_{X,V} + R_U\delta_{X,H}. \tag{30}$$

This leads to a duplication of the nonnull quadruple correlations, from four to eight. Using **Eqs 11**, **23**, and **29**, we have the following:

$$\begin{aligned}\langle F^{(+)}_{4,X}F^{(+)}_{1P,U}F^{(+)}_{2,W}F^{(+)}_{3,Z}\rangle &= \langle F^{(+)}_{4,X}F^{(+)}_{1P,U}\rangle\langle F^{(+)}_{2,W}F^{(+)}_{3,Z}\rangle \\ &= (-1)^{n(X)+n(W)+1}g^2VV'\nu^2(0)F(X,U)[1-\delta_{WZ}].\end{aligned} \tag{31}$$

Let us now calculate the fields at Alice's station. Beams $\mathbf{F}^{(+)}_{1P}$ and $\mathbf{F}^{(+)}_{2}$ are superposed at a balanced beam splitter (see **Figure 1**) so that the number of sets of amplified modes entering the Bell state analyzer is as follows (see **Eq. 15**) [33]:

$$N_{ZPF,A} = \frac{N_{ZPF,S}}{2} = 4. \tag{32}$$

From **Eqs 18**, **27**, and **28**, the exiting beam $(\mathbf{F}^{(+)}_{fj}j = 1,2)$ is given by the following superposition:

$$\mathbf{F}^{(+)}_{fj} = -i^j\frac{(-1)^j\mathbf{F}^{(+)}_{1P} + i\mathbf{F}^{(+)}_{2}}{\sqrt{2}} = -\frac{i^j}{\sqrt{2}}\begin{bmatrix}(-1)^jP_H\left(F^{(+)}_s,F^{(+)}_p\right) + iF'^{(+)}_s\\ (-1)^jP_V\left(F^{(+)}_s,F^{(+)}_p\right) + iF'^{(+)}_p\end{bmatrix}. \tag{33}$$

Now, to get the electric field at the detector f_{jX} (X= {H, V}), a ZPF component coming from the idle channel of PBSfj must be included. That is,

$$\mathbf{F}^{(+)}_{fjH} = -\frac{i^j}{\sqrt{2}}\left[(-1)^jP_H\left(F^{(+)}_s,F^{(+)}_p\right) + iF'^{(+)}_s\right] + iF^{(+)}_{ZPFfj,V}, \tag{34}$$

$$\mathbf{F}^{(+)}_{fjV} = -\frac{i^{j+1}}{\sqrt{2}}\left[(-1)^jP_V\left(F^{(+)}_s,F^{(+)}_p\right) + iF'^{(+)}_p\right] + F^{(+)}_{ZPFfj,H}. \tag{35}$$

In the standard description of quantum teleportation [1], Alice informs Bob of her measurement result via a classical communication channel. In this way, Bob can apply a linear transformation on beam $\mathbf{F}^{(+)}_3$ by means of the optical device C (see **Figure 1**), to reproduce the prepared state. Then, in order to verify that teleportation has been successfully carried out, the signal $\mathbf{F}'^{(+)}_3 = \widehat{C}\mathbf{F}^{(+)}_3$ enters an analyzer consisting of a linear optical device A followed by a polarizing beam splitter, PBSA. Let $\mathbf{F}^{(+)}_{3A}$ be the signal entering PBSA, that is, $\mathbf{F}^{(+)}_{3A} = \widehat{A}\mathbf{F}'^{(+)}_3 = \widehat{A}\widehat{C}\mathbf{F}^{(+)}_3$; then, we have the following:

$$\mathbf{F}^{(+)}_{3A} = \begin{bmatrix}\tilde{L}_H & \tilde{R}_H\\ \tilde{L}_V & \tilde{R}_V\end{bmatrix}\begin{bmatrix}F'^{(+)}_q\\ -F'^{(+)}_r\end{bmatrix} = \begin{bmatrix}\tilde{A}_H\left(F'^{(+)}_q,F'^{(+)}_r\right)\\ \tilde{A}_V\left(F'^{(+)}_q,F'^{(+)}_r\right)\end{bmatrix}, \tag{36}$$

$$\tilde{A}_H\left(F'^{(+)}_q,F'^{(+)}_r\right) = \tilde{L}_HF'^{(+)}_q - \tilde{R}_HF'^{(+)}_r, \tag{37}$$

$$\tilde{A}_V\left(F'^{(+)}_q,F'^{(+)}_r\right) = \tilde{L}_VF'^{(+)}_q - \tilde{R}_VF'^{(+)}_r, \tag{38}$$

where the matrix $\widehat{A}\widehat{C}$ is represented by parameters $\tilde{L}_H$, $\tilde{L}_V$, $\tilde{R}_H$, and $\tilde{R}_V$. It has been considered that neither $\widehat{C}$ nor $\widehat{A}$ introduces additional ZPF modes.

Finally, by considering the ZPF entering the idle channel of PBSA, the field amplitudes at detectors d_1 and d_2 are given by

$$\mathbf{F}^{(+)}_{d_2} = \begin{bmatrix}\tilde{A}_H\left(F'^{(+)}_q,F'^{(+)}_r\right)\\ iF^{(+)}_{ZPF,AV}\end{bmatrix};\ \mathbf{F}^{(+)}_{d_1} = \begin{bmatrix}F^{(+)}_{ZPF,AH}\\ i\tilde{A}_V\left(F'^{(+)}_q,F'^{(+)}_r\right)\end{bmatrix}. \tag{39}$$

From **Eqs 18**, **20**, **37**, and **38**, the following four cross-correlations, involving beams $F^{(+)}_2$ and $F^{(+)}_{3A}$, are obtained:

$$\langle F^{(+)}_{2,W}F^{(+)}_{3A,Z}\rangle = (-1)^{n(W)+1}gV'\nu(0)\tilde{F}(W,Z), \tag{40}$$

where

$$\tilde{F}(W,Z) = \tilde{L}_Z\delta_{W,V} + \tilde{R}_Z\delta_{W,H}. \tag{41}$$

3.1 Analysis of the Quadruple Correlations

The quadruple correlations play a fundamental role in the calculation of fourfold detection probabilities (see **Eq. 10**). Given that the zero-point beams entering the idle channels of the PBSs placed before the detectors are uncorrelated with the signals and with each other, the understanding of the Innsbruck experiment requires a detailed analysis of the correlation $\langle F^{(+)}_{4,X}F^{(+)}_{fj,U}F^{(+)}_{fk,W}F^{(+)}_{3A,Z}\rangle$ involving the fields given in **Eqs 17**, **33**, and **36**. Using **Eq. 11** and taking into consideration that beam 4 (3) is only correlated with 1 (2), the following expression is obtained:

$$\begin{aligned}\langle F^{(+)}_{4,X}F^{(+)}_{fj,U}F^{(+)}_{fk,W}F^{(+)}_{3A,Z}\rangle = \frac{1}{2}i^{j+k+1}(-1)^j\big[&\langle F^{(+)}_{4,X}F^{(+)}_{1P,U}\rangle\langle F^{(+)}_{2,W}F^{(+)}_{3A,Z}\rangle \\ &+ (-1)^{k-j}\langle F^{(+)}_{4,X}F^{(+)}_{1P,W}\rangle\langle F^{(+)}_{2,U}F^{(+)}_{3A,Z}\rangle\big].\end{aligned} \tag{42}$$

Now, substituting **Eqs 29** and **40** into **Eq. 42**, we get

$$\begin{aligned}\langle F^{(+)}_{4,X}F^{(+)}_{fj,U}F^{(+)}_{fk,W}F^{(+)}_{3A,Z}\rangle = \frac{1}{2}i^{j+k+1}(-1)^jg^2VV'\nu^2(0)(-1)^{n(X)+n(W)+1} \\ \times\big[F(X,U)\tilde{F}(W,Z) \\ + (-1)^{k-j}(-1)^{n(U)-n(W)}F(X,W)\tilde{F}(U,Z)\big].\end{aligned} \tag{43}$$

As will be demonstrated below, a detailed analysis of **Eqs 42** and **43** provides an understanding of physics behind teleportation without the necessity of collapse as a crucial ingredient. Let us divide this study into two parts: (i) the properties of the quadruple correlations in terms of the fields at Alice's station will provide a better understanding of the indistinguishability of the four Bell states given in **Eq. 12** [11, 32]; (ii) the analysis of quadruple correlations by looking at beams $\mathbf{F}^{(+)}_4$ and $\mathbf{F}^{(+)}_3$, that is, by putting $\widehat{A}\widehat{C} = \widehat{I}$, will offer a complete comprehension of the Innsbruck experiment in terms of correlated modes.

3.1.1 Quadruple Correlations and Bell State Measurement

Let us consider the following situations, according to the values of the polarizations U and W given in **Eq. 42**:

(a) First let us focus on the case of U=W. We have the following:

$$\langle F^{(+)}_{4,X}F^{(+)}_{fj,U}F^{(+)}_{fk,U}F^{(+)}_{3A,Z}\rangle = \frac{1}{2}i^{j+k+1}(-1)^j\langle F^{(+)}_{4,X}F^{(+)}_{1P,U}\rangle\langle F^{(+)}_{2,U}F^{(+)}_{3A,Z}\rangle\left[1+(-1)^{k-j}\right]. \tag{44}$$

a.1. The above expression is equal to zero in the case of $j \neq k$, that is when the field amplitudes corresponding to the same polarization of different beams are considered. This result justifies that a double detection in detectors f_{1H} and f_{2H}, or in f_{1V} and f_{2V}, cannot be produced (see **Figure 1**).

a.2. In the case of $j = k$, **Eq. 44** leads to

$$\langle F^{(+)}_{4,X}F^{(+)}_{fj,U}F^{(+)}_{fj,U}F^{(+)}_{3A,Z}\rangle = i\langle F^{(+)}_{4,X}F^{(+)}_{1P,U}\rangle\langle F^{(+)}_{2,U}F^{(+)}_{3A,Z}\rangle. \tag{45}$$

This situation corresponds to a joint detection at any of the four detectors located in Alice's station and is related to the detection of one of the two indistinguishable states $|\phi^+\rangle_{12}$ or $|\phi^-\rangle_{12}$ [32].

b. Let us now analyze the $U \neq W$ situation; that is, the amplitudes at Alice's station have orthogonal polarization.

b.1. Let us first consider the case of j=k, where both polarizations of the same beam, namely, $F^{(+)}_{fj,H}$ and $F^{(+)}_{fj,V}$, are involved. From **Eq. 42**, we have the following:

$$\langle F^{(+)}_{4,X}F^{(+)}_{fj,U}F^{(+)}_{fj,W}F^{(+)}_{3A,Z}\rangle = \frac{i}{2}\left[\langle F^{(+)}_{4,X}F^{(+)}_{1P,U}\rangle\langle F^{(+)}_{2,W}F^{(+)}_{3A,Z}\rangle + \langle F^{(+)}_{4,X}F^{(+)}_{1P,W}\rangle \times \langle F^{(+)}_{2,U}F^{(+)}_{3A,Z}\rangle\right]. \tag{46}$$

From the above equation, the following symmetry property is derived:

$$\langle F^{(+)}_{4,X}F^{(+)}_{fj,U}F^{(+)}_{fj,W}F^{(+)}_{3A,Z}\rangle = \langle F^{(+)}_{4,X}F^{(+)}_{fj,W}F^{(+)}_{fj,U}F^{(+)}_{3A,Z}\rangle, \tag{47}$$

which implies that the correlation remains invariant under the exchange $U \leftrightarrow W$. This property is related to the detection of the state $|\psi^+\rangle_{12}$ when a joint detection is produced in f_{1H} and f_{1V} or in f_{2H} and f_{2V}.

b.2. Finally, the cases of $U \neq W$ and $j \neq k$ correspond to the situation in which the orthogonal polarization of different beams is involved. From **Eq. 42**, the corresponding quadruple correlation is

$$\langle F^{(+)}_{4,X}F^{(+)}_{fj,U}F^{(+)}_{fk,W}F^{(+)}_{3A,Z}\rangle = \frac{1}{2}(-1)^j\left[\langle F^{(+)}_{4,X}F^{(+)}_{1P,U}\rangle\langle F^{(+)}_{2,W}F^{(+)}_{3A,Z}\rangle - \langle F^{(+)}_{4,X}F^{(+)}_{1P,W}\rangle\langle F^{(+)}_{2,U}F^{(+)}_{3A,Z}\rangle\right], \tag{48}$$

and the following antisymmetric property can be easily deduced:

$$\langle F^{(+)}_{4,X}F^{(+)}_{fj,U}F^{(+)}_{fk,W}F^{(+)}_{3A,Z}\rangle = -\langle F^{(+)}_{4,X}F^{(+)}_{fj,W}F^{(+)}_{fk,U}F^{(+)}_{3A,Z}\rangle. \tag{49}$$

This sign difference under the exchange $U \leftrightarrow W$ is related to the detection of the state $|\psi^-\rangle_{12}$ when a joint detection is produced at detectors f_{1H} and f_{2V}, or in f_{1V} and f_{2H}.

3.1.2 Quadruple Correlations and Teleportation

From now on, let us focus on the situation in which no transformation is applied on beam $\mathbf{F}^{(+)}_3$, that is, $\widehat{C} = \widehat{A} = \widehat{I}$, so that $\mathbf{F}^{(+)}_{3A} = \mathbf{F}^{(+)}_3$. In Ref. 32, it is demonstrated that, for $\widehat{P} = \widehat{I}$, a joint detection in f_{1H} and f_{2V} (f_{1V} and f_{2H}) leads to the transfer of the correlation properties that characterize the singlet state $|\Psi^-\rangle_{12}$ to the beams $\mathbf{F}^{(+)}_4$ and $\mathbf{F}^{(+)}_3$, mediated by the quadruple correlations of the field, even when $\mathbf{F}^{(+)}_4$ and $\mathbf{F}^{(+)}_3$ are uncorrelated (entanglement swapping in the WRHP approach). The key point in that analysis is the sign flip in the correlations involving orthogonal polarization components of beams $\mathbf{F}^{(+)}_4$ and $\mathbf{F}^{(+)}_3$, for $j \neq k$ and $U \neq W$, under the exchange $X \leftrightarrow Z$ (see equations (33)–(36) of Ref. 32).

Let us now address the action of a linear polarizer on beam $\mathbf{F}^{(+)}_1$, so that $\mathbf{F}^{(+)}_{1P}$ represents linearly polarized light. Given that the correlation properties corresponding to the beams exiting the crystal (see **Eqs 16–19**) are rotationally invariant [29], $\mathbf{F}^{(+)}_4$ behaves like a polarized beam with orthogonal polarization to the one corresponding to $\mathbf{F}^{(+)}_{1P}$, mediated by the cross-correlation properties given in **Eq. 29**. As demonstrated below, once detection is produced at the trigger area, a joint detection in f_{1H} (f_{1V}) and f_{2V} (f_{2H}) gives rise to the teleportation of the polarization properties from $\mathbf{F}^{(+)}_{1P}$ to $\mathbf{F}^{(+)}_3$.

To demonstrate teleportation in the WRHP approach, a sign flip is required under the exchange $X \leftrightarrow Z$ in **Eq. 48**, for $\widehat{C} = \widehat{A} = \widehat{I}$. In this case, $\tilde{L}_H = \tilde{R}_V = 1$ and $\tilde{R}_H = \tilde{L}_V = 0$, so that $\tilde{F}(U, W) = 1 - \delta_{UW}$ (see **Eq. 41**). In this situation, **Eq. 43**, for $j \neq k$ and $U \neq W$, leads to

$$\langle F^{(+)}_{4,X}F^{(+)}_{fj,U}F^{(+)}_{fk,W}F^{(+)}_{3,Z}\rangle = \frac{(-1)^j}{2}(-1)^{n(X)+n(W)+1}g^2VV'\nu^2(0) \times [F(X,U)(1-\delta_{WZ}) + F(X,W)(1-\delta_{UZ})]. \tag{50}$$

Given that $U \neq W$, one of the two addends must be zero. Let us take, for instance, $Z=U$. Then, $X=W$; that is,

$$\langle F^{(+)}_{4,W}F^{(+)}_{fj,U}F^{(+)}_{fk,W}F^{(+)}_{3,U}\rangle = \frac{(-1)^{j+1}}{2}g^2VV'\nu^2(0)F(W,U). \tag{51}$$

Exchanging X and Z in **Eq. 50** and taking $U=Z$, we get

$$\langle F^{(+)}_{4,U}F^{(+)}_{fj,U}F^{(+)}_{fk,W}F^{(+)}_{3,W}\rangle = \frac{(-1)^j}{2}g^2VV'\nu^2(0)F(U,W). \tag{52}$$

Now, dividing **Eqs 51** and **52**, the searched result is found:

$$\frac{\langle F^{(+)}_{4,W}F^{(+)}_{fj,U}F^{(+)}_{fk,W}F^{(+)}_{3,U}\rangle}{\langle F^{(+)}_{4,U}F^{(+)}_{fj,U}F^{(+)}_{fk,W}F^{(+)}_{3,W}\rangle} = -\frac{F(W,U)}{F(U,W)}. \tag{53}$$

The minus sign in the above expression is independent of the concrete matrix $\widehat{P}$ representing the transformation of beam $\mathbf{F}^{(+)}_1$.

Equation 53 is only fulfilled in the cases of $U \neq W$ and $j \neq k$. In the cases of $U \neq W$ and $j = k$, there is no sign flip under the exchange $X \leftrightarrow Z$, as it can be easily demonstrated using **Eq. 43**, by putting $\tilde{F}(U, W) = 1 - \delta_{UW}$. We have the following:

$$\frac{\langle F^{(+)}_{4,W}F^{(+)}_{fj,U}F^{(+)}_{fj,W}F^{(+)}_{3,U}\rangle}{\langle F^{(+)}_{4,U}F^{(+)}_{fj,U}F^{(+)}_{fj,W}F^{(+)}_{3,W}\rangle}=\frac{F(W,U)}{F(U,W)}. \tag{54}$$

In this case, Alice must only inform Bob about her result via a classical communication channel, and Bob would modify beam $\mathbf{F}^{(+)}_3$ by applying a phase shift of p between the vertical and horizontal components of $\mathbf{F}^{(+)}_3$; that is,

$$\widehat{C}=\begin{pmatrix}1 & 0\\ 0 & -1\end{pmatrix}\Rightarrow F'^{(+)}_3=\widehat{C}\mathbf{F}^{(+)}_3=\begin{pmatrix}F'^{(+)}_q\\ F'^{(+)}_r\end{pmatrix}. \tag{55}$$

In this situation, using **Eq. 43** for $\widehat{A}=\widehat{I}$, that is, $\mathbf{F}^{(+)}_{3A}=\mathbf{F}_{I3}{}^{(+)}$, the following result was obtained:

$$\frac{\langle F^{(+)}_{4,W}F^{(+)}_{fj,U}F^{(+)}_{fj,W}F'^{(+)}_{3,U}\rangle}{\langle F^{(+)}_{4,U}F^{(+)}_{fj,U}F^{(+)}_{fj,W}F'^{(+)}_{3,W}\rangle}=-\frac{F(W,U)}{F(U,W)}. \tag{56}$$

At this point, a comment is in order. Given that Bob must wait to receive the classical information coming from Alice's station, the description of teleportation in the WRHP formalism admits a causal interpretation. Let T_{cc} be the time interval corresponding to the classical communication. If, for instance, the field amplitudes $\mathbf{F}^{(+)}_4$ and $\mathbf{F}^{(+)}_{fj}(j=1,2)$ are defined at time t_A, then the signal at Bob's station, $F'^{(+)}_3$, must be defined at time $t_B=t_A+T_{cc}$. For simplicity, let us consider an identical path length, d_{SA}, between the source and any of the detectors TH, TV, f_{jH}, and f_{jV}. And let d_{SB} be the corresponding path length between the crystal and the position where Bob applies the transformation given in **Eq. 55**. From **Eqs 7** and **20**, the following condition must be fulfilled to achieve the teleportation protocol [33]:

$$\left|T_{cc}+\frac{d_{SA}-d_{SB}}{c}\right|\leq\tau. \tag{57}$$

4 ZERO-POINT FIELD INPUTS AND BELL STATE MEASUREMENT IN THE INNSBRUCK EXPERIMENT

The role of the ZPF inputs in Bell state analysis has been investigated in previous works [31, 33, 34] by focusing on Bell state distinguishability of two photons, entangled in n dichotomic degrees of freedom, which are not mixed at the analyzer, and BSM of the one-photon polarization-momentum Bell states. The common denominator is the relationship between distinguishability of Bell states and an adequate balance between the number of amplified sets of ZPF modes entering the analyzer and the number of the sets of ZPF modes entering the idle channels located inside the analyzer.

The situation described in **Figure 1** is more involved. The information concerning the two couples of downconverted photos is carried out by the eight sets of ZPF modes entering the crystal. Two uncorrelated beams, $\mathbf{F}^{(+)}_{1P}$ and $\mathbf{F}^{(+)}_2$, are brought together at the beam splitter for Bell state analysis. Although this situation needs further consideration, the impossibility of measuring the four polarization Bell states will be addressed on the basis of the arguments set out below.

Let us analyze the interference of beams $\mathbf{F}^{(+)}_{1P}$ and $\mathbf{F}^{(+)}_2$ at the beam splitter (see **Eqs 18** and **26**) to give the exiting fields $\mathbf{F}^{(+)}_{f1}$ and $\mathbf{F}^{(+)}_{f2}$ shown in **Eq. 33**. The intensity corresponding to $\mathbf{F}^{(+)}_{fj}$ $(j=1,2)$ is

$$I_j=\mathbf{F}^{(+)}_{fj}\cdot\mathbf{F}^{(-)}_{fj}=I_{H,j}+I_{V,j}, \tag{58}$$

where $I_{X,j}$ $(X=\{H,V\})$ is the intensity corresponding to the polarization component X. By putting $F^{(+)}_{1P,X}=\left|F^{(+)}_{1P,X}\right|\exp(i\varphi_{1P,X})$ and $F^{(+)}_{2,X}=\left|F^{(+)}_{2,X}\right|\exp(i\varphi_{2,X})$, it is immediate that

$$I_{X,j}=\frac{1}{2}\left[\left|F^{(+)}_{1P,X}\right|^2+\left|F^{(+)}_{2,X}\right|^2+2(-1)^{j+1}\left|F^{(+)}_{1P,X}\right|\left|F^{(+)}_{2,X}\right|\sin\left(\varphi_{2,X}-\varphi_{1P,X}\right)\right], \tag{59}$$

where $I_{X,1}$ and $I_{X,2}$ contain an identical contribution, $(\left|F^{(+)}_{1P,X}\right|^2+\left|F^{(+)}_{2,X}\right|^2)/2$, along with an addend that represents the interference between $F^{(+)}_{1P,X}$ and $F^{(+)}_{2,X}$, with opposite values for $I_{X,1}$ and $I_{X,2}$. This result is similar to the anticorrelation after a beam splitter described in stochastic optics [28], the only difference being that, in this case, both input channels contain one photon.

By taking into consideration the zero-point beam entering PBSfj and **Eqs 34** and **35**, the intensity at the detector $f_{j,X}$ is

$$I_{fj,X}=I_{X,j}+\left|F^{(+)}_{ZPFfj,Y}\right|^2;\ Y\neq X. \tag{60}$$

Given that detection implies noise subtraction (see **Eq. 8**), the intensity above the zero-point background is

$$I_{fj,X}-\left(I_{fj,X}\right)_{vac}=I_{X,j}-\left(I_{X,j}\right)_{vac}, \tag{61}$$

so that the zero-point contribution coming from $\mathbf{F}_{ZPFf_j}$ and the pure zero-point contribution coming from the beams entering Alice's station are subtracted.

At this point, the following conjecture is applied: for an ideal detector f_{jX} $(K_{f_{jX}}=1)$, a detection is produced when a constructive interference between $F^{(+)}_{1P,X}$ and $F^{(+)}_{2,X}$ is produced; that is, $(-1)^{j+1}\sin(\varphi_{2,X}-\varphi_{1P,X})=1$, which necessarily implies a destructive interference at detector $f_{k,X}$ $(k\neq j)$. For this reason, a joint detection in detectors $f_{1,H}$ $(f_{1,V})$ and $f_{2,H}$ $(f_{2,V})$ cannot be produced. In terms of the quadruple correlations properties of the field, this result is explained in **Eq. 44**.

If detection is produced in, for example, $f_{1,H}$, it is revealed that $\varphi_{2,H}-\varphi_{1P,H}=\pi(1+4n)/2$, $n=0,1,2....$ Then, the second detection event could be produced at the same detector $f_{1,H}$ or in one of the detectors $f_{1,V}$ and $f_{2,V}$. The question that arises is how many sets of ZPF modes, coming from the idle channels located inside the analyzer, must be subtracted to complete the phase information at Alice's station? The answer is as follows: as a minimum, one of the sets of ZPF modes entering $f_{1,V}$ and $f_{2,V}$, coming from the PBSs placed at Alice's station, should be subtracted, so that the different possibilities for the second detection would be identified.

The classical information that can be obtained in the measurement entails the subtraction of a sufficient number of sets of ZPF modes entering the idle channels inside the analyzer

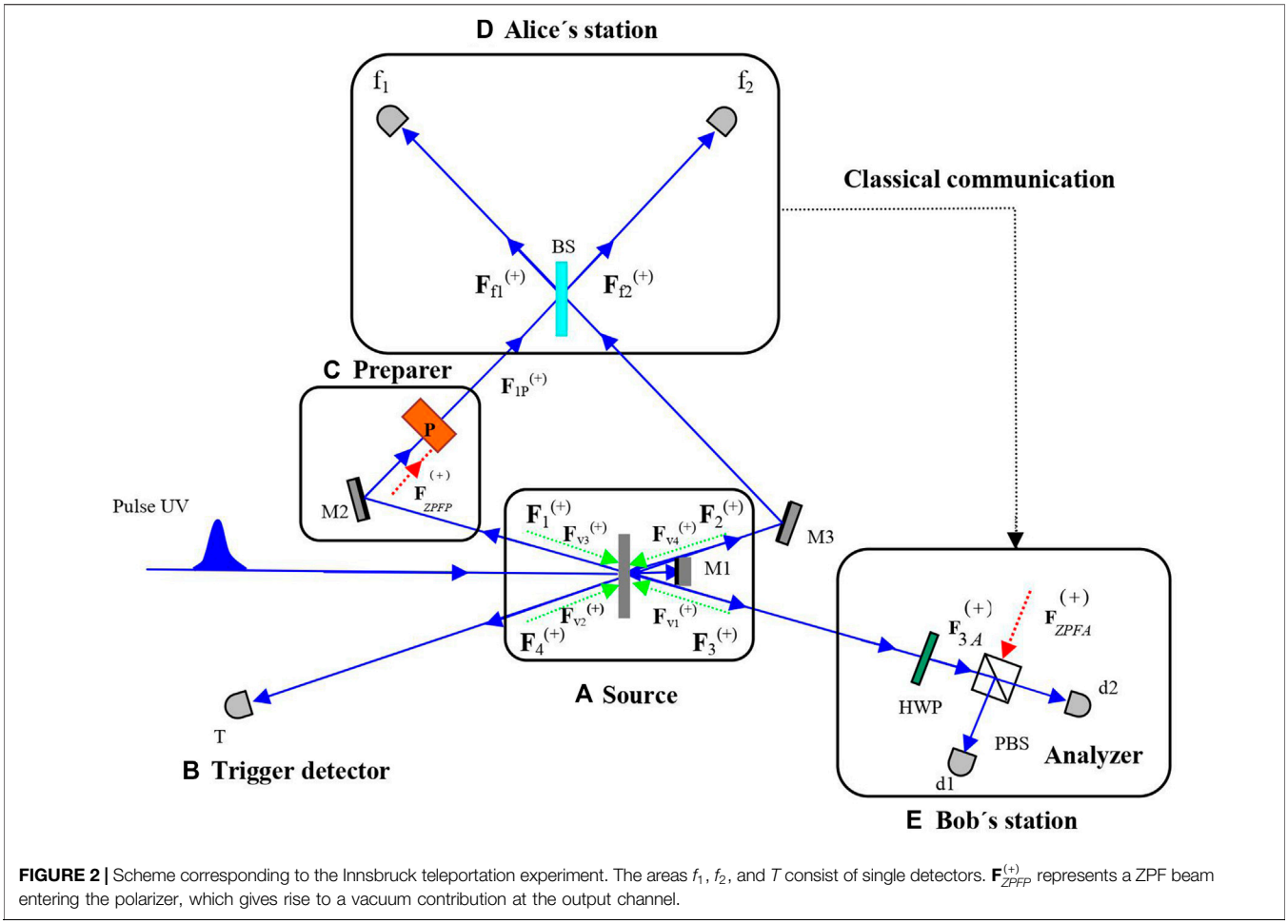

FIGURE 2 | Scheme corresponding to the Innsbruck teleportation experiment. The areas f_1, f_2, and T consist of single detectors. $\mathbf{F}^{(+)}_{ZPFP}$ represents a ZPF beam entering the polarizer, which gives rise to a vacuum contribution at the output channel.

from the number of amplified sets of modes that enter the analyzer (see **Eq. 32**). Hence, the difference $4 - 1 = 3$ gives the maximum distinguishability, which corresponds to the experimental situation.

5 FOURFOLD COINCIDENCES IN THE INNSBRUCK EXPERIMENT

Let us consider the experimental arrangement in **Figure 2** [5]. The signal $\mathbf{F}_1^{(+)}$ is sent to a polarizer P of angle $\theta = 45°$ ($\theta = -45°$) with respect to horizontal. The corresponding expression for $\mathbf{F}_{1P}^{(+)}$ is given by **Eqs 27** and **28**, where $L_H = R_V = 1/2$ and $R_H = L_V = 1/2$ ($-1/2$). In this situation, **Eq. 30** leads to $F(U, W) = F(W, U)$, so that (see **Eq. 53**)

$$\langle F^{(+)}_{4,W} F^{(+)}_{fj,U} F^{(+)}_{fk,W} F^{(+)}_{3,U} \rangle = -\langle F^{(+)}_{4,U} F^{(+)}_{fj,U} F^{(+)}_{fk,W} F^{(+)}_{3,W} \rangle. \tag{62}$$

The polarization analyzer consists of a half-wave plate (HWP) that rotates the polarization plane of $\mathbf{F}_3^{(+)}$ by an angle of 45° around the propagation direction and a PBS that transmits (reflects) horizontal (vertical) polarization. The field amplitudes at the detectors $d1$ and $d2$ are given by **Eq. 39**, where $\tilde{A}_H$ and $\tilde{A}_V$ are given by **Eqs 37** and **38**, respectively, with $\tilde{L}_H = \tilde{R}_H = \tilde{L}_V = 1/\sqrt{2}$ and $\tilde{R}_V = -1/\sqrt{2}$. In this particular setting, a fourfold detection in T, f_1, f_2, and $d2$ ($d1$) is produced for $\theta = 45°$ ($\theta = -45°$).

The quadruple correlations can be calculated by using **Eq. 43**. We get the following:

Case I ($\theta = +45°$).

$$\langle F^{(+)}_{4,V} F^{(+)}_{fj,H} F^{(+)}_{fk,V} F^{(+)}_{3A,H} \rangle = \frac{g^2 V V' \nu^2(0)}{2\sqrt{2}} (-1)^j, \tag{63}$$

$$\langle F^{(+)}_{4,H} F^{(+)}_{fj,H} F^{(+)}_{fk,V} F^{(+)}_{3A,H} \rangle = \frac{g^2 V V' \nu^2(0)}{2\sqrt{2}} i(-1)^j, \tag{64}$$

$$\langle F^{(+)}_{4,V} F^{(+)}_{fj,H} F^{(+)}_{fk,V} F^{(+)}_{3A,V} \rangle = \langle F^{(+)}_{4,H} F^{(+)}_{fj,H} F^{(+)}_{fk,V} F^{(+)}_{3A,V} \rangle = 0. \tag{65}$$

Case II ($\theta = -45°$).

$$\langle F^{(+)}_{4,H} F^{(+)}_{fj,H} F^{(+)}_{fk,V} F^{(+)}_{3A,V} \rangle = \frac{g^2 V V' \nu^2(0)}{2\sqrt{2}} (-1)^j, \tag{66}$$

$$\langle F^{(+)}_{4,V} F^{(+)}_{fj,H} F^{(+)}_{fk,V} F^{(+)}_{3A,V} \rangle = \frac{g^2 V V' \nu^2(0)}{2\sqrt{2}} i(-1)^j, \tag{67}$$

$$\langle F^{(+)}_{4,H} F^{(+)}_{fj,H} F^{(+)}_{fk,V} F^{(+)}_{3A,H} \rangle = \langle F^{(+)}_{4,V} F^{(+)}_{fj,H} F^{(+)}_{fk,V} F^{(+)}_{3A,H} \rangle = 0. \tag{68}$$

A quick look at **Eqs 63–65** shows that only the two correlations involving the horizontal component of $\mathbf{F}_{3A}^{(+)}$ are different from zero. This situation reveals the teleportation of the polarization properties of beam $\mathbf{F}_{1P}$ (polarized at +45°) to $F_{3A,H}$ (detection in $d2$). Similarly, the teleportation from $\mathbf{F}_{1P}^{(+)}$ (polarized at −45°) to $F_{3A,V}^{(+)}$ can be inferred from **Eqs 66–68**.

To obtain the fourfold detection probabilities in the WRHP formalism, **Eq. 10** must be used, with $a \equiv T$, $b \equiv f_1$, $c \equiv f_2$, and $d = d_i\,(i = 1, 2)$. Each summation has sixteen addends. Given that the vacuum contribution at $d_i\,(i = 1, 2)$ coming from $\mathbf{F}_{ZPFA}^{(+)}$ is uncorrelated with the other signals and the quadruple correlations involving the same polarization at detectors f_1 and f_2 are zero (see **Eq. 44**), the sum is reduced to four addends. By using **Eqs 63–68**, the corresponding detection probabilities are as follows:

- For $\theta = 45°$,

$$P_{T,f1,f2,d1} = 0, \tag{69}$$

$$\frac{P_{T,f1,f2,d2}}{K_T K_{f1} K_{f2} K_{d2}} = \frac{g^4 |V|^4 |\nu(0)|^4}{8}. \tag{70}$$

- For $\theta = -45°$,

$$\frac{P_{T,f1,f2,d1}}{K_T K_{f1} K_{f2} K_{d1}} = \frac{g^4 |V|^4 |\nu(0)|^4}{8}, \tag{71}$$

$$P_{T,f1,f2,d2} = 0. \tag{72}$$

6 DISCUSSION AND CONCLUSION

In this article, it has been shown that the quintessential experiment on quantum teleportation, the Innsbruck experiment, can be understood without the consideration of collapse and entanglement as necessary ingredients. Compared to the classical theoretical treatment of this experiment, the consideration of the ZPF as a real field adds new physical insights that were not previously discovered. First of all, the quantum information is carried out by eight sets of ZPF modes entering the crystal, so that the physical meaning of entanglement can be found in the correlations that characterize vacuum amplitudes distributed in the emitted signals. Second, the projection postulate is closely related to the subtraction of the zero-point intensity at the detectors, in such a way that the vacuum inputs located at the idle channels inside the analyzer limit the distinguishability at Alice's station. In this sense, the WRHP formalism provides a more complete description than the one provided by the standard particle-like image in terms of photons. This is in consonance with recent approaches to the quantum jumps, where a deeper insight into the projection postulate is obtained [36].

In the WRHP approach, the teleportation of the prepared state once the trigger detector fires, under the condition of a joint detection in areas $f1$ and $f2$, is discovered by means of the quadruple correlation properties of the field and its propagation throughout the setup. The antisymmetry requirements, fulfilled in **Eqs 49** and **62**, constitute the mathematical properties leading to teleportation in the Innsbruck experiment [5]. In a general transformation represented by the matrix $\widehat{P}$, teleportation is explained based on **Eqs 49** and **53**. Moreover, **Eq. 53** is required for understanding the possibility of reproducing the prepared state, in the case of a joint detection at separated detectors in areas $f1$ or $f2$ (see **Eq. 56**). In this sense, the consideration of the classical communication time in the quadruple correlation (see **Eq. 57**) reinforces the idea of a causal interpretation of teleportation.

The role of the zero-point intensity as a threshold for detection has been applied elsewhere to Bell state analysis [31, 33, 34]. In this article, new advances have been made in this area. The maximum Bell state distinguishability of two photons that are mixed at a beam splitter has been treated in this work for the first time, in the special situation of two uncorrelated beams entering the analyzer, of the four two-by-two correlated photons emitted by the source in the Innsbruck experiment. The possibility of measuring only three classes of the four polarization Bell states is based on the subtraction between the four sets of amplified modes entering the analyzer and one of the four sets of ZPF modes that enter the idle channels inside Alice's station. The role of the phases of the signals entering the analyzer as hidden variables and the consideration of the ZPF entering the vacuum channels of the PBSs as a source of noise that limits the capacity for distinguishing Bell states provide new insights that require further consideration.

At this point, some comments are in order. The statement that the information about teleportation is carried out by field amplitudes and supported by the quadruple correlations sharply contrasts with the standard description in the Hilbert space. The collapse of the four-photon state mediated by detection at the trigger detection area leads to a three-particle state (see **Eq. 12**) that constitutes the starting point of the teleportation protocol [11]. The projection of this vector via BSM at Alice's station results in a nonlocal change of the physical properties of light at Bob's side, which is identified throughout the classical communication between Alice and Bob. This conundrum of the quantum theory, which conjugates nonlocality and the superposition principle, can be solved using the WRHP formalism. On the one hand, the odd-order correlations are identically zero for Gaussian processes, so that no information about teleportation can be extracted by looking at the "triple" correlation properties of the fields $\mathbf{F}_{1P}^{(+)}$, $\mathbf{F}_{2}^{(+)}$, and $\mathbf{F}_{3}^{(+)}$. Furthermore, the Wigner distribution of the four-photon state is positive, so that a picture in terms of stochastic processes is plausible. In contrast, the corresponding one to the state given in **Eq. 12** is not positive-definite. In this sense, we emphasize that the physical properties of photon 1 are inherently linked to photon 4 through the cross-correlation properties of the light field. Hence, the consideration of the prepared state as a single-photon state is an oversimplification that hides the essential nature of teleportation, that is, the possibility of transferring the physical properties from one location to another, mediated by the zero-point fluctuations of the electromagnetic field.

The WRHP formalism bridges the gap between quantum optics and stochastic optics [37] by considering the vacuum field as a real stochastic field. Moreover, one of the main advantages of using this approach is the possibility of investigating the role of ZPF amplitudes as hidden variables to obtain information regarding the internal mechanism leading to teleportation. This analysis will be further developed in future studies.

DATA AVAILABILITY STATEMENT

The original contributions presented in the study are included in the article/Supplementary Material; further inquiries can be directed to the corresponding author.

AUTHOR CONTRIBUTIONS

AC has conducted the whole research in the article, the organization of the manuscript, calculations, and the main ideas in the text. SG has contributed to the calculations, figures, and text elaboration, along with useful discussions concerning the essential ideas. JP has contributed to the discussions of the main ideas related to this research.

ACKNOWLEDGMENTS

The authors thank R. Risco-Delgado for his interest, comments, and careful reading of the manuscript.

REFERENCES

1. Bennett CH, Brassard G, Crépeau C, Jozsa R, Peres A, Wootters WK. Teleporting an unknown quantum state via dual classical and Einstein-Podolsky-Rosen channels. *Phys Rev Lett* (1993) 70:1895–9. doi:10.1103/PhysRevLett.70.1895
2. Llewellyn DM, Ding Y, Faruque II, Paesani S, Bacco D, Santagati R, et al. Chip-to-chip quantum teleportation and multi-photon entanglement in silicon. *Nat Phys* (2020) 16:148–53. doi:10.1038/s41567-019-0727-x
3. Luo Y-H, Zhong H-S, Erhard M, Wang X-L, Peng L-C, Krenn M, et al. Quantum Teleportation in high dimensions. *Phys Rev Lett* (2019) 123:070505. doi:10.1103/PhysRevLett.123.070505
4. Einstein A, Podolsky B, Rosen N. Can quantum-mechanical description of physical reality be considered complete? *Phys Rev* (1935) 47:777. doi:10.1103/PhysRev.47.777
5. Bouwmeester D, Pan J-W, Mattle K, Eibl M, Weinfurter H, Zeilinger A. Experimental quantum teleportation. *Nature* (1997) 390:575–9. doi:10.1038/37539
6. Boschi D, Branca S, De Martini F, Hardy L, Popescu S. Experimental realization of teleporting an unknown pure quantum state via dual classical and Einstein-Podolsky-Rosen channels. *Phys Rev Lett* (1998) 80:1121–5. doi:10.1103/PhysRevLett.80.1121
7. De Martini F. Teleportation: who was first? *Phys World* (1998) 11:23–4. doi:10.1088/2058-7058/11/3/21
8. Bouwmeester D, Pan J-W, Weinfurter H, Zeilinger A. High-fidelity teleportation of independent qubits. *J Mod Optic* (2000) 47:279–89. doi:10.1080/09500340008244042
9. Yurke B, Stoler D. Einstein-Podolsky-Rosen effects from independent particle sources. *Phys Rev Lett* (1992) 68:1251–4. doi:10.1103/PhysRevLett.68.1251
10. Pan J-W, Bouwmeester D, Weinfurter H, Zeilinger A. Experimental entanglement swapping: entangling photons that never interacted. *Phys Rev Lett* (1998) 80:3891. doi:10.1103/PhysRevLett.80.3891
11. Mattle K, Weinfurter H, Kwait PG, Zeilinger A. Dense coding in experimental quantum communication. *Phys Rev Lett* (1996) 76:4656–9. doi:10.1103/PhysRevLett.76.4656
12. Braunstein SL, Kimble HJ. A posterior teleportation. *Nature* (1998) 394:840–41. doi:10.1038/29674
13. Bouwmeester D, Pan J-W, Daniell M, Weinfurter H, Zukowski M, Zeilinger A. Reply: a posterior teleportation. *Nature* (1998) 394:841. doi:10.1038/29678
14. Kok P, Braunstein SL. Postselected versus nonpostselected quantum teleportation using parametric down-conversion. *Phys Rev* (2000) 61:042304. doi:10.1103/PhysRevA.61.042304
15. Popescu S. An optical method for teleportation (1995) arxiv:9501020.
16. Michler M, Risco-Delgado R, Weinfurter H. Remote state preparation. *Technical. Digest. EQEC* (1998) 1:99. doi:10.1109/EQEC.1998.714868
17. Casado A, Marshall TW, Santos E. Parametric downconversion experiments in the Wigner representation. *J Opt Soc Am B* (1997) 14:494–502. doi:10.1364/JOSAB.14.000494
18. Casado A, Fernández-Rueda A, Marshall TW, Risco-Delgado R, Santos E. Fourth-order interference in the Wigner representation for parametric down-conversion experiments. *Phys Rev* (1997) 55:3879–90. doi:10.1103/PhysRevA.55.3879
19. Casado A, Marshall TW, Santos E. Type-II parametric downconversion in the Wigner function formalism: entanglement and Bell's inequalities. *J Opt Soc Am B* (1998) 15:1572–7. doi:10.1364/JOSAB.15.001572
20. Casado A, Fernández-Rueda A, Marshall TW, Risco-Delgado R, Santos E. Dispersion cancellation and quantum eraser experiments analyzed in the Wigner function formalism. *Phys Rev* (1997) 56:2477–80. doi:10.1103/PhysRevA.56.2477
21. Casado A, Fernández-Rueda A, Marshall TW, Martínez J, Risco-Delgado R, Santos E. Dependence on crystal parameters of the correlation time between signal and idler beams in parametric down conversion calculated in the Wigner representation. *Eur Phys J D* (2000) 11:465–72. doi:10.1007/s100530070074
22. Casado A, Marshall TW, Risco-Delgado R. Spectrum of the parametric down converted radiation calculated in the Wigner function formalism. *Eur Phys J D* (2001) 13:109–19. doi:10.1007/s100530170292
23. Dechoum K, Marshall TW, Santos E. Parametric down and up conversion in the Wigner representation of quantum optics. *J Mod Optic* (2000) 47:1273–87. doi:10.1080/095003400147575
24. Casado A, Risco-Delgado R, Santos E. Local realistic theory for PDC experiments based on the Wigner formalism. *Z Naturforsch* (2001) 56A:178–81. doi:10.1515/zna-2001-0129
25. Casado A, Marshall TW, Risco-Delgado R, Santos E. A Local hidden variables model for experiments involving photon pairs produced in parametric down conversion (2002) arXiv:quant-ph/0202097v1.
26. Santos E. Local realistic interpretation of entangled photon pairs in the Weyl-Wigner formalism (2020) arXiv:1908.03924v4 [quant-ph].
27. Santos E. Can quantum vacuum fluctuations be considered real? (2002) arxiv:0206161.
28. Santos E. Photons are fluctuations of a random (zeropoint) radiation filling the whole space. *Proc SPIE* (2005) 5866:36–7. doi:10.1117/12.619611
29. Casado A, Guerra S, Plácido J. Wigner representation for experiments on quantum cryptography using two-photon polarization entanglement produced in parametric down-conversion. *J Phys B Atom Mol Opt Phys* (2008) 41:045501. doi:10.1088/0953-4075/41/4/045501
30. Casado A, Guerra S, Plácido J. Partial Bell-state analysis with parametric down conversion in the Wigner function formalism. *J Adv Math Phys* (2010) 2010:501521. doi:10.1155/2010/501521
31. Casado A, Guerra S, Plácido J. Wigner representation for polarization-momentum hyperentanglement generated in parametric down-conversion,

and its application to complete Bell-state measurement. *Eur Phys J D* (2014) 68: 338. doi:10.1140/epjd/e2014-50368-y

32. Casado A, Guerra S, Plácido J. Wigner representation for entanglement swapping using parametric down conversion: the role of vacuum fluctuations in teleportation. *J Mod Optic* (2015) 62:377–86. doi:10.1080/09500340.2014.983571
33. Casado A, Guerra S, Plácido J. Rome teleportation experiment analysed in the Wigner representation: the role of the zeropoint fluctuations in complete one-photon polarization-momentum Bell-state analysis. *J Mod Optic* (2018) 65:1960–74. doi:10.1080/09500340.2018.1478009
34. Casado A, Guerra S, Plácido J. From stochastic optics to the Wigner formalism: the role of the vacuum field in optical quantum communication experiments. *Atoms* (2019) 7:76. doi:10.3390/atoms7030076
35. Clauser JF, Horne M. Experimental consequences of objective local theories. *Phys Rev D.* (1974) 10:526–35. doi:10.1103/PhysRevD.10.526
36. Minev ZK, Mundhada SO, Shankar S, Reinhold P, Gutiérrez-Jáuregui R, Schoelkopf RJ, et al. To catch and reverse a quantum jump mid-flight. *Nature* (2019) 570:200–204. doi:10.1038/s41586-019-1287-z
37. Marshall TW, Santos E. Stochastic optics: a reaffirmation of the wave nature of light. *Found Phys* (1988) 18:185–223. doi:10.1007/BF01882931

Conflict of Interest: The authors declare that the research was conducted in the absence of any commercial or financial relationships that could be construed as a potential conflict of interest.

frontiers in Physics

ORIGINAL RESEARCH
published: 12 April 2021
doi: 10.3389/fphy.2020.580869

Probability Calculations Within Stochastic Electrodynamics

Daniel C. Cole *

Department of Mechanical Engineering, Boston University, Boston, MA, United States

Several stochastic situations in stochastic electrodynamics (SED) are analytically calculated from first principles. These situations include probability density functions, as well as correlation functions at multiple points of time and space, for the zero-point (ZP) electromagnetic fields, as well as for ZP plus Planckian (ZPP) electromagnetic fields. More lengthy analytical calculations are indicated, using similar methods, for the simple harmonic electric dipole oscillator bathed in ZP as well as ZPP electromagnetic fields. The method presented here makes an interesting contrast to Feynman's path integral approach in quantum electrodynamics (QED). The present SED approach directly entails probabilities, while the QED approach involves summing weighted paths for the wave function.

Keywords: stochastic electrodynamics, probabilistic, classical, multivariate, probability density

OPEN ACCESS

Edited by:
Andrea Valdés-Hernández, National Autonomous University of Mexico, Mexico

Reviewed by:
Kaled Dechoum, Fluminense Federal University, Brazil
Emilio Santos, University of Cantabria, Spain

***Correspondence:**
Daniel C. Cole
dccole@bu.edu

Specialty section:
This article was submitted to Mathematical and Statistical Physics, a section of the journal Frontiers in Physics

Received: *07 July 2020*
Accepted: *27 August 2020*
Published: *12 April 2021*

Citation:
Cole DC (2021) Probability Calculations Within Stochastic Electrodynamics. Front. Phys. 8:580869. doi: 10.3389/fphy.2020.580869

1 INTRODUCTION

This article is largely intended for providing a new calculational method for deducing the stochastic properties of electromagnetic radiation and classical charged particles in the theory called stochastic electrodynamics (SED). This new calculational method to be described here might well be useful in some contexts outside of SED; nevertheless, the main focus here will indeed be SED.

Summarizing quickly, SED is a classical physical theory involving classical charged particles and classical electromagnetic (E&M) radiation, where Maxwell's classical, microscopic electromagnetic equations hold. The motion of point charges is assumed to be described by the relativistic Lorentz–Dirac classical equation of motion. What is particularly interesting about SED is that the basic assumptions of SED are few, they are not complicated, and their basis makes clear physical sense. A number of physicists over the years, including the author, have felt that SED might not only be a substitute for the part of quantum theory (QT) consisting of quantum mechanics (QM) and quantum electrodynamics (QED), but much more so, provide the basis to derive or deduce QM and QED, or, at the very least, to provide a deeper physical understanding of QM and QED.

To emphasize this point, many well-known systems traditionally analyzed in QM, such as the simple harmonic oscillator (SHO) in either one, two, or three dimensions, fluctuating electric dipole SHOs, including interacting systems of such electric dipoles, plus van der Waals forces, Casimir forces, the thermal-like behavior of electrodynamic systems uniformly accelerated through the "vacuum," diamagnetism, aspects of hydrogen, and blackbody radiation dynamics [1, 2], have all been analyzed within the classical theory of SED. This range of "QM" phenomena, that has always been considered outside the domain of classical physics, became understandable in a coherent, consistent, and logical manner in SED, without needing to draw on any extraneous "physical or phenomenological" concepts. Moreover, not only did these classical physics, calculations with ZP or ZPP classical E&M radiation provide close connections with QED results, in some cases, the SED results also preceded QED calculations, such as pioneered by Boyer in the case of uniformly electrodynamic system through the "vacuum" [3–7], or even in the case of Casimir and van der

Waals forces, where the physics in SED seems clearer, and changing from $T = 0$ calculations to $T > 0$ calculations is much simpler in the case of SED than QED [8].

Recently, Boyer made a strong argument [9] that SED is the best classical physical theory for describing physical phenomena, as it contains a range of QM and QED predictions, in addition to the expected classical physics. Moreover, these QT predictions by SED are remarkable, not just in their prediction *via* classical physics, but also that the supposed faults of classical physics, such as the collapse of Rutherford's orbital model of the atom, or no explanation for van der Waals or Casimir forces, are "repaired" by taking into account the full interaction between classical charges and classical electromagnetic radiation.

Some of the key original articles on SED were in the 1960s, by Marshall [10, 11] and Boyer [12, 13]. As expected for a classical physical theory, SED recognizes that accelerated and de-accelerated charges create E&M radiation; in turn, E&M radiation effects the motion of charged particles *via* the Lorentz force term. However, what is significantly different for SED from classical physics as typically taught, is the recognition that if classical charged particles can exist in a thermodynamic equilibrium state, such as for atoms and molecules, then this can only be done in a stochastic equilibrium between charges and E&M fields. The E&M fields fluctuate, as expected in blackbody radiation, but the charges also fluctuate in position, since the two entities are connected together. Fluctuations of one result in fluctuations of the other. In other words, the dilemma that Rutherford immediately recognized after proposing his "miniature solar system" model of the atom, with electrons orbiting the nucleus, is addressed in SED. If only classical charges are present, then Rutherford's model will result in E&M energy radiated off as the electrons orbit, and the orbits will collapse. We now know that the time for decay, for a classical hydrogen atom, is about 1.3×10^{-11} s, starting from the Bohr radius [14]. Moreover, if the charges were attempted to be held in some static configuration (no orbiting), we know from Earnshaw's theorem that a stable stationary equilibrium configuration is also not possible [15]. Thus, classical E&M radiation and classical charged particles must both be present if there is any hope for equilibrium, with of course radiation effecting the particles, and particles creating radiation, and a stochastic balance resulting.

What the early SED researchers recognized is that to obtain thermodynamic equilibrium between radiation and charges, there must be special stochastic properties of the radiation, and consequently also of the charges. They deduced that these interesting relationships must logically be deductible at all temperatures, indeed, even at $T = 0$, which gave rise to the notion of classical electromagnetic zero-point (ZP) radiation.

Several good reviews exist on all of this work: Ref. [16] provides an excellent history on the development of SED. Other reviews of interest are [9, 17–19]. These reviews discuss the deductions made by researchers about the properties of classical electromagnetic ZP radiation, such as Lorentz invariant [12, 20], and that the fundamental definition of $T = 0$ must be obeyed by ZP radiation [1, 21, 22]. Some of the more recent work, such as on hydrogen in SED, is briefly outlined in Ref. [23].

The outline of this article is as follows. In **Sections 2.1** and **2.2**, certain stochastic properties will be calculated for the E&M radiation fields in SED, first using a new technique that was covered to a lesser extent in Section 3 of Ref. [23]. Some comparisons of this approach will also be made to earlier n-point correlation function approaches by others, particularly by Boyer [24], as well as Marshall [20], the results of which have been used extensively, and extended, by others, including this author. **Section 2** has several subsections, including **Section 2.3**, which provides checks on the results derived in **Section 2.2**. **Section 2.4** relates results in **Section 2.2** to the multivariate normal distribution, and why the latter applies to the stochastic fields described here.

Section 3 ends with some concluding remarks. In particular, some brief comments are first made about extending this calculational method to the electric dipole oscillator immersed in these stochastic fields, meaning either ZP or ZPP fields as treated in SED. The electric dipole oscillator, one of the first systems analyzed in SED, is discussed in terms of why this system "easily" lends itself to the stochastic method discussed here. The calculations are long with this method, but can be carried out. In contrast, a system like the classical hydrogen atom is far more difficult and has not yet been shown to be tractable. The point is made that a similar situation existed for the Feynman path integral approach.

2 PROBABILITY DENSITY FUNCTION CALCULATIONS FOR ELECTRIC AND MAGNETIC RADIATION FIELDS

2.1 Introduction to the Calculational Method

We will begin the calculations in this article by determining the probability density functions for various stochastic properties of the classical electromagnetic ZP radiation fields in SED, as well as the zero-point plus Planckian (ZPP) fields. Actually, both situations can be treated at once, with the temperature T in the expressions allowing the distinction, with $0 \leq T$.

The present **Section 2** will address how to determine the probabilistic functions of the E&M stochastic fields in SED. The subsequent section, 3, will then turn to calculating the stochastic properties of a classical electric dipole SHO within ZPP radiation. The main difference between what will be done in this article and what is typically done in SED is that normally the mean, the variance, and correlation quantities of the stochastic E&M fields, and the position and momentum of the oscillator's fluctuating particle are directly calculated. These quantities are sometimes, although not always, calculated at different times and positions in SED. For some problems, the correlations at different times and positions are critical, although this is not the case for many other types of SED problems. One place where clearly the different times and positions were essential in the system analysis, had to do with the uniform acceleration of electrodynamic systems through the vacuum, such as in Refs. [3–7].

Of course, given any probability distribution or density function associated with a single random variable X, one can calculate an infinite number of moments, such as $\langle (X - \langle X \rangle)^N \rangle = \int_{-\infty}^{\infty} dx P(x) (x - \langle x \rangle)^N$, for $N = 1, 2, 3, \ldots$, where the angled brackets mean "expectation value," and where $P(x)$ is the probability density function associated with X. However, for a Gaussian probability density distribution of a single random variable, there are only two defining parameters, namely, the mean, or $\mu \equiv \langle X \rangle$, and the variance, $\sigma^2 \equiv \langle (X - \langle X \rangle)^2 \rangle$. All other moments $\langle (X - \langle X \rangle)^N \rangle$, for $N = 1, 2, 3, \ldots$, can be expressed in terms of just μ and σ.

For a multivariate Gaussian distribution, which actually defines the classical ZP and ZPP E&M radiation, each frequency and polarization component of the radiation is assumed to be governed by an independent Gaussian process. Thus, the situation is more complicated. Nevertheless, the previous paragraph helps to identify the difference between past work in SED involving stochastic process calculations, which largely dealt with moment calculations like $\langle (X - \langle X \rangle)^N \rangle$, whereas here we will directly calculate quantities like $P(x)$.

Early on in SED, the "two-point correlation functions" of the stochastic fields, at different times and positions, were calculated in detail, and were used to deduce "n point" correlation functions, again where different times and spatial positions were included when calculating these correlation functions. An excellent source for investigating deeply these "n point" correlation functions was by Boyer in Ref. [24], where not only were the SED correlation functions determined, but also compared to the expectation values of the corresponding QED functions, involving annihilation and creation operators. The quantities were shown to be in agreement, provided the quantum operators were symmetrized. In contrast, in this article, the probabilities of these quantities will be directly calculated, rather than calculating individual moments of fields and oscillator coordinates. This same approach can also be used in a similar manner for the probability distribution for linear nonrelativistic electric dipole SHOs, although the calculations become even longer than for the fields. Brief comments will be made on this topic in **Section 3**.

As often done in SED, where the ZP and ZPP fields are critically important to the final physics results, the radiation fields at temperature $T \geq 0$ are characterized by T of course, but must also be thought of as having a rapid variation in space and time. This aspect was tackled by Planck using classical physics, covered in the first half of his famous book [25], "The Theory of Heat Radiation," which is still basically represented by the SED theory. The second half of his book, however, introduces quantum concepts involving energy and frequency related to what QT now treats as photons. SED certainly avoids this direction, but the first part of Planck's work, which was also used later by Einstein and Hopf [26, 27], still applies to the beginnings of SED. Indeed, the work by Marshall and Boyer in SED has parallels to this early work by Planck and Einstein and Hopf, with the important caveat that equilibrium radiation must exist at $T = 0$ [12, 13], and the recognition that ZP radiation is key to getting the stochastic thermodynamic behavior of classical charged particles and classical E&M correct.

To adequately describe the "radiation dynamics" in SED, usually a large region of space is considered, where "large" means compared to the size that any charged particles representing atomic systems are encompassing or traversing. Thus, in the same vein as Planck, Einstein, and Hopf, SED typically considers a rectangular parallelepiped region in space, with dimensions L_x, L_y, and L_z, along the x, y, and z axes. Other shapes can in principle be used, but a rectangular parallelepiped offers mathematical simplicity, without effecting the physical description if the volume is large. The radiation fields representing ZP or ZPP conditions are typically expressed as an infinite sum of plane waves, with periodic boundary conditions (bcs) imposed. The imposition of periodic bcs makes use of the Fourier analysis process for representing the fields, such that if the region is large enough, then the imposition of periodicity does not affect the physical analysis, but does simplify the subsequent mathematical analysis.

Thus, the following expressions for the "free" electric $\mathbf{E}(\mathbf{x}, t)$ and magnetic $\mathbf{B}(\mathbf{x}, t)$ radiation fields in this large parallelepiped volume can be written as the following sum of plane waves [16]:

$$\mathbf{E}(\mathbf{x}, t) = \frac{1}{\left(L_x L_y L_z\right)^{1/2}} \sum_{n_x, n_y, n_z = -\infty}^{\infty} \sum_{\lambda = 1,2} \widehat{\varepsilon}_{\mathbf{k_n}, \lambda} \left[A_{\mathbf{k_n}, \lambda} \cos(\mathbf{k_n} \cdot \mathbf{x} - \omega_{\mathbf{n}} t) + B_{\mathbf{k_n}, \lambda} \sin(\mathbf{k_n} \cdot \mathbf{x} - \omega_{\mathbf{n}} t) \right], \tag{1}$$

$$\mathbf{B}(\mathbf{x}, t) = \frac{1}{\left(L_x L_y L_z\right)^{1/2}} \sum_{n_x, n_y, n_z = -\infty}^{\infty} \sum_{\lambda = 1,2} \left(\widehat{k}_{\mathbf{n}} \times \widehat{\varepsilon}_{\mathbf{k_n}, \lambda} \right) \left[A_{\mathbf{k_n}, \lambda} \cos(\mathbf{k_n} \cdot \mathbf{x} - \omega_{\mathbf{n}} t) + B_{\mathbf{k_n}, \lambda} \sin(\mathbf{k_n} \cdot \mathbf{x} - \omega_{\mathbf{n}} t) \right], \tag{2}$$

where

$$\mathbf{k_n} = \frac{2\pi n_x}{L_x} \widehat{\mathbf{x}} + \frac{2\pi n_y}{L_y} \widehat{\mathbf{y}} + \frac{2\pi n_z}{L_z} \widehat{\mathbf{z}}, \tag{3}$$

and n_x, n_y, and n_z are integers, and $\omega_{\mathbf{n}} = c|\mathbf{k_n}|$, $\mathbf{k_n} \cdot \widehat{\varepsilon}_{\mathbf{k_n}, \lambda} = \mathbf{k_n} \cdot \widehat{\varepsilon}_{\mathbf{k_n}, \lambda'} = 0$, and $\widehat{\varepsilon}_{\mathbf{k_n}, \lambda} \cdot \widehat{\varepsilon}_{\mathbf{k_n}, \lambda'} = 0$ for $\lambda \neq \lambda'$, where λ and λ' indicate the linear polarization direction. Specifically, λ might be represented by the values 1 or 2, and the same for λ'. Also, $\widehat{\mathbf{k}}_{\mathbf{n}} = \mathbf{k_n}/|\mathbf{k_n}|$. **Equations 1** and **2** satisfy the wave equations of $\nabla^2 \mathbf{E}(\mathbf{x}, t) = \frac{1}{c^2} \frac{\partial^2}{\partial t^2} \mathbf{E}(\mathbf{x}, t)$ and $\nabla^2 \mathbf{B}(\mathbf{x}, t) = \frac{1}{c^2} \frac{\partial^2}{\partial t^2} \mathbf{B}(\mathbf{x}, t)$, which can be deduced from Maxwell's equations for free space (charge density and current charge density both equal to zero). Moreover, the presence of $\widehat{\varepsilon}_{\mathbf{k_n}, \lambda}$ and $(\widehat{\mathbf{k}}_{\mathbf{n}} \times \widehat{\boldsymbol{\varepsilon}}_{\mathbf{k_n}, \lambda})$ in **Eqs. 1**, **2** respectively, and the cited relationships of $\mathbf{k_n} \cdot \widehat{\varepsilon}_{\mathbf{k_n}, \lambda} = \mathbf{k_n} \cdot \widehat{\varepsilon}_{\mathbf{k_n}, \lambda'} = 0$, and $\widehat{\varepsilon}_{\mathbf{k_n}, \lambda} \cdot \widehat{\varepsilon}_{\mathbf{k_n}, \lambda'} = 0$ for $\lambda \neq \lambda'$, provide the other needed relationships for satisfying the four Maxwell's equations for free fields, such as Faraday's law of $\nabla \times \mathbf{E} = -\frac{\partial}{c \partial t} \mathbf{B}$.

Following more or less the lead of Planck's first half of Ref. [25], the above radiation fields represent the stochastic fluctuations of thermal radiation, for $0 \leq T$ (i.e., including $T = 0$), with the following assumptions. The coefficients of the expressions for $\mathbf{E}(\mathbf{x}, t)$ and $\mathbf{B}(\mathbf{x}, t)$ in **Eqs. 1** and **2**, namely, $A_{\mathbf{k_n}, \lambda}$ and $B_{\mathbf{k_n}, \lambda}$, were assumed to be randomly distributed in the following way initially, but once fixed, they stay fixed in all physical analysis, such as in the interaction of charged oscillators and radiation, as in simulations of [28–31]. In the case of simulations, the physical

picture is conceptually fairly simple, although of course computationally intensive. Each time a charged particle system, such as an "oscillator or atom," undergoes its motion due to an atomic binding force, and due to the radiation fields in **Eqs. 1** and **2**, the subsequent scenario of particle motion and radiation fluctuations would represent a real situation of say, the classical atom inside a large cavity kept at temperature T. However, "redoing" the simulation or "experiment" would be carried out with a different set of $A_{\mathbf{k_n},\lambda}$ and $B_{\mathbf{k_n},\lambda}$ coefficients, to represent a similar but different initial set of conditions.

Each time a similar "experiment" of radiation and charges is considered, the experiment is treated as another member of the ensemble of similar experiments. This part of SED coincides with the thoughts in the first half of Planck's major treatise [25] and later by Einstein's and Hopf [26, 27]. Related SED discussions can be found in Refs. [16, 17]. However, most of the following relationships make physical sense without even referring to these references.

Specifically, the expectation value of these coefficients characterizing the ensemble of ZPP radiation fields is of course zero:

$$\langle A_{\mathbf{k_n},\lambda}\rangle = \langle B_{\mathbf{k_n},\lambda}\rangle = 0. \tag{4}$$

Moreover, the "A and B coefficients" are considered to be both independent and uncorrelated random variables in this ensemble, so

$$\langle A_{\mathbf{k_n},\lambda} B_{\mathbf{k_{n'}},\lambda'}\rangle = 0, \tag{5}$$

as are the "A coefficients" with different indices, and the same for the "B coefficients":

$$\langle A_{\mathbf{k_n},\lambda} A_{\mathbf{k_{n'}},\lambda'}\rangle = \langle B_{\mathbf{k_n},\lambda} B_{\mathbf{k_{n'}},\lambda'}\rangle = 0, \quad \text{if } \mathbf{n}\neq\mathbf{n}' \text{ or } \lambda\neq\lambda'. \tag{6}$$

However, for two "A coefficients" with the same indices, and similarly for the "B coefficients," then of course, these quantities cannot be zero, but are assumed to be functions of the frequency of the radiation and of the temperature T:

$$\langle A_{\mathbf{k_n},\lambda} A_{\mathbf{k_n},\lambda}\rangle = \langle B_{\mathbf{k_n},\lambda} B_{\mathbf{k_n},\lambda}\rangle = [\sigma(\omega_{\mathbf{n}}, T)]^2. \tag{7}$$

Although **Eqs. 4**–**7** are indeed assumed in SED, the more general relationship that includes all these relationships, plus more, is that the $A's$ and $B's$ coefficients are assumed to be independent random variables, with zero mean as in **Eq. 4**, with variance $[\sigma(\omega_{\mathbf{n}}, T)]^2$, and with probability density distributions characterizing the ensemble of possible radiation situations characterizing thermal radiation at temperature T, for $0 \le T$, as being Gaussian distributions. Specifically:

$$P(A_{\mathbf{k_n},\lambda}) = \frac{1}{\sqrt{2\pi[\sigma(\omega_{\mathbf{n}}, T)]^2}} \exp\left\{-\frac{1}{2}\left[\frac{A_{\mathbf{k_n},\lambda}}{\sigma(\omega_{\mathbf{n}}, T)}\right]^2\right\}, \tag{8}$$

with the same also holding for $P(B_{\mathbf{k_n},\lambda})$. From these independent Gaussian distributions, **Eqs. 4**–**7** also follow.

Initial understanding of the importance of the statistical properties of ZP and ZPP in SED, and how these properties relate to the resulting fluctuating and equilibrium properties of charged particles interacting with this radiation, focused a fair bit on $[\sigma(\omega_{\mathbf{n}}, T)]^2$ [16]. The Lorentz invariant property of ZP found independently by Marshall [20] and Boyer [12], is due to the functional form connected to this function. Similarly, the thermodynamic connection of the meaning of $T = 0$ to this radiation and interacting particles is also tied to $[\sigma(\omega_{\mathbf{n}}, T)]^2$ [1, 21, 22]. Other work by Boyer deduced additional symmetry properties of the required classical E&M nature of ZP and ZPP radiation that involved scaling and conformal invariances [32].

All of these analyses have led to the following in SED for the ZPP spectrum:

$$[\sigma(\omega_{\mathbf{n}}, T)]^2 = 2\pi\hbar\omega_{\mathbf{n}} + \frac{4\pi\hbar\omega_{\mathbf{n}}}{\exp\left(\frac{\hbar\omega_{\mathbf{n}}}{k_B T}\right) - 1} = 2\pi\hbar\omega_{\mathbf{n}} \coth\left(\frac{\hbar\omega_{\mathbf{n}}}{2k_B T}\right). \tag{9}$$

Note: $\lim_{T\to 0} \coth\left(\frac{\hbar\omega_{\mathbf{n}}}{2k_B T}\right) = 1$. Consequently, the term $2\pi\hbar\omega_{\mathbf{n}}$ constitutes the ZP ($T \to 0$) spectrum contribution, while the $\frac{4\pi\hbar\omega_{\mathbf{n}}}{\exp\left(\frac{\hbar\omega_{\mathbf{n}}}{k_B T}\right)-1}$ term is the Planckian part. Using **Eqs. 9**, **1**, and **2**, the ensemble average of the net energy due to these thermal radiation fields for $0 \le T$, within the $L_x \times L_y \times L_z$ rectilinear parallelepiped, can be calculated. Specifically, using the relationships above, and the usual relationship between electromagnetic energy in free space and the E&M fields [15], yields

$$\mathcal{E} = \int \mathrm{d}V \frac{1}{8\pi}\langle \mathbf{E}^2(\mathbf{x}, t) + \mathbf{B}^2(\mathbf{x}, t)\rangle = \sum_{\mathbf{n}} \left[\frac{\hbar\omega_{\mathbf{n}}}{2} + \frac{\hbar\omega_{\mathbf{n}}}{\exp\left(\frac{\hbar\omega_{\mathbf{n}}}{k_B T}\right) - 1}\right], \tag{10}$$

where $\omega_{\mathbf{n}} = c|\mathbf{k_n}|$ follows from **Eq. 3**; $\mathbf{n}$ is composed of $\{n_x, n_y, n_z\}$, where n_x, n_y, n_z are each integers, ranging from $-\infty$ to ∞. The term in **Eq. 10** of $\frac{\hbar\omega_{\mathbf{n}}}{2}$ is considered the ZP radiation contribution, since as $T \to 0$, the second term of $\frac{\hbar\omega_{\mathbf{n}}}{\exp\left(\frac{\hbar\omega_{\mathbf{n}}}{k_B T}\right)-1}$ vanishes. This second term is what Planck concentrated his efforts upon, and of course is connected to the Planck spectrum. We will refer to **Eq. 10** as being due to the ZP plus Planckian spectrum, or as the ZPP spectrum.

Now, we are in a position to calculate the probability distributions of $\mathbf{E}(\mathbf{x}, t)$ and $\mathbf{B}(\mathbf{x}, t)$ in **Eqs. 1** and **2**, as well as consider much more complicated joint probabilities involving $\mathbf{E}(\mathbf{x}, t)$ and $\mathbf{B}(\mathbf{x}, t)$. We will carry this analysis out now; again, in **Section 3**, we will apply these ideas to electric dipole oscillators in SED.

We start by calculating the probability density function of realizing a specific value of the electric field, for the ZPP situation. Our ensemble varies of course due to its ensemble members, meaning by the ensemble distribution of the $A's$ and $B's$ in **Eqs. 1** and **2** each time a new radiation situation is considered, then new $A's$ and $B's$ are realized according to the probability density distribution in **Eq. 8**, that then remain of constant values over the course of the subsequent physical analysis involving charged particles and fields.

As a start, the probability density distribution at position $\mathbf{x}$ and time t in **Eq. 1** is

$$P(\mathbf{E}\text{ at }\mathbf{x},t)=\int_{-\infty}^{\infty}\mathrm{d}A_1\cdots\int_{-\infty}^{\infty}\mathrm{d}A_N\cdots\int_{-\infty}^{\infty}\mathrm{d}B_1\cdots\int_{-\infty}^{\infty}\mathrm{d}B_N\cdots P(A_1,\ldots,A_N,\ldots,B_N,\ldots)\delta^3\left[\mathbf{E}-\mathbf{E}_{\mathrm{ZPP}}(\mathbf{x},t)\right],\tag{11}$$

where $A's$ and $B's$ here are symbolically written to represent the coefficients in **Eq. 1**, but as labeled there by $A_{\mathbf{k_n},\lambda}$ and $B_{\mathbf{k_n},\lambda}$. In **Eq. 11**, $P(A_1,\ldots,A_N,B_1,\ldots,B_N)$ represents the probability density function of all these coefficients. In the end, we would let $N\to\infty$. By $\mathbf{E}_{\mathrm{ZPP}}(\mathbf{x},t)$ in the Dirac delta function, we mean **Eq. 1**, but where the ZPP conditions of **Eqs. 8**-**9** hold.

The key variables being integrated over in **Eq. 11** are $A_{\mathbf{k_n},\lambda}$ and $B_{\mathbf{k_n},\lambda}$ variables. The integrations from $-\infty$ to $+\infty$ cover the range of their full possible values, while $P(A_1,\ldots,A_N,B_1,\ldots,B_N)$ provides the probability density associated with those values, and $\delta^3\left[\mathbf{E}-\mathbf{E}_{\mathrm{ZPP}}(\mathbf{x},t)\right]$ selects the values such that the probability density $P(\mathbf{E}\text{ at }\mathbf{x},t)$ arises from all the possible matches of $\mathbf{E}_{\mathrm{ZPP}}(\mathbf{x},t)$ to the electric field value in question of $\mathbf{E}$ at $\mathbf{x},t$. As a side comment, in a sense, **Eq. 11** has something in common with the Feynman path integral method in QM and QED, as the latter integrates over all weighted "path" contributions of a wave function evolving from one state to another. In contrast, **Eq. 11** considers all the "paths," or allowed values of the $A_{\mathbf{k_n},\lambda}$ and $B_{\mathbf{k_n},\lambda}$ coefficients in the ensemble of radiation possibilities, that result in the condition $\mathbf{E}$ at $\mathbf{x},t$. While **Eq. 11** directly involves probabilities, the Feynman path integral involves the QM wave function Ψ, with $|\Psi|^2$ more indirectly providing the probability aspect.

Returning back to our present calculation involving **Eq. 11**, if either $\mathbf{n}\neq\mathbf{n}'$, or $\lambda\neq\lambda'$, then $A_{\mathbf{k_n},\lambda}$ and $A_{\mathbf{k_n},\lambda'}$ represent independent random variables, as do $B_{\mathbf{k_n},\lambda}$ and $B_{\mathbf{k_n},\lambda'}$; moreover, $A_{\mathbf{k_n},\lambda}$ and $B_{\mathbf{k_n},\lambda'}$ are also independent random variables, even when $\mathbf{n}=\mathbf{n}'$ and $\lambda=\lambda'$. Using the Fourier representation for the Dirac delta function in **Eq. 11** of

$$\delta^3\left[\mathbf{E}-\mathbf{E}_{\mathrm{ZPP}}(\mathbf{x},t)\right]=\frac{1}{2\pi}\int_{-\infty}^{\infty}\mathrm{d}s_x e^{is_x\left(E_x-E_{x,\mathrm{ZPP}}\right)}\frac{1}{2\pi}\int_{-\infty}^{\infty}\mathrm{d}s_y e^{is_y\left(E_y-E_{y,\mathrm{ZPP}}\right)}\frac{1}{2\pi}\int_{-\infty}^{\infty}\mathrm{d}s_z e^{is_z\left(E_z-E_{z,\mathrm{ZPP}}\right)},\tag{12}$$

in addition to the Gaussian distribution in **Eq. 8**, then **Eq. 11** becomes:

$$\begin{aligned}P(\mathbf{E}\text{ at }\mathbf{x},t)=&\int_{-\infty}^{\infty}\mathrm{d}A_1\cdots\int_{-\infty}^{\infty}\mathrm{d}A_N\cdots\frac{1}{\sqrt{2\pi\sigma_{\mathbf{n}_1}^2}}\exp\left[-\frac{(A_1)^2}{2\sigma_{\mathbf{n}_1}^2}\right]\cdots\frac{1}{\sqrt{2\pi\sigma_{\mathbf{n}_N}^2}}\exp\left[-\frac{(A_N)^2}{2\sigma_{\mathbf{n}_N}^2}\right]\cdots\\&\times\int_{-\infty}^{\infty}\mathrm{d}B_1\cdots\int_{-\infty}^{\infty}\mathrm{d}B_N\cdots\frac{1}{\sqrt{2\pi\sigma_{\mathbf{n}_1}^2}}\exp\left[-\frac{(B_1)^2}{2\sigma_{\mathbf{n}_1}^2}\right]\cdots\frac{1}{\sqrt{2\pi\sigma_{\mathbf{n}_N}^2}}\exp\left[-\frac{(B_N)^2}{2\sigma_{\mathbf{n}_N}^2}\right]\cdots\\&\times\frac{1}{2\pi}\int_{-\infty}^{\infty}\mathrm{d}s_x e^{is_x\left(E_x-E_{x,\mathrm{ZPP}}\right)}\frac{1}{2\pi}\int_{-\infty}^{\infty}\mathrm{d}s_y e^{is_y\left(E_y-E_{y,\mathrm{ZPP}}\right)}\frac{1}{2\pi}\int_{-\infty}^{\infty}\mathrm{d}s_z e^{is_z\left(E_z-E_{z,\mathrm{ZPP}}\right)},\end{aligned}\tag{13}$$

where to simplify notation, $\omega_{\mathbf{n}}$ and T will be suppressed here:

$$\left[\sigma(\omega_{\mathbf{n}},T)\right]^2\equiv\sigma_{\mathbf{n}}^2\ .\tag{14}$$

To evaluate **Eq. 13**, **Eq. 1** needs to be substituted in three places on the last line. To simplify notation yet again, let us replace **Eq. 1** *via*

$$\mathbf{E}_{\mathrm{ZPP}}(\mathbf{x},t)=\sum_q A_q\mathbf{E}_{cq}+\sum_q B_q\mathbf{E}_{sq},\tag{15}$$

where q represents all the indices of n_x,n_y,n_z,λ, with their appropriate ranges, A_q still represents $A_{\mathbf{k_n},\lambda}$, and likewise for B_q and $B_{\mathbf{k_n},\lambda}$, and we will also refer to $\sigma_{\mathbf{n}}^2$ as σ_q^2 from here on, again to simplify notation. Also, in **Eq. 15**, the expression has been abbreviated using

$$\mathbf{E}_{cq}\equiv\frac{1}{\left(L_xL_yL_z\right)^{1/2}}\widehat{\boldsymbol{\varepsilon}}_{\mathbf{k_n},\lambda}\cos\left(\mathbf{k_n}\cdot\mathbf{x}-\omega_{\mathbf{n}}t\right),\tag{16}$$

and

$$\mathbf{E}_{sq}\equiv\frac{1}{\left(L_xL_yL_z\right)^{1/2}}\widehat{\boldsymbol{\varepsilon}}_{\mathbf{k_n},\lambda}\sin\left(\mathbf{k_n}\cdot\mathbf{x}-\omega_{\mathbf{n}}t\right).\tag{17}$$

Hence:

$$\begin{aligned}P(\mathbf{E}\text{ at }\mathbf{x},t)=&\int\mathrm{d}A_1\cdots\int\mathrm{d}A_N\ldots\frac{1}{\sqrt{2\pi\sigma_1^2}}\exp\left[-\frac{(A_1)^2}{2\sigma_1^2}\right]\ldots\frac{1}{\sqrt{2\pi\sigma_N^2}}\exp\left[-\frac{(A_N)^2}{2\sigma_N^2}\right]\ldots\\&\times\int\mathrm{d}B_1\cdots\int\mathrm{d}B_N\ldots\frac{1}{\sqrt{2\pi\sigma_1^2}}\exp\left[-\frac{(B_1)^2}{2\sigma_1^2}\right]\ldots\frac{1}{\sqrt{2\pi\sigma_N^2}}\exp\left[-\frac{(B_N)^2}{2\sigma_N^2}\right]\ldots\\&\times\frac{1}{2\pi}\int_{-\infty}^{\infty}\mathrm{d}s_x e^{is_x\left(E_x-\sum_q\left(A_qE_{cq,x}+B_qE_{sq,x}\right)\right)}\times\frac{1}{2\pi}\int_{-\infty}^{\infty}\mathrm{d}s_y e^{is_y\left(E_y-\sum_q A_qE_{cq,y}+B_qE_{sq,y}\right)}\\&\times\frac{1}{2\pi}\int_{-\infty}^{\infty}\mathrm{d}s_z e^{is_y\left(E_z-\sum_q A_qE_{cq,z}+B_qE_{sq,z}\right)}.\end{aligned}\tag{18}$$

These integrals can be done by completing the squares of the A_q and B_q variables, then integrating over the resulting Gaussian expressions, followed by the integrals over s_1, s_2, s_3. For example, completing the square:

$$\begin{aligned}&-\frac{\left(A_q\right)^2}{2\sigma_q^2}-is_xA_qE_{cq,x}-is_yA_qE_{cq,y}-is_zA_qE_{cq,z}\\&=-\frac{1}{2\sigma_q^2}\left[A_q+i\left(s_xE_{cq,x}+s_yE_{cq,y}+s_zE_{cq,z}\right)\sigma_q^2\right]^2\\&\quad-\left(s_xE_{cq,x}+s_yE_{cq,y}+s_zE_{cq,z}\right)^2\frac{\sigma_q^2}{2}\end{aligned}\tag{19}$$

results in:

$$\begin{aligned}&\int_{-\infty}^{\infty}\mathrm{d}A_q\frac{1}{\sqrt{2\pi\sigma_q^2}}\exp\left[-\frac{\left(A_q\right)^2}{2\sigma_q^2}\right]e^{-is_xA_qE_{cq,x}}e^{-is_yA_qE_{cq,y}}e^{-is_zA_qE_{cq,z}}\\&=\int_{-\infty}^{\infty}\mathrm{d}A_q\frac{1}{\sqrt{2\pi\sigma_q^2}}\exp\left\{-\frac{1}{2\sigma_q^2}\left[A_q+i\left(s_xE_{cq,x}+s_yE_{cq,y}+s_zE_{cq,z}\right)\sigma_q^2\right]^2\right\}\\&\times\exp\left[-\left(s_xE_{cq,x}+s_yE_{cq,y}+s_zE_{cq,z}\right)^2\frac{\sigma_q^2}{2}\right]\\&=\exp\left[-\left(s_xE_{cq,x}+s_yE_{cq,y}+s_zE_{cq,z}\right)^2\frac{\sigma_q^2}{2}\right],\end{aligned}\tag{20}$$

since the Gaussian integral in the second line equals unity.

Continuing for each A_q and B_q results in:

$$P(\mathbf{E}\text{ at }\mathbf{x},t)=\frac{1}{2\pi}\int_{-\infty}^{\infty}\mathrm{d}s_x e^{is_xE_x}\frac{1}{2\pi}\int_{-\infty}^{\infty}\mathrm{d}s_y e^{is_yE_y}\frac{1}{2\pi}\int_{-\infty}^{\infty}\mathrm{d}s_z e^{is_zE_z}$$
$$\times\exp\left[-\sum_q\left(s_xE_{cq,x}+s_yE_{cq,y}+s_zE_{cq,z}\right)^2\frac{\sigma_q^2}{2}\right] \quad (21)$$
$$\times\exp\left[-\sum_q\left(s_xE_{sq,x}+s_yE_{sq,y}+s_zE_{sq,z}\right)^2\frac{\sigma_q^2}{2}\right].$$

Three integrals remain, namely, over s_x, s_y, s_z. The arguments of the two exponential terms in the second and third lines of **Eq. 21**, become, after making use of **Eqs. 16** and **17**:

$$\left(s_xE_{cq,x}+s_yE_{cq,y}+s_zE_{cq,z}\right)^2+\left(s_xE_{sq,x}+s_yE_{sq,y}+s_zE_{sq,z}\right)^2$$
$$=\frac{1}{\left(L_xL_yL_z\right)}\left(s_x^2\varepsilon_{q,x}^2+s_y^2\varepsilon_{q,y}^2+s_z^2\varepsilon_{q,z}^2+2s_xs_y\varepsilon_{q,x}\varepsilon_{q,y}\right.$$
$$\left.+2s_xs_z\varepsilon_{q,x}\varepsilon_{q,z}+2s_ys_z\varepsilon_{q,y}\varepsilon_{q,z}\right). \quad (22)$$

Still, the three integrals in **Eq. 21** are nontrivial to evaluate, because of the cross terms in **Eq. 22**. However, the integrals can be greatly simplified by first summing over the polarization indices of $\lambda=1,2$ as part of the "q" set of indices, and making use of the following identities for the three perpendicular unit vectors of $\widehat{\boldsymbol{\varepsilon}}_{\mathbf{k_n},1}$, $\widehat{\boldsymbol{\varepsilon}}_{\mathbf{k_n},2}$, and $\mathbf{k_n}$:

$$\sum_{\lambda=1,2}\left[\left(\widehat{\boldsymbol{\varepsilon}}_{\mathbf{k_n},\lambda}\right)_i\right]^2=1-\left[\frac{(\mathbf{k_n})_i}{k_\mathbf{n}}\right]^2, \quad (23)$$

$$\sum_{\lambda=1,2}\left(\widehat{\boldsymbol{\varepsilon}}_{\mathbf{k_n},\lambda}\right)_i\left(\widehat{\boldsymbol{\varepsilon}}_{\mathbf{k_n},\lambda}\right)_j=\delta_{ij}-\frac{(\mathbf{k_n})_i(\mathbf{k_n})_j}{k_\mathbf{n}^2}. \quad (24)$$

After summing over the λ part of the q indices, one obtains:

$$\sum_q\left(s_x^2\varepsilon_{q,x}^2+s_y^2\varepsilon_{q,y}^2+s_z^2\varepsilon_{q,z}^2+2s_xs_y\varepsilon_{q,x}\varepsilon_{q,y}+2s_xs_z\varepsilon_{q,x}\varepsilon_{q,z}+2s_ys_z\varepsilon_{q,y}\varepsilon_{q,z}\right)\sigma_q^2$$
$$=\sum_\mathbf{n}\left\{s_x^2\left[1-\left(\frac{k_{\mathbf{n},x}}{k_\mathbf{n}}\right)^2\right]+s_y^2\left[1-\left(\frac{k_{\mathbf{n},y}}{k_\mathbf{n}}\right)^2\right]+s_z^2\left[1-\left(\frac{k_{\mathbf{n},z}}{k_\mathbf{n}}\right)^2\right]\right\}\sigma_\mathbf{n}^2 \quad (25)$$
$$-2\sum_\mathbf{n}\left[s_xs_y\frac{k_{\mathbf{n},x}k_{\mathbf{n},y}}{k_\mathbf{n}^2}+s_xs_z\frac{k_{\mathbf{n},x}k_{\mathbf{n},z}}{k_\mathbf{n}^2}+s_ys_z\frac{k_{\mathbf{n},y}k_{\mathbf{n},z}}{k_\mathbf{n}^2}\right]\sigma_\mathbf{n}^2.$$

Although the "cross terms" involving s_xs_y, s_xs_z, s_ys_z still remain, upon summing over $\mathbf{n}$ in the last three terms, we obtain

$$\sum_\mathbf{n}\frac{k_{\mathbf{n},i}k_{\mathbf{n},j}}{k_\mathbf{n}^2}\sigma_\mathbf{n}^2=0\text{ for }i\neq j, \quad (26)$$

since n_x, n_y, n_z each vary as integers symmetrically from $-\infty$ to $+\infty$, where $\mathbf{k_n}$ is given in **Eq. 3**.

Consequently, from **Eqs. 21**, **25** and **26**:

$$P(\mathbf{E}\text{ at }\mathbf{x},t)=I_1I_2I_3, \quad (27)$$

where

$$I_i\equiv\frac{1}{2\pi}\int_{-\infty}^{\infty}\mathrm{d}s_i\exp\left(is_iE_i-\frac{1}{2}\frac{s_i^2}{\left(L_xL_yL_z\right)}\sum_\mathbf{n}\left[1-\left(\frac{k_{\mathbf{n},i}}{k_\mathbf{n}}\right)^2\right]\sigma_\mathbf{n}^2\right). \quad (28)$$

Simplifying notation, let

$$\alpha_i\equiv\frac{1}{\left(L_xL_yL_z\right)}\sum_\mathbf{n}\left[1-\left(\frac{k_{\mathbf{n},i}}{k_\mathbf{n}}\right)^2\right]\sigma_\mathbf{n}^2. \quad (29)$$

By then completing the square in **Eq. 28** and carrying out the integral, yields

$$I_i=\frac{1}{2\pi}\int_{-\infty}^{\infty}\mathrm{d}s_i\exp\left(-s_i^2\alpha_i\frac{1}{2}+is_iE_i\right)$$
$$=\frac{1}{2\pi}\exp\left(-\frac{E_i^2}{2\alpha_i}\right)\int_{-\infty}^{\infty}\mathrm{d}s_i\exp\left[-\frac{\alpha_i}{2}\left(s_i-\frac{iE_i}{\alpha_i}\right)^2\right]$$
$$=\frac{1}{2\pi}\exp\left(-\frac{E_i^2}{2\alpha_i}\right)\left(\frac{2\pi}{\alpha_i}\right)^{1/2}, \quad (30)$$

resulting in

$$P(\mathbf{E}\text{ at }\mathbf{x},t)=I_1I_2I_3$$
$$=\frac{1}{(2\pi)^{\frac{3}{2}}}\frac{1}{(\alpha_1\alpha_2\alpha_3)^{1/2}}\exp\left(-\frac{E_x^2}{2\alpha_1}-\frac{E_y^2}{2\alpha_2}-\frac{E_z^2}{2\alpha_3}\right). \quad (31)$$

More insight into **Eq. 31** can be gained by relating α_i in **Eq. 29**, to $\langle\mathbf{E}_{\mathrm{ZPP},i}^2(\mathbf{x},t)\rangle$, using **Eqs. 6, 7**, and **23**:

$$\langle\mathbf{E}_{\mathrm{ZPP},i}^2(\mathbf{x},t)\rangle=\left\langle\left\{\frac{1}{\left(L_xL_yL_z\right)^{1/2}}\sum_{n_x,n_y,n_z=-\infty}^{\infty}\sum_{\lambda=1,2}\left(\widehat{\boldsymbol{\varepsilon}}_{\mathbf{k_n},\lambda}\right)_i\right.\right.$$
$$\left.\left.\times\left[A_{\mathbf{k_n},\lambda}\cos\left(\mathbf{k_n}\cdot\mathbf{x}-\omega_\mathbf{n}t\right)+B_{\mathbf{k_n},\lambda}\sin\left(\mathbf{k_n}\cdot\mathbf{x}-\omega_\mathbf{n}t\right)\right]\right\}^2\right\rangle$$
$$=\frac{1}{\left(L_xL_yL_z\right)}\sum_{n_x,n_y,n_z=-\infty}^{\infty}\sum_{\lambda=1,2}\left[\left(\widehat{\boldsymbol{\varepsilon}}_{\mathbf{k_n},\lambda}\right)_i\right]^2\sigma_\mathbf{n}^2\left[\cos^2\left(\mathbf{k_n}\cdot\mathbf{x}-\omega_\mathbf{n}t\right)\right.$$
$$\left.+\sin^2\left(\mathbf{k_n}\cdot\mathbf{x}-\omega_\mathbf{n}t\right)\right]$$
$$=\frac{1}{\left(L_xL_yL_z\right)}\sum_{n_x,n_y,n_z=-\infty}^{\infty}\left[1-\left(\frac{k_{\mathbf{n},i}}{k_\mathbf{n}}\right)^2\right]\sigma_\mathbf{n}^2. \quad (32)$$

Combining **Eqs. 29**, **31** and **32** and noting

$$\alpha_i=\langle\mathbf{E}_{\mathrm{ZPP},i}^2(\mathbf{x},t)\rangle, \quad (33)$$

we obtain:

$$P(\mathbf{E}\text{ at }\mathbf{x},t)=\frac{\exp\left[-\frac{E_x^2}{2\langle E_{\mathrm{ZPP},x}^2\rangle}\right]}{\sqrt{2\pi\langle E_{\mathrm{ZPP},x}^2\rangle}}\frac{\exp\left[-\frac{E_y^2}{2\langle E_{\mathrm{ZPP},y}^2\rangle}\right]}{\sqrt{2\pi\langle E_{\mathrm{ZPP},y}^2\rangle}}\frac{\exp\left[-\frac{E_z^2}{2\langle E_{\mathrm{ZPP},z}^2\rangle}\right]}{\sqrt{2\pi\langle E_{\mathrm{ZPP},z}^2\rangle}}. \quad (34)$$

Note that the mathematically detailed development of **Eq. 34**, and shortly **Eq. 37** for the magnetic field case, agree nicely with the less detailed, but still the same result from Ref. [16].

In the symmetrical situation, with $L_x = L_y = L_z$ chosen for the rectilinear parallelepiped, then

$$\langle \mathbf{E}^2_{\mathrm{ZPP},x}\rangle = \langle \mathbf{E}^2_{\mathrm{ZPP},y}\rangle = \langle \mathbf{E}^2_{\mathrm{ZPP},z}\rangle = \langle \mathbf{E}^2_{\mathrm{ZPP},i}\rangle$$
$$= \frac{1}{\left(L_xL_yL_z\right)}\sum_{n_x,n_y,n_z=-\infty}^{\infty}\left\{1-\left[\frac{(\mathbf{k_n})_i}{k_\mathbf{n}}\right]^2\right\}\sigma^2_\mathbf{n} = \frac{2}{3\left(L_xL_yL_z\right)}\sum_{n_x,n_y,n_z=-\infty}^{\infty}\sigma^2_\mathbf{n} \tag{35}$$

and

$$P_{L_x=L_y=L_z}(\mathbf{E}\text{ at }\mathbf{x},t) = \frac{1}{\left(2\pi\langle E_i^2\rangle\right)^{3/2}}\exp\left[-\frac{\left(E_x^2+E_y^2+E_z^2\right)}{2\langle E_i^2\rangle}\right]. \tag{36}$$

Thus, the probability density for the radiation electric field **E** at position **x** and time *t*, from either **Eqs. 34** or **36**, equals the product of three Gaussian functions. Moreover, the probability density of **E** is independent of position **x** and time *t*. If material walls existed, as in a cavity of arbitrary shape, as opposite to this free space situation treated by periodic bcs, then the probability density function for the fields could well be dependent on position. In Planck's original treatment of blackbody radiation [25], he considered a cavity with smooth walls and a size that was large compared to the key wavelengths of interest. Since his work, researchers have probed on variations of these concerns, including small cavities, often referred to as the areas of quantum cavity electrodynamics [33, 34]. To treat these problems in SED, one would need to take into account the precise nodal structure due to the cavity shape, and likely not take continuum approximation limits.

Looking back at the calculations, it is fairly easy to show that when analyzing magnetic fields, but now using **Eq. 2**, that:

$$P(\mathbf{B}\text{ at }\mathbf{x},t) = \frac{\exp\left[-\frac{B_x^2}{2\langle B^2_{\mathrm{ZPP},x}\rangle}\right]}{\sqrt{2\pi\langle B^2_{\mathrm{ZPP},x}\rangle}}\frac{\exp\left[-\frac{B_y^2}{2\langle B^2_{\mathrm{ZPP},y}\rangle}\right]}{\sqrt{2\pi\langle B^2_{\mathrm{ZPP},y}\rangle}}\frac{\exp\left[-\frac{B_z^2}{2\langle B^2_{\mathrm{ZPP},z}\rangle}\right]}{\sqrt{2\pi\langle B^2_{\mathrm{ZPP},z}\rangle}}. \tag{37}$$

Finally, a caution needs to be made upon understanding **Eqs. 32–37**. When ZP radiation is included in the analysis, which is indeed a cornerstone of SED, $\langle \mathbf{E}^2_{\mathrm{ZPP},i}(\mathbf{x},t)\rangle$ is infinite, as the energy spectrum monotonically grows with larger values of frequency. If one only considers the Planckian part of the spectrum, then this infinity does not happen. However, for calculating quantities like Casimir forces, van der Waals forces, and prevention of hydrogen collapse, it is absolutely essential to include the ZP spectrum. Cutoffs of the spectrum have been considered, but to date, the usual treatment has been to examine changes in regions between material boundaries, such as plates or cavity walls, when these are displaced. Such changes in energy due to wall displacements are finite, even with ZP fields [2]. Moreover, the results agree with experiments carried out to date. However, when considering the calculation in the next section, involving the probability of the electric field at two different positions and/or times, this infinity problem does not occur, unless the two points are chosen to be the same point both in space and time, or if $|\Delta\mathbf{x}| = c|\Delta t|$.

2.2 Joint Probability Density for Two Electric Field Values

The method just used can in principle be carried out for a wide range of probabilistic situations, with the key starting point being a similar condition to **Eq. 11**. A second calculation for a more complicated situation will be carried out here to illustrate this point. Before beginning, it is interesting to note that a number of "two-point" correlation functions of fields in SED have been calculated before by researchers, with the key reference being [24], but also [20], as well as by the present author in Ref. [35] and even for two-point correlation functions involving points in space and time following uniformly accelerated trajectories [7]. Clearly, probability density distributions such as in **Eqs. 34** and **37** are more general, since they can be used to deduce all possible moments of the probability distribution; however, their calculation is in general much more involved.

Here, we will calculate the joint probability density function of

$$P(\mathbf{E}_1\text{ at }\mathbf{x}_1,t_1;\mathbf{E}_2\text{ at }\mathbf{x}_2,t_2)$$
$$= \int \mathrm{d}A_1\cdots\int \mathrm{d}A_N\cdots\int \mathrm{d}B_1\cdots\int \mathrm{d}B_N\cdots P(A_1,\ldots,A_N,\ldots,B_N,\ldots) \tag{38}$$
$$\times\delta^3\left[\mathbf{E}_1-\mathbf{E}_{\mathrm{ZPP}}(\mathbf{x}_1,t_1)\right]\delta^3\left[\mathbf{E}_2-\mathbf{E}_{\mathrm{ZPP}}(\mathbf{x}_2,t_2)\right], \tag{39}$$

where the semicolon in the first line is intended as a shortened meaning for the logical "AND" symbol of $\cap$.

Again, we make use of the random variable independence of the $A's$ and $B's$ for a normal thermodynamic radiation situation, and impose the distribution **Eq. 8**, plus use **Eq. 12**, to obtain:

$$\begin{aligned}
&P(\mathbf{E}_1\text{ at }\mathbf{x}_1,t_1;\mathbf{E}_2\text{ at }\mathbf{x}_2,t_2)\\
&=\int \mathrm{d}A_1\cdots\int \mathrm{d}A_N\cdots\frac{1}{\sqrt{2\pi\sigma^2_{\mathbf{n}_1}}}\exp\left[-\frac{(A_1)^2}{2\sigma^2_{\mathbf{n}_1}}\right]\cdots\frac{1}{\sqrt{2\pi\sigma^2_{\mathbf{n}_N}}}\exp\left[-\frac{(A_N)^2}{2\sigma^2_{\mathbf{n}_N}}\right]\cdots\\
&\times\int \mathrm{d}B_1\cdots\int \mathrm{d}B_N\cdots\frac{1}{\sqrt{2\pi\sigma^2_{\mathbf{n}_1}}}\exp\left[-\frac{(B_1)^2}{2\sigma^2_{\mathbf{n}_1}}\right]\cdots\frac{1}{\sqrt{2\pi\sigma^2_{\mathbf{n}_N}}}\exp\left[-\frac{(B_N)^2}{2\sigma^2_{\mathbf{n}_N}}\right]\cdots\\
&\times\frac{1}{2\pi}\int_{-\infty}^{\infty}\mathrm{d}s_{1x}e^{is_{1x}\left(E_{1x}-E_{1x,\mathrm{ZPP}}\right)}\frac{1}{2\pi}\int_{-\infty}^{\infty}\mathrm{d}s_{1y}e^{is_{1y}\left(E_{1y}-E_{1y,\mathrm{ZPP}}\right)}\frac{1}{2\pi}\int_{-\infty}^{\infty}\mathrm{d}s_{1z}e^{is_{1z}\left(E_{1z}-E_{1z,\mathrm{ZPP}}\right)}\\
&\times\frac{1}{2\pi}\int_{-\infty}^{\infty}\mathrm{d}s_{2x}e^{is_{2x}\left(E_{2x}-E_{2x,\mathrm{ZPP}}\right)}\frac{1}{2\pi}\int_{-\infty}^{\infty}\mathrm{d}s_{2y}e^{is_{2y}\left(E_{2y}-E_{2y,\mathrm{ZPP}}\right)}\frac{1}{2\pi}\int_{-\infty}^{\infty}\mathrm{d}s_{2z}e^{is_{2z}\left(E_{2z}-E_{2z,\mathrm{ZPP}}\right)},
\end{aligned} \tag{40}$$

where the positions $\mathbf{x}_1$ and $\mathbf{x}_2$ and times t_1 and t_2 are contained in the radiation field expressions of **Eq. 1** or **15**. Thus, in **Eq. 40**, $E_{1x,\mathrm{ZPP}}$, $E_{1y,\mathrm{ZPP}}$, and $E_{1z,\mathrm{ZPP}}$ refer to $\mathbf{E}_{\mathrm{ZPP}}(\mathbf{x}_1,t_1)$ as in **Eq. 15**, and similarly for $\mathbf{E}_{\mathrm{ZPP}}(\mathbf{x}_2,t_2)$. Again abbreviating expressions, as in **16** and **17**, with $a = 1, 2$, as below:

$$\begin{aligned}
\mathbf{E}_{\mathrm{ZPP}}(\mathbf{x}_a,t_a) &= \frac{1}{\left(L_xL_yL_z\right)^{1/2}}\sum_{n_x,n_y,n_z=-\infty}^{\infty}\sum_{\lambda=1,2}\widehat{\varepsilon}_{\mathbf{k_n},\lambda}\left[A_{\mathbf{k_n},\lambda}\cos\left(\mathbf{k_n}\cdot\mathbf{x_a}\right.\right.\\
&\left.\left.-\boldsymbol{\omega}_\mathbf{n}t_a\right)+B_{\mathbf{k_n},\lambda}\sin\left(\mathbf{k_n}\cdot\mathbf{x_a}-\omega_\mathbf{n}t_a\right)\right]\\
&= \sum_q A_q\mathbf{E}_{a,cq}+\sum_q B_q\mathbf{E}_{a,sq}.
\end{aligned} \tag{41}$$

Collecting the A_q-related terms in **Eq. 40** as in the following manner, then later doing similarly for the B_q terms:

$$
\begin{aligned}
&-\frac{\left(A_q\right)^2}{2\sigma_q^2} - is_{1x}A_qE_{1,cq,x} - is_{1y}A_qE_{1,cq,y} - is_{1z}A_qE_{1,cq,z} - is_{2x}A_qE_{2,cq,x}\\
&- is_{2y}A_qE_{2,cq,y} - is_{2z}A_qE_{2,cq,z}\\
&= \frac{1}{2\sigma_q^2}\Big[A_q + i\Big(s_{1x}E_{1,cq,x} + s_{1y}E_{1,cq,y} + s_{1z}E_{1,cq,z}\\
&+ s_{2x}E_{2,cq,x} + s_{2y}E_{2,cq,y} + s_{2z}E_{2,cq,z}\Big)\sigma_q^2\Big]^2 - \Big(s_{1x}E_{1,cq,x} + s_{1y}E_{1,cq,y}\\
&+ s_{1z}E_{1,cq,z} + s_{2x}E_{2,cq,x} + s_{2y}E_{2,cq,y} + s_{2z}E_{2,cq,z}\Big)^2\frac{\sigma_q^2}{2}.
\end{aligned}
\tag{42}
$$

Now integrating over each A_q term, followed later by integrating over the related B_q term expression, results in:

$$
\begin{aligned}
&\int_{-\infty}^{\infty} dA_q \frac{1}{\sqrt{2\pi\sigma_q^2}} \exp\left[-\frac{\left(A_q\right)^2}{2\sigma_q^2}\right] e^{-i\left(s_{1x}A_qE_{1,cq,x}+s_{1y}A_qE_{1,cq,y}+s_{1z}A_qE_{1,cq,z}+s_{2x}A_qE_{2,cq,x}+s_{2y}A_qE_{2,cq,y}+s_{2z}A_qE_{2,cq,z}\right)}\\
&= \int_{-\infty}^{\infty} dA_q \frac{1}{\sqrt{2\pi\sigma_q^2}} \exp\left[-\frac{1}{2\sigma_q^2}\left[A_q + i\left(\begin{array}{l} s_{1x}E_{1,cq,x} + s_{1y}E_{1,cq,y} + s_{1z}E_{1,cq,z} \\ +s_{2x}E_{2,cq,x} + s_{2y}E_{2,cq,y} + s_{2z}E_{2,cq,z}\end{array}\right)\sigma_q^2\right]^2\right]\\
&\times \exp\left[-\left(s_{1x}E_{1,cq,x} + s_{1y}E_{1,cq,y} + s_{1z}E_{1,cq,z} + s_{2x}E_{2,cq,x} + s_{2y}E_{2,cq,y} + s_{2z}E_{2,cq,z}\right)^2\frac{\sigma_q^2}{2}\right]\\
&= \exp\left[-\left(s_{1x}E_{1,cq,x} + s_{1y}E_{1,cq,y} + s_{1z}E_{1,cq,z} + s_{2x}E_{2,cq,x} + s_{2y}E_{2,cq,y} + s_{2z}E_{2,cq,z}\right)^2\frac{\sigma_q^2}{2}\right].
\end{aligned}
\tag{43}
$$

Integrating over each A_q and B_q results in:

$$
\begin{aligned}
&P(\mathbf{E}_1 \text{ at } \mathbf{x}_1, t_1; \mathbf{E}_2 \text{ at } \mathbf{x}_2, t_2)\\
&= \frac{1}{(2\pi)^6}\int_{-\infty}^{\infty} ds_{1x}e^{is_{1x}E_{1x}}\int_{-\infty}^{\infty} ds_{1y}e^{is_{1y}E_{1y}}\int_{-\infty}^{\infty} ds_{1z}e^{is_{1z}E_{1z}}\int_{-\infty}^{\infty} ds_{2x}e^{is_{2x}E_{2x}}\int_{-\infty}^{\infty} ds_{2y}e^{is_{2y}E_{2y}}\int_{-\infty}^{\infty} ds_{2z}e^{is_{2z}E_{2z}}\\
&\times \exp\left[-\sum_q\left(s_{1x}E_{1,cq,x} + s_{1y}E_{1,cq,y} + s_{1z}E_{1,cq,z} + s_{2x}E_{2,cq,x} + s_{2y}E_{2,cq,y} + s_{2z}E_{2,cq,z}\right)^2\frac{\sigma_q^2}{2}\right]\\
&\times \exp\left[-\sum_q\left(s_{1x}E_{1,sq,x} + s_{1y}E_{1,sq,y} + s_{1z}E_{1,sq,z} + s_{2x}E_{2,sq,x} + s_{2y}E_{2,sq,y} + s_{2z}E_{2,sq,z}\right)^2\frac{\sigma_q^2}{2}\right]
\end{aligned}
\tag{44}
$$

Six integrals remain, namely, over s_{1x}, s_{1y}, s_{1z}, s_{2x}, s_{2y}, and s_{2z}. The arguments of the exponential terms in the last lines of **Eq. 44**, using **Eq. 41** as well as **Eqs. 16** and **17**, and recognizing that many of the terms below have the simplification factor of

$$
\cos^2(\mathbf{k}_\mathbf{n}\cdot\mathbf{x}_a - \omega_\mathbf{n}t_a) + \sin^2(\mathbf{k}_\mathbf{n}\cdot\mathbf{x}_a - \omega_\mathbf{n}t_a) = 1\,, \tag{45}
$$

for either $a = 1$ or 2, then:

$$
\begin{aligned}
&\left(s_{1x}E_{1,cq,x} + s_{1y}E_{1,cq,y} + s_{1z}E_{1,cq,z} + s_{2x}E_{2,cq,x} + s_{2y}E_{2,cq,y} + s_{2z}E_{2,cq,z}\right)^2\\
&+\left(s_{1x}E_{1,sq,x} + s_{1y}E_{1,sq,y} + s_{1z}E_{1,sq,z} + s_{2x}E_{2,sq,x} + s_{2y}E_{2,sq,y} + s_{2z}E_{2,sq,z}\right)^2\\
&= \frac{1}{\left(L_xL_yL_z\right)}\left(s_{1x}^2\varepsilon_{q,x}^2 + s_{1y}^2\varepsilon_{q,y}^2 + s_{1z}^2\varepsilon_{q,z}^2 + s_{2x}^2\varepsilon_{q,x}^2 + s_{2y}^2\varepsilon_{q,y}^2 + s_{2z}^2\varepsilon_{q,z}^2\right)\\
&+\frac{2}{\left(L_xL_yL_z\right)}\left(s_{1x}\varepsilon_{q,x}s_{1y}\varepsilon_{q,y} + s_{1x}\varepsilon_{q,x}s_{1z}\varepsilon_{q,z} + s_{1y}\varepsilon_{q,y}s_{1z}\varepsilon_{q,z}\right)\\
&+\frac{2}{\left(L_xL_yL_z\right)}\left(s_{2x}\varepsilon_{q,x}s_{2y}\varepsilon_{q,y} + s_{2x}\varepsilon_{q,x}s_{2z}\varepsilon_{q,z} + s_{2y}\varepsilon_{q,y}s_{2z}\varepsilon_{q,z}\right)\\
&+\frac{2s_{1x}\varepsilon_{q,x}}{\left(L_xL_yL_z\right)}\left(s_{2x}\varepsilon_{q,x} + s_{2y}\varepsilon_{q,y} + s_{2z}\varepsilon_{q,z}\right)(C_1C_2 + S_1S_2)\\
&+\frac{2s_{1y}\varepsilon_{q,y}}{\left(L_xL_yL_z\right)}\left(s_{2x}\varepsilon_{q,x} + s_{2y}\varepsilon_{q,y} + s_{2z}\varepsilon_{q,z}\right)(C_1C_2 + S_1S_2)\\
&+\frac{2s_{1z}\varepsilon_{q,z}}{\left(L_xL_yL_z\right)}\left(s_{2x}\varepsilon_{q,x} + s_{2y}\varepsilon_{q,y} + s_{2z}\varepsilon_{q,z}\right)(C_1C_2 + S_1S_2)
\end{aligned}
\tag{46}
$$

The meaning of the abbreviated terms $(C_1C_2 + S_1S_2)$ is:

$$
\begin{aligned}
(C_1C_2 + S_1S_2) &= \cos(\mathbf{k}_\mathbf{n}\cdot\mathbf{x}_1 - \omega_\mathbf{n}t_1)\cos(\mathbf{k}_\mathbf{n}\cdot\mathbf{x}_2 - \omega_\mathbf{n}t_2)\\
&+\sin(\mathbf{k}_\mathbf{n}\cdot\mathbf{x}_1 - \omega_\mathbf{n}t_1)\sin(\mathbf{k}_\mathbf{n}\cdot\mathbf{x}_2 - \omega_\mathbf{n}t_2)\\
&= \cos[\mathbf{k}_\mathbf{n}\cdot(\mathbf{x}_1 - \mathbf{x}_2) - \omega_\mathbf{n}(t_1 - t_2)] \equiv C_{12,\mathbf{n}}.
\end{aligned}
\tag{47}
$$

Again summing over the polarization indices of $\lambda = 1, 2$ as part of the "q" set of indices in the last lines of **Eq. 44**, and making use **Eqs. 23** and **24**, plus noting that the cross terms of $\varepsilon_{q,i}\varepsilon_{q,j}$ for $i \neq j$, will drop out due to the sum in **Eq. 26**, results in:

$$
\begin{aligned}
&\sum_q\left(s_{1x}E_{1,cq,x} + s_{1y}E_{1,cq,y} + s_{1z}E_{1,cq,z} + s_{2x}E_{2,cq,x} + s_{2y}E_{2,cq,y} + s_{2z}E_{2,cq,z}\right)^2\\
&+\sum_q\left(s_{1x}E_{1,sq,x} + s_{1y}E_{1,sq,y} + s_{1z}E_{1,sq,z} + s_{2x}E_{2,sq,x} + s_{2y}E_{2,sq,y} + s_{2z}E_{2,sq,z}\right)^2\\
&= \frac{1}{\left(L_xL_yL_z\right)}\sum_{n_x,n_y,n_z=-\infty}^{\infty}\left[\left(s_{1x}^2 + s_{2x}^2\right)\left(1 - \frac{\mathbf{k}_{\mathbf{n},x}^2}{k_\mathbf{n}^2}\right) + \left(s_{1y}^2 + s_{2y}^2\right)\left(1 - \frac{\mathbf{k}_{\mathbf{n},y}^2}{k_\mathbf{n}^2}\right)\right.\\
&\left.+\left(s_{1z}^2 + s_{2z}^2\right)\left(1 - \frac{\mathbf{k}_{\mathbf{n},z}^2}{k_\mathbf{n}^2}\right)\right] + \frac{2}{\left(L_xL_yL_z\right)}\sum_{n_x,n_y,n_z=-\infty}^{\infty}\left[s_{1x}s_{2x}\left(1 - \frac{\mathbf{k}_{\mathbf{n},x}^2}{k_\mathbf{n}^2}\right)\right.\\
&\left.+ s_{1y}s_{2y}\left(1 - \frac{\mathbf{k}_{\mathbf{n},y}^2}{k_\mathbf{n}^2}\right) + s_{1z}s_{2z}\left(1 - \frac{\mathbf{k}_{\mathbf{n},z}^2}{k_\mathbf{n}^2}\right)\right]C_{12,\mathbf{n}}\,.
\end{aligned}
\tag{48}
$$

Hence:

$$
\begin{aligned}
&P(\mathbf{E}_1 \text{ at } \mathbf{x}_1, t_1; \mathbf{E}_2 \text{ at } \mathbf{x}_2, t_2) = \frac{1}{(2\pi)^6}\int_{-\infty}^{\infty} ds_{1x}e^{is_{1x}E_{1x}}\int_{-\infty}^{\infty} ds_{1y}e^{is_{1y}E_{1y}}\\
&\int_{-\infty}^{\infty} ds_{1z}e^{is_{1z}E_{1z}}\int_{-\infty}^{\infty} ds_{2x}e^{is_{2x}E_{2x}}\int_{-\infty}^{\infty} ds_{2y}e^{is_{2y}E_{2y}}\int_{-\infty}^{\infty} ds_{2z}e^{is_{2z}E_{2z}}\\
&\times\exp\left[-\frac{1}{\left(L_xL_yL_z\right)}\sum_{n_x,n_y,n_z=-\infty}^{\infty}\left\{\begin{array}{l}\left(s_{1x}^2 + 2s_{1x}s_{2x}C_{12,\tilde{\mathbf{n}}} + s_{2x}^2\right)\left(1 - \frac{\mathbf{k}_{\mathbf{n},x}^2}{k_\mathbf{n}^2}\right)\\ +\left(s_{1y}^2 + 2s_{1y}s_{2y}C_{12,\tilde{\mathbf{n}}} + s_{2y}^2\right)\left(1 - \frac{\mathbf{k}_{\mathbf{n},y}^2}{k_\mathbf{n}^2}\right)\\ +\left(s_{1z}^2 + 2s_{1z}s_{2z}C_{12,\tilde{\mathbf{n}}} + s_{2z}^2\right)\left(1 - \frac{\mathbf{k}_{\mathbf{n},z}^2}{k_\mathbf{n}^2}\right)\end{array}\right\}\frac{\sigma_q^2}{2}\right]\\
&= I_{1x2x}I_{1y2y}I_{1z2z}
\end{aligned}
\tag{49}
$$

where

$$
\begin{aligned}
&I_{1x2x} \equiv \frac{1}{(2\pi)^2}\int_{-\infty}^{\infty} ds_{1x}\int_{-\infty}^{\infty} ds_{2x}\\
&\exp\left[-\frac{1}{\left(L_xL_yL_z\right)}\sum_{n_x,n_y,n_z=-\infty}^{\infty}\left(s_{1x}^2 + 2s_{1x}s_{2x}C_{12,\mathbf{n}} + s_{2x}^2\right)\left(1 - \frac{\mathbf{k}_{\mathbf{n},x}^2}{k_\mathbf{n}^2}\right)\frac{\sigma_\mathbf{n}^2}{2} + is_{1x}E_{1x} + is_{2x}E_{2x}\right],
\end{aligned}
\tag{50}
$$

$$
\begin{aligned}
&I_{1y2y} \equiv \frac{1}{(2\pi)^2}\int_{-\infty}^{\infty} ds_{1y}\int_{-\infty}^{\infty} ds_{2y}\\
&\exp\left[-\frac{1}{\left(L_xL_yL_z\right)}\sum_{n_x,n_y,n_z=-\infty}^{\infty}\left(s_{1y}^2 + 2s_{1y}s_{2y}C_{12,\mathbf{n}} + s_{2y}^2\right)\left(1 - \frac{\mathbf{k}_{\mathbf{n},y}^2}{k_\mathbf{n}^2}\right)\frac{\sigma_\mathbf{n}^2}{2} + is_{1y}E_{1y} + is_{2y}E_{2y}\right],
\end{aligned}
\tag{51}
$$

$$I_{1z2z} \equiv \frac{1}{(2\pi)^2}\int_{-\infty}^{\infty} ds_{1z}\int_{-\infty}^{\infty} ds_{2z} \exp\left[\begin{array}{c} is_{1z}E_{1z} + is_{2z}E_{2z} \\ -\frac{1}{\left(L_xL_yL_z\right)}\sum_{n_x,n_y,n_z=-\infty}^{\infty}\left(s_{1z}^2 + 2s_{1z}s_{2z}C_{12,\mathbf{n}} + s_{2z}^2\right)\left(1-\frac{\mathbf{k}_{\mathbf{n},z}^2}{k_{\mathbf{n}}^2}\right)\frac{\sigma_{\mathbf{n}}^2}{2} \end{array}\right]. \tag{52}$$

Now to evaluate one of these integrals, it does not matter which we pick, as they all have the same form. Choosing I_{1x2x}, we can first complete the square in s_{1x}, then integrate over s_{1x}, followed by completing the square in s_{2x}, and then integrating over s_{2x}.

$$I_{1x2x} = \frac{1}{(2\pi)^2}\int_{-\infty}^{\infty} ds_{1x}\int_{-\infty}^{\infty} ds_{2x} \exp\left[\begin{array}{c} -s_{1x}^2\frac{1}{\left(L_xL_yL_z\right)}\sum_{n_x,n_y,n_z=-\infty}^{\infty}K_{\mathbf{n},x}^2\frac{\sigma_{\mathbf{n}}^2}{2} \\ +s_{1x}\left(iE_{1x} - 2s_{2x}\frac{1}{\left(L_xL_yL_z\right)}\sum_{n_x,n_y,n_z=-\infty}^{\infty}C_{12,\mathbf{n}}K_{\mathbf{n}}^2\frac{\sigma_{\mathbf{n}}^2}{2}\right) \\ +is_{2x}E_{2x} \quad -s_{2x}^2\frac{1}{\left(L_xL_yL_z\right)}\sum_{n_x,n_y,n_z=-\infty}^{\infty}K_{\mathbf{n},\mathbf{x}}^2\frac{\sigma_{\mathbf{n}}^2}{2} \end{array}\right] \tag{53}$$

where

$$K_{\mathbf{n},x}^2 \equiv \left(1-\frac{\mathbf{k}_{\mathbf{n},x}^2}{k_{\mathbf{n}}^2}\right). \tag{54}$$

Let

$$A_x \equiv \frac{1}{\left(L_xL_yL_z\right)}\sum_{n_x,n_y,n_z=-\infty}^{\infty}K_{\mathbf{n},x}^2\sigma_{\mathbf{n}}^2 \tag{55}$$

and

$$B_x \equiv \left(iE_{1x} - \frac{s_{2x}}{\left(L_xL_yL_z\right)}\sum_{n_x,n_y,n_z=-\infty}^{\infty}C_{12,\mathbf{n}}K_{\mathbf{n},x}^2\sigma_{\mathbf{n}}^2\right), \tag{56}$$

where $C_{12,\mathbf{n}}$ was defined in **Eq. 47**. Then:

$$I_{1x2x} = \frac{1}{(2\pi)^2}\int_{-\infty}^{\infty} ds_{1x}\int_{-\infty}^{\infty} ds_{2x}\exp\left[-\frac{1}{2}s_{1x}^2A_x + s_{1x}B_x + is_{2x}E_{2x} - \frac{1}{2}s_{2x}^2A_x\right]$$
$$= \frac{1}{(2\pi)^2}\int_{-\infty}^{\infty} ds_{2x}\exp\left(is_{2x}E_{2x} - \frac{1}{2}s_{2x}^2A_x\right)\times\int_{-\infty}^{\infty} ds_{1x}\exp\left(-\frac{1}{2}s_{1x}^2A_x + s_{1x}B_x\right) \tag{57}$$

Completing the square with

$$-\mathfrak{u}u^2 + \mathfrak{B}u = -\left(\mathfrak{u}u^2 - \mathfrak{B}u\right) = -\left(\sqrt{\mathfrak{u}}\,u - \frac{\mathfrak{B}}{2\sqrt{\mathfrak{u}}}\right)^2 + \frac{\mathfrak{B}^2}{4\mathfrak{u}}\ , \tag{58}$$

results in:

$$I_{1x2x} = \frac{1}{(2\pi)^2}\int_{-\infty}^{\infty} ds_{2x}\exp\left(is_{2x}E_{2x} - \frac{1}{2}s_{2x}^2A_x\right)$$
$$\times\left\{\exp\left(\frac{B_x^2}{2A_x}\right)\int_{-\infty}^{\infty} ds_{1x}\exp\left[-\left(\sqrt{\frac{A_x}{2}}s_{1x} - \frac{B_x}{2\sqrt{\frac{A_x}{2}}}\right)^2\right]\right\}$$
$$= \frac{1}{(2\pi)^2}\int_{-\infty}^{\infty} ds_{2x}\exp\left(is_{2x}E_{2x} - \frac{1}{2}s_{2x}^2A_x\right)\left[\exp\left(\frac{B_x^2}{2A_x}\right)\frac{\sqrt{\pi}}{\left(\frac{1}{2}A_x\right)^{1/2}}\right]. \tag{59}$$

To now carry out the integration over s_2, B_x in **Eq. 56** must be expanded, as B_x contains s_2. Also, let

$$C_x \equiv \frac{1}{\left(L_xL_yL_z\right)}\sum_{n_x,n_y,n_z=-\infty}^{\infty}C_{12,\mathbf{n}}K_{\mathbf{n},x}^2\sigma_{\mathbf{n}}^2, \tag{60}$$

so that

$$B_x \equiv iE_{1x} - s_{2x}C_x. \tag{61}$$

Then:

$$I_{1x2x} = \frac{\sqrt{2\pi}}{(2\pi)^2}\frac{1}{A_x^{1/2}}\int_{-\infty}^{\infty} ds_{2x}\exp\left(is_{2x}E_{2x} - \frac{1}{2}s_{2x}^2A_x\right)$$
$$\times\exp\left[\frac{1}{2A_x}(iE_{1x} - s_{2x}C_x)^2\right]$$
$$= \frac{1}{(2\pi)^{3/2}A_x^{1/2}}\int_{-\infty}^{\infty} ds_{2x}\exp\left(is_{2x}E_{2x} - \frac{1}{2}s_{2x}^2A_x\right)$$
$$\times\exp\left[-\frac{E_{1x}^2}{2A_x} - \frac{s_{2x}iE_{1x}C_x}{A_x} + \frac{s_{2x}^2C_x^2}{2A_x}\right]$$
$$= \frac{1}{(2\pi)^{3/2}A_x^{1/2}}\int_{-\infty}^{\infty} ds_{2x}\exp\left\{-s_{2x}^2\left[\frac{1}{2}A_x - \frac{C_x^2}{2A_x}\right]\right.$$
$$\left. + s_{2x}\left(iE_{2x} - \frac{iE_{1x}C_x}{A_x}\right) - \frac{E_{1x}^2}{2A_x}\right\}.$$

Applying **Eq. 58** again:

$$I_{1x2x} = \frac{\exp\left(-\frac{E_{1x}^2}{2A_x}\right)}{(2\pi)^{3/2}A_x^{1/2}}\int_{-\infty}^{\infty} ds_{2x}$$
$$\times\exp\left(-\left[s_{2x}\left(\frac{A_x}{2} - \frac{C_x^2}{2A_x}\right)^{1/2} - \frac{\left(iE_{2x} - \frac{iE_{1x}C_x}{A_x}\right)}{2\left(\frac{A_x}{2} - \frac{C_x^2}{2A_x}\right)^{1/2}}\right]^2 + \frac{\left(iE_{2x} - \frac{iE_{1x}C_x}{A_x}\right)^2}{4\left(\frac{A_x}{2} - \frac{C_x^2}{2A_x}\right)}\right)$$
$$= \frac{\exp\left(-\frac{E_{1x}^2}{2A_x}\right)}{(2\pi)^{3/2}A_x^{1/2}}\frac{\sqrt{\pi}}{\left[\frac{1}{2}A_x - \frac{C_x^2}{2A_x}\right]^{1/2}}\exp\left\{-\frac{\left(E_{2x} - \frac{E_{1x}C_x}{A_x}\right)^2}{4\left[\frac{1}{2}A_x - \frac{C_x^2}{2A_x}\right]}\right\}$$
$$= \frac{1}{2\pi A_x\left(1-\frac{C_x^2}{A_x^2}\right)^{1/2}}\exp\left[\frac{-E_{1x}^2 - E_{2x}^2 + 2E_{2x}E_{1x}\frac{C_x}{A_x}}{2A_x\left(1-\frac{C_x^2}{A_x^2}\right)}\right] \tag{62}$$

As will be discussed in more detail in **Section 2.4**, our deduction of **Eq. 62** is actually a multivariate normal (Gaussian) distribution involving E_{1x} and E_{2x}. Moreover, this distribution depends on the spatial and time differences, $(\mathbf{x}_1 - \mathbf{x}_2)$ and $(t_1 - t_2)$, between the two space time points, through the quantity C_x. Moreover, since I_{1x2x}, I_{1y2y}, and I_{1z2z} will all have the same form as in **Eq. 62**, and the final probability density $P(\mathbf{E}_1 \text{ at } \mathbf{x}_1, t_1; \mathbf{E}_2 \text{ at } \mathbf{x}_2, t_2)$ in **Eq. 49** is just the product $I_{1x2x} \cdot I_{1y2y} \cdot I_{1z2z}$, then we will have obtained a multivariate normal distribution involving six field values at two points in space and time: $E_{1x}, E_{1y}, E_{1z}, E_{2x}, E_{2y}$, and E_{2z}. Again, these points will be made clearer in **Section 2.4**.

2.3 Checks on Behavior of I_{1x2x}

To be a probability density for E_{1x} and E_{2x}, as given by I_{1x2x}, certain probabilistic properties must hold. We will examine some of them here, such as

$$\int_{-\infty}^{\infty} \mathrm{d}E_{2x} \int_{-\infty}^{\infty} \mathrm{d}E_{1x} I_{1x2x}$$

should equal unity. Checking:

$$\begin{aligned}
&\int_{-\infty}^{\infty} dE_{2x} \int_{-\infty}^{\infty} dE_{1x} I_{1x2x} = \int_{-\infty}^{\infty} dE_{2x} \int_{-\infty}^{\infty} dE_{1x} \frac{1}{2\pi A_x \left(1 - \frac{C_x^2}{A_x^2}\right)^{1/2}} \\
&\times \exp\left\{ \frac{-E_{1x}^2 - E_{2x}^2 + 2E_{2x}E_{1x}\frac{C_x}{A_x}}{2A_x\left(1 - \frac{C_x^2}{A_x^2}\right)} \right\} \\
&= \frac{1}{2\pi A_x \left(1 - \frac{C_x^2}{A_x^2}\right)^{1/2}} \int_{-\infty}^{\infty} dE_{2x} \exp\left[- \frac{E_{2x}^2}{2A_x\left(1 - \frac{C_x^2}{A_x^2}\right)} \right] \\
&\times \int_{-\infty}^{\infty} dE_{1x} \exp\left[\frac{-\left(E_{1x} - E_{2x}\frac{C_x}{A_x}\right)^2 + E_{2x}^2 \frac{C_x^2}{A_x^2}}{2A_x\left(1 - \frac{C_x^2}{A_x^2}\right)} \right] \\
&= \frac{1}{2\pi A_x \left(1 - \frac{C_x^2}{A_x^2}\right)^{1/2}} \int_{-\infty}^{\infty} dE_{2x} \exp\left[\frac{-E_{2x}^2}{2A_x\left(1 - \frac{C_x^2}{A_x^2}\right)} \right] \\
&\times \exp\left[\frac{+E_{2x}^2 \frac{C_x^2}{A_x^2}}{2A_x\left(1 - \frac{C_x^2}{A_x^2}\right)} \right] \times \int_{-\infty}^{\infty} dE_{1x} \exp\left[\frac{-\left(E_{1x} - E_{2x}\frac{C_x}{A_x}\right)^2}{2A_x\left(1 - \frac{C_x^2}{A_x^2}\right)} \right] \\
&= \frac{1}{2\pi A_x \left(1 - \frac{C_x^2}{A_x^2}\right)^{1/2}} \int_{-\infty}^{\infty} dE_{2x} \exp\left(- \frac{E_{2x}^2}{2A_x} \right) \left[\sqrt{\pi} \sqrt{2A_x\left(1 - \frac{C_x^2}{A_x^2}\right)} \right] \\
&= \frac{1}{\sqrt{2\pi A_x}} \int_{-\infty}^{\infty} dE_{2x} \exp\left(- \frac{E_{2x}^2}{2A_x} \right) = \frac{1}{\sqrt{2\pi A_x}} \sqrt{\pi 2A_x} = 1 \ ,
\end{aligned} \tag{63}$$

so this is fine.

Another check is whether

$$\int_{-\infty}^{\infty} \mathrm{d}E_{2i} I_{1i2i} = P(E_{1i}), \tag{64}$$

and of course the opposite situation of $\int_{-\infty}^{\infty} \mathrm{d}E_{1i} I_{1i2i} = P(E_{2i})$. In **Eq. 64**, we have already deduced from earlier work, including **Eq. 34**, that

$$P(E_i \text{ at } \mathbf{x}_1, t_1) = \frac{\exp\left[- \frac{E_i^2}{2\langle E_{\mathrm{ZPP},i}^2 \rangle} \right]}{\sqrt{2\pi \langle E_{\mathrm{ZPP},i}^2 \rangle}}. \tag{65}$$

As shown earlier, **Eq. 65** turns out to be independent of $\mathbf{x}_1, t_1$, where $i = 1, 2, 3$ refers to x, y, z, respectively. Mathematically, this independence on $\mathbf{x}_1, t_1$ arises because $\langle E_{\mathrm{ZPP},i}^2 \rangle$ is independent of $\mathbf{x}_1, t_1$, as seen in **Eq. 32**. A more "physical" view of this result is that the stochastic properties of the ZP and ZPP fields are homogeneous and isotropic in space and independent of time origin. In any case, from **Eqs. 32**, **54**, and **55**, and if we generalize A_x to A_i for $i = 1, 2,$ and 3, to include all three x, y, z cases, then:

$$\langle E_{\mathrm{ZPP},i}^2 \rangle = \frac{1}{\left(L_x L_y L_z\right)} \sum_{n_x, n_y, n_z = -\infty}^{\infty} \left(1 - \frac{\mathbf{k}_{\mathbf{n},i}^2}{k_{\mathbf{n}}^2}\right) \sigma_{\mathbf{n}}^2 = A_i. \tag{66}$$

Returning to **Eq. 64** and using **50**:

$$\begin{aligned}
&\int_{-\infty}^{\infty} dE_{2i} I_{1i2i} = \frac{\exp\left[\frac{-E_{1i}^2}{2A_i\left(1 - \frac{C_i^2}{A_i^2}\right)} \right]}{2\pi A_i \left(1 - \frac{C_i^2}{A_i^2}\right)^{1/2}} \int_{-\infty}^{\infty} dE_{2i} \exp\left[\frac{-E_{2i}^2 + 2E_{2i}E_{1i}\frac{C_i}{A_i}}{2A_i\left(1 - \frac{C_i^2}{A_i^2}\right)} \right] \\
&= \frac{\exp\left[\frac{-E_{1i}^2}{2A_i\left(1 - \frac{C_i^2}{A_i^2}\right)} \right]}{2\pi A_i \left(1 - \frac{C_i^2}{A_i^2}\right)^{1/2}} \exp\left[\frac{E_{1i}^2 \frac{C_i^2}{A_i^2}}{2A_i\left(1 - \frac{C_i^2}{A_i^2}\right)} \right] \int_{-\infty}^{\infty} dE_{2i} \\
&\times \exp\left[- \left(\frac{1}{\sqrt{2A_i\left(1 - \frac{C_i^2}{A_i^2}\right)}} E_{2i} - \frac{E_{1i}\frac{C_i}{A_i}}{\sqrt{2A_i\left(1 - \frac{C_i^2}{A_i^2}\right)}} \right)^2 \right] \\
&= \frac{1}{2\pi A_i \left(1 - \frac{C_i^2}{A_i^2}\right)^{1/2}} \exp\left[\frac{-E_{1i}^2}{2A_i} \right] \sqrt{\pi 2A_i\left(1 - \frac{C_i^2}{A_i^2}\right)} \\
&= \frac{1}{\sqrt{2\pi A_i}} \exp\left[\frac{-E_{1i}^2}{2A_i} \right] = \frac{\exp\left[- \frac{E_{1i}^2}{2\langle E_{\mathrm{ZPP},1i}^2 \rangle} \right]}{\sqrt{2\pi \langle E_{\mathrm{ZPP},1i}^2 \rangle}},
\end{aligned}$$

using **Eq. 66** at the end. By symmetry, $\int_{-\infty}^{\infty} \mathrm{d}E_{1i} I_{1i2i} = P(E_{2i})$ then also holds.

Another obvious item to check is whether $\int_{-\infty}^{\infty} \mathrm{d}E_{2x} \int_{-\infty}^{\infty} \mathrm{d}E_{1x} E_{1x} I_{1x2x} = 0$ (or *vice versa* $\langle E_{2x} \rangle = 0$, by symmetry):

$$\int_{-\infty}^{\infty} dE_{2x} \int_{-\infty}^{\infty} dE_{1x} E_{1x} I_{1x2x} = \frac{1}{2\pi A_x \left(1 - \frac{C_x^2}{A_x^2}\right)^{1/2}} \int_{-\infty}^{\infty} dE_{2x} \times \exp\left(- \frac{E_{2x}^2}{2A_x \left(1 - \frac{C_x^2}{A_x^2}\right)} \right) \int_{-\infty}^{\infty} dE_{1x} E_{1x} \exp\left[\frac{-E_{1x}^2 + 2E_{2x} E_{1x} \frac{C_x}{A_x}}{2A_x \left(1 - \frac{C_x^2}{A_x^2}\right)} \right]$$

$$= \frac{1}{2\pi A_x \left(1 - \frac{C_x^2}{A_x^2}\right)^{1/2}} \int_{-\infty}^{\infty} dE_{2x} \exp\left(- \frac{E_{2x}^2}{2A_x \left(1 - \frac{C_x^2}{A_x^2}\right)} \right) \int_{-\infty}^{\infty} dE_{1x} E_{1x} \times \exp\left[\frac{-\left(E_{1x} - E_{2x} \frac{C_x}{A_x}\right)^2 + E_{2x}^2 \frac{C_x^2}{A_x^2}}{2A_x \left(1 - \frac{C_x^2}{A_x^2}\right)} \right] = \frac{1}{2\pi A_x \left(1 - \frac{C_x^2}{A_x^2}\right)^{1/2}} \int_{-\infty}^{\infty} dE_{2x} \times \exp\left(- \frac{E_{2x}^2}{2A_x} \right) \int_{-\infty}^{\infty} dE_{1x} E_{1x} \exp\left[\frac{-\left(E_{1x} - E_{2x} \frac{C_x}{A_x}\right)^2}{2A_x \left(1 - \frac{C_x^2}{A_x^2}\right)} \right]. \tag{67}$$

In the integral on the far right, bottom line, let $E_{1x} - E_{2x} \frac{C_x}{A_x} = u$ and $\mathrm{d}u = \mathrm{d}E_{1x}$:

$$\int_{-\infty}^{\infty} dE_{2x} \int_{-\infty}^{\infty} dE_{1x} E_{1x} I_{1x2x} = \frac{1}{2\pi A_x \left(1 - \frac{C_x^2}{A_x^2}\right)^{1/2}} \int_{-\infty}^{\infty} dE_{2x} \exp\left(- \frac{E_{2x}^2}{2A_x} \right) \times \int_{-\infty}^{\infty} du \left(u + E_{2x} \frac{C_x}{A_x} \right) \exp\left[\frac{-u^2}{2A_x \left(1 - \frac{C_x^2}{A_x^2}\right)} \right]$$

$$= \frac{1}{2\pi A_x \left(1 - \frac{C_x^2}{A_x^2}\right)^{1/2}} \int_{-\infty}^{\infty} dE_{2x} \times \exp\left(- \frac{E_{2x}^2}{2A_x} \right) \left\{ 0 + E_{2x} \frac{C_x}{A_x} \left[\pi 2A_x \left(1 - \frac{C_x^2}{A_x^2}\right) \right]^{1/2} \right\} = \frac{\frac{C_x}{A_x}}{(2\pi A_x)^{1/2}} \int_{-\infty}^{\infty} dE_{2x} E_{2x} \exp\left(- \frac{E_{2x}^2}{2A_x} \right) = 0 \ , \tag{68}$$

since the integral is odd in E_{2x}.

Now trying a check that is more involved, we will compute a 2-point correlation function in the fields, using the probability density I_{1x2x}. We will calculate an example, along the lines of Ref. [24], but also carrying the calculations to a final analytical expression, more along [7, 35]. Hence, this will be an example, with of course many other two point sets of coordinates in time and space that could be carried out, but even this single example is nontrivial to carry out. Most importantly, however, this example shows how to carry out the analysis in Ref. [24] *via* the probability density method discussed here.

Following roughly along Refs. [24, 35], and [7], then:

$$\begin{aligned}
&\langle E_{\mathrm{ZPP},x}(0,0) E_{\mathrm{ZPP},x}(\hat{\mathbf{y}}R, t) \rangle \\
&= \left(\frac{1}{\left(L_x L_y L_z\right)^{1/2}} \right)^2 \sum_{n_x, n_y, n_z = -\infty}^{\infty} \sum_{\lambda=1,2} \left(\hat{\varepsilon}_{\mathbf{k_n}\lambda}\right)_x \sum_{n_x', n_y', n_z' = -\infty}^{\infty} \sum_{\lambda'=1,2} \left(\hat{\varepsilon}_{\mathbf{k}_{\mathbf{n}'}\lambda'} \right)_x \times \\
&\times \left\langle \begin{array}{c} \left[A_{\mathbf{k_n}\lambda} \cos\left(\mathbf{k_n} \cdot 0 - \omega_{\mathbf{n}} 0\right) + B_{\mathbf{k_n}\lambda} \sin\left(\mathbf{k_n} \cdot 0 - \omega_{\mathbf{n}} 0\right) \right] \times \\ \times \left[A_{\mathbf{k}_{\mathbf{n}'}\lambda'} \cos\left(\mathbf{k}_{\mathbf{n}'} \cdot \hat{\mathbf{y}} R - \omega_{\mathbf{n}'} t\right) + B_{\mathbf{k}_{\mathbf{n}'}\lambda'} \sin\left(\mathbf{k}_{\mathbf{n}'} \cdot \hat{\mathbf{y}} R - \omega_{\mathbf{n}'} t\right) \right] \end{array} \right\rangle \\
&= \frac{1}{\left(L_x L_y L_z\right)} \sum_{\substack{n_x, n_y, n_z = -\infty \\ \lambda=1,2}}^{\infty} \left(\hat{\varepsilon}_{\mathbf{k_n},\lambda}\right)_x \sum_{\substack{n_x', n_y', n_z' = -\infty \\ \lambda'=1,2}}^{\infty} \left(\hat{\varepsilon}_{\mathbf{k}_{\mathbf{n}'},\lambda'} \right)_x \delta_{\mathbf{n}_{\mathbf{n}'}} \delta_{\lambda,\lambda'} \cos\left(\mathbf{k}_{\mathbf{n}'} \cdot \hat{\mathbf{y}} R \right. \\
&\quad \left. - \omega_{\mathbf{n}'} t\right) \sigma^2\left(\omega_{\mathbf{n}}, T\right) \\
&= \frac{1}{\left(L_x L_y L_z\right)} \sum_{n_x, n_y, n_z = -\infty}^{\lambda=1,2} \left(\hat{\varepsilon}_{\mathbf{k_n},\lambda}\right)_x^2 \cos\left(\mathbf{k_n} \cdot \hat{\mathbf{y}} R - \omega_{\mathbf{n}} t\right) \sigma^2\left(\omega_{\mathbf{n}}, T\right) \\
&= \frac{1}{\left(L_x L_y L_z\right)} \sum_{n_x, n_y, n_z = -\infty}^{\infty} \left[1 - \left(\frac{\mathbf{k}_{\mathbf{n},x}}{k_{\mathbf{n}}} \right)^2 \right] \cos\left(\mathbf{k}_{\mathbf{n},y} R - \omega_{\mathbf{n}} t \right) \sigma^2\left(\omega_{\mathbf{n}}, T\right)
\end{aligned} \tag{69}$$

Making the change of discrete to continuous variables, with $\mathbf{k_n} = \frac{2\pi n_x}{L_x} \hat{\mathbf{x}} + \frac{2\pi n_y}{L_y} \hat{\mathbf{y}} + \frac{2\pi n_z}{L_z} \hat{\mathbf{z}}$, for large values of L_x, L_y, L_z, with

$$\Delta n_x \approx \frac{L_x}{2\pi} \mathrm{d}k_x, \Delta n_y \approx \frac{L_y}{2\pi} \mathrm{d}k_y, \Delta n_z \approx \frac{L_z}{2\pi} \mathrm{d}k_z \tag{70}$$

enables integrals to be carried out. Moreover, although the ZPP spectrum in the integral could be evaluated, the ZP spectrum is certainly much easier to do so analytically. Since this is just an example, we will proceed with restriction to the ZP case, or $[\sigma(\omega, T)]^2 \rightarrow 2\pi\hbar\omega = 2\pi\hbar kc$:

$$\begin{aligned}
&\langle E_{\mathrm{ZP},x}(0,0) E_{\mathrm{ZP},x}(\hat{\mathbf{y}}R, t) \rangle \\
&\approx \frac{1}{(2\pi)} \int_{-\infty}^{\infty} dk_x \frac{1}{(2\pi)} \int_{-\infty}^{\infty} dk_y \frac{1}{(2\pi)} \int_{-\infty}^{\infty} dk_z \left[1 - \left(\frac{\mathbf{k}_{\mathbf{n},x}}{k_{\mathbf{n}}} \right)^2 \right] \\
&\times \cos\left(k_y R - \omega t\right) 2\pi\hbar\omega \\
&= \frac{2\pi\hbar}{(2\pi)^3} \int_{-\infty}^{\infty} dk_x \int_{-\infty}^{\infty} dk_y \int_{-\infty}^{\infty} dk_z kc \left[1 - \left(\frac{k_x}{k} \right)^2 \right] \\
&\times \left[\cos\left(k_y R\right) \cos\left(\omega t\right) + \sin\left(k_y R\right) \sin\left(\omega t\right) \right].
\end{aligned}$$

The second term of $\sin(k_y R)\sin(\omega t)$ makes the integrand odd in k_y. Hence:

$$\langle E_{\mathrm{ZP},x}(0,0) E_{\mathrm{ZP},x}(\hat{\mathbf{y}}R, t) \rangle = \frac{\hbar c}{(2\pi)^2} \int_{-\infty}^{\infty} \mathrm{d}k_x \int_{-\infty}^{\infty} \mathrm{d}k_y \int_{-\infty}^{\infty} \mathrm{d}k_z \times K \left[1 - \left(\frac{k_x}{k} \right)^2 \right] \cos\left(k_y R\right) \cos\left(kct\right).$$

Next, we will make k_y be the axis where the polar angle is measured from, so that $k_y = k\cos\theta$. Consequently, $k_x = k\sin\theta\sin\phi$ and $k_z = k\sin\theta\cos\phi$. Hence:

$$\langle E_{\mathrm{ZP},x}(0,0) E_{\mathrm{ZP},x}(\hat{\mathbf{y}}R, t) \rangle = \frac{\hbar c}{(2\pi)^2} \int_0^{\infty} \mathrm{d}k k^2 \int_0^{\pi} \mathrm{d}\theta \sin\theta \times \int_0^{2\pi} \mathrm{d}\phi k \left[1 - \sin^2\theta \sin^2\phi \right] \cos\left(R k \cos\theta\right) \cos\left(kct\right). \tag{71}$$

Since

$$\frac{1}{2\pi}\int_0^{2\pi} \mathrm{d}\phi \sin^2\phi = \frac{1}{2},$$

then:

$$\langle E_{ZP,x}(0,0)E_{ZP,x}(\hat{\mathbf{y}}R,t)\rangle = \frac{\hbar c\pi}{(2\pi)^2}\int_0^{\infty}\mathrm{d}k k^3\cos(kct)\int_0^{\pi}\mathrm{d}\theta\sin\theta[2-\sin^2\theta]\cos(Rk\cos\theta). \tag{72}$$

Using

$$\int_0^{\pi}\mathrm{d}\theta\sin\theta[2-\sin^2\theta]\cos(Rk\cos\theta) = 2\int_0^{\pi}\mathrm{d}\theta\sin\theta\cos(Rk\cos\theta) - \int_0^{\pi}\mathrm{d}\theta\sin^3\theta\cos(Rk\cos\theta), \tag{73}$$

with $u = Rk\cos\theta$, $du = -Rk\sin\theta d\theta$, the first term in **Eq. 73** becomes:

$$2\int_0^{\pi}\mathrm{d}\theta\sin\theta\cos(Rk\cos\theta) = 2\int_{Rk}^{-Rk}\left(-\frac{\mathrm{d}u}{Rk}\right)\cos(u) = -\frac{2}{Rk}\sin u\Big|_{Rk}^{-Rk} = \frac{4}{Rk}\sin(Rk). \tag{74}$$

The second term in **Eq. 73** becomes:

$$\begin{aligned}
&-\int_0^{\pi} d\theta\sin^3\theta\cos(Rk\cos\theta) = -\int_{-Rk}^{+Rk}\frac{du}{Rk}[1-\cos^2\theta]\cos(u)\\
&= -\frac{1}{Rk}\int_{-Rk}^{+Rk} du\cos(u) + \frac{1}{(Rk)^3}\int_{-Rk}^{+Rk} du\cdot u^2\cos(u)\\
&= -\frac{1}{Rk}\sin(u)\Big|_{-Rk}^{Rk} + \frac{1}{(Rk)^3}\left[4Rk\cos(Rk) - 4\sin(Rk) + 2(Rk)^2\sin(Rk)\right]\\
&= +\frac{4}{(Rk)^2}\cos(Rk) - \frac{4}{(Rk)^3}\sin(Rk)\ .
\end{aligned} \tag{75}$$

From **Eqs. 73–75**:

$$\begin{aligned}
&\int_0^{\pi}\mathrm{d}\theta\sin\theta[2-\sin^2\theta]\cos(Rk\cos\theta) = 2\int_0^{\pi}\mathrm{d}\theta\sin\theta\cos(Rk\cos\theta)\\
&-\int_0^{\pi}\mathrm{d}\theta\sin^3\theta\cos(Rk\cos\theta) = \frac{4}{Rk}\sin(Rk) + \frac{4}{(Rk)^2}\cos(Rk)\\
&-\frac{4}{(Rk)^3}\sin(Rk).
\end{aligned}$$

Consequently, **Eq. 72** becomes:

$$\begin{aligned}
&\langle E_{ZP,x}(0,0)E_{ZP,x}(\hat{\mathbf{y}}R,t)\rangle = \frac{\hbar c\pi}{(2\pi)^2}\int_0^{\infty}\mathrm{d}k k^3\cos(kct)\\
&\left[\frac{4}{Rk}\sin(Rk) + \frac{4}{(Rk)^2}\cos(Rk) - \frac{4}{(Rk)^3}\sin(Rk)\right]\\
&= \frac{\hbar c\pi}{(2\pi)^2}\frac{1}{R^4}\int_0^{\infty}\mathrm{d}w w^3\cos\left(w\frac{ct}{R}\right)\\
&\times\left[\frac{4}{w}\sin(w) + \frac{4}{w^2}\cos(w) - \frac{4}{w^3}\sin(w)\right].
\end{aligned} \tag{76}$$

Substituting $\frac{ct}{R} = b$, and using an integral table [36] (p. 504, No. 8), also discussed in the limiting sense in Ref. [7], Appendix C:

$$\int_0^{\infty}\mathrm{d}w\cos(wb)\sin(w) = \frac{1}{(1-b^2)}, \tag{77}$$

$$\int_0^{\infty}\mathrm{d}w w\cos(wb)\cos(w) = -\left[\frac{1}{(1-b^2)} + \frac{2b^2}{(1-b^2)^2}\right], \tag{78}$$

$$\int_0^{\infty}\mathrm{d}w w^2\cos(wb)\sin(w) = -2\left[\frac{1}{(1-b^2)} + \frac{5b^2}{(1-b^2)^2} + \frac{4b^4}{(1-b^2)^3}\right], \tag{79}$$

enables **Eq. 76** to be evaluated:

$$\begin{aligned}
&\langle E_{ZP,x}(0,0)E_{ZP,x}(\hat{\mathbf{y}}R,t)\rangle = \frac{\hbar c\pi}{(2\pi)^2}\frac{1}{R^4}4\left\{-2\left[\frac{1}{(1-b^2)}\right.\right.\\
&\left.\left.+\frac{5b^2}{(1-b^2)^2} + \frac{4b^4}{(1-b^2)^3}\right] - \left[\frac{1}{(1-b^2)} + \frac{2b^2}{(1-b^2)^2}\right] - \frac{1}{(1-b^2)}\right\}
\end{aligned} \tag{80}$$

$$\begin{aligned}
&= \frac{\hbar c\pi}{(2\pi)^2}\frac{1}{R^4}4\frac{1}{(1-b^2)^3}\left\{-2(1-b^2)^2 - 10b^2(1-b^2) - 8b^4\right.\\
&\left.-(1-b^2)^2 - 2b^2(1-b^2) - (1-b^2)^2\right\}\\
&= \frac{\hbar c\pi}{(2\pi)^2}\frac{1}{R^4}4\frac{1}{(1-b^2)^3}(-4b^2-4) = -4\frac{\hbar c\pi}{\pi^2}\frac{1}{R^4}\frac{\left[1+\left(\frac{ct}{R}\right)^2\right]}{\left(1-\left(\frac{ct}{R}\right)^2\right)^3}\\
&= -\frac{4\hbar c}{\pi}\frac{\left[R^2+(ct)^2\right]}{\left[R^2-(ct)^2\right]^3}
\end{aligned} \tag{81}$$

As mentioned earlier, unless $R = ct$, this two-point correlation function is not singular.

The above calculation has typically been, roughly, the means for calculating such "two-point correlation" functions in SED, or even "n-point correlation functions" [24]. We will proceed to calculate the same quantity as in **Eq. 81**, but by using the joint probability density function for two electric field values, I_{1x2x}, **Eq. 62**, deduced in **Section 2.2**. Of course the two results should agree, but it is interesting to see the difference in methods.

$$\begin{aligned}
&\langle E_{ZP,x}(0,0)E_{ZP,x}(\hat{\mathbf{y}}R,t)\rangle = \int_{-\infty}^{\infty} dE_{1x}\int_{-\infty}^{\infty} dE_{2x}E_{1x}E_{2x}I_{1x2x}\Big|_{\text{at }\mathbf{x}_1,t_1\ \&\ \mathbf{x}_2,t_2}\\
&= \int_{-\infty}^{\infty} dE_{1x}\int_{-\infty}^{\infty} dE_{2x}E_{1x}E_{2x}\\
&\left\{\frac{1}{2\pi A_x\left(1-\frac{C_x^2}{A_x^2}\right)^{1/2}}\left[\frac{-E_{1x}^2 - E_{2x}^2 + 2E_{2x}E_{1x}\left(\frac{C_x}{A_x}\right)}{2A_x\left(1-\frac{C_x^2}{A_x^2}\right)}\right]\right\}_{\mathbf{x}_1,t_1;\mathbf{x}_2,t_2}.
\end{aligned}$$

Here, the meaning of the subscript at the end of $\mathbf{x}_1, t_1; \mathbf{x}_2, t_2$ is that the two electric field points E_{1x} and E_{2x} are to be evaluated at the two space and time points, $\mathbf{x}_1, t_1$ and $\mathbf{x}_2, t_2$, respectively, in the function $C_{12,\mathbf{n}}$, **Eq. 47**, contained within C_x, in **Eq. 60**.

Thus,

$$\int_{-\infty}^{\infty} dE_{2x} \int_{-\infty}^{\infty} dE_{1x} (E_{1x}E_{2x}) I_{1x2x}$$

$$= \left\{ \frac{1}{2\pi A_x \left(1 - \frac{C_x^2}{A_x^2}\right)^{1/2}} \int_{-\infty}^{\infty} dE_{2x} E_{2x} \exp\left[- \frac{E_{2x}^2}{2A_x\left(1 - \frac{C_x^2}{A_x^2}\right)} \right] \times \right.$$
$$\left. \times \int_{-\infty}^{\infty} dE_{1x} E_{1x} \exp\left[\frac{-E_{1x}^2 + 2E_{2x}E_{1x}\frac{C_x}{A_x}}{2A_x\left(1 - \frac{C_x^2}{A_x^2}\right)} \right] \right\}_{\mathbf{x}_1,t_1;\mathbf{x}_2,t_2}$$

$$= \left\{ \frac{1}{2\pi A_x \left(1 - \frac{C_x^2}{A_x^2}\right)^{1/2}} \int_{-\infty}^{\infty} dE_{2x} E_{2x} \exp\left[\frac{-E_{2x}^2 + E_{2x}^2\frac{C_x^2}{A_x^2}}{2A_x\left(1 - \frac{C_x^2}{A_x^2}\right)} \right] \times \right.$$
$$\left. \times \int_{-\infty}^{\infty} dE_{1x} E_{1x} \exp\left[\frac{-\left(E_{1x} - E_{2x}\frac{C_x}{A_x}\right)^2}{2A_x\left(1 - \frac{C_x^2}{A_x^2}\right)} \right] \right\}_{\mathbf{x}_1,t_1;\mathbf{x}_2,t_2}$$

$$= \left\{ \frac{1}{2\pi A_x \left(1 - \frac{C_x^2}{A_x^2}\right)^{1/2}} \int_{-\infty}^{\infty} dE_{2x} E_{2x} \exp\left(\frac{-E_{2x}^2}{2A_x} \right) \int_{-\infty}^{\infty} dE_{1x} E_{1x} \exp\left[\frac{-\left(E_{1x} - E_{2x}\frac{C_x}{A_x}\right)^2}{2A_x\left(1 - \frac{C_x^2}{A_x^2}\right)} \right] \right\}_{\mathbf{x}_1,t_1;\mathbf{x}_2,t_2}$$

The integral over E_{1x} on the right can be broken up as:

$$\int_{-\infty}^{\infty} dE_{1x} E_{1x} \exp\left[\frac{-\left(E_{1x} - E_{2x}\frac{C_x}{A_x}\right)^2}{2A_x\left(1 - \frac{C_x^2}{A_x^2}\right)} \right]_{\mathbf{x}_1,t_1;\mathbf{x}_2,t_2}$$
$$= \int_{-\infty}^{\infty} dE_{1x} \left\{ \left(E_{1x} - E_{2x}\frac{C_x}{A_x} \right) \exp\left[\frac{-\left(E_{1x} - E_{2x}\frac{C_x}{A_x}\right)^2}{2A_x\left(1 - \frac{C_x^2}{A_x^2}\right)} \right] \right\}_{\mathbf{x}_1,t_1;\mathbf{x}_2,t_2}$$
$$+ \int_{-\infty}^{\infty} dE_{1x} E_{2x} \left\{ \frac{C_x}{A_x} \exp\left[\frac{-\left(E_{1x} - E_{2x}\frac{C_x}{A_x}\right)^2}{2A_x\left(1 - \frac{C_x^2}{A_x^2}\right)} \right] \right\}_{\mathbf{x}_1,t_1;\mathbf{x}_2,t_2}$$
$$= \int_{-\infty}^{\infty} dx \cdot x \exp\left[\frac{-x^2}{2A_x\left(1 - \frac{C_x^2}{A_x^2}\right)} \right]_{\mathbf{x}_1,t_1;\mathbf{x}_2,t_2}$$
$$+ \left\{ E_{2x}\frac{C_x}{A_x} \int_{-\infty}^{\infty} dE_{1x} \exp\left[\frac{-\left(E_{1x} - E_{2x}\frac{C_x}{A_x}\right)^2}{2A_x\left(1 - \frac{C_x^2}{A_x^2}\right)} \right] \right\}_{\mathbf{x}_1,t_1;\mathbf{x}_2,t_2}$$

The first integral equals zero, as it is odd in x. Hence:

$$\int_{-\infty}^{\infty} \mathrm{d}E_{1x} E_{1x} \exp\left[\frac{-\left(E_{1x} - E_{2x}\frac{C_x}{A_x}\right)^2}{2A_x\left(1 - \frac{C_x^2}{A_x^2}\right)} \right]_{\mathbf{x}_1,t_1;\mathbf{x}_2,t_2}$$
$$= E_{2x} \left\{ \frac{C_x}{A_x} \left[\pi 2A_x \left(1 - \frac{C_x^2}{A_x^2} \right) \right]^{1/2} \right\}_{\mathbf{x}_1,t_1;\mathbf{x}_2,t_2}$$

and

$$\int_{-\infty}^{\infty} dE_{2x} \int_{-\infty}^{\infty} dE_{1x} (E_{1x}E_{2x}) I_{1x2x}$$
$$= \left[\frac{1}{2\pi A_x \left(1 - \frac{C_x^2}{A_x^2}\right)^{1/2}} \int_{-\infty}^{\infty} dE_{2x} E_{2x} \exp\left(- \frac{E_{2x}^2}{2A_x} \right) \right.$$
$$\left. \times \left\{ E_{2x}\frac{C_x}{A_x} \left[\pi 2A_x \left(1 - \frac{C_x^2}{A_x^2} \right) \right]^{1/2} \right\} \right]_{\mathbf{x}_1,t_1;\mathbf{x}_2,t_2}$$
$$= \left\{ \frac{1}{2\pi A_x \left(1 - \frac{C_x^2}{A_x^2}\right)^{1/2}} \int_{-\infty}^{\infty} dE_{2x} E_{2x}^2 \exp\left(- \frac{E_{2x}^2}{2A_x} \right) \frac{C_x}{A_x} \left[\pi 2A_x \left(1 - \frac{C_x^2}{A_x^2} \right) \right]^{1/2} \right\}_{\mathbf{x}_1,t_1;\mathbf{x}_2,t_2}$$
$$= \frac{1}{(2\pi A_x)^{1/2}} \frac{(C_x)_{\mathbf{x}_1,t_1;\mathbf{x}_2,t_2}}{A_x} \int_{-\infty}^{\infty} dE_{2x} E_{2x}^2 \exp\left(- \frac{E_{2x}^2}{2A_x} \right)$$
$$= \frac{1}{(2\pi A_x)^{1/2}} \frac{(C_x)_{\mathbf{x}_1,t_1;\mathbf{x}_2,t_2}}{A_x} \frac{\pi^{1/2}}{2} (2A_x)^{3/2} = (C_x)_{\mathbf{x}_1,t_1;\mathbf{x}_2,t_2}$$
$$= \frac{1}{\left(L_x L_y L_z\right)} \sum_{n_x,n_y,n_z=-\infty}^{\infty} (C_{12,\mathbf{n}})_{\mathbf{x}_1,t_1;\mathbf{x}_2,t_2} K_{\mathbf{n},x}^2 \sigma_{\mathbf{n}}^2.$$

The last expression for C_x came from **Eq. 60**.

Hence, using **Eqs. 47** and **54** replacing the coordinates $\mathbf{x}_1$ and t_1 with 0, 0, and $\mathbf{x}_2$ and t_2 with $\hat{\mathbf{y}}R$ and t, respectively, and $\sigma_{\mathbf{n}}^2$ with ZP of $2\pi\hbar\omega_{\mathbf{n},\lambda}$:

$$\int_{-\infty}^{\infty} \mathrm{d}E_{2x} \int_{-\infty}^{\infty} \mathrm{d}E_{1x} (E_{1x}E_{2x}) I_{1x2x}$$
$$= \frac{1}{\left(L_x L_y L_z\right)} \sum_{n_x,n_y,n_z=-\infty}^{\infty} \cos[\mathbf{k}_{\mathbf{n}} \cdot (\mathbf{x}_1 - \mathbf{x}_2) - \omega_{\mathbf{n}}(t_1 - t_2)] \left[1 - \left(\frac{\mathbf{k}_{\mathbf{n},x}}{k_{\mathbf{n}}} \right)^2 \right] \sigma_{\mathbf{n}}^2$$
$$= \frac{1}{\left(L_x L_y L_z\right)} \sum_{n_x,n_y,n_z=-\infty}^{\infty} \cos\left[k_y R - ckt \right] \left[1 - \left(\frac{\mathbf{k}_{\mathbf{n},x}}{k_{\mathbf{n}}} \right)^2 \right] 2\pi\hbar\omega_{\mathbf{n},\lambda} \ .$$

Implementing the same continuum approximation as with the other method, **Eq. 70**, then results in:

$$\int_{-\infty}^{\infty} dE_{2x} \int_{-\infty}^{\infty} dE_{1x} (E_{1x}E_{2x}) I_{1x2x} \approx \frac{1}{(2\pi)} \int_{-\infty}^{\infty} dk_x \frac{1}{(2\pi)} \int_{-\infty}^{\infty} dk_y \frac{1}{(2\pi)}$$
$$\times \int_{-\infty}^{\infty} dk_z \cos\left(k_y R - ckt \right) \left[1 - \left(\frac{k_x}{k} \right)^2 \right] 2\pi\hbar\omega$$
$$= \frac{1}{(2\pi)^3} \int_{-\infty}^{\infty} dk_x \int_{-\infty}^{\infty} dk_y \int_{-\infty}^{\infty} dk_z \left[\cos\left(k_y R \right) \cos(ckt) \right.$$
$$\left. + \sin\left(k_y R \right) \sin(ckt) \right] \left[1 - \left(\frac{k_x}{k} \right)^2 \right] 2\pi\hbar\omega$$

The second integral with $\sin(k_y R)$ is odd in k_y and equals zero by symmetry. Hence:

$$\int_{-\infty}^{\infty} dE_{2x} \int_{-\infty}^{\infty} dE_{1x}\,(E_{1x}E_{2x})I_{1x2x} = \frac{1}{(2\pi)^3} \int_{-\infty}^{\infty} dk_x \int_{-\infty}^{\infty} dk_y \times \int_{-\infty}^{\infty} dk_z \cos\left(k_y R\right)\cos(\omega t)\left[1-\left(\frac{k_x}{k}\right)^2\right] 2\pi\hbar\omega \tag{82}$$

$$= \frac{1}{(2\pi)^3} \int_0^{\infty} k^2 dk \int_0^{\pi} d\theta \sin\theta \int_0^{2\pi} d\phi \cos(kR\cos\theta)\cos(\omega t) \times \left(1-\sin^2\theta\sin^2\phi\right)(2\pi\hbar kc) = \frac{\hbar c}{(2\pi)^2} \int_0^{\infty} k^3 dk \int_0^{\pi} d\theta \sin\theta \tag{83}$$

$$\times \int_0^{2\pi} d\phi \cos(kR\cos\theta)\cos(\omega t)\left(1-\sin^2\theta\sin^2\phi\right).$$

However, this result agrees exactly with the earlier result, **Eq. 71**, obtained partway through the ensemble derivation of $\langle E_{\mathrm{ZP},x}(0,0)E_{\mathrm{ZP},x}(\hat{\mathbf{y}}R,t)\rangle$. Thus, continuing with further steps in evaluating **Eq. 83** will provide a final result, using the joint probability density approach of $\int_{-\infty}^{\infty} dE_{2x} \int_{-\infty}^{\infty} dE_{1x}\,(E_{1x}E_{2x})I_{1x2x}$, that exactly agrees with the ensemble derivation $\langle E_{\mathrm{ZP},x}(0,0)E_{\mathrm{ZP},x}(\hat{\mathbf{y}}R,t)\rangle$ of $-\frac{4\hbar c}{\pi}\frac{[R^2+(ct)^2]}{[R^2-(ct)^2]^3}$ in **Eq. 81**.

2.4 Multivariate Normal Distribution

Much of the work carried out here can be generalized using the multivariate normal distribution. The two key expressions for us here are the Fourier decomposition of the radiation fields in **Eqs. 1** and **2** not just because they are Fourier decompositions, but also that they are a linear sum of the random variables $A_{\mathbf{k_n},\lambda}$ and $B_{\mathbf{k_n},\lambda}$. To put this in better perspective, if we imagine an ensemble of boxes $L_x \times L_y \times L_z$, each the same size, but existing at different points in space and/or in time, then electromagnetic field fluctuations of $\mathbf{E}_{\mathrm{ZPP}}$ and $\mathbf{B}_{\mathrm{ZPP}}$ will occur at each point within each box. However, for each box, there is only one set of coefficients $A_{\mathbf{k_n},\lambda}$ and $B_{\mathbf{k_n},\lambda}$, as these coefficients do not change from the initial point of field evolution. However, as viewed over the entire ensemble of boxes, the coefficients are assumed to be independent random variables obeying Gaussian distributions. The mean for each, over the ensemble, is zero, as in **Eq. 4**, and the normal distribution for either $A_{\mathbf{k_n},\lambda}$ or $B_{\mathbf{k_n},\lambda}$ is given by **Eq. 8**, while the variance of each is given by $[\sigma(\omega_{\mathbf{n}},T)]^2$, as in **Eq. 8**.

Thus, $\mathbf{E}_{\mathrm{ZPP}}$ and $\mathbf{B}_{\mathrm{ZPP}}$ can be viewed as the linear transformation of the random variables $A_{\mathbf{k_n},\lambda}$ and $B_{\mathbf{k_n},\lambda}$. However, the coefficients multiplying $A_{\mathbf{k_n},\lambda}$ and $B_{\mathbf{k_n},\lambda}$ in these linear sums in **Eqs. 1** and **2** are not constants, as they depend on time and space. In particular, $\frac{1}{(L_xL_yL_z)^{1/2}}\hat{\boldsymbol{\varepsilon}}_{\mathbf{k_n},\lambda}\cos(\mathbf{k_n}\cdot\mathbf{x}-\omega_{\mathbf{n}}t)$ and $\frac{1}{(L_xL_yL_z)^{1/2}}\hat{\boldsymbol{\varepsilon}}_{\mathbf{k_n},\lambda}\sin(\mathbf{k_n}\cdot\mathbf{x}-\omega_{\mathbf{n}}t)$ are the coefficients multiplying the random variables of $A_{\mathbf{k_n},\lambda}$ and $B_{\mathbf{k_n},\lambda}$ for $\mathbf{E}(\mathbf{x},t)$ in **Eq. 1**. An exactly similar situation occurs for $A_{\mathbf{k_n},\lambda}$ and $B_{\mathbf{k_n},\lambda}$ regarding $\mathbf{B}(\mathbf{x},t)$ in **Eq. 2**, except that $\hat{\boldsymbol{\varepsilon}}_{\mathbf{k_n},\lambda}$ is replaced by $\hat{\mathbf{k}}_{\mathbf{n}}\times\hat{\boldsymbol{\varepsilon}}_{\mathbf{k_n},\lambda}$. Thus, although the probabilistic properties for the random variables $A_{\mathbf{k_n},\lambda}$ and $B_{\mathbf{k_n},\lambda}$ are independent of time and space, as expressed by **Eq. 8**, the same is not true for the probabilistic/stochastic properties of $\mathbf{E}_{\mathrm{ZPP}}$ and $\mathbf{B}_{\mathrm{ZPP}}$, as seen for example in **Eq. 81** and other related results discussed in this subsection.

A multivariate normal expression for the probability density of a set of field values would be represented by:

$$P\left(\begin{array}{c}\mathbf{E}_1 \text{ at } \mathbf{x}_1, t_1; \mathbf{E}_2 \text{ at } \mathbf{x}_2, t_2; \ldots; \mathbf{E}_n \text{ at } \mathbf{x}_n, t_n; \mathbf{B}_{n+1} \text{ at } \mathbf{x}_{n+1}, t_{n+1}; \\ \mathbf{B}_{n+2} \text{ at } \mathbf{x}_{n+2}, t_{n+2}; \ldots; \mathbf{B}_{n+m} \text{ at } \mathbf{x}_{n+m}, t_{n+m}\end{array}\right), \tag{84}$$

where there are n electric field vector values (i.e., $3\times n$ component values, as indicated below) and m magnetic field vector values ($3\times m$ component values), at respective positions in space and time, as indicated. However, since this is a multivariate normal distribution, where all $\langle\mathbf{E}_i\rangle$ and all $\langle\mathbf{B}_i\rangle$ ensemble averages equal zero, then by probability theory, the above would be represented by [37]:

$$P(\mathbf{X}) = \frac{\exp\left[-\frac{1}{2}\mathbf{X}^T\Sigma^{-1}\mathbf{X}\right]}{\sqrt{(2\pi)^{n+m}|\Sigma|}}, \tag{85}$$

where $\mathbf{X}$ is the vector of

$$\left(E_{1x}, E_{1y}, E_{1z}, \ldots, E_{nx}, E_{ny}, E_{nz}, B_{(n+1)x}, B_{(n+1)y}, B_{(n+1)z}, \ldots, B_{(n+m)x}, B_{(n+m)y}, B_{(n+m)z}\right)$$

values. Moreover, Σ is the covariant matrix as expressed by

$$\Sigma_{ij} = \langle X_iX_j\rangle, \tag{86}$$

since $\langle X_i\rangle = 0$ for all E_i and B_i values, due to **Eqs. 4**, **1** and **2**. Also, $|\Sigma|$ and Σ^{-1} represent the determinant and inverse matrix of the covariant matrix, Σ, respectively.

If we calculated all the components of the covariant matrix, meaning all combinations $\Sigma_{ij} = \langle X_iX_j\rangle$ of pairs of electric and magnetic field expectation values, then the probability density, **Eq. 85**, could be evaluated for any vector $\mathbf{X}$ of electric and magnetic field components at different space and time points. Two comparisons can immediately be made with work already covered here. In **Section 2.1**, the probability density was deduced for $P(\mathbf{E}\text{ at }\mathbf{x},t)$ in **Eq. 34**, but this also follows from **Eq. 85** with $\mathbf{X}$ being the vector (E_{1x},E_{1y},E_{1z}), then using **Eq. 86** plus earlier relations in **Section 2.1**, and

$$\Sigma_{ij} = \begin{bmatrix}\langle E_{1x}^2\rangle & 0 & 0\\ 0 & \langle E_{1y}^2\rangle & 0\\ 0 & 0 & \langle E_{1z}^2\rangle\end{bmatrix},$$

which leads to **Eq. 34**.

Similarly, **Eq. 85** can be used to deduce the probability density function for two electric field points that was covered in **Section 2.2**. For a multivariate normal distribution for two field points, although **Eq. 85** is certainly the correct equation to use, it is usually rewritten in the following simplified form in probability textbooks, and referred to as the "bivariate" normal distribution [38]:

$$P(E_{1x},E_{2x}) = \frac{\exp\left\{-\frac{1}{2\left(1-\rho_{1x2x}^2\right)}\left[\frac{\left(E_{1x}-\mu_{1x}\right)^2}{\sigma_{1x}^2}+\frac{\left(E_{2x}-\mu_{2x}\right)^2}{\sigma_{2x}^2}-\frac{2\rho_{1x2x}\left(E_{1x}-\mu_{1x}\right)\left(E_{2x}-\mu_{2x}\right)}{\sigma_{1x}\sigma_{2x}}\right]\right\}}{2\pi\sigma_{1x}\sigma_{2x}\sqrt{1-\rho_{1x2x}^2}}. \tag{87}$$

Here, $\mu_{1x} \equiv \langle E_{1x} \rangle$ and $\mu_{2x} \equiv \langle E_{2x} \rangle$ are both zero for our ZP and ZPP cases. Also, $\sigma_{1x}^2 \equiv \langle (E_{1x} - \mu_{1x})^2 \rangle = \langle E_{1x}^2 \rangle$, for our situation, and similarly for $(\sigma_{2x})^2 = \langle (E_{2x})^2 \rangle$, while

$$\rho_{1x2x} \equiv \frac{\langle (E_{1x} - \mu_{1x})(E_{2x} - \mu_{2x}) \rangle}{\sigma_{1x}\sigma_{2x}} \tag{88}$$

is called the Pearson's correlation coefficient of E_{1x} and E_{2x}. With $\mu_{1x} = \mu_{2x} = 0$ for our case, then

$$\rho_{1x2x} \rightarrow \frac{\langle E_{1x}E_{2x} \rangle}{\sqrt{\langle E_{1x}^2 \rangle \langle E_{2x}^2 \rangle}}. \tag{89}$$

Putting these expressions into **Eq. 87** results in:

$$P(E_{1x}, E_{2x}) = \frac{\exp\left\{ -\frac{1}{2\left(1 - \frac{\langle E_{1x}E_{2x} \rangle^2}{\langle E_{1x}^2 \rangle \langle E_{2x}^2 \rangle}\right)} \left[\frac{E_{1x}^2}{\langle E_{1x}^2 \rangle} + \frac{E_{2x}^2}{\langle E_{2x}^2 \rangle} - 2E_{1x}E_{2x} \frac{\langle E_{1x}E_{2x} \rangle}{\langle E_{1x}^2 \rangle \langle E_{2x}^2 \rangle} \right] \right\}}{2\pi \langle E_{1x}^2 \rangle \langle E_{2x}^2 \rangle \sqrt{1 - \frac{\langle E_{1x}E_{2x} \rangle^2}{\langle E_{1x}^2 \rangle \langle E_{2x}^2 \rangle}}} \tag{90}$$

This is then readily related to our result of I_{1x2x} in **Section 2.2**, **Eq. 62**, since from **Eq. 66**, $A_i = \langle E_{\mathrm{ZPP},i}^2 \rangle$ for $(i \rightarrow x, y, z)$, and is independent of space and time, so $\langle E_{1x}^2 \rangle = \langle E_{2x}^2 \rangle$, for example. Moreover, C_x in **Eq. 60** can be shown to be the two-point correlation function of the x component of the electric field at two different space/time points, or, $\langle E_{1x}E_{2x} \rangle$. Thus,

$$\frac{C_x}{A_x} = \frac{\langle E_{1x}E_{2x} \rangle}{\sqrt{\langle E_{1x}^2 \rangle \langle E_{2x}^2 \rangle}},$$

which is just ρ_{1x2x} in **Eq. 89**. Thus, **Eq. 90** agrees with I_{1x2x} in **Eq. 62**.

Extending this result to the discussion at the end of **Section 2.2** involving x, y, and z components of two electric field values:

$$\begin{aligned} &P(\mathbf{E}_1 \text{ at } \mathbf{x}_1, t_1; \mathbf{E}_2 \text{ at } \mathbf{x}_2, t_2) \\ &= I_{1x2x} \cdot I_{1y2y} \cdot I_{1z2z} \\ &= \frac{\exp\left[\frac{-E_{1x}^2 - E_{2x}^2 + 2E_{1x}E_{2x}\rho_{1x,2x}}{2\left(1 - \rho_{1x,2x}^2\right)\langle E_{1x}^2 \rangle} \right]}{2\pi \langle E_{1x}^2 \rangle \left(1 - \rho_{1x,2x}^2\right)^{1/2}} \\ &\times \frac{\exp\left[\frac{-E_{1y}^2 - E_{2y}^2 + 2E_{1y}E_{2y}\rho_{1y,2y}}{2\left(1 - \rho_{1y,2y}^2\right)\langle E_{1y}^2 \rangle} \right]}{2\pi \langle E_{1y}^2 \rangle \left(1 - \rho_{1y,2y}^2\right)^{1/2}} \\ &\times \frac{\exp\left[\frac{-E_{1z}^2 - E_{2z}^2 + 2E_{1z}E_{2z}\rho_{1z,2z}}{2\left(1 - \rho_{1z,2z}^2\right)\langle E_{1z}^2 \rangle} \right]}{2\pi \langle E_{1z}^2 \rangle \left(1 - \rho_{1z,2z}^2\right)^{1/2}} \end{aligned} \tag{91}$$

3 CONCLUDING REMARKS

The technique used here in **Eq. 11** for one electric field value **E**, or three component values E_x, E_y, E_z, or with **Eq. 40** for $P(\mathbf{E}_1 \text{ at } \mathbf{x}_1, t_1; \mathbf{E}_2 \text{ at } \mathbf{x}_2, t_2)$, for two electric field values, or six component values, was clearly understood to be extendable to n electric and/or m magnetic field values. Various tests and examinations were carried out in **Section 2.3** to provide further understanding of the results derived here. **Section 2.4** showed how to more easily use the multivariate normal distribution to obtain the same probability densities.

However, although the methods of **Eqs. 11** and **40** and the obvious generalizations to far more electric and magnetic radiation field values, result in long calculations, there are a few aspects that should be noted. As briefly discussed in Ref. [23], these techniques can readily be applied to the electric dipole simple harmonic oscillator, in either one, two, or three oscillatory degrees of freedom. For example, for a 1-D oscillator,

$$\begin{aligned} &P(x_1 \text{ at } t_1; x_2 \text{ at } t_2) = \int dA_1 \cdots \int dA_N \ldots \int dB_1 \cdots \int dB_N \ldots \\ &P(A_1, \cdots, A_N, \cdots, B_N, \ldots) \delta[x_1 - x(t_1)] \delta[x_2 - x(t_2)] \ , \end{aligned} \tag{92}$$

represents the probability density of finding an oscillator extension of x_1 at time t_1, and extension of x_2 at time t_2. The subtle point here is the expressions for $x(t_1)$ and $x(t_2)$ must be inserted into **Eq. 92**, and these depend on the A_n and B_n values. **Equation 92** is similar to **Eq. 40**, but more complicated. The electric dipole oscillator system, often phrased in terms of the simple harmonic oscillator (SHO), was a key early system that was studied in SED. However, the drawback is that the oscillator computations are even longer than in **Sections 2.1–2.3**, which only involved the probability states of electric radiation values in ZP and ZPP conditions.

Another interesting aspect of the present method is that, in principle, the method can begin to tackle other systems, particularly one that has not yet been solved analytically in SED: the classical hydrogen problem. Now, for that system, there is no simplification, such as the multivariate normal distribution, to provide a simpler method of solution. The classical hydrogen atom is not a linear SHO system; it is nonlinear, and the multivariate normal distribution only becomes possible for linear sums of random variables that each obey the normal distribution. Possibly, the classical hydrogen system in SED is intractable with the present method, but as far as the author knows, this approach has not yet been tried.

This brings us back to brief comments made in **Section 2.1** about the Feynman path integral for QM and QED, and how there is a slight connection to the present method for SED. Although Feynman developed the technique by 1948, it was initially applied only to some relatively simple systems, such as discussed in [39]. The hydrogen atom escaped solution by Feynman and others until about 1979, by Duru and Kleinert. In analogy, at first blush, although the present method for classical hydrogen in SED may be too difficult, still it seems an interesting perspective to consider.

Finally, a last comment: many of the computations shown here for field values could likely be extended to far more field points, simply by writing the correct code to make a versatile program of n-point correlation functions, such as with the aid of a symbolic mathematic program, as has been done in some cases for Feynman diagram calculations.

DATA AVAILABILITY STATEMENT

All datasets presented in this study are included in the article/ Supplementary Material.

AUTHOR CONTRIBUTIONS

The author confirms being the sole contributor of this work and has approved it for publication.

REFERENCES

1. Cole DC. Reinvestigation of the thermodynamics of blackbody radiation via classical physics. *Phys Rev A* (1992) 45:8471–89. doi:10.1103/physreva.45.8471
2. Cole DC. Thermodynamics of blackbody radiation via classical physics for arbitrarily shaped cavities with perfectly conducting walls. *Found Phys* (2000) 30(11):1849–67. doi:10.1023/a:1003706320972
3. Boyer TH. Thermal effects of acceleration for a classical dipole oscillator in classical electromagnetic zero-point radiation. *Phys Rev D* (1984) 29(6): 1089–95. doi:10.1103/physrevd.29.1089
4. Boyer TH. Thermal effects of acceleration through random classical radiation. *Phys Rev D* (1980) 21(8):2137–48. doi:10.1103/physrevd.21.2137
5. Boyer TH. Thermal effects of acceleration for a classical spinning magnetic dipole in classical electromagnetic zero-point radiation. *Phys Rev D* (1984) 30(6):1228–32. doi:10.1103/physrevd.30.1228
6. Cole DC. Properties of a classical charged harmonic oscillator accelerated through classical electromagnetic zero-point radiation. *Phys Rev D* (1985) 31(8):1972–81. doi:10.1103/physrevd.31.1972
7. Cole DC. Thermal effects of acceleration for a spatially extended electromagnetic system in classical electromagnetic zero-point radiation: transversely positioned classical oscillators. *Phys Rev D* (1987) 35:562–83. doi:10.1103/physrevd.35.562
8. Boyer TH. Temperature dependence of Van der Waals forces in classical electrodynamics with classical electromagnetic zero-point radiation. *Phys Rev A* (1975) 11:1650–63. doi:10.1103/physreva.11.1650
9. Boyer T. Stochastic electrodynamics: the closest classical approximation to quantum theory. *Atoms* (2019) 7(1):29–39. doi:10.3390/atoms7010029
10. Marshall TW. Random electrodynamics. *Proc R Soc London, Ser A* (1963) 276: 475–91.
11. Marshall TW. A classical treatment of blackbody radiation. *Nuovo Cim* (1965) 38:206–15. doi:10.1007/bf02750449
12. Boyer TH. Derivation of the blackbody radiation spectrum without quantum assumptions. *Phys Rev* (1821) 1374–83. doi:10.1103/phyRev.182.1374
13. Boyer TH. Classical statistical thermodynamics and electromagnetic zero-point radiation. *Phys Rev* (1861) 1304–18. doi:10.1103/phyRev. 186.1304
14. Cole DC, Zou Y. Simulation study of aspects of the classical hydrogen atom interacting with electromagnetic radiation: circular orbits. *J Scientific Comput* (2004) 20(1):43–68. doi:10.1023/a:1025846412872
15. Jackson JD. *Classical electrodynamics*. 2nd ed.. New York , NY John Wiley & Sons (1975).
16. de la Peña L, Cetto AM. *The quantum dice - an introduction to stochastic electrodynamics*. Kluwer Dordrecht: Kluwer Acad. Publishers (1996).
17. Boyer TH. Random electrodynamics: the theory of classical electrodynamics with classical electromagnetic zero-point radiation. *Phys Rev D* (1975) 11(4): 790–808. doi:10.1103/physrevd.11.790
18. Cole DC, Lakhtakia A. *Compendium book, "essays on formal aspects of electromagnetic theory*. edited. Singapore: World Scientific (1993). p. 501–32.
19. Boyer TH. The classical vacuum. *Sci Am* (1985) 253:70–8. doi:10.1038/ scientificamerican0885-70
20. Marshall TW. Statistical electrodynamics. *Math Proc Camb Phil Soc* (1965) 61: 537–46. doi:10.1017/s0305004100004114
21. Cole DC. Derivation of the classical electromagnetic zero-point radiation spectrum via a classical thermodynamic operation involving van der Waals forces. *Phys Rev A* (1990) 42:1847–62. doi:10.1103/physreva.42.1847
22. Cole DC. Entropy and other thermodynamic properties of classical electromagnetic thermal radiation. *Phys Rev A* (1990) 42:7006–24. doi:10. 1103/physreva.42.7006
23. Cole DC. Energy considerations of classical electromagnetic zero-point radiation and a specific probability calculation in stochastic electrodynamics. *Atoms* (2019) 7(2):50. doi:10.3390/atoms7020050
24. Boyer TH. `General connection between random electrodynamics and quantum electrodynamics for free electromagnetic fields and for dipole oscillator systems. *Phys Rev D* (1975) 11(4):809–30. doi:10.1103/physrevd. 11.809
25. Planck M. *The theory of Heat radiation*. New York: Dover (1959). This publication is an English translation of the second edition of Planck's work entitled Waermestrahlung, published in 1913. A more recent republication of this work is Vol. 11 of the series The History of Modern Physics 1800–1950 (AIP, New York, 1988).
26. Einstein A, Hopf L. Über einen Satz der Wahrscheinlichkeitsrechnung und seine Anwendung in der Strahlungstheorie. *Ann Phys* (1910) 338: 1096–104.doi:10.1002/andp.19103381603
27. Einstein A, Hopf L. Statistische Untersuchung der Bewegung eines Resonators in einem Strahlungsfeld. *Ann Phys* (1910) 338:1105–15. doi:10.1002/andp.19103381604
28. Cole DC, Zou Y. Quantum mechanical ground state of hydrogen obtained from classical electrodynamics. *Phys Lett A* (2003) 317(1–2):14–20. doi:10. 1016/j.physleta.2003.08.022
29. Cole DC. Simulation results related to stochastic electrodynamics. In AIP Conference Proceedings, USA. 810 99 – 113(.) 2006.
30. Nieuwenhuizen TM, Liska MTP. Simulation of the hydrogen ground state in stochastic electrodynamics. *Phys Scr* (2015) T165:014006. doi:10.1088/0031-8949/2015/t165/014006
31. Nieuwenhuizen TM, Liska MTP. Simulation of the hydrogen ground state in stochastic electrodynamics-2: inclusion of relativistic corrections. *Found Phys* (2015) 45(10):1190–202. doi:10.1007/s10701-015-9919-0
32. Boyer TH. Conformal symmetry of classical electromagnetic zero-point radiation. *Found Phys* (1989) 19(4):349–65. doi:10.1007/bf00731830
33. Haroche S, Kleppner D. Cavity quantum electrodynamics. *Phys Today* (1989) 42(1):24–30. doi:10.1063/1.881201
34. Haroche S, Raimond J-M. Cavity quantum electrodynamics. *Sci Am* (1993) 268(4):26–33. doi:10.1038/scientificamerican0493-54
35. Cole DC. Correlation functions for homogeneous, isotropic random classical electromagnetic radiation and the electromagnetic fields of a fluctuating classical electric dipole. *Phys Rev D* (1986) 33:2903–15. doi:10.1103/ physrevd.33.2903
36. Gradshteyn IS, Ryzhik IM. *Tables of integrals, series, and products*. New York: Academic (1980).
37. Taboga M. *Lectures on probability theory and mathematical statistics*. 3rd ed.. Scotts Valley, California, US: CreateSpace Independent Publishing Platform (2017).
38. Shirazi AN, Fleck I. *Bivariate normal distribution for finding inliers in hough space for a time projection chamber*, 150. EPJ Web Conf (2017). 00010.
39. Feynman RP, Hibbs AR. *Quantum mechanics and path integrals*. New York: McGraw-Hill (1965).

Conflict of Interest: The author declares that the research was conducted in the absence of any commercial or financial relationships that could be construed as a potential conflict of interest.

frontiers in Physics

ORIGINAL RESEARCH
published: 23 October 2020
doi: 10.3389/fphy.2020.00335

Stochastic Electrodynamics: Renormalized Noise in the Hydrogen Ground-State Problem

*Theo M. Nieuwenhuizen**

Institute for Theoretical Physics, University of Amsterdam, Amsterdam, Netherlands

The hydrogen ground-state problem is a touchstone for the theory of Stochastic Electrodynamics. Recently, we have shown numerically and theoretically that the H-atom self-ionizes after a characteristic time. In another approach, we reconsidered the harmonic oscillator and renormalized the stochastic force in order to suppress high-frequency tails so that all frequency integrals are dominated by the physical resonances. In the present work, we consider the regularization of the noise in the hydrogen ground-state problem. Several renormalization schemes are considered. Some are well-behaved, whereas in others the high frequency renormalization induces pathologies at low frequencies. In no situation did we find a way to escape from the previously signaled self-ionization.

Keywords: stochastic electrodynamics, hydrogen problem, hydrogen ground state, self-ionization, renormalization

OPEN ACCESS

Edited by:
Ana Maria Cetto, Universidad Nacional Autónoma de México, Mexico

Reviewed by:
Luis De La Peña, National Autonomous University of Mexico, Mexico
Yilun Shang, Northumbria University, United Kingdom
Daniel C. Cole, Boston University, United States

***Correspondence:**
Theo M. Nieuwenhuizen
t.m.nieuwenhuizen@uva.nl

Specialty section:
This article was submitted to Mathematical and Statistical Physics, a section of the journal Frontiers in Physics

Received: *09 March 2020*
Accepted: *20 July 2020*
Published: *23 October 2020*

Citation:
Nieuwenhuizen TM (2020) Stochastic Electrodynamics: Renormalized Noise in the Hydrogen Ground-State Problem. Front. Phys. 8:335. doi: 10.3389/fphy.2020.00335

1. INTRODUCTION

Stochastic electrodynamics (SED) is a classical theory that aims to explain quantum phenomena. Particles move in classical orbits. The basic assumption is the existence of a physical stochastic electromagnetic force that fills the universe and acts as an environment on charged particles and causes their quantum behavior at a statistical level. There is much literature on this field, and it can be summarized in the excellent books [1, 2].

The two celebrated touchstones of quantum physics, the harmonic oscillator [3–6] and the hydrogen problem [7–9], have received much attention within SED. The harmonic oscillator leads to a reasonable agreement, though not all details coincide. While the outcomes of various frequency integrals were routinely taken from their resonances, we have recently introduced a renormalization of the stochastic force such that high-frequency pathologies do not occur [10].

Our studies of the H-problem go back two decades. In [11], we showed how a classical phase space distribution can produce the shape of the quantum ground state, even Dirac's square-root shape, including relativistic corrections.

Stability of circular orbits was demonstrated by [12–14]. The numerics of the hydrogen ground state were performed in 2002 by [15] with a modestly optimistic outlook. With the aim to reconsider the problem, new simulations were performed in our group in 2016. Various schemes for treating the stochastic force numerically were formulated analytically. Liska employed video cards and a modern computer code, speeding up the simulations significantly. They were carried out for the non-relativistic problem [16] and with the inclusion of relativistic corrections [17]. Many CPU hours were spent to achieve long run times and to incorporate many frequency modes. Ongoing findings of self-ionization led to simulation of a variety of formulations of the problem. The bottom

line was that there was always self-ionization, suggesting that SED is not a basis for quantum mechanics.

On another track, Huang and Batelaan [18] reported that quantum interferences do not show up in the SED version of a double-slit-like quantum model.

Nieuwenhuizen [19] showed analytically for the H atom that there is a trend for self-ionization when the energy of the elliptic orbit is close to zero and the dimensionless angular momentum lies below a critical value of order unity, thus supporting the numerics and the non-recurrence of orbits found by [8].

The question of whether a proper definition of SED can describe the hydrogen atom is of fundamental interest. It is the purpose of the present work to reinspect stability in the hydrogen ground-state problem, inspired by our recent renormalization of the stochastic force for the harmonic oscillator. In section 2, we recall some properties of elliptic orbits in the Kepler problem. In section 3, we consider energy absorption from the stochastic field for various renormalizations of the force. We close with a discussion.

2. KEPLER ORBITS

We consider an electron bound to a nucleus with charge Ze and employ the notation of our recent work [19]. Lengths are expressed in terms of the Bohr radius $\hbar/\alpha Zm_ec$, times in the Bohr time $\hbar/\alpha^2Z^2m_ec^2$, speeds in the Bohr speed of αZc, energy in the Bohr energy $\alpha^2Z^2m_ec^2$, and angular momentum in terms of $\hbar$. Here, $\hbar$ is the reduced Planck constant, $\alpha \approx 1/137$ the fine structure constant, Z the atomic number, m_e the electron mass, and c the speed of light.

We start recalling the essential details of the dynamics. In Bohr units the classical Newton equation reads

$$\ddot{\mathbf{r}} = -\frac{\mathbf{r}}{r^3}. \tag{2.1}$$

The Kepler orbit is solved in the parametric forms

$$\begin{aligned}\mathbf{r} &= \frac{1-\varepsilon\cos a}{k^2}(\cos\phi, \sin\phi, 0)\\ &= \frac{(c_a-\varepsilon, \kappa s_a, 0)}{k^2}.\end{aligned} \tag{2.2}$$

Here, ϕ is the angle of the orbit with respect to the x-axis, a is a time-like parameter, ε is the ellipticity, and $\kappa = \sqrt{1-\varepsilon^2}$. Furthermore, c_a is a shorthand for $\cos a$ and s_a for $\sin a$. The orbit lies on the ellipse

$$(k^2x+\varepsilon)^2 + \frac{k^4}{\kappa^2}y^2 = 1 \tag{2.3}$$

Its perihelion lies at $\mathbf{r} = \mathbf{0}$, the location of the nucleus, and the aphelion at $(-2\varepsilon/k^2, 0, 0)$.

Time t and a second time s are parameterized as

$$\begin{aligned}t &= \frac{\tau_a}{k^3}, \quad \tau_a = a - \varepsilon\sin a,\\ s &= \frac{\tau_b}{k^3}, \quad \tau_b = b - \varepsilon\sin b.\end{aligned} \tag{2.4}$$

For circular orbits ($\varepsilon = 0$), $\tau_a = a$ is a scaled time. In general, (2.4) exhibits an oscillation on top of this.

The angle ϕ is related to the variable a as

$$c_\phi = \frac{c_a-\varepsilon}{1-\varepsilon c_a}, \quad s_\phi = \frac{\kappa s_a}{1-\varepsilon c_a}, \tag{2.5}$$

and reads explicitly

$$\phi = 2\arctan\left(\sqrt{\frac{1+\varepsilon}{1-\varepsilon}}\tan\frac{a}{2}\right). \tag{2.6}$$

It exhibits the ongoing revolutions; for circular orbits ($\varepsilon = 0$) it equals $\phi = a = k^3t$. For general ε, the orbit and t are thus explicit in terms of a.

In Bohr units, the energy is $E = -\frac{1}{2}k^2$ and $\kappa = kL$ with L being the angular momentum in units of $\hbar$. The period reads $P = 2\pi/k^3$. While the QM ground state corresponds to $k = 1$, in SED, k takes any value between 0 and ∞, that is, ranging from loosely to strongly bound, respectively. In the philosophy of SED, the time average of E produces the ground state energy $E_0 = -\frac{1}{2}$ as the average of E over the stationary distribution of E-values. Presuming that it exists, its form has been determined in [11].

Linear perturbations $\mathbf{h}$ to the Kepler orbit satisfy

$$\ddot{\mathbf{h}}(t) = -\mathbf{W}(t)\cdot\mathbf{h}(t), \quad \mathbf{W} = \frac{\mathbf{1}-3\hat{\mathbf{r}}\hat{\mathbf{r}}}{r^3}. \tag{2.7}$$

In [10], we presented a set of eigenmodes in the rotating frame. A linear combination of these solutions reads, in the laboratory frame,

$$\begin{aligned}\mathbf{h}^{(1)}(t) &= \frac{1}{\rho_a}(-s_a, \kappa c_a, 0),\\ \mathbf{h}^{(2)}(t) &= 2(\varepsilon - c_a, -\kappa s_a, 0) + 3\tau_a\mathbf{h}^{(1)}(t),\\ \mathbf{h}^{(3)}(t) &= \frac{1}{2\rho_a}(-\kappa s_{2a}, 3 - 4\varepsilon c_a + c_{2a}),\\ \mathbf{h}^{(4)}(t) &= \frac{\kappa}{2\rho_a}(3 - 2\varepsilon c_a - c_{2a}, \frac{2\varepsilon s_a - s_{2a}}{\kappa}, 0),\\ \mathbf{h}^{(5)}(t) &= (0, 0, s_a),\\ \mathbf{h}^{(6)}(t) &= (0, 0, c_a - \varepsilon).\end{aligned} \tag{2.8}$$

The benefit of these modes is that the limits $\varepsilon \to 0$ or $\kappa \to 0$ to be taken in each of them.

The Greens function satisfies

$$\begin{aligned}\ddot{\mathbf{G}}(t,s) + \mathbf{W}(t)\cdot\mathbf{G}(s,t) &= \mathbf{1}\,\delta(t-s),\\ \mathbf{G}''(t,s) + \mathbf{G}(t,s)\cdot\mathbf{W}(s) &= \mathbf{1}\,\delta(t-s),\end{aligned} \tag{2.9}$$

where dots denote derivatives to t and primes to s. Generally, it holds that

$$\dot{\mathbf{G}}(t,t^-) = -\mathbf{G}'(t,t^-) = \mathbf{1}, \quad \dot{\mathbf{G}}'(t,t^-) = \mathbf{0}. \tag{2.10}$$

Following the approach of [19], we verify that for $s < t$, the Greens function reads explicitly

$$\mathbf{G}(t,s) = \sum_{i=1,3,5} \frac{\mathbf{h}^{(i)}(t)\mathbf{h}^{(i+1)}(s) - \mathbf{h}^{(i+1)}(t)\mathbf{h}^{(i)}(s)}{k^3}.$$

while causality imposes $\mathbf{G} = \mathbf{0}$ for $s \geq t$.

3. STOCHASTIC ELECTRODYNAMICS

In SED the Kepler orbit is perturbed by the stochastic electric field $\mathbf{E}$ and the damping $\mathbf{D}$,

$$\ddot{\mathbf{r}} = -\frac{\mathbf{r}}{r^3} - \beta\mathbf{E} + \mathbf{D}, \tag{3.1}$$

The small parameter β is related to the fine structure constant

$$\beta = \sqrt{\frac{2}{3}}\alpha^{3/2}Z \approx \frac{Z}{1965}. \tag{3.2}$$

with charge $Z = 1$ for hydrogen. The damping $\mathbf{D}(t)$ has been analyzed in full detail in [10]; Here, the standard approximation $\mathbf{D} = \beta^2\,\dddot{\mathbf{r}}$ suffices. The stochastic field satisfies

$$\mathbf{E}(t) = -\dot{\mathbf{A}}(t) = -\ddot{\mathbf{C}}(t). \tag{3.3}$$

It has zero average and correlation functions

$$\begin{aligned}
C_{EE}(t-s) &= \langle \mathbf{E}(t)\mathbf{E}(s)\rangle = \Re\frac{6\times\mathbf{1}}{\pi(t-s-i\tau_c)^4},\\
C_{AA}(t-s) &= \langle \mathbf{A}(t)\mathbf{A}(s)\rangle = \Re\frac{-\mathbf{1}}{\pi(t-s-i\tau_c)^2},\\
C_{CE}(t-s) &= \langle \mathbf{E}(t)\mathbf{C}(s)\rangle = \Re\frac{-\mathbf{1}}{\pi(t-s-i\tau_c)^2},\\
C_{CC}(t-s) &= \langle \mathbf{C}(t)\mathbf{C}(s)\rangle\\
&= \frac{-\mathbf{1}}{\pi}\,\Re\log\omega_c(t-s-i\tau_c),
\end{aligned} \tag{3.4}$$

where $\tau_c = \alpha^2Z^2$ is the Compton time $\hbar/mc$ in Bohr units and $\omega_c \sim \alpha^3\log 1/\alpha$ is a low frequency cutoff. These correlators are large at $s = t$.

The energy radiation is well-understood. Per revolution there is an energy loss

$$(\Delta E)_{rad} = -\beta^2k^5\pi\frac{3-\kappa^2}{\kappa^5}. \tag{3.5}$$

The theme of the present work is the average energy gained from the field. It occurs at the rate

$$\langle \dot{E}_{\rm field}\rangle = \beta^2\int_{s_0}^{t} \mathrm{d}s\,\langle \mathbf{E}(t)\cdot\dot{\mathbf{G}}(t,s)\cdot\mathbf{E}(s)\rangle \tag{3.6}$$

where we must take $s_0 \to -\infty$. Integrated over a period $P = 2\pi/k^3$, it brings

$$\langle \Delta E_{\rm field}\rangle = \beta^2\int_{-P/2}^{P/2}\mathrm{d}t\int_{s_0}^{t}\mathrm{d}s\,I_1(t,s) \tag{3.7}$$

with

$$I_1(t,s) = C_{EE}(t-s)\,\mathrm{tr}\,\dot{\mathbf{G}}(t,s), \tag{3.8}$$

This expression has been studied in our previous work. The s-integral has potentially dangerous behavior at $s = t$ where $\dot{\mathbf{G}} = \mathbf{1}$ and $C_{EE}(0)$ is very large. But the shape (3.4) of C_{EE} implies that this high frequency effect has a vanishing contribution. Just leaving it out corresponds to a motivated short-time ($t \approx s$) or high frequency renormalization. The remaining integrand

$$\dot{g}(t,s) = \mathrm{tr}\,\dot{\mathbf{G}}(t,s) - 3 = O[(t-s)^4], \tag{3.9}$$

decays rapidly enough to set $\tau_c \to 0$ in C_{EE} so that the integral is well behaved in this limit.

3.1. Short-Time Regularization

In our recent study of the harmonic oscillator we introduced a high-frequency regularization of the ultraviolet contributions [10]. Leaving out the subleading damping $\mathbf{D}$, it amounts to replace $\mathbf{E} \to \overline{\mathbf{E}}$, where the frequency components are related as

$$\overline{\mathbf{E}}_\omega \equiv \frac{\omega_0^2}{\omega^2}\mathbf{E}_\omega = \omega_0^2\mathbf{C}_\omega, \tag{3.10}$$

with the equality from $\mathbf{E}(t) = -\ddot{\mathbf{C}}(t)$. At the resonance frequency $\omega = \omega_0$, the $\overline{\mathbf{E}}_\omega$ and $\mathbf{E}_\omega$ coincide. For nonlinear potentials this demands a generalization. The definition of $\mathbf{G}$ is $\ddot{\mathbf{G}} + \mathbf{W}\cdot\mathbf{G} = \mathbf{1}\,\delta(t-s)$ in the hydrogen problem, while $\mathbf{W}(t) \to \mathbf{1}\,\omega_0^2$ in the harmonic case. A natural and simple generalization is therefore

$$\overline{\mathbf{E}}(t) = \mathbf{W}(t)\cdot\mathbf{C}(t). \tag{3.11}$$

Indeed, this reduces to (3.10) for the harmonic case. With $\overline{\mathbf{E}}$ instead of $\mathbf{E}$ inserted in (3.1), there will now appear in (3.7) the renormalized integrand

$$\begin{aligned}
I_2 &= \langle \overline{\mathbf{E}}(t)\cdot\dot{\mathbf{G}}(t,s)\cdot\overline{\mathbf{E}}(s)\rangle\\
&= C_{CC}(t-s)\,\mathrm{tr}\,\mathbf{W}(t)\cdot\dot{\mathbf{G}}(t,s)\cdot\mathbf{W}(s).
\end{aligned} \tag{3.12}$$

We also consider the expressions with one $\mathbf{E}$ and one $\overline{\mathbf{E}}$, which result in

$$\begin{aligned}
I_3 &= C_{CE}(t-s)\,\mathrm{tr}\,\dot{\mathbf{G}}(t,s)\cdot\mathbf{W}(s),\\
I_4 &= C_{CE}(t-s)\,\mathrm{tr}\,\mathbf{W}(t)\cdot\dot{\mathbf{G}}(t,s).
\end{aligned} \tag{3.13}$$

By partial integration we can generally relate the s-integral over I_1 to one over I_4.

$$\begin{aligned}
&\int_{-\infty}^{t}\mathrm{d}s\,\dot{\mathbf{G}}(t,s)\Re\frac{6}{\pi(t-s+i\tau_c)^4} =\\
&\int_{-\infty}^{t}\mathrm{d}s\,\dot{\mathbf{G}}(t,s)\mathbf{W}(s)\Re\frac{-1}{\pi(t-s+i\tau_c)^2}.
\end{aligned} \tag{3.14}$$

In the boundary terms, we used $\dot{\mathbf{G}}'(t,t) = \mathbf{0}$ and inserted $\dot{\mathbf{G}}''(t,s) = -\dot{\mathbf{G}}(t,s)\cdot\mathbf{W}(s)$. But when we do the same to relate I_3 to I_2, we cannot omit the boundary terms at large negative s_0,

$$\int_{s_0}^{t} \mathrm{d}s\, \Re \frac{-\dot{\mathbf{G}}(t,s)}{\pi(t-s+i\tau_c)^2} = \frac{\dot{\mathbf{G}}(t,s_0)}{\pi(t-s_0)} + \dot{\mathbf{G}}'(t,s_0)\frac{\log\omega_1(t-s_0)}{\pi} - \int_{s_0}^{t} \mathrm{d}s\, \dot{\mathbf{G}}(t,s)\cdot\mathbf{W}(s)\frac{\log\omega_1(t-s)}{\pi}, \tag{3.15}$$

where we took $\tau_c \to 0$ in the right-hand side. The main reason for the complication is that $\mathbf{G}(t,s)$, as well as its derivatives, contain an explicit factor $t-s$ arising from the secular part $3k^3 t\,\mathbf{h}^{(1)}(t)$ of the $\mathbf{h}^{(2)}(t)$ mode, see (2.8). With the left-hand side of (3.15) well-behaved for $s_0 \to -\infty$, it follows that the integral in the right hand side must have an $s_0 + s_0\log|s_0|$ divergency in this limit. This is confirmed by inspection and implies that the short-time regularization (2.8) creates a long-time divergency. It is related to the $1/\omega^2$ factor in (3.10) and already led for the harmonic oscillator to a divergency; this was, however, subdominant. For the hydrogen problem it is more cumbersome and leads to an ill-defined leading order integral over I_2. Similar computational methods of integral calculation have been used in other settings (see e.g., [20]).

Though C_{CC} in Equation (3.4) involves a cutoff ω_c, Equation (3.15) is valid for any ω_1. But even the awkward choice $\omega_1 \sim -1/s_0$ would not eliminate the boundary terms that regularize the integral.

3.2. Nearing the Self-Ionization

The important question of whether the H ground state is stable in SED is analyzed for orbits in the limit where $E = -\frac{1}{2}k^2$ vanishes. In our previous works, we showed that this amounts to studying the orbits in the limit where $\kappa = kL$ vanishes, at fixed L, in an order unity. From (3.5), one has the energy loss by radiation per orbit

$$(\Delta E)_{rad} \approx -3\pi\frac{\beta^2}{L^5}. \tag{3.16}$$

To study this limit, the scaling $a \to \kappa u$, $b \to \kappa v$ for $\kappa \to 0$ is introduced, expressing that the main contribution, described by u and v of the order unity, comes from the part of the Kepler orbit near the pericenter at $u = 0$. Indeed, it holds that

$$\mathbf{r} = \frac{L^2}{2}(1-u^2, 2u, 0),\ r = \frac{L^2}{2}(1+u^2). \tag{3.17}$$

Clearly, this part of the orbit is in its $k \to 0$ limit, while the farthest point, lying at $((1+\varepsilon)/k^2, 0, 0) \approx (2/k^2, 0, 0)$, exhibits a self-ionization for $k \to 0$. For further details of the method we refer to [19]. We reproduce its equations (2.24)–(2.26) for $\kappa \to 0$ and multiplied by P,

$$\langle \Delta E^{(1)}_{\rm field}\rangle = \frac{144}{5\pi}\frac{\beta^2}{L^6}\int_{-\infty}^{\infty}\mathrm{d}u\int_{-\infty}^{u}\mathrm{d}v \times \frac{27}{2}\frac{5+3u^2+4(2+u^2)uv+(u^2-1)v^2}{(1+u^2)^2(3+u^2+uv+v^2)^4}. \tag{3.18}$$

Continuing along these lines, we find that $\langle \Delta E^{(3)}_{\rm field}\rangle$ is equal to this, while $\langle \Delta E^{(4)}_{\rm field}\rangle$ comes out with the second line replaced by

$$\frac{15+20u^2+3u^4+4(5+8u^2+u^4)uv}{(1+u^2)^5(3+u^2+uv+v^2)^2} + \frac{5+u^2+8u^4+2(5+u^2)uv+(u^2-1)v^2}{(1+u^2)^5(3+u^2+uv+v^2)^2}\,v^2. \tag{3.19}$$

Its v-integral is linearly divergent with logarithms, as it is for $\langle \Delta E^{(2)}_{\rm field}\rangle$. This all results in

$$\begin{aligned} \langle \Delta E^{(1)}_{\rm field}\rangle &= \frac{16\sqrt{3}}{5}\frac{\beta^2}{L^6} \\ \langle \Delta E^{(2)}_{\rm field}\rangle &= \text{divergent} \\ \langle \Delta E^{(3)}_{\rm field}\rangle &= \frac{16\sqrt{3}}{5}\frac{\beta^2}{L^6} \\ \langle \Delta E^{(4)}_{\rm field}\rangle &= \text{divergent} \end{aligned} \tag{3.20}$$

The equality of the first and third case yields some justification for the renormalization method we investigated.

In case 1 and 3, the average total energy change per orbit thus comes out as

$$\begin{aligned} \Delta E &= 3\pi\frac{\beta^2}{L^6}(L_c - L), \\ L_c &= \frac{16}{5\pi\sqrt{3}} = 0.588057. \end{aligned} \tag{3.21}$$

Orbits that have achieved a small k and $L < L_c$ will gain energy on average, which explains the self-ionization observed in all our numerics.

3.3. Other Renormalization Schemes

The renormalization $\mathbf{E} \to \bar{\mathbf{E}} = \mathbf{W}(t)\cdot\mathbf{C}(t)$ involves $\mathbf{W} = (\mathbf{1} - 3\hat{\mathbf{r}}\hat{\mathbf{r}})/r^3$, of which the numerator has eigenvalues -2 and 1 (twice). One may wonder whether the "absolute value" $|\mathbf{W}| \equiv (\mathbf{1} + \hat{\mathbf{r}}\hat{\mathbf{r}})/r^3$, with the eigenvalues +2 and 1 (twice), fares better. Inspection shows that the divergence does not disappear; if anything, it becomes worse.

A renormalization with a broken power of $|\mathbf{W}|$ fares better at large times. One may replace $\mathbf{E} = -\dot{\mathbf{A}}$ by $\overline{\mathbf{E}}(t) = -\sqrt{|\mathbf{W}|(t)}\cdot\mathbf{A}(t)$ with the expression $\sqrt{|\mathbf{W}|} = (\mathbf{1} + (\sqrt{2}-1)\hat{\mathbf{r}}\hat{\mathbf{r}})/r^{3/2}$ squaring to $|\mathbf{W}|$. Like (3.11), this approach softens the short time behavior, but it does not ruin the long time regime. This leads to a contribution to $\langle\dot{E}\rangle_{\rm field}$ of the form

$$\int_{-\infty}^{t}\mathrm{d}s\,\Re\frac{-f(t,s)}{(t-s+i\tau_c)^2} = f'(t,t)|\log\tau_c| + \int_{-\infty}^{t}\mathrm{d}s\, f''(t,s)\log(t-s) + O(\tau_c). \tag{3.22}$$

Using $\dot{\mathbf{G}} = \mathbf{1}$ and $\dot{\mathbf{G}}' = \mathbf{0}$ at $s = t$, the boundary term leads to

$$\frac{\delta\langle\dot{E}\rangle_{\rm field}}{|\log\tau_c|} = \frac{\beta^2}{2\pi}\frac{\mathrm{d}}{\mathrm{d}t}\mathrm{tr}\,|\mathbf{W}| = -\frac{6\beta^2}{2\pi}\frac{\dot{r}}{r^4}. \tag{3.23}$$

It expresses energy gain (i.e., the electron becomes less bound, on the average) on the approach to the pericenter, and loss (becoming more bound) on departure. This cutoff dependence is unexpected. Nevertheless, when integrated over a full period, the effect averages out.

Next, we calculate, in analogy with (3.7), the energy gain per period. In the scaling limit, the t, s integrals become u, v integrals, of which the latter can be performed analytically. Its $v = u$ boundary term vanishes upon u-integration, while the integral over the $v = -\infty$ boundary term leads to a finite result,

$$\langle \Delta E_{\rm field} \rangle = 2.99842 \, \langle \Delta E^{(1)}_{\rm field} \rangle. \tag{3.24}$$

Hence it also leads to self-ionization.

The combination $\overline{\mathbf{E}} = (1-x)\mathbf{E} - x\sqrt{|\mathbf{W}|}\cdot\mathbf{A}$ involves from the **AE** and **EA** cross terms, a new contribution of the form

$$\int_{-\infty}^{t} {\rm d}s\, \Re \frac{-2f(t,s)}{(t-s+i\tau_c)^3} = f''(t,t)\log\tau_c + \int_{-\infty}^{t} {\rm d}s f'''(t,s)\log(t-s) + O(\tau_c). \tag{3.25}$$

with a lengthy f having $f(t,t) = 0$. The $\log\tau_c$ again drops out when integrated over a full period. After scaling, the v-integral can be performed analytically; now, the primitive for $v \to -\infty$ is odd in u, while the result comes from the $v = u$ term. This ends up in

$$\langle \Delta E^{(x)}_{\rm field} \rangle = \frac{16\sqrt{3}}{5}\frac{\beta^2}{L^6} \times [(1-x)^2 - 0.876444(1-x)x + 2.99842x^2]. \tag{3.26}$$

Its minimum at $x = 0.295028$ leads to $L_c^{min} = 0.33855$, smaller than $L_c = 0.58808$ from (3.21). For all x, this still leads to self-ionization.

The above "absolute" value $|\mathbf{W}|$ looks unnatural, but it was necessary to define a real valued version of $\sqrt{\mathbf{W}}$. The third roots are real however:

$$\mathbf{W}^{1/3} = (\mathbf{1} - (2^{1/3}+1)\hat{\mathbf{r}}\hat{\mathbf{r}})/r, \quad \mathbf{W}^{2/3} = (\mathbf{1} + (2^{2/3}-1)\hat{\mathbf{r}}\hat{\mathbf{r}})/r^2, \tag{3.27}$$

It is easily verified that $(\mathbf{W}^{1/3})^2 = \mathbf{W}^{2/3}$ and $(\mathbf{W}^{1/3})^3 = \mathbf{W}$. They thus permit the renormalization

$$\mathbf{E} \to \bar{\mathbf{E}} = (1-x)\mathbf{W}^{1/3}\cdot\mathbf{B}_1 + x\mathbf{W}^{2/3}\cdot\mathbf{B}_2, \tag{3.28}$$

for some real valued x, with the stochastic fields

$$\mathbf{B}_1 = \partial_t^{-2/3}\mathbf{E}, \qquad \mathbf{B}_2 = \partial_t^{-4/3}\mathbf{E}, \tag{3.29}$$

defined by having $e^{-i\omega t}$ frequency components

$$(\mathbf{B}_1)_\omega = \frac{\mathbf{E}_\omega}{(-i\omega)^{2/3}}, \quad (\mathbf{B}_2)_\omega = \frac{\mathbf{E}_\omega}{(-i\omega)^{4/3}}. \tag{3.30}$$

In the notation of [10], their correlation functions $\langle \mathbf{B}_i(t)\mathbf{B}_j(s)\rangle = \mathbf{1}B_{ij}(t-s)$ emerge as

$$\begin{aligned} B_{11}(t) &= \int_{-\infty}^{\infty}\frac{{\rm d}\omega}{2\pi}\frac{|\omega|^3}{|\omega|^{4/3}}e^{-i\omega t-|\omega|\tau_c} \\ &= \frac{1}{\pi}\Gamma_{8/3}\Re\frac{1}{(it+\tau_c)^{8/3}}, \\ B_{22}(t) &= \frac{1}{\pi}\Gamma_{4/3}\Re\frac{1}{(it+\tau_c)^{4/3}}, \\ B_{12}(t) &= B_{21}(-t) = \frac{1}{\pi}\Re\frac{e^{-\pi i/3}}{(it+\tau_c)^2}. \end{aligned} \tag{3.31}$$

The difficulty is again to deal with the singularities in the limit $\tau_c \to 0$. To proceed, we perform partial integrations. We introduce $B^{(3)}_{11}$ and $B^{(1)}_{22}$ to get

$$\begin{aligned} &B_{11} = \dddot{B}^{(3)}_{11}, \quad B^{(3)}_{11}(t) = -\frac{27}{20\pi}\Gamma_{8/3}\, t^{1/3}, \\ &B_{22} = \dot{B}^{(1)}_{22}, \quad B^{(1)}_{22}(t) = \frac{3}{2\pi}\Gamma_{4/3}\, t^{-1/3}, \\ &B_{12}(t) = B_{21}(t) = -\frac{1}{2\pi t^2}, \end{aligned} \tag{3.32}$$

where we took $\tau_c \to 0$. In view of (3.21) we define

$$\begin{aligned} L_c^{ij} &= \frac{L^6}{3\pi}\int_{-P/2}^{P/2}{\rm d}t\int_{s_0}^{t}{\rm d}s\, B_{ij}(t-s)\Gamma_{ij}(t,s), \\ \Gamma_{ij}(t,s) &= {\rm tr}\,\mathbf{W}^{i/3}(t)\cdot\dot{\mathbf{G}}(t,s)\cdot\mathbf{W}^{j/3}(s), \end{aligned} \tag{3.33}$$

for $i,j = 1,2$. For L_c^{11} we perform a partial integration w.r.t. s. Next we write the t-integral as the difference between two integrals starting at s_0 and switch the t and s integrals. Then we do a partial integration w.r.t. t, switch back and do a final one w.r.t. s. This leads to a t, s integral over $-\dot{\Gamma}''_{11}B^{(3)}_{11}$. One boundary term at $t = s$ is non-trivial, namely

$$\begin{aligned} \delta L_c^{11} &= \frac{3\Gamma_{8/3}L^6}{10\pi^2\,\tau_c^{2/3}}\int_{-P/2}^{P/2}{\rm d}s\,\Gamma'_{11}(s,s) \\ &= -\frac{3(1-2^{-1/3})\Gamma_{8/3}L^6}{5\pi^2\,\tau_c^{2/3}}\int_{-P/2}^{P/2}{\rm d}s\frac{r'(s)}{r(s)^3}. \end{aligned} \tag{3.34}$$

This vanishes again since it involves a total derivative integrated over a full period. But the integrand itself is moderately large, so that, as before, the average rate of energy exchange with the field results in gain on approach to the pericenter and loss on departure. While weakened by the prefactor and canceling over a period, this cutoff dependence is unexpected.

For L_c^{22} we perform a partial integration w.r.t. s and evaluate the double integral in the limit $\tau_c \to 0$. The boundary term at $s = t$ vanishes identically. With $\Gamma^{12} \sim \Gamma^{21} \sim (t-s)^2$ for $s \to t$, the L_c^{12} and L_c^{21} integrands are already regular for $\tau_c \to 0$.

We are interested in these results in the scaling limit $\kappa = kL \to 0$ at fixed L. The resulting integrals are of the type (3.18). Numerical evaluation yields

$$L_c^{11} = 8.5191, \quad L_c^{22} = 2.1944, \qquad (3.35)$$
$$L_c^{12} = 0.3182, \quad L_c^{21} = -0.5615.$$

The combined L_c corresponding to (3.28) reads

$$L_c^{11}(1-x)^2 + (L_c^{12} + L_c^{21})x(1-x) + L_c^{22}x^2. \qquad (3.36)$$

It has a minimum at $x = 0.7886$,

$$L_c^{min} = 1.7048, \qquad (3.37)$$

which sets the boundary for self-ionizing orbits because (3.36) exceeds this for other x-values.

4. DISCUSSION

Previous studies, both analytical and numerical, have pointed out that the hydrogen problem in Stochastic Electrodynamics leads to a self-ionization of the electron. The present work investigates whether "easy fixes" of the stochastic force may improve the situation. We consider a short time or high frequency renormalization of the stochastic force that we recently proposed for the harmonic oscillator problem and generalized it for the hydrogen ground-state problem. To achieve this, we consider several options, of which some do, and some do not, lead to a well-defined approach. We find that the renormalization does not help to stabilize the situation, and that its impact on long time behavior actually makes the situation worse.

Next, we study various further renormalization schemes which lead to well behaved dynamics, but neither heal the self-ionization problem. Our approach generally puts forward that stability of orbits with energy near $E = 0$ can only be achieved for a scheme in which the parameter L_c in (3.21) vanishes. On physical grounds one expects that it can be proven that this quantity is positive. However, we are not aware of such a proof, not even in the scaling limit $E \to 0$.

In our view, the problem does not lie in the Kepler orbits but in the close enough approach to the nucleus where a relatively high amount of energy is absorbed from the stochastic force. Indeed, Kepler orbits *can* be stable in SED. Nieuwenhuizen [19] adds an $L_0^2/2r^2$ potential to the $-1/r$ Newton potential. It induces an effective angular momentum $L_{eff} = (L^2 + L_0^2)^{1/2}$, which, if $L_0 \gtrsim 6$ is large enough, leads to a stable system without self-ionization. Then L_{eff}, and with it the distance between the pericenter and the nucleus, is large enough to prevent orbits that keep on gaining energy on the average.

In the absence of such an extra potential, we confirm previous findings that the hydrogen self-ionizes in Stochastic Electrodynamics. When the orbit has nearly zero energy and the angular momentum lies below some critical value, then, on the average, more energy gets absorbed from the field than is radiated away, making the orbit more and more delocalized so that ultimately self-ionization occurs. To circumvent this, a fundamental reformulation of Stochastic Electrodynamics seems to be necessary.

AUTHOR CONTRIBUTIONS

The author confirms being the sole contributor of this work and has approved it for publication.

REFERENCES

1. Cetto A, de la Peña L. The quantum dice, an introduction to stochastic electrodynamics. In: *Fundamental Theories of Physics*. Vol. 75 (1996). p. 1–512. doi: 10.1007/978-94-015-8723-5
2. de la Peña L, Cetto AM, Vald'es-Hern'andez A. *The Emerging Quantum: The Physics Behind Quantum Mechanics*. Berlin: Springer (2014).
3. Surdin M. Derivation of Schrödinger's equation from stochastic electrodynamics. *IJTP*. (1971) **4**:117–23. doi: 10.1007/BF00670387
4. Santos E. The harmonic oscillator in stochastic electrodynamics. *Il Nuovo Cimento B (1971-1996)* (1974) **19**:57–89. doi: 10.1007/BF02749757
5. De la Peña L, Cetto A. The quantum harmonic oscillator revisited: a new look from stochastic electrodynamics. *J Math Phys*. (1979) **20**:469–83. doi: 10.1063/1.524098
6. Boyer TH. A brief survey of stochastic electrodynamics. In: *Foundations of Radiation Theory and Quantum Electrodynamics*. Boston, MA: Springer (1980). p. 49–63. doi: 10.1007/978-1-4757-0671-0_5
7. Claverie P, Pesquera L, Soto F. Existence of a constant stationary solution for the hydrogen atom problem in stochastic electrodynamics. *Phys Lett A*. (1980) **80**:113–6. doi: 10.1016/0375-9601(80)90198-X
8. Claverie P, Soto F. Nonrecurrence of the stochastic process for the hydrogen atom problem in stochastic electrodynamics. *J Math Phys*. (1982) **23**:753–9. doi: 10.1063/1.525431
9. França H, Franco H, Malta, C. A stochastic electrodynamics interpretation of spontaneous transitions in the hydrogen atom. *Eur J Phys*. (1997) **18**:343. doi: 10.1088/0143-0807/18/5/006
10. Nieuwenhuizen TM. Stochastic electrodynamics: lessons from regularizing the harmonic oscillator. *Atoms*. (2019) **7**:59. doi: 10.3390/atoms7020059
11. Nieuwenhuizen TM. Classical phase space density for the relativistic hydrogen atom. *AIP Conf Proc*. (2006) **810**:198. doi: 10.1063/1.2158722
12. de la Peña L. *Introducción a la Mecánica Cuántica*. Mexico City: UNAM-FCE (1980).
13. Puthoff HE. Ground state of hydrogen as a zero-point-fluctuation-determined state. *Phys Rev D*. (1987) **35**:3266. doi: 10.1103/PhysRevD.35.3266
14. Puthoff HE. Quantum ground states as equilibrium particle–vacuum interaction states. *Quant Stud*. (2012) 1–6.
15. Cole DC, Zou Y. Quantum mechanical ground state of hydrogen obtained from classical electrodynamics. *Phys Lett A* (2003) **317**:14–20. doi: 10.1016/j.physleta.2003.08.022
16. Nieuwenhuizen TM, Liska MT. Simulation of the hydrogen ground state in stochastic electrodynamics. *Phys Scripta* (2015) **2015**:014006. doi: 10.1088/0031-8949/2015/T165/014006
17. Nieuwenhuizen TM, Liska MT. Simulation of the hydrogen ground state in stochastic electrodynamics-2: inclusion of relativistic

corrections. *Found Phys.* (2015) **45**:1190–202. doi: 10.1007/s10701-015-9919-0
18. Huang WCW, Batelaan H. Testing quantum coherence in stochastic electrodynamics with squeezed schrödinger cat states. *Atoms.* (2019) **7**:42. doi: 10.3390/atoms7020042
19. Nieuwenhuizen TM. On the stability of classical orbits of the hydrogen ground state in Stochastic Electrodynamics. *Entropy*. (2016) **18**:135. doi: 10.3390/e18040135
20. Shang Y. The limit behavior of a stochastic logistic model with individual time-dependent rates. *J Math.* (2013) **2013**:502635. doi: 10.1155/2013/502635

Conflict of Interest: The author declares that the research was conducted in the absence of any commercial or financial relationships that could be construed as a potential conflict of interest.

frontiers in Physics

ORIGINAL RESEARCH
published: 12 May 2020
doi: 10.3389/fphy.2020.00162

Connecting Two Stochastic Theories That Lead to Quantum Mechanics

Luis de la Peña, Ana María Cetto and Andrea Valdés-Hernández*

Departamento de Física Teórica, Instituto de Física, Universidad Nacional Autónoma de México, Mexico City, Mexico

The connection is established between two theories that have developed independently with the aim to describe quantum mechanics as a stochastic process, namely stochastic quantum mechanics (SQM) and stochastic electrodynamics (SED). Important commonalities and complementarities between the two theories are identified, notwithstanding their dissimilar origins and approaches. Further, the dynamical equation of SQM is completed with the radiation terms that are an integral element in SED. The central problem of the transition to the quantum dynamics is addressed, pointing to the key role of diffusion in the emergence of quantization.

Keywords: stochastic theories, foundations of quantum mechanics, stochastic electrodynamics (SED), stochastic mechanics, quantum fluctuations

1. INTRODUCTION

A whole and diverse series of stochastic theories have been developed with the aim to throw some light on the nature of the quantum phenomenon [for some representative work see Fényes [1–16]]. In this paper we pay attention to two theories in particular that have developed separately with the common purpose of describing the quantum phenomenon as a stochastic process. On one hand we have stochastic quantum mechanics, SQM (also known as stochastic mechanics), a phenomenological theory initiated by E. Nelson, and further developed and extended independently by several groups; a sample of related works is provided in Nelson [2], de la Peña [3], Guerra [4], Gaveau et al. [5], Nelson [6], de la Peña and Cetto [7], and Nelson [8], and references therein. On the other hand we have stochastic electrodynamics, SED, a first-principles theory pioneered by Marshall [11, 12] and Boyer [13] and further developed and completed with the contributions from a number of other authors, as shown in de la Peña and Cetto [7, 16], de la Peña et al. [17] Claverie [14], and Santos [15], and references contained therein. A common feature of these two theories is the explicit introduction of stochasticity as an ontological element missing in the quantum theory, with the aim to address many of the historical—and still current—conceptual difficulties associated with quantum mechanics. It is in a way astounding that the two theories have lived parallel lives for decades, virtually in isolation from one another.

In both SQM and SED the dynamics of a representative particle of mass m is considered, for simplicity. In the phenomenological approach of SQM the (statistical) concepts of a flux velocity $\boldsymbol{v}$ and a diffusive velocity $\boldsymbol{u}$ are introduced on an equal footing, without the need to specify the source of stochasticity. A generic equation of motion is obtained, which serves to describe the dynamics of two distinct types of stochastic process, in the Markov approximation: the classical, Brownian-motion type and the quantum one. The mathematics are simple and straightforward, and their physical meaning is clear.

The approach of SED, on the other hand, is guided by the hypothesis of the existence of the (random) zero-point radiation field, ZPF[1]. This rather more elaborate approach goes through a

[1]In the atomic, non-relativistic case it is sufficient to consider the electromagnetic vacuum; for other particles different kinds of vacua may have to be considered. A general formulation embracing all kinds of particles could be envisaged, based on a fluctuating spacetime; the different vacuum fields would then be manifestations of these primordial fluctuations.

OPEN ACCESS

Edited by:
Manuel Asorey,
University of Zaragoza, Spain

Reviewed by:
Gastao Inacio Krein,
São Paulo State University, Brazil
Andrei Khrennikov,
Linnaeus University, Sweden

****Correspondence:***
Luis de la Peña
luis@fisica.unam.mx

Specialty section:
This article was submitted to Mathematical Physics, a section of the journal Frontiers in Physics

Received: *12 February 2020*
Accepted: *20 April 2020*
Published: *12 May 2020*

Citation:
de la Peña L, Cetto AM and Valdés-Hernández A (2020) Connecting Two Stochastic Theories That Lead to Quantum Mechanics. Front. Phys. 8:162. doi: 10.3389/fphy.2020.00162

statistical evolution equation (a generalized Fokker-Planck-type equation, GFPE) in phase space, to arrive at a description in $\boldsymbol{x}$-space, in which the dissipative and diffusive terms are seen to bring about a definitive departure from the classical Hamiltonian dynamics. The interplay between these two terms is what allows the system to eventually reach equilibrium and thus attain the quantum regime; the dynamics is then described by the Schrödinger equation, and the operators become a natural tool for its description. Planck's constant enters into the picture through the spectral density of the ZPF, and this allows to determine uniquely the value of the only free parameter introduced in SED, as well as in SQM.

The purpose of the present work is to establish the connection between SQM and SED and, by so doing, to identify the strengths and limitations of the two theories, as well as certain commonalities and complementarities between them. With this aim, we first present the basic elements of SQM leading to the dynamical law that governs both classical and quantum stochastic processes in the Markov approximation. Secondly, we briefly review the statistical treatment followed in SED to arrive at a description in configuration space, and discuss the conditions under which the system attains equilibrium and thus reaches the quantum regime as described by the Schrödinger equation, which corresponds to the radiationless approximation of SED. The discussion of the connections between the two theories provides an opportunity to highlight the role played by diffusion in quantum mechanics. The more complete dynamical description provided by SED, which includes the radiative terms, serves in its turn to complete the corresponding dynamical equation of SQM. The distinct nature of the diffusive terms allows us to address the central problem of the transition from the initially classical dynamics with ZPF, to the quantum one. It is concluded that this more complete ontology which includes the ZPF as the source of stochasticity, leads in a natural process to the quantum description.

2. THE UNDERLYING EQUATIONS OF STOCHASTIC QUANTUM MECHANICS

Stochastic quantum mechanics is a phenomenological theory that considers a particle of mass m undergoing a stochastic motion. It is general enough as to accommodate a range of physical phenomena in which an underlying stochastic process, considered in the Markov (second-order) approximation, takes place. The stochastic nature of the dynamics calls for a statistical treatment, which is carried out in $\boldsymbol{x}$-space. The basic kinematic elements for the description are obtained by applying an average over the ensemble of particles in the neighborhood of $\boldsymbol{x}$ at times close to t. By taking the time interval Δt small but different from zero, two different velocities are obtained, namely the flux (or *systematic*) velocity [see e.g., [2, 7]]

$$\boldsymbol{v}(\boldsymbol{x},t)=\frac{\overline{\boldsymbol{x}(t+\Delta t)-\boldsymbol{x}(t-\Delta t)}}{2\Delta t}=\hat{\mathcal{D}}_c\boldsymbol{x}, \tag{1}$$

with

$$\hat{\mathcal{D}}_c=\frac{\partial}{\partial t}+\boldsymbol{v}\cdot\boldsymbol{\nabla}, \tag{2}$$

and the diffusive (or *osmotic*) velocity

$$\boldsymbol{u}(\boldsymbol{x},t)=\frac{\overline{\boldsymbol{x}(t+\Delta t)+\boldsymbol{x}(t-\Delta t)-2\boldsymbol{x}(t)}}{2\Delta t}=\hat{\mathcal{D}}_s\boldsymbol{x}, \tag{3}$$

with

$$\hat{\mathcal{D}}_s=\boldsymbol{u}\cdot\boldsymbol{\nabla}+D\boldsymbol{\nabla}^2, \tag{4}$$

and

$$D=\frac{\overline{(\Delta x)^2}}{2\Delta t} \tag{5}$$

the diffusion coefficient, assumed to be constant. The symbol $\overline{(\cdot)}$ denotes the aforementioned ensemble averaging.

By considering the forward and backward Fokker-Planck equations for the probability density in $\boldsymbol{x}$-space $\rho(\boldsymbol{x},t)$ [see, e.g., [18]], and combining them appropriately, it follows that $\rho(\boldsymbol{x},t)$ is related to the flux velocity through the continuity equation

$$\frac{\partial\rho}{\partial t}+\boldsymbol{\nabla}\cdot(\rho\boldsymbol{v})=0, \tag{6}$$

and to the diffusive velocity according to

$$\boldsymbol{u}(\boldsymbol{x},t)=D\frac{\boldsymbol{\nabla}\rho}{\rho}. \tag{7}$$

This most important relation confirms the diffusive meaning of the velocity $\boldsymbol{u}$.

The two time derivatives (2) and (4), applied to the velocities (1) and (3), give rise to four different accelerations, thus leading to a couple of generic dynamical equations, which are, respectively, the time-reversal invariant generalization of Newton's Second Law, and the time-reversal non-invariant equation, namely

$$m\left(\hat{\mathcal{D}}_c\boldsymbol{v}-\lambda\hat{\mathcal{D}}_s\boldsymbol{u}\right)=\boldsymbol{f}_+, \tag{8a}$$

$$m\left(\hat{\mathcal{D}}_c\boldsymbol{u}+\hat{\mathcal{D}}_s\boldsymbol{v}\right)=\boldsymbol{f}_-, \tag{8b}$$

where λ is a free, real parameter, and the net force acting on the particle $\boldsymbol{f}$ decomposes as $\boldsymbol{f}=\boldsymbol{f}_++\boldsymbol{f}_-$, such that $\boldsymbol{f}_-$ and $\boldsymbol{f}_+$ do and do not change sign, respectively, under time reversal (notice that $\boldsymbol{v}$ changes its sign whereas $\boldsymbol{u}$ remains invariant).

Since Equations (8) hold simultaneously and together they describe the dynamics of the system, it is convenient to combine them into a single equation. This is readily achieved by introducing the symbol $\kappa=\sqrt{-\lambda}$ and multiplying the second equation by κ; the result is

$$\hat{\mathcal{D}}_\kappa\boldsymbol{p}_\kappa=\boldsymbol{f}_\kappa, \tag{9}$$

with

$$\boldsymbol{p}_\kappa=m\boldsymbol{w}_\kappa+\frac{e}{c}\boldsymbol{A},\quad \boldsymbol{w}_\kappa=\boldsymbol{v}+\kappa\boldsymbol{u}, \tag{10}$$

$$\boldsymbol{f}_\kappa=\boldsymbol{f}_++\kappa\boldsymbol{f}_-, \tag{11}$$

and

$$\hat{\mathcal{D}}_\kappa = \hat{\mathcal{D}}_c + \kappa\hat{\mathcal{D}}_s = \frac{\partial}{\partial t} + \frac{1}{m}\boldsymbol{p}_\kappa \cdot \boldsymbol{\nabla} + \kappa\, D\,\boldsymbol{\nabla}^2. \tag{12}$$

Equation (9) is the equation of motion appropriate for the description of an ensemble of electrically charged particles immersed in an external electromagnetic field $\boldsymbol{A}$, and subject to stochastic forces. The Newtonian limit (or equivalently, the classical Hamiltonian description) corresponds to $D = 0$ and hence $\boldsymbol{u} = \boldsymbol{0}$, which means no diffusion at all.

For simplicity in the derivations we shall assume no external electromagnetic field $\boldsymbol{A}$, so that the momentum is simply $\boldsymbol{p}_\kappa = m\boldsymbol{w}_\kappa$ and the external force components reduce to

$$\boldsymbol{f}_+ = \boldsymbol{f} = -\boldsymbol{\nabla}V,\ \boldsymbol{f}_- = 0. \tag{13}$$

Equations (9)–(12) show that the specific dynamical properties of the system strongly depend on the sign of the parameter λ, which in its turn determines whether κ is real or imaginary. Since only the sign of λ is relevant [its magnitude can be absorbed into the value of D, as explained in de la Peña et al. and Cetto [17, 19]] one can take $\lambda = \pm 1$. The value $\lambda = -1$ ($\kappa = 1$) implies an irreversible dynamics, of the Brownian-motion type. In contrast, by setting $\lambda = 1$ ($\kappa = -i$) one obtains after some algebra the Schrödinger-like equation

$$-2mD^2\boldsymbol{\nabla}^2\psi(\boldsymbol{x},t) + V(\boldsymbol{x})\psi(\boldsymbol{x},t) = 2imD\frac{\partial\psi(\boldsymbol{x},t)}{\partial t}, \tag{14}$$

and its complex conjugate, where $\psi(\boldsymbol{x},t)$ is a complex function such that

$$\rho(\boldsymbol{x},t) = |\psi(\boldsymbol{x},t)|^2 \tag{15}$$

and

$$\boldsymbol{v} = iD\left(\frac{\nabla\psi^*}{\psi^*} - \frac{\nabla\psi}{\psi}\right),\ \boldsymbol{u} = D\left(\frac{\nabla\psi^*}{\psi^*} + \frac{\nabla\psi}{\psi}\right), \tag{16}$$

whence

$$\boldsymbol{w} = \boldsymbol{v} - i\boldsymbol{u} = -2iD\frac{\nabla\psi}{\psi}. \tag{17}$$

3. THE UNDERLYING EQUATIONS OF STOCHASTIC ELECTRODYNAMICS

3.1. The Generalized Fokker-Planck Equation

We recall that the equation of motion of SED for a (non-relativistic) particle of mass m and electric charge e is the Langevin equation, also known in SED as Braffort-Marshall equation [7, 14, 15],

$$m\ddot{\boldsymbol{x}} = \boldsymbol{f}(\boldsymbol{x}) + m\tau\dddot{\boldsymbol{x}} + e\boldsymbol{E}_0(t), \tag{18}$$

where $\tau = 2e^2/3mc^3$, and $\boldsymbol{f} = -\boldsymbol{\nabla}V$. The (random) electromagnetic ZPF is usually taken in the dipole approximation and is therefore represented by $\boldsymbol{E}_0(t)$. With the momentum defined as

$$\boldsymbol{p} = m\dot{\boldsymbol{x}}, \tag{19}$$

Equation (18) transforms into

$$\dot{\boldsymbol{p}} = \boldsymbol{f} + m\tau\dddot{\boldsymbol{x}} + e\boldsymbol{E}_0(t). \tag{20}$$

Since the dynamics of the system becomes stochastic due to the ZPF, its evolution can only be described in statistical terms. We therefore follow a standard procedure [see de la Peña et al. [17]; section 4.2] that leads to the following generalized Fokker-Planck equation (GFPE) for the phase-space distribution $Q(\boldsymbol{x},\boldsymbol{p},t)$,

$$\hat{L}Q = \left(\hat{L}_c + e^2\hat{L}_r\right)Q = 0, \tag{21}$$

where

$$\hat{L}_c = \frac{\partial}{\partial t} + \frac{1}{m}\boldsymbol{\nabla}\cdot\boldsymbol{p} + \boldsymbol{\nabla}_p\cdot\boldsymbol{f} \tag{22}$$

and

$$\hat{L}_r = \boldsymbol{\nabla}_p\cdot\left(\frac{m\tau}{c^2}\dddot{\boldsymbol{x}} - \hat{\mathscr{D}}\right). \tag{23}$$

The operator $\hat{L}_c$ contains the classical (i.e., conservative and nondiffusive) Liouvillian terms, and $\hat{L}_r$ the radiative and diffusive terms, the latter being represented by the integro-differential operator $\hat{\mathscr{D}}$. To lowest order in e^2, this operator takes the form

$$\hat{\mathscr{D}} = \int_{-\infty}^{t} dt'\varphi(t-t')\nabla_{p'}, \tag{24}$$

where

$$\varphi(t) = \frac{2\hbar}{3\pi c^3}\int_0^\infty d\omega\,\omega^3\cos\omega t \tag{25}$$

denotes the ZPF covariance, and $\boldsymbol{p}' = \boldsymbol{p}(t')$ evolves toward $\boldsymbol{p}(t)$ under the action of $\hat{L}$. Notice that it is through this diffusive term that Planck's constant appears in the description.

3.2. Evolution Equations in Configuration Space

From Equation (21) follows the equation of evolution in $\boldsymbol{x}$-space for any dynamical variable $G(\boldsymbol{x},\boldsymbol{p})$ of interest without explicit time-dependence, by left-multiplying the equation by G and integrating over the momentum space. The local mean value of G is

$$\langle G\rangle_x \equiv \frac{1}{\rho}\int d\boldsymbol{p}\,G(\boldsymbol{x},\boldsymbol{p})Q(\boldsymbol{x},\boldsymbol{p},t), \tag{26}$$

where $\rho = \rho_x = \rho(\boldsymbol{x},t) = \int d\boldsymbol{p}\,Q(\boldsymbol{x},\boldsymbol{p},t)$ stands for the probability density. Here we consider only the results corresponding to $G = 1$ and $G = \boldsymbol{p}$. In the first case, a direct integration of Equation (21) over $\boldsymbol{p}$ gives the continuity equation for ρ,

$$\frac{\partial\rho}{\partial t} + \boldsymbol{\nabla}\cdot\boldsymbol{j} = 0,\ \boldsymbol{j} = \rho\boldsymbol{v}, \tag{27}$$

with $\boldsymbol{v} = \boldsymbol{v}(\boldsymbol{x},t)$ the flux (or current) velocity,

$$\boldsymbol{v} = \frac{1}{m}\langle\boldsymbol{p}\rangle_x. \tag{28}$$

For $G = \boldsymbol{p}$ one gets, using (19) and summing over repeated indices,

$$\frac{\partial}{\partial t} m\boldsymbol{v}\rho + m^2 \partial_j \left\langle \dot{x}_j \dot{\boldsymbol{x}} \right\rangle_x \rho - \left\langle \boldsymbol{f} \right\rangle_x \rho = \boldsymbol{R}, \tag{29}$$

with

$$\boldsymbol{R} = m\tau \left\langle \ddot{\boldsymbol{x}} \right\rangle_x \rho - e^2 \langle \hat{\mathscr{D}} \rangle_x \rho \tag{30}$$

containing the radiative and diffusive terms, which are of the order of e^2.

As is shown in detail in de la Peña et al. [17] (Chapter 4) and de la Peña et al. [20], the left-hand side of Equation (29) can be transformed into the Schrödinger-like equation

$$-\frac{2\eta^2}{m}\nabla^2\psi(\boldsymbol{x},t) + V(\boldsymbol{x})\psi(\boldsymbol{x},t) = 2i\eta\frac{\partial\psi(\boldsymbol{x},t)}{\partial t} \tag{31}$$

with $\psi(\boldsymbol{x},t)$ a complex function such that

$$\rho(\boldsymbol{x},t) = |\psi(\boldsymbol{x},t)|^2, \tag{32}$$

η a free (undetermined) parameter, and

$$\boldsymbol{v}(\boldsymbol{x},t) = \frac{1}{m}\mathrm{Re}\left(\frac{-2i\eta\nabla\psi}{\psi}\right) = -\frac{i\eta}{m}\left(\frac{\nabla\psi}{\psi} - \frac{\nabla\psi^*}{\psi^*}\right). \tag{33}$$

It is important to note that neither the left-hand side of (29) nor the resulting Equation (31), contain any element that is explicitly related with the ZPF nor with radiation reaction. In fact it is just through the balance eventually achieved between the average energy lost by radiation reaction and that gained from the ZPF (the two terms deriving from the action of $\hat{L}_r$, Equation 23), that the value of the parameter η is determined. It is thus found that [17, 20]

$$\eta = \hbar/2, \tag{34}$$

which transforms (31) into the true Schrödinger equation; the term on the right-hand side of Equation (29) represents the radiative corrections. We shall come back to this crucial point in section 5.4.

4. CONNECTING SED WITH SQM

4.1. Comparing the Dynamical Equations

To explore the connection between the two theories we start by noticing that (33) relates the flux velocity with the real part of the complex vector $(-i\hbar\nabla\psi)/\psi$, while the corresponding imaginary term, on its part, gives the velocity vector

$$\begin{aligned}\boldsymbol{u}(\boldsymbol{x},t) &= -\frac{1}{m}\mathrm{Im}\left(\frac{-i\hbar\nabla\psi}{\psi}\right)\\ &= \frac{\hbar}{2m}\left(\frac{\nabla\psi}{\psi} + \frac{\nabla\psi^*}{\psi^*}\right) = \frac{\hbar}{2m}\frac{\nabla\rho}{\rho}.\end{aligned} \tag{35}$$

These expressions coincide precisely with those obtained for the two velocities of SQM, namely Equation (16), if the diffusion coefficient appearing in these equations is assigned the value

$$D = \frac{\hbar}{2m}.$$

In SED—as in quantum mechanics—$\boldsymbol{v}$ and $\boldsymbol{u}$ represent local ensemble averages; the SQM expressions (1) and (3) represent averages over the ensemble of particles in the neighborhood of $\boldsymbol{x}$, which is a different way of saying the same.

In terms of these velocities, the full SED Equation (29) reads

$$\begin{aligned}m\frac{\partial v_i}{\partial t} - mv_i\left(\frac{2m}{\hbar}\boldsymbol{u}\cdot\boldsymbol{v} + \nabla\cdot\boldsymbol{v}\right)\\ +m\left(\frac{2m}{\hbar}\boldsymbol{u}\cdot\left\langle\dot{\boldsymbol{x}}\dot{x}_i\right\rangle_x + \nabla\cdot\left\langle\dot{\boldsymbol{x}}\dot{x}_i\right\rangle_x\right) = f_i + \frac{1}{\rho}R_i.\end{aligned} \tag{36}$$

For clarity we introduce the tensor T_{ij}, given by the (local) correlation between the i-th and j-th components of the vector $\dot{\boldsymbol{x}}$,

$$T_{ij} = -\frac{2m}{\hbar}\left(\left\langle\dot{x}_i\dot{x}_j\right\rangle_x - v_iv_j\right) = -\frac{2m}{\hbar}\left(\left\langle\dot{x}_i\dot{x}_j\right\rangle_x - \left\langle\dot{x}_i\right\rangle_x\left\langle\dot{x}_j\right\rangle_x\right), \tag{37}$$

so that Equation (36) takes the form

$$m\left(\frac{\partial v_i}{\partial t} - T_{ij}u_j - \frac{\hbar}{2m}\partial_jT_{ij} + v_j\partial_jv_i\right) = f_i + \frac{1}{\rho}R_i. \tag{38}$$

Barring the radiative corrections, represented by the last term, this dynamical equation reduces to

$$m\left(\frac{\partial v_i}{\partial t} - T_{ij}u_j - \frac{\hbar}{2m}\partial_jT_{ij} + v_j\partial_jv_i\right) = f_i. \tag{39}$$

The SQM dynamical equation (8a), in its turn, reads explicitly

$$m\left(\frac{\partial v_i}{\partial t} + v_j\partial_jv_i - u_j\partial_ju_i - D\partial_j\partial_ju_i\right) = f_i \tag{40}$$

in the absence of an external field, when Equation (13) holds. This coincides with the (non-radiative) dynamical equation of SED, Equation (39), with T_{ij} given by

$$T_{ij} = \partial_ju_i. \tag{41}$$

Hence, by inserting (41) into (38) we obtain an extended equation for SQM that includes the radiative contributions represented by R_i,

$$m\left(\frac{\partial v_i}{\partial t} + v_j\partial_jv_i - u_j\partial_ju_i - D\partial_j\partial_ju_i\right) = f_i + \frac{1}{\rho}R_i. \tag{42}$$

On the other hand, the SQM Equation (8b) leads after one integration to the continuity equation, which is equivalent to the SED Equation (27).

In this form the connection between SQM and SED is established. The theories are seen to complement one another: while SQM offers the advantage of naturally incorporating from the beginning the couple of velocities $\boldsymbol{v}$ and $\boldsymbol{u}$ to describe the dynamics due to an (unidentified) stochastic source, SED recognizes the ZPF as the determining ingredient that serves to precise the origin of the (quantum) fluctuations, and introduces Planck's constant into the ultimate quantum description. The specific value of D constitutes a postulate in SQM, since in this theory the nature of the stochastic source remains unidentified. Things change when making the connection of SQM with SED, since in the latter theory the ZPF with energy per mode $\hbar\omega/2$, is the natural carrier of $\hbar$.

4.2. Evidence of Diffusion in Quantum Mechanics

A significant hint of the direct connection of SED and SQM with quantum mechanics follows by observing that the quantum momentum operator is directly related with the velocity $\boldsymbol{w}_\kappa$ for $\kappa = -i$ (Equation 17),

$$\hat{\boldsymbol{p}}\psi = -i\hbar\nabla\psi = (\boldsymbol{v} - i\boldsymbol{u})\psi. \tag{43}$$

This result reveals that both velocities $\boldsymbol{v}$ and $\boldsymbol{u}$ are a natural part of quantum mechanics, even if $\boldsymbol{v}$ is rarely used [see however Ballentine [21], and $\boldsymbol{u}$ remains virtually ignored]. In terms of these velocities, the (quantum) expectation value of the squared momentum reads

$$\left\langle \hat{\boldsymbol{p}}^2 \right\rangle = m^2 \left\langle \boldsymbol{v}^2 + \boldsymbol{u}^2 \right\rangle, \tag{44}$$

and the quantum variance

$$\sigma^2_{\hat{\boldsymbol{p}}} = \left\langle \hat{\boldsymbol{p}}^2 \right\rangle - \left\langle \hat{\boldsymbol{p}} \right\rangle^2 \tag{45}$$

is given by

$$\sigma^2_{\hat{\boldsymbol{p}}} = \sigma^2_{m\boldsymbol{v}} + \sigma^2_{m\boldsymbol{u}}, \tag{46}$$

where the variance of a generic vector $\boldsymbol{b}(\boldsymbol{x}, t)$ is given by $\sigma^2_{\boldsymbol{b}} = \langle \boldsymbol{b}^2 \rangle - \langle \boldsymbol{b} \rangle^2$, with $\langle \cdot \rangle = \int d\boldsymbol{x}\, (\cdot)\, \rho(\boldsymbol{x}, t)$.

Since

$$\sigma^2_{\boldsymbol{u}} = \left\langle \boldsymbol{u}^2 \right\rangle = \int d\boldsymbol{x}\, \rho(\boldsymbol{x}, t)\, \boldsymbol{u}^2(\boldsymbol{x}, t) > 0, \tag{47}$$

momentum dispersion is unavoidable in quantum mechanics—the single exception being the free particle in a $\boldsymbol{p}$-eigenstate, in which case the position dispersion is infinite. A well-known manifestation of this is the Heisenberg inequality $\Delta x \Delta p \geq \hbar/2$.

Another distinctive and persisting manifestation of the diffusive velocity $\boldsymbol{u}$ is the so-called quantum potential,

$$V_Q = -\hbar^2 \left(\nabla^2 \sqrt{\rho}\right) / 2\sqrt{\rho} = -\frac{1}{2}\left(m\boldsymbol{u}^2 + \hbar\nabla \cdot \boldsymbol{u}\right). \tag{48}$$

This energy contribution totally due to fluctuations is of paramount importance in determining much of the quantum behavior; we recall that it plays a central role in Bohm's interpretation of quantum mechanics [22].

Along the present discussion we have met the confluence of both theories, SQM and SED, with quantum mechanics, through the equivalence of their statistical nature as being described by the Schrödinger equation. But there is more, since results such as (43)–(46) furnish convincing evidence that, along with the Schrödinger equation, the whole Hilbert-space formalism is involved in such correspondence.

5. THE MECHANISM OF THE CLASSICAL-TO-QUANTUM TRANSITION

5.1. Radiation and Diffusion

Let us now pay attention to the radiative contributions, represented by the term $e^2\hat{L}_r Q$ in the GFPE (21). For this purpose we multiply this equation by any constant of motion $G(\boldsymbol{x}, \boldsymbol{p}) = \xi$ and integrate over $\boldsymbol{p}$. The terms associated with the classical Liouvillian, $\hat{L}_c\xi$, cancel out automatically, and only the two terms associated with $\hat{L}_r\xi$ remain. For equilibrium to be reached, these terms must eventually balance each other. By resorting to Equations (24) and (25), one obtains for the balance condition

$$-\left\langle \dddot{\boldsymbol{x}} \cdot \boldsymbol{g} \right\rangle_x = \frac{\hbar}{\pi}\int_0^\infty d\omega\, \omega^3 \int_{-\infty}^t dt \cos\omega(t - t') \left\langle \nabla_{p'} \cdot \boldsymbol{g} \right\rangle_x, \tag{49}$$

with $\boldsymbol{g}(\boldsymbol{x}, \boldsymbol{p}) = \nabla_p \xi(\boldsymbol{x}, \boldsymbol{p})$ and $\boldsymbol{p}' = \boldsymbol{p}(t')$, $t' < t$.

Although the equality in (49) holds only under equilibrium, each side of it can be analyzed separately for all times. It is clear that the two terms reflect different dynamical properties of the system. Whereas, initially (at $t = -\infty$, when particle and ZPF start to interact and there is no diffusion) the radiation term (left-hand side) obviously dominates over the diffusive one (right-hand side), with time the diffusion of the momentum increases due to the action of the ZPF. Thus, while the system starts from a non-equilibrium condition, the two dynamical processes allow it to converge toward a balance regime in which the ξ are indeed constant.

Fundamental to the analysis is the factor $\nabla_{p'} \cdot \boldsymbol{g}$, which is at the core of the mechanism of evolution toward the balance regime. This coefficient signals the effects on $\boldsymbol{g}(\boldsymbol{x}, \boldsymbol{p})$, of the diffusion of the particles activated by the ZPF through its direct action on the momentum $\boldsymbol{p}$. In classical mechanics, the quantity $\nabla_{p'} \cdot \boldsymbol{g}$ can be expressed in terms of a Poisson bracket involving $\boldsymbol{g}$ at time t and $\boldsymbol{p}$ at time t',

$$\frac{\partial g_i}{\partial p'_j} = \left[x'_j, g_i\right]. \tag{50}$$

The Poisson bracket represents an abridged description of the Hamiltonian evolution, controlled by the classical Liouvillian L_c; in this case the dynamics is purely deterministic. By contrast, the dynamics contained in Equation (49) is controlled by the entire Liouvillian, and is therefore deterministic in a statistical sense only. This means that although the motion of each particle follows deterministic rules, the fact that it is acted upon by a stochastic field makes the evolution of the ensemble of particles *statistically deterministic*, hence not amenable to a purely Hamiltonian description. The conforming (modified) Newton equations of motion are of a nature akin to that discussed in section 2 and reflected in Equation (9), which appropriately incorporates the effects of diffusion. As a consequence, the right-hand side of Equation (49)—and with it the entire equation—ceases to obey Hamiltonian laws as soon as the diffusion enters into force.

In conclusion, although initially the dynamics is controlled by Hamiltonian laws, as the interaction develops diffusion eventually takes control. At this point Equation (49) acquires validity, signaling the passage to classical+ZPF physics in the balance regime. The new laws, which are statistical in nature by virtue of the action of the ZPF, coincide with those of quantum mechanics. This means that the Poisson brackets have been replaced by their corresponding commutator. The presence of $\hbar$ in the commutator provides an important clue—although rarely appreciated if at all in its daily use: it is a direct result of the

crucial role played by the ZPF in the dynamics, and evinces the transition from initially conventional classical to classical+ZPF physics, and eventually to SED in the balance regime, i.e., to quantum physics. That this qualitative change stems from an underlying physical mechanism of transition mastered by the ZPF, may sound natural to some, radical to others; in fact, it is both. Interestingly, however, a qualitative change due to a transition from an initially classical dynamics into one which is fundamentally quantum in nature, has already been observed in experiments with open photonic systems [23].

5.2. Two Brands of Stochastic Processes

In the general approach to SQM as briefly discussed in section 2 [and more extensively in, e.g., [3, 17, 19]], the description of the dynamics involves the undetermined coefficient λ that can take the values $+1$ or -1, thereby opening the way to the study of two essentially different dynamics. Indeed, this parameter defines the sign of an acceleration related to the diffusion that is to be either added or subtracted to the drift-related acceleration (as shown in Equation 8a), so that the dynamical laws differ from one another, and from the classical (Newtonian) law, due precisely to the diffusive terms. In the referred works and as discussed above, it is shown that the selection $\lambda = -1$ corresponds to Brownian motion, whereas $\lambda = 1$ leads to quantum mechanics (through the Schrödinger equation). The close relationship between SQM and SED shows that, despite their dissimilarities, both stochastic processes share certain laws, such as Equations (9–13).

A natural question that emerges from the previous discussion is, how is it that the transition to quantum mechanics occurs in the SED system but not in the case of Brownian motion, which is the most characteristic classical stochastic process? There are several physical features that distinguish the two stochastic processes, a first obvious one being the scale. Whereas, Brownian systems are normally microscopic or macroscopic in size, the quantum ones are of atomic or subatomic size, and many orders of magnitude more sensitive to the relatively high intensity of the stochastic background—in this case the ZPF—which induces significant fluctuations on the dynamical variables of the system. This difference in the response is so noticeable that one of the first quantum rules to be established (already during 1927) were the Heisenberg uncertainty relations, which in the present understanding express properties of *causal* stochastic motions, rather than the familiar "inherent" indeterminism. But of course the most important difference refers to the source of the stochasticity, which in the Brownian system is a white noise, free of any self-correlation, whereas in the quantum case it is, according to our description, an intense colored field (due to its ω^3-spectrum) with important spatial and temporal self-correlations. In fact, as has been shown in the relevant literature [see de la Peña et al. [17] and references therein], it is the radiation field endowed with these high correlations that can be identified as the source of the (statistical) wavelike behavior of quantum particles.

5.3. Precising the Ontology of Quantum Mechanics

The question of whether the dynamics of a system can transit from classical to quantum may result misleading or baffling if taken loosely. A legitimate answer requires that the starting theory contain already the ontological elements proper of quantum mechanics. Now, the miscellany of conceptual problems and difficulties that beset conventional quantum mechanics, when closely looked at, point toward the possibility of a common origin, namely some critical component that has been left aside. Here we are proposing to consider the zero-point radiation field as the key missing element in the quantum ontology, and the transition, therefore, not from plain classical physics but from classical-plus-zero-point-radiation-field physics to quantum physics. As seen from the above analysis, this more complete ontology leads in a natural process to the quantum description.

Equation (31), along with Equations (43–46), imply that once the balance (or quantum) regime is established, the dynamical variables can legitimately be treated via the corresponding usual operators in Hilbert space. This perspective stands in contrast with the historical one, in which the founders of the theory felt compelled to introduce operators (in their matrix representation) to account for the observed facts—just as Newton's law of gravitation was proposed to save the phenomenon—without any acknowledgment (nor knowledge) of the role played by the underlying cause, the theoretical weight of which remained—and still remains—largely unrecognized, adding its part to the opacity of quantum mechanics.

The perspective to be drawn from these results is that the ZPF not only plays a significant role in explaining quantum indeterminism as the result of an induced stochasticity, but that its presence provides the basis for an explanation of the quantum behavior of matter altogether. [A more extensive discussion and substantiation of these matters is presented in de la Peña et al. [17]].

A note about the reverse transition from quantum to classical seems appropriate at this point. It is usual to consider classical physics as a limiting case of the quantum description, attained e.g., by allowing $\hbar$ to go to zero, with the argument that in this limit all operators commute. This is however a formal transition; the fundamental difference in the nature of the classical-vs-quantum dynamics demands a more in-depth consideration of this apparently simple "change of scale."

5.4. Some Words About the Radiative Corrections

Equation (42) is the dynamical law of both SED and SQM, including the radiative corrections to second order in e. This more complete description allows one to obtain several important results pertaining to the realm of quantum electrodynamics (in the non-relativistic approximation), such as the formulas for the Einstein coefficients, which determine in particular the lifetimes of atomic states. The corresponding calculations and results can be seen in de la Peña et al. [17] and references therein. In the context of the present work, the most interesting application has been the determination of the diffusion coefficient D of SQM.

We recall that according to the SED Equation (49), a balance must be achieved in the quantum regime between the radiative and dissipative effects on the dynamics. In particular, for $\xi = \boldsymbol{p}^2/2m + V$, Equation (49) represents the energy-balance

condition, meaning that the mean power absorbed by the particle from the ZPF is compensated by the mean power radiated by the former. While the radiation reaction term contains parameters deriving from (classical) electrodynamics only, Planck's constant enters into the second term through the spectral energy density of the ZPF. A detailed calculation of the two terms shows that it is precisely this balance condition what fixes uniquely the value of the free parameter η used in section 3.2, and hence of the diffusion coefficient D in terms of $\hbar$.

6. FINAL REMARKS AND CONSIDERATIONS

For several decades already, two theories have coexisted which arrive at quantum mechanics from an (assumed) classical context that includes stochasticity as an essential ingredient. Historically they were developed by different and virtually independent clusters of researchers, with little intersection. Hence their coexistence has been more than peaceful. Also their philosophies are quite distant, SQM having been conceived of as a Brownian-type theory for the particle subject to a *white noise* from an unidentified source. By contrast, SED has been developed as a statistical description for the particle subject to the ZPF with a *colored* spectrum. As shown here, the two theories complement each other and both lead to the Schrödinger equation after appropriate workings; thus, in the global scenario quantum mechanics emerges from a classical+stochastic context. Leaving aside the theoretical body here developed, one could ask, why so?

The reason for the success of such parallel constructs is traced to the role played by diffusion. In SQM the velocity $\boldsymbol{u}$ is introduced from the very start as a dynamical variable that encapsulates the diffusive effect of the random force on the particle motion. Both the diffusive velocity $\boldsymbol{u}$ and the flux velocity $\boldsymbol{v}$ are of course statistical concepts, and together with the ensuing four accelerations they modify Newton's Second Law in an essential way. Also SED starts by considering the appropriate statistical description by means of the GFPE, which ensues from the (stochastic) Langevin-type equation—equally modifying the Second Law in an essential way.

In this work we have established the equivalence between the equations of motion derived in SED—a fundamental theory—and those of SQM—a phenomenological theory. One may say that SQM becomes thus *explained* by SED, and completed by it. This is reinforced by recalling that the value of the diffusion constant $D = \hbar/2m$—a free postulate in SQM, which has no natural place for Planck's constant—is derived from a consideration of the radiative terms of SED, as explained in section 5.4.

A final important point is that the coherence between the SQM and SED theories unravels in the former the presence of an undulatory element, which it lacks of in its usual strictly corpuscular treatments [by Nelson and followers; see Nelson and Guerra [2, 4]]. This provides a natural answer to the well-known objection against SQM by Wallstrom [24, 25], who deems the known derivations incorrect, based on the argument that they require an *ad hoc* (wave-like) quantization condition on the velocity potential (the gradient of which gives the velocity $\boldsymbol{v}$) in order to derive Schrödinger's equation; of course such condition appears artificial in a strictly corpuscular framework, but it acquires a natural place in a theory that embodies a radiation field as its substantial source of stochasticity.

AUTHOR CONTRIBUTIONS

All authors listed have made a substantial, direct and intellectual contribution to the work, and approved it for publication.

ACKNOWLEDGMENTS

Useful comments from the referees are acknowledged. The authors acknowledge financial support from DGAPA.UNAM through project PAPIIT IN113720.

REFERENCES

1. Fényes I. Eine wahrscheinlichkeitstheoretische Begründung und Interpretation der Quantenmechanik. *Zeits Physik*. (1952) **132**:81–106. doi: 10.1007/BF01338578
2. Nelson E. *Dynamical Theories of Brownian Motion*. Princeton, NJ: Princeton University Press (1967).
3. de la Peña L. New formulation of stochastic theory and quantum mechanics. *J Math Phys*. (1969) **10**:1620. doi: 10.1063/1.1665009
4. Guerra F. Structural aspects of stochastic mechanics and stochastic field theory. *Phys Rep*. (1981) **77**:263–321. doi: 10.1016/0370-1573(81)90078-8
5. Gaveau B, Jakobson T, Kac M, Schulman LS. Relativistic extension of the analogy between quantum mechanics and Brownian motion. *Phys Rev Lett*. (1984) **53**:419–22. doi: 10.1103/PhysRevLett.53.419
6. Nelson E. *Quantum Fluctuations*. Princeton, NJ: Princeton University Press (1985).
7. de la Peña L, Cetto AM. *The Quantum Dice*. Dordrecht: Kluwer Academic Publishers (1996).
8. Nelson E. Review of stochastic mechanics. *JPCS*. (2012) **361**:012011. doi: 10.1088/1742-6596/361/1/012011
9. Khrennikov AY. *Beyond Quantum*. Taylor & Francis; Boca Raton, FL: CRC Press (2014).
10. t'Hooft G. *The Cellular Automaton Interpretation of Quantum Mechanics*. Berlin: Springer Verlag (2016).
11. Marshall TW. Random electrodynamics. *Proc R Soc A*. (1963) **276**:475. doi: 10.1098/rspa.1963.0220
12. Marshall TW. Statistical electrodynamics. *Proc Camb Philos Soc*. (1965) **61**:537.
13. Boyer TH. Random electrodynamics: the theory of classical electrodynamics with classical electromagnetic zero-point radiation. *Phys Rev D*. (1975) **11**:790–808. doi: 10.1103/PhysRevD.11.790
14. Claverie P. Stochastic electrodynamics versus quantum theory: recent advances in the study of non-linear systems. In: Moore SM, et al., editors. *Proceedings of Einstein Centennial Symposium on Fundamental Physics*. Bogotá: Universidad de los Andes (1981). p. 229.
15. Santos E. Locality in stochastic electrodynamics. In: Moore SM, et al., editors. *Proceedings of Einstein Centennial Symposium on Fundamental Physics*. Bogotá: Universidad de los Andes (1981). p. 213.
16. de la Peña L, Cetto AM. Derivation of quantum mechanics from stochastic electrodynamics. *J Math Phys*. (1977) **18**:1612. doi: 10.1063/1.523448
17. de la Peña L, Cetto AM, Valdés-Hernández A. *The Emerging Quantum*. Berlin: Springer Verlag (2015).

18. Risken H. *The Fokker-Planck Equation. Methods of Solution and Applications*. Berlin: Springer Verlag (1984).
19. Cetto AM, de la Peña L, Valdés-Hernández A. Specificity of the Schrödinger equation. *Quant Stud Math Found*. (2015) **2**:275–87. doi: 10.1007/s40509-015-0047-5
20. de la Peña L, Cetto AM, Valdés-Hernández A. The zero-point field and the emergence of the quantum. *Int J Mod Phys E*. (2014) **23**:1450049. doi: 10.1142/S0218301314500499
21. Ballentine LE. *Quantum Mechanics: A Modern Development*. Singapore: World Scientific (1998).
22. Bohm D, Hiley BJ. *The Undivided Universe*. New York, NY: Routledge (1995).
23. Raftery J, Sadri D, Schmidt S, Türeci HE, Houck AA. Observation of a dissipation-induced quantum transition. *Phys Rev X*. (2014) **4**:031043. doi: 10.1103/PhysRevX.4.031043
24. Wallstrom TC. On the derivation of the Schrödinger equation from stochastic mechanics. *Found Phys Lett*. (1989) **2**:113.
25. Wallstrom TC. Inequivalence between the Schrödinger equation and the Madelung hydrodynamic equation. *Phys Rev A*. (1994) **49**:1613. doi: 10.1103/PhysRevA.49.1613

Conflict of Interest: The authors declare that the research was conducted in the absence of any commercial or financial relationships that could be construed as a potential conflict of interest.

frontiers in Physics

ORIGINAL RESEARCH
published: 11 August 2020
doi: 10.3389/fphy.2020.00300

Hydrodynamic Quantum Field Theory: The Onset of Particle Motion and the Form of the Pilot Wave

*Matthew Durey and John W. M. Bush**

Department of Mathematics, Massachusetts Institute of Technology, Cambridge, MA, United States

We consider the hydrodynamic quantum field theory proposed by Dagan and Bush, a model of quantum dynamics inspired by Louis de Broglie and informed by the hydrodynamic pilot-wave system discovered by Couder and Fort. According to this theory, a quantum particle has an internal vibration at twice the Compton frequency that generates disturbances in an ambient scalar field, the result being self-propulsion of the particle through a resonant interaction with its pilot-wave field. Particular attention is given here to providing theoretical rationale for the geometric form of the wave field generated by steady, rectilinear particle motion at a prescribed speed, where signatures of both the de Broglie and Compton wavelengths are generally evident. While focus is given to the one-dimensional geometry considered by Dagan and Bush, we also deduce the form of the pilot wave in two dimensions. We further consider the influence on the pilot-wave form of the details of the particle-induced wave generation, specifically the spatial extent and vibration frequency of the particle. Finally, guided by analogous theoretical descriptions of the hydrodynamic system, we recast the particle dynamics in terms of an integro-differential trajectory equation. Analysis of this equation in the non-relativistic limit reveals a critical wave-particle coupling parameter, above which the particle self-propels. Our results provide the foundation for subsequent theoretical investigations of hydrodynamic quantum field theory, including the stability analysis of various dynamical states.

Keywords: Klein-Gordon equation, de Broglie relation, matter waves, Compton scale, hydrodynamic quantum analogs

OPEN ACCESS

Edited by:
Ana Maria Cetto, Universidad Nacional Autónoma de México, Mexico

Reviewed by:
Catalina Stern, National Autonomous University of Mexico, Mexico
Sania Qureshi, Mehran University of Engineering and Technology, Pakistan

***Correspondence:**
John W. M. Bush
bush@math.mit.edu

Specialty section:
This article was submitted to Mathematical and Statistical Physics, a section of the journal Frontiers in Physics

Received: *25 April 2020*
Accepted: *30 June 2020*
Published: *11 August 2020*

Citation:
Durey M and Bush JWM (2020) Hydrodynamic Quantum Field Theory: The Onset of Particle Motion and the Form of the Pilot Wave. Front. Phys. 8:300. doi: 10.3389/fphy.2020.00300

1. INTRODUCTION

In his double-solution pilot-wave theory [1–4], Louis de Broglie proposed a physical picture of quantum dynamics, according to which quantum particles move in concert with a guiding or "pilot" wave. In its rest frame, a particle of mass m_0 was imagined to have an associated vibration at a frequency prescribed by the Einstein-de Broglie relation, $m_0c^2 = \hbar\omega_c$, an internal clock with the Compton frequency, $\omega_c = m_0c^2/\hbar$, where $\hbar = h/(2\pi)$ is the reduced Planck constant and c the speed of light. This vibration was imagined to be responsible for generating a wave form, the particle's "pilot wave," ϕ, responsible for propelling the particle. It was hoped, though never demonstrated, that the resulting particle dynamics would give rise to statistical behavior consistent with the predictions of the standard quantum formalism, as described by the wavefunction, Ψ. Owing to the distinct forms of ϕ and Ψ in de Broglie's original conception, this is widely referred to as his double-solution pilot-wave theory [5].

De Broglie's theory had a number of successes, including the Einstein-de Broglie relation, the de Broglie relation, $p = \hbar k_B$, between particle momentum, p, and its associated wavenumber, k_B, and his prediction of electron diffraction, the experimental confirmation of which [6] earned him the Nobel Prize in 1929. Nevertheless, his double-solution theory was incomplete on several fronts [5]. First, he did not specify the physical nature of the pilot wave. Second, he failed to specify either the mechanism for pilot-wave generation or its resulting form. Initially, he posited that the pilot wave be monochromatic, from which $p = \hbar k_B$ follows directly. Subsequently, he followed the lead of Bohm [7, 8] in asserting that the pilot wave, ϕ, is linearly related to the wavefunction, Ψ. This concession was made with the caveat that there is an unspecified singularity in ϕ in the vicinity of the particle; however, it otherwise reduced de Broglie's double-solution theory to Bohmian mechanics, hence, the two are often conflated into the so-called 'de Broglie-Bohm' theory. In Bohmian mechanics, the mechanism for pilot-wave generation is also absent: particles move in response to both the classical potential and the quantum potential, whose form is uniquely prescribed by the wavefunction, Ψ. The possibility of the particle playing a more active role, specifically acting as the source of its own pilot wave as originally proposed by de Broglie, was discussed by Holland [9].

The most substantial efforts to extend de Broglie's mechanics have come from workers in stochastic electrodynamics (also known as SED) [10, 11], according to which de Broglie's pilot wave may be sought in the electromagnetic quantum vacuum field [12, 13]. The geometry of the pilot-wave field in SED is relatively difficult to characterize, as it requires consideration of the vector electromagnetic field. Nevertheless, de la Peña and Cetto [10] assert that the de Broglie wave may be understood in terms of the Lorentz-transformed Doppler shifting of a pilot wave with the Compton frequency. Kracklauer [14] also speculated as to the form of the pilot wave in SED. We here adopt a simpler approach by following de Broglie in assuming that the pilot wave may be characterized in terms of a single scalar field. Doing so allows us to characterize the form of the resulting pilot-wave field, and so make clear the geometric significance of the de Broglie and Compton wavelengths on its structure.

In the hydrodynamic pilot-wave system discovered by Couder et al. [15], a bouncing droplet self-propels along the surface of a vertically vibrating fluid, guided by the pilot-wave form generated by its resonant interaction with the bath. This pilot wave is the superposition of two distinct wave forms generated at each impact: a traveling disturbance propagating radially outward from each impact, and an axisymmetric standing Faraday wave form centered on the point of impact [16]. The spatio-temporal extent of both the propagating and stationary wave forms is limited by the fluid viscosity. Consequently, the number of prior impacts that influence the droplet is limited by viscous damping. The most striking quantum features arise in the limit of weak viscous damping, also referred to as the "high-memory" limit, where the critical non-Markovian nature of the droplet dynamics is most pronounced [17]. In this limit, the walking droplet is dressed by a quasi-monochromatic wave form with the Faraday wavelength; the pilot wave propagates with the particle, as may be seen by strobing the system at the Faraday frequency [18]. The quantum-like features of the system emerge owing to the quasi-monochromatic form of the pilot wave deduced by superposing the standing wave forms generated at impact, and are only weakly influenced by the traveling waves [17].

Informed by the walking-droplet system, Dagan and Bush [19] presented a model of quantum dynamics, the so-called hydrodynamic quantum field theory (henceforth HQFT), inspired by de Broglie's double-solution pilot-wave theory [1, 4]. Specifically, they adopted de Broglie's notion that quantum particles have an internal clock, a vibration at the Compton frequency that interacts with a scalar background field that satisfies the Klein-Gordon equation. To describe the particle propulsion, de Broglie considered a guidance equation in which the particle velocity is proportional to the gradient of the phase of the monochromatic guiding wave. Dagan and Bush [19] explored a variant of this guidance equation, according to which the particle moves at a velocity proportional to the gradient of the pilot wave. As de Broglie did not specify the precise manner in which the particle vibration generates its associated pilot wave, Dagan and Bush [19] followed the physical analogy between pilot-wave hydrodynamics and de Broglie's mechanics proposed by Bush [20]. Specifically, they considered particle vibration at $2\omega_c$ to serve as a localized disturbance, acting over the scale of the Compton wavelength, $\lambda_c = h/(m_0 c)$, of a scalar field, ϕ, that evolves according to the Klein-Gordon equation.

Dagan and Bush [19] restricted their attention to a one-dimensional geometry: the particle motion was restricted to a line. Nevertheless, their simulations revealed two striking features. First, the particle moves in concert with its pilot wave in such a way that its mean momentum satisfies the de Broglie relation, $p = \hbar k_B$. Second, the free particle is characterized by in-line speed oscillations at the frequency ck_B, over a length scale comparable to the de Broglie wavelength. Here, we shall rationalize the emergence of the de Broglie relation by elucidating the precise form of the wave field in the immediate vicinity of the particle.

In the special case of prescribed particle motion at a constant speed, the simulations of Dagan and Bush [19] also indicated the form of the emergent pilot-wave field, which had two salient features. First, the leading and trailing forms were significantly different. Second, the relative prominence of the de Broglie and Compton wavelengths was seen to depend markedly on the particle speed. These two features, and their analogs arising for a two-dimensional pilot wave, will be rationalized through the theoretical developments presented herein. Finally, our theoretical developments allow us to derive an integro-differential trajectory equation for the particle motion, which we analyze in the non-relativistic limit. As in the hydrodynamic system, this integro-differential form will provide the theoretical basis for examining the stability of various dynamical states, including the in-line speed oscillations of the free particle reported by Dagan and Bush [19].

This paper is arranged as follows: In section 2, we review the theoretical model proposed by Dagan and Bush [19]. We also highlight a number of fundamental features of the Klein-Gordon equation that form the foundations of our analysis. In

section 3, we derive an analytic solution of the pilot wave for the kinematic case of steady particle motion at a prescribed speed. Particular attention is given to rationalizing the salient features reported by Dagan and Bush [19]. Our theoretical developments are then extended to describe the two-dimensional pilot wave generated by rectilinear particle motion in the plane. Finally, in section 4, we derive an integro-differential trajectory equation for the particle motion, analysis of which indicates the onset of self-propulsion for sufficiently strong wave-particle coupling. This trajectory equation represents the starting point for future investigations of this new pilot-wave system.

2. HYDRODYNAMIC QUANTUM FIELD THEORY

2.1. Formulation

We examine the model of one-dimensional quantum dynamics proposed by Dagan and Bush [19], according to which the pilot wave, $\phi(x,t)$, and particle position, $x_p(t)$, evolve according to:

$$\frac{\partial^2\phi}{\partial t^2} - c^2\frac{\partial^2\phi}{\partial x^2} + \omega_c^2\phi = \epsilon_p f(t)g(x - x_p(t)), \tag{1a}$$

$$\gamma(x_p')x_p' = -\alpha\left.\frac{\partial\phi}{\partial x}\right|_{x=x_p}, \tag{1b}$$

where primes denote differentiation with respect to time, t, and ϕ satisfies $\phi \to 0$ as $x \to \pm\infty$. The pilot wave, $\phi(x,t)$, evolves according to the Klein-Gordon equation subject to a localized, periodic forcing, and the particle moves in response to the local gradient of its pilot-wave field. We note that the novelty of HQFT is the wave-particle coupling, as manifest in the forcing of the Klein-Gordon equation and the particle trajectory equation. It is this coupling that distinguishes our work from the numerous studies of the Klein-Gordon equation with a potential [21, 22]. The strength of the wave-particle coupling is governed by the free parameter α. The standard Lorentz factor is defined in terms of the particle velocity, $v = x_p'$, via $\gamma(v) = (1 - (v/c)^2)^{-1/2}$. We define $\epsilon_p = \phi_0\omega_c^2/k_c$, where ϕ_0 is a characteristic value of ϕ and $k_c = 2\pi/\lambda_c$ is the Compton wavenumber. We recall that the Compton wavelength, λ_c, is the distance light travels in one Compton period, $\tau_c = 2\pi/\omega_c$; thus, $\lambda_c = c\tau_c$ and $\omega_c = ck_c$.

Following the suggestion of Schrödinger [23], and in order to achieve wave-particle resonance, Dagan and Bush [19] considered the special case of particle vibration at twice the Compton frequency, $f(t) = \sin(2\omega_c t)$. They further localized the influence of the particle-induced forcing to the Compton wavelength by choosing

$$g(x) = \frac{1}{\sqrt{\pi a^2}}\mathrm{e}^{-(x/a)^2}, \tag{2}$$

with $a = \lambda_c/2$. For the numerical examples presented herein, we adopt these two forms; however, we note that our analysis is not specific to these forms. In section 3, we investigate the influence of the forms of $f(t)$ and $g(x)$ on the resultant pilot wave. Specifically, we consider a more general periodic vibration, $f(t)$, with dominant angular frequency ω_0, and $g(x)$ corresponding to any symmetric function exhibiting a peak about $x = 0$ and decaying as $|x| \to \infty$, normalized such that $\int_{\mathbb{R}} g = 1$.

2.2. The Klein-Gordon Equation

To aid our analysis of the periodically-forced Klein-Gordon equation (Equation 1a), we first recall some of the fundamental features of the unforced Klein-Gordon equation,

$$\frac{\partial^2\phi}{\partial t^2} - c^2\frac{\partial^2\phi}{\partial x^2} + \omega_c^2\phi = 0. \tag{3}$$

The $\omega_c^2\phi$ term in Equation (3) renders this wave equation dispersive: the propagation speed of a wave depends on its wavelength. This dispersion relation is derived through consideration of traveling wave solutions to Equation (3) of the form $\phi(x,t) = \mathrm{e}^{\mathrm{i}(\omega t - kx)}$, where i is the imaginary unit. (As the wave form is unchanged under the mapping $\omega \to -\omega$ and $k \to -k$, we consider $\omega > 0$ without loss of generality). We thus obtain the dispersion relation

$$\omega^2(k) = \omega_c^2 + c^2k^2 \Rightarrow \omega(k) = \sqrt{\omega_c^2 + c^2k^2},$$

which relates the wave angular frequency, ω, and the wavenumber, k.

Since the group velocity, $\frac{\mathrm{d}\omega}{\mathrm{d}k}$, increases monotonically from $-c$ to $+c$ as k is increased, for any prescribed particle velocity, $v \in (-c, c)$, there is a unique wavenumber satisfying $\frac{\mathrm{d}\omega}{\mathrm{d}k} = v$. This wavenumber is precisely the de Broglie wavenumber, $k_B(v)$, defined as

$$k_B = \frac{v/c}{\sqrt{1-(v/c)^2}}k_c = \frac{v}{c}\gamma(v)k_c. \tag{4}$$

As such, the particle is accompanied by a moving wave packet with wavelength $\lambda_B = 2\pi/|k_B|$ in the vicinity of the particle. We note that the de Broglie wavelength, λ_B, and the Compton wavelength, λ_c, differ in general, but are identical when the particle speed is such that $|v/c| = 1/\sqrt{2}$. The dependence of k_B on the particle velocity, v, is illustrated in **Figure 1**, where asymptotes are evident as the particle speed approaches the speed of light. Notably, the de Broglie wavelength is infinite for a stationary particle. Finally, we remark that the phase speed,

$$C_p(k) = \left|\frac{\omega(k)}{k}\right| = \sqrt{(\omega_c/k)^2 + c^2},$$

is superluminal for any wavenumber, k; in particular, the de Broglie phase speed is $C_p(k_B) = c^2/|v|$. However, as the propagating crests do not carry energy, the principle of relativity is not violated.

2.3. The Form of the Pilot Wave

Dagan and Bush [19] considered two forms of particle motion: *kinematics*, in which the particle motion is prescribed as steady translation at a fixed velocity, v; and *dynamics*, where the particle is free to move in response to the gradient of the pilot wave according to Equation (1b). Our study of the pilot wave, ϕ, is

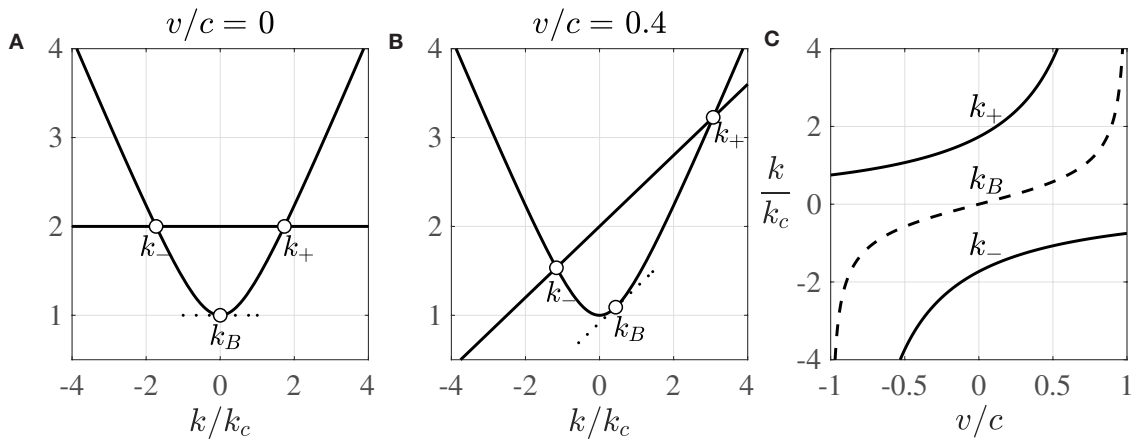

FIGURE 1 | The wavenumbers excited by a particle moving at a prescribed, constant velocity, v, and vibrating at an angular frequency $\omega_0 = 2\omega_c$. Here k_B is the de Broglie wavenumber (Equation 4) and $k_\pm$ are the wavenumbers of the traveling waves [see Equation (9)]. **(A,B)** The curve $\sqrt{1+(k/k_c)^2}$ and line $(\omega_0 + kv)/\omega_c$ intersect at $k_+ > 0$ and $k_- < 0$, and have equal slope at k_B. The dotted line also has slope v/ω_c. **(A)** $v/c = 0$. **(B)** $v/c = 0.4$. **(C)** Dependence of $k_\pm$ (solid curves) and k_B (dashed curve) on v.

similarly split into consideration of particle kinematics (section 3) and particle dynamics (section 4).

To demonstrate the richness and variety in the form of the pilot wave, we present snapshots of $\phi(x,t)$ for particle kinematics in **Figure 2**. These wave forms are similar to those deduced numerically by Dagan and Bush [19] and possess a number of intriguing features. First, there is a clear manifestation of the de Broglie wavelength, λ_B, most visible in advance of the particle: however, upon closer inspection, this wavelength modulates weakly in space, as is most apparent in **Figure 2A**, and the amplitude of this wave *decreases* as the particle speed increases. Second, we see the emergence of an additional wavelength, comparable (but not equal) to the Compton wavelength, λ_c. Such waves are visible only in the wake of the particle, and the amplitude of these waves *increases* with particle speed. We proceed by rationalizing these wave forms through a systematic theoretical analysis of the periodically-forced, one-dimensional Klein-Gordon equation, before demonstrating numerically that these salient features are also apparent in two dimensions.

3. PILOT-WAVE KINEMATICS

We first consider the kinematic case in which particle motion is prescribed, so we need not consider the partial trajectory equation (Equation 1b). Specifically, we consider the particle trajectory $x_p(t) = vt$, where $v > 0$ corresponds to motion in the x-direction. The form of the pilot-wave field is thus described by the periodically-forced Klein-Gordon equation,

$$\frac{\partial^2\phi}{\partial t^2} - c^2\frac{\partial^2\phi}{\partial x^2} + \omega_c^2\phi = \epsilon_p f(t)g(x-vt). \tag{5}$$

Example wave forms are presented in **Figure 2**. We consider the initial conditions $\phi = \partial_t\phi = 0$ at $t = 0$ (for all x) and explore the dynamics of the waves generated in the vicinity of the particle after a long time. Our analysis in sections 3.1 and 3.2 is for a one-dimensional wave form. In section 3.4, we demonstrate that the salient features of the one-dimensional pilot wave persist in two dimensions. For simplicity, we consider the forcing $f(t) = \sin(\omega_0 t)$ in the following analysis, but the wave form for a more general periodic forcing may be derived similarly through the linear superposition of the harmonics $n\omega_0$, for any integer n. Our analysis coincides with the simulations of Dagan and Bush [19] for $\omega_0 = 2\omega_c$.

As the Klein-Gordon equation is linear, we decompose the solution of Equation (5) into two parts: the time-periodic particular solution, ϕ_p, which arises due to the periodic particle forcing; and the homogeneous solution, ϕ_h, whose initial wave form is chosen so that, when combined with the particular solution, the initial conditions for $\phi = \phi_p + \phi_h$ are satisfied. Our analysis reveals that the particular solution gives rise to emitted waves that propagate away from the particle, where the wavelengths in advance of and behind the particle differ and depend on the particle speed. However, both the leading and trailing propagating waves oscillate with the angular frequency, ω_0, of the particle vibration. The homogeneous solution appears as a slowly decaying carrier wave whose local wavelength and angular frequency in the vicinity of the particle are precisely the de Broglie wavelength, λ_B, and the reduced angular frequency ω_c/γ. In general, the propagating and carrier waves thus oscillate at different frequencies.

3.1. The Propagating Waves

We first derive the particular solution, ϕ_p, to the periodically-forced Klein-Gordon equation (Equation 5) for a prescribed particle velocity, v. To allow for generality in the spatial form, $g(x)$, we first seek the Green's function, $\bar{\phi}_p$, satisfying

$$\frac{\partial^2\bar{\phi}_p}{\partial t^2} - c^2\frac{\partial^2\bar{\phi}_p}{\partial x^2} + \omega_c^2\bar{\phi}_p = \epsilon_p \sin(\omega_0 t)\delta(x-vt), \tag{6}$$

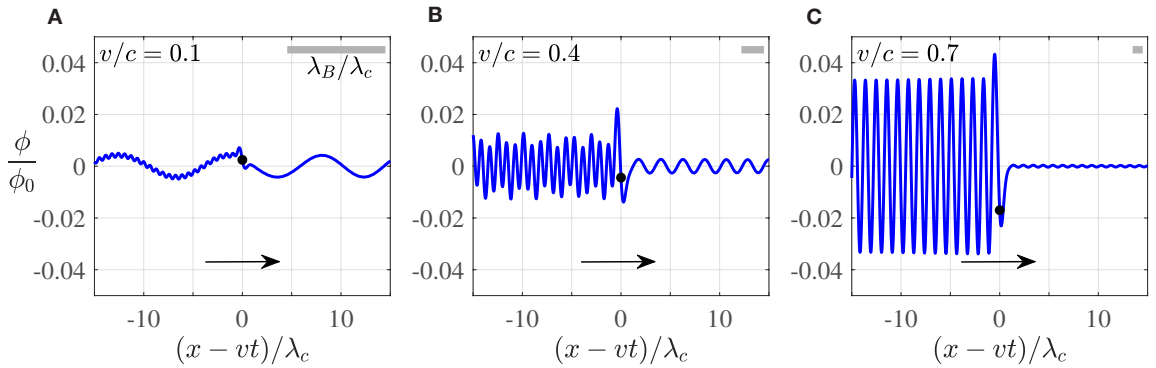

FIGURE 2 | Snapshots of the pilot wave, ϕ, generated by a particle (black dot) moving at a prescribed velocity, v, such that **(A)** $v/c = 0.1$, **(B)** $v/c = 0.4$, **(C)** $v/c = 0.7$. The wave field oscillates in time and is sampled at $t/\tau_c = 600$. The arrow denotes the direction of particle motion. The gray bar (top right of each panel) indicates the ratio λ_B/λ_c, which decreases as the particle speed increases, in accord with Equation (4). The solution was found analytically via a Fourier transform on an infinite domain (see **Appendix 1**), where the inversion was performed numerically using a Gauss-Kronrod quadrature routine built into MATLAB.

where $\delta(x)$ is the Dirac delta function, yielding the following spatial convolution for ϕ_p:

$$\phi_p(x,t) = \int_{-\infty}^{\infty} g(x-y)\bar{\phi}_p(y,t)\,\mathrm{d}y. \tag{7}$$

We find that this particular solution corresponds to emitted plane waves that propagate away from the moving particle, and that the form of $g(x)$ determines the far-field amplitude of these waves.

To derive $\bar{\phi}_p$, we first consider periodic solutions to the unforced Klein-Gordon equation (Equation 3) of the form

$$\phi(x,t) = \mathrm{e}^{\mathrm{i}(\omega t - k(x-vt))} = \mathrm{e}^{\mathrm{i}((\omega+kv)t-kx)}.$$

In the frame of reference moving with the particle, the angular frequency shifts according to $\omega \mapsto \omega + kv$, yielding the dispersion relation

$$(\omega + kv)^2 = \omega_c^2 + c^2k^2. \tag{8}$$

When the angular frequency is that of the vibrating particle, $\omega = \omega_0$, Equation (8) yields two corresponding wavenumbers,

$$k_\pm = \frac{1}{c^2 - v^2}\left[v\omega_0 \pm \sqrt{c^2(\omega_0^2 - \omega_c^2) + v^2\omega_c^2}\right]. \tag{9}$$

The dependence of $k_\pm$ on the particle velocity, v, is presented in **Figure 1** for the special case of $\omega_0 = 2\omega_c$ considered by Dagan and Bush [19].

We now utilize the dispersion relation (Equation 8) in order to determine the wave forms of the particular solution, ϕ_p, when the angular frequency of the particle vibration exceeds the Compton angular frequency, $\omega_0 > \omega_c$, which encompasses the special case $\omega_0 = 2\omega_c$ explored by Dagan and Bush [19]. (We shall demonstrate in section 3.3 that unphysical wave forms arise in the case of $\omega_0 \leq \omega_c$). Equation (9) indicates that $k_+ > 0$, corresponding to wave propagation in the positive x-direction, while $k_- < 0$, corresponding to wave propagation in the negative x-direction. It thus follows that, for the case of $v > 0$ considered here, the leading and trailing wavenumbers are k_+ and k_-, respectively. Moreover, as $k_+ > |k_-|$ for $v > 0$, the trailing wavelength is longer than the leading wavelength, a feature characteristic of a Doppler shift. Finally, we note that the phase speed, $\omega_0/|k_\pm|$, of these propagating waves is comparable, but not precisely equal, to the de Broglie phase speed, $C_p(k_B) = c^2/|v|$, as was evident in the simulations of Dagan and Bush [19].

We demand that the waves propagate away from the vibrating particle. This radiation condition suggests that $\bar{\phi}_p$ has the form

$$\bar{\phi}_p(x,t) = A_+\cos\big(\omega_0 t - k_+(x-vt)\big) + B_+\sin\big(\omega_0 t - k_+(x-vt)\big)$$

for $x > vt$. When $x < vt$, the form is similar, but k_+ is replaced by k_- (and similarly for A_+ and B_+). The coefficients, $A_\pm$ and $B_\pm$, are determined by the assumed continuity of $\bar{\phi}_p$ at $x = vt$ and the jump condition

$$\partial_x\bar{\phi}_p(vt^+,t) - \partial_x\bar{\phi}_p(vt^-,t) = -\frac{\epsilon_p}{c^2}\sin(\omega_0 t),$$

which follows from (6). The Green's function is then

$$\bar{\phi}_p(x,t) = \frac{\epsilon_p}{c^2(k_- - k_+)}\cos\big(\omega_0 t - K(x-vt)\big), \tag{10}$$

where $K = k_+$ for $x > vt$ and $K = k_-$ for $x < vt$.

For a stationary particle ($v = 0$), Equation (9) determines $k_\pm = \pm k_0$ (where $ck_0 = \sqrt{\omega_0^2 - \omega_c^2}$) and the Green's function (Equation 10) reduces to

$$\bar{\phi}_p(x,t) = \frac{-\epsilon_p}{2k_0c^2}\cos(\omega_0 t - k_0|x|).$$

Since $k_0 \neq k_c$, the wavelength of the propagating waves differs from the Compton wavelength. Instead, k_0 depends on the vibrational angular frequency, ω_0. For the special case of interest, $\omega_0 = 2\omega_c$, the propagating waves are shorter than the Compton wavelength, with $k_0 = \sqrt{3}k_c$.

When the particle moves at a constant speed, symmetry is broken and the propagating waves exhibit a Doppler shift: shorter waves propagate ahead of the particle and longer waves are emitted in its wake. Since $k_+/k_c \to \infty$ as $v \to c$, we conclude that waves ahead of the particle are further compressed as the particle speed increases. Conversely, the waves behind the particle are stretched: the wavelength $\lambda_- = 2\pi/|k_-|$ has the limiting form

$$\frac{\lambda_-}{\lambda_c} \to \frac{2\omega_0\omega_c}{\omega_0^2 - \omega_c^2} \quad \text{as} \quad v \to c.$$

In the special case of interest, $\omega_0 = 2\omega_c$, the far-field wavelength behind the particle approaches $4\lambda_c/3$ in this limit.

The effect of the convolution (Equation 7) is to diminish rapid spatial oscillations arising in Equation (10). We define the Fourier transform of $g(x)$ as

$$\hat{g}(k) = \int_{-\infty}^{\infty} g(x) e^{ikx}\, dx, \tag{11}$$

where the symmetry of $g(x)$ implies that $\hat{g}$ is a real and even function of k. Combining Equations (7) and (11), and applying the convolution theorem, reveals that, far from the particle, the trailing (−) and leading (+) propagating waves are approximated by

$$\phi_p(x,t) \approx \hat{g}(k_\pm)\bar{\phi}_p(x,t)$$

for $v > 0$, since $\bar{\phi}_p$ is sinusoidal and $g(x)$ acts over a localized region in space. For the case where $g(x)$ is a Gaussian function [19], $\hat{g}(k)$ is also a Gaussian; thus, short waves are diminished in amplitude to a greater extent than long waves. The amplitude of ϕ_p is thus less ahead of the particle, where waves are shorter, than in its wake, where waves are longer, as is evident in **Figure 3**.

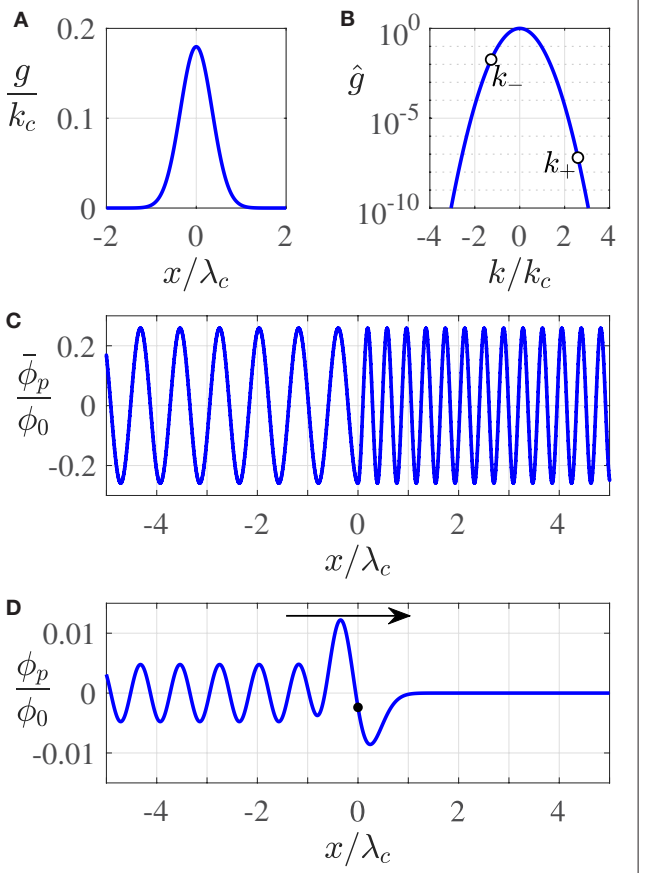

FIGURE 3 | The propagating waves. **(A,B)** The Gaussian shape function, $g(x)$, defined in (2), and its Fourier transform, $\hat{g}(k) = e^{-a^2k^2/4}$. **(C)** The Green's function, $\bar{\phi}_p$, at $t = 0$ for $v/c = 0.3$. **(D)** The particular solution, $\phi_p = \bar{\phi}_p * g$, yields the form of the propagating waves at $t = 0$. The arrow denotes the direction of particle motion. The white circles in **(B)** at $k = k_\pm$ determine the trailing (−) and leading (+) wavelength of $\bar{\phi}_p$, where $\phi_p \approx \hat{g}(k_\pm)\bar{\phi}_p$ far from the particle.

3.2. The Carrier Wave

We now deduce the accompanying homogeneous solution, $\phi_h(x,t)$, to Equation (5), from which we demonstrate that the de Broglie wavelength is the local wavelength of a carrier wave propagating at the particle speed. As shown in **Appendix 1**, the homogeneous solution, ϕ_h, may be expressed as the inverse Fourier transform

$$\phi_h(x,t) = \frac{1}{2\pi}\int_{-\infty}^{\infty}\left(a(k)\cos\left(\sqrt{\omega_c^2 + c^2k^2}\, t\right) + b(k)\sin\left(\sqrt{\omega_c^2 + c^2k^2}\, t\right)\right)e^{-ikx}\, dk, \tag{12}$$

where the functions $a(k)$ and $b(k)$ are defined in **Appendix 1**. Evaluating this integral analytically is intractable. However, we may proceed by exploiting the highly oscillatory form of the integrand for $\omega_c t \gg 1$ in order to derive the integral's asymptotic behavior using the method of stationary phase [24], as outlined in **Appendix 2**. By applying this asymptotic procedure to Equation (12), we obtain that the long-time form of the carrier wave is

$$\phi_h(x,t) \sim \mathcal{A}(x/ct)\frac{\sin(\sqrt{\omega_c^2t^2 - k_c^2x^2} + \pi/4)}{\sqrt{\omega_c t}}, \tag{13}$$

an approximation valid for $|x| < ct$ and $\omega_c t \gg 1$. The form of the slowly varying envelope, $\mathcal{A}(x/ct)$, depends only weakly on the particle speed [see **Appendix 2**].

We present the carrier wave, ϕ_h, in **Figure 4**, where its envelope, $\mathcal{A}(x/ct)$, may be seen to exhibit weak asymmetry about the origin. Notably, the wavelength of the carrier wave varies significantly in space, with compression ahead of the particle and elongation in its wake, characteristic of a Doppler shift. Moreover, we note that ϕ_h decays algebraically in time, so the significance of the carrier wave decreases as $\omega_c t \to \infty$. Nevertheless, this algebraic decay is sufficiently slow for the amplitude of ϕ_h to remain appreciable at finite time and so be evident in the pilot-wave forms presented in **Figure 2**.

We now elucidate the manifestation of the de Broglie wavelength in the carrier wave, ϕ_h. For a particle moving with velocity v, we define $\chi = x - vt$ as the displacement from the particle. As the envelope, $\mathcal{A}$, is slowly varying, the dominant spatial oscillations in ϕ_h arise from the sinusoid in Equation

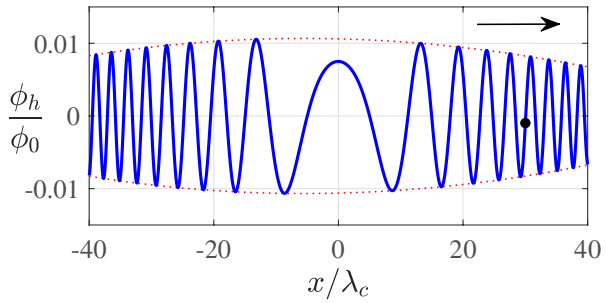

FIGURE 4 | The carrier wave. The asymptotic homogeneous solution, ϕ_h [blue curve, see Equation (13)], for $v/c = 0.3$ and $t/\tau_c = 100$, corresponding to a particle position $x_p/\lambda_c = 30$ (black dot). In the vicinity of the particle, waves are contracted ahead of the particle and elongated behind it. The dotted curve denotes the slowly varying envelope, $\pm\mathcal{A}(x/ct)/\sqrt{\omega_c t}$, where $\mathcal{A}$ is defined in **Appendix 2**.

(13), whose argument we expand in the vicinity of the particle ($|\chi/vt| \ll 1$). Specifically, we obtain

$$\sqrt{\omega_c^2 t^2 - k_c^2 x^2} = \omega_c t\sqrt{1-(v/c)^2} - \mathcal{K}(\chi)\chi, \qquad (14)$$

where the slowly varying wavenumber is

$$\mathcal{K}(\chi) = k_c\left[\frac{k_B}{k_c} + \frac{\chi/vt}{2(1-(v/c)^2)^{3/2}} + O((\chi/vt)^2)\right], \qquad (15)$$

and k_B is the de Broglie wavenumber (Equation 4). The first term on the right-hand side of Equation (14) corresponds to the temporal oscillation of the carrier wave at the reduced angular frequency ω_c/γ. At the particle position ($\chi = 0$), the local wavenumber, $\mathcal{K}$, of the carrier wave is *precisely* the de Broglie wavenumber, as might have been anticipated by the relationship $\frac{d\omega}{dk}(k_B) = v$ [see Equation (4)]. Moreover, the local wavenumber varies slowly in space, as described by the correction term of size $O(|\chi/vt|)$ in Equation (15). This variation serves to compress the wavelength ahead of the particle and elongate it in the particle's wake (see **Figures 2**, **4**). This wavenumber modulation decreases over time, and is also reduced for faster moving particles.

We may also infer why the local amplitude of the carrier wave decreases as the particle speed increases, a trend evident in **Figure 2**. We first recall from Equation (4) that $|k_B|$ increases with the particle speed. Moreover, the variations from the de Broglie wavelength in the vicinity of the particle become weaker as the particle speed increases, a trend due to the aforementioned correction term of size $O(|\chi/vt|)$. Consequently, there is a strong signature of the de Broglie wavelength in the vicinity of the particle, where the amplitude of this wave is governed by the value of $\hat{g}(k_B)$, akin to the dependence of the amplitude of the propagating waves on $\hat{g}(k_\pm)$ discussed in section 3.1. As $|k_B|$ increases with $|v|$, and $\hat{g}(k)$ decreases with $|k|$ (when $g(x)$ is a Gaussian function), the local amplitude of the carrier wave is thus diminished with increasing particle speed, consistent with the trend apparent in **Figure 2**.

3.3. Summary

By combining the foregoing results, specifically superposing the propagating (Equation 7) and carrier (Equation 13) wave forms, we deduce that the one-dimensional wave form generated by particle motion at uniform speed is

$$\phi(x,t) \sim \int_{-\infty}^{\infty} g(x-y)\bar{\phi}_p(y,t)\,dy + \mathcal{A}(x/ct)\frac{\sin(\sqrt{\omega_c^2 t^2 - k_c^2 x^2} + \pi/4)}{\sqrt{\omega_c t}}, \qquad (16)$$

an approximation valid for $\omega_c t \gg 1$ and $|x| < ct$. The Green's function, $\bar{\phi}_p$, is defined in Equation (10), and the envelope, $\mathcal{A}(x/ct)$, is defined in **Appendix 2**. As the asymptotic temporal decay of the carrier wave is algebraic, the signature of the de Broglie wavelength becomes imperceptible only at very large times. It is thus apparent why λ_B is evident in **Figure 2** and the finite-duration simulations of Dagan and Bush [19], but is expected to vanish in the long-time limit.

In **Figure 5**, we present an example of the superposition $\phi = \phi_p + \phi_h$, representing the full pilot-wave field. The particular solution, ϕ_p, describes waves that propagate away from the moving particle, where the approximate trailing (−) and leading (+) form is $\phi_p \approx \hat{g}(k_\pm)\bar{\phi}_p$ for $v > 0$. The shorter propagating waves ahead of the particle are imperceptible, but the longer propagating waves in the particle's wake remain appreciable. The homogeneous solution, ϕ_h, represents a carrier wave exhibiting local wavelength contraction and elongation ahead of and behind the particle, respectively. At the particle position, the local wavelength of the carrier wave is precisely the de Broglie wavelength. The asymptotic approximation (Equation 16) of the full pilot-wave field, ϕ, is in excellent agreement with the numerical solution of Equation (5), lending credence to our analytic approach.

We proceed by examining the effects of changing the form of the spatial forcing, $g(x)$. For Gaussian forcing of the form given in Equation (2), increasing the breadth, a, of the spatial forcing diminishes the amplitude of the propagating waves, ϕ_p, both ahead of and behind the moving particle, as the far-field wave amplitudes, $\phi_p \approx \hat{g}(k_\pm)\bar{\phi}_p$, accordingly decrease due to the form $\hat{g}(k) = e^{-a^2k^2/4}$. When the particle forcing is localized to a point ($a \to 0$), we obtain $\bar{\phi}_p = \phi_p$, whose form, portrayed in **Figure 3C**, has leading and trailing propagating waves of equal amplitude. When $g(x)$ is other than Gaussian, the far-field wave amplitudes, $\phi_p \approx \hat{g}(k_\pm)\bar{\phi}_p$, may vary in a more complex manner as a function of the localization breadth, a, or particle speed, $|v|$. Nevertheless, since $k_+ \to \infty$ as $v \to c$, and $\hat{g}(k) \to 0$ as $k \to \infty$, the amplitude of the propagating waves far ahead of the particle approaches zero as the particle speed approaches the speed of light.

We next examine the influence of the angular frequency, ω_0, of the particle vibration, $f(t) = \sin(\omega_0 t)$, on the form of the propagating waves. We first consider the case in which this frequency exceeds the Compton frequency, $\omega_0 > \omega_c$, which incorporates the case of resonant superharmonics of the form $\omega_0 = n\omega_c$ for integers $n > 1$. We recall that Dagan and Bush [19]

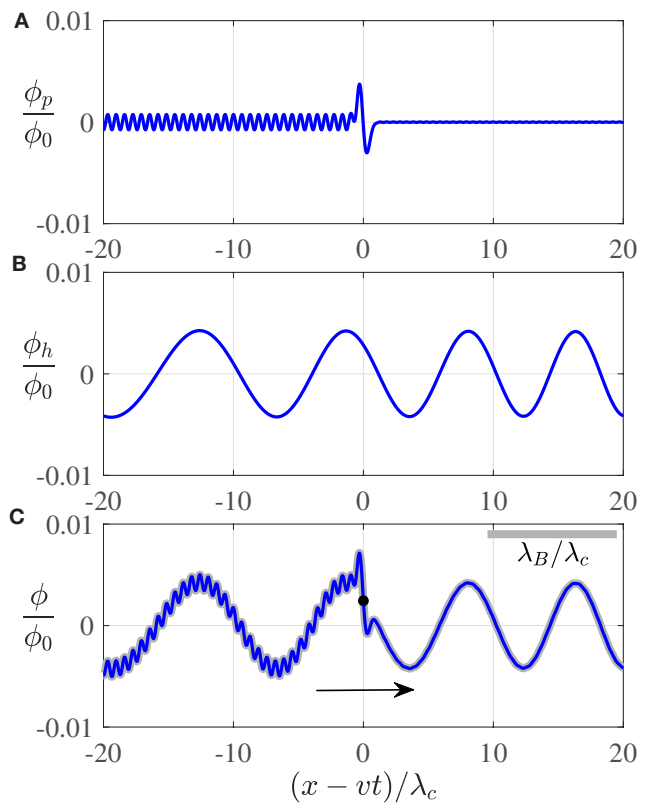

FIGURE 5 | Wave forms accompanying a particle moving at constant velocity $v = 0.1c$ after a time $600\tau_c$. **(A)** The analytic particular solution, ϕ_p [see Equations (7) and (10)], corresponding to propagating waves. **(B)** The long-time asymptotic approximation (Equation 13) of the homogeneous solution, ϕ_h, corresponding to the carrier wave. **(C)** The total wave field deduced analytically, $\phi = \phi_p + \phi_h$ (blue curve), coincides with the numerical solution (gray curve) shown in **Figure 2A**. The gray bar indicates the ratio λ_B/λ_c. The arrow indicates the direction of particle motion.

restricted their attention to the case $n = 2$. As ω_0 is increased, the wavenumbers k_+ and k_- both increase monotonically in magnitude [see Equation (9) and **Figure 1**], resulting in a decrease in the far-field amplitude of the propagating waves, $\phi_p \approx \hat{g}(k_\pm)\bar{\phi}_p$. Consequently, the inclusion of higher harmonics results in a relatively small change in the form of the propagating waves, justifying the decision of Dagan and Bush [19] to consider only the superharmonic $n = 2$.

For the special case arising when the angular frequency of the particle vibration is equal to the Compton angular frequency, $\omega_0 = \omega_c$, it follows from Equation (9) that $k_- = 0$ and $k_+ = 2\gamma k_B$ for $v > 0$. In this case, the wavelength of the propagating wave is infinite in the particle's wake and at most half the de Broglie wavelength in advance of the particle, giving rise to markedly different wave forms from those presented in **Figures 2**, **5**. However, since $k_- = 0$, the propagating waves generated in this special case of harmonic forcing exhibit the unphysical feature of an infinite-wavelength oscillation in the particle's wake.

Finally, we consider the case where the angular frequency of the particle vibration is less than the Compton angular frequency, $\omega_0 < \omega_c$, such as for the subharmonic vibration $\omega_0 = \frac{1}{2}\omega_c$. Then, Equation (9) indicates that the wavenumbers $k_\pm$ are real for $|v| > v_*$, where $v_*/c = 1 - \omega_0^2/\omega_c^2$, and complex for $|v| < v_*$. For fast-moving particles, $|v| > v_*$, waves thus propagate ahead of the particle over two distinct length scales and no waves propagate in the particle's wake. Conversely, for slow-moving particles, $|v| < v_*$, waves grow exponentially in space ahead of the particle (over a length scale determined by the imaginary part of $k_\pm$), which renders the case $\omega_0 < \omega_c$ unsuitable for the generation of a finite-amplitude pilot wave.

As a caveat, we note that our analysis is only valid within the light cone: the particular solution, ϕ_p, extends beyond the light cone at any finite time since ϕ_p is sinusoidal in the far field. Our analytic results are therefore invalid beyond a distance $O((c - |v|)t)$ from the particle. Nevertheless, since we are chiefly interested in the wave form in the vicinity of the particle, as is necessarily responsible for guiding the particle, this limitation does not undermine the key results of our study as they pertain to HQFT.

3.4. The Two-Dimensional Pilot Wave

The approach developed here may be extended to higher spatial dimensions. We do so here in order to briefly characterize the two-dimensional pilot wave emerging for rectilinear particle motion in the plane $\boldsymbol{x} = (x, y)$, with particle velocity $\boldsymbol{v} = (v, 0)$. We restrict our attention to the case of superharmonic forcing, $\omega_0 = 2\omega_c$. Notably, the salient features of the one-dimensional pilot wave, specifically the propagation of waves away from the particle and the emergence of the de Broglie wavelength in the carrier wave, persist in two dimensions. In **Appendix 3**, we analytically determine the two-dimensional wave form of the periodically-forced Klein-Gordon equation [the equivalent of Equation (5)] in Fourier space, before inverting back to physical space numerically.

Figures 6, **7** both indicate that, as in one dimension, two clear length scales emerge, comparable to the Compton and de Broglie wavelengths. The separation in scales between λ_c and λ_B is most evident at low speeds, consistent with Equation (4). **Figure 6** illustrates the wave form in the transient case, for which the particle is initialized at the origin, where the carrier wave forms about the particle's initial position. For a stationary or slowly moving particle, the particle is surrounded by its pilot wave. However, for faster particles, the amplitude of the waves ahead of the particle is diminished, as is evident in **Figure 6F**. **Figure 7** illustrates the long-time form of the pilot wave, composed of propagating waves of characteristic wavelength λ_c emitted by the particle, and a carrier wave of the de Broglie wavelength propagating at the particle speed. Notably, the carrier wave ahead of the particle approaches a plane wave with the de Broglie wavelength as $\omega_c t \to \infty$. A more extensive exploration of HQFT in two dimensions will be left for future consideration.

4. PILOT-WAVE DYNAMICS

We proceed by transforming the coupled system (Equation 1) into an integro-differential trajectory equation governing the particle position. We do so by following Oza et al.'s [25]

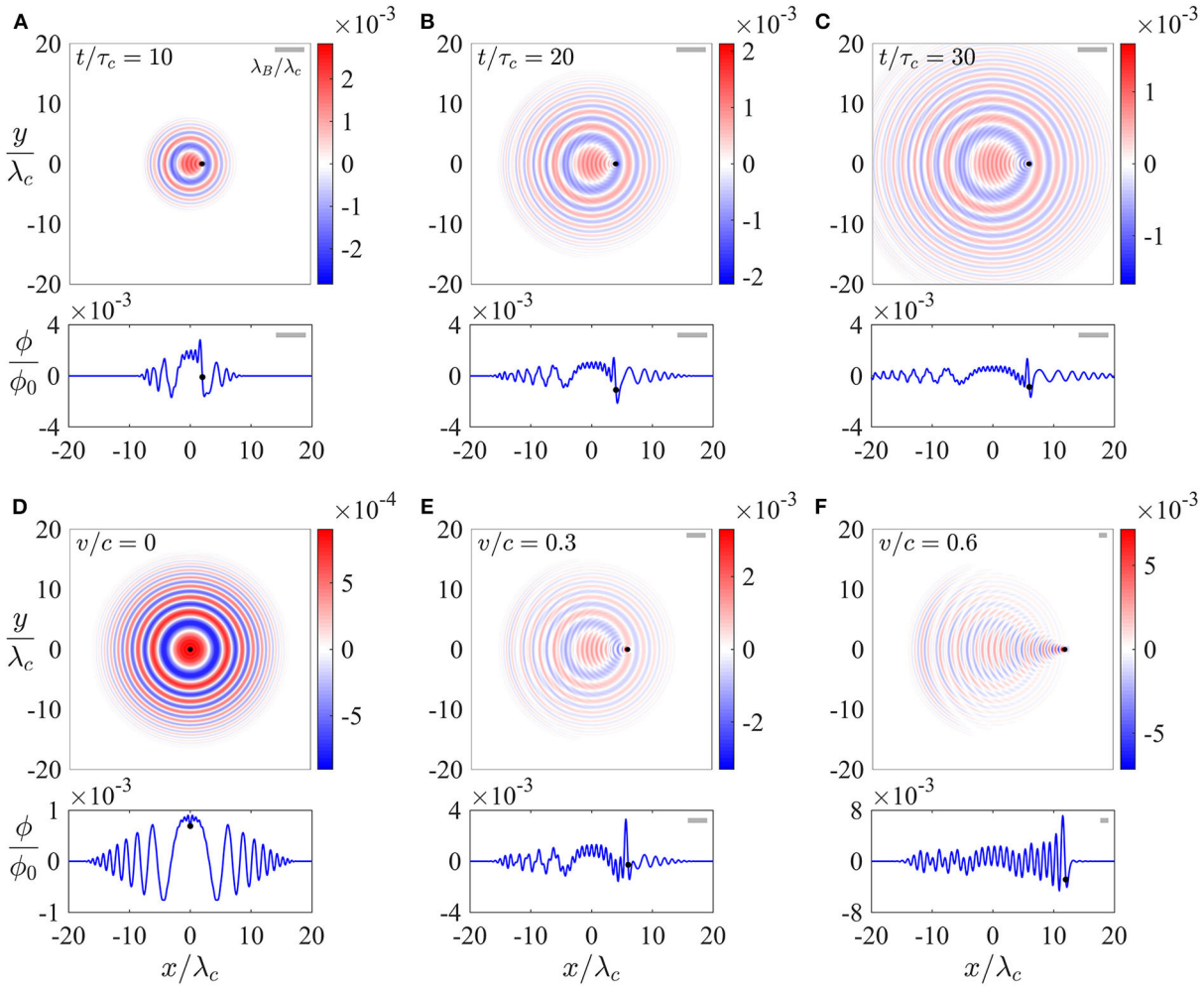

FIGURE 6 | The two-dimensional wave forms generated by particle motion along the x-axis at a prescribed velocity, $\boldsymbol{v} = (v, 0)$, initiated at $t = 0$, when $\phi = \partial_t \phi = 0$. The normalized wave amplitude, ϕ/ϕ_0, is color-coded. The cross section of the wave form along the particle path ($y = 0$) is shown below. **(A–C)** A particle moves along the x-axis with $v/c = 0.2$, with snapshots at **(A)** $t/\tau_c = 10$, **(B)** $t/\tau_c = 20$, and **(C)** $t/\tau_c = 30$. **(D–F)** The wave field generated at time $t/\tau_c = 20$, where the propagation velocity is such that **(D)** $v/c = 0$, **(E)** $v/c = 0.3$, and **(F)** $v/c = 0.6$. The black dot denotes the particle position and the gray bar (top right of each panel) denotes λ_B/λ_c, which is necessarily infinite for $v = 0$. The wave forms were obtained by numerically inverting the Fourier transform solution of the two-dimensional periodically-forced Klein-Gordon equation, as described in **Appendix 3**.

theoretical description of walking droplets, wherein the memory of the pilot-wave system is manifest in the wave force, and appears in the form of an integral over the particle path. This formulation has two principal benefits. First, the integro-differential equation provides a framework for mathematical analysis of the particle dynamics, including an assessment of the stability of various dynamical states. Second, since the influence of the pilot wave is felt only along the particle trajectory, one need not solve the Klein-Gordon equation numerically for all space, which will be particularly beneficial in higher dimensions. One may thus side-step the requirement of an increasingly large computational domain when the simulation duration is increased, a shortcoming of the numerical approach of Dagan and Bush [19]. We proceed by using the Green's function of the Klein-Gordon equation in order to derive a trajectory equation valid for arbitrary particle speed. We then simplify the resulting trajectory equation in the non-relativistic limit, $|v| \ll c$. Analysis of the resulting dimensionless equation allows us to deduce the critical wave-particle coupling parameter required to support sustained particle self-propulsion.

4.1. The Green's Function

By definition, the Green's function, $\varphi_0(x, t)$, for the Klein-Gordon equation is the solution of

$$\frac{\partial^2 \varphi_0}{\partial t^2} - c^2 \frac{\partial^2 \varphi_0}{\partial x^2} + \omega_c^2 \varphi_0 = \delta(x)\delta(t).$$

Its form may be determined exactly using standard analytic methods. To obtain the solution, $\phi(x, t)$, to the forced Klein-Gordon equation (Equation 1a), one then convolves (in space and time) $\varphi_0(x, t)$ with the right-hand side of Equation (1a). To side-step the complexity of the resulting double integral, we instead

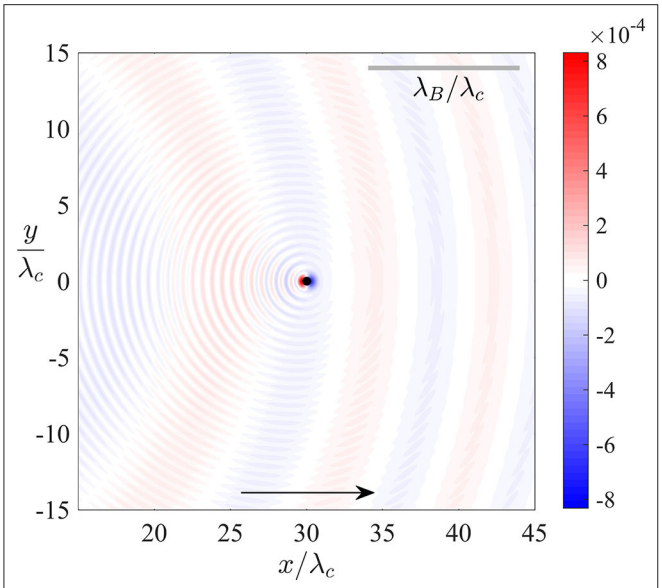

FIGURE 7 | The two-dimensional pilot-wave field generated by particle (black dot) motion along the x-axis at a prescribed velocity, $\boldsymbol{v} = (0.1c, 0)$, after a time $300\tau_c$. The dimensionless wave amplitude, ϕ/ϕ_0, is color-coded. Compton-scale propagating waves are evident in the particle's wake, and a de Broglie-scale, quasi-planar carrier wave propagates at the particle speed.

seek a modified Green's function (valid for $\omega_c t \gg 1$) that accounts for the form of the spatial forcing, allowing for a convolution in time only.

Specifically, we seek $\varphi(x, t)$ satisfying

$$\frac{\partial^2 \varphi}{\partial t^2} - c^2 \frac{\partial^2 \varphi}{\partial x^2} + \omega_c^2 \varphi = \epsilon_p g(x)\delta(t), \tag{17}$$

with $\varphi(x, 0) = \partial_t \varphi(x, 0^-) = 0$. For initial conditions $\phi = \partial_t \phi = 0$ at $t = 0$, the solution, $\phi(x, t)$, of (1a) is then given by the temporal convolution

$$\phi(x, t) = \int_0^t f(s)\varphi(x - x_p(s), t - s)\, \mathrm{d}s, \tag{18}$$

where we have used translational invariance to recenter φ about the particle position.

To determine φ, we apply a Fourier transform in space to Equation (17), yielding an evolution equation for $\hat{\varphi}(k, t)$, specifically

$$\hat{\varphi}'' + (\omega_c^2 + c^2 k^2)\hat{\varphi} = \epsilon_p \hat{g}(k)\delta(t),$$

with $\hat{\varphi}(k, 0) = \hat{\varphi}'(k, 0^-) = 0$. This equation is readily solved, yielding

$$\hat{\varphi}(k, t) = \epsilon_p \hat{g}(k) \frac{\sin(\sqrt{\omega_c^2 + c^2 k^2}\, t)}{\sqrt{\omega_c^2 + c^2 k^2}}.$$

To obtain φ, we must then apply the inverse Fourier transform to $\hat{\varphi}$: this process is simplified for $\omega_c t \gg 1$, where the highly oscillatory integrand may be approximated using the method of stationary phase [24], akin to the procedure outlined in **Appendix 2**. For $|x| < ct$, the asymptotic result is

$$\varphi(x, t) \sim \frac{\epsilon_p}{c\sqrt{2\pi}} \frac{\sin(\sqrt{\omega_c^2 t^2 - k_c^2 x^2} + \pi/4)}{(\omega_c^2 t^2 - k_c^2 x^2)^{1/4}} \hat{g}(k_*),$$

where $k_* = k_c/\sqrt{(tc/x)^2 - 1}$. At any given time, the local wavelength is longest at $x = 0$ and decreases as the light cone is approached ($|x| \to ct$). Moreover, the function $\hat{g}(k_*)$ modulates the amplitude of the wave, and the decay of $\hat{g}(k)$ as $|k| \to \infty$ ensures that φ is not singular at $|x| = ct$.

To further simplify the form of φ, we recall that the Bessel function of the first kind with order zero has asymptotic form $J_0(z) \sim \sqrt{2/\pi z}\sin(z + \pi/4)$ as $|z| \to \infty$. As the large-argument decay of $\hat{g}$ diminishes the amplitude of φ for $|x| \lesssim ct$ (see **Figure 8**), we may modify the asymptotic Green's function to the more tractable form

$$\varphi(x, t) \sim \frac{\epsilon_p}{2c} J_0\left(\sqrt{\omega_c^2 t^2 - k_c^2 x^2}\right) \hat{g}\left(\frac{k_c}{\sqrt{(tc/x)^2 - 1}}\right). \tag{19}$$

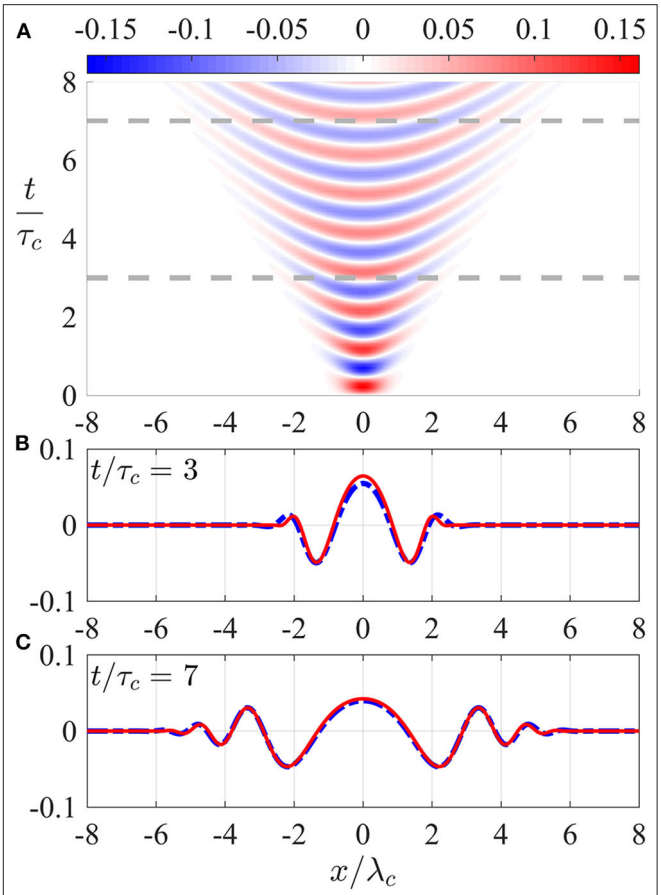

FIGURE 8 | The Green's function. **(A)** Space-time wave evolution of φ, normalized by $\phi_0\omega_c$, as computed numerically. The dashed lines correspond to the profiles presented in **(B,C)**. **(B,C)** φ (blue dash-dotted curve) and its asymptotic approximation (Equation 19) (red solid curve) at times **(B)** $t/\tau_c = 3$ and **(C)** $t/\tau_c = 7$.

The validity of this approximation is demonstrated in **Figure 8**, where we see an excellent agreement between the evolution of the asymptotic and numerical forms of φ.

4.2. The Trajectory Equation

We proceed by combining Equations (1b), (18), and (19) in order to obtain the following integro-differential trajectory equation describing the evolution of the particle position, $x_p(t)$:

$$\gamma(x_p')x_p' = -\alpha \int_{-\infty}^{t} f(s)\partial_x \varphi(x_p(t) - x_p(s), t-s)\,\mathrm{d}s. \qquad (20)$$

The only difference between this integral formulation (Equation 20) and the differential formulation (Equation 1) considered by Dagan and Bush [19] is the approximation of the Green's function, φ, by its asymptotic form (Equation 19). However, as in the stroboscopic model of walking droplets [25], the integral is extended to account for the particle's entire history, specifically its trajectory for $t < 0$.

We next derive a reduced trajectory equation, valid in the non-relativistic limit, in which $|x_p'(t)|/c < \eta$ for all time, t, where $0 < \eta \ll 1$. Equivalently,

$$\frac{|x_p(t) - x_p(s)|}{c(t-s)} < \eta$$

for all time, t, and all $s < t$. To derive the non-relativistic trajectory equation, we expand Equation (20) in powers of η, where $\gamma(x_p') \sim 1 + O(\eta^2)$ and

$$\frac{\partial \varphi}{\partial x}(x,t) \sim \frac{\epsilon_p k_c}{2c}\left[J_1(\omega_c t)\frac{x}{ct} + O(|x/ct|^3)\right],$$

for $|x/ct| \ll 1$. In this latter expansion, we have used the symmetry and normalization of $g(x)$ to exploit that $\hat{g}(k) \sim 1 + O(a^2k^2)$ for $|ak| \ll 1$. As a result, the precise form of the localized particle forcing, g, only appears as a higher-order correction to the near-field slope of φ.

By combining the foregoing expansions and introducing the dimensionless variables $\hat{t} = \omega_c t$, $\hat{x}_p(\hat{t}) = k_c x_p(t)$ and $\hat{f}(\hat{t}) = f(t)$, we reduce Equation (20) to the non-relativistic trajectory equation

$$\frac{\mathrm{d}\hat{x}_p}{\mathrm{d}\hat{t}} = -\kappa \int_{-\infty}^{\hat{t}} \hat{f}(s)\big(\hat{x}_p(\hat{t}) - \hat{x}_p(s)\big)\frac{J_1(\hat{t}-s)}{\hat{t}-s}\,\mathrm{d}s, \qquad (21)$$

where the resultant terms are all of size $O(\eta)$ and we have neglected the correction terms of size $O(\eta^3)$. The dimensionless parameter, $\kappa = \alpha\epsilon_p/2c^3$, determines the strength of the wave-particle coupling, with larger κ resulting in higher particle speeds. We thus require $\kappa > 0$ to be sufficiently small that relativistic effects remain negligible. The non-relativistic trajectory equation (Equation 21) represents a convenient form for exploring non-relativistic pilot-wave dynamics in one dimension: We proceed by characterizing the onset of motion at the critical threshold $\kappa = \kappa_c$.

4.3. The Onset of Particle Motion

For the special case of superharmonic forcing, $\hat{f}(\hat{t}) = \sin(2\hat{t})$, we determine the critical wave-particle coupling parameter, $\kappa_c > 0$, beyond which the particle rest state, $\hat{x}_p = $ constant, is unstable and the system supports sustained particle self-propulsion. We first recast Equation (21) in the form

$$\frac{1}{\kappa}\frac{\mathrm{d}\hat{x}_p}{\mathrm{d}\hat{t}} + \hat{x}_p(\hat{t})\left[\int_0^\infty \sin(2(\hat{t}-s))\frac{J_1(s)}{s}\,\mathrm{d}s\right] = \int_0^\infty \sin(2(\hat{t}-s))\hat{x}_p(\hat{t}-s)\frac{J_1(s)}{s}\,\mathrm{d}s. \qquad (22)$$

By noting that the coefficient of $\hat{x}_p(\hat{t})$ on the left-hand side is periodic with period π, we deduce that this linear trajectory equation is of Floquet form. We thus expect, and may verify numerically, that the onset of motion at $\kappa = \kappa_c$ arises through lateral particle oscillation that is subharmonic relative to the particle's vibration, with a period of 2π corresponding precisely to the Compton period in our non-dimensionalization.

To determine κ_c, we expand $\hat{x}_p(\hat{t})$ using the Floquet ansatz

$$\hat{x}_p(\hat{t}) = \sum_{\substack{n=-\infty \\ n\,\mathrm{odd}}}^{\infty} X_n \mathrm{e}^{\mathrm{i}n\hat{t}}, \qquad (23)$$

where the reality condition for $\hat{x}_p$ is $X_{-n} = X_n^*$ for all n, and $*$ denotes complex conjugation. We substitute the Floquet ansatz (Equation 23) into (22) and evaluate the resultant integrals analytically, before grouping together powers of $\mathrm{e}^{\mathrm{i}\hat{t}}$ to form an infinite-dimensional system of equations for the unknown coefficients, X_n. The critical threshold, κ_c, is the value of κ at which the X_n coefficients have a non-trivial solution, for which the determinant of the corresponding matrix vanishes. Following the procedure outlined by Kumar and Tuckerman [26] and Kumar [27] for the study of the Faraday wave instability, we then truncate this system to a specified number of leading-order harmonics, at which we evaluate an approximation of κ_c numerically.

After substituting Equation (23) into (22), following the aforementioned procedure and evaluating integrals using the identity [28]

$$\int_0^\infty \mathrm{e}^{\pm\mathrm{i}\mu s}\frac{J_1(s)}{s}\,\mathrm{d}s = \pm\mathrm{i}[\mu - \sqrt{\mu^2-1}] \quad \text{for} \quad \mu \geq 1,$$

we obtain the infinite-dimensional, tridiagonal system

$$X_{n-2}(c_n - c_2) - \frac{2\mathrm{i}n}{\kappa}X_n - X_{n+2}(c_n + c_2) = 0$$

for all odd n, where $c_n = \mathrm{sgn}(n)[-|n| + \sqrt{n^2-1}]$. We truncate this system to $(N+1)$ dimensions for the terms $X_{-N}, X_{-N+2}, \ldots, X_N$, where $N \geq 1$ is an odd integer, and we set $X_n = 0$ for $|n| > N$. We define the corresponding critical threshold, κ_N, as the value of κ at which the truncated system is singular, where $\kappa_N \to \kappa_c \sim 2.97579\ldots$ as $N \to \infty$. Since a satisfactory approximation of κ_c is afforded by $\kappa_3 \sim 2.97894\ldots$,

we deduce that the particle oscillation is dominated by the two leading-order harmonics, $e^{\pm i\hat{t}}$ and $e^{\pm 3i\hat{t}}$, corresponding to lateral perturbations at ω_c and $3\omega_c$, respectively.

As may be confirmed numerically by direct simulation of Equation (22), the static state is stable for $0 < \kappa < \kappa_c$ and unstable for $\kappa > \kappa_c$. Similar lateral oscillations were observed in the simulations of Dagan and Bush [19], who described free particle motion in terms of lateral oscillations at the Compton frequency, superimposed on a slowly varying net drift. Our analytic results lend support to their inference that lateral oscillations at the Compton frequency are a fundamental feature of particle motion in HQFT. A fruitful avenue of future research may thus be to exploit the disparity between the time scale of particle translation and lateral oscillation, with a view to further simplifying the trajectory equation.

5. DISCUSSION

The wave forms deduced herein have a number of striking similarities with those arising in pilot-wave hydrodynamics. The propagating waves arising in HQFT are similar to the traveling disturbances in the walker system, which typically play a relatively minor role in the hydrodynamic system, particularly in the guidance of a single droplet. In both systems, the moving particle is dressed in a quasi-monochromatic wave form, which has proven to be the critical feature for the emergence of quantum-like behavior in the hydrodynamic system [17, 20]. Both systems exhibit a Doppler shift, in which the pilot wavelength is compressed ahead of the moving particle, and elongated in the particle's wake [16, 29–31]. Strobing the carrier wave in the walking-droplet system at the Faraday frequency reveals a steady, quasi-monochromatic wave form with the Faraday wavelength, propagating with the droplet: strobing the carrier wave in HQFT at the reduced Compton angular frequency, ω_c/γ, reveals a quasi-steady, quasi-monochromatic wave form with the de Broglie wavelength, propagating with the particle.

The wave forms explored herein also differ substantially from those arising in the walking-droplet system [15]. Most notably, the carrier waves in the two systems take markedly different forms. For rectilinear particle motion in HQFT, the carrier wave of local wavelength λ_B is centered on the particle's initial position (see **Figure 6**) and so may be considered as a relic of the initial conditions. However, in the vicinity of the particle, this carrier wave propagates at the particle speed, qualifying it as a viable candidate for a pilot wave in the fully dynamic treatment. In two spatial dimensions, the carrier wave approaches, in the long-time limit, a plane wave whose wavelength is precisely the de Broglie wavelength at the particle position. We note that a similar pilot-wave form was deduced by Andersen et al. [32], who described a quantum particle in terms of a wave packet solution to the forced Schrödinger equation subject to Galilean invariance. In the hydrodynamic system, the quasi-monochromatic carrier wave instead consists of the superposition of the stationary Faraday wave forms generated at each impact, giving rise to its characteristic horseshoe-like form [16]. Finally, the Faraday waves in the walker system decay exponentially in time owing to the influence of viscosity. In HQFT, the carrier wave is relatively long lived, exhibiting algebraic temporal decay; specifically, in one spatial dimension, the amplitude of the carrier wave decreases over time according to $(\omega_c t)^{-1/2}$. One expects this relatively slow decay to result in a relatively pronounced influence of the particle's past trajectory on the instantaneous wave form in HQFT.

The dependence of the pilot-wave form on the particle speed elucidated here is both intriguing and encouraging. In the non-relativistic limit, the pilot-wave form is effectively monochromatic, with the de Broglie wavelength. Our analysis has shown that, in the special case of rectilinear motion, the carrier wave is a transient, dependent on the initialization of the system, and decays algebraically as $\omega_c t \to \infty$. While the form of this carrier wave was derived only for the special case of rectilinear particle motion at a prescribed speed, we anticipate that similar wave forms will arise for free particle dynamics [19]. Moreover, for different dynamical configurations, such as for in-line speed oscillations of the free particle [19] or orbital dynamics, the carrier wave form may in fact be more persistent than the case of rectilinear motion, producing a robust signature of the de Broglie wavelength in the pilot wave. The dynamics and emergent statistics might then be similar to those arising in pilot-wave hydrodynamics, where the Faraday wavelength plays a role analogous to the de Broglie wavelength in numerous settings, including orbital pilot-wave systems [33–36] and corrals [37, 38].

While the nonrelativistic trajectory equation (Equation 21) yields a convenient mathematical form, preliminary simulations have revealed that the particle has a propensity for speed fluctuations on the Compton time scale, at speeds approaching the speed of light [19]. These relativistic speed fluctuations are similar in form to the jittering modes arising in generalized pilot-wave hydrodynamics [39], the *Zitterbewegung* predicted in early models of quantum dynamics [23, 40], and the speed fluctuations evident in simulations of the free particle in HQFT [19]. Thus, while the mean particle speed may be slow relative to the speed of light, relativistic effects may still be significant on the Compton time scale, necessitating alternative simplifications of the relativistic trajectory equation (Equation 20). In the hydrodynamic system, one may average the droplet trajectory over one bouncing period, giving rise to a stroboscopic trajectory equation that requires no consideration of the droplet's vertical motion [25]. Analogous averaging of Equation (20) over the Compton period of lateral oscillations might give rise to a reduced trajectory equation for HQFT, similar in spirit to the stroboscopic model of pilot-wave hydrodynamics. Another potentially fruitful direction would be to consider the limit in which the intrinsic particle vibration, $f(t)$, is characterized in terms of a periodically applied delta function. One might thus deduce a discrete-time iterative map similar in form to the hydrodynamic pilot-wave model of Durey Milewski [29].

Our theoretical developments have shown that, in the relativistic limit, $|v| \to c$, the pilot-wave form is dominated by the Compton wavelength, suggesting the possibility of quantization arising on this scale. A tantalizing possibility thus presents itself of HQFT being able to capture structure on the scale of

the Compton wavelength. For example, while hydrodynamic spin states are known to be unstable in the laboratory [41, 42], their analog in HQFT may correspond to the classical model of the electron, wherein a charge executes a circular orbit with the Compton frequency on a radius corresponding to the Compton wavelength [43]. HQFT thus promises the possibility of accounting for the emergence of both quantization and quantum statistics on the de Broglie wavelength for non-relativistic dynamics, and structure on the Compton scale for relativistic dynamics.

6. CONCLUSION

We have performed a detailed analysis of the one-dimensional pilot-wave model proposed by Dagan and Bush [19], an attempt to advance de Broglie's double-solution theoretical program [1–4] by exploiting insights gained from the walking-droplet system [15, 20]. Particular attention has been given to rationalizing the forms of the emergent pilot-wave fields reported by Dagan and Bush [19]. Our analysis has shown that the pilot wave is the combination of short, Compton-scale waves that propagate away from the moving particle, and a de Broglie-scale carrier wave. The wavelength of the carrier wave is precisely the de Broglie wavelength at the particle position, independent of the particle speed, which is consistent with the validity of the de Broglie relation, $p = \hbar k_B$. Moreover, in the vicinity of the particle, the frequency of the carrier wave is ω_c/γ and the local wavelength exhibits a Doppler shift: this carrier wave thus has features of the pilot wave described by de la Peña and Cetto [10] in the context of stochastic electrodynamics. Notably, as the local wavelength is precisely the de Broglie wavelength, the gradient of the wave phase is simply proportional to the gradient of the wave amplitude, indicating that the wave-particle coupling considered by Dagan and Bush [19] is consistent with that proposed by de Broglie [1–4].

Our study of particle kinematics (section 3.3) has shown that increasing the spatial extent of the localized forcing of the particle on its pilot wave decreases the amplitude of both the propagating and carrier waves, thus presumably decreasing the efficacy of particle self-propulsion. Furthermore, the form of the pilot wave also varies significantly with the angular frequency, ω_0, of the particle vibration. In the hydrodynamic system, resonance between the droplet's vertical motion and its subharmonic Faraday wave field is a prerequisite for a quasi-monochromatic wave field and the concomitant emergence of quantum-like behavior [17, 20]. We therefore expect that a similar resonance between particle and wave vibration will be necessary in HQFT: ω_0 must be an integer multiple of ω_c. Our deductions in section 3.3 indicate that the amplitude of the pilot wave is decreased when ω_0 is large compared to ω_c. To maximize the particle's propensity for self-propulsion, the choice $\omega_0 = 2\omega_c$ considered by Dagan and Bush [19] thus appears to be the most propitious.

Finally, we have laid the foundations for deeper study of HQFT through the derivation of an integro-differential trajectory equation (Equation 20) similar in form to that derived for walking droplets [25, 44]. This formulation will enable more efficient simulation of the associated pilot-wave dynamics in a range of one-dimensional settings. Moreover, it will allow for the analysis of the stability of various dynamical states, including the free self-propelling state [19] and the oscillatory particle motion arising in the presence of a harmonic potential [45]. Of particular interest is the stability of the free self-propelling state to speed oscillations with the de Broglie wavelength [39], as may result in a commensurate statistical signature [46]. The extension of our analysis to two dimensions, as outlined in section 3.4, follows through a similar procedure, and has allowed for a comparison between the wave forms in HQFT and those arising in pilot-wave hydrodynamics. We expect the extension of HQFT to three dimensions to be straightforward, and to open up exciting new vistas in pilot-wave modeling.

DATA AVAILABILITY STATEMENT

The original contributions presented in the study are included in the article/**Supplementary Material**, further inquiries can be directed to the corresponding author/s.

AUTHOR CONTRIBUTIONS

JB proposed the study. MD performed the mathematical analysis, numerical computations, and created the figures. All authors wrote the paper, gave final approval for publication, and agree to be held accountable for the work performed therein.

FUNDING

The authors gratefully acknowledge the NSF for financial support through grant CMMI-1727565.

ACKNOWLEDGMENTS

We acknowledge valuable discussions with, and input from, Yuval Dagan.

SUPPLEMENTARY MATERIAL

The Supplementary Material for this article can be found online at: https://www.frontiersin.org/articles/10.3389/fphy.2020.00300/full#supplementary-material

REFERENCES

1. de Broglie L. *Recherches sur la thÉorie des Quanta*. Migration-Université en Cours D'affectation (1924).
2. de Broglie L. *An Introduction to the Study of Wave Mechanics*. London, UK: Methuen, MA (1930). Available online at: https://catalog.hathitrust.org/Record/001477720
3. de Broglie L. The reinterpretation of wave mechanics. *Found Phys.* (1970) **1**:1–15. doi: 10.1007/BF00708650

4. de Broglie L. Interpretation of quantum mechanics by the double solution theory. *Ann Fond*. (1987) **12**:1–23.
5. Colin S, Durt T, Willox R. L. de Broglie's double solution program: 90 years later. *Ann Fond Louis de Broglie*. (2017) **42**:19–71. Available online at: https://arxiv.org/pdf/1703.06158.pdf
6. Davisson CJ, Germer LH. Reflection of electrons by a crystal of nickel. *Proc Natl Acad Sci USA*. (1928) **14**:317–22. doi: 10.1073/pnas.14.4.317
7. Bohm D. A suggested interpretation of the quantum theory in terms of "hidden" variables. I. *Phys Rev*. (1952) **85**:166–79. doi: 10.1103/PhysRev.85.166
8. Bohm D. A suggested interpretation of the quantum theory in terms of "hidden" variables. II. *Phys Rev*. (1952) **85**:180–93. doi: 10.1103/PhysRev.85.180
9. Holland PR. *The Quantum Theory of Motion: An Account of the de Broglie-Bohm Causal Interpretation of Quantum Mechanics*. Cambridge, MA: Cambridge University Press (2008).
10. de la Peña L, Cetto AM. *The Quantum Dice: An Introduction to Stochastic Electrodynamics*. Dordrecht: Kluwer Academic (1996). doi: 10.1007/978-94-015-8723-5
11. de la Peña L, Cetto AM, Valdés-Hernández A. *The Emerging Quantum: The Physics Behind Quantum Mechanics*. New York, NY: Springer (2015).
12. Boyer TH. Any classical description of nature requires classical electromagnetic zero-point radiation. *Am J Phys*. (2011) **79**:1163–7. doi: 10.1119/1.3630939
13. Milonni PW. *The Quantum Vacuum: An Introduction to Quantum Electrodynamics*. Cambridge, MA: Academic Press (1994). doi: 10.1016/B978-0-08-057149-2.50014-X
14. Kracklauer AF. Pilot-wave steerage: a mechanism and test. *Found Phys Lett*. (1999) **12**:441–53. doi: 10.1023/A:1021629310707
15. Couder Y, Protiére S, Fort E, Boudaoud A. Walking and orbiting droplets. *Nature*. (2005) **437**:208. doi: 10.1038/437208a
16. Eddi A, Sultan E, Moukhtar J, Fort E, Rossi M, Couder Y. Information stored in Faraday waves: the origin of a path memory. *J Fluid Mech*. (2011) **674**:433–63. doi: 10.1017/S0022112011000176
17. Bush JWM, Couder Y, Gilet T, Milewski PA, Nachbin A. Introduction to focus issue on hydrodynamic quantum analogs. *Chaos*. (2018) **28**:096001. doi: 10.1063/1.5055383
18. Harris DM, Bush JWM. The pilot-wave dynamics of walking droplets. *Phys Fluids*. (2013) **25**:091112. doi: 10.1063/1.4820128
19. Dagan Y, Bush JWM. Hydrodynamic Quantum Field Theory: The Free Particle. Comptes Rendus Mécanique. (2020). doi: 10.5802/crmeca.34
20. Bush JWM. Pilot-wave hydrodynamics. *Annu Rev Fluid Mech*. (2015) **47**:269–92. doi: 10.1146/annurev-fluid-010814-014506
21. Alhaidari AD, Bahlouli H, Al-Hasan A. Dirac and Klein-Gordon equations with equal scalar and vector potentials. *Phys Lett A*. (2006) **349**:87–97. doi: 10.1016/j.physleta.2005.09.008
22. Shinbrot T. Dynamic pilot wave bound states. *Chaos*. (2019) **29**:113124. doi: 10.1063/1.5116695
23. Schrödinger E. About the force-free motion in relativistic quantum mechanics. *Prus Acad Sci*. (1930) **31**:418–28.
24. Bender CM, Orszag SA. *Advanced Mathematical Methods for Scientists and Engineers I*. New York, NY: Springer (1999). doi: 10.1007/978-1-4757-3069-2
25. Oza AU, Rosales RR, Bush JWM. A trajectory equation for walking droplets: hydrodynamic pilot-wave theory. *J Fluid Mech*. (2013) **737**:552–70. doi: 10.1017/jfm.2013.581
26. Kumar K, Tuckerman LS. Parametric instability of the interface between two fluids. *J Fluid Mech*. (1994) **279**:49–68. doi: 10.1017/S0022112094003812
27. Kumar K. Linear theory of Faraday instability in viscous fluids. *Proc R Soc Lond A*. (1996) **452**:1113–26. doi: 10.1098/rspa.1996.0056
28. Abramowitz M, Stegun I. *Handbook of Mathematical Functions*. New York, NY: Dover Publications (1964).
29. Durey M, Milewski PA. Faraday wave-droplet dynamics: discrete-time analysis. *J Fluid Mech*. (2017) **821**:296–329. doi: 10.1017/jfm.2017.235
30. Milewski PA, Galeano-Rios CA, Nachbin A, Bush JWM. Faraday pilot-wave dynamics: modelling and computation. *J Fluid Mech*. (2015) **778**:361–88. doi: 10.1017/jfm.2015.386
31. Tadrist L, Shim JB, Gilet T, Schlagheck P. Faraday instability and subthreshold Faraday waves: surface waves emitted by walkers. *J Fluid Mech*. (2018) **848**:906–45. doi: 10.1017/jfm.2018.358
32. Andersen A, Madsen J, Reichelt C, Rosenlund Ahl S, Lautrup B, Ellegaard C, et al. Double-slit experiment with single wave-driven particles and its relation to quantum mechanics. *Phys Rev E*. (2015) **92**:013006. doi: 10.1103/PhysRevE.92.013006
33. Fort E, Eddi A, Boudaoud A, Moukhtar J, Couder Y. Path-memory induced quantization of classical orbits. *Proc Natl Acad Sci USA*. (2010) **107**:17515–20. doi: 10.1073/pnas.1007386107
34. Harris DM, Bush JWM. Droplets walking in a rotating frame: from quantized orbits to multimodal statistics. *J Fluid Mech*. (2014) **739**:444–64. doi: 10.1017/jfm.2013.627
35. Oza AU, Harris DM, Rosales RR, Bush JWM. Pilot-wave dynamics in a rotating frame: on the emergence of orbital quantization. *J Fluid Mech*. (2014) **744**:404–29. doi: 10.1017/jfm.2014.50
36. Perrard S, Labousse M, Miskin M, Fort E, Couder Y. Self-organization into quantized eigenstates of a classical wave-driven particle. *Nat Commun*. (2014) **5**:3219. doi: 10.1038/ncomms4219
37. Harris DM, Moukhtar J, Fort E, Couder Y, Bush JWM. Wavelike statistics from pilot-wave dynamics in a circular corral. *Phys Rev E*. (2013) **88**:011001. doi: 10.1103/PhysRevE.88.011001
38. Sáenz PJ, Cristea-Platon T, Bush JWM. Statistical projection effects in a hydrodynamic pilot-wave system. *Nat Phys*. (2018) **14**:315–9. doi: 10.1038/s41567-017-0003-x
39. Durey M, Turton SE, Bush JWM. Speed oscillations in classical pilot-wave dynamics. *Proc R Soc A*. (2020) 476:20190884. doi: 10.1098/rspa.2019.0884
40. Hestenes D. The zitterbewegung interpretation of quantum mechanics. *Found Phys*. (1990) **20**:1213–32. doi: 10.1007/BF01889466
41. Labousse M, Perrard S, Couder Y, Fort E. Self-attraction into spinning eigenstates of a mobile wave source by its emission back-reaction. *Phys Rev E*. (2016) **94**:042224. doi: 10.1103/PhysRevE.94.042224
42. Oza AU, Rosales RR, Bush JWM. Hydrodynamic spin states. *Chaos*. (2018) **28**:096106. doi: 10.1063/1.5034134
43. Burinskii A. The Dirac-Kerr-Newman electron. *Gravit Cosmol*. (2008) **14**:109–22. doi: 10.1134/S0202289308020011
44. Moláček J, Bush JWM. Drops walking on a vibrating bath: towards a hydrodynamic pilot-wave theory. *J Fluid Mech*. (2013) **727**:612–47. doi: 10.1017/jfm.2013.280
45. Durey M, Milewski PA, Bush JWM. Dynamics, emergent statistics, and the mean-pilot-wave potential of walking droplets. *Chaos*. (2018) **28**:096108. doi: 10.1063/1.5030639
46. Sáenz PJ, Cristea-Platon T, Bush JWM. A hydrodynamic analog of Friedel oscillations. *Sci Adv*. (2020) **6**:eaay9234. doi: 10.1126/sciadv.aay9234

Conflict of Interest: The authors declare that the research was conducted in the absence of any commercial or financial relationships that could be construed as a potential conflict of interest.

frontiers in Physics

ORIGINAL RESEARCH
published: 17 July 2020
doi: 10.3389/fphy.2020.00213

Electron Mass Predicted From Substructure Stability in Electrodynamical Model

Stéphane Avner[1]* *and Florence Boillot*[2]

[1] CNRS, Univ Rennes, IGDR-UMR 6290, Rennes, France, [2] COSYS-GRETTIA, Univ Gustave Eiffel, IFSTTAR, Marne-la-Vallée, France

Modern physics has characterized spacetime, the interactions between particles, but not the nature of the particles themselves. Previous models of the electron have not specified its substance nor justified its cohesion. Here we present a relativistic electrodynamical model of the electron at rest, founded on natural interpretations of observables. Essentially intertwined positively and negatively charged subparticles revolve at light velocity in coplanar circular orbits, forming some coherent "*envelope*" and "*nucleus*", possibly responsible for its wavelike and corpuscular behaviors, respectively. We show that the model can provide interpretations of fundamental constants, satisfy the Virial theorem, and exhibit cohesion and stability without invoking Poincaré stresses. Remarkably, the stability condition allows predicting electron mass, regarded as being a manifestation of its total (kinetic and potential) electromagnetic cohesion energy, and muon mass, directly from the substructure. Our study illustrates the possibility of constructing causal and objectively realist models of particles beneath the Compton scale. Finally, wave-corpuscle duality and the relation to quantum mechanics are discussed in the light of our electron model.

Keywords: electron substructure, fundamental constants, electromagnetic mass, wave-corpuscle duality, objective reality

OPEN ACCESS

Edited by:
Ana Maria Cetto, National Autonomous University of Mexico, Mexico

Reviewed by:
Xing Lu, Beijing Jiaotong University, China
Kazuharu Bamba, Fukushima University, Japan

***Correspondence:**
Stéphane Avner
stephane.avner@univ-rennes1.fr

Specialty section:
This article was submitted to Mathematical Physics, a section of the journal Frontiers in Physics

Received: *24 March 2020*
Accepted: *19 May 2020*
Published: *17 July 2020*

Citation:
Avner S and Boillot F (2020) Electron Mass Predicted From Substructure Stability in Electrodynamical Model. Front. Phys. 8:213. doi: 10.3389/fphy.2020.00213

INTRODUCTION

Depending on the experiment, the most emblematic subatomic particle, the electron, has been found to interact as a point-like corpuscle in scattering experiments [1], or to behave as an extensible wave [2]. Elaborating on Bohr's interpretation of Quantum Mechanics [3], Heisenberg concluded that particles could neither be represented nor even apprehended by the human mind, and that only their abstract mathematical description existed [4]. For de Broglie however, "abstract presentations have no physical reality. Only the movement of elements localized in space, in the course of time, has physical reality" [5]. Hence, modern physics has identified with unprecedented precision the interactions and their underlying principles, has successfully described its environment, spacetime, but still lacks a characterization of the nature of its "objects," the particles themselves.

Consequently, several kinds of electron models have been proposed: extended models [6], point-like models, and mixed models in which a point-like corpuscle follows an extended trajectory [7]. Early attempts included the *spherical models* of Abraham [8] and Lorentz [9], which led to theories of electromagnetic mass [10–13]. Spherical models soon evolved into the so-called *ring models* of Parson [14], Webster [15], Allen [16], and Compton [17], constituted of rotating

infinitesimal charges and verifying the properties of classical magnetic moment and Compton scattering. Essential constraints however, such as electron cohesion and stability, could not be satisfied: new putative forces, denoted Poincaré stresses [18], were suggested to maintain the cohesion of the negatively charged electron. The abstract descriptions of quantum mechanical theories [19, 20] then successfully accounted for the wave-like behavior of the electron and probabilistically predicted [21] the values of most observables by considering a point-like particle, yet failed at interpreting fundamental constants or explaining how a point-like corpuscle could have spin or a finite energy density. Paradoxically, quantum mechanics revived geometric models when Schrödinger noticed within the Dirac equation itself a rapid oscillatory trembling motion, which he called Zitterbewegung (*zbw*) [22], exhibiting microcurrents arising at light velocity *c*. Surprisingly, the electron seemed to follow a helical trajectory of radius $\lambda\!\!\!^{-}_c$, the reduced Compton wavelength, surrounding the average travel direction (**Figure 1A**). Several such *zbw models*, identifying spin with orbital angular momentum, were interpreted classically [27–29]. Subsequent electrodynamical or hydrodynamical models involved fluids with spin [30], current loops of a certain thickness [31], Dirac-like Equations [32, 33], moving charged membranes [34], plasmoid fibers [35], or toroidal geometry [35, 36]. Wondering whether *zbw* could be a real phenomenon, Hestenes emphasized the need to investigate the electron substructure, suggested *zbw* could originate in the electron self-interaction [37], and showed *zbw* was compatible with the ring models [38].

With the development of realist models of the electron emerged theories of electromagnetic mass. At first, the spherical models of Abraham [8], and Lorentz [9] seemed to fail to recover Einstein's relation $E = mc^2$ due to the appearance of a factor 4/3, but later proved to be compatible, once relativistic corrections were accounted for [12]. Stability of the sphere however still relied on Poincaré stresses or unknown surface tension [34], and electron mass could not be predicted from an objective criterion, but depended on the value taken by an arbitrary parameter, whose value is unconstrained, i.e., the radius of the sphere. Of note, the mass of subatomic particles is not predicted by quantum theories, and their values need to be inserted in calculations [12]. Most ring models [14–17] are prior to the discoveries of the spin, anomalous magnetic moment, and quantum mechanics. The ring model of Bergman and Wesley [31] exhibited cohesion and stability, but the expression for mass still involved an arbitrary parameter (i.e., width of current loop), and the substance constituting the electron remained indeterminate. More recently, Consa proposed a point-like electron following a toroidal trajectory [36], recovered mass independently of any arbitrary parameter, but did not specify how the trajectory developed nor demonstrated its stability. To our knowledge, the Virial theorem, which should be satisfied since the electron is a bound system, has not been considered in electron models. Potential energy is often equated to $+mc^2$, although cohesion potential energy should be negative for a bound system [as it is for the atom for instance [19]]. Kinetic energy is not usually accounted for, even though Lorentz [9], Hestenes [38] and others [e.g., [32]] noted the existence of a rotating motion and wondered whether kinetic energy did not contribute to rest mass. For Barut and Bracken, rest mass energy of the particle is the energy of the internal motion in the rest frame [29].

Hence, several issues remain to be addressed regarding the electron: for instance, which forces could cause the puzzling helical trajectory? What could be the nature of the substance constituting the electron? Could an electrodynamical description account for electron cohesion and stability? And could Lorentz' hypothesis advocating the electromagnetic origin of mass be simultaneously implemented from an objective criterion, instead of an arbitrary parameter?

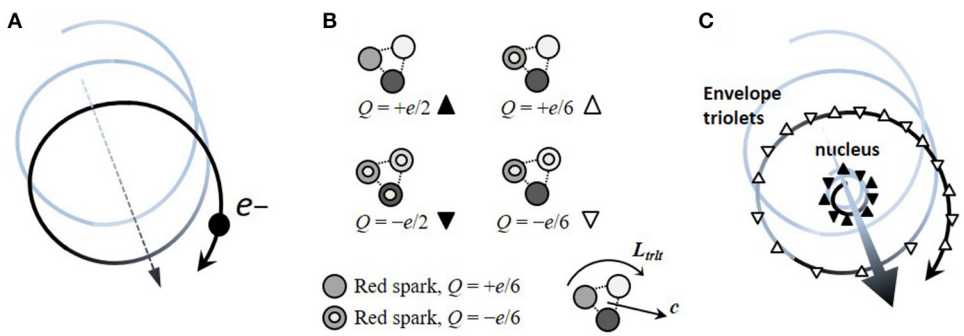

FIGURE 1 | Triolets and the helical trajectory. **(A)** In Schrödinger's Zitterbewegung (*zbw*) model, the wavefunction associated to the electron seems to revolve at light velocity along a helical trajectory of radius $\lambda\!\!\!^{-}_c$, the reduced Compton wavelength, surrounding the average travel direction, and to exhibit microcurrents. Quantum mechanics does not specify which forces could cause the electron, which is assumed to be point-like, to follow such a peculiar helical trajectory. **(B)** Triolets are colorless particles composed of three sparks, each bearing electric charge $\pm e/6$ and a specific strong interaction color charge. Thus triolets bear electric charge $\pm e/6$ or $\pm e/2$ depending on their combination of sparks. They travel at light velocity *c*, possess angular momentum L_{trlt}, and triolets will thereafter be represented as upward or downward, filled or hollow triangles depending on their electric charge, as depicted here. **(C)** In our model, the electron is composed of triolets forming a nucleus and an envelope. It is conceivable that, in the absence of perturbation, the nucleus of the moving electron attracts envelope triolets and maintains them bound, thus explaining their helical trajectory. Conversely, envelope triolets would revolve at light velocity on an orbit of radius $\lambda\!\!\!^{-}_c$ around the nucleus, exhibiting the zbw microcurrents, and guide the nucleus, as in pilot-wave theories [23–26], sensing the electromagnetic fields generated by the envelopes of other particles.

In this study, we present a relativistic electrodynamical model of the electron at rest, in which charged subparticles follow definite trajectories. The model is based on two main hypotheses: (*i*) the existence of charged colorless subparticles called *triolets*, (*ii*) the assumption that triolets revolve at light velocity on coplanar circular orbits, constituting an *envelope* and *nucleus*, depending on their electromagnetic charges. As the electron is coherent, it is assumed that the model satisfies the Virial theorem. Constraints capturing the measured values of several observables (classical and anomalous magnetic moments, spin, Compton wavelength, kinetic energy) are formulated. Using Liénard-Wichert potentials, we then determine the specific kinds and numbers of triolets satisfying envelope and nucleus stability. Remarkably, we find that these kinds and numbers are precisely those that allow predicting electron mass and muon mass electromagnetically directly from the substructure, thus implementing Lorentz' hypothesis. Electron mass is effectively derived from an expression of substructure stability, which constitutes an objective criterion in our view. Our system also illustrates the possibility of constructing causal, local, objective, and realist models of particles beneath the Compton scale. Finally, we discuss novel perspectives suggested by the model, relative to the understanding of wave-corpuscle duality and to its relation to quantum theory.

DESCRIPTION OF THE MODEL AND HYPOTHESES

In a previous study, we proposed that just six kinds of *indestructible* elementary subparticles denoted *sparks*, bearing electric charge $\pm e/6$ and a specific strong interaction color charge, are necessary and sufficient to reconstruct all subatomic particles, so that sparks are conserved and reorganized across particle decays and annihilations [Avner, Boillot, Richard, submitted]. Since sparks are subject to both the strong and electromagnetic interactions, with the former dominating at short distances [20], groups of three sparks could presumably assemble beforehand to form composite colorless particles, thereafter called *triolets*, bearing charge $+e/6$, $-e/6$, $+e/2$, or $-e/2$ (**Figure 1B**). Henceforth, we shall suppose that the electron is exclusively composed of triolets, which travel at light velocity [7], exhibit some intrinsic angular momentum L_{trlt}, and being colorless, are submitted to electromagnetic and centrifugal forces only (hypothesis A).

Following de Broglie's proposition, we aim at constructing a plausible electrodynamical model of the electron at rest, in which positive and negative triolets form an electromagnetically bound system, exhibit the *zbw* microcurrents, and account for all experimentally measured observables. The electron is considered here as a particle of a certain extension, composed of revolving charged subparticles, the triolets, thereby exhibiting magnetic moment and intrinsic angular momentum (its spin) sensed by other particles. We know that the measured value of the electron magnetic moment is the sum of Bohr magneton $\mu_B = -e\hbar/2m$, predicted by both classical physics and quantum mechanics, where $\hbar$ is reduced Planck constant, m the electron mass, and e the elementary charge, and an *anomalous* magnetic moment [39], which accounts for a small fraction $a_{anml} \backsimeq 0.001159$ of the previous and is only predicted by quantum electrodynamics [20]. Remarkably, the value of the classical magnetic moment of the electron can be derived by considering a charge $(-e)$ revolving on a circular orbit of radius $\lambda\!\!\!^{-}_c$ [19]. Hence, we reckoned the classical and anomalous magnetic moments could, respectively, be produced by two different *components* of the electron, namely a negatively charged *envelope* and a neutrally charged *nucleus*, also possibly responsible for the electron's wavelike and corpuscular behaviors, respectively. The peculiar helical trajectory of the electron predicted by *zbw* could then be naturally apprehended by considering that *zbw* describes the dynamics of envelope triolets, which are attracted and bound to the nucleus (**Figure 1C**). Electron spin could correspond to the sum of angular momenta of envelope triolets. Moreover, we shall regard electron mass as being a manifestation of the total electromagnetic cohesion energy E of the particle, as Lorentz hypothesized [9], through Einstein's formula $m = E/c^2$. The latter interpretation of the mass is naturally suggested by the observation that the muon possesses a mass ∼206.77 times bigger than that of the electron, while its Compton wavelength is ∼206.77 times smaller, as would be the case for a mass of electromagnetic origin, presenting a potential proportional to inverse distance.

The net electromagnetic forces acting on any particular envelope triolet should mostly depend on its surrounding triolets. The envelope could be organized into a complex structure, with triolets irregularly distributed along the orbits, or revolving at various radii, or experiencing fluctuations. To facilitate calculations however, we chose to make approximations and consider triolets at radial equilibrium rotating in the same direction on four coplanar circular orbits of different radii depending on their four different electromagnetic charges (hypothesis B, **Figure 2**). In our model, positive and negative nucleus triolets are intertwined to maintain their cohesion and could rotate along two close yet separate orbits due to the charged envelope. This could cause in turn a similar arrangement in the envelope, which would exhibit predominantly intertwined triolets, in spite of the excess of negative triolets. We are aware our model is only an approximation, even if we reckon that a collection of fluctuating $\pm e/6$ and $\pm e/2$ triolets traveling at light velocity could possibly converge toward such a configuration. Because of their stronger charges, $\pm e/2$ triolets could be more tightly bound and form a condensed nucleus, while $\pm e/6$ triolets would be bound more loosely and constitute the envelope.

In addition, as the electron is a bound system whose inner potentials allegedly depend on position coordinates only and not velocities (justification is given below), the Virial theorem should be verified [40]: for inverse square law electromagnetic interactions, one typically has $E = U/2$ and $E = -T$, where T is the total internal kinetic energy and U the internal potential energy. Therefore, T and U should, respectively, amount to $+mc^2$ and $-2mc^2$, resulting in total internal energy

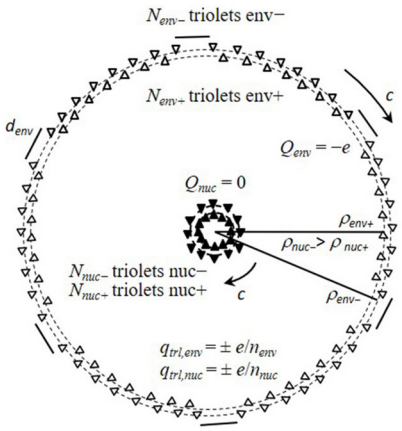

FIGURE 2 | Model of the electron at rest. In our simplified model, triolets rotate at light velocity in the same direction along four different coplanar circular orbits depending on their electric charge, constituting an envelope, and nucleus. Negative triolets are more numerous at the envelope, while the nucleus is neutrally charged. Due to the charged envelope, nucleus triolets are separated into two close orbits depending on their charge. Envelope triolets similarly revolve on separated orbits whose radii are close to the reduced Compton wavelength. Possible triolet configurations (triolet kinds and numbers, angular distributions, orbital radii) must fulfill constraints expressing radial stability and the measured values of charge, spin, magnetic moments, and mass. Due to consecutive negative triolets in the envelope, intertwined envelope triolets assemble into stretches separated by a distance d_{env}.

$E = T + U = -mc^2$ corresponding to electron mass, the minus sign being indicative of a bound system. Finally, we shall admit that, for the electron at rest, envelope triolets approximately follow a circular trajectory of radius $\lambda\!\!\!^{-}_{c} = \hbar/mc$, as suggested by the classical derivation of Bohr's magneton, and by *zbw*-like models. Interpretations of fundamental constants associated to the electron, such as reduced Planck constant $\hbar$ and fine-structure constant $\alpha = e^2/4\pi\varepsilon_0\hbar c$ (where ε_0 designates vacuum permittivity), should also emerge from the model.

FORMULATION OF THE MODEL

Our system captures the measured values of charge, magnetic moments, spin and kinetic energy, and will be validated by showing that cohesion and stability can be satisfied, and potential energy (and thus electron mass) can be recovered. Let us here mathematically formulate the constraints: (*i*) a charge $-e$ carried by $N_{env} = N_{env+} + N_{env-}$ triolets of charge $\pm e/n_{env}$ at the envelope; (*ii*) a classical magnetic moment μ_B generated by envelope triolets rotating at radii $\rho_{env+} = \eta_{env+}\lambda\!\!\!^{-}_{c}$, $\rho_{env-} = \eta_{env-}\lambda\!\!\!^{-}_{c}$, and producing currents I_{env+}, I_{env-}; (*iii*) an anomalous magnetic moment $a_{anml.}\mu_B$ generated by N_{nuc} nucleus triolets ($N_{nuc+} = N_{nuc-}$) of charge $\pm e/n_{nuc}$ rotating in the same direction as envelope triolets at radii $\rho_{nuc+} = \eta_{nuc+}\lambda\!\!\!^{-}_{c}$, $\rho_{nuc-} = \eta_{nuc-}\lambda\!\!\!^{-}_{c}$, with momentum $p_{nuc+} \simeq p_{nuc-} = p_{nuc}$ and producing currents I_{nuc+}, I_{nuc-}; (*iv*) an internal kinetic energy $T = \sum_i p_i c = +mc^2$; (*v*) a spin $S_{env} = +\hbar/2$ generated by envelope triolets of momentum p_{env+}, p_{env-}:

$$-e = e\left[\left(\frac{N_{env+}}{n_{env}}\right) - \left(\frac{N_{env-}}{n_{env}}\right) + \left(\frac{N_{nuc+}}{n_{nuc}}\right) - \left(\frac{N_{nuc-}}{n_{nuc}}\right)\right], \quad (1)$$

$$\frac{-e\hbar}{2m} = I_{env+}\pi\rho_{env+}^2 + I_{env-}\pi\rho_{env-}^2, \quad (2)$$

$$\frac{-a_{anml}e\hbar}{2m} = I_{nuc+}\pi\rho_{nuc+}^2 + I_{nuc-}\pi\rho_{nuc-}^2, \quad (3)$$

$$\sum_i p_i c = \left(N_{env+}p_{env+} + N_{env-}p_{env-} + N_{nuc}p_{nuc}\right)c, \quad (4)$$

$$\frac{\hbar}{2} = N_{env+}\rho_{env+}p_{env+} + N_{env-}\rho_{env-}p_{env-}. \quad (5)$$

The fact that the muon has same spin as the electron, despite possessing a smaller Compton wavelength and the same number of triolets according to our chemical theory [Avner, Boillot, Richard, submitted], suggests that the angular momentum of envelope triolets could be a constant $\rho_{env+}p_{env+} \simeq \rho_{env-}p_{env-} \equiv L_{trlt,env}$, yielding from (5):

$$\hbar = 2N_{env}L_{trlt,env}. \quad (6)$$

$L_{trlt,env}$ is possibly determined by the triangular substructure of envelope triolets made of three strongly interacting sparks, and could be at the basis of Planck's constant. Further constraints are also deduced (see Values of Observables) from Equations (1–5):

$$n_{env} = N_{env-} - N_{env+}, \quad (7)$$

$$n_{env} = \left(N_{env-}\eta_{env-} - N_{env+}\eta_{env+}\right), \quad (8)$$

$$a_{anml}n_{nuc} = N_{nuc+}\left(\eta_{nuc-} - \eta_{nuc+}\right), \quad (9)$$

$$\frac{T_{env} + T_{nuc}}{mc^2} = 1 \simeq \frac{1}{b_{env}}\left(\frac{N_{env+}}{\eta_{env+}} + \frac{N_{env-}}{\eta_{env-}}\right) + \frac{N_{nuc}}{b_{nuc}\eta_{nuc}}, \quad (10)$$

$$b_{env} = 2N_{env}, \quad (11)$$

where b_{env} and b_{nuc} are dimensionless numbers. Assuming that $\eta_{env+} \simeq \eta_{env-} \equiv \eta_{env} \simeq 1$, we deduce (in Values of Observables) from Equations (10–11) that the kinetic energies of the envelope and nucleus are approximately equal $T_{env+} \simeq T_{nuc} \simeq +mc^2/2$, leading to relation:

$$b_{nuc}\eta_{nuc} = 2N_{nuc}. \quad (12)$$

Furthermore, the electromagnetic force acting on a nucleus triolet due to the envelope charge and current and the electromagnetic force exerted on an envelope triolet due to the net nucleus magnetic moment were derived but found to be negligible when compared to intra-component interactions. This suggests that each component is only loosely bound to the other, almost constituting an independent

system, and thus verifies the Virial theorem independently (see Values of Observables), yielding for potential energies $U_{env} \simeq U_{nuc} \simeq -mc^2$ and total energies $E_{env} \simeq E_{nuc} \simeq -mc^2/2$. The system of Equations (9–11) further allows to determine η_{nuc+} (Values of Observables) for each value of N_{nuc+}:

$$\eta_{nuc+} = \frac{N_{nuc+}}{b_{nuc}} \left[2 - \frac{a_{anml} b_{nuc} n_{nuc}}{2N_{nuc+}^2} + \sqrt{4 + \left(\frac{a_{anml} b_{nuc} n_{nuc}}{2N_{nuc+}^2} \right)^2} \right], \tag{13}$$

while η_{nuc-} is then given by Equation (9).

System cohesion and stability can be formulated by ensuring triolets are at radial equilibrium. As triolets are electrically charged and travel at light velocity, we use Liénard-Wichert potentials from relativistic electrodynamics [41] to express the radial components of electric field $\boldsymbol{E_{ij\perp}}$ and magnetic field $\boldsymbol{B_{ij}}$ emitted by triolet T_j of charge q_j at retarded time t', radius ρ_j and retarded angle θ'_j, and sensed at distance R_{ij}—electromagnetic fields traveling at light velocity in vacuum—by triolet T_i arriving at the vertical (angle 0), radius ρ_i, at time t (**Figure 3A**). From known electrodynamical expressions [41] for these fields, using cylindrical unit vectors and coordinates, and **Figure 3B**, we deduce (Forces and Potentials):

$$\mathbf{E_{ij\perp}} = \frac{q_j \sin\gamma_j}{4\pi\varepsilon_0 R_{ij}\rho_i \left(1+\sin\gamma_j\right)^2} \hat{\boldsymbol{\rho}}, \tag{14}$$

$$\mathbf{B_{ij}} = \frac{-q_j}{4\pi\varepsilon_0 c R_{ij}\rho_j \left(1+\sin\gamma_j\right)^2} \hat{\mathbf{z}}, \tag{15}$$

where R_{ij} and γ_j are defined by:

$$R_{ij}^2 = \rho_i^2 + \rho_j^2 - 2\rho_i\rho_j \cos\theta_j', \tag{16}$$

$$\sin\gamma_j = \frac{\rho_i}{R_{ij}} \sin\theta_j'. \tag{17}$$

Note that these fields depend on position coordinates only, not velocities, thereby justifying the use of the Virial theorem. We then derive expressions (Forces and Potentials) for the net radial Lorentz force $\boldsymbol{F_{ij\perp}}$ due to triolet T_j exerted on triolet T_i belonging to the same component, and for the centrifugal force $\boldsymbol{F}_{ctfg,i}$ experienced by triolet T_i:

$$\mathbf{F_{ij\perp}} = \frac{q_i q_j}{4\pi\varepsilon_0 R_{ij}\left(1+\sin\gamma_j\right)^2} \left[\frac{\sin\gamma_j}{\rho_i} + \frac{1}{\rho_j} \right] \hat{\boldsymbol{\rho}}, \tag{18}$$

$$\overrightarrow{\mathbf{F}}_{ctfg,i} = \frac{hc}{b_i \rho_i^2} \hat{\boldsymbol{\rho}}, \tag{19}$$

where b_i stands for b_{env} (respectively, b_{nuc}) when T_i belongs to the envelope (resp. the nucleus). In the electron at rest, assuming triolets remain at radial equilibrium, the net radial component of the Lorentz force exerted by other triolets should compensate the centrifugal force. Neglecting the small contribution of the envelope onto the nucleus and vice-versa, and expressing equilibrium for triolet T_i along the radial direction

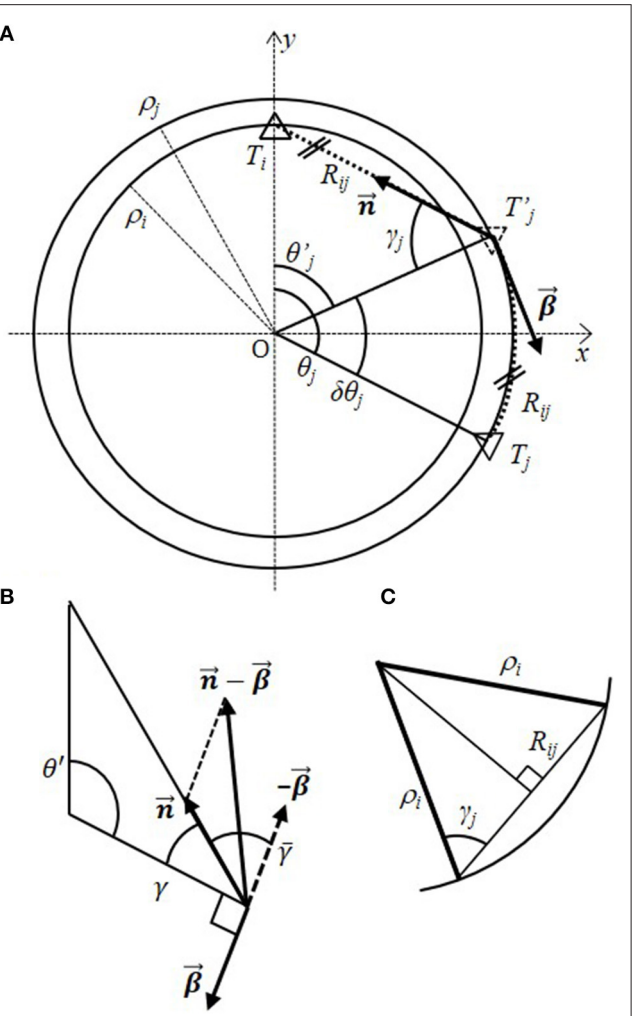

FIGURE 3 | Geometric diagrams. **(A)** The influence of electromagnetic fields due to triolet T_j onto T_i: let triolets T_i and T_j belong to the same component (envelope or nucleus). Triolet T_j rotates at light velocity along circular orbit of radius ρ_j and arrives at angle θ_j at time t, but was at position T_j' at retarded angle θ_j' and time t' when it emitted electromagnetic fields that reached triolet T_i revolving along coplanar circular orbit of radius ρ_i and arriving at angle 0 (vertical y axis) at time t. The retarded electromagnetic fields can be expressed using Liénard-Wichert potentials. This figure applies to all envelope and nucleus triolets. **(B)** Diagram showing vectors and angles involved in the demonstration of the expressions of electromagnetic fields and potentials. **(C)** Diagram depicting the case $\rho_j = \rho_i$.

and rearranging (Triolets at Radial Equilibrium), we obtain for the envelope and nucleus:

$$\frac{1}{\alpha} \simeq \frac{-b_{env}}{n_{env}^2} \sum_{j\in env}^{N_{env}-1} \frac{\rho_i^2 \mathrm{sgn}\left(i\cdot j\right)}{R_{ij}\left(1+\sin\gamma_j\right)^2} \left(\frac{\sin\gamma_j}{\rho_i} + \frac{1}{\rho_j} \right) \equiv G_{i\in env}\left(\eta_i\right), \tag{20}$$

$$\frac{1}{\alpha} \simeq \frac{-b_{nuc}}{n_{nuc}^2} \sum_{j\in nuc}^{N_{nuc}-1} \frac{\rho_i^2 \mathrm{sgn}\left(i\cdot j\right)}{R_{ij}\left(1+\sin\gamma_j\right)^2} \left(\frac{\sin\gamma_j}{\rho_i} + \frac{1}{\rho_j} \right) \equiv G_{i\in nuc}\left(\eta_i\right), \tag{21}$$

where sgn(i·j) is the sign of the product of the charges of triolets T_i and T_j, and α is the fine-structure constant, which is found to be related to the ratio between the centrifugal force and the net radial electromagnetic force experienced by any single triolet inside the electron. We assume positive and negative triolets are intertwined and uniformly distributed along the orbits except—as negative triolets are more numerous at the envelope—consecutive negative envelope triolets, which presumably repel to produce stretches of alternatively charged triolets separated by empty space (**Figure 2**). Let d_{env} designate the distance (using the number of missing triolets as units) between the stretches. The expressions under the sums in Equations (20–21) can be calculated by first considering the non-retarded angular positions θ_j of triolets distributed along the circular orbit, then by determining the corresponding retarded angles θ'_j, as illustrated in Retarted Angles, using Newton's recursion method for instance onto transcendental equation:

$$\left(\theta_j - \theta_j^{'}\right)^2 = 1 - 2\frac{\rho_i}{\rho_j}\cos\theta_j^{'} + \left(\frac{\rho_i}{\rho_j}\right)^2, \tag{22}$$

and then deriving γ_j from Equation (17). Equations (20–21) will help us derive adequate values for N_{env}, N_{nuc}, n_{env}, n_{nuc}, b_{env}, b_{nuc}.

The potential energy due to interactions between the nucleus and envelope being negligible, the total potential energy of our system is approximately $U_{tot} \simeq U_{env} + U_{nuc}$, where U_{env}, and U_{nuc} are, respectively, the envelope and nucleus potential energies, which are evaluated in Potential Energy:

$$U_{env} \simeq \frac{2\alpha mc^2}{n_{env}^2}\sum_{i\in env}^{N_{env}}\sum_{j\neq i}^{N_{env}-1}\frac{\mathrm{sgn}\left(i\cdot j\right)}{H_{ij}\left(1+\sin\gamma_j\right)}, \tag{23}$$

$$U_{nuc} \simeq \frac{2\alpha mc^2}{n_{nuc}^2}\sum_{i\in nuc}^{N_{nuc}}\sum_{j\neq i}^{N_{nuc}-1}\frac{\mathrm{sgn}\left(i\cdot j\right)}{H_{ij}\left(1+\sin\gamma_j\right)}, \tag{24}$$

where $H_{ij} = R_{ij}/\lambda_c$. Assuming $\eta_{env+} \simeq \eta_{env-} \simeq 1$, we demonstrate (Potential Energy) from b_{env}=$2N_{env}$ (11) and Equation (20), which expresses the radial stability of every envelope triolet, that Equation (23) yields $U_{env} \simeq -mc^2$. Likewise, assuming $\eta_{nuc+} \simeq \eta_{nuc-}$, we demonstrate (Potential Energy) from $b_{nuc}\eta_{nuc} = 2N_{nuc}$ (12) and Equation (21), which expresses the radial stability of every nucleus triolet, that Equation (24) yields $U_{nuc} \simeq -mc^2$. Hence, we find: $U_{tot} \simeq U_{env} + U_{nuc} \simeq -2mc^2$, as expected from the Virial theorem, and recover electron mass. As substructure stability implies radial equilibrium for all envelope and nucleus triolets (20–21), it allows predicting electron mass. We find it remarkable that the same number of triolets allows to recover both substructure stability and electron mass.

DETERMINATION OF SUITABLE CONFIGURATIONS

The problem then reduces to determining triolet configurations, i.e., sets of values for {n_{env}, n_{nuc}, N_{env+}, N_{env-}, N_{nuc}, b_{env}, b_{nuc}, η_{env+}, η_{env-}, η_{nuc+}, η_{nuc-}, d_{env}}, that verify radial equilibrium for every triolet and correctly predict the total energy. We shall estimate the stability and total energy in three different models of the envelope successively, each lying at a different level of approximation. The three models are: the *one-orbit* model, where all envelope triolets rotate on the same orbit $\eta_{env+} \simeq \eta_{env-} \equiv \eta_{env}$; the *two-orbits* model, where positively-charged envelope triolets revolve on orbit of radius η_{env+} and negative triolets at radius η_{env-}; the *n-orbits* model where every envelope triolet i rotates on a circular orbit of specific but fixed radius η_i.

We shall first estimate the number of triolets N_{env} present in the envelope by considering the one-orbit model. Assuming $\eta_{env+} \simeq \eta_{env-}$ and $\eta_{nuc+} \simeq \eta_{nuc-}$, we have $R_{ij} \simeq 2\rho_i\cos\gamma_j$ (**Figure 3C**) both at the envelope and nucleus, and Equations (20–21) can be approximated to:

$$\frac{1}{\alpha} \simeq \frac{-b_{env}}{2n_{env}^2}\sum_{j\in env}^{N_{env}-1}\frac{\mathrm{sgn}\left(i\cdot j\right)}{\cos\gamma_j\left(1+\sin\gamma_j\right)} \simeq G_{i\in env}\left(\eta_i\right), \tag{25}$$

$$\frac{1}{\alpha} \simeq \frac{-b_{nuc}}{2n_{nuc}^2}\sum_{j\in nuc}^{N_{nuc}-1}\frac{\mathrm{sgn}\left(i\cdot j\right)}{\cos\gamma_j\left(1+\sin\gamma_j\right)} \simeq G_{i\in nuc}\left(\eta_i\right). \tag{26}$$

Recalling that b_{env} is related to N_{env} via $b_{env} = 2N_{env}$ (11), and setting values for input parameters {n_{env}, d_{env}}, the iteration over N_{env} values in Equation (25) enabled us to determine values for b_{env} and N_{env} approximately verifying Equations (25) and (11) simultaneously. Due to the asymmetry in the arrangement of envelope triolets, we found these Equations were satisfied for different values of N_{env} depending on the triolet T_i under consideration. In the case $n_{env} = 6$, $d_{env} = 0$ for instance, we found positive triolets approximatively satisfied these conditions for $N_{env} \simeq 108$, while negative triolets did so for $N_{env} \simeq 144$, thus justifying the necessity of considering two distinct orbits in the envelope. Although these figures should be regarded as merely indicative, cases $d_{env} = 1$ and $d_{env} = 2$ also pointed at average value $N_{env} = 126$, corresponding to $N_{env+} = 60$ and N_{env-}= 66, and we shall be considering only this case in the remainder of our analysis. For the nucleus, in the absence of a constraint like Equation (11), values for b_{nuc} and η_{nuc} satisfying Equations (26) and (12) simultaneously were determined for every iterated value of N_{nuc}. However, when accounting for the correction due to envelope current (first two terms, Triolets at Radial Equilibrium):

$$G_{env>i\in nuc} \approx \frac{b_{nuc}\mathrm{sgn}\left(i\right)}{n_{nuc}}\left[\frac{\eta_{nuc}^3}{2} + \frac{3\eta_{nuc}^4}{8}\right], \tag{27}$$

the best estimate appeared to be $N_{nuc} = 18$ (**Table 1**). Note that input values other than $n_{env} = 6$, $n_{nuc} = 2$ did not yield any possible solutions.

Now, considering $n_{env} = 6$, $n_{nuc} = 2$, $d_{env} = 2$, $\eta_{env+} \simeq \eta_{env-} \simeq 1$ (one-orbit model), and putting in the value obtained above for N_{env}, we evaluated potential energies U_{env}, U_{nuc} using Equations (13, 23–24) and found $U_{env} = -0.997{\cdot}mc^2$ (**Table 2**), $U_{nuc} \simeq -1.000{\cdot}mc^2$ (**Table 1**). The total potential energy therefore amounts to $U_{tot} \simeq -1.997{\cdot}mc^2$, close to our expected result. Hence, recalling that kinetic energies satisfy $T_{env} \simeq T_{nuc} \simeq$

TABLE 1 | Stability and energy of various nucleus configurations.

N_{nuc}	b_{nuc}	η_{nuc+}	η_{nuc-}	G_{nuc+}	G_{nuc-}	$G_{env>nuc}$	U_{nuc}	T_{nuc}
6	553.42	0.0213	0.0221	127.69	146.51	±0.001	−0.9996	+0.5001
8	425.49	0.0373	0.0379	132.47	141.62	±0.006	−0.9998	+0.4999
12	290.89	0.0823	0.0827	135.02	138.21	±0.043	−1.0000	+0.5000
16	221.03	0.1446	0.1449	136.29	137.78	±0.186	−1.0002	+0.5001
18	197.35	0.1823	0.1825	136.49	137.58	±0.340	−1.0005	+0.5000
20	178.27	0.2243	0.2245	136.63	137.45	±0.588	−0.9999	+0.5000
22	162.55	0.2706	0.2708	136.71	137.35	±0.970	−1.0003	+0.4999
24	149.39	0.3212	0.3214	136.79	137.29	±1.538	−1.0000	+0.5000

At the nucleus, setting $n_{nuc} = 2$, values for b_{nuc} and nucleus radii η_{nuc+}, η_{nuc-} are determined for several values of N_{nuc}, the number of nucleus triolets, according to Equations (9, 12, 13, 26), so as to yield $U_{nuc} \simeq -mc^2$, $T_{nuc} \simeq +mc^2/2$ and satisfactory stability values G_{nuc+}, G_{nuc-} (value 137.03 stands for stability). Accounting for first correction terms $G_{env>nuc}$ due to envelope current and specified by Equation (27), the best estimate seems to be $N_{nuc} = 18$. Nucleus potential energy U_{nuc} and kinetic energy T_{nuc} are expressed in terms of mc^2.

TABLE 2 | Stability and energy of various envelope models.

Model	η_{env+}	η_{env-}	N_{env}	$<G_i>$	K	U_{env}	T_{env}
One orbit	1.0	1.0	120	131.4	41.7	−0.949	+0.5000
			126	136.7	48.0	−0.996	+0.5000
			132	157.5	46.5	−1.139	+0.5000
Two fixed orbits	0.977	1.023	120	124.6	17.3	−0.962	+0.4997
			126	130.0	16.1	−1.011	+0.4997
			132	148.7	16.1	−1.155	+0.4997
Specific orbits	various	various	126	137.7	3.2	−0.975	+0.5020

The potential energy U_{env}, kinetic energy T_{env}, and average absolute stability deviation K are shown for the three considered envelope models, involving triolets revolving on (i) a single orbit at reduced Compton wavelength, (ii) two fixed envelope orbits η_{env+} and η_{env-}, (iii) N_{env} orbits of specific but fixed radii, with parameters set to $n_{env} = 6$, $d_{env} = 2$. Energies are expressed in terms of mc^2, where m is the mass of the electron and c is light velocity. It can be seen that for the single orbit and two fixed orbits models, the solution $N_{env+} = 60$, $N_{env-} = 66$ yields accurate potential energy values. Although in the one-orbit or two-orbits models, total energy of the envelope E_{env} is close to $-mc^2/2$, K stability values strongly diverge from 0, indicating that triolets do not verify radial equilibrium. A configuration of fixed specific orbits yielding overall satisfactory energy and average stability values (value 137.03 stands for stability) has been determined using our optimization algorithm.

TABLE 3 | Stability of individual envelope triolets.

Triolet		One orbit		Two fixed orbits		Specific orbits	
#	+/−	η_i	G_i	η_i	G_i	η_i	G_i
1	−	1.0	75.4	1.023	108.4	1.761	137.0
2	+	1.0	189.4	0.977	145.4	0.861	114.0
3	−	1.0	105.2	1.023	134.5	0.880	137.0
4	+	1.0	178.8	0.977	134.3	0.931	139.5
5	−	1.0	110.4	1.023	139.7	0.915	137.0
6	+	1.0	176.0	0.977	131.3	0.947	145.3
7	−	1.0	111.9	1.023	141.1	0.925	137.3
8	+	1.0	175.4	0.977	130.7	0.958	137.0
9	−	1.0	111.8	1.023	141.0	0.987	143.6
10	+	1.0	176.0	0.977	131.4	0.974	137.0
11	−	1.0	110.6	1.023	139.7	1.012	142.0
12	+	1.0	177.8	0.977	133.2	0.977	141.7
13	−	1.0	108.2	1.023	137.1	0.968	143.1
14	+	1.0	181.0	0.977	136.5	0.975	137.0
15	−	1.0	103.9	1.023	132.5	1.019	137.5
16	+	1.0	186.7	0.977	142.3	0.998	137.0
17	−	1.0	96.1	1.023	124.0	1.045	137.0
18	+	1.0	198.2	0.977	154.0	1.004	144.0
19	−	1.0	78.0	1.023	104.4	1.017	133.8
20	+	1.0	231.7	0.977	188.2	1.043	137.0
21	−	1.0	−12.0	1.023	1.0	1.130	137.0
K			48.0		16.1		3.2

*The stability of individual envelope triolets belonging to the first stretch—the five other stretches of 21 triolets being identical in the $N_{env} = 126$ case—is evaluated by determining G_i and comparing it to $1/\alpha \simeq 137.036$, in the three envelope models (single orbit, two fixed orbits, n fixed orbits of specific radii), with input parameters set to $n_{env} = 6$, $N_{env+} = 60$, $N_{env-} = 66$, $d_{env} = 2$. The one-orbit model was evaluated at η_{env}=1 corresponding to radius $\lambda\!\!\!^{-}_c$, the reduced Compton wavelength. The two-orbits model was evaluated for radii $\eta_{env+} = 0.977$, $\eta_{env-} = 1.023$, that yielded acceptable energy value (**Table 2**). In the model with specific radii, our optimization algorithm converged toward the 21 different radii shown here, together with their corresponding individual stability value G_i (value 137.03 stands for stability). The average absolute deviation K to $1/\alpha$ is supplied for the three envelope models.*

$+mc^2/2$, then $T_{tot} \simeq T_{env} + T_{nuc} \simeq +mc^2$, $E_{tot} \simeq T_{tot} + U_{tot} \simeq -mc^2$, and the mass of the electron is deduced directly from our model substructure. Likewise, since the muon is seen as an excited state of the electron [6] according to our chemical theory [Avner, Boillot, Richard, submitted], presumably displaying a similar arrangement of triolets albeit on a smaller scale, muon mass can also be successfully calculated by replacing m by muon mass m_μ in expressions (23–24), or equivalently $\lambda\!\!\!^{-}_c$ by the reduced muonic Compton Wavelength $\lambda\!\!\!^{-}_{\mathrm{muon}}$.

We next evaluated the cohesion and stability of individual triolets. For the symmetric nucleus, we computed the right-hand side G_{nuc} of Equation (21) for every triolet; for $n_{nuc} = 2$, $N_{nuc} = 18$ for instance, accounting for the correction due to the envelope current, we obtained $G_{nuc}(\eta_{nuc+}) \simeq 136.83$, $G_{nuc}(\eta_{nuc-}) \simeq 137.24$ (**Table 1**). For the asymmetric envelope, which can be divided into six identical stretches of 21 triolets in the case $N_{env} = 126$, we computed the right-hand sides G_{env} of Equation (20) for every triolet belonging to the first stretch and compared the results with the left-hand side $1/\alpha \simeq 137.036$, which they should yield if triolets were truly at radial equilibrium. For the one-orbit model, setting $n_{env} = 6$, values of G_{env} disagreed with the expected value for all values of d_{env} (the case $d_{env} = 2$ is given in **Table 3**). Clearly, in these conditions at least, the centrifugal and net electromagnetic forces fail to compensate and to ensure radial equilibrium, one dominating over the other, and triolets would be moving radially as well as azimuthally. Therefore, we considered the two-orbits model with $\eta_{env+} \simeq 0.977$, $\eta_{env-} \simeq 1.023$, for which we obtained an acceptable energy value (**Table 2**). Once again, we found that radial equilibrium was not verified for many envelope triolets, especially for consecutive negative triolets or those adjacent to them (**Table 3**). Hence, we decided to complicate our model again and considered envelope triolets orbiting at various but fixed radii ρ_i (n-orbits model) instead of the probably too general ρ_{env+} and ρ_{env-}. We heuristically determined fixed radii exhibiting reasonable stability

for all envelope triolets, then used an optimization algorithm, described in Optimization Algorithm, to make every triolet tend toward radial equilibrium, minimizing criterion K, the average absolute deviation from $1/\alpha$ per triolet:

$$K = \frac{1}{N_{env}} \sum_{i}^{N_{env}} \left| G_{i \in env}(\eta_i) - \frac{1}{\alpha} \right|, \tag{28}$$

which effectively constitutes a measure of global stability of envelope triolets. Our algorithm converged toward a solution yielding acceptable energy and global stability (**Table 2**). The stability values $G_{env}(\eta_i)$ of individual envelope triolets belonging to the first stretch in the n-orbits model are shown in **Table 3**: most values appeared to be close to $1/\alpha$. We found that our optimization algorithm nicely converged toward stable solutions. However, the latter were highly dependent on initial conditions, and a thorough optimization study is needed to ensure local minima are avoided.

DISCUSSION

In this study, we presented a relativistic electrodynamical model of the electron based on natural interpretations of its associated observables. Our electron model is composed of triolets that revolve along coplanar circular orbits constituting an envelope and nucleus, which could be responsible for its wavelike and corpuscular behaviors, respectively. These two components would thus constitute a natural solution to wave-corpuscle duality. Capturing the values of charge, spin, magnetic moments, Compton wavelength and kinetic energy, we created a triolet-based configuration that verified cohesion and stability without invoking Poincaré stresses, and predicted electron and muon mass, defined as electromagnetic cohesion energy, directly from substructure stability. Importantly, our model accounts for kinetic energy and presents a negative cohesion potential energy, in agreement with the Virial theorem. In our model, the numbers of triolets in the envelope and nucleus are the adjusting parameters, and the same numbers are found to account both for substructure stability and electron mass. Notably, electron mass can be derived directly from an expression of substructure stability. Our study therefore implements Lorentz' hypothesis, which advocates the electromagnetic origin of mass, from an objective criterion, even if satisfaction of the criterion itself relies on two parameters, i.e., the numbers of triolets in the envelope and nucleus. Noteworthy, these parameters are not arbitrary, but instead are strongly constrained by several relations (11, 12, 20, 21, 27) that fix their values in our model. Altogether, we believe our study establishes that deterministic electrodynamical models of subatomic particles can be constructed beneath the Compton scale, in agreement with an objectively realist conception of physics.

Envelope triolets could also fluctuate radially or otherwise in time, possibly constituting a periodic wave that revolves at light velocity. This system has not been investigated here, but is of interest because this periodic wave could correspond to the wave associated to the electron, first imagined by de Broglie and later represented by wavefunction $|\psi>$ in Schrödinger's wave mechanics or Dirac's quantum mechanics. It is conceivable that a wave made of envelope triolets, if it exists, attracts and drives the nucleus in the manner of the de Broglie-Bohm guiding wave [23, 24], sensing the electromagnetic fields generated by the envelopes belonging to other particles. Hence, envelope triolets could undulate and incarnate wavefunction $|\psi>$, whose concrete existence has recently been reconsidered [42]. Note further that nucleus triolets could also form a wave, reminiscent of the second wave described in de Broglie's double solution theory [23]. Specifically, triolets could propagate in a highly dynamical manner and experience irregular fluctuations, as in the hydrodynamical model of Bohm and Vigier [25]. Importantly, it has been suggested that solutions of this type could account both for quantum phenomena [26] and for quantum principles [37]. Bell also wrote that such solutions were compatible with the predictions of quantum mechanics [43]. Further, it is conceivable that such a complex envelope can exhibit several stable states, much like modes for a vibrating rope. These could correspond to the eigenstates of quantum mechanics. In the general case, the envelope would be in an unstable state, but could converge toward one of its eigenstates upon measurement, which could be conceived as the sum of interactions between system subparticles and apparatus subparticles. Such propositions constitute an interpretation of von Neumann's *reduction of the wave packet* [44], and would provide a possible solution to *the measurement problem* of quantum mechanics [45].

These considerations suggest that quantum theories, which encompass all subatomic phenomena and whose standard interpretation states that everything is intrinsically probabilistic, could eventually emerge [46, 47] from a relativistic electrodynamical description in agreement with the deterministic paradigm, which supports the causality principle, objective reality, and governs macroscopic physics. In this perspective, Schrödinger and Dirac Equations would constitute high-level descriptions of the dynamics of envelope triolets. Our study therefore provides new insight regarding the unification of the two apparently irreconcilable paradigms in physics: the deterministic and quantum paradigms.

Now, how exactly does the electron appear to be point-like in corpuscular interactions? How does our model relate to the observation that the electron seems spherical [48], or that its spin, charge and orbital components seem to be separable [49–51]? How would the moving electron, which exhibits a wave satisfying de Broglie relation $p=h/\lambda$, be described? Could our description be regarded as an attempt to create a corpuscular counterpart to wave mechanics? Could analogous electrodynamical models be similarly constructed for other subatomic particles [52]? Could our extended model of the electron bring insight to the nature of molecular bonding, or to the arrangement of electrons inside atoms? And finally, what would be the implications for the interpretation of quantum mechanics [45]? How would quantum properties, such as the existence of eigenstates, the measurement problem or entanglement, and quantum phenomena, such as the two-slits experiment or the one-dimensional potential well, be understood in the light of our model? We believe the

aforementioned questions should stimulate discussion and foster novel investigations.

METHODS

Values of Observables

Charge

The charge of the electron is given by the N_{env+} triolets of charge $(+e/n_{env})$, the N_{env-} triolets of charge $(-e/n_{env})$, the N_{nuc+} triolets of charge $(+e/n_{nuc})$ and the N_{nuc-} triolets of charge $(-e/n_{nuc})$:

$$-e = e\left[\left(\frac{-N_{env-}}{n_{env}}\right) + \left(\frac{N_{env+}}{n_{env}}\right) + \left(\frac{-N_{nuc-}}{n_{nuc}}\right) + \left(\frac{N_{nuc+}}{n_{nuc}}\right)\right].$$

Assuming the nucleus is neutrally charged (hypothesis B), implying $N_{nuc+} = N_{nuc-}$, we deduce:

$$n_{env} = N_{env-} - N_{env+}. \tag{A1}$$

Nucleus and Envelope Orbits

Let us suppose triolets of charges $(+e/n_{env})$, $(-e/n_{env})$, $(+e/n_{nuc})$, $(-e/n_{nuc})$ revolve along four coplanar circular orbits of radii:

$$\begin{cases} \rho_{env+} = \eta_{env+}\lambda\!\!\!^{-}_{C} \\ \rho_{env-} = \eta_{env-}\lambda\!\!\!^{-}_{C} \\ \rho_{nuc+} = \eta_{nuc+}\lambda\!\!\!^{-}_{C} \\ \rho_{nuc-} = \eta_{nuc-}\lambda\!\!\!^{-}_{C} \end{cases} \tag{A2}$$

where $\lambda\!\!\!^{-}_{c} = \hbar/mc$ is the reduced Compton wavelength, and η's are dimensionless real numbers.

Classical and Anomalous Magnetic Moments

Let us express the classical magnetic moment $\mu_B = -e\hbar/2m = \sum_i I_i A_i = \sum_i Q_i A_i/t_i$, where I_i is the current generated by triolet T_i, Q_i its charge, $t_i = c/2\pi\rho_i$ the time taken to go through a full orbit at light velocity c, and A_i the area formed by this orbit. The magnetic moment is due to a net charge $(-e)$ made of $N_{env} = N_{env+} + N_{env-}$ triolets revolving in the same direction along envelope orbits of radii ρ_{env+} and ρ_{env-}:

$$\begin{aligned} \mu_B &= \frac{-e\hbar}{2m} = \frac{Q_{env+}A_{env+}}{t_{env+}} + \frac{Q_{env-}A_{env-}}{t_{env-}}, \\ \frac{-e\hbar}{2m} &= \frac{N_{env+}e}{n_{env}}\frac{c\pi\,\rho_{env+}^2}{2\pi\rho_{env+}} + \frac{N_{env-}(-e)}{n_{env}}\frac{c\pi\rho_{env-}^2}{2\pi\rho_{env-}}, \\ \frac{-e\hbar}{2m} &= \frac{ec}{2n_{env}}\left(N_{env+}\eta_{env+} - N_{env-}\eta_{env-}\right)\frac{\hbar}{mc}, \\ &\left(N_{env-}\eta_{env-} - N_{env+}\eta_{env+}\right) = n_{env}. \end{aligned} \tag{A3}$$

As the anomalous magnetic moment $\mu_{nuc} = -a_{anml}(e\hbar/2m)$, with $a_{anml} \simeq 0.001159$, is relatively small, let us assume it is produced by an equal number $N_{nuc+} = N_{nuc-}$ of positive and negative triolets of charge $(\pm e/n_{nuc})$ revolving in the same direction as envelope triolets along nucleus orbits of slightly different radii due to the net envelope charge:

$$\mu_{nuc} = -a_{anml}\frac{e\hbar}{2m} = \frac{Q_{nuc+}A_{nuc+}}{t_{nuc+}} + \frac{Q_{nuc-}A_{nuc-}}{t_{nuc-}},$$

$$N_{nuc+}\left(\eta_{nuc-} - \eta_{nuc+}\right) = a_{anml}n_{nuc}. \tag{A4}$$

Virial Theorem

The virial theorem states that if a system remains bound, and if its inner potentials do not depend on velocities but only on positions, then the kinetic and potential energies take on definite shares in the total energy, depending on the degree n of the forces that apply. As the electron is a bound system, and as in our system the magnetic force will be found to depend on position coordinates ρ and γ only, the theorem applies and, for electromagnetic interactions in r^{-2}, it stipulates that:

$$\begin{cases} T = mc^2 \\ U = -2mc^2 \\ E = T + U = -mc^2 \end{cases} \tag{A5}$$

where T, U, and E, respectively, designate the internal kinetic energy, internal potential energy, and total internal energy of the system. Note that the potential and total energies are negative, as they should be for a bound system.

Kinetic Energy

The kinetic energy is given by:

$$\begin{aligned} T = mc^2 \;&=\; \sum_i p_i c = N_{env+}p_{env+}c + N_{env-}p_{env-}c \\ &+\; N_{nuc+}p_{nuc+}c + N_{nuc-}p_{nuc-}c, \end{aligned} \tag{A6}$$

suggesting:

$$\begin{cases} p_{env+} = mc/K_{env+} \\ p_{env-} = mc/K_{env-} \\ p_{nuc+} = mc/K_{nuc+} \\ p_{nuc-} = mc/K_{nuc-} \end{cases}, \tag{A7}$$

where the K's remain to be determined, thus yielding from Equation (A6):

$$1 = \frac{N_{env+}}{K_{env+}} + \frac{N_{env-}}{K_{env-}} + \frac{N_{nuc+}}{K_{nuc-}} + \frac{N_{nuc+}}{K_{nuc-}}. \tag{A8}$$

Note that we may assume that nucleus triolets possess comparable momentum $p_{nuc+} \simeq p_{nuc-} = p_{nuc}$, and that their orbit radius is approximately $\rho_{nuc+} \simeq \rho_{nuc-} = \rho_{nuc}$, since $(\rho_{nuc+} - \rho_{nuc-})$ is very small according to Equation (A4).

Spin

Since particles as different as quarks and leptons (which possess different numbers of sparks according to our chemical model [Avner, Boillot, Richard, submitted]) share same spin, the latter can be interpreted as being the total angular momentum the particle conveys to the objects it encounters, i.e., the sum of the angular momenta of its envelope triolets. For the electron, assuming all triolets revolve in the same positive direction, it is written using Equations (A2, A6):

$$S = +\frac{\hbar}{2} = \sum_i \rho_i p_i = N_{env+}\rho_{env+}p_{env+} + N_{env-}\rho_{env-}p_{env-}, \tag{A9}$$

$$\frac{1}{2} = \frac{N_{env+}\eta_{env+}}{K_{env+}} + \frac{N_{env-}\eta_{env-}}{K_{env-}}, \tag{A10}$$

Further, as the muon is composed of the same number of triolets as the electron according to our chemical model and exhibits a Compton length much smaller than that of the electron [Avner, Boillot, Richard, submitted], spin $\hbar/2$ is thus independent of the radii of triolets' orbits. A necessary and sufficient condition is then that variables K's be proportional to η's:

$$\begin{cases} K_{env+} = b_{env+}\eta_{env+} \\ K_{env-} = b_{env-}\eta_{env-} \\ K_{nuc+} = b_{nuc}\eta_{nuc+} \\ K_{nuc-} = b_{nuc}\eta_{nuc-} \end{cases} \tag{A11}$$

where b_{env+}, b_{env-}, b_{nuc+}, b_{nuc-} are values independent of radii, in order that the η's cancel out in Equation (A10), yielding:

$$\frac{1}{2} = \frac{N_{env+}}{b_{env+}} + \frac{N_{env-}}{b_{env-}}. \tag{A12}$$

The angular momentum of triolet i is given by:

$$L_i = p_i\rho_i = \frac{mc}{b_i\eta_i}\cdot\eta_i\frac{\hbar}{mc} = \frac{\hbar}{b_i}, \tag{A13}$$

implying for spin and kinetic energy:

$$\frac{b_{env}}{2} = N_{env+} + N_{env-}, \tag{A14}$$

$$1 = \frac{N_{env+}}{b_{env}\eta_{env+}} + \frac{N_{env-}}{b_{env}\eta_{env-}} + \frac{N_{nuc+}}{b_{nuc}\eta_{nuc+}} + \frac{N_{nuc-}}{b_{nuc}\eta_{nuc-}}. \tag{A15}$$

Definition of Planck's Constant

Supposing angular momentum $L_{trlt,env}$ is a constant common to every envelope triolet, the expression for the spin, from Equation (A9), due to the envelope is:

$$\frac{\hbar}{2} = N_{env+}L_{trlt,env} + N_{env-}L_{trlt,env} = N_{env}L_{trlt,env},$$

and thus:

$$\hbar = 2N_{env}L_{trlt,env}, \tag{A16}$$

meaning that the constant angular momentum $L_{trl,env}$ common to every envelope triolet could be at the basis of Planck's constant.

Kinetic Energy of the Nucleus and Envelope

From Equations (A6, A7, A11), the kinetic energy of the nucleus is given by:

$$\begin{aligned} T_{nuc} &= N_{nuc+}p_{nuc+}c + N_{nuc-}p_{nuc-}c \\ &= \frac{mc^2N_{nuc+}}{b_{nuc}}\left(\frac{1}{\eta_{nuc+}} + \frac{1}{\eta_{nuc-}}\right). \end{aligned} \tag{A17}$$

Likewise, the kinetic energy of the envelope is:

$$T_{env} = N_{env+}p_{env+}c + N_{env-}p_{env-}c,$$

$$T_{env} = \frac{mc^2}{b_{env}}\left(\frac{N_{env+}}{\eta_{env+}} + \frac{N_{env-}}{\eta_{env-}}\right). \tag{A18}$$

Now, assuming $\eta_{env+} \simeq \eta_{env-} \simeq 1$ according to Schrödinger's Zitterbewegung, T_{env} becomes, using Equation (A14):

$$T_{env} \simeq \frac{mc^2}{b_{env}}(N_{env-} + N_{env+}) \simeq \frac{1}{2}mc^2, \tag{A19}$$

and thus:

$$T_{nuc} = T - T_{env} \simeq \frac{1}{2}mc^2. \tag{A20}$$

The forthcoming study of the interactions between the nucleus and envelope will show that they are negligible compared to intra-component forces (nucleus onto itself, envelope onto itself). The two components therefore almost behave as two bound independent systems, and thus presumably obey the Virial theorem separately. Hence, since we have $T_{nuc} \simeq T_{env} \simeq mc^2/2$, we should also obtain $U_{nuc} \simeq U_{env} \simeq -mc^2$ so that the total energies amount to: $E_{nuc} \simeq E_{env} \simeq -mc^2/2$ and $E_{tot} \simeq -mc^2$.

Determination of η_{nuc}+ and η_{nuc}-

In order to determine η_{nuc^+} and η_{nuc^-}, considering Equations (A17) and (A20), we have:

$$\left(\frac{1}{\eta_{nuc+}} + \frac{1}{\eta_{nuc-}}\right) \simeq \frac{b_{nuc}}{2N_{nuc+}}. \tag{A21}$$

The latter expression, together with Equation (A4), can allow us to determine η_{nuc+} and η_{nuc-} in terms of N_{nuc+}, a_{anml}, n_{nuc}, and b_{nuc}:

$$\begin{aligned} &\frac{b_{nuc}}{2N_{nuc+}} \simeq \frac{1}{\eta_{nuc+}} + \frac{1}{\left(\eta_{nuc+} + \frac{a_{anml}n_{nuc}}{N_{nuc+}}\right)}, \\ &\frac{1}{\eta_{nuc+}}\left(\frac{b_{nuc}\eta_{nuc+}}{2N_{nuc+}} - 1\right) = \frac{1}{\eta_{nuc+}}\left(\frac{1}{1 + \frac{a_{anml}n_{nuc}}{N_{nuc+}\eta_{nuc+}}}\right), \\ &1 = \left(1 + \frac{a_{anml}n_{nuc}}{N_{nuc+}\eta_{nuc+}}\right)\left(\frac{b_{nuc}\eta_{nuc+}}{2N_{nuc+}} - 1\right), \\ &\eta_{nuc+}^2\left(\frac{b_{nuc}}{2N_{nuc+}}\right) + \eta_{nuc+}\left(\frac{a_{anml}b_{nuc}n_{nuc}}{2N_{nuc+}^2} - 2\right) \\ &\qquad - \left(\frac{a_{anml}n_{nuc}}{N_{nuc+}}\right) = 0, \\ &\Delta = 4 + \left(\frac{a_{anml}b_{nuc}n_{nuc}}{2N_{nuc+}^2}\right)^2, \end{aligned}$$

and taking the positive solution, we find:

$$\eta_{nuc+} = \frac{N_{nuc+}}{b_{nuc}}\left(2 - \frac{a_{anml}b_{nuc}n_{nuc}}{2N_{nuc+}^2} + \sqrt{4 + \left(\frac{a_{anml}b_{nuc}n_{nuc}}{2N_{nuc+}^2}\right)^2}\right), \tag{A22}$$

and η_{nuc-} can then be derived from Equation (A4).

Forces and Potentials

Centrifugal Force of a Triolet

Assuming triolets travel at light velocity, the centrifugal force [16] of triolet T_i, revolving along orbit of radius $\rho_i = \eta_i \lambda\!\!\!^{-}_C$, is in cylindrical coordinates:

$$F_{ctf,i} = \frac{p_i v_i}{\rho_i} = \frac{mc \cdot c}{b_i \eta_i \rho_i} = \frac{\hbar c}{b_i \rho_i^2}, \tag{B1}$$

where b_i stands for b_{env} (respectively, b_{nuc}) when T_i belongs to the envelope (resp. the nucleus). This expression applies both to nucleus and envelope triolets.

Electromagnetic Force Exerted on Nucleus Triolet *i* Due to Current at Envelope

The electromagnetic force exerted onto nucleus triolet i is given by the Lorentz force written using scalar potential V and vector potential $\mathbf{A}$:

$$\overrightarrow{\mathbf{F}}_{env\pm>i} = \frac{\mathrm{sgn}(i)\cdot e}{n_{nuc}}\left[-\overrightarrow{\nabla} V_{env\pm>i} - \frac{\partial}{\partial t}\overrightarrow{\mathbf{A}}_{env\pm>i} + c\hat{\theta} \times \left(\overrightarrow{\nabla} \times \overrightarrow{\mathbf{A}}_{env\pm>i}\right)\right], \tag{B2}$$

if all triolets revolve in the same positive direction. The expressions for the scalar and vector potentials and their derivatives must be determined.

As a net charge $(-e)$ circulates around the envelope, the scalar potential and vector potential, for $r_{nuc} < r_{env}$ and $\cos\theta = 0$ (since the orbit is in the plane $z = 0$), are given [41] by:

$$V_{env\pm>i\in nuc} = \frac{Q_{env\pm}}{4\pi\varepsilon_0 r_{env\pm}} \sum_{l=0,2,4\ldots}^{\infty} [P_l(0)]^2 \left(\frac{\rho_i}{\rho_{env\pm}}\right)^l, \tag{B3}$$

$$A_{env\pm>i\in nuc} = \frac{\mu_0 I_{env\pm}}{2} \sum_{l=1,3,5\ldots}^{\infty} \frac{\left[P_l^1(0)\right]^2}{l(l+1)} \left(\frac{\rho_i}{\rho_{env\pm}}\right)^l, \tag{B4}$$

where the $P_l(x)$ and $P_l{}^1(x)$, respectively, designate the Legendre polynomials and associated Legendre polynomials, yielding:

$$V_{env\pm>i\in nuc} \simeq \frac{Q_{env\pm}}{4\pi\varepsilon_0}\left[\frac{1}{\rho_{env\pm}} + \frac{1}{4}\frac{\rho_i^2}{\rho_{env\pm}^3} + \frac{9}{64}\frac{\rho_i^4}{\rho_{env\pm}^5}\right], \tag{B5}$$

$$\frac{\partial V_{env\pm>i\in nuc}}{\partial \rho_{nuc\pm}} \simeq \frac{Q_{env\pm}}{4\pi\varepsilon_0}\left[\frac{1}{2}\frac{\rho_i}{\rho_{env\pm}^3} + \frac{9}{16}\frac{\rho_i^3}{\rho_{env\pm}^5}\right]. \tag{B6}$$

Recalling $\mu_0 = 1/(\varepsilon_0 c^2)$, $v = c$ and $Q_{env\pm} = \pm N_{env\pm} e / n_{env}$:

$$\frac{\mu_0 I_{env\pm}}{2} = \frac{\mu_0 Q_{env\pm}}{2t_{env\pm}} \simeq \frac{1}{2\varepsilon_0 c^2}\left(\frac{\pm N_{env\pm} e}{n_{env}}\right)\left(\frac{c}{2\pi\rho_{env\pm}}\right), \tag{B7}$$

$$A_{env\pm>i\in nuc} \simeq \frac{\pm N_{env\pm} e}{4\pi\varepsilon_0 c n_{env}}\left[\frac{1}{2}\frac{\rho_i}{\rho_{env\pm}^2} + \frac{3}{16}\frac{\rho_i^3}{\rho_{env\pm}^4}\right], \tag{B8}$$

$$\frac{\partial\left(A_{env\pm>i\in nuc}\hat{\boldsymbol{\theta}}\right)}{\partial t_{nuc}} = -A_{env\pm>i\in nuc}\frac{c}{\rho_{nuc}}\hat{\boldsymbol{\rho}} \simeq \frac{-(\pm N_{env\pm} e)}{4\pi\varepsilon_0 n_{env}}\left[\frac{1}{2\rho_{env\pm}^2} + \frac{3}{16}\frac{\rho_i^2}{\rho_{env\pm}^4}\right]\hat{\boldsymbol{\rho}}, \tag{B9}$$

$$\overrightarrow{\nabla} \times \overrightarrow{\mathbf{A}} = \begin{vmatrix} \hat{\boldsymbol{\rho}} & \hat{\boldsymbol{\theta}} & \hat{\mathbf{k}} \\ \frac{\partial}{\partial\rho} & \frac{\partial}{\rho\partial\theta} & \frac{\partial}{\partial z} \\ 0 & A_{env\pm>i\in nuc} & 0 \end{vmatrix} = \frac{\partial\left(A_{env\pm>i\in nuc}\right)}{\partial\rho_{nuc}}\hat{\boldsymbol{k}} \simeq \frac{(\pm N_{env\pm} e)}{4\pi\varepsilon_0 c n_{env}}\left[\frac{1}{2\rho_{env\pm}^2} + \frac{9}{16}\frac{\rho_i^2}{\rho_{env\pm}^4}\right]\hat{\mathbf{k}}. \tag{B10}$$

The electromagnetic force (B2) exerted on a nucleus triolet T_i by the envelope is then given by:

$$\overrightarrow{\mathbf{F}}_{env\pm>i\in nuc} \simeq \frac{-\mathrm{sgn}(i)}{n_{nuc}}\frac{\left(\pm N_{env\pm} e^2\right)}{4\pi\varepsilon_0 n_{env}\rho_{env\pm}^2}\left[\frac{1}{2}\frac{\rho_i}{\rho_{env\pm}} + \frac{3}{8}\frac{\rho_i^2}{\rho_{env\pm}^2} + \frac{9}{16}\frac{\rho_i^3}{\rho_{env\pm}^3}\right]\hat{\boldsymbol{\rho}}. \tag{B11}$$

Electromagnetic Force Exerted on Envelope Triolet *i* Due to Current Flowing at Nucleus

According to Equation (A3), the magnetic moment due to the nucleus is:

$$\mu_{nuc} = \frac{-a_{anml} e\hbar}{2m} = \frac{N_{nuc+} ec}{2n_{nuc}}\left(\rho_{nuc+} - \rho_{nuc-}\right). \tag{B12}$$

The vector potential and its derivatives are given [41] by:

$$\overrightarrow{\mathbf{A}}_{nuc>i\in env} \simeq \frac{\mu_0}{4\pi}\frac{\mu_{nuc}}{\rho_i^2}\hat{\boldsymbol{\theta}}, \tag{B13}$$

$$\overrightarrow{\mathbf{A}}_{nuc>i\in env} \simeq \frac{1}{8\pi\varepsilon_0 c}\frac{N_{nuc+} e}{n_{nuc}}\frac{\left(\rho_{nuc+} - \rho_{nuc-}\right)}{\rho_i^2}\hat{\boldsymbol{\theta}}, \tag{B14}$$

$$\frac{\partial\left(A_{nuc>i\in env}\hat{\boldsymbol{\theta}}\right)}{\partial t_i} = -A_{nuc>i\in env}\frac{c}{\rho_i}\hat{\boldsymbol{\rho}} = \frac{-1}{8\pi\varepsilon_0}\frac{N_{nuc+} e}{n_{nuc}}\frac{\left(\rho_{nuc+} - \rho_{nuc-}\right)}{\rho_i^3}\hat{\boldsymbol{\rho}} \tag{B15}$$

$$\overrightarrow{\nabla} \times \overrightarrow{\mathbf{A}} = \begin{vmatrix} \hat{\boldsymbol{\rho}} & \hat{\boldsymbol{\theta}} & \hat{\mathbf{k}} \\ \frac{\partial}{\partial\rho} & \frac{\partial}{\rho\partial\theta} & \frac{\partial}{\partial z} \\ 0 & A_{nuc>i\in env} & 0 \end{vmatrix} = \frac{\partial\left(A_{nuc>i\in env}\right)}{\partial\rho_i}\hat{\boldsymbol{k}} = \frac{(-1)}{4\pi\varepsilon_0 c}\frac{N_{nuc+} e}{n_{nuc}}\frac{\left(\rho_{nuc+} - \rho_{nuc-}\right)}{\rho_i^3}\hat{\mathbf{k}}. \tag{B16}$$

As the net nucleus charge is zero, and using Equation (A4), the force is defined by:

$$\overrightarrow{\mathbf{F}}_{nuc>i\in env} = \frac{\mathrm{sgn}(i)\cdot e}{n_{env}}\left[-\frac{\partial}{\partial t}\overrightarrow{\mathbf{A}}_{nuc>i} + c\hat{\theta}_j\left(\overrightarrow{\nabla} \times \overrightarrow{\mathbf{A}}_{nuc>i}\right)\right],$$

$$\overrightarrow{\mathbf{F}}_{nuc>i\in env} = \frac{3}{8\pi\varepsilon_0}\frac{\mathrm{sgn}(i)\, e^2 N_{nuc+}}{n_{nuc} n_{env}}\frac{\left(\eta_{nuc+} - \eta_{nuc-}\right)\lambda\!\!\!^{-}_C}{\rho_i^3}\hat{\boldsymbol{\rho}},$$

$$\overrightarrow{\mathbf{F}}_{nuc>i\in env} = \frac{-3}{8\pi\varepsilon_0}\frac{\mathrm{sgn}(i)\, e^2}{n_{env}}\frac{a_{anml}\lambda\!\!\!^{-}_C}{\rho_i^3}\hat{\boldsymbol{\rho}}. \tag{B17}$$

Electromagnetic Force Exerted on Triolet *i* at Radius ρ_i Due to Triolet *j* at Radius ρ_j

Every triolet experiences the fields emitted by all other triolets belonging to the same or adjacent orbit in the same component. Here we estimate the electromagnetic field and force exerted by a single triolet revolving on the same or adjacent orbit.

Let triolet T_j' ($\rho_j \sin\theta'_j$, $\rho_j \cos\theta'_j$) of charge q_j, revolving at light velocity on circular orbit of radius ρ_j, be positioned at angle θ'_j at retarded time t', and emitting an electromagnetic field received at time t by triolet $T_i(0, \rho_i)$ of charge q_i revolving at light velocity on circular orbit of radius ρ_i, and arriving at angle $\theta_i = 0$ on vertical axis y (**Figure 3A**). We have:

$$\overrightarrow{\mathbf{T_j T_i}} \begin{pmatrix} -\rho_j \ \sin\theta'_j \\ \rho_i - \rho_j \ \cos\theta'_j \end{pmatrix},$$

$$T_j T_i{}^2 = \rho_i^2 + \rho_j^2 - 2\rho_i\rho_j \cos\theta'_j \equiv R_{ij}^2, \tag{B18}$$

$$\hat{\mathbf{n}}_{ji} = \frac{\overrightarrow{\mathbf{T_j T_i}}}{T_j T_i} \begin{pmatrix} -\frac{\rho_j}{R_{ij}} \sin\theta'_j \\ \frac{\rho_i - \rho_j \ \cos\theta'_j}{R_{ij}} \end{pmatrix}, \tag{B19}$$

$$R_{ij} = \sqrt{\rho_i^2 + \rho_j^2 - 2\rho_i\rho_j \cos\theta'_j}. \tag{B20}$$

The trajectory, velocity and acceleration of triolet T_j are, respectively, given by:

$$\overrightarrow{\mathbf{w}}_j\left(t'\right) = \rho_j\left(\sin\omega t'\,\hat{\mathbf{x}} + \cos\omega t'\,\hat{\mathbf{y}}\right), \tag{B21}$$

$$\overrightarrow{\mathbf{v}}_j\left(t'\right) = \rho_j\omega\left(\cos\omega t'\,\hat{\mathbf{x}} - \sin\omega t'\,\hat{\mathbf{y}}\right), \tag{B22}$$

$$\overrightarrow{\mathbf{a}}_j\left(t'\right) = -\rho_j\omega^2\left(\sin\omega t'\,\hat{\mathbf{x}} + \cos\omega t'\,\hat{\mathbf{y}}\right), \tag{B23}$$

with ω being the angular velocity, satisfying relations $c = \rho\omega$ and $\theta' = \omega t'$. Since $v = c$, $\beta = v/c = 1$, we also have:

$$\hat{\boldsymbol{\rho}}_\mathbf{j}\begin{pmatrix}\sin\theta'_j\\ \cos\theta'_j\\ 0\end{pmatrix}, \quad \boldsymbol{\beta}_\mathbf{j}\begin{pmatrix}\cos\theta'_j\\ -\sin\theta'_j\\ 0\end{pmatrix}, \quad \dot{\boldsymbol{\beta}}_\mathbf{j}\begin{pmatrix}-c\sin\theta'_j/\rho_j\\ -c\cos\theta'_j/\rho_j\\ 0\end{pmatrix}$$

$$= \frac{-c}{\rho_j}\,\hat{\rho}_\mathbf{j}, \tag{B24}$$

$$g = 1 - \beta_\mathbf{j}\cdot\hat{\mathbf{n}}_{ji} = 1 - \cos\left(\frac{\pi}{2} + \gamma_j\right) = 1 + \sin\gamma_j. \tag{B25}$$

The electric and magnetic fields emitted by T_j and received by T_i are given [41] by:

$$\boldsymbol{E}_\mathbf{j} = \frac{q_j}{4\pi\varepsilon_0}\left[\frac{\left(\hat{\mathbf{n}}_{ji} - \boldsymbol{\beta}_\mathbf{j}\right)\left(1-\beta^2\right)}{g^3 R_{ij}^2} + \frac{\hat{\mathbf{n}}_{ji}\times\left[\left(\hat{\mathbf{n}}_{ji} - \boldsymbol{\beta}_\mathbf{j}\right)\times\dot{\boldsymbol{\beta}}_\mathbf{j}\right]}{cg^3 R_{ij}}\right] \tag{B26}$$

$$\boldsymbol{B}_\mathbf{j} = \frac{\mu_0 q_j}{4\pi}\left[\frac{\left(\mathbf{v_j}\times\hat{\mathbf{n}}_{ji}\right)\left(1-\beta^2\right)}{g^3 R_{ij}^2} + \frac{\left(\boldsymbol{\beta}_\mathbf{j}\times\hat{\mathbf{n}}_{ji}\right)\left(\dot{\boldsymbol{\beta}}_\mathbf{j}\cdot\hat{\mathbf{n}}_{ji}\right) + g\dot{\boldsymbol{\beta}}_\mathbf{j}\times\hat{\mathbf{n}}_{ji}}{g^3 R_{ij}}\right]. \tag{B27}$$

From **Figure 3B**, it can be seen that:

$$\dot{\boldsymbol{\beta}}_\mathbf{j}\cdot\hat{\mathbf{n}}_{ji} = \frac{c}{\rho_j}\cos\gamma_j, \tag{B28}$$

$$\cos\frac{\bar{\gamma}_j}{2} = \frac{1}{2}\left|\hat{\mathbf{n}}_{ji} - \boldsymbol{\beta}_\mathbf{j}\right|, \tag{B29}$$

$$\cos\frac{\bar{\gamma}_j}{2} = \sqrt{\frac{1}{2}\left(1+\cos\bar{\gamma}_j\right)} = \sqrt{\frac{1}{2}\left(1+\sin\gamma_j\right)}. \tag{B30}$$

And thus:

$$\hat{\mathbf{n}}_{ji}\cdot\left(\hat{\mathbf{n}}_{ji} - \boldsymbol{\beta}_\mathbf{j}\right) = \left|\hat{\mathbf{n}}_{ji} - \boldsymbol{\beta}_\mathbf{j}\right|\cdot\cos\frac{\gamma_j}{2} = 2\cos^2\frac{\gamma_j}{2} = 1 + \sin\gamma_j. \tag{B31}$$

From Equations (B25, B28) and identity: $\boldsymbol{a}\times(\boldsymbol{b}\times\boldsymbol{c}) = (\boldsymbol{a}\cdot\boldsymbol{c})\boldsymbol{b} - (\boldsymbol{a}\cdot\boldsymbol{b})\boldsymbol{c}$, we deduce:

$$\begin{aligned}\hat{\boldsymbol{n}}_{ji}\times\left[\left(\hat{\boldsymbol{n}}_{ji} - \boldsymbol{\beta}_\mathbf{j}\right)\times\dot{\boldsymbol{\beta}}_j\right] &= \left(\dot{\boldsymbol{\beta}}_j\cdot\hat{\boldsymbol{n}}_{ji}\right)\left(\hat{\boldsymbol{n}}_{ji} - \boldsymbol{\beta}_j\right) - \left[\hat{\boldsymbol{n}}_{ji}\cdot\left(\hat{\boldsymbol{n}}_{ji} - \boldsymbol{\beta}_j\right)\right]\dot{\boldsymbol{\beta}}_\mathbf{j},\\ \hat{\boldsymbol{n}}_{ji}\times\left[\left(\hat{\boldsymbol{n}}_{ji} - \boldsymbol{\beta}_\mathbf{j}\right)\times\dot{\boldsymbol{\beta}}_\mathbf{j}\right] &= \frac{c}{\rho_j}\cos\gamma_j\left(\hat{\boldsymbol{n}}_{ji} - \boldsymbol{\beta}_j\right) - \left(1+\sin\gamma_j\right)\dot{\boldsymbol{\beta}}_\mathbf{j},\end{aligned} \tag{B32}$$

implying, since $1-\beta^2 = 0$ and using Equations (B24, B25, B32):

$$\begin{aligned}\boldsymbol{E}_\mathbf{j} &= \frac{q_j}{4\pi\varepsilon_0}\left[\frac{\hat{\mathbf{n}}_{ji}\times\left[\left(\hat{\mathbf{n}}_{ji} - \boldsymbol{\beta}_j\right)\times\dot{\boldsymbol{\beta}}_j\right]}{cg^3 R_{ij}}\right],\\ \boldsymbol{E}_\mathbf{j} &= \frac{q_j}{4\pi\varepsilon_0 R_{ij}\rho_j}\left[\left(\hat{\mathbf{n}}_{ji} - \boldsymbol{\beta}_j\right)\frac{\cos\gamma_j}{\left(1+\sin\gamma_j\right)^3} + \hat{\boldsymbol{\rho}}_\mathbf{j}\frac{1}{\left(1+\sin\gamma_j\right)^2}\right].\end{aligned} \tag{B33}$$

From **Figure 3B**, we also have:

$$\boldsymbol{\beta}_j\times\hat{\mathbf{n}}_{ji} = -\sin\left(\frac{\pi}{2} + \gamma_j\right)\hat{\mathbf{z}} = -\cos\gamma_j\hat{\mathbf{z}}, \tag{B34}$$

$$\dot{\boldsymbol{\beta}}_j\times\hat{\mathbf{n}}_{ji} = -\frac{c\hat{\rho}_\mathbf{j}}{\rho_j}\times\hat{\mathbf{n}}_{ji} = -\frac{c}{\rho_j}\sin\left(\pi - \gamma_j\right)\hat{\mathbf{z}} = -\frac{c}{\rho_j}\sin\gamma_j\hat{\mathbf{z}}, \tag{B35}$$

yielding, using Equations (B27, B28) and $\mu_0 = 1/(\varepsilon_0 c^2)$:

$$\begin{aligned}\mathbf{B}_\mathbf{j} &= \frac{\mu_0 q_j}{4\pi}\left[\frac{-\frac{c}{\rho_j}\cos\gamma_j\cos\gamma_j - \frac{c}{\rho_j}(1+\sin\gamma_j)\sin\gamma_j}{(1+\sin\gamma_j)^3 R_{ij}}\right]\hat{\mathbf{z}},\\ \mathbf{B}_\mathbf{j} &= \frac{-q_j}{4\pi\varepsilon_0 c R_{ij}\rho_j\left(1+\sin\gamma_j\right)^2}\hat{\mathbf{z}}.\end{aligned} \tag{B36}$$

The magnetic force is directed along $\boldsymbol{\rho_i}$ since $\boldsymbol{B}_j$ is along $\boldsymbol{z}$. But to express the equilibrium we need to find the component of $\boldsymbol{E_j}$ along $\boldsymbol{\rho_i}$, and thus we need:

$$\hat{\mathbf{n}}_{ji}\cdot\hat{\boldsymbol{\rho}}_\mathbf{i} = \frac{1}{R_{ij}}\left(\rho_i - \rho_j\ \cos\theta'_j\right), \tag{B37}$$

$$\hat{\boldsymbol{\rho}}_\mathbf{i}\cdot\left(-\boldsymbol{\beta}_\mathbf{j}\right) = \cos\left(\theta'_j - \frac{\pi}{2}\right) = \sin\theta'_j, \tag{B38}$$

$$\hat{\boldsymbol{\rho}}_\mathbf{i}\cdot\hat{\boldsymbol{\rho}}_\mathbf{j} = \cos\theta'_j, \tag{B39}$$

yielding from Equation (B33):

$$\boldsymbol{E}_{\mathbf{ji}\perp} = \frac{q_j}{4\pi\varepsilon_0 R_{ij}\rho_j}\left[\frac{1}{R_{ij}}\left(\rho_i - \rho_j\ \cos\theta'_j\right)\frac{\cos\gamma_j}{\left(1+\sin\gamma_j\right)^3}\right.$$

$$+\frac{\sin\theta_j^{'}\cos\gamma_j}{\left(1+\sin\gamma_j\right)^3}+\frac{\cos\theta_j^{'}}{\left(1+\sin\gamma_j\right)^2}\Bigg]\hat{\boldsymbol{\rho}}. \quad \text{(B40)}$$

This can be rearranged by expressing θ'_j as a function of γ_j and vice versa. From Equations (B19, B24):

$$\begin{aligned}\cos\gamma_j &= -\hat{\boldsymbol{\rho}}_{\mathbf{j}}\cdot\hat{\mathbf{n}}_{ji} = -\sin\theta_j^{'}\left(-\frac{\rho_j}{R_{ij}}\sin\theta_j^{'}\right)\\ &\quad -\cos\theta_j^{'}\left(\frac{\rho_i-\rho_j\cos\theta_j^{'}}{R_{ij}}\right),\\ \cos\gamma_j &= \frac{1}{R_{ij}}\left(\rho_j-\rho_i\cos\theta_j^{'}\right). \quad \text{(B41)}\end{aligned}$$

Similarly, from Equation (B28):

$$\begin{aligned}\sin\gamma_j\,\hat{\mathbf{z}} &= \hat{\boldsymbol{\rho}}_{\mathbf{j}}\times\hat{\mathbf{n}}_{ji} = \begin{vmatrix}\hat{\boldsymbol{x}} & \hat{\boldsymbol{y}} & \hat{\boldsymbol{z}}\\ \sin\theta_j^{'} & \cos\theta_j^{'} & 0\\ -\frac{\rho_j}{R_{ij}}\sin\theta_j^{'} & \frac{\rho_i-\rho_j\cos\theta_j^{'}}{R_{ij}} & 0\end{vmatrix},\\ \sin\gamma_j &= \frac{\rho_i}{R_{ij}}\sin\theta_j^{'}. \quad \text{(B42)}\end{aligned}$$

Relations (B41) and (B42) may be reversed:

$$\sin\theta_j^{'} = \frac{R_{ij}}{\rho_i}\sin\gamma_j, \quad \text{(B43)}$$

$$\cos\theta_j^{'} = \frac{1}{\rho_i}\left(\rho_j-R_{ij}\cos\gamma_j\right). \quad \text{(B44)}$$

Then, using these to rearrange Equation (B40) and developing:

$$\begin{aligned}&\frac{1}{R_{ij}^2}\left(\rho_i-\rho_j\cos\theta_j^{'}\right)\left(\rho_j-\rho_i\cos\theta_j^{'}\right)\\ &\quad=\frac{1}{R_{ij}^2}\left[\rho_i\rho_j\sin^2\theta_j^{'}-R_{ij}^2\cos\theta_j^{'}\right],\\ &\frac{\sin\theta_j^{'}}{R_{ij}}\left(\rho_j-\rho_i\cos\theta_j^{'}\right)+\cos\theta_j^{'}\left(1+\frac{\rho_i}{R_{ij}}\sin\theta_j^{'}\right)\\ &\quad=\cos\theta_j^{'}+\frac{\rho_j}{R_{ij}}\sin\theta_j^{'},\end{aligned}$$

we obtain using Equation (B42):

$$\begin{aligned}\boldsymbol{E}_{\mathbf{ji}\perp} &= \frac{q_j\sin\theta_j^{'}}{4\pi\varepsilon_0R_{ij}^2\left(1+\sin\gamma_j\right)^3}\left[\frac{\rho_i}{R_{ij}}\sin\theta_j^{'}+1\right]\hat{\boldsymbol{\rho}},\\ \boldsymbol{E}_{\mathbf{ji}\perp} &= \frac{q_j\sin\gamma_j}{4\pi\varepsilon_0R_{ij}\rho_i\left(1+\sin\gamma_j\right)^2}\hat{\boldsymbol{\rho}}. \quad \text{(B45)}\end{aligned}$$

The Lorentz force is then:

$$\begin{aligned}\boldsymbol{F}_{\mathbf{ij}\perp} &= q_i\left(\boldsymbol{E}_{\mathbf{ij}\perp}+c\hat{\theta}_i\times\boldsymbol{B}_{\mathbf{ij}}\right),\\ \boldsymbol{F}_{\mathbf{ij}\perp} &= \frac{q_iq_j}{4\pi\varepsilon_0R_{ij}\rho_i}\left[\frac{\sin\gamma_j}{\left(1+\sin\gamma_j\right)^2}\right]\hat{\boldsymbol{\rho}}\\ &\quad+\frac{q_iq_j}{4\pi\varepsilon_0R_{ij}\rho_j}\left[\frac{1}{\left(1+\sin\gamma_j\right)^2}\right]\hat{\boldsymbol{\rho}},\\ \boldsymbol{F}_{\mathbf{ij}\perp} &= \frac{q_iq_j}{4\pi\varepsilon_0R_{ij}\left(1+\sin\gamma_j\right)^2}\left[\frac{\sin\gamma_j}{\rho_i}+\frac{1}{\rho_j}\right]\hat{\boldsymbol{\rho}}. \quad \text{(B46)}\end{aligned}$$

The scalar and vector Liénard-Wichert retarded electromagnetic potentials [41] are:

$$V_{ij} = \frac{q_j}{4\pi\varepsilon_0\left(R_{ij}-\boldsymbol{\beta}_{\mathbf{j}}\cdot\mathbf{R}_{\mathbf{ij}}\right)_{rtrd}} = \frac{q_j}{4\pi\varepsilon_0R_{ij}\left(1+\sin\gamma_j\right)}, \quad \text{(B47)}$$

$$\boldsymbol{A}_{\mathbf{ij}} = \frac{\mu_0}{4\pi}\left(\frac{q_jv_j\hat{\theta}_j}{R_{ij}-\boldsymbol{\beta}_{\mathbf{j}}\cdot\mathbf{R}_{\mathbf{ij}}}\right)_{rtrd} = \frac{q_j\hat{\theta}_j}{4\pi\varepsilon_0cR_{ij}\left(1+\sin\gamma_j\right)}. \quad \text{(B48)}$$

Approximation ρ_i=ρ_j. When making this approximation (one-orbit model), from **Figure 3C**, R_{ij} becomes:

$$R_{ij} = 2\rho_i\cos\gamma_j. \quad \text{(B49)}$$

Note that if ρ_i= ρ_j, Equation (B46) then becomes:

$$\mathbf{F}_{\mathbf{ij}\perp}=\frac{q_iq_j}{8\pi\varepsilon_0\rho_i^2\cos\gamma_j\left(1+\sin\gamma_j\right)}\hat{\boldsymbol{\rho}}. \quad \text{(B50)}$$

Triolets at Radial Equilibrium

Equilibrium of Envelope Triolets

Envelope triolets are submitted to the centrifugal force (B1), the magnetic force due to the net nucleus magnetic moment (B17), and the net electromagnetic force due to the other envelope triolets (B46). Equilibrium for env– triolets can be written:

$$\begin{aligned}0 = \frac{\hbar c}{b_{env}\rho_{env-}^2}+\frac{(-e)}{n_{env}}\sum_j^{N_{env}-1}\frac{e}{n_{env}}\frac{1}{4\pi\varepsilon_0}\frac{\mathrm{sgn}\left(j\right)}{R_{ij}(1+\sin\gamma_j)^2}\\ \times\left[\frac{\sin\gamma}{\rho_{env-}}+\frac{1}{\rho_j}\right]+\frac{3}{8\pi\varepsilon_0}\frac{e^2}{n_{env}}\frac{a_{anml}\lambda\!\!\!^{-}_C}{\rho_{env-}^3}.\end{aligned}$$

And rearranging to isolate the fine-structure constant:

$$\begin{aligned}\frac{4\pi\varepsilon_0\hbar c}{e^2} = \frac{1}{\alpha} = \frac{b_{env}\rho_{env-}^2}{n_{env}}\Bigg[\sum_j^{N_{env}-1}\frac{1}{n_{env}}\frac{\mathrm{sgn}\left(j\right)}{R_{ij}(1+\sin\gamma_j)^2}\\ \times\left(\frac{\sin\gamma}{\rho_{env-}}+\frac{1}{\rho_j}\right)-\frac{3a_{anml}\lambda\!\!\!^{-}_C}{2\rho_{env-}^3}\Bigg]. \quad \text{(C1)}\end{aligned}$$

Likewise, equilibrium for env+ triolets can be written:

$$\begin{aligned}\frac{1}{\alpha} = \frac{b_{env}\rho_{env+}^2}{n_{env}}\Bigg[-\sum_j^{N_{env}-1}\frac{1}{n_{env}}\frac{\mathrm{sgn}\left(j\right)}{R_{ij}(1+\sin\gamma_j)^2}\left(\frac{\sin\gamma}{\rho_{env+}}+\frac{1}{\rho_j}\right)\\ +\frac{3a_{anml}\lambda\!\!\!^{-}_C}{2\rho_{env+}^3}\Bigg]. \quad \text{(C2)}\end{aligned}$$

Neglecting the term due to the nucleus magnetic moment, the equations become:

$$\frac{1}{\alpha} = \frac{-b_{env}}{n_{env}^2}\left[\sum_{j}^{N_{env}-1}\frac{\rho_i^2 \mathrm{sgn}\left(i\cdot j\right)}{R_{ij}(1+\sin\gamma_j)^2}\left(\frac{\sin\gamma}{\rho_i}+\frac{1}{\rho_j}\right)\right] \equiv G_{env}. \quad \text{(C3)}$$

The fine structure constant therefore appears to be naturally related to the ratio between the centrifugal force and the net electromagnetic force experienced by a single triolet. Making the ρ_i=ρ_j approximation (B49), we obtain:

$$\frac{1}{\alpha} = \frac{-b_{env}}{2n_{env}^2}\left[\sum_{j}^{N_{env}-1}\frac{\mathrm{sgn}\left(i\cdot j\right)}{\cos\gamma_j(1+\sin\gamma_j)}\right]. \quad \text{(C4)}$$

Equilibrium of Nucleus Triolets

Nucleus triolets are submitted to the centrifugal force (B1), the electromagnetic force due to the envelope (B11), and the net electromagnetic force due to the other nucleus triolets (B46). Equilibrium for nuc– triolets is thus written:

$$\frac{1}{\alpha} \simeq \frac{b\rho_{nuc-}^2}{n_{nuc}}\left[\frac{\rho_{nuc-}}{2n_{env}}\left(\frac{N_{env+}}{\rho_{env+}^3}-\frac{N_{env-}}{\rho_{env-}^3}\right) + \sum_{j}^{N_{nuc}-1}\frac{1}{n_{nuc}}\frac{\mathrm{sgn}\left(j\right)}{R_{ij}\left(1+\sin\gamma_j\right)^2}\left(\frac{\sin\gamma}{\rho_{nuc-}}+\frac{1}{\rho_j}\right)\right]. \quad \text{(C5)}$$

Similarly we have for the nuc+ triolets:

$$\frac{1}{\alpha} \simeq \frac{b\rho_{nuc+}^2}{n_{nuc}}\left[\frac{\rho_{nuc+}}{2n_{env}}\left(\frac{N_{env+}}{\rho_{env+}^3}-\frac{N_{env-}}{\rho_{env-}^3}\right) - \sum_{j}^{N_{nuc}-1}\frac{1}{n_{nuc}}\frac{\mathrm{sgn}\left(j\right)}{R_{ij}\left(1+\sin\gamma_j\right)^2}\left(\frac{\sin\gamma}{\rho_{nuc+}}+\frac{1}{\rho_j}\right)\right]. \quad \text{(C6)}$$

Neglecting the term due to the envelope current, the equations become:

$$\frac{1}{\alpha} = \frac{-b_{nuc}}{n_{nuc}^2}\left[\sum_{j}^{N_{nuc}-1}\frac{\rho_i^2 \mathrm{sgn}\left(i\cdot j\right)}{R_{ij}(1+\sin\gamma_j)^2}\left(\frac{\sin\gamma}{\rho_i}+\frac{1}{\rho_j}\right)\right] \equiv G_{nuc}. \quad \text{(C7)}$$

Making the ρ_i=ρ_j approximation (B49), we obtain:

$$\frac{1}{\alpha} = \frac{-b_{nuc}}{2n_{nuc}^2}\left[\sum_{j}^{N_{nuc}-1}\frac{\mathrm{sgn}\left(i\cdot j\right)}{\cos\gamma_j(1+\sin\gamma_j)}\right]. \quad \text{(C8)}$$

Also, the correction due to envelope current (first two terms) is:

$$G_{env>i\in nuc} \approx \frac{-b_{nuc}\mathrm{sgn}\,(i)\,(-n_{env})}{n_{nuc}n_{env}}\left[\frac{\rho_{nuc}^3}{2\rho_{env}^3}+\frac{3\rho_{nuc}^4}{8\rho_{env}^4}\right] \approx \frac{b_{nuc}\mathrm{sgn}\,(i)}{n_{nuc}}\left[\frac{\eta_{nuc}^3}{2}+\frac{3\eta_{nuc}^4}{8}\right]. \quad \text{(C9)}$$

Retarted Angles

Evaluating the Values of Retarded Angle θ_j' From Non-retarded Angle θ_j

If we suppose triolets are uniformly distributed along the circular orbits (this is certainly true of the nucleus since we have N_{nuc+} = N_{nuc-}, but is an approximation in the case of the envelope, as there are more negative than positive triolets), then angle θ_j (expressed in radians) determining the position of the j^{th} triolet (starting at 1) at non-retarded time t on the orbit is defined by:

$$\theta_{j\in nuc} = 2\pi\frac{j}{N_{nuc}}. \quad \text{(D1)}$$

Note that, for the envelope, we also need to account for the empty space of length d_{env} (using the number of missing triolets as units) separating the n_{env} stretches of triolets, yielding for triolets T_j belonging to the first stretch:

$$\theta_{j\in 1stStretch} = 2\pi\frac{j}{\left(N_{env}+n_{env}d_{env}\right)}. \quad \text{(D2)}$$

To evaluate θ_j' determining the angular position T_j' at retarded time t' when the electromagnetic field was emitted toward triolet T_i, which arrives at angle 0 (vertical y axis) at time t to receive the field, we use the following relation, derived from **Figure 3A**:

$$R_{ij} = \rho_j\delta\theta_j = \rho_j\left(\theta_j-\theta_j^{'}\right). \quad \text{(D3)}$$

Then squaring Equations (B20) and (D3) and equating, we obtain:

$$\left(\theta_j-\theta^{'}{}_j\right)^2 = 1-2\left(\frac{\rho_i}{\rho_j}\right)\cos\theta^{'}{}_j+\left(\frac{\rho_i}{\rho_j}\right)^2. \quad \text{(D4)}$$

Given ρ_i, ρ_j, and θ_j, the retarded angles θ'$_j$ may be numerically determined by recurrence, using a computer program that implements Newton method for instance, to resolve transcendental Equation (D4) for all triolets of angular position θ_j expressed in radians. The corresponding values of γ_j are then estimated using Equation (B42).

Potential Energy

Electric Potential Energy

By definition, the electric potential energies at the envelope and nucleus are defined by:

$$U_{elec,env} = \sum_{i}^{N_{env}}\sum_{j\neq i}^{N_{env}-1} q_iV_{ij} = \sum_{i\in env}\sum_{j\neq i}\frac{q_iq_j}{4\pi\varepsilon_0R_{ij}\left(1+\sin\gamma_j\right)}, \quad \text{(E1)}$$

$$U_{elec,env} = \frac{\alpha mc^2}{n_{env}^2}\sum_{i\in env}\sum_{j\neq i}\frac{\mathrm{sgn}(i\cdot j)}{H_{ij}\left(1+\sin\gamma_j\right)}, \quad \text{(E2)}$$

where $H_{ij} = R_{ij}/\lambda\!\!\!^{-}_c$. Likewise, we have:

$$U_{elec,nuc} = \frac{\alpha mc^2}{n_{nuc}^2}\sum_{i\in nuc}\sum_{j\neq i}\frac{\mathrm{sgn}(i\cdot j)}{H_{ij}\left(1+\sin\gamma_j\right)}. \quad \text{(E3)}$$

Making the $\rho_i = \rho_j$ approximation (B49), we obtain:

$$U_{elec,env} = \frac{\alpha mc^2}{2n_{env}^2} \sum_{i\in env} \sum_{j\neq i} \frac{\mathrm{sgn}(i\cdot j)}{\eta_j \cos\gamma_j \left(1+\sin\gamma_j\right)}, \quad \text{(E4)}$$

$$U_{elec,nuc} = \frac{\alpha mc^2}{2n_{nuc}^2} \sum_{i\in nuc} \sum_{j\neq i} \frac{\mathrm{sgn}(i\cdot j)}{\eta_j \cos\gamma_j \left(1+\sin\gamma_j\right)}. \quad \text{(E5)}$$

Magnetic Potential Energy

The magnetic potential energy U_{mag} and electric potential energy U_{elec} are, respectively, the opposite of the magnetic work and electric work [41] given by:

$$W_{mag} = \frac{1}{2\mu_0} \int_{all\ space} B^2 d\tau = -U_{mag}, \quad \text{(E6)}$$

$$W_{elec} = \frac{\varepsilon_0}{2} \int_{all\ space} E^2 d\tau = -U_{elec}. \quad \text{(E7)}$$

Now, the vector expression relating the magnetic field to the electric field:

$$\overrightarrow{\boldsymbol{B}} = \frac{1}{c}\hat{\boldsymbol{n}} \times \overrightarrow{\boldsymbol{E}} \quad \text{(E8)}$$

holds in relativistic electrodynamics with particles going at light velocity, yielding:

$$W_{mag} = \frac{1}{2\mu_0 c^2} \int_{all\ space} E^2 d\tau, \quad \text{(E9)}$$

and since we know that $c^2 = 1/\varepsilon_0\mu_0$, we have:

$$W_{mag} = \frac{\varepsilon_0}{2} \int_{all\ space} E^2 d\tau = W_{elec}. \quad \text{(E10)}$$

Therefore:

$$U_{mag} = U_{elec}. \quad \text{(E11)}$$

Total Potential Energy

Neglecting the potential energy of the envelope acting on the nucleus $U_{env>nuc}$, and the potential energy of the nucleus acting on the envelope $U_{nuc>env}$, the electron potential energy is approximately:

$$U_{tot} \simeq U_{env} + U_{nuc}, \quad \text{(E12)}$$

where U_{env} is the envelope potential energy and U_{nuc} the nucleus potential energy. Using Equations (E2, E11), we obtain:

$$U_{env} = U_{env,mag} + U_{env,elec} = 2U_{env,elec}, \quad \text{(E13)}$$

$$U_{env} = \frac{2\alpha mc^2}{n_{env}^2} \sum_{i\in env} \sum_{j\neq i} \frac{\mathrm{sgn}(i\cdot j)}{H_{ij}\left(1+\sin\gamma_j\right)}, \quad \text{(E14)}$$

where $H_{ij} = R_{ij}/\lambda\!\!\!^{-}_c$. Likewise, using Equation (E.3) we have:

$$U_{nuc} = \frac{2\alpha mc^2}{n_{nuc}^2} \sum_{i\in nuc} \sum_{j\neq i} \frac{\mathrm{sgn}(i\cdot j)}{H_{ij}\left(1+\sin\gamma_j\right)}. \quad \text{(E15)}$$

Compatibility Between Potential Energies and Radial Equilibrium Equations

It can be shown that Equations (E14, E15) are compatible with Equations (C4, C8) if we assume $\eta_{nuc+} \simeq \eta_{nuc-}$ and $\eta_{env+} \simeq \eta_{env-} \simeq 1$. Indeed, Equation (C4) becomes:

$$\left[\sum_{j}^{N_{env}-1} \frac{\mathrm{sgn}\left(i\cdot j\right)}{2\cos\gamma_j(1+\sin\gamma_j)}\right] \simeq \frac{-n_{env}^2}{\alpha b_{env}}.$$

Then, by replacing the relation above into Equation (98), since $\eta_{env+} \simeq \eta_{env-} \simeq 1$, we obtain:

$$U_{env} = \frac{2\alpha mc^2}{n_{env}^2} \sum_{i\in env} \sum_{j\neq i} \frac{\mathrm{sgn}\left(i\cdot j\right)}{2\eta_i \cos\gamma_j \left(1+\sin\gamma_j\right)}$$

$$\simeq \frac{-2\alpha mc^2}{n_{env}^2} N_{env} \frac{n_{env}^2}{\alpha b_{env}},$$

$$U_{env} \simeq \frac{-2N_{env}mc^2}{b_{env}}.$$

Since $b_{env} = 2N_{env}$, this yields: $U_{env} \simeq -mc^2$ as expected. Likewise, Equation (C8) becomes:

$$\left[\sum_{j}^{N_{nuc}-1} \frac{\mathrm{sgn}\left(i\cdot j\right)}{2\cos\gamma_j(1+\sin\gamma_j)}\right] \simeq \frac{-n_{nuc}^2}{\alpha b_{nuc}}.$$

Then, by replacing the relation above into Equation (E15), we obtain:

$$U_{nuc} = \frac{2\alpha mc^2}{n_{nuc}^2} \sum_{i\in nuc} \sum_{j\neq i} \frac{\mathrm{sgn}(i\cdot j)}{2\eta_i \cos\gamma_j \left(1+\sin\gamma_j\right)} \simeq \frac{-2\alpha mc^2}{n_{nuc}^2} \frac{N_{nuc}}{\eta_{nuc}} \frac{n_{nuc}^2}{\alpha b_{nuc}},$$

$$U_{nuc} \simeq \frac{-2N_{nuc}mc^2}{b_{nuc}\eta_{nuc}}.$$

Since $2N_{nuc} = b_{nuc}\eta_{nuc}$ (A21), we obtain: $U_{nuc} \simeq -mc^2$ as expected.

Optimization Algorithm

An optimization algorithm has been devised and implemented to determine a set of optimum orbital radii for envelope triolets by minimizing average absolute deviation K, in the n-orbits model where each triolet possesses a specific radii η_i at the envelope. An approximate solution is determined heuristically before applying this algorithm. The algorithm next considers in turn every envelope triolet belonging to the first stretch, tries five different radii surrounding the current radius, and computes for each the stability of all envelope triolets. The radius yielding best overall stability is then attributed to the corresponding triolets in all six stretches. Once the procedure has been applied to all triolets of the first stretch, it is run again, considering five closer radii this time (thus slowly reducing the noise), until convergence toward an optimum solution is reached. The corresponding pseudocode is shown below. The algorithm was applied with the following values: delta = 0.00201, step = 0.00005, n_{env}= 6, N_{env+} = 60, N_{env-} = 66, $d_{env} = 2$.

```
Function optimize_env_radii( radius[126], delta, step ):
    for d in range( delta to 0.00001 by –step ):
        for i in range( 0 to 20 by +1 ):
            previous_radius = radius[ i ]
            R = previous_radius
            best_r = R
            best_K = 10000
            list_new_radii = { R−2d, R–d, R, R+d, R+2d }
            for r in list_new_radii:
                set_radius( i to r in all six stretches )
                clear( list_inv_alphas )
                for j in range( 1 to 20 by +1 ):
                    G = compute_inv_alpha( i, j )
                    add( G to list_inv_alphas )
                K = compute_error_K( list_inv_alphas )
                if K < best_K:
                    best_K = K
                    best_r = r
            set_radius( i to best_r in all six stretches )
return radius[126]
```

DATA AVAILABILITY STATEMENT

All datasets generated for this study are included in the article/supplementary material.

AUTHOR CONTRIBUTIONS

SA conceived the study, formed the hypotheses, constructed the model, wrote down and solved the equations, implemented the computations, and wrote the manuscript. FB helped solve the equations, devised the optimization algorithm, independently implemented the computations, and reviewed the manuscript. All authors approved the submitted version.

ACKNOWLEDGMENTS

The authors wish to thank Patrick Richard (IFSTTAR, University Gustave Eiffel) for helpful advice and Gilles Salbert (IGDR, University of Rennes 1) for support and reading the manuscript.

REFERENCES

1. Bourilkov D. Hint for axial-vector contact interactions in the data on $e^+e^- \rightarrow e^+e^-(\gamma)$ at center-of-mass energies 192-208 GeV. *Phys Rev* D. (2001) **64:**071701. doi: 10.1103/PhysRevD.64.071701
2. Davisson CJ, Germer LH. Diffractions of electrons by a crystal of Nickel. *Phys. Rev*. (1927) **30**:705.
3. Bohr N. The quantum postulate and the recent development of atomic theory. *Nature*. (1928) **121:**580–90.
4. Heisenberg W. Das naturgesetz und die struktur der materie, belser-presse, 1967. trans. *Natural Law and The Structure of Matter*. Belser: Warm Wind Books (1981).
5. de Broglie L. Treize remarques sur divers sujets de physique théorique. *Ann. Fond. L. de Broglie*. (1976) **1**:116–28.
6. Dirac P. An extensible model of the electron. *Proc. Royal Soc. Lond A*. (1962) **268**:57–67.
7. Bunge M. A picture of the electron. *Nuovo Cimento*. (1955) **1**:977–85.
8. Abraham M. Prinzipien der dynamik des elektrons. *Ann Phys*. (1903) **1**:105–79.
9. Lorentz HA. *The Theory of Electrons*. 2nd ed. Leipzig: Teubner (1916).
10. Fermi E. Über einen Widerspruch zwischen der elektrodynamischen und relativistischen theorie der elektromagnetischen masse. *Phys Zeitschrift*. (1922) **23:**341–4.
11. Dirac P. Classical theory of radiating electrons. *Proc Royal Soc Lond A*. (1938) **167**:148.
12. Rohrlich F. Self-energy and stability of the classical electron. *Am J Phys*. (1960) **28:**639.
13. Schwinger J. Electromagnetic mass revisited. *Found Phys*. (1983) **13**:373–83.
14. Parson AL. A magneton theory of the structure of the atom smithson. *Misc Collect*. (1915) **65**:1–80.
15. Webster LW. The theory of electromagnetic mass of the parson magneton and other non-spherical systems. *Phys Rev*. (1917) **9**:484–99.
16. Allen HS. The case for a ring electron. *Proc Phys Soc Lond*. (1918) **31**:49.
17. Compton AH. The size and shape of the electron. *Phys Rev*. (1919) **14**:247.
18. Poincaré H. Sur la dynamique de l'électron. *Rend Circolo Mat Palermo*. (1906) **21**:129–76.
19. Eisberg R, Resnick R. *Quantum Physics of Atoms, Molecules, Solids, Nuclei and Particles*, 2nd ed. Hamilton, ON: John Wiley and Sons (1985).
20. Griffiths DJ. *Introduction to Elementary Particles*, 2nd ed. Weinheim: Wiley-VCH. (2008). doi: 10.1002/9783527618460. index
21. Born M. Quantenmechanik der Stoßvorgänge. *Zeitschrift für Physik*. (1926) **38:**803–27.
22. Schrödinger E. Uber die kraftefreie Bewegung in der relativistischen Quantum-mechanik, Sitz. *Preuss. Akad. Wiss. Physik-Math*. (1930) **24**:418.
23. de Broglie L. La mécanique ondulatoire et la structure atomique de la matière et du rayonnement. *J Phys Radium*. (1927) **8**:225–41.
24. Bohm D. A suggested interpretation of the quantum theory in terms of hidden variables. *Phys Rev*. (1952) **85**:166. doi: 10.1103/PhysRev.85.166
25. Bohm D, Vigier JP. Model of the causal interpretation of quantum theory in terms of a fluid with irregular fluctuations. *Phys Rev*. (1954) **96**:208–16.
26. Bohm D, Dewdney C, Hiley BH. A quantum approach to the Wheeler delayed-choice experiment. *Nature*. (1985) **315**:294–7.
27. Weyssenhoff J. On two relativistic models of dirac's electron. *Acta Phys Pol*. (1947) **9**:47–53.
28. Huang K. On the zitterbewegung of the dirac electron. *Am J Phys*. (1952) **20**:479–84.
29. Barut AO, Bracken AJ. Zitterbewegung and the internal geometry of the electron. *Phys Rev D*. (1981) **23**:10.
30. Barut AO, Zanghi N. Classical model of the dirac electron. *Phys Rev Lett*. (1984) **52**:2009.
31. Bergman DL, Wesley JP. Spinning charge ring model of electron yielding anomalous magnetic moment. *Galilean Electrodynamics*. (1990) **1**:63–7.
32. Pavšič M, Recami E, Rodrigues WA Jr, Maccarrone GD, Raciti F, Salesi G. Spin and electron structure. *Phys Lett B*. (1993) **318**:481–8.
33. Salesi G, Recami E. Hydrodynamical reformulation and quantum limit of the barut-zanghi theory, found. *Phys Lett*. (1997) **10**:533–46.
34. Barut AO, Pavšič M. Radiation reaction and the electromagnetic energy-momentum of moving relativistic charged membranes. *Phys Lett B*. (1994) **331**:45–50.
35. Bostick WH. Mass, charge and current: the essence and morphology. *Physics Essays*. (1991) **4**:45.
36. Consa O. Helical solenoid model of the electron. *Progr Phys*. (2018) **14**:80–89.
37. Hestenes D. Quantum mechanics from self-interaction. *Found Phys*. (1985) **15**:63–87.
38. Hestenes D. The zitterbewegung interpretation of quantum mechanics. *Found Phys*. (1990) **20**:1213–32.
39. Odom B, Hanneke D, D'Urso B, Gabrielse G. New measurement of the electron magnetic moment using a one-electron quantum cyclotron. *Phys Rev Lett*. (2006) **97**:030801.

40. Goldstein H, Poole C, Safko J. *Classical Mechanics*, 3rd ed. Longman: Addison Wesley (2002). doi: 10.1119/1.1484149
41. Zangwill A. *Modern Electrodynamics*. Cambridge: Cambridge University Press (2013).
42. Pusey MF, Barrett J, Rudolph T. On the reality of the quantum state. *Nat Phys*. (2012) **8**:475–8.
43. Bell JS. On the impossible pilot wave. *Found Phys*. (1982) **12**:989–99.
44. von Neumann J. *Mathematical Foundations of Quantum Mechanics*. Princeton, NJ: Princeton Univ. Press (1955).
45. Wheeler JA, Zurek WH. *Quantum Theory and Measurement*. Princeton, NJ: Princeton University Press (1983).
46. Einstein A. Physics and reality. *J Franklin Institute*. (1936) **221**:349–82.
47. Dürr D, Goldstein S, Zanghi N. Quantum equilibrium and the origin of absolute uncertainty. *J Stat Phys*. (1992) **67**:843–907. doi: 10.1007/BF01049004
48. Hudson JJ, Kara DM, Smallman IJ, Sauer BE, Tarbutt MR, Hinds EA. Improved measurement of the shape of the electron. *Nature*. (2011) **473:**493–6. doi: 10.1038/nature10104
49. Kim BJ, Koh H, Rotenberg E, Oh SJ, Eisaki H, Motoyama N, et al. Distinct spinon and holon dispersions in photoemission spectral functions from one-dimensional $SrCuO_2$. *Nat Phys*. (2006) **2**:397–401. doi: 10.1038/nphys316
50. Jompol Y, Ford CJB, Griffiths JP, Farrer I, Jones GAC, Anderson D, et al. Probing spin-charge separation in a tomonaga-luttinger liquid. *Science*. (2009) **325**:597–601. doi: 10.1126/science.1171769
51. Schlappa J, Wohlfeld K, Zhou KJ, Mourigal M, Haverkort MW, Strocov VN, et al. Spin-orbital separation in the quasi-one-dimensional Mott insulator Sr_2CuO_3. *Nature*. (2012) **485**:82–5. doi: 10.1038/nature10974
52. Eidelman S, Hayes KG, Olive KA, Aguilar-Benitez M, Amsler C, Asner D. (Particle Data Group). Review of particle physics. *Phys Lett B*. (2004) **592**:1–5.

Conflict of Interest: The authors declare that the research was conducted in the absence of any commercial or financial relationships that could be construed as a potential conflict of interest.

Advantages of publishing in Frontiers

OPEN ACCESS
Articles are free to read for greatest visibility and readership

FAST PUBLICATION
Around 90 days from submission to decision

HIGH QUALITY PEER-REVIEW
Rigorous, collaborative, and constructive peer-review

TRANSPARENT PEER-REVIEW
Editors and reviewers acknowledged by name on published articles

Frontiers
Avenue du Tribunal-Fédéral 34
1005 Lausanne | Switzerland

Visit us: www.frontiersin.org
Contact us: frontiersin.org/about/contact

REPRODUCIBILITY OF RESEARCH
Support open data and methods to enhance research reproducibility

DIGITAL PUBLISHING
Articles designed for optimal readership across devices

FOLLOW US
@frontiersin

IMPACT METRICS
Advanced article metrics track visibility across digital media

EXTENSIVE PROMOTION
Marketing and promotion of impactful research

LOOP RESEARCH NETWORK
Our network increases your article's readership